Genetic determinants of tomato response to abiotic stresses

Isidore Diouf

THÈSE POUR OBTENIR LE GRADE DE DOCTEUR DE MONTPELLIER SUPAGRO

En Génétique et Amélioration des Plantes

École doctorale GAIA – Biodiversité, Agriculture, Alimentation, Environnement, Terre, Eau
Portée par l'Université de Montpellier

Unité de recherche GAFL (Génétique et Amélioration des Fruits et Légumes)

Architecture Génétique de la Réponse aux Stress Abiotiques chez la Tomate

Présentée par Isidore DIOUF
Le 20 Décembre 2019

Sous la direction de Mathilde CAUSSE

Devant le jury composé de

Alain CHARCOSSET, Directeur de Recherche, INRA Le Moulon (UMR GQE)	Rapporteur
Gilles CHARMET, Directeur de Recherche, INRA Clermont-Ferrand (UMR GDEC)	Rapporteur
Hélène GAUTIER, Directrice de Recherche, INRA Avignon (UR PSH)	Présidente du jury
Jacques DAVID, Professeur à Montpellier SupAgro	Examinateur
Mathilde CAUSSE, Directrice de Recherche, INRA Avignon (UR GAFL)	Directrice de thèse

UNIVERSITÉ DE MONTPELLIER

Montpellier SupAgro

THÈSE POUR OBTENIR LE GRADE DE DOCTEUR DE MONTPELLIER SUPAGRO

En Génétique et Amélioration des Plantes

École doctorale GAIA – Biodiversité, Agriculture, Alimentation, Environnement, Terre, Eau
Portée par l'Université de Montpellier

Unité de recherche GAFL (Génétique et Amélioration des Fruits et Légumes)

Architecture Génétique de la Réponse aux Stress Abiotiques chez la Tomate

Présentée par Isidore DIOUF
Le 20 Décembre 2019

Sous la direction de Mathilde CAUSSE

Devant le jury composé de

Alain CHARCOSSET, Directeur de Recherche, INRA Le Moulon (UMR GQE)	**Rapporteur**
Gilles CHARMET, Directeur de Recherche, INRA Clermont-Ferrand (UMR GDEC)	**Rapporteur**
Hélène GAUTIER, Directrice de Recherche, INRA Avignon (UR PSH)	**Présidente du jury**
Jacques DAVID, Professeur à Montpellier SupAgro	**Examinateur**
Mathilde CAUSSE, Directrice de Recherche, INRA Avignon (UR GAFL)	**Directrice de thèse**

Combien acquérir la sagesse vaut mieux que l'or ! Combien acquérir l'intelligence est préférable à l'argent !

Proverbe 16 :16

Xamul aay na wànte laajtewul a ka yéés. *Ne pas savoir n'est pas recommandé, mais ne pas questionner c'est pire.*

Proverbe Wolof

Remerciements

J'aimerais ici remercier toutes les personnes qui de près ou de loin ont participé à l'aboutissement de ce travail.

Tout d'abord j'adresse mes sincères remerciements à Mathilde Causse de m'avoir accueilli d'abord en tant que stagiaire dans son équipe et de m'avoir par la suite accordé sa confiance pour engager ces trois années de thèse. Si cette aventure arrive aujourd'hui à bon terme c'est aussi grâce à sa patience, ses conseils précieux, sa bienveillance et surtout son encadrement très didactique. J'ai beaucoup appris en tant que jeune chercheur et en tant que personne auprès de toi. Merci d'avoir su très vite m'orienter vers la bonne direction et de n'avoir pas hésité à me partager toutes les opportunités intéressantes qui m'ont permis de compléter ma formation et de m'épanouir pleinement dans mon travail.

Je remercie très cordialement les membres de mon jury de thèse en l'occurrence Alain Charcosset et Gilles Charmet d'avoir accepté d'être les rapporteurs pour évaluer ce travail et Hélène Gautier, Jacques David et Daniel Fonceka en tant qu'Examinateurs.

Mes différents comités de thèse m'ont également beaucoup apporté et inspiré dans mes recherches et pour cela merci à Nadia Bertin, Guillem Rigaill, Bénédicte Quilot-Turion, Jacques David et Daniel Fonceka. Daniel F. et Jacques D. vous n'avez pas hésité à aucune occasion de suivre mon parcours depuis mes premiers pas dans la génétique et l'amélioration des plantes à SupAgro ; et pour cela je vous dis encore un grand merci.

Je n'ai pas réalisé cette thèse tout seul non plus il faut le reconnaître j'ai aussi reçu une aide précieuse, notamment de la part de Laurence Moreau qui m'a accueilli au Moulon et aidé pour la modélisation statistique des interactions GxE, Frédérique Bitton pour les analyses bio-informatiques et la recherche des gènes candidats et Yolande Carretero pour tout le travail en serre et pour m'avoir appris à faire pousser des tomates. Merci à Christopher Sauvage, Rebecca Stevens, Emmanuel Szadkowski, chercheurs au GAFL avec qui j'ai pu échanger sur divers sujets scientifiques.

La thèse est une aventure humaine aussi et qui commence et s'entretient avec ses collègues de tous les jours. Merci à toute l'unité du GAFL (Génétique et Amélioration des Fruits et Légumes) pour ces trois années passées avec vous. Je voudrais d'abord commencer par mon équipe anciennement « QUALITOM » et aujourd'hui « DADI ».

Justine Gricourt, à toi je décerne le prix de la meilleure collègue de bureau☺. Merci d'avoir toujours veillé à ce que le placard à gâteaux ne soit jamais vide et surtout merci pour la *Zen' attitude* et les encouragements quotidiens ces derniers moments qui étaient un peu stressant pour moi. Avec toi Esther Pelpoir on ne s'ennuie jamais et j'ai tellement appris de chose à travers nos discussions toujours intéressantes (mais aussi pour les gâteaux au carambar). Et toi Laure (toujours à la recherche du plus beau motif de tissus Wax) merci pour les « repas autour du monde » et le tee-shirt «*Mômyandfamily*». Merci à Renaud (le King du Labo), Marie-Noël, Naïma, Rémy, Caroline, Henry, Hélène, Karine et Cécile pour les pause-café au CPER qui étaient souvent accompagnés de très bons gâteaux.

Merci à l'équipe administrative du GAFL : Evelyne Joubert-Mazellier, Sébastien Le Pioufle, Astrid Bourret, Philippe Marchand, Catherine Dogimont (actuelle Directrice) et Véronique Lefebvre

(Directrice à mon arrivée), pour avoir bien organisé tous mes déplacements et assisté dans toutes les démarches administratives durant ces trois ans.

Ces années passées à Avignon ont été aussi l'occasion pour moi de m'exercer à la guitare avec le meilleur groupe d'Avignon les « RATATOUILLES ». Merci à vous Mariem.O et Lucie.T pour ces agréables moments passés à la gratte et pour les concerts.

J'ai également eu l'occasion de croiser les anciens doctorants qui ont tous été des sortes de Maître Yoda pour moi, notamment Elise.A, Stéphanie A., Gaëtan M., Leandro O., Anna B et tout récemment Zoé T. Et aux doctorants actuels, Pierre S., Hussein K., Aimeric A., Estelle B., Delyan Z., Mamoudou D. Sévérine M. et Mariem N. je dis merci pour les sessions de journal club et tenez-bon. Et à mon presque jumeau de thèse 剑涛朝 (Jiantao) je dis 谢谢 我的 朋友. Aux amis que j'ai rencontrés à Avignon, Maxime Bocquentin (merci pour les apéros et ta grande culture botanique☺), Koffi B., Honoré, Amath, Cathleen, Hélène, Camille, Anne So, Enrico, Neus, Chandro, Alexandre, Typhaine, merci pour les apéros et les bons moments passés ensemble.

A la best team de la Paroisse St Symphorien, merci pour m'avoir fait découvrir l'Afrique à travers ces mémoriaux voyages culinaires, je veux citer par-là Dave, Prune, Olivia, Jules et Tatiana.

L'idée de faire une thèse s'est structurée surtout au cours de ma formation APIMET-SEPMET et c'est l'occasion pour moi de remercier tous mes camarades de promo et l'équipe pédagogique de la formation (Isabelle M.G, Jean-Luc R. et Jacques D.).

Merci à Corinne Picket, Muriel Fromont, Madeleine Aidi, Denis Grivel et Jean-Luc Bosio, vous qui vous êtes toujours occupés de la gestion de mes allocations WAAPP durant toute ma formation à Montpellier et à Avignon.

Et enfin, je dédie ce travail à ma famille. J'aimerais adresser un grand MERCI à vous Marthe, Rosalie, Hélène et Aloyse pour votre soutien sans faille malgré la distance. Maman et Papa, je ne pourrais jamais assez vous remercier pour tout ce que vous avez fait pour moi et pour avoir encourager et soutenu toutes mes entreprises. Je ne peux qu'être d'accord avec l'assertion de Victor Hugo qui disait *« L'amour d'une famille, le centre autour duquel tout gravite et tout brille »*.

*Et sans oublier ceux qui ont financé cette thèse : le programme **PPAAO/WAAPP** et les ANR **ADAPTOM** et **TOM-EPISET**.*

Résumé

Les plantes peuvent exprimer des réponses phénotypiques très variables en fonction des conditions environnementales auxquelles elles sont soumises. Cette aptitude généralement décrite sous le terme de **plasticité phénotypique** influence de manière très importante la productivité des espèces cultivées. La compréhension des bases moléculaires de la plasticité phénotypique est de ce fait un enjeu crucial pour l'amélioration variétale, notamment en raison des prédictions sur les changements climatiques. Cette thèse a pour objectif principal d'évaluer la réponse de la **tomate (*Solanum lycopersicum*)** aux stress hydrique, salin et thermique de caractériser l'architecture génétique de la plasticité phénotypique.

Pour ce faire, une population multi-parentale (**MAGIC**) issue du croisement de huit lignées parentales a été évaluée dans un dispositif d'**essais multi-environnement (MET)** incluant des conditions optimales de culture avec une irrigation suffisante et des conditions de stress hydrique (WD), stress salin (SS) et stress thermique (HT) en France, en Israël et au Maroc. Au total 12 environnements ont été testés, chaque environnement constituant une combinaison de Traitement x Lieu géographique x Année. Plusieurs caractères phénotypiques ont été mesurés en lien avec la vigueur de la plante, la qualité du fruit, la phénologie et des traits liés au rendement.

Les analyses phénotypiques ont révélé des **interactions génotype-environnement (GxE)** significatives pour la majorité des traits évalués. Ces interactions GxE ont par la suite été décomposées à travers différentes mesures de plasticité phénotypique en estimant la sensibilité génotypique des lignées MAGIC aux variations environnementales. Une analyse de cartographie de liaison a été réalisée en utilisant des modèles prenant en compte la probabilité haplotypique de l'origine parentale des allèles, pour identifier les locus contrôlant la variation des caractères quantitatifs **(QTL)** impliqués dans les variations de la moyenne et de la plasticité phénotypique. L'étude a mis en évidence la complexité de l'architecture génétique de la plasticité phénotypique chez la tomate, qui est en majorité (66% des QTLs de plasticité) contrôlée par des locus différents de ceux qui affectent la variation moyenne des traits.

Nous avons pu proposer des gènes candidats de plasticité qui nécessitent des études plus approfondies pour leur validation et la compréhension de leur mode de fonctionnement. Dans le contexte agronomique, les résultats présentés dans cette étude ouvrent des perspectives intéressantes pour la création de variétés de tomate adaptées aux stress abiotiques en présentant d'une part des marqueurs génétiques intéressant pour les programmes de sélection assistée par marqueurs et d'autre part, des génotypes intéressants à évaluer dans de futurs programmes d'amélioration variétale.

Abstract

Plants can express different phenotypic responses when exposed to different environmental conditions. This ability, commonly described as phenotypic plasticity, has a very important impact on crop productivity and performance. Understanding the molecular basis of phenotypic plasticity is therefore a crucial issue for plant breeding in the coming years, particularly challenged by climate change predictions. The main objective of this thesis was to assess the impact of tomato (*Solanum lycopersicum*) response to water deficit, high temperature and salinity stresses at the phenotypic level, and to characterize the genetic architecture of phenotypic plasticity.

To this end, a multi-parental (MAGIC) population, derived from the cross of eight parental lines was evaluated in a multi-environment trial (MET) design including optimal culture conditions with adequate water irrigation and water deficit (WD), salinity stress (SS) and high temperature stress (HT) in France, Israel and Morocco. A total of 12 environments were tested, each environment being regarded as a combination of Treatment x Location x Year. Several phenotypic traits were measured in relation to plant vigor, fruit quality, phenology and yield component traits.

Phenotypic analyses revealed significant genotype-environment (GxE) interactions for the majority of traits assessed. These GxE interaction were subsequently decomposed through various parameters of phenotypic plasticity by estimating the genotypic sensitivities of MAGIC lines to environmental variations. A linkage mapping analysis was performed using regression and mixed linear models, accounting for the haplotype probabilities of the inheritance of parental alleles, to identify the loci (QTL) involved in the variation of mean and phenotypic plasticity phenotypes. The study highlighted a complex genetic architecture of phenotypic plasticity in tomato, which is predominantly (66% of QTLs of plasticity) controlled by loci different from those affecting the phenotypic means.

We proposed several plasticity candidate genes that require further investigation for functional validation and a clear understanding of their mode of action. In the agronomic context, the results presented in this study open interesting perspectives for the development of tomato varieties adapted to abiotic stresses by presenting on the one hand, interesting genetic markers for marker-assisted or genomic selection programs and, on the other hand, interesting genotypes to evaluate in future breeding programs.

Communications scientifiques

Congrès international:

XIV Solanaceae and 3rd Cucurbitaceae Joint Conference at Valencia in Spain (Poster presentation), Sep 3-6, 2017

CROPS-2019, Conference about "Genomic based techniques to crop improvement and plant molecular breeding" at Hudson Alpha Institute for Biotechnology (Huntsville-Alabama, US) (Oral presentation), June 3-6, 2019

Posters:

Isidore Diouf, Laurent Derivot, Frédérique Bitton, Laura Pascual, Mathilde Causse (2017). *Tomato MAGIC population: Linkage mapping under water deficit and salinity stress*; XIV Solanaceae and 3rd Cucurbitaceae Joint Conference; Valencia, Spain

Riccini Alessandro, **Diouf Isidore**, Tizon François, Pons Clara., Monforte Antonio, Blanca José, Granell Antonio., Causse Mathilde., Mazzucato Andrea (2018). *Dissecting genetic factors underlying style position in tomato;* LXII SIGA Annual Congress; Verona, Italy

Articles acceptés :

Isidore A. Diouf, Laurent Derivot, Frédérique Bitton, Laura Pascual and Mathilde Causse (2018). *Water Deficit and Salinity Stress Reveal Many Specific QTL for Plant Growth and Fruit Quality Traits in Tomato* Frontiers in Plant Science, 9, **https://doi.org/10.3389/fpls.2018.00279**

Christophe Rothan, **Isidore Diouf** and Mathilde Causse (2018). Trait discovery and editing in tomato the plant journal, **https://onlinelibrary.wiley.com/doi/abs/10.1111/tpj.14152**

Chapitre de livre soumis :

Mathilde Causse, Jiantao Zhao, **Isidore Diouf**, Wuqian Wang, Véronique Lefebvre, Bernard Caromel, Nadia Bertin. *Genomic designing of climate-smart crops*

Preamble

Organisation du manuscrit :

Le manuscrit sera présenté sous forme d'articles organisés suivant sept chapitres, les chapitres 1 et 7 étant réservés à l'introduction et à la discussion générale. Le format de la rédaction de la thèse sous forme d'articles m'a poussé à choisir de rédiger les différents chapitres en anglais. Un résumé en Français reprenant le contexte général de la thèse, les principaux résultats et les perspectives de notre étude sera présenté en Annexe **(Appendix 1)**. Le plan ci-dessous présente les titres et un bref aperçu des différents chapitres.

Annexes

- **Annexe 1 :** Résumé substantiel de la Thèse en Français
- **Annexe 2 :** Article de revue Rothan C, Diouf I et Causse M ***"Trait discovery and editing in tomato". Plant J***
- **Annexe 3 :** Données supplémentaires du chapitre 3
- **Annexe 4 :** Données supplémentaires du chapitre 4
- **Annexe 5 :** Données supplémentaires du chapitre 5
- **Annexe 6 :** Données supplémentaires du chapitre 6
- **Annexe 7 :** Liste des QTLs détectés dans la population MAGIC depuis sa création (données publiées, en cours de publication et non publiées)

Chapter 1

General Introduction

Chapter 1 presents a general introduction contextualizing the objectives of this thesis. Tomato is presented both as an economically important and as a model species for genetic studies. The tomato genetic resources available are presented and the state of art of what is known about tomato response to some of the main environmental stresses depicted. This chapter also outlines the challenges and priorities of breeding for adaptation to abiotic stress for crop species in general. A short review of the importance of genotype-by-environment interaction (GxE) and methodologies available for its estimation is presented. Finally, multi-parental populations are presented with their major benefits as mapping populations for genetic studies.

Outline

Tomato (*Solanum lycopersicum L.)* is a major food crop which belongs to the large *Solanaceae* family. It is a self-pollinated crop and has a medium genome size (~950 Mb), a rapid cycle (2-3 cycles per year) and a relatively high rate of successful genetic transformation. All these attributes make it a model plant species.

Tomato is cultivated worldwide and intended for human consumption with two main types of production: the fresh market and processing tomatoes. Tomato fruit is an important source of micronutrients and antioxidants giving a high nutritional value to the crop. The last five decades were marked by a steady increase of tomato production (**Figure 1**) emphasizing the considerable world-wide consumption and the economic importance of the crop.

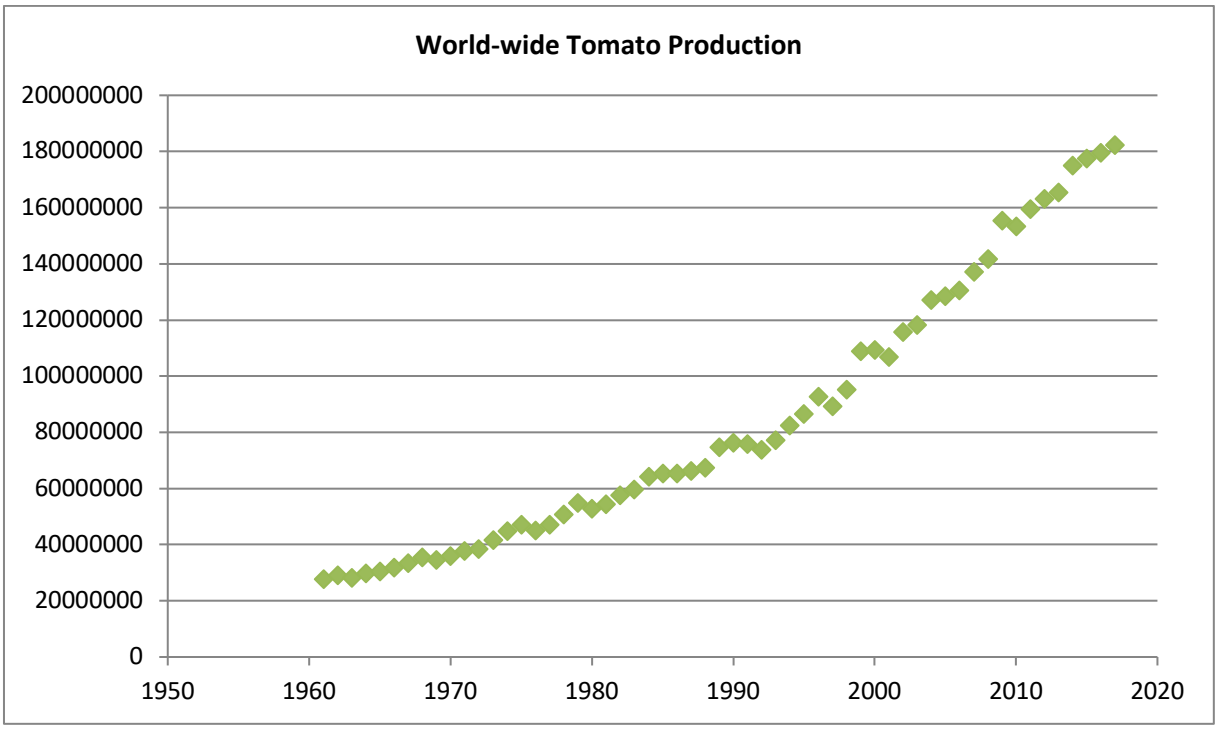

Figure 1: Total tomato production (in tons) per year over the world.

A long breeding history has shaped the current diversity observed within the species. Domestication followed by local adaptation and more recently by molecular breeding always targeted agronomic traits mainly associated to increased yield and tolerance to biotic and/or abiotic stresses. Tomato production for fresh market consumption covers a range of environmental conditions and cultural practices; be it within greenhouse or field conditions, highlighting a high adaptability. Indeed, substantial genotype-by-environment interactions (GxE) have been noticed in response to different geographical location, years or conditions of cultivation. Tomato covers an extensive diversity of genetic and genomic resources that contributed greatly in the understanding of genotype-phenotype

association within the species. The main phenotypic traits studied in tomato are summarized in **Figure 2.**

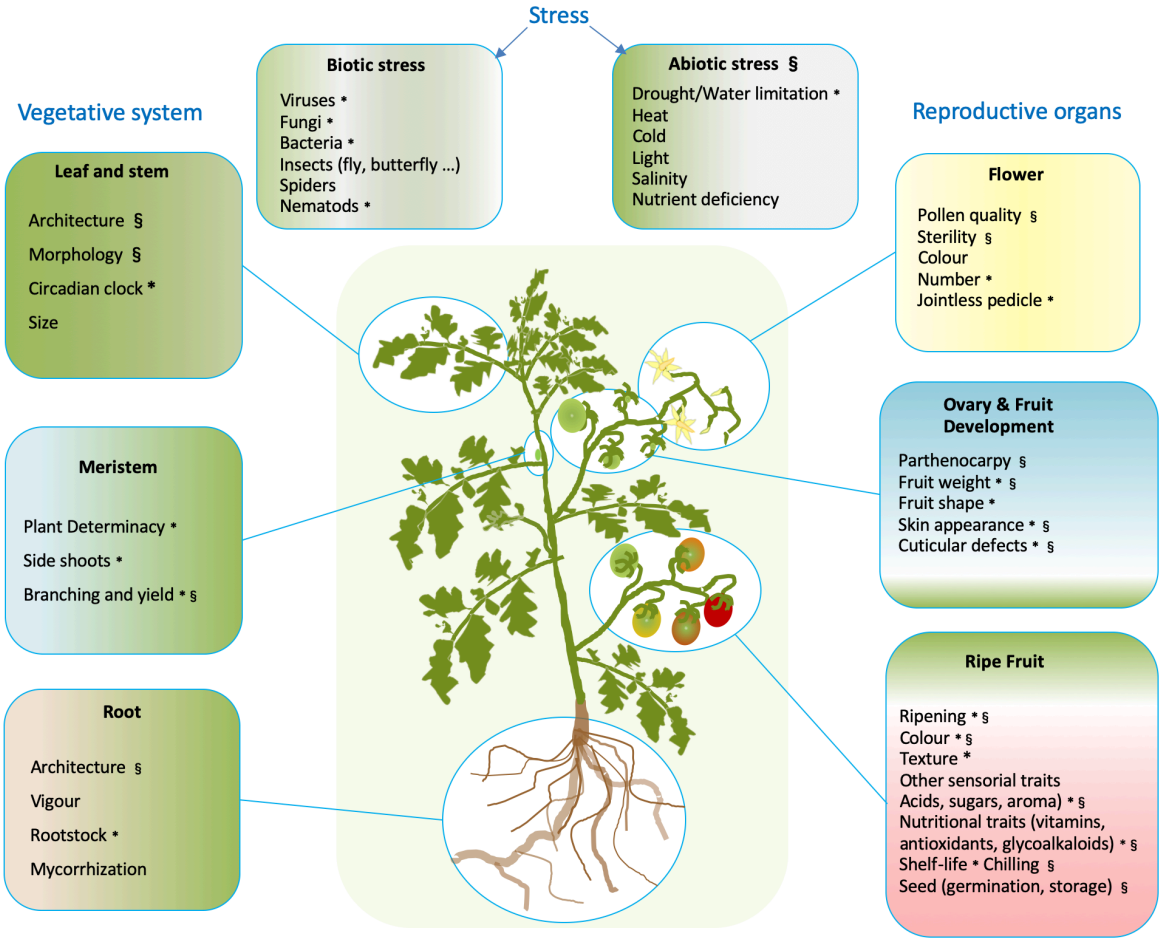

Figure 2: Main phenotypic traits studied in cultivated tomato. Left and right boxes: main tissues and associated phenotypic traits studied in tomato for their agricultural importance. Center boxes: main stresses that tomato is facing. ***** Traits selected during tomato domestication and improvement. **§** Traits highly susceptible to variations in environmental conditions.**Figure 2**

1 Genetic and Genomic resources

Tomato domestication and diversification triggered a lot of phenotypic diversity which have been deeply characterized at the genetic level and increasingly depicted at the whole genome level. Databases exist for the tomato community gathering phenotypic, genetic and genomic information from different cultivars/mutant accessions.

1.1 Tomato and its wild relatives

Tomato clade species originated in the Andean region and 12 wild related species have been distinguished according to the classification in Peralta et al., (2008). The most closely related species to the cultivated clade is *Solanum pimpinellifolium* (SP) (**Figure 3**) from which started the process of

domestication resulting to *Solanum lycopersicum* var. *cerasiforme* (SLC, the cherry tomato) at first and *Solanum lycopersicum lycopersicum* (SLL) lately (Lin et al., 2014; Blanca et al., 2015). Possible crossing between the wild and cultivated tomatoes allowed to develop experimental populations and enhanced our understanding of the genetic basis of tomato diversity. This gave also opportunity to transfer specific alleles from wild species to modern varieties, notably for disease resistances. In addition, the wild species have distinct ecological habitats and are widely distributed, from desert to equatorial regions and in variable altitudes (Pease et al., 2016). This highlights a huge potential of evolution of environmentally adaptive alleles. Indeed abiotic stress tolerance genes have been characterized in *S. habrochaites* (Liu et al., 2015; Munir et al., 2016) and *S. pennellii* (Li et al., 2013; Egea et al., 2018). These wild species represent therefore an important reservoir for biotic and abiotic stresses and have been successfully used to this end (Rothan et al., 2019). Tomato genetic resources are conserved in a wide range of germplasm collections – the TGRC being the largest collection – which include the conservation of diverse wild species (Labate et al., 2007).

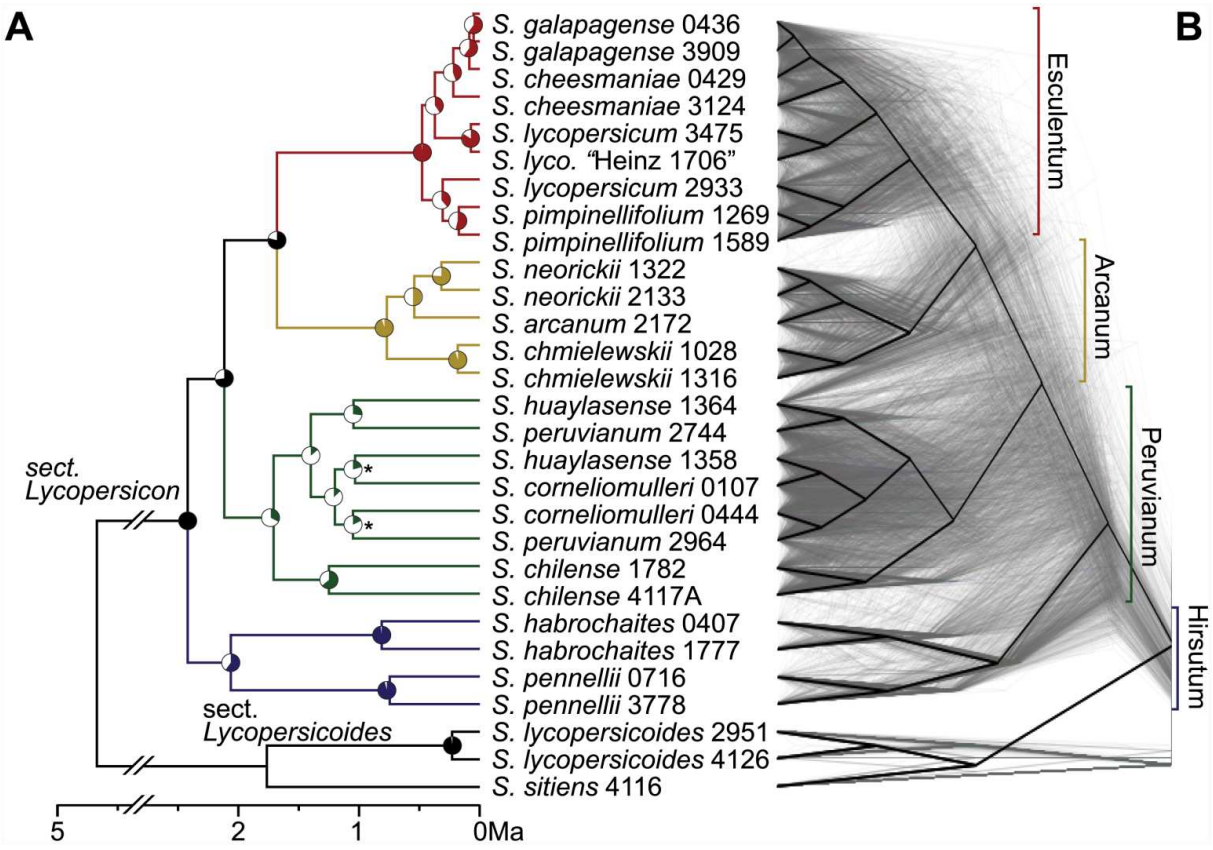

Figure 3: The phylogeny of Solanum section Lycopersicon. (A) A whole-transcriptome concatenated molecular clock phylogeny with section Lycopersicoides as outgroup. Branch colors indicate the four major subgroups (labels on right). (B) A "cloudogram" of 2,745 trees (grey) inferred from non-overlapping 100-kb genomic windows. For contrast, the consensus phylogeny is shown in black. Adapted from Pease et al., (2016).

1.2 Mutant collections

Mutant collections provide an allelic series on a uniform genetic background and also constitute important resources for enhancing our genetic understanding of tomato phenotypic diversity. Different mutagenic agents are successfully applicable in tomato for mutant induced phenotypes (Rothan et al., 2019). Mutant accessions possibly express phenotypic variation not found in natural lines which may prove helpful for forward-genetic studies. For instance, a TILLING (targeting induced local lesions in genomes) approach allowed getting more insight into the functional mechanisms of genes involved in potyviruses resistance in tomato (Gauffier et al., 2016). A large variety of mutant resources in tomato are presented in Rothan et al., (2016) who reviewed besides the wide range of biological processes successfully depicted through the use of tomato mutant collections.

1.3 Mapping populations

Mapping populations used for gene/QTL discovery in tomato are very diverse and display specific and complementary features (Labate et al., 2007). The genomic era with cheaper and high throughput sequencing capacity facilitated the access to large number of polymorphisms between individuals even between closely related species or within cultivated tomato (which was impossible before SNP availability). This opens up a lot of possibilities for new population designs. The traditional populations used for gene discovery in tomato involved crosses between two parental lines and are commonly called bi-parental populations. Among these, we can count the early generation segregating population notably the F2 populations, the backross (BC) and advanced backcross (AB), the recombinant inbreed lines (RILs) and introgression lines (ILs/NILs/BILs). Significant genomic regions involved in the regulation of tomato for a range of phenotypes have been dissected through the use of such populations (Grandillo et al., 2013; Grandillo and Cammareri, 2016). Each of these bi-parental progenies has its specificity which could result in different genetic architecture regulation (Fulton et al., 2002). Introgression lines (ILs) are derived from two parental lines in a way that all the lines have almost all the genome similar to the recurrent parent except one or few fragments of the donor line. If there is just a single region studied, we refer to NILs and BILs. An ultra-high density genotyping of a BIL tomato population increased the fine mapping resolution and allowed to point several candidate genes for leaf morphology and flowering time traits (Fulop et al., 2016).

Compared to bi-parental populations, multi-parental populations are generated from the cross of more than two parental lines, carrying a wider allelic diversity. Until now, two Multi-parental tomato populations have been developed, both generated from intraspecific and interspecific crosses of eight diverse lines. The first tomato MAGIC population involved the cross between four cherry accessions and four large fruit accessions and generated about 400 MAGIC lines (Pascual et al., 2015). The most recent tomato MAGIC population included seven parental lines selected within the cultivated species

for their resistance to fungi, bacteria and viruses and one wild relative belonging to *Solanum cheesmaniae* species and which was selected for tolerance to biotic and abiotic stresses (Campanelli et al., 2019). These two populations constitute highly relevant resources for genetic and genomic studies. Pascual et al., (2015) already demonstrated the potential of the MAGIC population to dissect quantitative trait variation in tomato. After the release of the tomato reference genome, genome wide association analysis (GWAS) was rapidly applied to the exploration of various traits. This has led to the establishment of different tomato GWAS panels encompassing core-collection of unrelated individuals from cultivated accessions, landraces and wild accessions (Ruggieri et al., 2014; Sauvage et al., 2014; Sacco et al., 2015; Bauchet et al, 2017; Albert et al., 2016b; Zhu et al., 2018). Genetic and genomic analyses using these panels furthered tomato understanding of genetic variation and allowed a meta-GWAS analysis (Zhao et al., 2019).The different populations mentioned above have different benefits and limits for studying the genetic basis of trait variation as depicted in **Figure 4**.

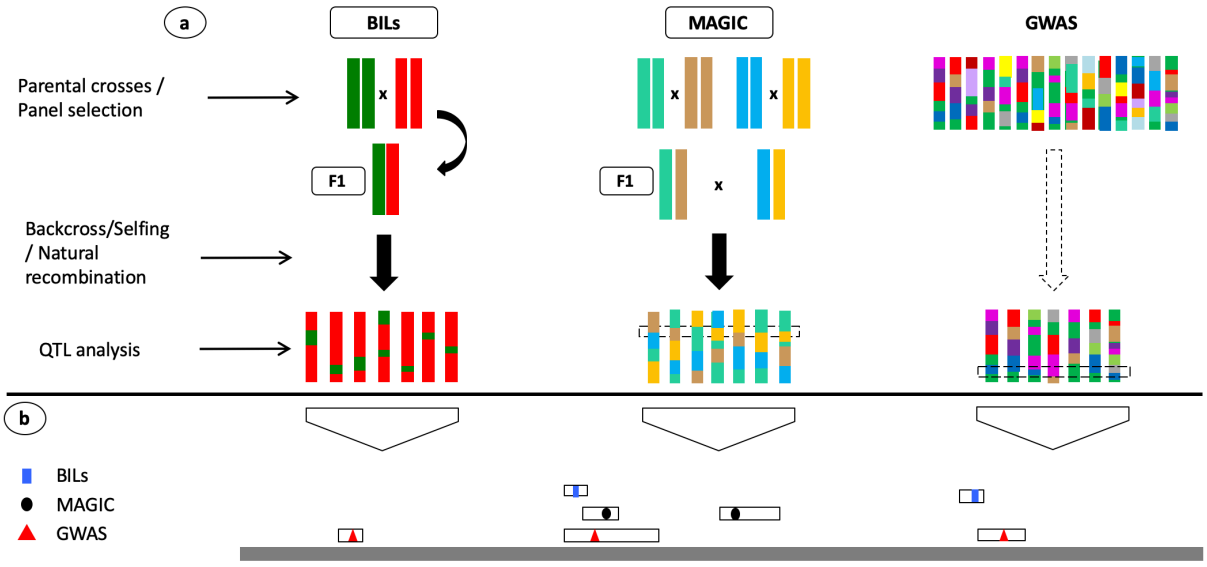

c

Time to set up	Time consuming	Time consuming	Short time
Allelic diversity	+	+++	++++
Population structure	No structure	No structure	Structure
Marker density required	++	+	+++
Mapping resolution	+++	+	++

Figure 4: New populations developed in tomato for gene/QTL mapping and identification. (a) Mapping population development and linkage/association analysis. BILs are created by backrossing the F1 hybrid into the recurrent parent, followed by several selfing generations. A single (or a few) portion of the wild recurrent parent is introgressed. MAGIC population here involved crossing four parental lines producing two F1 hybrids thereafter crossed together. The derived progeny then follows several generations of selfing to reach inbred MAGIC lines. GWAS panels are constituted by natural accessions each of which has its own recombination history. For each population and the GWAS panel, appropriate statistical models are used to decipher the linkage/association between DNA polymorphism and the observed phenotypic variation. (b) The confidence intervals around the identified QTL can be aligned onto the physical map of the reference tomato genome and compared according to their positions. Candidate genes can be suggested when the intervals are not too large. (c) Key characteristics differentiating BIL, MAGIC and GWAS populations.

1.4 Genome sequences

The improvement in sequencing technologies allowed successful completion of genome sequence in diverse animal and plant species (Goodwin et al., 2016). The first tomato genome reference was achieved thanks to the contribution of an international consortium and was published in 2012 (The Tomato Genome Consortium, 2012). The reference genome was sequenced from the inbred tomato cultivar 'Heinz 1706'. About 900 megabase (Mb) of the genome was predicted across the 12 chromosomes resulting in the assembly SL2.40 and ITAG2.3 annotation. The tomato community feedbacks and new annotation tools allowed improvements and the release of new assembly version (SL2.50) and ITAG2.4 which were used in most of the analysis carried on this thesis project. Different versions of the reference genome are available in the Solgenomic (SGN) database (https://solgenomics.net/) outlining the major differences between versions. A total of 34,727 protein-coding genes were successfully predicted. A high proportion of gene similarity was noticed with Arabidopsis which is a model in plant genetics with a high quality reference genome (Cheng et al., 2017) and the strong synteny with potato, eggplant and pepper underlined. Recently, Hosmani et al., (2019) published the last version of the reference genome (SL4.0; annotation ITAG4.0) with improved *de novo* assembly from PacBio long reads. From this assembly, 4,794 novel genes were described, and 29,281 genes conserved from the ITAG2.4 annotation. Unmapped contigs from the different genome assembly are standardly referred as chromosome 0 which measured 21.8 Mbp vs 9.6 Mbp considering SL2.50 and the last SL4.0 genome versions, respectively.

Following the availability of the reference genome, whole-genome resequencing of several other genotypes from cultivated and wild tomato species have been achieved. For instance, the genome of the stress-tolerant wild tomato *S. pennellii* (LA716) was published (Bolger et al., 2014). This species is characterized by extreme drought tolerance and unusual morphology. Many stress-related candidate genes were mapped in this species. In addition to *S. pennellii* (LA716), the reference genome of two other wild species, *S. habrochaites* (LYC4) and S. *arcanum* (LA2157) were made available (Aflitos et al., 2014). Interestingly, these species belong to the different subgroups of tomato species (**Figure 3** from (Pease et al., 2016)). The full genome sequences of eight diverse cultivated accessions was also made available from Causse et al., (2013). Almost at the same time, Lin et al., (2014) re-sequenced at low depth 360 tomato accessions from SLL, SLC and wild SP accessions allowing a comprehensive analysis of domestication process in tomato. In an effort to achieve a better characterization of tomato gene function, Gao et al., (2019) presented the first pan-genome reference. A total of 725 phylogenetically and geographically diverse accessions were included in this study and allowed to capture 4,873 novel genes absent from the reference genome 'Heinz 1706'. Next generation sequencing technologies has allowed a better characterization of genome complexity in several species (Goodwin et al., 2016). This

has led to a substantial evolution of the genomic resources developed in tomato these last decades (**Figure 5**). Up to now, around 900 tomato accessions have been re-sequenced, with the sequence depth ranging from low (3-4x) to high (>20x) (The Tomato Genome Consortium et al., 2012; Causse et al., 2013; Aflitos et al., 2014; Bolger et al., 2014b; Lin et al., 2014; Ye et al., 2017; Tranchida-Lombardo et al., 2018).These genomic resources are freely available (https://solgenomics.net) and will greatly facilitate modern breeding of tomato cultivars.

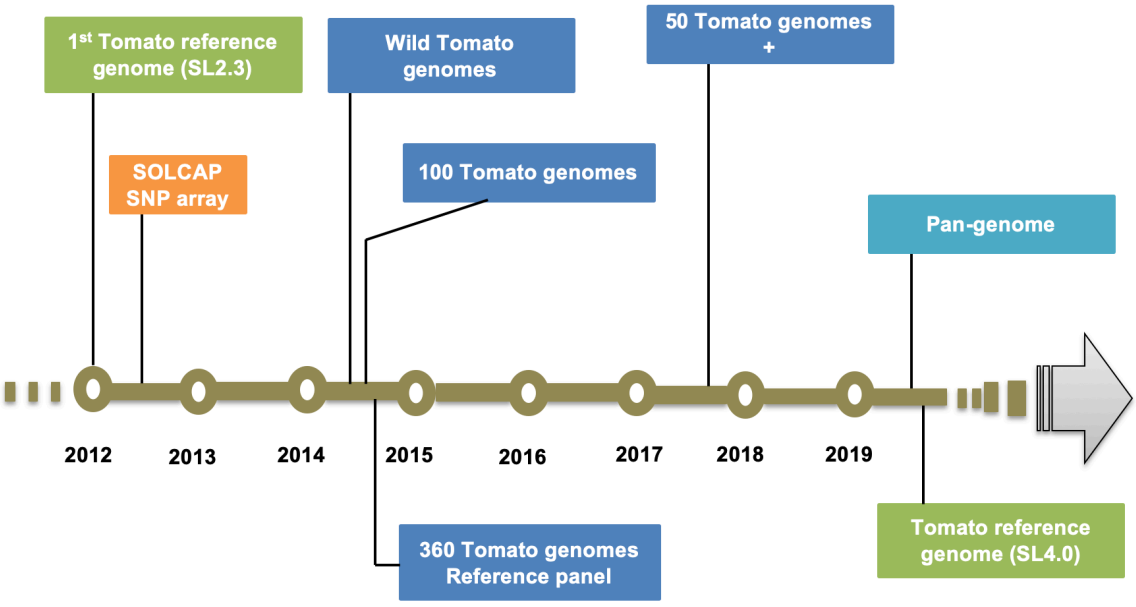

Figure 5: Evolution of the genomic resources developed in tomato

1.5 Omics data

The genomic era changed geneticist's approaches to address the phenotype-genotype association analysis, notably through the integration of information from the related fields of transcriptomics, proteomics, metabolomics and phenomics (Edwards and Batley, 2004). Complex phenotypic traits result from multiple molecular factor interactions notably the allelic variants, transcript regulation, post-translational modifications, metabolic pathways networking, which besides may potentially vary according to the environment (**Figure 6**). Numerous studies have been conducted on tomato at these different levels to achieve better understanding of phenotypic variation. For instance, Zhu et al., (2018) generated a large dataset of genomes, transcriptomes, and metabolomes from hundreds of tomato genotypes providing a valuable resource for further studies. Multi-omics datasets usually allow the identification of hundreds and thousands of genes potentially acting as important regulators of key phenotypic traits. Tomato proteome dataset have been generated to characterize proteins involved in

variation at fruit pericarp level (Faurobert et al., 2007; Xu et al., 2013), for tomato pollen (Lopez-Casado et al., 2012; Chaturvedi et al., 2013) and for abiotic stress response (Jegadeesan et al., 2018; Parrine et al., 2018). Tomato transcriptome is deeply characterized for different organs and under different environmental conditions. Efforts to assemble the large amount of transcriptomic data resulted in the creation of some database such as the Tomato Expression Atlas (http://tea.solgenomics.net/) developed through a project funded by the National Science Foundation Plant Genome Research Program and the TomExpress platform (http://tomexpress.toulouse.inra.fr/), a friendly web interface developed by Zouine et al., (2017).

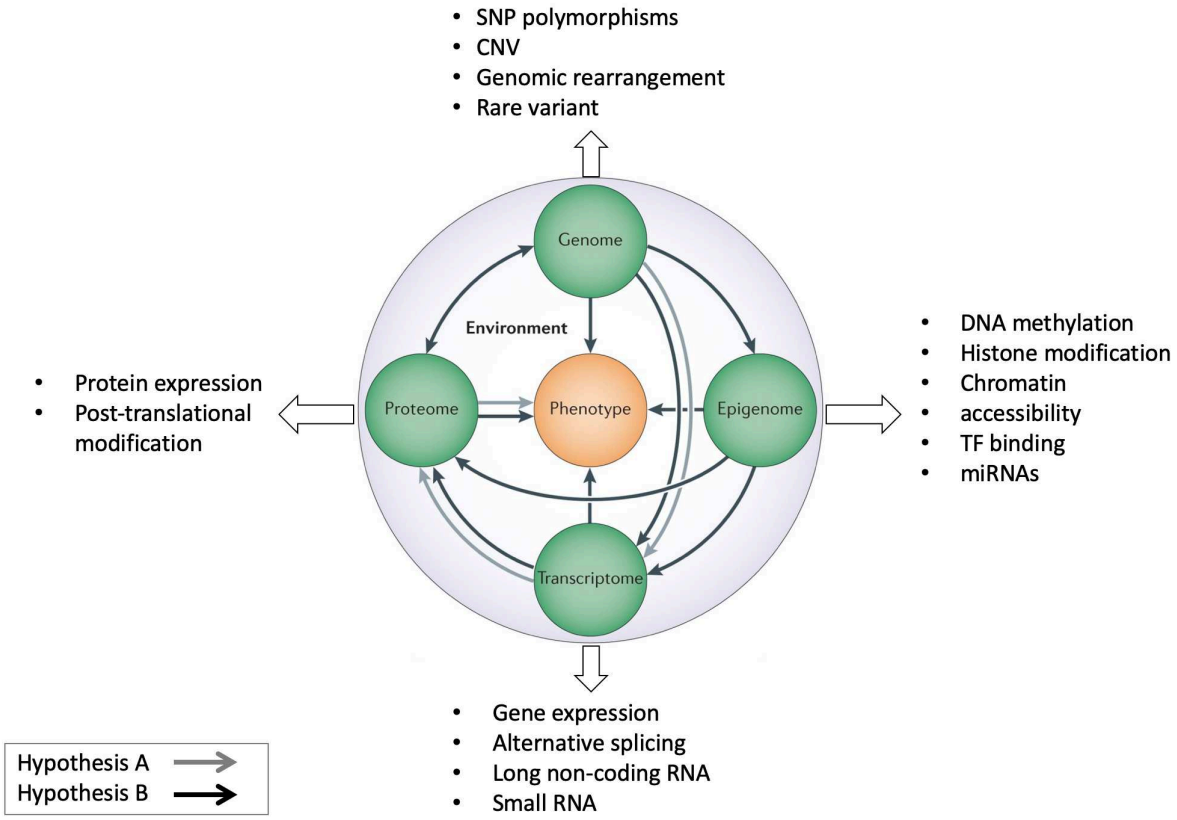

Figure 6: Hypothesis A (grey arrow) is the theory that variation is hierarchical, such that variation in DNA leads to variation in RNA and so on in a linear manner. Hypothesis B (black arrow) is the idea that it is the combination of variation across all possible omic levels in concert that leads to phenotype. Adapted from Ritchie et al., (2015).

2 Abiotic stress response in plants

Plants are non-mobile organisms subjected to frequent environmental fluctuations in their growing habitats. Reproduction success and long-term survival for these organisms require sophisticated adaptive behaviors against the variety of environmental stimuli perceived throughout their life cycle. Environmental fluctuations arising mostly from climate variation are generally referred to abiotic

stresses when they lead to serious disruption of plant metabolism and homeostasis (Munns and Gilliham, 2015). Upon exposure to abiotic stress, plant responses involve regulation at the physiological, metabolic, biochemical and molecular levels which are ultimately related to visible morphological changes. Yield reduction is a symptomatic character of abiotic stress consequences in cultivated crops. It results from the activation of the multi-level plant's defense mechanisms. Deciphering the complexity of plant response to abiotic stress is hence of primary importance for crop breeding under uneven growing conditions. Indeed, the climate change predictions expect rises in the temperatures in many areas over the world and the 2019 report of the Intergovernmental Panel on Climate Change (IPPC) group enumerated multiple potential risks of 1.5-2°C increase on crop yield (Hoegh-Guldberg et al., 2019). Indeed, considering four major cultivated crops (rice, wheat, maize and soybean) Zhao et al., (2017) predicted a significant yield decrease for 1°C of global increase of the mean temperature. The IPPC report also mentioned the emerging risk of the increase in frequency and intensity of abiotic stresses notably drought (changes in evapotranspiration and precipitation timing) and salinization of agricultural lands (rises of sea water level) (Hoegh-Guldberg et al., 2019). Several studies attempting to quantify the impact of abiotic stresses on crop productivity unequivocally come to the conclusion of a significant yield decrease, economic loss regarding crop production and potential food insecurity in some regions (Fuller et al., 2018; Kabubo-Mariara et al., 2018; Lv et al., 2018).

Thus, important efforts have been deployed by the plant biology community for better characterizing how plants respond to abiotic stresses and the multi-level activation of defense mechanisms. Indeed, more precise description of the major physiological process and molecular regulation leading to plant adaptation to abiotic stresses have been produced. Water deficit (WD) – commonly referring to drought stress in plants – high-temperature (HT) and salinity stress (SS) are among the major abiotic stress affecting crop production across species. Extensive researches dedicated in understanding the defense mechanisms against these stresses emphasized their highly polygenic nature. They are interrelated and usually co-occur, especially under field conditions. Common and specific regulatory mechanisms may interfere, depending on the stress intensity, the stage of occurrence and the potential interaction with other environmental factors.

2.1 Morphological consequences of WD, HT and SS in plants

Drought stress (WD) is probably the most documented abiotic stress for plants in the literature. Bosco De Oliveira et al., (2013) defined it as a situation of water scarcity where water potential and cell turgor are reduced under levels altering the plant metabolism and homeostasis. Water deficit primarily affects germination potential and early seedling growth (Farooq et al., 2009). This is reflected by major morphological injuries commonly observed across species encompassing reduced hypocotyl length, vegetative growth and shoot and dry weight (Fahad et al., 2017). Stress symptoms are visible at the

vegetative growth stage where leaf development is altered with effects on leaf rolling, leaf wilting and leaf bleaching (Joshi et al., 2016), which might be related to impairment of mitosis and cell elongation inhibition. Indeed, when plants are exposed to WD, water flow from different cellular compartments is disturbed, leading to a loss of turgor and reduced cell expansion. Farooq et al., (2012) attested that crops are generally more sensitive to WD stress occurring during the flowering time stage which is particularly detrimental to reproduction and yield performance.

Soil salinity has become problematic in agriculture, especially in the Mediterranean region where desertification and non-sustainable irrigation practices tend to increase the surface area of salty soils (Munns and Tester, 2008). Munns and Gilliham (2015) defined SS as the level of salinity up to which the energy for plant growth is redirected into defense response. Plants respond to SS in two distinct processes involving osmotic stress at first, occurring due to a limited ability of water uptake from the root medium and internal toxicity later, related to an excess of ion accumulation in cellular compartments (Parihar et al., 2015). Salinity may arise from the soil or the water irrigation causing in any case an excess of ion accumulation such as sodium (Na^+) and chloride (Cl^-), the two ions most used to study SS in plants. Seedling and early vegetative growth are particularly affected by salinity in plants. Poor germination rate under saline conditions have been recorded and linked to lower osmotic potential of germination media, changes in the activities of enzymes of nucleic acid metabolism, alteration in protein metabolism, hormonal imbalance and reduced utilization of seed reserves (Troyo-Diéguez and Murillo-Amador, 2000; Parihar et al., 2015). An immediate response of SS is the reduction in the rate of leaf surface expansion consequently leading to stunted growth (Parida and Das, 2005). The accumulation of ions during SS in the roots prevents from optimal water uptake causing osmotic stress, stomatal closure and reduced growth rate. Besides, high Na^+ concentration in the roots may concurrence the uptake of K^+ ion, which is necessary for proper plant development. Long-term SS or failure to osmotic stress adaptation results in the accumulation of ion at a toxic level with cell death in older leaves (Munns and Tester, 2008). Negative correlation of the salinity level and yield component traits such as numbers of pods per plant, seeds per pod, seed weight and grain yield have been documented (Parida and Das, 2005). As well, yield reduction under SS could be associated to fertility impairment.

Rising temperatures is among the most visible effect of climate change in different areas of the world. When plants are exposed to high temperatures (HT), ensuing stress are considered as short-term heat stress when the period of exposure to HT is short or long-term heat stress if plants experienced the HT for several consecutive days. The latter has more dramatic effects on agronomic performances of crops, especially when it occurs during the entire cropping season. In open field trials, seed germination is more generally impaired by HT of the soil and can differ to effects of elevated air temperatures. However, the flowering period is described as the most critical stage under HT stress

(Wahid et al., 2007). Severe yield decrease caused by HT stress arises from hampered reproduction performance with a high impact of HT on reproductive organs (Nadeem et al., 2018). In cereals however, HT stress during the period of grain filling highly impacts final yield. Nadeem et al., (2018) also documented reduced sucrose synthesis upon HT stress in sink organs which may be crucial in preventing fruit abortion. HT stress triggers osmotic stress through reduced water content induced by high transpiration rate. Wahid (2007) documented several morphological responses to HT stress in plants among which the most notable are delayed germination, loss of vigor, decline in growth rate (limit of leaf expansion, reduced inter-node); yield decrease (loss in kernel density, grain weight and grain number) and decreased fruit set (impairment of pollen and anther development).

In summary, WD, HT and SS are all responsible of reproduction alteration and yield decrease across crop species. Morphological changes imposed by these stress usually show similar injuries as presented in **Figure 7**. Crop species show different level of tolerance regarding how they are affected for yield component traits **Table 1**. Besides, there is a large genetic variability within species for the different abiotic stresses in general. However, the molecular bases of these responses are highly polygenic and emphasize the action of hundreds of genes.

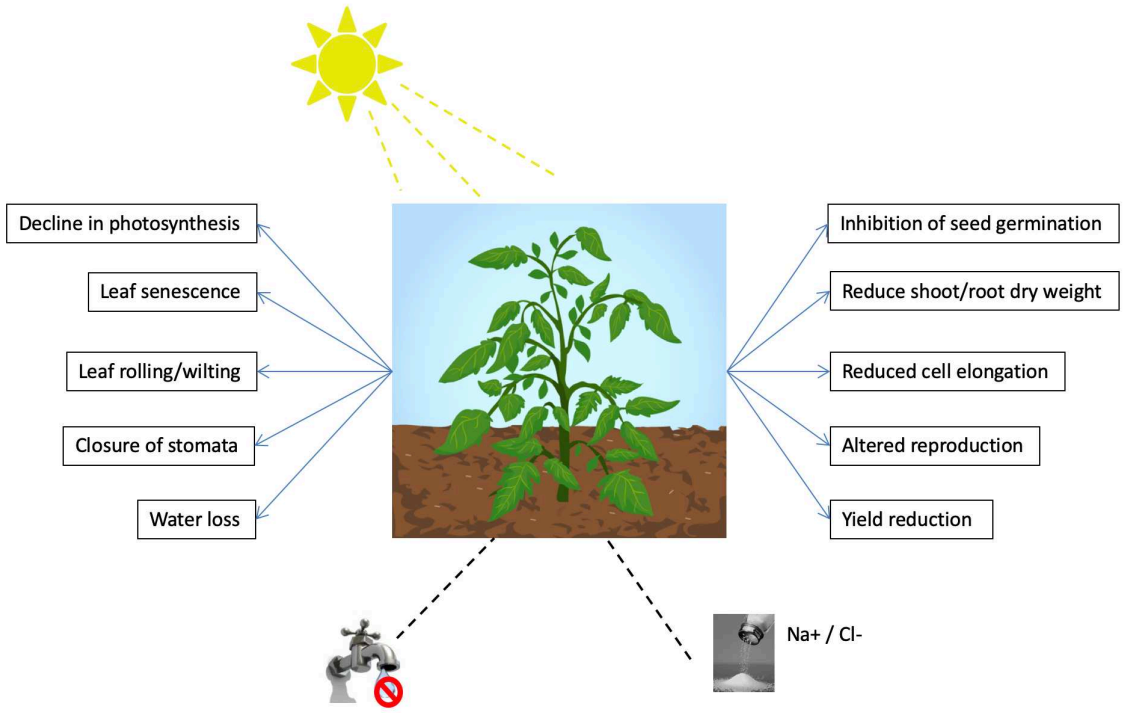

Figure 7: Morphological consequences of water deficit (WD), high temperature (HT) and salinity stress (SS) in plants.

2.2 Physiological responses

Abiotic stresses induce many physiological disorders in plants, interplaying with signal perception and transduction and homeostasis restoration. These disorders mainly relate to the occurrence of

secondary stress such as osmotic and oxidative stresses which both arise upon exposure to WD, HT and SS.

Plasma membrane is among the main cellular sites where the first impact of abiotic stresses occurs. As reviewed by many authors, WD, HT and SS all alleviate membrane fluidity favoring ion leakage from the cells which in turn lead to stress signal activation through the ionic imbalance. Solute uptake and efflux in mature guard cells occurs usually via ion channels and ion transporters located in the plasma membrane (Pandey et al., 2007). The Ca^{2+} ion is among the most well described which acts as a secondary messenger in the cell signaling network initiation (Bose et al., 2011). Variation in the cytosolic Ca^{2+} concentration opens various Ca^{2+} permeable channels on plasma membrane and triggers stress signaling. For instance, a transient Ca^{2+} increase have been described as a means to potentiate stress signal transduction and induce salt adaptation (Parida and Das, 2005). Rise in the cytosolic Ca^{2+} concentration is among the primary stress sensing activating the downstream responses in many abiotic stresses. Abiotic stress injuries importantly involve deleterious effects on photosynthesis activity. Photosynthesis is a vital function in plants and its maintenance is required for better stress adaptation (Farooq et al., 2012). Alteration in photosynthesis efficiency is related to the activation of secondary stresses, notably osmotic and oxidative stresses both occurring upon exposure to WD, HT and SS. Indeed, osmotic stress induced over limited water uptake modifies the plant water status leading to reduced stomatal conductance, leaf area, chlorophyll content and photosystem II (PSII) activity that are all important for proper photosynthesis activity. Moreover, the reduced leaf area and the closure of stomata for water-loss limitation consequently result in an increased level of internal CO_2 increasing photorespiration and hampering photosynthesis activity. Oxidative stress is widely described as a consequence of many abiotic and/or biotic stresses. It is generated by an overproduction of reactive oxygen species (ROS) which could be amplified by the photorespiration activity. A variety of ROS have been described in the literature encompassing superoxide anions (O_2^-), singlet oxygen (O_2^1), hydrogen peroxide (H_2O_2) and hydroxyl radical (OH^-) (You and Chan, 2015). However, although the accumulation of ROS products might be important in signal transduction and plant adaptation, its maintenance in non-toxic level is necessary to preserve cells from damaging effect of ROS. This implies an efficient activity of the antioxidative system of plants to alleviate the negative effect of ROS. Physiological consequences of WD, HT and SS involve mostly similar responses even though the ensuing molecular regulation activates different set of stress response genes some of which possibly stress specific.

Table 1: Abiotic stress threshold documented in the literature for major crops

A) Salinity stress			
Crop	levels of salinity	Yield reduction	Reference

Rice	150mM NaCl	36 - 50%	(Hasanuzzaman et al., 2009)
Maize	7.4dS.m-1	34%	(Cucci et al., 2019)
Wheat	18dsm	50%	(Chamekh et al., 2015)
Bell Pepper	3-7dSm	61 - 98%	(Kurunc et al., 2011)
Eggplant	5-7dsm	47 - 63%	(Ünlükara et al., 2008)
Brassica	4.5-6.76dsm	57 - 83%	(Chakraborty et al., 2016)
Cowpea	9dsm	50%	(Wests and Francois, 1982)
Tomato (SLL)	6-14dSm	36 - 70%	(Caro et al., 1991)
Tomato (SLC)	6-14dSm	4-67%	(Caro et al., 1991)
Potato	40mM Nacl	63-87%	(Zhang et al., 2005)

B) Water deficit

Crop	Growth stage	Yield reduction	Reference
Barley	Seed filling	49 - 57%	in (Farooq et al., 2009)
Maize	Reproductive	63 - 87%	in (Farooq et al., 2009)
Maize	Vegetative	25 - 60%	in (Farooq et al., 2009)
Rice	Grain filling (mild stress)	30 - 55%	in (Farooq et al., 2009)
Rice	Reproductive	24 - 84%	in (Farooq et al., 2009)
Chickpea	Reproductive	45 - 69%	in (Farooq et al., 2009)
Common beans	Reproductive	58 - 87%	in (Farooq et al., 2009)
Soybean	Reproductive	46 - 71%	in (Farooq et al., 2009)
Cowpea	Reproductive	60 - 11%	in (Farooq et al., 2009)
Sunflower	Reproductive	60%	in (Farooq et al., 2009)
Potato	Flowering	13%	in (Farooq et al., 2009)
Pepper	Vegetative	19 - 35%	(Dorji et al., 2005)
Eggplant	Whole growing season	12-60%	(Karam et al., 2011)
Tomato	Vegetative-Flowering	42 - 52%	(Patanè and Cosentino, 2010)

C) HT stress

Crop	Growth stage	T° threshold	Reference
Cowpea	Flowering	41°C	in (Wahid et al., 2007)
Corn	Grain filling	38°C	in (Wahid et al., 2007)
Rice	Grain yield	34°C	in (Wahid et al., 2007)
Pepper	Yield per plant	29°C	(Saha et al., 1970)
Tomato	Emergence	30°C	in (Wahid et al., 2007)
Brassica	Flowering	29°C	in (Wahid et al., 2007)
Wheat	Post-anthesis	26°C	in (Wahid et al., 2007)
Cotton	Reproductive	45°C	in (Wahid et al., 2007)
Potato	Flowering	38°C	(Krystyna, 2017)

2.3 Molecular responses

A plethora of stress response genes have been dissected in plants, showing altered levels of gene expression upon signalization of abiotic stresses (Zhu, 2016). Acclimation regarding different abiotic stresses generally involves common molecular responses (**Figure 8**). However, stress-specific adaptive

responses have been also documented (Muthuramalingam et al., 2017; Shaar-Moshe et al., 2017). Three major types of gene categories are recognized as important under abiotic stresses referring to: i) water uptake and ion transports; ii) osmotic and protective function and iii) signaling cascades and transcriptional regulation related genes (Munns, 2005; Fang and Xiong, 2015).

2.3.1 Water uptake and ion transports

Osmotic stress and ion toxicity subsequently occurring after exposure to abiotic stresses are responsible of cellular homeostasis disequilibrium. Plant response to re-establish homeostasis implies the activation of different classes of ion transporters to guide ion movements through cell compartments. These involve among others the HKT1, mostly important for passive transport; the NHX family of antiporters, selective for Na^+ especially under SS; the plasma/vacuole-type H^+ ATPases, which hydrolyses ATP to pump H^+ into the cell wall/vacuole; the salt overly sensitive genes (SOS) notably involved in efflux Na^+/H^+ antiporters and the cation /proton antiporter CHX which might be related to chloroplast envelope membrane (Wang et al., 2003; Munns, 2005).

2.3.2 Osmotic and protective function

Osmoprotectants are solute molecules synthesized to play a metabolic protective role, notably for membrane protein stabilization. For instance, osmoprotectants allow maintenance of cellular turgor pressure to improve stomatal conductance. The major solutes with known protective roles under abiotic stresses are proline, glycine betaine, sucrose, raffinose, mannitol, sorbitol and cyclic alcohols (Singh et al., 2015). Protective functions against abiotic stress injuries also involve the activity of genes preserving cells from ROS damaging effects (You and Chan, 2015). Proteins with protective roles in plant response to abiotic stresses are widely documented (**Figure 8**). These include essentially the glutamic-Ɣ-semialdehyde (GSA) and D1-pyrroline-5-carboxylate (P5C) for proline synthesis; betaine aldehyde dehydrogenase (BADH); choline monooxygenase (CMO); catalase, superoxide dismutase (SOD), ascorbate peroxidase (APX) and glutathione reductase for ROS scavenging, the late-embryogenesis-abundant proteins (LEAs) and their close relatives, dehydrins; and also chaperonins and Heat shock proteins (Hsp) in general.

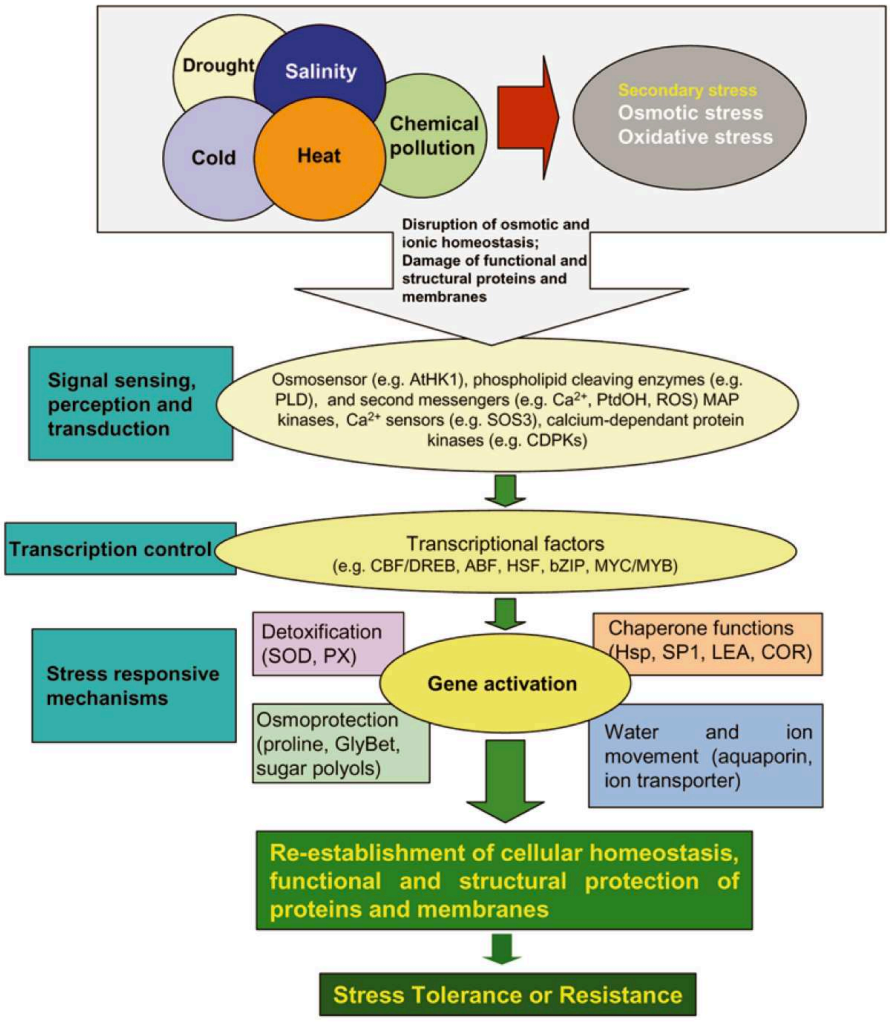

Figure 8: The complexity of the plant response to abiotic stress. Primary stresses, such as drought, salinity and heat cause cellular damage and secondary stresses, such as osmotic and oxidative stress. The initial stress signals (e.g. osmotic and ionic effects, or temperature, membrane fluidity changes) trigger the downstream signaling process and transcription controls which activate stress-responsive mechanisms to re-establish homeostasis and protect and repair damaged proteins and membranes. Inadequate response at one or several steps in the signaling and gene activation may ultimately result in irreversible changes of cellular homeostasis and in the destruction of functional and structural proteins and membranes, leading to cell death; adapted from Wang et al., (2003).

2.3.3 Signaling cascades and transcriptional regulation

Signalization is an important step in plant defense mechanisms against abiotic stresses. Calcium is an important nutrient for plant metabolism and an ubiquitous ion for plant signaling and regulatory mechanisms. Abiotic stress signaling pathways involve many calcium-dependent protein kinases (CDPKs) and calcium-regulated phosphatases which are activated following Ca^{2+} increase. Indeed, phosphatases are important for triggering stress adaptation and are implicated in different abiotic stress responses. Mitogen activated protein kinases (MAPK) cascades are kinase proteins activated by

numerous abiotic stresses which could interact with hydrogen peroxide (involved in oxidative stress response) (Knight and Knight, 2001).

Transcription factors (TFs) are specialized proteins which can bind to specific DNA elements in gene promoters and modulate gene expression in response to various external and internal stimuli (Spitz and Furlong, 2012). TFs are classified in different families based on their DNA-binding domains, some involved in stress regulation (Shaar-Moshe et al., 2017). Plant genomes contain multiple TFs some of which have been recognized as active in stress response mechanisms with conserved roles across species (**Figure 8**). Several transcriptomic analyses distinguished the major class of TFs with regulatory role under multiple abiotic stresses in plants, including AREB, AP2/ERF, NAC, bZIP, MYC, and MYB among others.

2.3.4 Post-translational regulation in response to abiotic stresses

Apart from transcription regulation, post-translational modifications are also involved in stress response mechanisms. It concerns notably epigenetic regulators and small RNAs which have been recently described with important roles in stress adaption.

Environmental perturbations can induce several epigenetic processes via specific gene regulations. Epigenetic modifications involve DNA methylation, chromatin and small RNA regulations, which can have heritable component and play different roles in response to environmental stimuli. DNA methylation and histone modifications both interfere with the regulation of stress-response gene expression (Grativol et al., 2012). Inhibition of gene transcription may occur with DNA methylation and histone modification can induce the regulation of different genes through enhancement or repression of gene expression (Chinnusamy and Zhu, 2009). A number of genes regulated under various abiotic stresses through DNA methylation and histone modification mechanisms have been documented in plants with their associated phenotypes (Kim et al., 2010). Epigenetic marks represent heritable and reversible changes that do not alter the original DNA sequence. According to Chinnusamy and Zhu (2009), heritable epigenetic modifications may provide within-generation and transgenerational stress memory.

MicroRNAs (miRNAs) are a class of small RNAs (about < 24 nucleotides) with effective roles in post-transcriptional regulation of gene expression. MiRNA biogenesis in eukaryotes has been well documented and their role in plants described (Kumar, 2014). The regulation activity of miRNAs is thought to occur via directing mRNA cleavage, translational repression, chromatin remodeling, and/or DNA methylation (Shriram et al., 2016). Two main mechanisms of miRNA action have been pinpointed by Sun et al., (2019). The first mechanism which is the main mode of action involved that the miRNA and the open reading frame (ORF) of the messenger RNA (mRNA) are completely complementary to

each other to cleave and degrade mRNA, resulting in the inability of the mRNA to be translated. Another mode of action implies that miRNAs do not fully bind to the 3'UTR region of the target mRNA leading to inhibition of the translation initiation or specific degradation of synthetic ribosomes for translational inhibition. Given the rising evidence of their important role in abiotic stress response, more and more researches are conducted to identify and characterize miRNA and their functional role in plant adaptation mechanisms. High-throughput sequencing technologies facilitates nowadays wide characterization of genomes and several miRNAs databases are now available Shriram et al., (2016). In tomato and more generally in the Solanaceae genus, interesting miRNA that could be targeted for stress tolerance improvement have been identified. For instance, miRNAs participating in the activation of stress-response genes such as MYB and WRKY TFs have been identified in tomato (López-Galiano et al., 2019) and pepper *Capsicum annuum* (Cheng et al., 2019). A tomato miRNA gene, Sp-miR396a-5p from *S. pimpinellifolium* was detected as promoting tolerance to drought, salinity and cold stress through interaction with growth-regulating factor (GRFs) genes (Chen et al., 2015). Luan et al., (2014) identified several micro-RNAs with potential role in regulating stress-related genes. Among these, the sly-miR398 was involved in drought and salinity response. Using tobacco, Rabara et al., (2015) highlighted several drought-response genes representing interesting targets for drought-tolerance improvement in Solanaceae. Salt stress altered the expression level of different ERF genes related to NICOTINE2 tobacco gene (Shoji and Hashimoto, 2015), and micro-RNA in wild eggplant (Zhuang et al., 2014).

3 Tomato response to abiotic stresses

Tomato domestication and improvement have focused for a long time on agronomic traits associated to productivity, quality and disease resistances. Crop resilience facing the global climate change nowadays represents one of the most challenging aspects in plant breeding, raising awareness in developing climate-smart crops. Understanding the complex genetic architecture of plant response to environmental changes appears to be central for the development of new cultivars. Indeed, crop's agronomic performance is altered to some extent, as a result of morphological, physiological and molecular disorders occurring with variations in environmental conditions. Stress adaptation in plants requires at the molecular level, the activation of multiple stress-response genes that are involved in different metabolic pathways for growth maintenance and whose expression is regulated by various transcription factors (TFs). The genomic era facilitated the characterization of such stress-response genes across plant species that were assigned to diverse family of TFs. The major families of TFs playing significant roles in stress tolerance that were described in the literature include the basic leucine zipper (bZIP), dehydration-responsive element-binding protein (DREB), APETALA 2 and ethylene-responsive

element binding factor (AP2/ERF), zinc fingers (ZFs), basic helix-loop-helix (bHLH), Heat-Shock proteins (HSP) and the NAC, WRKY, MYB among others (Lindemose *et al.* 2013). The functions covered by these TFs are very common in the plant kingdom, however each species present specificities. In tomato, Bai *et al.* (2018) characterized for instance 83 WRKY genes identified in previous studies and displayed their different roles in response to pathogen infection, drought, salt, heat and cold stresses. Some genes were highlighted with expression level variation under different stresses such as drought and salinity stress (*SlWRKY3; SlWRKY3 and SlWRKY33*) pointing pertinent candidates for further investigation. The expression profiles of other tomato stress-response genes were also investigated for a class of genes belonging to the ERFs family (Klay et al., 2018) and Hsp20 gene family (Yu et al., 2016). Examples of single genes involved in tomato tolerance to abiotic stress were also described including the *SlJUB1* promoting drought tolerance; *DREB1A* and *VP1.1* playing a role in salinity tolerance and *ShDHN, MYB49* and *SlWRKY39* for tolerance to multi-stress factors (Liu et al., 2015; Sun et al., 2015; Cui et al., 2018).

Water deficit (WD), high temperature (HT) and salinity (SS) represent the most important abiotic stresses threatening tomato productivity and fruit quality. A brief review of the impact of these stresses on tomato will be presented below.

3.1 Water deficit (WD)

Tomato is a high water-demanding crop (Heuvelink, 2005) making water resource management one of the key factors essential for the crop. The amount of irrigation water in tomato production is usually managed according to the reference evapotranspiration (ET_0) and the developmental stage. When water deficit (WD) occurs during the cropping period, morphological and molecular changes are usually observed that hamper the final yield production. Several studies assessed the impact of WD stress on tomato, most of which establishing WD as a percentage of water restriction, according to the optimal water requirement (Albert *et al.* 2016a,b; Ripoll *et al.* 2016).

From an agronomic point of view, the main consequence of WD on tomato is yield reduction, that can be severe when stress occurs during fruit development (Chen et al., 2013). However, all developmental stages are susceptible to WD to a level depending on the cultivar and stress intensity. Seed germination is the first step exposed to environmental stress. In tomato, a delay or even an inhibition of seed germination was observed with the application of osmotic stress (Bhatt and Rao 1987). Water deficit during vegetative and reproductive development negatively affects the overall economic performance of the crop but positive effects on fruit quality are documented. Indeed, Costa *et al.* (2007) described some trade-off between yield decrease and increase in quality component on fruit trees and vegetables including tomato, where enhancement in fruit quality compounds such as vitamin C, antioxidants and soluble sugars was observed under WD stress (Albert *et al.* 2016a; Ripoll *et al.* 2014;

Patanè and Cosentino 2010; Zegbe-Domínguez *et al.* 2003). The two groups of accessions constituted of cherry tomato and large fruit accessions usually show different sensitivity to environmental stresses. For instance, a study using a panel of unrelated lines tested under control and WD conditions revealed that large fruit tomato accessions were more susceptible and show higher response to WD (Albert *et al.* 2016b). This study also showed that the increase in the sugar content in fruit under WD is linked to the reduction in fruit water content and not to an increased synthesis of sugars. However, Ripoll *et al.* (2016) found higher fructose and glucose synthesis in tomato fruits submitted to WD stress at different stages of fruit development, indicating that both dilution effect and higher sugar synthesis are responsible of fruit quality enhancement in tomato under WD. Targeting specific genes for reverse genetic studies is now possible with the evolution of omics approaches. Variation in the expression level of several genes has been assessed under different environmental conditions and some examples are documented for water deficit response in tomato. This is the case for *SlSHN1* gene that induces tolerance to drought by activating downstream genes involved in higher cuticular wax accumulation on leaves (Al-Abdallat *et al.* 2014). Wang *et al.* (2018) identified a drought-induced gene (*SlMAPK1*) playing an active role in the antioxidant enzymes activities and ROS scavenging leading to higher drought tolerance.

3.2 Salinity stress (SS)

Considering yield as a measure of tolerance to SS, tomato is a crop that can tolerate up to 2.5dS.m^{-1} of salinity and cherry tomatoes are less salt sensitive than large fruit accessions (Caro et al., 1991; Scholberg and Locascio, 1999). Over the above-mentioned threshold, a significant yield decrease is observed. Yield reduction under SS in tomato was found to be associated to a reduction in both fruit size and fruit number (Scholberg and Locascio, 1999). As for WD, SS also leads to an increase in sugar content in tomato fruits (Mitchell *et al.* 1991). Besides, SS leads to changes in the cation/anion ratio and the increase in sugar content in fruits of salinized plants likely results from the interaction between reduced fruit water content, increased ion content, and maintained hexose accumulation (Navarro et al., 2005). These changes are the consequences of tomato response to osmotic adjustment. The threshold for salinity tolerance defined above was set upon the characterization of few selected tomato cultivars. However, Alian *et al.* (2000) noticed a high genotypic variability in response to salinity in fresh market tomato cultivars. This highlights the possibility and the potentiality for the crop to breed salt-tolerant cultivars.

Facing SS, plants deploy a variety of response to rebalance and reestablish the cellular homeostasis. Physiological responses to SS involve the ionic channel transporters as they are highly needed to regulate the ionic imbalance (Apse et al., 1999). Rajasekaran *et al.* (2000) screened salinity tolerance in a number of tomato wild relatives and associated salinity tolerance mainly to a higher K^+/NA^+ ratio

in roots. High genetic variability was observed in *S.pimpinellifolium* accessions for yield and survival traits in response to SS (Rao et al., 2013). Among the yield component traits, fruit number was the most affected in both wild and cultivated populations (Rao et al., 2013; Diouf et al., 2018). Breeding salt-tolerant variety therefore seems possible by using either physiological traits or agronomic performance under salinity, as sufficient genetic variability is available in several tomato genetic resources.

3.3 High-temperature stress

All crop species have an optimal temperature range for growth. Tomato is known as a crop that can grow in a wide range of environments, from elevated areas with low temperatures to tropical and arid zones where high temperatures usually occur. Based on crop simulation model, Boote et al., (2012) indicated that the optimal growth for tomato and its fruit development is about 25°C. Temperatures below 6°C and above 30°C severely limit growth, pollination and fruit development and could negatively impact final fruit yield. Studies on different accessions and wild relative species of tomato helped understanding how the crop is responding to low and high temperature stresses.

In tomato, HT stress around flowering was shown to inhibit reproduction by altering male fertility at high degree and female fertility at a lower rate (Xu et al., 2017). Tomato male fertility could be considered as the main factor limiting reproduction success under HT stress. This has led some studies to use pollen traits as a measure of heat tolerance instead of only final yield (Driedonks et al., 2018). Male reproductive traits were highly variable among wild species and some accessions showed high pollen viability compared to cultivated cultivars. This emphasizes possibilities for transferring heat-tolerance alleles from wild donors to cultivated tomato. A reduction of fruit setting was observed in cultivated tomato with a high rate of parthenocarpic fruits noticed under HT stress at 26°C in growth chambers (Adams *et al.* 2001). These authors noticed that fruit maturation is accelerated under higher temperature mostly when fruits are exposed themselves to heating periods, that could alter final fruit quality composition.

Considering the important effect of HT on agriculture, numerous studies successfully tackled and identified several heat-response genes (Fragkostefanakis et al., 2016; Waters et al., 2017; Keller and Simm, 2018). Heat-response genes are commonly regulated by the activity of heat stress transcription factors (HSFs) as earlier described for different organisms. This has led to the investigation of the roles played by HSFs in thermo-tolerance and majors HSFs depicted across plant species could lead to the development of heat-tolerant tomato via genome editing (Fragkostefanakis *et al.* 2015).

In addition to the major abiotic stresses, tomato is also affected for several traits by chilling stress (Heuvelink, 2005; Meena et al., 2018) and mineral nutrition deficiency (Sainju et al., 2003; de Groot et al., 2004). Essential and non-essential mineral elements required for normal plant growth have been

classified (Marschner, 1983). Their relative importance and their limiting effect in tomato are discussed in more details in Causse et al., (2019) (submitted).

3.4 Stress combination

Plant responses to individual stress at specific growth stage are well documented and avenues for crop breeding to enhance tolerance to a particular stress were provided. However, observations in the nature and in open field conditions clearly brought to light that stress combination is a common phenomenon, especially with the climate change that has an incidence on co-occurring environmental stresses such as WD and HT stress. Climate change trend has also an impact on pathogen spreading and new disease appearance and distribution (Harvell et al., 2002). Different scenarios of biotic and abiotic stress combination are then expected to arise, according to the geographical regions and areas of crop cultivation. Suzuki *et al.* (2014) presented a stress matrix with the potential positive and negative effects of various patterns of stress combination (**Figure 9**). The global effect of combined stresses on yield, morphological and physiological traits on plants can be highly different from those of a single stress. Thus the stress matrix proposed by Suzuki *et al.* (2014) would be highly useful if specified for tomato, to achieve a global view of how stress combinations could be managed in breeding programs.

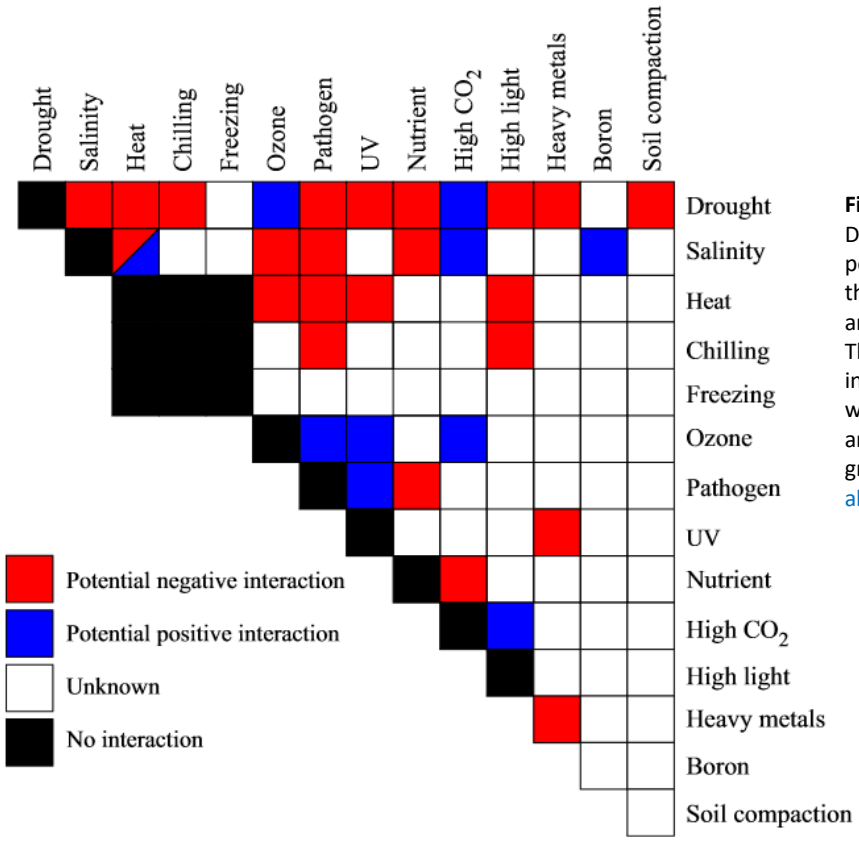

Figure 9: The stress matrix. Different combinations of potential environmental stresses that can affect crops in the field are shown in the form of a matrix. The matrix is color-coded to indicate stress combinations that were studied with a range of crops and their overall effect on plant growth and yield. From Suzuki et al., (2014).

Examples of studies conducted in tomato to assess the impact of combined stress on different traits are available in the literature. Zhou *et al.* (2017) showed that physiological and growth responses to the combined WD and HT stresses had a similar pattern across different cultivars, but the response was different from the single heat response. Combination of HT stress and SS on tomato showed however less damage on growth than the application of SS alone (Rivero *et al.* 2014). Beside morphological changes, some studies conducted on the model species *Arabidopsis thaliana* demonstrated that variations in gene expression under stress combination are highly independent of variation induced by single stress application (Rasmussen et al., 2013).

4 Genotype-by-environment (GxE) analyses in plant

4.1 GxE definition

Genotype-by-environment interaction (GxE) is a common phenomenon in crops that has received considerable attention particularly because of its profound implication in breeding (Allard and Bradshaw, 1964). It occurs when different genotypes exposed to different environmental conditions exhibit distinct phenotypic responses (El-Soda et al., 2014). The presence of GxE is closely related to the concept of phenotypic plasticity as illustrated in **Figure 10**. Crop production suffers from the phenomenon of GxE when the commonly used varieties display non-stable agronomic performance from different growing conditions. Variation in the environment may arise from year-to-year cultivation, different cropping systems or different geographical locations. Moreover, the global climate change also affects greatly environmental fluctuations leading to GxE, especially in open field conditions. The analysis of GxE in the context of plant breeding usually include a set of genotypes selected by a breeder to test in a targeted population of environments (TPE) where the cropping are intended to take place. This might imply on one side elite varieties that have been selected for agronomic characters earlier and on the other side different locations or abiotic stress conditions (Admassu et al., 2008; Rodriguez et al., 2008; Tonk et al., 2011). This strategy allows to identify interesting genotypes that perform well in specific growing conditions and others that are more stable showing non-significant variation from one environment to another. Exploring the extent of GxE in a panel of genotypes from the breeder's collection is judicious for the selection of environmentally adapted varieties. A more comprehensive approach for the study of GxE is to use experimental immortal populations with fixed lines that can be grown in different environments. Mapping populations such as RILs, MAGIC, NAM and GWAS panels are interesting because they also offer the possibility for including genotypic information in GxE modelling and dissect directly the genomic regions related to the occurrence of GxE (van Eeuwijk et al., 2010). Thus, molecular breeding could be

conducted on GxE component. Different analytical tools were proposed to analyze GxE in crops which will be developed below.

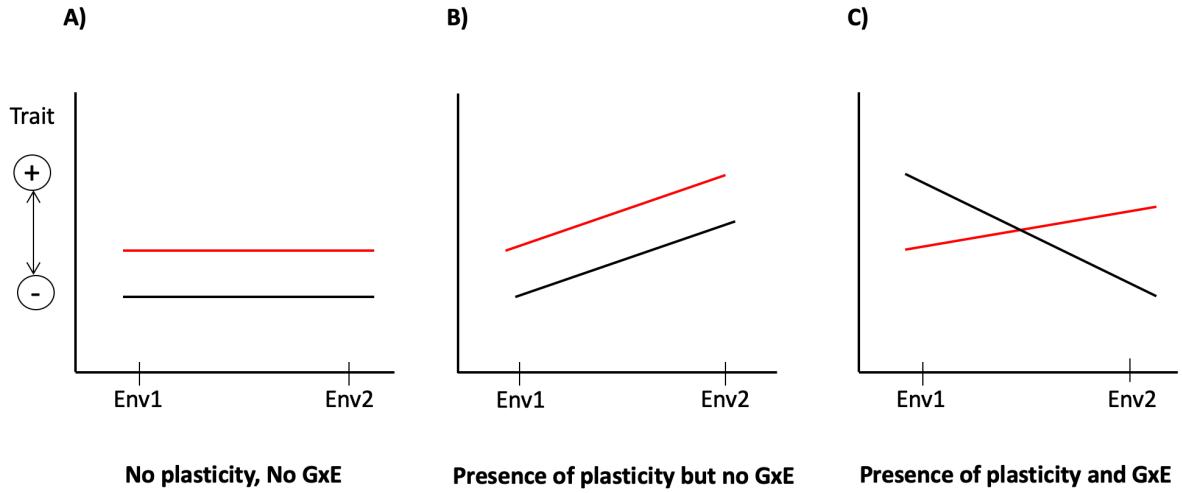

Figure 10: Graphical representation of GxE and phenotypic plasticity. This graph depicts different situation for two genotypes (black and green line) in two environmental conditions (Env1 and Env2). In A) both genotypes show no response to the environment thus denoting no plasticity and no GxE. B) Represents a situation where both genotypes have positive response to Env2 hence the presence of plasticity, but the response was similar so denoting absence of GxE. In the situation C) the genotypes show different response (antagonistic in this case) showing in this way both plasticity and GxE.

4.2 Methods for GxE estimation

The characterization of GxE in plants requires the evaluation of a set of genotypes (or a population) in a range of environmental conditions for one or multiple traits referred as phenotypes. A statistical decomposition of the phenotype has been proposed via the following equation: P = G + E + GxE where a phenotype (P) is the sum of the combined effects of genetic (G), environment (E) and their interaction (GxE) factors (Lynch and Walsh, 1998). Malosetti et al., (2013) reviewed a series of model that can be used to explore, describe and predict GxE in plant. **Table 2** present different models used in the literature for the analysis of GxE encompassing linear, bilinear and mixed models.

The full factorial analysis of variance (ANOVA) model (1) describes the simplest and starting model to explore GxE. In this model, Y_{ij} represents the phenotype for genotype i (G_i) in environment j (E_j) and GE_{ij} and ε_{ijk} represents GxE interaction and error terms, respectively. This model allows accounting simultaneously for the within and between environment variation. All the dataset is used for this purpose, although unbalanced dataset may lead to misinterpretation. Constant residual variances are assumed from the different environments which might not reflect the reality. Besides, this model does not allow accounting for any complexity of the trial design. Thus, its use is mainly restricted for GxE exploration.

Table 2: Commonly used statistical models for GxE analysis

Model name	Model formulation	Model
Full factorial	$Y_{ij} = \mu + G_i + E_j + GE_{ij} + \varepsilon_{ijk}$	(1)
Additive model	$Y_{ij} = \mu + G_i + E_j + \varepsilon_{ij}$	(2)
Joint regression	$Y_{ij} = \mu + G_i + \beta i E_j + \varepsilon_{ij}$	(3)
Factorial regression	$Y_{ij} = \mu + G_i + E_j + \sum_{k=1}^{K} \beta_{ik} C_{jk} + \varepsilon_{ij}$	(4)
AMMI	$Y_{ij} = \mu + G_i + E_j + \sum_{k=1}^{K} \beta_{ik} \delta_{jk} + \varepsilon_{ij}$	(5)
GGE	$Y_{ij} = \mu + E_j + \sum_{k=1}^{K} \beta_{ik} \delta_{jk} + \varepsilon_{ij}$	(6)
Linear mixed models	$Y_{ij} = \mu + \underline{G_i} + E_j + \underline{GE}_{ij} + \varepsilon_{ijk}$	(7)

The additive ANOVA model (2) is preferably applied than the full factorial ANOVA. Here, the dataset input is summarized to the two-way table consisting of single values (average) per genotype and environment. These values are usually estimated by calculating the adjusted means derived from single environment analysis. Within-environment modelling is an important first step in GxE analysis as it allows environment-specific quality control and spatial heterogeneity correction which may arise from local effects of genotype positions (row/block effect) in the trial. The additive model (2) depicts the variation of a trait into parts attributed to intrinsic genotypic effect and external environmental effect. It is also an explorative model and do not allow to go beyond in interpreting what causes the observed GxE nor to assess directly the GxE significance. From this model, GxE is not directly estimated but rather it is incorporated in the residual errors from which it can be inferred (Malosetti et al., 2013).

An attractive and widely used model for GxE analyses from the plant breeding perspective is the joint regression also called Finlay-Wilkinson model (Finlay and Wilkinson, 1963). The popularity of this model in crops lies in the fact that both the general performance and stability, within the range of environments recorded can be estimated for a given genotype (Romagosa et al., 2013). The joint regression model (3) uses the average performance of all genotypes in every environment as a proxy measuring a hypothetic environmental quality index. Environments are then ranked from the poorest to the highest environment and the GEI described by genotype-specific regression slopes on the environmental quality indexes (Malosetti et al., 2013). The estimated βi terms represent the environmental sensitivity of the genotypes which is a measure of adaptability. Genotypes are then classified from the most adaptable (highest βi) with a high potential of performance in good environments to the least adaptable, which do not increase performance in good environments

compared to the vast majority of the genotypes tested. The expected average performance of a genotype is represented by the sum of the intercept (μ) and the estimated genotypic effect (G_i).

Factorial regression model is an alternative of the joint regression model in the case where environmental variables have been measured and the environments characterized according to embedded biological information. Environmental covariates are then used as explanatory variables and GxE described as differential genotypic sensitivity (β_{ik} terms in model 4) to these covariates (C_{jk} terms in model 4) which could represent temperatures, water irrigation or soil characteristic (Malosetti et al., 2013). An important aspect for factorial regression model is the selection of the environmental covariates which could greatly impact the interpretation of the GxE. Using a high number of covariates is not straightforward for linear regression models. Thus covariates should be selected only if relevant and not correlated for parsimony and better interpretation of GxE (Brancourt-Hulmel et al., 2000; Leflon et al., 2005).

Other models have been proposed with the particularity of including multiplicative terms to characterize the GxE. The additive main effects and multiplicative interaction (AMMI) model (5) for example allows to use K multiplicative terms referring to the product of a genotypic sensitivity (β_{ik}) environmental quality (δ_{jk}). The multiplicative terms in the AMMI model are derived from the singular decomposition of the GxE interaction matrix which is computed from the residuals of the additive model (van Eeuwijk et al., 1995). The different PCA axes are then retrieved and used to depict GxE. A slight modification of the AMMI model (5) was proposed to consider GxE and the main genotype effect together leading to the Genotype main effects and GxE (GGE) model (6) described in (Yan et al., 2000). This model is very useful for visualizing the overall performance of the genotypes through biplot tools (Malosetti et al., 2013). Biplots exploration can help to dissect the relationships between genotypes and environments for a given phenotypic trait.

Linear mixed models allowed substantial improvement in quantitative genetic modelling through the inclusion of random effect for complex dataset (Smith et al., 2005). Malosetti et al., (2013) outlined the interest of considering genotype as random in the context of GxE modelling as it allows considering genetic covariances and correlations between performances in different environments. These models are useful to compare the relative importance of GxE regarding the main genotype effect. Mixed model's framework offers a large flexibility in modelling variance structure in GxE. A simple and unrealistic model is the compound symmetry model which only considers genotype effects as random without structuration of the residual variances. When environments are highly heterogeneous (*e.g* stress vs non-stress environments), the heterogeneous model is more interesting for allowing environment specific residual variances (Malosetti et al., 2013; Romagosa et al., 2013). Besides, more complex models have been documented, notably the unstructured and factor analytic models which accounts for specific structure in the MET design (Boer et al., 2007).

4.3 Phenotypic plasticity

Phenotypic plasticity is commonly defined as the ability of a single genotype to produce different phenotypes in response to the environment (Des Marais et al., 2013). When multiple genotypes and different environments are considered, differences in their plasticity lead to GxE phenomenon. Plasticity has been considered as playing an important role in evolution given that it may procure adaptive features when the new phenotypes produced in new environments tend towards the optimum (Ghalambor et al., 2007). In crops, plasticity is intrinsically linked to the concept of stability which is important in the agronomic point of view. A stable or environmentally canalized genotype refers to individual with little or no phenotypic variation when exposed to new environments while a plastic genotype will display larger phenotypic variation in new environments. Phenotypic plasticity and environmental canalization may be viewed as two opposed concepts (Flatt, 2005) and could both be related to stability. The concept of canalization was first reported by (Waddington, 1942) who considers it as developmental adjustment occurring in variation of the physical and/or genetic environment leading to conserved phenotypic expression. For crop production, plant breeders and farmers may prefer a canalized/stable genotype with considerably predictable behaviors compared to plastic genotypes. Various statistical methods for the estimation of stability have been documented and classified in three groups according to Lin et al., (1986). Three stability concepts were proposed by these authors who considered a genotype as stable when i) its among-environment variance is small; ii) its response to environments is parallel to the average response relatively to the test set of genotypes; iii) the residual mean-squares from the regression model on the environmental index (joint regression model defined in section 4.2 above) is small. These different concepts of stability have different implications. The first stability concept for example only teaches us about the extent of which a genotype is plastic /canalized with no inference about its performance. Thus, the second and third concepts have more implication for plant breeders; however, they are estimated relatively to the set of the genotypes included in the analysis and are then highly sensitive to the number and diversity of the selected genotypes test set. A variety of methods for quantification of phenotypic plasticity have been proposed in the literature (Valladares et al., 2006) and could be grouped in one of the three concept of stability proposed by (Lin et al., 1986).

The genetic basis of phenotypic plasticity have been investigated and (Bradshaw, 2006) proposed the presence of specific genes controlling phenotypic plasticity of an organism that might be distinct from constitutive genes. This opens up the possibility for considering plasticity as a trait *per se* on which breeding could be carried out. However, phenotypic plasticity have different features that should be considered when studying it, notably its great dependence on the environmental range, the phenotype measured and the method used for its quantification (Pigliucci et al., 2006).

4.4 Genetic dissection of GxE

From the genetic point of view, Des Marais et al., (2013) defined GxE as the effect of a locus that changes in magnitude or direction across environments. Different statistical models have been proposed in the literature to identify the genetic loci governing the expression of GxE, which are commonly referred as interactive QTLs or QTLxE (El-Soda et al., 2014). The simplest way to test for the presence of QTLxE is to compare QTL effects from the single environment QTL analyses. This strategy was applied by Paterson et al., (1991) for example, who was among the first describing QTLxE by comparing tomato QTLs detected in three different environments. Different QTLs types can be distinguished with this approach (**Figure 11**). Des Marais et al., (2013) reviewed 37 QTLxE analysis published before 2013 for 11 species and observed that about 57% of the QTLs identified were environment specific. However, whether these QTLs were undetectable in other environments due to methodological limitation or real QTLxE is not always evident.

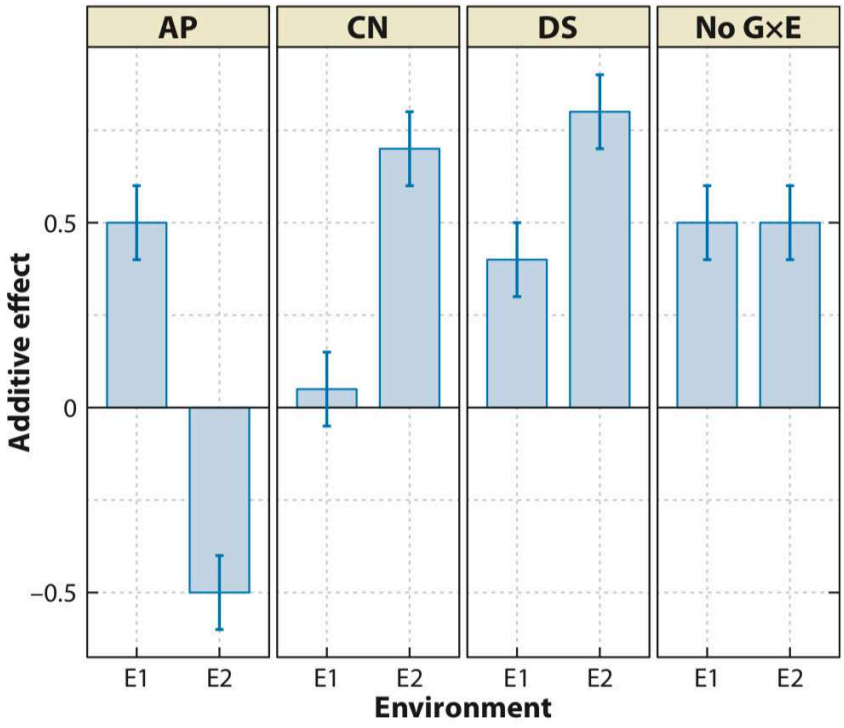

Figure 11: Patterns of quantitative trait loci additive effects for traits that show genotype-by-environment interactions (G×E) can fall into four main categories: (a) antagonistic pleiotropy (AP), the result of sign changing additive effects; (b) conditional neutrality (CN), additive effects limited to only specific environmental conditions; (c) differential sensitivity (DS), the result of changes in magnitude of additive effects; and (d)no G×E, no detectable change in additive effects across environments; adapted from Des Marais et al., (2013).

More sophisticated methods to test for the presence of QTLxE have been proposed, most of them being based on the models used to describe GxE at the phenotypic level. Mixed models for instance are powerful for detecting QTLxE as they allow defining either fixed or random term for modelling

complex data sets. Indeed, Malosetti et al., (2013) extended the framework of mixed model analysis of GxE by integrating molecular marker information to detect the genomic regions governing QTLxE in maize. A review presenting the potentiality offered by mixed models to dissect QTLxE was proposed by (van Eeuwijk et al., 2010). Different steps are required for multi-environment QTLs detection through the use of mixed models. At first, the best variance-covariance model fitting the phenotypic data needs to be determined. This selection will mainly rely on detecting the best parsimonious variance structure regarding the quality of the model and the number of parameters integrated. A genome-wide QTL scan is then conducted using the genomic marker information for QTL detection where the QTLxE effects could be tested jointly or independently for the marker and marker-by-environment interaction (van Eeuwijk et al., 2010; El-Soda et al., 2014).

Recently, approaches for detecting QTLxE using phenotypic plasticity emerged in plants yielding promising results for crop breeding in the context of GxE. These methods use the estimates of phenotypic plasticity which is further considered as phenotype denoting trait-response to environment variation. Valladares et al., (2006) proposed different quantification of plasticity and presented the conditions of relevance of each. For instance, phenotypic plasticity could be computed by the difference or relative proportion of the phenotypic values in stress vs control condition when only two environmental conditions are considered. When a high number of environments are screened, relative approaches for plasticity quantification could be used based on the joint regression or factorial regression models (Laitinen and Nikoloski, 2019). Numerous studies explored the genetic basis of phenotypic plasticity with such approaches across species (Lacaze et al., 2009; Kusmec et al., 2017; Mangin et al., 2017; Xavier et al., 2018).

5 Multi-parental mapping populations

Multi-parental populations have been proposed as alternative to overcome the limiting allelic diversity present in bi-parental mapping populations. Different types of multi-parental populations exist and are mostly categorized in Nested Association Mapping (NAM) or Multi-parent Advanced Generation Intercrosses (MAGIC) populations. These populations have interesting characteristics making them suitable resources for genetic studies in plants.

5.1 NAM populations

The Nested Association Mapping (NAM) populations are achieved by a complex mating design where multiple parental lines are crossed with a common parental line. The first NAM population in crops was developed for maize (Yu et al., 2008) and was characterized as a powerful experimental population exploiting the advantages of linkage and association mapping analyses. It was developed from the

crossing of 25 inbreed lines to a common reference parent 'B73' (**Figure 12**), selected from the important US inbreed lines and according to agronomic and physiological characteristics. NAM populations were also developed in soybean (Diers et al., 2018), sorghum (Jordan et al., 2011), barley (Maurer et al., 2015) and wheat (Bajgain et al., 2016). The genetic architecture of a lot of traits have been dissected in the NAM populations, highlighting interesting genomic regions for breeding perspectives and allowing the identification of candidate genes underlying trait variation in crops (Tian et al., 2011; Cook et al., 2012; Bajgain et al., 2016; Bouchet et al., 2017).

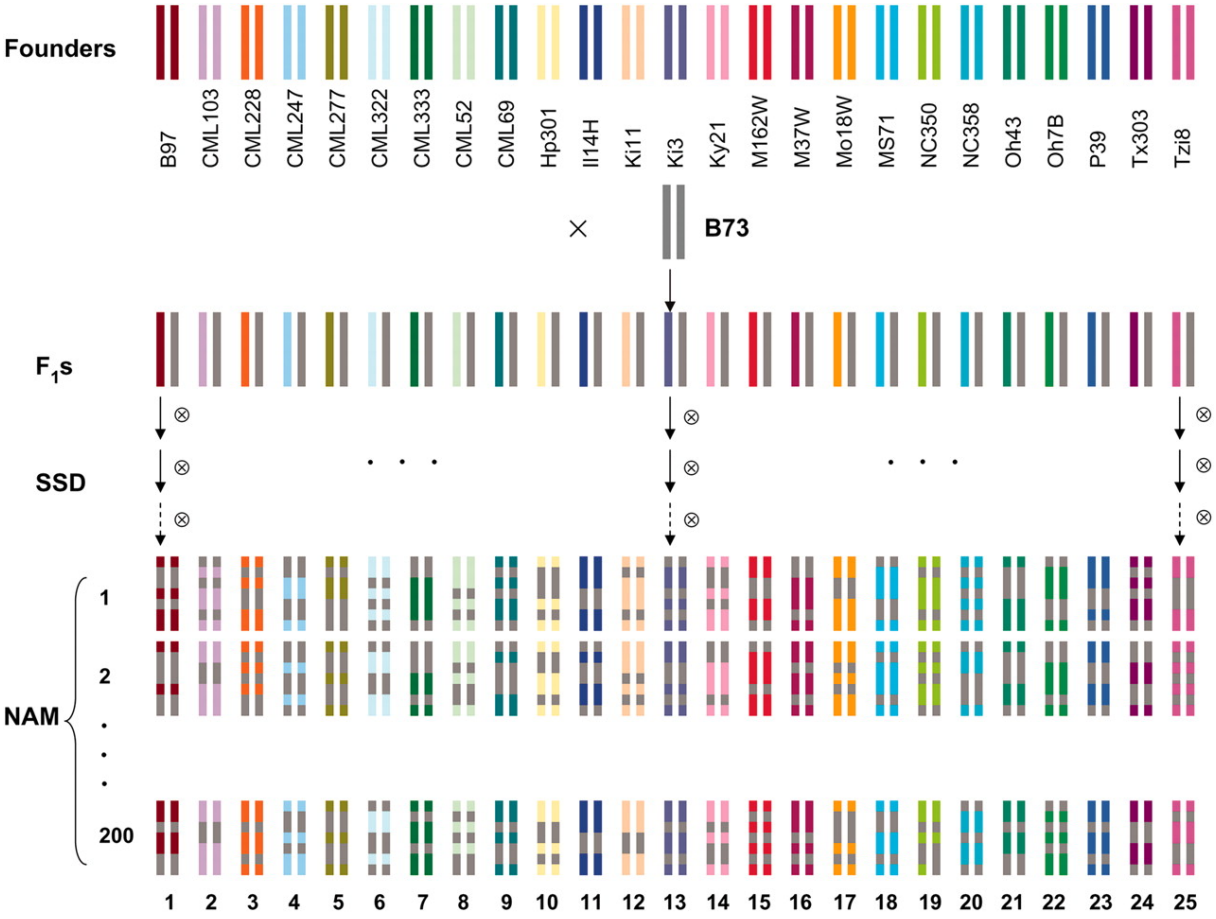

Figure 12: Crossing design between 25 diverse founders and the common B73 generating 5000 immortal genotypes. Due to diminishing chances of recombination over short genetic distance and a given number of generations, the genomes of these recombinant inbred lines (RILs) are essentially mosaics of the founder genomes; X crossing; ⊗ selfing (SSD); adapted from Yu et al., (2008).

5.2 MAGIC populations

Multi-parent Advanced Generation Intercrosses (MAGIC) populations are issued from the crossing of multiple parental lines (> two parental lines) followed by intercrossing of the first generations of descendant lines then allele fixation of the whole offspring to generate recombinant inbreed lines (RILs). These populations are characterized by an important allelic diversity dependent on the genetic

distance between the selected parental lines. Each MAGIC RIL's genome comprises an approximately equal proportion of alleles from every parent.

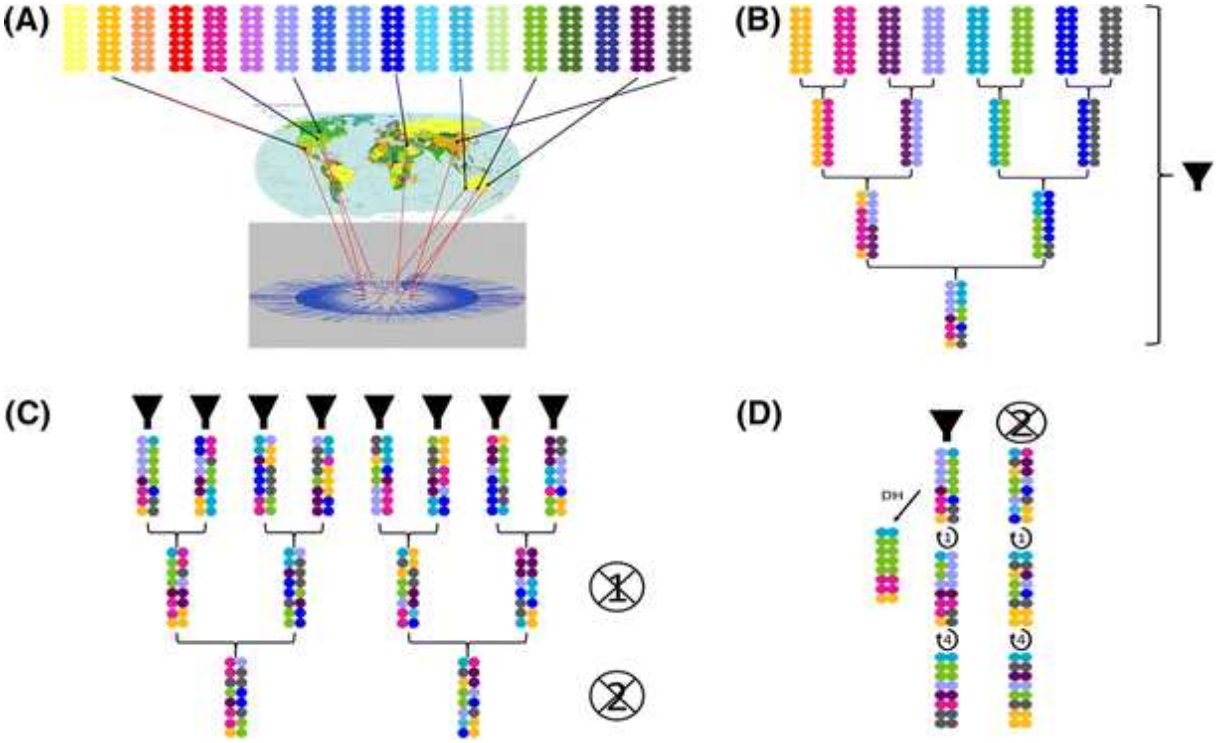

Figure 13: Stages of an 8-way MAGIC population development from eight founders. A) Selection of founders based on geographic, genetic, phenotypic diversity. The maternal pedigree tree is presented at the bottom for an eight-way MAGIC population with each ring representing a subsequent generation; B) mixing of parents together in predefined patterns, or funnels (denoted by symbol on right); C) intercrossing of individuals (generations denoted by number within crossed circle) derived from different funnels for additional generations; D) selfing (generations denoted by number within circular arrow) or double haploidization of individuals either directly from funnels or after advanced intercrossing to form inbred lines; From Huang et al., (2015).

5.2.1 MAGIC populations in plants

Genetic analyses of MAGIC population was first described in mouse (Mott et al., 2000). Thereupon, MAGIC populations disseminated in plants and were developed for *Arabidopsis thaliana* (Kover et al., 2009), wheat (Huang et al., 2012), rice (Bandillo et al., 2013) and tomato (Pascual et al., 2015) among other species. MAGIC populations accumulate a high number of recombination events rising the power and precision of quantitative trait loci mapping. The development of MAGIC populations takes relatively long time and requires different steps. At first, the selection of the parental lines must be carefully operated. Parental lines might be selected upon different characteristics, notably for disease or abiotic stress resistance (Bandillo et al., 2013; Stadlmeier et al., 2018; Campanelli et al., 2019) or for agronomic performance and breeding objectives (Mackay et al., 2014; Pascual et al., 2015). However, parents should always include the maximum diversity if genetic and genomic analyses are intended.

Multiple two-way crossing is then carried from the chosen parental lines to generate the first hybrids (F1) generation. Ensuing intercrossing between the F1 and their direct descendent may happen through different strategies; with the most common – for a balanced allele distribution in the final offspring – presented in **Figure 13**. A brief comparison between MAGIC and other mapping populations have been presented in section 1.3 (**Figure 3**). Besides, MAGIC populations advantages have been documented in the literature including high accuracy of genetic maps (Pascual et al., 2015; Gardner et al., 2016); potential resource for pre-breeding/breeding (Mackay et al., 2014); great diversity for high order epistasis detection (Mathew et al., 2018; Ogawa et al., 2018) and ability to capture GxE (Diouf et al., 2018; Xavier et al., 2018).

5.2.2 QTL detection in the MAGIC population

Although MAGIC populations present multiple advantages, the use of suitable statistical models is required for genetic analyses especially in the QTL mapping. A review of different statistical modelling for quantitative analyses of MAGIC populations was proposed by (Huang et al., 2015). Two main approaches can be used for QTL mapping in MAGIC populations lying in the use of i) marker scores such as in bi-parental populations referring to the bi-allelic approach, or ii) the haplotype probabilities of parental allele's origin referring to the parental probabilities approach, where the probabilities of parental allele affiliation are inferred at each marker positions. Mott et al., (2000) depicted some limits with the bi-allelic approach mainly because not all information of the parental polymorphisms is taken into account. Indeed, for n progenitor lines and for a given position, each MAGIC RIL has 1/n chance to inherit one of the parental alleles. Thus, assigning alleles to one of the parents may be ambiguous since different parents carrying the same allelic status might be observed. The limits with the bi-allelic approach is well illustrated in **Figure 14** from Verbyla et al., (2014).

Methods for reconstruction of the parental probabilities have been proposed (Huang and George, 2011) and attested efficient in different analyses with real data (Huang et al., 2012; Pascual et al., 2015). The R/mpMap package proposed by Huang and George, (2011) allows mapping QTLs through simple linear regression model where QTL effects are estimated for every parent at each marker position where parental probabilities are computed. On the basis of parental probabilities, Broman et al., (2019) proposed new methods allowing to account for more complex designs of MAGIC populations and implemented them in R/qtl2 package. This package offers possibility to use regression models based on the Haley-Knott regression method (Haley and Knott, 1992) or to perform genome scan with a linear mixed model which could account for polygenic residual variance by modelling genetic relatedness between individuals. Previous studies had already proposed the use of linear mixed model in the MAGIC population which modelled also the polygenic variance and allowed for

detection of more than one QTL per chromosome or linkage group (Verbyla et al., 2014; Wei and Xu, 2016). Mixed models are highly powerful for MAGIC populations because of the flexibility they offer for modeling any complexity from the mating design. In maize for instance, Giraud et al., (2017) applied mixed model for QTL analysis and considered the structure from the parental belonging to different heterotic groups.

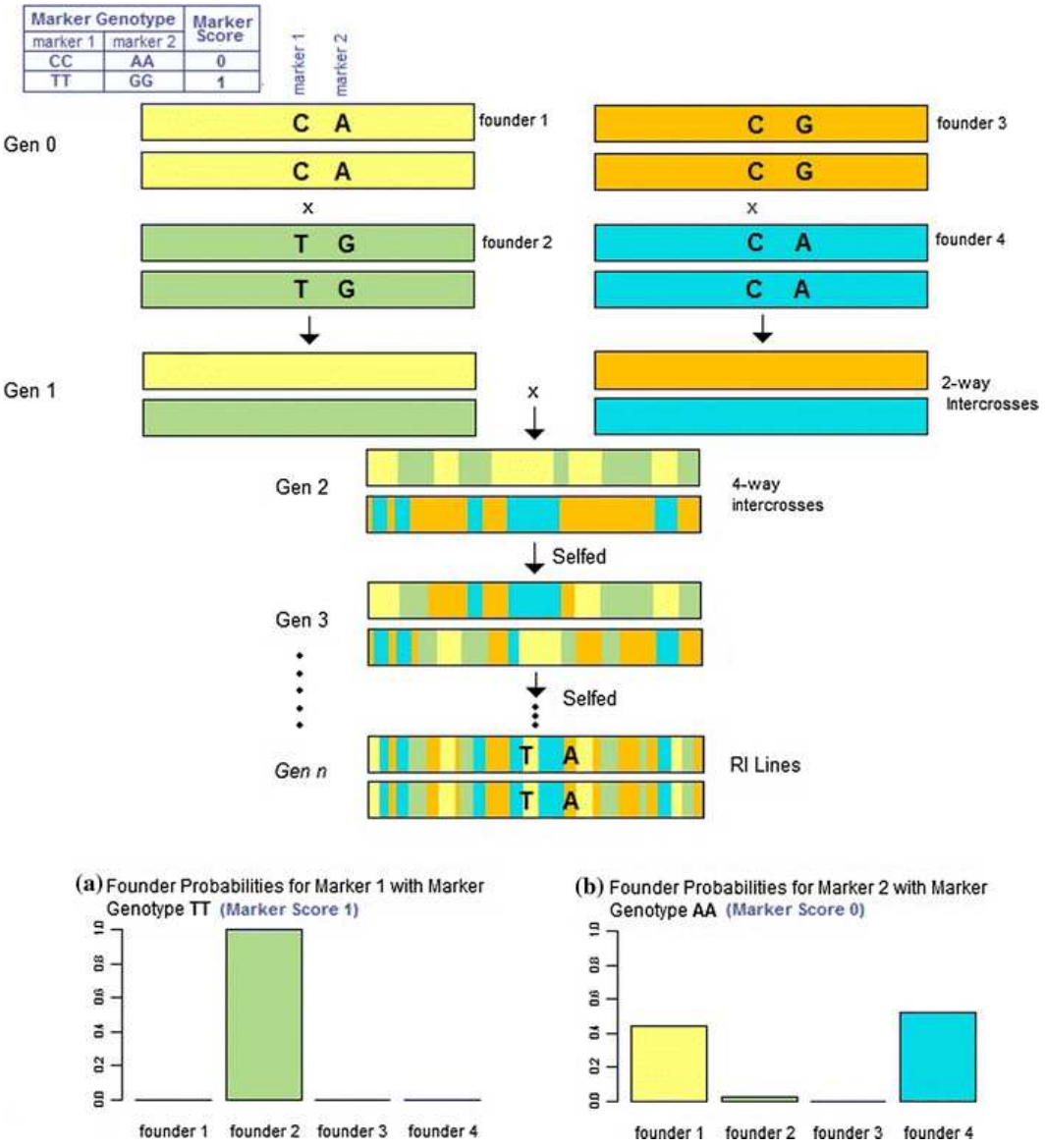

Figure 14: MAGIC population generation for four founders and two loci tracked through the process. The histograms in a and b present the probability that the marker represents each founder allele

6 Context and objectives of the thesis

This study was conducted with the general objective of identifying QTLs/genes, genotypes and phenotypes involved in tomato adaptation to several stresses, water deficit and salinity (in the frame of the ANR project ADAPTOM) and heat stress (in the frame of the ANR project TomEpiset). Indeed, tomato yield and fruit quality have been shown to vary under different abiotic stress conditions and the climate change is expected to exacerbate the occurrence of abiotic stresses pointing the needs to find new strategies for tomato breeding under unfavorable climatic conditions. The two ANR projects were funded by the French National Agency for Research (ANR) with the contribution of multiple research groups and private breeding companies.

I was funded by the West Africa Agricultural Productivity Program (WAAPP) project through collaboration between the World Bank (WB) and the Senegalese National Institute for Agricultural Research (ISRA)

Research questions

The aim of the thesis was to assess the impact of abiotic stresses on tomato *fruit quality, plant development* and *phenology* traits and study their genetic control

Three scientific questions were proposed to reach this objective:

1. To what extent water deficit, salinity and heat stress affect tomato at phenotypic level?
2. How do the genetic background and the amount of water irrigation affect the transcriptome variation on tomato?
3. What are the genetic bases of tomato plasticity and GxE under abiotic stresses?

References:

Adams, S.R., Cockshull, K.E., and Cave, C.R.J. (2001) Effect of Temperature on the Growth and Development of Tomato Fruits. *Ann Bot*. 88: 869–877.

Admassu, S., Nigussie, M., and Zelleke, H. (2008) Genotype-Environment Interaction and Stability Analysis for Grain Yield of Maize (Zea mays L.) in Ethiopia. *Asian J Plant Sci*. 7: 163–169.

Aflitos, S., Schijlen, E., de Jong, H., de Ridder, D., Smit, S., Finkers, R., et al. (2014) Exploring genetic variation in the tomato (Solanum section Lycopersicon) clade by whole-genome sequencing. *Plant J*. 80: 136–148.

Al-Abdallat, A., Al-Debei, H., Ayad, J., Hasan, S., Al-Abdallat, A.M., Al-Debei, H.S., et al. (2014) Over-Expression of SlSHN1 Gene Improves Drought Tolerance by Increasing Cuticular Wax Accumulation in Tomato. *Int J Mol Sci*. 15: 19499–19515.

Albert, E., Gricourt, J., Bertin, N., Bonnefoi, J., Pateyron, S., Tamby, J.-P.P., et al. (2016a) Genotype by watering regime interaction in cultivated tomato: lessons from linkage mapping and gene expression. *Theor Appl Genet*. 129: 395–418.

Albert, E., Segura, V., Gricourt, J., Bonnefoi, J., Derivot, L., and Causse, M. (2016b) Association mapping reveals the genetic architecture of tomato response to water deficit: focus on major fruit quality traits. *J Exp Bot*. 67: 6413–6430.

Alian, A., Altman, A., and Heuer, B. (2000) Genotypic difference in salinity and water stress tolerance of fresh market tomato cultivars. *Plant Sci*. 152: 59–65.

Allard, R.W., and Bradshaw, A.D. (1964) Implications of Genotype-Environmental Interactions in Applied Plant Breeding1. *Crop Sci*. 4: 503.

Apse, M.P., Aharon, G.S., Snedden, W.A., and Blumwald, E. (1999) Salt tolerance conferred by overexpression of a vacuolar Na+/H+ antiport in Arabidopsis. *Science*. 285: 1256–8.

Bai, Y., Sunarti, S., Kissoudis, C., Visser, R.G.F., and van der Linden, C.G. (2018) The Role of Tomato WRKY Genes in Plant Responses to Combined Abiotic and Biotic Stresses. *Front Plant Sci*. 9: 801.

Bajgain, P., Rouse, M.N., Tsilo, T.J., Macharia, G.K., Bhavani, S., Jin, Y., et al. (2016) Nested Association Mapping of Stem Rust Resistance in Wheat Using Genotyping by Sequencing. *PLoS One*. 11: e0155760.

Bandillo, N., Raghavan, C., Muyco, P.A., Sevilla, M.A.L., Lobina, I.T., Dilla-Ermita, C.J., et al. (2013) Multi-parent advanced generation inter-cross (MAGIC) populations in rice: progress and potential for genetics research and breeding. *Rice (N Y)*. 6: 11.

Bauchet, G., Grenier, S., Samson, N., Bonnet, J., Grivet, L., and Causse, M. (2017) Use of modern tomato breeding germplasm for deciphering the genetic control of agronomical traits by Genome Wide Association study. *Theor Appl Genet*. 130: 875–889.

Bhatt, R.M., and Srinivasa Rao, N.K. (1987) Seed germination and seedling growth responses of tomato cultivars to imposed water stress. *J Hortic Sci*. 62: 221–225.

Blanca, J., Montero-Pau, J., Sauvage, C., Bauchet, G., Illa, E., Díez, M.J., et al. (2015) Genomic variation in tomato, from wild ancestors to contemporary breeding accessions. *BMC Genomics*. 16: 257.

Boer, M.P., Wright, D., Feng, L., Podlich, D.W., Luo, L., Cooper, M., et al. (2007) A mixed-model quantitative trait loci (QTL) analysis for multiple-environment trial data using environmental covariables for QTL-by-environment interactions, with an example in maize. *Genetics*. 177: 1801–13.

Bolger, A., Scossa, F., Bolger, M.E., Lanz, C., Maumus, F., Tohge, T., et al. (2014a) The genome of the stress-tolerant wild tomato species Solanum pennellii. *Nat Genet*. 46: 1034–1038.

Bolger, A., Scossa, F., Bolger, M.E., Lanz, C., Maumus, F., Tohge, T., et al. (2014b) The genome of the stress-tolerant wild tomato species Solanum pennellii. *Nat Genet*. 46: 1034–1038.

Bosco De Oliveira, A., de Oliveira, A.B., Mendes Alencar, N.L., Gomes-filho, E.E., Oliveira, A.B. De, Alencar, N.L.M., et al. (2013) Comparison Between the Water and Salt Stress Effects on Plant Growth and Development, Responses of Organisms to Water Stress. InTech.

Bose, J., Pottosin, I.I., Shabala, S.S., Palmgren, M.G., and Shabala, S. (2011) Calcium Efflux Systems in Stress Signaling and Adaptation in Plants. *Front Plant Sci*. 2: 85.

Bouchet, S., Olatoye, M.O., Marla, S.R., Perumal, R., Tesso, T., Yu, J., et al. (2017) Increased Power To Dissect Adaptive Traits in Global Sorghum Diversity Using a Nested Association Mapping Population. *Genetics*. 206: 573–585.

Bradshaw, A.D. (2006) Unravelling phenotypic plasticity ? why should we bother? *New Phytol*. 170: 644–648.

Brancourt-Hulmel, M., Denis, J.-B., and Lecomte, C. (2000) Determining environmental covariates which explain genotype environment interaction in winter wheat through probe genotypes and biadditive factorial regression. *Theor Appl Genet*. 100: 285–298.

Broman, K.W., Gatti, D.M., Simecek, P., Furlotte, N.A., Prins, P., Sen, Ś., et al. (2019) R/qtl2: Software for Mapping Quantitative Trait Loci with High-Dimensional Data and Multiparent Populations. *Genetics*. 211: 495–502.

Campanelli, G., Sestili, S., Acciarri, N., Montemurro, F., Palma, D., Leteo, F., et al. (2019) Multi-Parental Advances Generation Inter-Cross Population, to Develop Organic Tomato Genotypes by Participatory Plant Breeding. *Agronomy*. 9: 119.

Caro, M., Cruz, V., Cuartero, J., Estañ, M.T., Bolarin, M.C., Esta / Q, M.T., et al. (1991) Salinity tolerance of normal-fruited and cherry tomato cultivars. *Plant Soil*. 136: 249–255.

Causse, M., Desplat, N., Pascual, L., Le Paslier, M.-C., Sauvage, C., Bauchet, G., et al. (2013) Whole genome resequencing in tomato reveals variation associated with introgression and breeding events. *BMC Genomics*. 14: 791.

Chakraborty, K., Sairam, R.K., and Bhaduri, D. (2016) Effects of different levels of soil salinity on yield attributes, accumulation of nitrogen, and micronutrients in *Brassica* spp. *J Plant Nutr*. 39: 1026–1037.

Chamekh, Z., Karmous, C., Ayadi, S., Sahli, A., Hammami, Z., Belhaj Fraj, M., et al. (2015) Stability analysis of yield component traits in 25 durum wheat (Triticum durum Desf.) genotypes under contrasting irrigation water salinity. *Agric Water Manag*. 152: 1–6.

Chaturvedi, P., Ischebeck, T., Egelhofer, V., Lichtscheidl, I., and Weckwerth, W. (2013) Cell-specific Analysis of the Tomato Pollen Proteome from Pollen Mother Cell to Mature Pollen Provides Evidence for Developmental Priming. *J Proteome Res*. 12: 4892–4903.

Chen, J., Kang, S., Du, T., Qiu, R., Guo, P., and Chen, R. (2013) Quantitative response of greenhouse tomato yield and quality to water deficit at different growth stages. *Agric Water Manag*. 129: 152–162.

Chen, L., Luan, Y., and Zhai, J. (2015) Sp-miR396a-5p acts as a stress-responsive genes regulator by conferring tolerance to abiotic stresses and susceptibility to Phytophthora nicotianae infection in transgenic tobacco. *Plant Cell Rep*. 34: 2013–2025.

Cheng, C.-Y., Krishnakumar, V., Chan, A.P., Thibaud-Nissen, F., Schobel, S., and Town, C.D. (2017) Araport11: a complete reannotation of the Arabidopsis thaliana reference genome. *Plant J*. 89: 789–804.

Cheng, Y., Ahammed, G.J., Yao, Z., Ye, Q., Ruan, M., Wang, R., et al. (2019) Comparative Genomic Analysis Reveals Extensive Genetic Variations of WRKYs in Solanaceae and Functional Variations of CaWRKYs in Pepper. *Front Genet*. 10: 492.

Chinnusamy, V., and Zhu, J.-K. (2009) Epigenetic regulation of stress responses in plants. *Curr Opin Plant Biol*. 12: 133–139.

Cook, J.P., McMullen, M.D., Holland, J.B., Tian, F., Bradbury, P., Ross-Ibarra, J., et al. (2012) Genetic architecture of maize kernel composition in the nested association mapping and inbred association panels. *Plant Physiol*. 158: 824–34.

Costa, J.M., Ortuño, M.F., and Chaves, M.M. (2007) Deficit Irrigation as a Strategy to Save Water: Physiology and Potential Application to Horticulture. *J Integr Plant Biol*. 49: 1421–1434.

Cucci, G., Lacolla, G., Boari, F., Mastro, M.A., and Cantore, V. (2019) Effect of water salinity and irrigation regime on maize (Zea mays L.) cultivated on clay loam soil and irrigated by furrow in Southern Italy. *Agric Water Manag*. 222: 118–124.

Cui, J., Jiang, N., Zhou, X., Hou, X., Yang, G., Meng, J., et al. (2018) Tomato MYB49 enhances resistance to Phytophthora infestans and tolerance to water deficit and salt stress. *Planta*. 248: 1487–1503.

Diers, B.W., Specht, J., Rainey, K.M., Cregan, P., Song, Q., Ramasubramanian, V., et al. (2018) Genetic

Architecture of Soybean Yield and Agronomic Traits. *G3 (Bethesda)*. 8: 3367–3375.

Diouf, I.A., Derivot, L., Bitton, F., Pascual, L., and Causse, M. (2018) Water Deficit and Salinity Stress Reveal Many Specific QTL for Plant Growth and Fruit Quality Traits in Tomato. *Front Plant Sci*. 9: 279.

Dorji, K., Behboudian, M.H., and Zegbe-Domínguez, J.A. (2005) Water relations, growth, yield, and fruit quality of hot pepper under deficit irrigation and partial rootzone drying. *Sci Hortic (Amsterdam)*. 104: 137–149.

Driedonks, N., Wolters-Arts, M., Huber, H., de Boer, G.-J., Vriezen, W., Mariani, C., et al. (2018) Exploring the natural variation for reproductive thermotolerance in wild tomato species. *Euphytica*. 214: 67.

Edwards, D., and Batley, J. (2004) Plant bioinformatics: from genome to phenome. *Trends Biotechnol*. 22: 232–237.

van Eeuwijk, F.A., Bink, M.C., Chenu, K., and Chapman, S.C. (2010) Detection and use of QTL for complex traits in multiple environments. *Curr Opin Plant Biol*. 13: 193–205.

van Eeuwijk, F.A., Keizer, L.C.P., and Bakker, J.J. (1995) Linear and bilinear models for the analysis of multi-environment trials: II. An application to data from the Dutch Maize Variety Trials. *Euphytica*. 84: 9–22.

Egea, I., Albaladejo, I., Meco, V., Morales, B., Sevilla, A., Bolarin, M.C., et al. (2018) The drought-tolerant Solanum pennellii regulates leaf water loss and induces genes involved in amino acid and ethylene/jasmonate metabolism under dehydration. *Sci Rep*. 8: 2791.

El-Soda, M., Malosetti, M., Zwaan, B.J., Koornneef, M., and Aarts, M.G.M. (2014) . Trends Plant Sci.

Fahad, S., Bajwa, A.A., Nazir, U., Anjum, S.A., Farooq, A., Zohaib, A., et al. (2017) Crop Production under Drought and Heat Stress: Plant Responses and Management Options. *Front Plant Sci*. 8: 1147.

Fang, Y., and Xiong, L. (2015) General mechanisms of drought response and their application in drought resistance improvement in plants. *Cell Mol Life Sci*. 72: 673–689.

Farooq, M., Hussain, M., Wahid, A., and Siddique, K.H.M. (2012) Plant Responses to Drought Stress.

Farooq, M., Wahid, A., Kobayashi, N., Fujita, D., and Basra, S.M.A. (2009) Plant Drought Stress: Effects, Mechanisms and Management. In *Sustainable Agriculture*. pp. 153–188 Springer Netherlands, Dordrecht.

Faurobert, M., Mihr, C., Bertin, N., Pawlowski, T., Negroni, L., Sommerer, N., et al. (2007) Major proteome variations associated with cherry tomato pericarp development and ripening. *Plant Physiol*. 143: 1327–46.

Finlay, B.K.W., and Wilkinson, G.N. (1963) The Analysis Of Adaptation In A Plant-Breeding Programme The ability of some crop varieties to perform well over a wide range of environ - mental conditions has lcng been appreciated by the agronomist and plant breeder . In the cereal belts of southern Au. .

Flatt, T. (2005) The Evolutionary Genetics of Canalization. *Q Rev Biol*. 80: 287–316.

Fragkostefanakis, S., Mesihovic, A., Simm, S., Paupière, M.J., Hu, Y., Paul, P., et al. (2016) HsfA2 Controls the Activity of Developmentally and Stress-Regulated Heat Stress Protection Mechanisms in Tomato Male Reproductive Tissues. *Plant Physiol*. 170: 2461–77.

Fragkostefanakis, S., Röth, S., Schleiff, E., and Scharf, K.-D. (2015) Prospects of engineering thermotolerance in crops through modulation of heat stress transcription factor and heat shock protein networks. *Plant Cell Environ*. 38: 1881–1895.

Fuller, T.L., Sesink Clee, P.R., Njabo, K.Y., Tróchez, A., Morgan, K., Meñe, D.B., et al. (2018) Climate warming causes declines in crop yields and lowers school attendance rates in Central Africa. *Sci Total Environ*. 610–611: 503–510.

Fulop, D., Ranjan, A., Ofner, I., Covington, M.F., Chitwood, D.H., West, D., et al. (2016) A New Advanced Backcross Tomato Population Enables High Resolution Leaf QTL Mapping and Gene Identification. *G3 (Bethesda)*. 6: 3169–3184.

Fulton, T.M., Bucheli, P., Voirol, E., López, J., Pétiard, V., and Tanksley, S.D. (2002) Quantitative trait loci (QTL) affecting sugars, organic acids and other biochemical properties possibly contributing to flavor, identified in four advanced backcross populations of tomato. *Euphytica*. 127: 163–177.

Gao, L., Gonda, I., Sun, H., Ma, Q., Bao, K., Tieman, D.M., et al. (2019) The tomato pan-genome uncovers new genes and a rare allele regulating fruit flavor. *Nat Genet*. 51: 1044–1051.

Gardner, K.A., Wittern, L.M., and Mackay, I.J. (2016) A highly recombined, high-density, eight-founder wheat MAGIC map reveals extensive segregation distortion and genomic locations of introgression segments. *Plant Biotechnol J*. 14: 1406–1417.

Gauffier, C., Lebaron, C., Moretti, A., Constant, C., Moquet, F., Bonnet, G., et al. (2016) A TILLING approach to generate broad-spectrum resistance to potyviruses in tomato is hampered by *eIF4E* gene redundancy. *Plant J*. 85: 717–729.

GHALAMBOR, C.K., McKAY, J.K., CARROLL, S.P., and REZNICK, D.N. (2007) Adaptive versus non-adaptive phenotypic plasticity and the potential for contemporary adaptation in new environments. *Funct Ecol*. 21: 394–407.

Giraud, H., Bauland, C., Falque, M., Madur, D., Combes, V., Jamin, P., et al. (2017) Reciprocal Genetics: Identifying QTL for General and Specific Combining Abilities in Hybrids Between Multiparental Populations from Two Maize (Zea mays L.) Heterotic Groups. *Genetics*. 207: 1167–1180.

Goodwin, S., McPherson, J.D., and McCombie, W.R. (2016) Coming of age: ten years of next-generation sequencing technologies. *Nat Rev Genet*. 17: 333–351.

Grandillo, S., and Cammareri, M. (2016) Molecular Mapping of Quantitative Trait Loci in Tomato pp. 39–73 Springer, Berlin, Heidelberg.

Grandillo, S., Termolino, P., and van der Knaap, E. (2013) Molecular Mapping of Complex Traits in Tomato. In *Genetics, Genomics, and Breeding of Tomato*. pp. 150–227 Science Publishers.

Grativol, C., Hemerly, A.S., and Ferreira, P.C.G. (2012) Genetic and epigenetic regulation of stress responses in natural plant populations. *Biochim Biophys Acta - Gene Regul Mech*. 1819: 176–185.

de Groot, C.C., Marcelis, L.F.M., van den Boogaard, R., and Lambers, H. (2004) Response Of Growth Of Tomato To Phosphorus And Nitrogen Nutrition. *Acta Hortic*. 357–364.

Haley, C.S., and Knott, S.A. (1992) A simple regression method for mapping quantitative trait loci in line crosses using flanking markers. *Heredity (Edinb)*. 69: 315–324.

Harvell, C.D., Mitchell, C.E., Ward, J.R., Altizer, S., Dobson, A.P., Ostfeld, R.S., et al. (2002) Climate warming and disease risks for terrestrial and marine biota. *Science*. 296: 2158–62.

Hasanuzzaman, M., Fujita, M., Islam, M.N., Ahamed, K.U., and Nahar, K. (2009) Performance of four irrigated rice varieties under different levels of salinity stress. *Int J Integr Biol*.

Heuvelink, E. (2005) Tomatoes. CABI Pub.

Hoegh-Guldberg, O., D. Jacob, M. Taylor, M. Bindi, S. Brown, I. Camilloni, A. Diedhiou, R. Djalante, K.L. Ebi, F. Engelbrecht, J. Guiot, Y. Hijioka, S. Mehrotra, A. Payne, S.I. Seneviratne, A. Thomas, R. Warren, and G. Zhou, 2018 (2019) Impacts of 1.5^{o}C Global Warming on Natural and Human Systems.

Hosmani, P.S., Flores-Gonzalez, M., Geest, H. van de, Maumus, F., Bakker, L. V., Schijlen, E., et al. (2019) An improved de novo assembly and annotation of the tomato reference genome using single-molecule sequencing, Hi-C proximity ligation and optical maps. *bioRxiv*. 767764.

Huang, B.E., and George, A.W. (2011) R/mpMap: A computational platform for the genetic analysis of multiparent recombinant inbred lines. *Bioinformatics*. 27: 727–729.

Huang, B.E., George, A.W., Forrest, K.L., Kilian, A., Hayden, M.J., Morell, M.K., et al. (2012) A multiparent advanced generation inter-cross population for genetic analysis in wheat. *Plant Biotechnol J*. 10: 826–839.

Huang, B.E., Verbyla, K.L., Verbyla, A.P., Raghavan, C., Singh, V.K., Gaur, P., et al. (2015) MAGIC populations in crops: current status and future prospects. *Theor Appl Genet*. 128: 999–1017.

Jegadeesan, S., Chaturvedi, P., Ghatak, A., Pressman, E., Meir, S., Faigenboim, A., et al. (2018) Proteomics of Heat-Stress and Ethylene-Mediated Thermotolerance Mechanisms in Tomato Pollen Grains. *Front Plant Sci*. 9: 1558.

Jordan, D.R., Mace, E.S., Cruickshank, A.W., Hunt, C.H., and Henzell, R.G. (2011) Exploring and Exploiting Genetic Variation from Unadapted Sorghum Germplasm in a Breeding Program. *Crop Sci*. 51: 1444.

Joshi, R., Wani, S.H., Singh, B., Bohra, A., Dar, Z.A., Lone, A.A., et al. (2016) Transcription Factors and Plants Response to Drought Stress: Current Understanding and Future Directions. *Front Plant Sci*. 7: 1029.

Kabubo-Mariara, J., Kabara, M., and Kabara, M. (2018) Climate change and food security in Kenya*. 55–80.

Karam, F., Saliba, R., Skaf, S., Breidy, J., Rouphael, Y., and Balendonck, J. (2011) Yield and water use of eggplants (Solanum melongena L.) under full and deficit irrigation regimes. *Agric Water Manag*. 98: 1307–1316.

Keller, M., and Simm, S. (2018) The coupling of transcriptome and proteome adaptation during development and heat stress response of tomato pollen. *BMC Genomics*. 19: 447.

Kenneth J. Boote; Maria R. Rybak; Johan M.S. Scholberg; James W. Jones (2012) Improving the CROPGRO-Tomato Model for Predicting Growth and Yield Response to Temperature. *HortScience*. 47.

Kim, J.-M., To, T.K., Nishioka, T., and Motoaki, S. (2010) Chromatin regulation functions in plant abiotic stress responses. *Plant Cell Environ*. 33: 604–611.

Klay, I., Gouia, S., Liu, M., Mila, I., Khoudi, H., Bernadac, A., et al. (2018) Ethylene Response Factors (ERF) are differentially regulated by different abiotic stress types in tomato plants. *Plant Sci*. 274: 137–145.

Knight, H., and Knight, M.R. (2001) Abiotic stress signalling pathways: specificity and cross-talk. *Trends Plant Sci*. 6: 262–267.

Kover, P.X., Valdar, W., Trakalo, J., Scarcelli, N., Ehrenreich, I.M., Purugganan, M.D., et al. (2009) A multiparent advanced generation inter-cross to fine-map quantitative traits in Arabidopsis thaliana. *PLoS Genet*. 5: e1000551.

Krystyna, R. (2017) Impact of heat and drought stresses on size and quality of the potato yield. *Plant, Soil Environ*. 63: 40–46.

Kumar, R. (2014) Role of MicroRNAs in Biotic and Abiotic Stress Responses in Crop Plants. *Appl Biochem Biotechnol*. 174: 93–115.

Kurunc, A., Unlukara, A., and Cemek, B. (2011) Salinity and drought affect yield response of bell pepper similarly. *Acta Agric Scand Sect B - Soil Plant Sci*. 61: 514–522.

Kusmec, A., Srinivasan, S., Nettleton, D., and Schnable, P.S. (2017) Distinct genetic architectures for phenotype means and plasticities in Zea mays. *Nat Plants*. 3: 715–723.

Labate, J.A., Grandillo, S., Fulton, T., Muños, S., Caicedo, A.L., Peralta, I., et al. (2007) Tomato. In *Vegetables*. pp. 1–125 Springer Berlin Heidelberg, Berlin, Heidelberg.

Lacaze, X., Hayes, P.M., and Korol, A. (2009) Genetics of phenotypic plasticity: QTL analysis in barley, Hordeum vulgare. *Heredity (Edinb)*. 102: 163–173.

Laitinen, R.A.E., and Nikoloski, Z. (2019) Genetic basis of plasticity in plants. *J Exp Bot*. 70: 739–745.

Leflon, M., Lecomte, C., Barbottin, A., Jeuffroy, M.H., Robert, N., and Brancourt-Hulmel, M. (2005) Characterization of Environments and Genotypes for Analyzing Genotype × Environment Interaction. *J Crop Improv*. 14: 249–298.

Li, J., Sima, W., Ouyang, B., Luo, Z., Yang, C., Ye, Z., et al. (2013) Identification and Expression Pattern of a ZPR1 Gene in Wild Tomato (Solanum Pennellii). *Plant Mol Biol Report*. 31: 409–417.

Lin, C.S., Binns, M.R., and Lefkovitch, L.P. (1986) Stability Analysis: Where Do We Stand?1. *Crop Sci*. 26: 894.

Lin, T., Zhu, G., Zhang, J., Xu, X., Yu, Q., Zheng, Z., et al. (2014) Genomic analyses provide insights into the history of tomato breeding. *Nat Genet*. 46: 1220–1226.

Lindemose, S., O'Shea, C., Jensen, M., Skriver, K., Lindemose, S., O'Shea, C., et al. (2013) Structure, Function and Networks of Transcription Factors Involved in Abiotic Stress Responses. *Int J Mol Sci*. 14: 5842–5878.

Liu, H., Yu, C., Li, H., Ouyang, B., Wang, T., Zhang, J., et al. (2015) Overexpression of ShDHN, a dehydrin gene from Solanum habrochaites enhances tolerance to multiple abiotic stresses in tomato. *Plant Sci*. 231: 198–211.

Lopez-Casado, G., Covey, P.A., Bedinger, P.A., Mueller, L.A., Thannhauser, T.W., Zhang, S., et al. (2012) Enabling proteomic studies with RNA-Seq: The proteome of tomato pollen as a test case. *Proteomics*. 12: 761–774.

López-Galiano, M.J., García-Robles, I., González-Hernández, A.I., Camañes, G., Vicedo, B., Real, M.D., et al. (2019) Expression of miR159 Is Altered in Tomato Plants Undergoing Drought Stress. *Plants*. 8: 201.

Luan, Y., Wang, W., and Liu, P. (2014) Identification and functional analysis of novel and conserved microRNAs

in tomato. *Mol Biol Rep*. 41: 5385–5394.

Lv, Z., Zhu, Y., Liu, X., Ye, H., Tian, Y., and Li, F. (2018) Climate change impacts on regional rice production in China. *Clim Change*. 147: 523–537.

Mackay, I.J., Bansept-Basler, P., Barber, T., Bentley, A.R., Cockram, J., Gosman, N., et al. (2014) An eight-parent multiparent advanced generation inter-cross population for winter-sown wheat: creation, properties, and validation. *G3 (Bethesda)*. 4: 1603–10.

Malosetti, M., Ribaut, J.-M., and van Eeuwijk, F.A. (2013) The statistical analysis of multi-environment data: modeling genotype-by-environment interaction and its genetic basis. *Front Physiol*. 4: 44.

Mangin, B., Casadebaig, P., Cadic, E., Blanchet, N., Boniface, M.-C., Carrère, S., et al. (2017) Genetic control of plasticity of oil yield for combined abiotic stresses using a joint approach of crop modelling and genome-wide association. *Plant Cell Environ*. 40: 2276–2291.

Des Marais, D.L., Hernandez, K.M., and Juenger, T.E. (2013) Genotype-by-environment interaction and plasticity: exploring genomic responses of plants to the abiotic environment. *Annu Rev Ecol Evol Syst*. 44: 5–29.

Marschner, H. (1983) General Introduction to the Mineral Nutrition of Plants. In *Inorganic Plant Nutrition*. pp. 5–60 Springer Berlin Heidelberg, Berlin, Heidelberg.

Mathew, B., Léon, J., Sannemann, W., and Sillanpää, M.J. (2018) Detection of Epistasis for Flowering Time Using Bayesian Multilocus Estimation in a Barley MAGIC Population. *Genetics*. 208: 525–536.

Maurer, A., Draba, V., Jiang, Y., Schnaithmann, F., Sharma, R., Schumann, E., et al. (2015) Modelling the genetic architecture of flowering time control in barley through nested association mapping. *BMC Genomics*. 16: 290.

Meena, Y.K., Khurana, D.S., and Singh, K. (2018) Towards enhanced low temperature stress tolerance in tomato : An approach. *J Environ Biol*. 39, N°4.

Mitchell, J., Shennan, C., and Grattan, S. (1991) Developmental-Changes in Tomato Fruit Composition in Response To Water Deficit and Salinity. *Physiol Plant*. 83: 177–185.

Mott, R., Talbot, C.J., Turri, M.G., Collins, A.C., and Flint, J. (2000) A method for fine mapping quantitative trait loci in outbred animal stocks. *Proc Natl Acad Sci U S A*. 97: 12649–54.

Munir, S., Liu, H., Xing, Y., Hussain, S., Ouyang, B., Zhang, Y., et al. (2016) Overexpression of calmodulin-like (ShCML44) stress-responsive gene from Solanum habrochaites enhances tolerance to multiple abiotic stresses. *Sci Rep*. 6: 31772.

Munns, R. (2005) Genes and salt tolerance: bringing them together. *New Phytol*. 167: 645–663.

Munns, R., and Gilliham, M. (2015) Salinity tolerance of crops - what is the cost? *New Phytol*. 208: 668–673.

Munns, R., and Tester, M. (2008) Mechanisms of Salinity Tolerance. *Annu Rev Plant Biol*. 59: 651–681.

Muthuramalingam, P., Krishnan, S.R., Pothiraj, R., and Ramesh, M. (2017) Global Transcriptome Analysis of Combined Abiotic Stress Signaling Genes Unravels Key Players in Oryza sativa L.: An In silico Approach. *Front Plant Sci*. 8: 759.

Nadeem, M., Li, J., Wang, M., Shah, L., Lu, S., Wang, X., et al. (2018) Unraveling Field Crops Sensitivity to Heat Stress：Mechanisms, Approaches, and Future Prospects. *Agronomy*. 8: 128.

Navarro, J.M., Flores, P., Carvajal, M., and Martinez, V. (2005) Changes in quality and yield of tomato fruit with ammonium, bicarbonate and calcium fertilisation under saline conditions. *J Hortic Sci Biotechnol*. 80: 351–357.

Ogawa, D., Yamamoto, E., Ohtani, T., Kanno, N., Tsunematsu, H., Nonoue, Y., et al. (2018) Haplotype-based allele mining in the Japan-MAGIC rice population. *Sci Rep*. 8: 4379.

Ohama, N., Sato, H., Shinozaki, K., and Yamaguchi-Shinozaki, K. (2017) Transcriptional Regulatory Network of Plant Heat Stress Response. *Trends Plant Sci*. 22: 53–65.

Pandey, S., Zhang, W., and Assmann, S.M. (2007) Roles of ion channels and transporters in guard cell signal transduction. *FEBS Lett*. 581: 2325–2336.

Parida, A.K., and Das, A.B. (2005) Salt tolerance and salinity effects on plants: a review. *Ecotoxicol Environ Saf*.

60: 324–349.

Parihar, P., Singh, S., Singh, R., Singh, V.P., and Prasad, S.M. (2015) Effect of salinity stress on plants and its tolerance strategies: a review. *Environ Sci Pollut Res*. 22: 4056–4075.

Parrine, D., Wu, B.-S., Muhammad, B., Rivera, K., Pappin, D., Zhao, X., et al. (2018) Proteome modifications on tomato under extreme high light induced-stress. *Proteome Sci*. 16: 20.

Pascual, L., Desplat, N., Huang, B.E., Desgroux, A., Bruguier, L., Bouchet, J.-P.P., et al. (2015) Potential of a tomato MAGIC population to decipher the genetic control of quantitative traits and detect causal variants in the resequencing era. *Plant Biotechnol J*. 13: 565–577.

Patanè, C., and Cosentino, S.L. (2010) Effects of soil water deficit on yield and quality of processing tomato under a Mediterranean climate. *Agric Water Manag*. 97: 131–138.

Paterson, A.H., Damon, S., Hewitt, J.D., Zamir, D., Rabinowitch, H.D., Lincoln, S.E., et al. (1991) Mendelian factors underlying quantitative traits in tomato: comparison across species, generations, and environments. *Genetics*. 127.

Pease, J.B., Haak, D.C., Hahn, M.W., and Moyle, L.C. (2016) Phylogenomics Reveals Three Sources of Adaptive Variation during a Rapid Radiation. *PLOS Biol*. 14: e1002379.

Peralta, I.E., Spooner, D.M., and Knapp, S. (2008) Taxonomy of wild tomatoes and their relatives (Solanum sect. Lycopersicoides, sect. Juglandifolia, sect. Lycopersicon ; Solanaceae). American Society of Plant Taxonomists.

Pigliucci, M., Murren, C.J., and Schlichting, C.D. (2006) Phenotypic plasticity and evolution by genetic assimilation. *J Exp Biol*. 209: 2362–7.

Rabara, R.C., Tripathi, P., Reese, R.N., Rushton, D.L., Alexander, D., Timko, M.P., et al. (2015) Tobacco drought stress responses reveal new targets for Solanaceae crop improvement. *BMC Genomics*. 16: 484.

Rajasekaran, L.R., Aspinall, D., and Paleg, L.G. (2000) Physiological mechanism of tolerance of *Lycopersicon* spp. exposed to salt stress. *Can J Plant Sci*. 80: 151–159.

Rao, E.S., Kadirvel, P., Symonds, R.C., and Ebert, A.W. (2013) Relationship between survival and yield related traits in Solanum pimpinellifolium under salt stress. *Euphytica*. 190: 215–228.

Rasmussen, S., Barah, P., Suarez-Rodriguez, M.C., Bressendorff, S., Friis, P., Costantino, P., et al. (2013) Transcriptome Responses to Combinations of Stresses in Arabidopsis. *PLANT Physiol*. 161: 1783–1794.

Ripoll, J., Urban, L., Brunel, B., and Bertin, N. (2016) Water deficit effects on tomato quality depend on fruit developmental stage and genotype. *J Plant Physiol*. 190: 26–35.

Ripoll, J., Urban, L., Staudt, M., Lopez-Lauri, F., Bidel, L.P.R., and Bertin, N. (2014) Water shortage and quality of fleshy fruits—making the most of the unavoidable. *J Exp Bot*. 65: 4097–4117.

Ritchie, M.D., Holzinger, E.R., Li, R., Pendergrass, S.A., and Kim, D. (2015) Methods of integrating data to uncover genotype–phenotype interactions. *Nat Rev Genet*. 16: 85–97.

Rivero, R.M., Mestre, T.C., Mittler, R., Rubio, F., Garcia-Sanchez, F., And Martinez, V. (2014) The combined effect of salinity and heat reveals a specific physiological, biochemical and molecular response in tomato plants. *Plant Cell Environ*. 37: 1059–1073.

Rodriguez, M., Rau, D., Papa, R., and Attene, G. (2008) Genotype by environment interactions in barley (Hordeum vulgare L.): different responses of landraces, recombinant inbred lines and varieties to Mediterranean environment. *Euphytica*. 163: 231–247.

Romagosa, I., Borràs-Gelonch, G., Slafer, G., and Eeuwijk, F. (2013) Genotype by Environment Interaction and Adaptation. In *Sustainable Food Production*. pp. 846–870 Springer New York, New York, NY.

Rothan, C., Bres, C., Garcia, V., and Just, D. (2016) Tomato Resources for Functional Genomics pp. 75–94 Springer, Berlin, Heidelberg.

Rothan, C., Diouf, I., and Causse, M. (2019) Trait discovery and editing in tomato. *Plant J*. 97: 73–90.

Ruggieri, V., Francese, G., Sacco, A., D'Alessandro, A., Rigano, M.M., Parisi, M., et al. (2014) An association mapping approach to identify favourable alleles for tomato fruit quality breeding. *BMC Plant Biol*. 14: 337.

Sacco, A., Ruggieri, V., Parisi, M., Festa, G., Rigano, M.M., Picarella, M.E., et al. (2015) Exploring a Tomato Landraces Collection for Fruit-Related Traits by the Aid of a High-Throughput Genomic Platform. *PLoS One*. 10: e0137139.

Saha, S., Hossain, M., Rahman, M., Kuo, C., and Abdullah, S. (1970) Effect of high temperature stress on the performance of twelve sweet pepper genotypes. *Bangladesh J Agric Res*. 35: 525–534.

Sainju, U.M., Dris, R., and Singh, B. (2003) Mineral nutrition of tomato. *Food Agric Environ*. 1: 176–183.

Sauvage, C., Segura, V., Bauchet, G., Stevens, R., Do, P.T., Nikoloski, Z., et al. (2014) Genome-Wide Association in Tomato Reveals 44 Candidate Loci for Fruit Metabolic Traits. *Plant Physiol*. 165: 1120–1132.

Scholberg, J.M.S., and Locascio, S.J. (1999) Growth response of snap bean and tomato as affected by salinity and irrigation method. *HortScience*. 34: 259–264.

Shaar-Moshe, L., Blumwald, E., and Peleg, Z. (2017) Unique Physiological and Transcriptional Shifts under Combinations of Salinity, Drought and Heat. *Plant Physiol*. 174: pp.00030.2017.

Shoji, T., and Hashimoto, T. (2015) Stress-induced expression of NICOTINE2-locus genes and their homologs encoding Ethylene Response Factor transcription factors in tobacco. *Phytochemistry*. 113: 41–49.

Shriram, V., Kumar, V., Devarumath, R.M., Khare, T.S., and Wani, S.H. (2016) MicroRNAs As Potential Targets for Abiotic Stress Tolerance in Plants. *Front Plant Sci*. 7: 817.

Singh, M., Kumar, J., Singh, S., Singh, V.P., and Prasad, S.M. (2015) Roles of osmoprotectants in improving salinity and drought tolerance in plants: a review. *Rev Environ Sci Bio/Technology*. 14: 407–426.

SMITH, A.B., CULLIS, B.R., and THOMPSON, R. (2005) The analysis of crop cultivar breeding and evaluation trials: an overview of current mixed model approaches. *J Agric Sci*. 143: 449–462.

Spitz, F., and Furlong, E.E.M. (2012) Transcription factors: from enhancer binding to developmental control. *Nat Rev Genet*. 13: 613–626.

Stadlmeier, M., Hartl, L., and Mohler, V. (2018) Usefulness of a Multiparent Advanced Generation Intercross Population With a Greatly Reduced Mating Design for Genetic Studies in Winter Wheat. *Front Plant Sci*. 9: 1825.

Sun, X., Gao, Y., Li, H., Yang, S., and Liu, Y. (2015) Over-expression of SlWRKY39 leads to enhanced resistance to multiple stress factors in tomato. *J Plant Biol*. 58: 52–60.

Sun, X., Lin, L., and Sui, N. (2019) Regulation mechanism of microRNA in plant response to abiotic stress and breeding. *Mol Biol Rep*. 46: 1447–1457.

Suzuki, N., Rivero, R.M., Shulaev, V., Blumwald, E., and Mittler, R. (2014) Abiotic and biotic stress combinations. *New Phytol*. 203: 32–43.

The Tomato Genome Consortium, T.T.G., Tomato Genome Consortium, T.T.G.C., Sato, S., Tabata, S., Hirakawa, H., Asamizu, E., et al. (2012) No Title. *Nature*. 485.

Tian, F., Bradbury, P.J., Brown, P.J., Hung, H., Sun, Q., Flint-Garcia, S., et al. (2011) Genome-wide association study of leaf architecture in the maize nested association mapping population. *Nat Genet*. 43: 159–162.

Tonk, F.A., Ilker, E., and Tosun, M. (2011) Evaluation of genotype x environment interactions in maize hybrids using GGE biplot analysis. *Crop Breed Appl Biotechnol*. 11: 01–09.

Tranchida-Lombardo, V., Aiese Cigliano, R., Anzar, I., Landi, S., Palombieri, S., Colantuono, C., et al. (2018) Whole-genome re-sequencing of two Italian tomato landraces reveals sequence variations in genes associated with stress tolerance, fruit quality and long shelf-life traits. *DNA Res*. 25: 149–160.

Troyo-Diéguez, E., and Murillo-Amador, B. (2000) Effects of salinity on the germination and seedling characteristics of cowpea [Vigna unguiculata (L.) Walp.]. *Aust J Exp Agric*. 40: 433.

Ünlükara, A., Kurunç, A., Kesmez, G.D., Yurtseven, E., and Suarez, D.L. (2008) Effects of salinity on eggplant (Solanum melongena L.) growth and evapotranspiration. *Irrig Drain*. 59: n/a-n/a.

Valladares, F., Sanchez-Gomez, D., and Zavala, M.A. (2006) Quantitative estimation of phenotypic plasticity: bridging the gap between the evolutionary concept and its ecological applications. *J Ecol*. 94: 1103–1116.

Verbyla, A.P., George, A.W., Cavanagh, C.R., and Verbyla, K.L. (2014) Whole-genome QTL analysis for MAGIC. *Theor Appl Genet*. 127: 1753–1770.

Waddington, C.H. (1942) Canalization Of Development And The Inheritance Of Acquired Characters. *Nature*. 150: 563–565.

Wahid, A. (2007) Physiological implications of metabolite biosynthesis for net assimilation and heat-stress tolerance of sugarcane (Saccharum officinarum) sprouts. *J Plant Res*. 120: 219–228.

Wahid, A., Gelani, S., Ashraf, M., and Foolad, M.R. (2007) Heat tolerance in plants: An overview. *Environ Exp Bot*. 61: 199–223.

Wang, L., Zhao, R., Li, R., Yu, W., Yang, M., Sheng, J., et al. (2018) Enhanced drought tolerance in tomato plants by overexpression of SlMAPK1. *Plant Cell, Tissue Organ Cult*. 133: 27–38.

Wang, W., Vinocur, B., and Altman, A. (2003) Plant responses to drought, salinity and extreme temperatures: Towards genetic engineering for stress tolerance. *Planta*. 218: 1–14.

Waters, A.J., Makarevitch, I., Noshay, J., Burghardt, L.T., Hirsch, C.N., Hirsch, C.D., et al. (2017) Natural variation for gene expression responses to abiotic stress in maize. *Plant J*. 89: 706–717.

Wei, J., and Xu, S. (2016) A Random-Model Approach to QTL Mapping in Multiparent Advanced Generation Intercross (MAGIC) Populations. *Genetics*. 202: 471–86.

Wests, D.W., and Francois, L.E. (1982) Effects of salinity on germination, growth and yield of cowpea. *Irrig Sci*. 3: 169–175.

Xavier, A., Jarquin, D., Howard, R., Ramasubramanian, V., Specht, J.E., Graef, G.L., et al. (2018) Genome-Wide Analysis of Grain Yield Stability and Environmental Interactions in a Multiparental Soybean Population. *G3 (Bethesda)*. 8: 519–529.

Xu, J., Pascual, L., Aurand, R., Bouchet, J.-P., Valot, B., Zivy, M., et al. (2013) An extensive proteome map of tomato (Solanum lycopersicum) fruit pericarp. *Proteomics*. 13: n/a-n/a.

Xu, J., Wolters-Arts, M., Mariani, C., Huber, H., and Rieu, I. (2017) Heat stress affects vegetative and reproductive performance and trait correlations in tomato (Solanum lycopersicum). *Euphytica*. 213: 156.

Yan, W., Hunt, L.A., Sheng, Q., and Szlavnics, Z. (2000) Cultivar Evaluation and Mega-Environment Investigation Based on the GGE Biplot. *Crop Sci*. 40: 597.

Ye, J., Wang, X., Hu, T., Zhang, F., Wang, B., Li, C., et al. (2017) An InDel in the Promoter of Al-Activated Malate Transporter9 Selected during Tomato Domestication Determines Fruit Malate Contents and Aluminum Tolerance. *Plant Cell*. 29: 2249–2268.

You, J., and Chan, Z. (2015) ROS Regulation During Abiotic Stress Responses in Crop Plants. *Front Plant Sci*. 6: 1092.

Yu, J., Cheng, Y., Feng, K., Ruan, M., Ye, Q., Wang, R., et al. (2016) Genome-Wide Identification and Expression Profiling of Tomato Hsp20 Gene Family in Response to Biotic and Abiotic Stresses. *Front Plant Sci*. 7: 1215.

Yu, J., Holland, J.B., McMullen, M.D., and Buckler, E.S. (2008) Genetic design and statistical power of nested association mapping in maize. *Genetics*. 178: 539–551.

Zegbe-Domínguez, J.., Behboudian, M.., Lang, A., and Clothier, B.. (2003) Deficit irrigation and partial rootzone drying maintain fruit dry mass and enhance fruit quality in 'Petopride' processing tomato (Lycopersicon esculentum, Mill.). *Sci Hortic (Amsterdam)*. 98: 505–510.

Zhang, Z., Mao, B., Li, H., Zhou, W., Takeuchi, Y., and Yoneyama, K. (2005) Effect of salinity on physiological characteristics, yield and quality of microtubers in vitro in potato. *Acta Physiol Plant*. 27: 481–489.

Zhao, C., Liu, B., Piao, S., Wang, X., Lobell, D.B., Huang, Y., et al. (2017) Temperature increase reduces global yields of major crops in four independent estimates. *Proc Natl Acad Sci*. 114: 9326–9331.

Zhao, Jiantao, Sauvage, C., Zhao, Jinghua, Bitton, F., Bauchet, G., Liu, D., et al. (2019) Meta-analysis of genome-wide association studies provides insights into genetic control of tomato flavor. *Nat Commun*. 10: 1534.

Zhou, R., Yu, X., Ottosen, C.-O., Rosenqvist, E., Zhao, L., Wang, Y., et al. (2017) Drought stress had a predominant effect over heat stress on three tomato cultivars subjected to combined stress. *BMC Plant Biol*. 17: 24.

Zhu, G., Wang, S., Huang, Z., Zhang, S., Liao, Q., Zhang, C., et al. (2018) Rewiring of the Fruit Metabolome in

Tomato Breeding. *Cell*. 172: 249-261.e12.

Zhu, J.-K. (2016) Abiotic Stress Signaling and Responses in Plants. *Cell*. 167: 313–324.

Zhuang, Y., Zhou, X.-H., and Liu, J. (2014) Conserved miRNAs and Their Response to Salt Stress in Wild Eggplant Solanum linnaeanum Roots. *Int J Mol Sci*. 15: 839–849.

Zouine, M., Maza, E., Djari, A., Lauvernier, M., Frasse, P., Smouni, A., et al. (2017) TomExpress, a unified tomato RNA-Seq platform for visualization of expression data, clustering and correlation networks. *Plant J*. 92: 727–735.

Chapter 2

Materials and Methods

This chapter presents a brief description of the materials and methods employed along the analyses process in this manuscript.

1. Plant material

The plant material used in this project consisted of a multi-parental advanced generation intercross (MAGIC) population released in 2012 through an ANR project coordinated by INRA-GAFL in collaboration with Limagrain. The MAGIC population was developed from a cross of eight tomato lines selected from a diverse panel of 360 accessions. These lines were selected for their diversity and their genetic distance regarding the reference genome line 'Heinz1706'. Four parental lines were selected from the genetic group of the cherry tomatoes: *Solanum lycopersicum* var. *cerasiforme* (SLC) and four from the large fruit group: *Solanum lycopersicum* var. *lycopersicum* (SLL). Whole genome resequencing of the eight lines yielded a total of 4 millions SNPs (Causse et al., 2013). The number of polymorphisms was higher between the small fruited accessions and the reference than for the large fruit accessions (**Table 1**). About 400 MAGIC lines were generated from the cross design depicted in **Figure 1**. Four pairs of two-way parental cross firstly generated four F1 hybrids from which two pairs of two-way crosses generated each 120 hybrids for each pair. Crosses between the 120 hybrids from the two series generated 480 F1-like hybrids. Three generation of single seed descent (SSD) were carried on and about 400 MAGIC RILs delivered (Pascual et al., 2015).

Among the 4M SNPs released from the whole resequencing of the parental lines, a total of 1486 SNPs were selected to be regularly spread and optimize parental haplotype identity for genotyping the whole population, which was performed using the Fluidigm 96.96 Dynamic Arrays according to the manufacturer's protocol manufacturing (Pascual et al., 2015). A genetic map was constructed using the R package *mpMap* version 1.24.3 (Huang & George, 2011). The genetic map was composed of 1345 SNPs all presenting less than 20% of missing data and presented an average number of recombination of 1.36 per Morgan (**Figure 2**). The linkage map obtained showed an 87% increase in recombination frequencies compared to EXPEN 2012 an earlier bi-parental genetic map (Pascual et al., 2015).

2. Experimental design

The MAGIC population was grown in three different geographical regions (France, Israel and Morocco) and four specific stress treatments were applied. Trials were conducted in order that in a given trial any stress treatment was applied aside a control trial (**Table 2**). Treatments consisted in water deficit (WD), two levels of salinity – considered here as low salinity (LS) and high salinity (HS) – and high temperature (HT) stress. A detailed description of the treatments is presented in chapter 3 (for WD and SS) and chapter 5 (for HT stress). For each trial, different phenotypic traits were recorded (**Table 3**). Climatic variables within greenhouses were recorded daily in each trial and

environmental covariate variables calculated to characterize the environments (see chapter 6 for details). The average values of all climatic covariates are presented in **Table 2**.

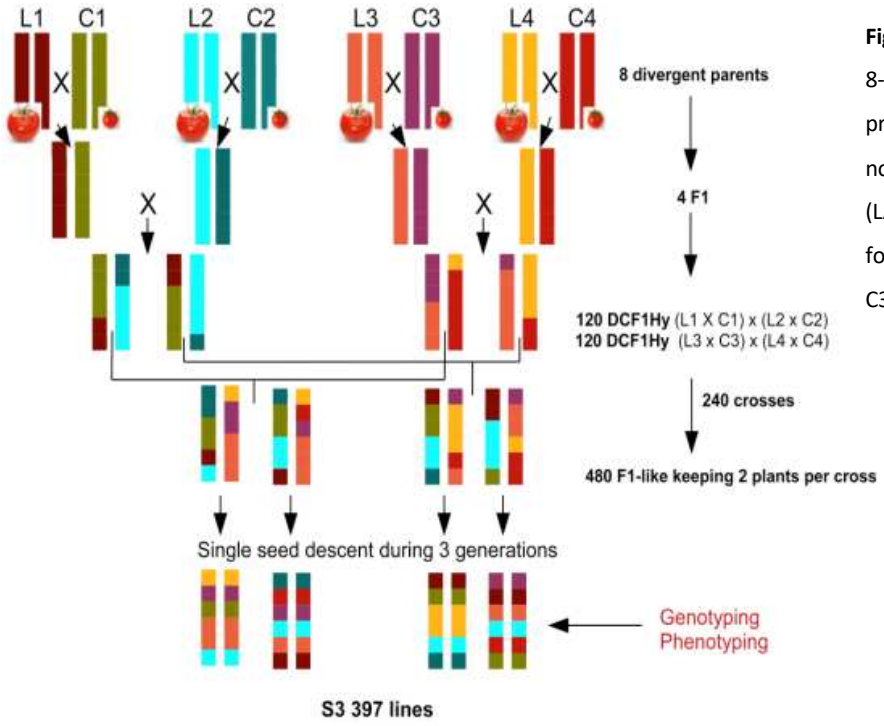

Figure 1: Construction of the tomato 8-way MAGIC population used in the present study. Large fruited founders noted as L1 (Levovil), L2 (Stupicke), L3 (LA0147), L4 (Ferum); Small fruited founders noted as C1 (Cervil), C2 (Criollo), C3 (Plovdiv24A), C4 (LA1420).

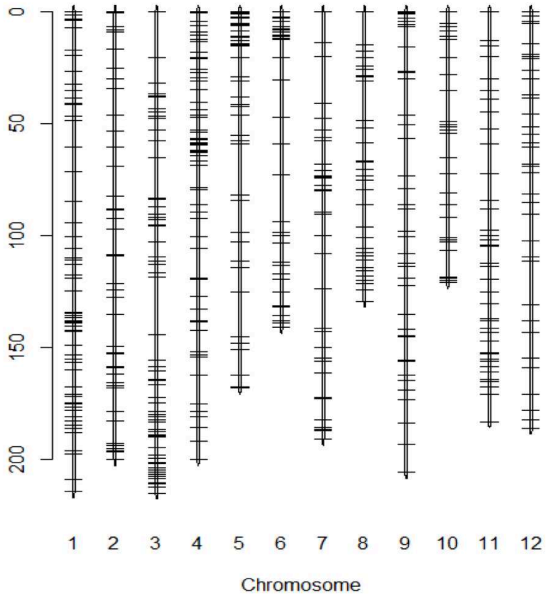

Summary information of the genetic map

0 markers had missing values in founders
0 markers had non-polymorphic founder genotypes

1345 markers were bi-allelic

1192 markers had >5% missing data.
495 markers had >10% missing data.
0 markers had >20% missing data.
---
2 markers had <1e-5 p-value for segregation distortion
0 markers had <1e-10 p-value for segregation distortion

Total genome length (in M): 21.56002
Average number of recombination (per M): 1.36

Figure 2:

3. Evaluation of stress impact at phenotypic level

Phenotypic plasticity (PP) and the relative stress impact (RSI) indexes were calculated for each trial separately to measure the effects of specific stresses for each MAGIC RIL and for the whole population. For each trait (*t*) the PP was computed using the general formula $PP = \frac{(t_{stress} - t_{control})}{t_{control}}$ and $RSI = 100\ x\ \frac{(T_{stress} - T_{control})}{T_{control}}$ where t and T represent the average phenotypic value per genotype and across all genotype (population average), respectively.

A global analysis of all trials together was conducted in chapter 6. Mixed linear models were used to estimate the level of genotype-by-environment interaction (GxE). Phenotypic plasticity was also computed in the multi-environment trial (MET) design through the factorial regression and joint regression models.

4. Evaluation of stress impact at the genetic level

Quantitative trait loci (QTL) mapping was conducted in the MAGIC population for every trait using the mean or plasticity phenotypes. Different QTL models were applied but all were based on the parental haplotype probabilities reconstruction. **Figure 3** summarizes the principle of QTL mapping in the MAGIC population using the parental haplotypes. The R packages *mpMap* (Huang & George, 2011), version 2.0 and *R/qtl2* (Broman et al., 2019) were used for QTL detection analysis in chapter 3 and chapters 5 and 6, respectively. These packages are designed for QTL mapping in MAGIC populations for single environment analysis. For the mapping of interactive QTLs (QEI), a home-made mixed model was developed which is an extension of the QTL model described by Giraud et al., (2017) to account for GxE in our case. The model is described in chapter 6 in details.

5. Evaluation of water-deficit impact at transcriptome level

RNA-sequencing was conducted on the eight parental lines used to generate the MAGIC population under control (fully irrigated) and WD conditions. Young leaf and fruit pericarp samples (at cell expansion stage) were collected and gene expression measured according to the sampling design depicted in **Figure 4**. The impact of WD and GxWD interaction on the transcriptome variation was evaluated through differentially expressed genes (DEG) analysis using the R-Bioconductor package *DESeq2 1.14.1* (Love et al., 2014), and through analysis of variance (ANOVA) of the transcript levels (see chapter 4).

6. Candidate genes identification

A general procedure for selecting candidate genes underlying QTLs was applied throughout the different sections of this document. The strategy coupled the QTL founder allele effects with the polymorphisms detected along the QTL region to narrow the candidate gene list (**Figure 5**). This

strategy was first applied in our MAGIC population by Pascual et al., (2015). Plasticity candidate genes were also screened by combining the QTL allelic effect with variation in the gene expression level under WD to shorten candidate gene list within the plasticity QTLs detected under WD and SS (details in chapter 4).

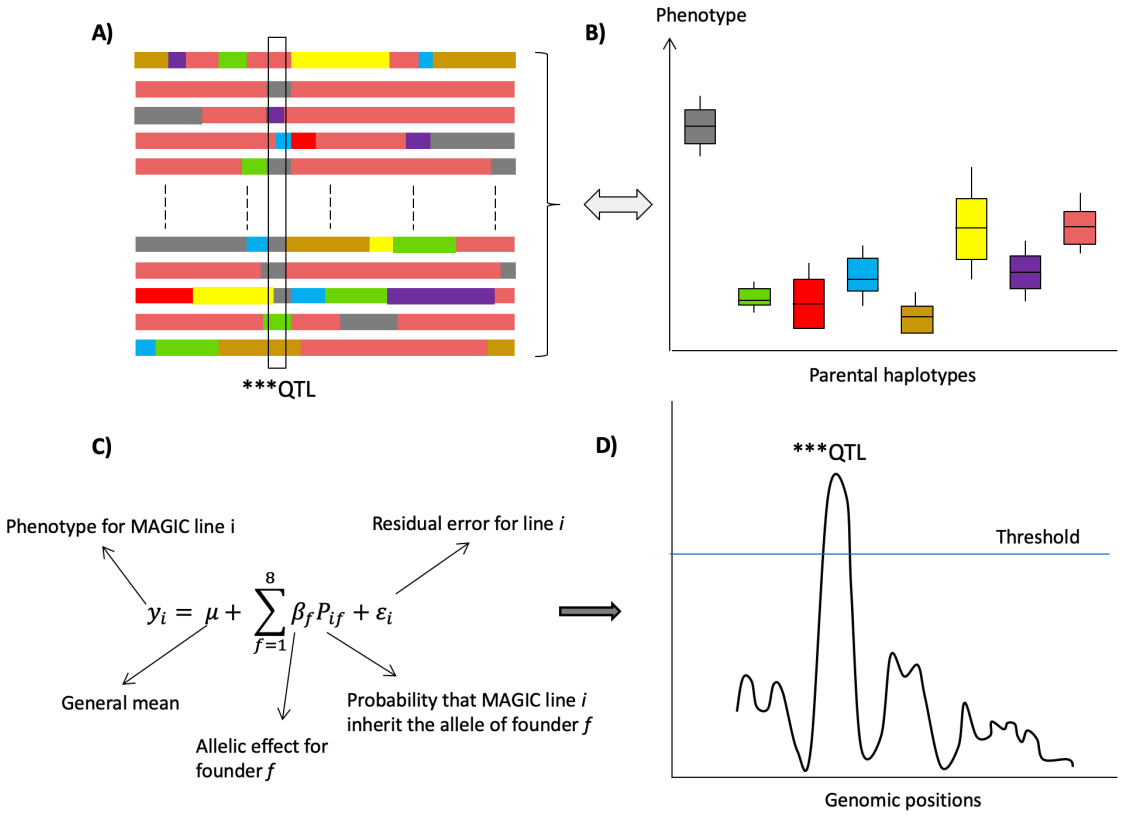

Figure 3: Principles of haplotype-based QTL mapping in MAGIC populations (example of an 8-way MAGIC population). Haplotype status of the MAGIC RILs denoting the inherited parental chromosome segments at the whole genome level. B) Phenotypic responses of the MAGIC RILs grouped according their haplotype status at a given region (*i.e* ***QTL). C) Statistical modelling to test for the presence of QTL. At every position where the genotypes are scored, the model test for significant association between the phenotypic variation and the parental haplotype status. Allelic effects could then be estimated for each parental line when a QTL is identified. D) The LOD score of the QTLs are derived along the whole genome scan and significance of the QTLs established through the estimation of a detection threshold.

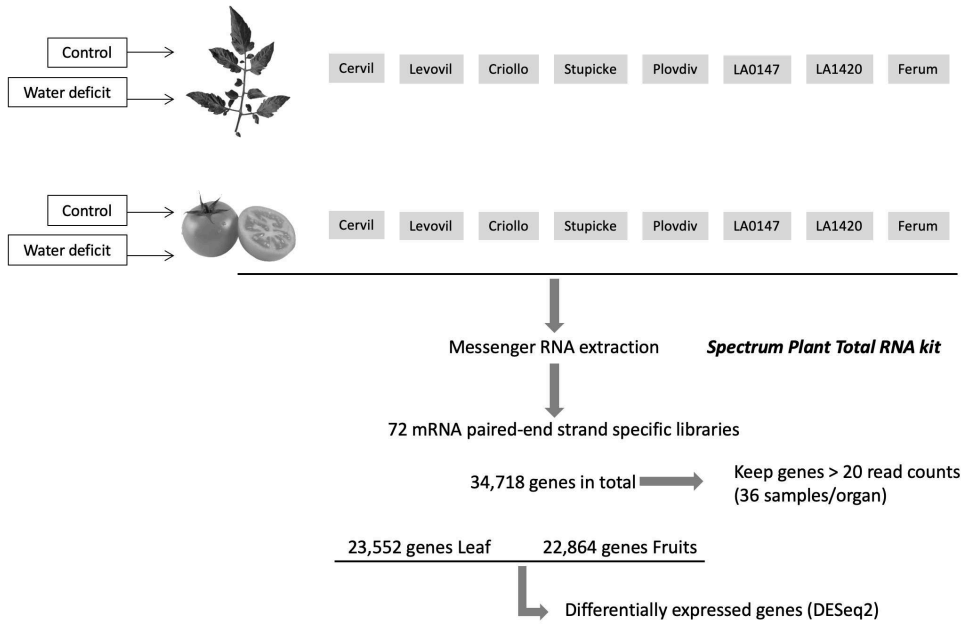

Figure 4: RNA-Seq experimental design. Sampling for the RNA-Seq analysis was carried on young leaves and fruit pericarp (at a green fruit stage). Samples were collected (2-3 biological replicates) for the eight MAGIC parental lines under fully irrigated (control) and water deficit (WD) conditions. A total of 72 mRNA libraries were constructed and expression level accounted for about 34K genes.

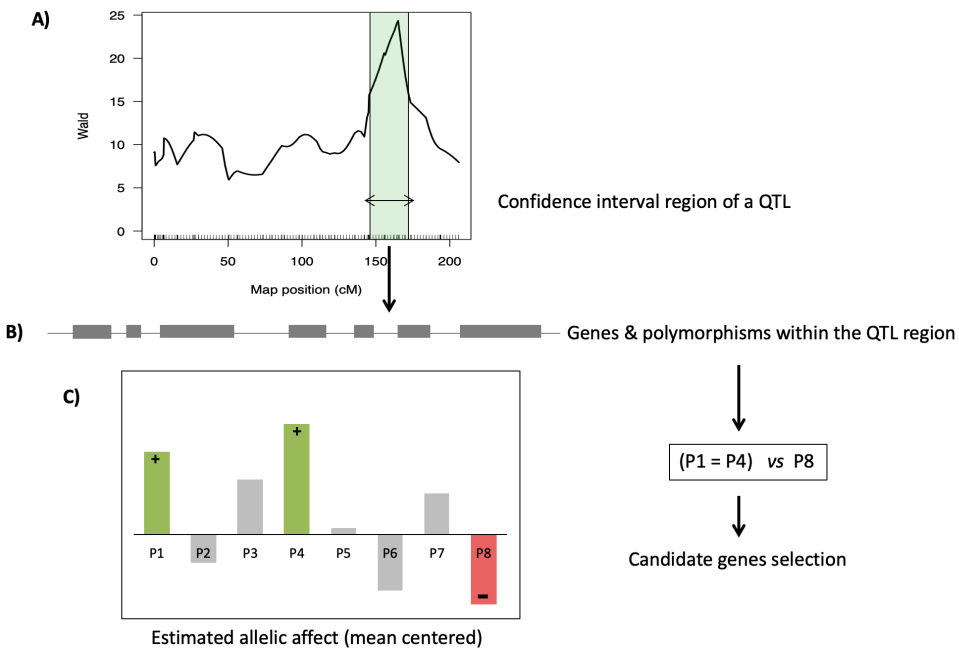

Figure 5: Schematic representation of the strategy used to narrow the candidate genes list for QTL detected in the MAGIC population. A) Represent a QTL significantly detected in a given genomic region. The confidence interval of the QTL (green region) hold many genes represnted in B). C) The mean centered of the estimated allelic effects for the eight parental lines at the pic QTL position. Parents likely carrying the positive allele are represented in green and parents with the negative allele in red. Candidate genes are selected then by filtering only genes affected by polymorphism varying according to the selected parents.

Table 1: Number of common SNP (upper diagonal) and InDel (lower diagonal) in all the pairs of comparisons (SNPs were defined with a depth higher than 4 in both accessions). Accessions consist in four S. lycopersicum (SLL) and four cherry-type (SLC) accessions. The first line and column indicate the number of SNP and InDel detected when compared to the reference genome

		Solanum lycopersicum lycopersicum				*Solanum lycopersicum cerasiforme*			
SNP InDel	**Nb vs Ref**	**LA0147**	**Levovil**	**Ferum**	**Stupicke**	**Criollo**	**LA1420**	**Plovdiv**	**Cervil**
Nb vs Ref		**182,371**	**271,458**	**306,083**	**356,655**	**1,042,928**	**1,358,257**	**1,457,098**	**2,028,568**
LA0147	**7,969**		82,46	85,695	116,904	63,915	79,616	76,642	87,389
Levovil	**2,894**	517		49,318	80,009	54,538	49,482	53,472	78,907
Ferum	**4,532**	715	353		71,995	122,094	116,987	68,448	64,689
Stupicke	**10,886**	1,544	540	738		70,024	217,565	244,284	111,531
Criollo	**13,898**	612	336	601	727		458,908	164,449	260,234
LA1420	**30,927**	1,298	468	910	2,366	2,666		310,635	222,517
Plovdiv	**33,966**	1,227	460	722	2,621	1,262	3,106		828,296
Cervil	**53,522**	1,521	534	807	1,746	1,811	2,532	8,441	

Table 2: Experimental design with the 12 environments and their respective names. The locations of the trials, the stress applied, and the average value of the climatic variables recorded/calculated during the vegetative and flowering stages are indicated. For each environment, the total number of genotypes used is given.

Environ-ments	Location	Water irrigation (%ETP)	Treatment	EC (dS/m)	Tmin (°C)	Tm (°C)	Tmax (°C)	Amp.Th (°C)	RH (%)	Vpd (kPa)	Sum of degree day (SDD)	Number of Genotypes
Avi12	France	100%	Control	1.33	15.48	20.5	26.4	10.92	70.83	1.71	466.94	397
Avi17	France	100%	Control	1.65	16.05	21.44	29.02	12.97	63.73	1.62	496.4	280
HAvi17	France	100%	Heat	1.47	20.35	26.9	34.34	13.99	70.72	2.52	664.06	356
Is14	Israel	100%	Control	NA	20.16	28.6	38.72	18.56	67.4	2.64	800.23	288
HIs14	Israel	100%	Heat	NA	21.92	33.05	48.33	26.41	55.02	2.78	1022.73	288
WDIs14	Israel	-70%	Water deficit	NA	20.53	29.28	40.83	20.3	63.48	2.59	835.57	288
Is15	Israel	100%	Control	NA	17.39	26.78	37.54	20.15	65.38	2.3	685.12	288
WDIs15	Israel	-30%	Water deficit	NA	17.27	25.97	35.38	18.11	65.94	2.21	638.54	288
Mor15	Morocco	100%	Control	2.17	8.11	18.17	35.91	27.8	62.42	1.3	484.9	241
WDMor15	Morocco	-50%	Water deficit	1.42	8.11	18.17	35.91	27.8	62.42	1.3	484.9	241
LSMor16	Morocco	100%	Salinity	3.76	11.54	19.99	34.11	22.57	59.56	1.39	583.06	253
HSMor16	Morocco	100%	Salinity	6.5	11.54	19.99	34.11	22.57	59.56	1.39	583.06	253

Table 3: Phenotypic traits evaluated per trial in the MAGIC-MET design

Trait	Avi12	Mor15 WDMor15	LSMor16 HSMor16	Is14 WDIs14 HIs14	Is15 WDIs15	Avi17 HAvi17
Fruit weight	x	x	x	x	x	x
Fruit number		x	x	x		x
Soluble solid content	x	x	x		x	x
Fruit firmness	x	x	x			x
pH	x					x
Color	x					x
Time to ripe	x	x	x			
Fruit length	x					
Fruit size	x					
Fruit width	x					
Titrable acidity	x					
Flowering time	x	x	x			x
Fruit set						x
Number of flowers		x	x	x		x
Leaf length		x	x	x		x
Stem diameter	x					x
Plant height	x			x		x
Style exertion	x					x

References:

Broman, K. W., Gatti, D. M., Simecek, P., Furlotte, N. A., Prins, P., Sen, Ś., … Churchill, G. A. (2019). R/qtl2: Software for Mapping Quantitative Trait Loci with High-Dimensional Data and Multiparent Populations. *Genetics*, *211*(2), 495–502. https://doi.org/10.1534/genetics.118.301595

Causse, M., Desplat, N., Pascual, L., Le Paslier, M.-C., Sauvage, C., Bauchet, G., … Bouchet, J.-P. (2013). Whole genome resequencing in tomato reveals variation associated with introgression and breeding events. *BMC Genomics*, *14*(1), 791. https://doi.org/10.1186/1471-2164-14-791

Giraud, H., Bauland, C., Falque, M., Madur, D., Combes, V., Jamin, P., … Moreau, L. (2017). Reciprocal Genetics: Identifying QTL for General and Specific Combining Abilities in Hybrids Between Multiparental Populations from Two Maize (Zea mays L.) Heterotic Groups. *Genetics*, *207*(3), 1167–1180. https://doi.org/10.1534/genetics.117.300305

Huang, B. E., & George, A. W. (2011). R/mpMap: A computational platform for the genetic analysis of multiparent recombinant inbred lines. *Bioinformatics*, *27*(5), 727–729. https://doi.org/10.1093/bioinformatics/btq719

Love, M. I., Huber, W., & Anders, S. (2014). Moderated estimation of fold change and dispersion for RNA-seq data with DESeq2. *Genome Biology*, *15*(12), 550. https://doi.org/10.1186/s13059-014-0550-8

Pascual, L., Desplat, N., Huang, B. E., Desgroux, A., Bruguier, L., Bouchet, J.-P. P., … Causse, M. (2015). Potential of a tomato MAGIC population to decipher the genetic control of quantitative traits and detect causal variants in the resequencing era. *Plant Biotechnology Journal*, *13*(4), 565–577. https://doi.org/10.1111/pbi.12282

CHAPTER 3

Water Deficit and Salinity Stress Reveal Many Specific QTL for Plant Growth and Fruit Quality Traits in Tomato

*Isidore A. Diouf[1], Laurent Derivot[2], Frédérique Bitton[1], Laura Pascual[1†] and Mathilde Causse[1]**

[1]INRA, UR1052, Génétique et Amélioration des Fruits et Légumes, Centre de Recherche PACA, Montfavet, France,

[2]GAUTIER Semences, Eyragues, France

Received: *22 August 2017*

Accepted: *19 February 2018*

Published: *06 March 2018 in Frontiers in Plant Science*

DOI : https://doi.org/10.3389/fpls.2018.00279

†Present Address: *Laura Pascual, Department of Biotechnology and Plant Biology, School of Agronomic Engineering, Polytechnic University of Madrid (UPM), Madrid, Spain*

****Correspondence:*** *Mathilde Causse*
mathilde.causse@inra.fr

frontiers in Plant Science

ORIGINAL RESEARCH
published: 06 March 2018
doi: 10.3389/fpls.2018.00279

Water Deficit and Salinity Stress Reveal Many Specific QTL for Plant Growth and Fruit Quality Traits in Tomato

Isidore A. Diouf[1], Laurent Derivot[2], Frédérique Bitton[1], Laura Pascual[1†] and Mathilde Causse[1]*

[1] INRA, UR1052, Génétique et Amélioration des Fruits et Légumes, Centre de Recherche PACA, Montfavet, France,
[2] GAUTIER Semences, Eyragues, France

OPEN ACCESS

Edited by:
Maarten Hertog,
KU Leuven, Belgium

Reviewed by:
Daniela Romano,
Università degli Studi di Catania, Italy
Francisco Perez-Alfocea,
Consejo Superior de Investigaciones Científicas (CSIC), Spain

****Correspondence:***
Mathilde Causse
mathilde.causse@inra.fr

†Present Address:
Laura Pascual,
Department of Biotechnology and Plant Biology, School of Agronomic Engineering, Polytechnic University of Madrid (UPM), Madrid, Spain

Specialty section:
This article was submitted to Plant Breeding, a section of the journal Frontiers in Plant Science

Received: *22 August 2017*
Accepted: *19 February 2018*
Published: *06 March 2018*

Citation:
Diouf IA, Derivot L, Bitton F, Pascual L and Causse M (2018) Water Deficit and Salinity Stress Reveal Many Specific QTL for Plant Growth and Fruit Quality Traits in Tomato. Front. Plant Sci. 9:279. doi: 10.3389/fpls.2018.00279

Quality is a key trait in plant breeding, especially for fruit and vegetables. Quality involves several polygenic components, often influenced by environmental conditions with variable levels of genotype × environment interaction that must be considered in breeding strategies aiming to improve quality. In order to assess the impact of water deficit and salinity on tomato fruit quality, we evaluated a multi-parent advanced generation intercross (MAGIC) tomato population in contrasted environmental conditions over 2 years, one year in control vs. drought condition and the other in control vs. salt condition. Overall 250 individual lines from the MAGIC population—derived from eight parental lines covering a large diversity in cultivated tomato—were used to identify QTL in both experiments for fruit quality and yield component traits (fruit weight, number of fruit, Soluble Solid Content, firmness), phenology traits (time to flower and ripe) and a vegetative trait, leaf length. All the traits showed a large genotype variation (33–86% of total phenotypic variation) in both experiments and high heritability whatever the year or treatment. Significant genotype × treatment interactions were detected for five of the seven traits over the 2 years of experiments. QTL were mapped using 1,345 SNP markers. A total of 54 QTL were found among which 15 revealed genotype × environment interactions and 65% (35 QTL) were treatment specific. Confidence intervals of the QTL were projected on the genome physical map and allowed identifying regions carrying QTL co-localizations, suggesting pleiotropic regulation. We then applied a strategy for candidate gene detection based on the high resolution mapping offered by the MAGIC population, the allelic effect of each parental line at the QTL and the sequence information of the eight parental lines.

Keywords: tomato, fruit quality, MAGIC population, genotype by environment interaction, QTL mapping

INTRODUCTION

Abiotic stress is one of the main factors limiting crop productivity and yield in agriculture. It occurs when plants experience any fluctuation in the growing habitat that alters or disrupts their metabolic homeostasis (de Oliveira et al., 2013). Among the abiotic stresses, drought and salinity are the most common threatening global food demand. Their adverse effect on agriculture is expected

to increase with the predicted climate change (Dai, 2011; Shrivastava and Kumar, 2015). Both drought and salinity stresses drive a series of morphological, physiological, and molecular changes in plants that are overall linked to adaptive mechanisms triggered by the plant to survive, or may simply be pathological consequences of stress injury (Zhu, 2002). Indeed, water deficit has several impacts on plant development due to the decrease of the plant's relative water content and water potential. Osmotic stress and limited nutrient uptake are then observed with stomatal closure, reduced photosynthesis activity, oxidative stress, and leaf growth inhibition. These behaviors are well reviewed by Farooq et al. (2012) and Chaves et al. (2003). For saline soil condition, plants are subjected to stress in two phases: a rapid osmotic stress phase starting immediately (due to the concentration of salt outside the roots) and a second ionic phase that starts when the accumulation of salt in the old leaves reaches a toxic level. The osmotic stress triggered by salinity has almost the same effect as drought with photosynthesis limitation, leaf growth inhibition, and ROS accumulation (Munns and Tester, 2008). Plants deploy a variety of adaptive strategies facing drought and salinity, including osmotic adjustment with the accumulation of osmo-protectants compounds, ROS detoxification, stomatal closure, and cellular signaling.

Drought and salinity arise with other adverse environmental factors threatening crop productivity in many species as a consequence of global climate changes. This has led plant breeders to renew their focus on understanding the molecular basis of plant adaptation to environment, in order to maintain high crop yielding by creating new varieties adapted to limited environmental conditions. As noted by Marais et al. (2013), plant responses to adverse conditions can be viewed as phenotypic plasticity (PP) and may lead to GxE when there is a genetic part shaping these responses. Understanding the molecular mechanism entailing PP and GxE is of great relevance in breeding strategies mainly if different growing areas (or cultural conditions) are targeted. For both PP and GxE, different underpinning models were suggested in the literature. PP can be viewed as additive effect of environmentally sensitive loci meaning that the same loci affect the phenotype in a set of environments at variable degrees, or specific regulatory loci altering differently the gene expression, in the different environments (Via et al., 1995). Non-additive effect such as over-dominance and epistasis or epigenetics can also be at the basis of the occurring GxE. El-Soda et al. (2014) present several statistical models to depict GxE into its individual genetic components through the identification of interactive QTL (QTLxE). Considering plasticity as an individual trait, some studies showed that loci linked to PP are in the vast majority also identified as QTLxE (Ungerer et al., 2003; Gutteling et al., 2007; Tétard-Jones et al., 2011).

Cultivated tomato is a crop moderately sensitive to salinity that can tolerate up to 2.5 dS/m EC, with minor negative impact on yield (Scholberg and Locascio, 1999). Caro et al. (1991) have found that small fruit accessions *S. lycopersicum* var *cerasiforme* are less sensitive to salinity than the large fruit group *S. lycopersicum* var *lycopersicum*. For drought, a negative impact on yield is observed from a limitation of water supply by 50% compared to control (well irrigated) (Ripoll et al., 2014; Albert et al., 2016a). Under such stresses, tomato yield components as well as fruit quality are greatly affected with different effects depending on the variety, the stage and duration of stress application and also the interaction with other environmental conditions like temperature, light, or relative humidity (Maas and Hoffman, 1977; Scholberg and Locascio, 1999; Ripoll et al., 2014). Furthermore, the genetic background may strongly modify the response to stress conditions (Albert et al., 2016b). This makes selection of genotypes tolerant to water deficit and salinity with high productivity and fruit quality a challenging task.

Several studies revealed that water deficit (WD) and salinity stress (SS) can improve fruit quality through higher accumulation of quality compounds and anti-oxidant (Mitchell et al., 1991; Du et al., 2008; Huang et al., 2009; Albert et al., 2016a; Ripoll et al., 2016). SS also increases inorganic ion content of salinized plants (Mitchell et al., 1991; Navarro et al., 2005). In many species, particularly for fruit and vegetables, quality is a main objective for variety improvement. Breeding for quality arose with the increasing demand of high quality products from consumers these last decades. Accordingly to its definition (Shewfelt, 1999; Causse et al., 2001), quality is complex and involves several chemical, physical, and organoleptic characteristics that can be directly related to consumer preferences or to the requirement of market-oriented production. Many quantitative trait loci (QTL) related to fruit quality traits were identified in several species (Causse et al., 2001; Monforte et al., 2004; Kenis et al., 2008; Eduardo et al., 2011). These studies revealed that most of the quality components are polygenic and based on multiple correlated traits, some of which being regulated by pleiotropic or linked QTLs (Monforte et al., 2004; Kenis et al., 2008).

Multi-parent populations require crosses between more than two inbred parental lines to generate RIL progeny. They include Nested Association Mapping (called NAM, Yu et al., 2008) or Multi-parent Advanced Generation Inter-cross (called MAGIC) populations (Kover et al., 2009; Huang et al., 2012). The interest of multi-parent populations relies on the mating design allowing more genetic diversity to occur in the offspring, which besides undergoes several recombination events. The first MAGIC population was developed in mouse (Threadgill et al., 2002) and expanded to several plant species (Kover et al., 2009; Huang et al., 2012; Bandillo et al., 2013; Milner et al., 2016). The MAGIC populations have some advantages with respect to association panel for GWAS because of the absence of structure and the balanced allelic frequencies. They already demonstrated their capacity to increase length of genetic maps and detect QTL with reduced confidence intervals compared to bi-parental progenies (Pascual et al., 2015; Gardner et al., 2016). Nevertheless, due to the complexity of the mating design, statistical methods used in bi-parental or GWAS populations are not efficient. A regression model estimating all parental effects was proposed by Huang and George (2011).

In the present study we investigated the effect of salinity stress and water deficit on tomato for quality, yield component, vegetative, and phenology traits, using a MAGIC population based on the cultivated tomato and which underwent several

recombination generations. Thus, the objectives were: (1) to assess and compare the impact of both WD and SS at phenotypic level and the trait plasticity, (2) to study the genetic determinants of tomato response to SS and WD and to identify interactive QTL using plasticity and (3) to select candidate genes, based on the parental allelic effect and their genomic sequences.

MATERIALS AND METHODS

Plant Materials

We analyzed the MAGIC tomato population created at INRA center of Avignon (France). It was derived from the cross of eight parental lines, four of them belonging to the small fruit group *S. lycopersicum* var. *cerasiforme* (Cervil, Criolo, Plovdiv24A, and LA1420) and four lines with large fruit from *S. lycopersicum* var. *lycopersicum* group (Levovil, Stupicke Polni Rane, LA0147 and Ferum). Parent's selection was carefully operated within a core collection of 360 cultivated tomatoes to comprise the maximum diversity, notably the genomes of the four *cerasiforme* accessions representing a mosaic between wild and cultivated tomato genomes. A population of 400 families was obtained following the crossing design detailed in Pascual et al. (2015). The genomes of all parental lines were fully sequenced allowing the identification of about 4 millions of single nucleotide polymorphisms (SNP) (Causse et al., 2013).

Greenhouse Trials

The MAGIC population was grown in contrasted conditions in Morocco (Gautier Semences breeding station) over 2 years in greenhouse with similar experimental procedures. Plants were grown in 5L plastic pots filled with loamy substrate (Klasmann 533) and treatments were applied by row. Stressed and control rows were placed side-by-side, each genotype in the stressed row facing its replicate in the control one. The first year of experiment (Exp.1), water deficit and control (well irrigated) treatment were applied, while the second year (Exp.2) was dedicated to salinity stress and its control treatment. The average temperature and relative humidity in the greenhouses were very similar in both experiment with 20.82°C and 60.68 HR for Exp.1 and 21.74°C and 61.60 HR for Exp.2. However, the management of electrical conductivity (EC) differed between the two experiments. In Exp.1, water supply was reduced for WD treatment with respect to the control treatment where plants were subjected to the optimal irrigation. WD treatment consisted in the reduction of irrigation by 25% at the first flowering truss of Cervil (the earliest parent) and by 50% at the second flowering truss. The EC of the loamy substrate was measured in the pots for each plant with a "GroSens HandHeld" instrument, giving an average value of 1.97 dS/m for the two treatments. In Exp.2, both control and salinity treatments were not restricted in the amount of water intake but differed in the EC application. A fertigation solution with a pH of 6.1 and EC of 3 dS/m was used for both treatments at the beginning of the culture until the 2nd truss flowering of at least half of the plants. Then, salt treatment was enriched with NaCl solution and salinity was evaluated by measuring the EC of the substrate every week. On average, the EC of the substrate was 3.76 dS/m in control treatment and 6.50 dS/m in salinity treatment. The average difference in EC between the controls treatments over the two experiments was thus 1.79 dS/m. First and last rows in the greenhouse were considered as border lines and border genotypes were also placed at the end of rows. The eight parental lines and four F1 hybrids were tested together with 241 MAGIC lines in Exp.1 and 253 MAGIC lines in Exp.2.

Plant Phenotyping

Seven traits were measured in both experiments. For phenology, flowering date (date of first open flower on 4th truss) and maturity date (first ripe fruit on the 4th truss) were recorded. Then time to flower (Flw) and time to ripe (RIP) were recorded as the day number between the sowing date and flowering date for Flw and between the flowering date and maturity date for RIP. Leaf length (Leaf) was measured as vegetative trait for each plant under the 5th truss. Fruits were harvested at maturity every week and for each genotype, fruit number was recorded on plants and fruit weight (FW) measured for at least 10 fruit per genotype on truss 3, 4, 5, and 6. For sugar content in Exp.1, 3 fruits harvested on truss 4 and 5 were pooled and crushed to obtain a fluid on which the soluble solid content (SSC) was measured with an electronic refractometer. In Exp.2 only fruits within each truss were pooled for SSC measurements. A durometer was used to measure fruit firmness (Firm), applying a pressure on the surface of the fruit measuring the strength needed to retract the durometer's tip. Five fruits per genotype were used with two measures per fruit.

For every trait in each experiment, phenotypic plasticity (PP) was measured by the relative difference between the control and stress treatments. For a trait (k) and for a single genotype, we calculated PP as $PP_k = (Stress_k – Control_k)/Control_k$ and used these data to identify interactive QTL between stress and control for each experiment. Considering all the genotypes, the average effect of the stress was evaluated in a single experiment by the mean relative variation as $(Mean\ Stress_k – Mean\ Control_k)/Mean\ Control_k$ and converted in percentage of increase or decrease due to the stress. For convenient comparison between salinity and water deficit effects on phenotypes, the mean variation was also calculated in a second step taking the control in Exp.1 as unique control and all other conditions as stress.

Statistical Analyses

Statistical analyses were performed with the free software R version 3.3.0. Data were firstly checked per trait and per treatment. FW and NFr were log-transformed for normality assumption. Analyses were conducted separately per experiment to allow the comparison of each stress treatment against its control. We tested the fixed effect of genotype and treatment and their interaction by a two way ANOVA following the model: $Yij = \mu + Gi + Tj + G^*Tij + \varepsilon ijk$, where Yij represents the phenotype of genotype i (Gi) and treatment j (Tj), G*Tij the interaction between genotype and treatment and εijk the residual error. Pearson's correlations were calculated between the mean trait values per treatment and for each trait between treatments within experiment and between the two control treatments. In each treatment, the broad sense heritability (h^2) was evaluated by means of the following ANOVA model where the genotype

was considered as random: $Yi = \mu + Gi + \varepsilon ij$. Gi and εij are the random effect of genotype and the residual error respectively. The broad sense heritability was then calculated as $h^2 = \sigma^2G/(\sigma^2G+\sigma^2E/r)$ where σ^2G and σ^2E are the genetic and residual variance respectively, and r is the average number of replicates per genotype.

Haplotype Prediction

The MAGIC population is characterized by the complex mating design of the eight parental lines. The parental origin of each allele in the offspring is not intuitive, on the contrary to the bi-parental population. To infer the allelic parental provenance, we estimated the probability of each parent being at the origin of each allele in the MAGIC lines with the function *mpprob* of the mpMap package 2.0 (Huang and George, 2011). We fixed a threshold of 50% above which allelic parental provenance is assigned. These probabilities were further used to perform the QTL identification.

QTL and QTL×E

The QTL were mapped by interval mapping (IM) procedure with the R package mpMap. Parental probabilities were computed every 2 cM along the genome and at each marker position and then used to estimate parental effects. The regression on the parental allelic effect, at each position where probabilities were computed, allowed the QTL identification. A LOD threshold of 3 was fixed to detect a significant QTL. Confidence interval (CI) of a QTL was estimated with one unit decreasing of the LOD threshold on both sides of a QTL position. Considering one trait, constitutive QTLs were defined when two (or more) QTLs were identified in different conditions (treatments) on the same chromosome with their CI overlapping. They were then considered as a unique QTL expressed in both conditions.

Then, PP was used as single trait for each phenotype, to identify interactive QTL (QTL×E). Before analysis, plasticity data were checked for normality and log transformed for FW and NFr.

Candidate Genes Identification

We screened for candidate genes under QTL for the QTL×E and QTL mapped in a CI shorter than 2Mb. For each QTL, we listed the number of polymorphisms and genes present within the CI region based on the sequence information of all parental lines (Causse et al., 2013) and the reference genome (Tomato Genome Consortium, 2012). We filtered the polymorphisms and genes listed in accordance with the parental allelic effects at the QTL. We focused on QTL that present pronounced divergence in the allelic effect of the eight parents, keeping all polymorphisms and genes commonly shared by the parents varying in the same direction and different from those shared by the parents varying in the opposite direction. The putative function of the remaining genes (when annotated) were then checked on the Sol Genomic Network (solgenomics.net) database in order to identify which candidate's annotated function is correlated to the QTL trait of interest.

RESULTS

Phenotypic Variation in the MAGIC Population

The phenotypic variation observed among the MAGIC lines showed transgressions in both directions in comparison to the eight parental values for every trait (**Table 1**; **Supplemental Figure 1**). Except FW in control of Exp.2, the highest value in MAGIC lines always exceeded the best parent in every trait by treatment combination.

The comparison of control treatments between the two experiments showed little mean differences for Firm, RIP and Leaf, which had a relative mean variation below 10%. FW, SSC, and NFr varied considerably between the controls by 38.54, 39.85, and 61.11% respectively (**Table 1**). Statistical analyses were thus conducted separately for each experiment to assess the impact of WD and SS compared to their specific control treatment.

All traits across treatments exhibited heritability above 0.4 except firmness in Exp.1. Heritability ranged from 0.09 for firmness in WD treatment to 0.92 for flowering time in control of Exp.1. In average, Flw, RIP and FW had the highest heritability. For both experiments, heritability varied between control and stress treatment with the highest variation observed for SSC in Exp.2 where h^2 SSC was 0.69 for the control and 0.48 for the salinity treatment. The heritability of a few traits like RIP was poorly impacted by the stress treatments.

The total sum of square of the two way ANOVAs was partitioned in proportion attributed to genotype, treatment and their interaction. A large part of the phenotypic variation was linked to genotype, accounting from 39 to 86% of the total sum of square in Exp.1 and 33 to 72% in Exp.2 (**Table 2**). Significant effects of treatment were found for every trait in Exp.1 while Exp.2 showed significant treatment effect only for FW, SSC, and Leaf. Similarly, all traits exhibited significant genotype × treatment interaction in both experiments except Firm in Exp.1 and NFr in Exp.2.

Significant correlations were observed between traits in each treatment revealing the link between quality, phenology, and vegetative traits. To assess the repeatability of phenotyping measurement, single trait correlations between treatments within each experiment and among control treatments were evaluated. Most of the correlations were significant at $P < 0.001$ (**Table 3**). The strongest Pearson's correlation was found between FW and leaf in Exp.1, which exhibited a positive correlation. In Exp.2, the correlation between Flw and RIP was the strongest correlation. For both experiments, Flw and RIP were significantly and negatively correlated indicating that the later the truss flowered, the shorter the time to ripe. FW was also negatively correlated to SSC in every treatment. Across experiments, the sign of correlations were conserved for all significant correlations.

Impact of Water Deficit and Salinity Stress at Phenotypic Level

The effect of stress treatment was assessed by the mean relative variation (MV) calculated as detailed in Materials and Methods. In a first step, salinity and water deficit were compared to their relative control treatment in each experiment. In accordance

TABLE 1 | Phenotypic variation among MAGIC lines for all traits and treatments.

Traits	Treatments	P. range	MAGIC lines			MV_WD	MV_Ctrl2	MV_SS	h^2
			Min	Max	Mean				
SSC	Ctrl1	3.50–7.30	2.80	8.20	5.56	11.78	39.85	75.91	0.72
	WD	4.30–10.10	3.10	10.10	6.21				0.80
	Ctrl2	7.50–9.50	4.00	13.00	7.74	25.96			0.69
	SS	8.50–11.00	6.00	12.5	9.75				0.48
Firm	Ctrl1	50.00–72.00	44.00	73.00	59.58	−2.18	2.02	6.92	0.32
	WD	50.00–68.00	45.50	73.00	58.28				0.09
	Ctrl2	38.50–76.00	36.00	82.00	60.60	4.93			0.64
	SS	57.00–70.00	31.00	84.00	63.58				0.57
FW	Ctrl1	6.88–92.00	10.71	110.00	38.75	−23.05	−38.54	−54.62	0.85
	WD	5.35–95.00	10.54	101.67	29.81				0.83
	Ctrl2	5.00–110.00	5.00	95.00	23.84	−26.52			0.77
	SS	5.00–23.84	2.50	74.28	17.52				0.60
NFr	Ctrl1	6.50–45.50	2.50	105.00	15.61	−15.32	−61.11	−59.85	0.75
	WD	3.00–47.00	3.00	50.00	13.22				0.56
	Ctrl2	2.00–12.50	2.00	23.50	6.20	3.70			0.42
	SS	2.00–15.50	2.00	21.00	6.43				0.40
Leaf	Ctrl1	23.50–42.00	18.00	55.00	32.24	−17.97	−7.92	−16.05	0.85
	WD	23.50–35.50	15.00	48.50	26.45				0.69
	Ctrl2	20.50–35.00	11.00	45.50	29.51	−8.66			0.66
	SS	25.00–31.00	11.50	40.00	26.97				0.58
Flw	Ctrl1	77.50–110.00	77.50	117.00	88.76	−0.77	−10.26	−10.74	0.92
	WD	76.50–107.00	75.50	124.00	88.07				0.92
	Ctrl2	80.50–102.00	75.00	102.00	79.74	−0.60			0.85
	SS	79.00–98.00	74.00	105.00	79.26				0.78
RIP	Ctrl1	51.00–71.50	43.50	74.00	57.88	−2.87	−5.30	−6.59	0.87
	WD	46.50–68.00	44.00	70.00	56.22				0.88
	Ctrl2	46.50–72.00	36.00	79.00	55.72	−0.22			0.64
	SS	47.00–66.00	35.50	75.00	55.59				0.75

Min, Max and mean are the minimum, maximum and mean values of MAGIC lines. P. range represents the range of the means of the eight parental lines. MV is the relative mean variation, with respect to control in Exp.1 due to treatments under WD (MV_WD), control in Exp.2 (MV_Ctrl2) and salinity (MV_SS). h^2 is the broad sense heritability calculated for each treatment.

to the results of ANOVA, FW, SSC, and Leaf were the traits most affected by stress treatments. Among all traits, SSC was the only one positively impacted by WD and SS with more than 10% increase compared to controls (**Table 1**). On average, when comparing each stress to its control, WD and SS affected all traits in the same direction except NFr. Indeed, NFr was reduced by WD condition (−15%) but slightly increased when comparing salinity to its control. FW and Leaf were both reduced in stress conditions while stress effects were less obvious for firmness and phenology traits.

For a convenient comparison of WD and SS applied in our study, we considered the control treatment in Exp.1 as reference, taking a subset of 241 lines commonly tested in all treatments. Indeed, the difference between the control in Exp.1 and treatments in Exp.2 lies mainly in the EC application that was 1.7 and 4.5 times higher in control of Exp.2 and SS, respectively. We then calculated the effect of those treatments compared to Ctrl1 and measured the effect of each of them in percentage of increase or decrease (**Supplemental Figure 2**). Using the same control revealed a growing negative effect of salt treatment while control in Exp.2 seemed to be intermediate between WD and SS.

Nevertheless, these average behaviors did not fully reflect the individual variations. FW plasticity was found negatively correlated to FW in control in both experiments, meaning that larger fruits were more affected by the stress. Indeed both stress decreased FW of accessions with fruits larger than 55g (**Figures 1A,B**). The plot of FW plasticity in SS against WD showed clearly that only one genotype had an increased FW

TABLE 2 | Phenotypic variation attributed to the genotype (G), the treatment (T) and the interaction (GxTreat) effects.

Traits	G	SSq G %	Treat	SSq Treat %	GxTreat	SSq GxTreat %	SSq Resid %
EXP.1 (CONTROL vs. WD)							
Firm	***	39.42	***	0.86	ns	18.75	40.97
Flw	***	86.04	***	0.44	***	6.48	7.04
FW	***	54.16	***	9.25	***	4.67	31.92
Leaf	***	47.75	***	14.85	***	23.91	13.48
NFr	***	55.53	*	0.62	*	17.88	25.98
RIP	***	73.27	***	2.77	***	13.62	10.34
SSC	***	61.75	***	6.7	***	15.8	15.75
EXP.2 (CONTROL vs. SS)							
Flw	***	68.76	ns	0.00	***	15.4	15.83
FW	***	47.14	***	6.87	***	26.2	19.78
Leaf	***	52.36	***	3.55	***	18.9	25.19
NFr	***	42.04	ns	0.18	ns	23.59	34.19
RIP	***	59.06	ns	0.01	*	17.56	23.36
SSC	***	33.45	***	27.24	***	23.01	16.29

For each quantitative trait the significance of the explaining factors: G, T and the interaction GxTreat, and their relative proportion of sum of square (SSq G, SSq Treat and SSq GxTreat, respectively) are shown.
****P < 0.001; *P < 0.05; ns = non significant.*

TABLE 3 | Correlations among traits in each treatment and experiment.

Ctrl1							**Ctrl1-Ctr2**	**Ctrl2**						
Firm	Firm						−0.17	Firm	Firm					
Flw	**0.15**	Flw					**0.61**	Flw	ns	Flw				
FW	ns	**0.24**	FW				**0.4**	FW	ns	ns	FW			
Leaf	ns	**0.18**	**0.37**	Leaf			0.19	Leaf	ns	−0.15	ns	Leaf		
NFr	ns	ns	**−0.33**	ns	NFr		ns	NFr	ns	−0.15	**−0.24**	0.11	NFr	
RIP	**0.17**	**−0.26**	**0.22**	ns	**−0.28**	RIP	**0.49**	RIP	ns	**−0.28**	0.13	ns	**−0.18**	RIP
SSC	−0.13	ns	**−0.17**	ns	ns	**−0.26**	**0.23**	SSC	ns	ns	**−0.25**	ns	ns	ns
WD							**Ctrl1-WD**	**Salt**						**Ctrl2-SS**
Firm	Firm						**0.34**	Firm	Firm					0.19
Flw	ns	Flw					**0.86**	Flw	ns	Flw				**0.62**
FW	**0.18**	**0.14**	FW				**0.84**	FW	ns	**−0.29**	FW			**0.26**
Leaf	ns	**0.29**	**0.4**	Leaf			**0.34**	Leaf	ns	**−0.29**	0.15	Leaf		**0.46**
NFr	−0.11	ns	**−0.38**	−0.14	NFr		**0.55**	NFr	ns	**−0.19**	ns	ns	NFr	**0.31**
RIP	**0.2**	**−0.31**	**0.23**	ns	−0.12	RIP	**0.68**	RIP	−0.12	**−0.38**	ns	ns	ns	RIP	**0.5**
SSC	**−0.17**	ns	**−0.33**	**−0.17**	ns	**−0.31**	**0.6**	SSC	ns	**0.33**	**−0.22**	ns	ns	0.13	0.16

Single trait correlation among controls (Ctrl1-Ctrl2) which is a measure of repeatability or between control and stress (Ctrl1-WD and Ctrl2-SS) is presented. Only significant correlations (P < 0.05) are indicated. They are in bold when significance is lower than 0.001. In bold P < 0.001; ns = non significant.

in both conditions while 23 genotypes increased FW under WD and decreased it under SS and 10 genotypes react in the opposite direction (**Figure 1C**). For SSC, all genotypes except H10_84 increased SSC with SS treatment. Altogether, 67% of the genotypes increased SSC under both stresses pointing the possibility to improve sugar content in fruit by irrigation practices. However, as for FW, some genotypes were affected inconsistently by the stress treatments with 55 genotypes (22.8%) that increased SSC only in SS and not under WD (**Figure 1D**).

QTL Detection and Stability

QTL Detection

QTL mapping was performed using a genetic map constructed with 1,345 polymorphic SNP selected from the parental line resequencing data. This genetic map covers more than 84% of the genome and measures 2,156 cM (details in Pascual et al., 2015). With the available information of parental polymorphisms, the offspring haplotype structure was predicted by inferring the parental origin of each allele. On average, 88.7% of founder allele origin was accurately predicted with

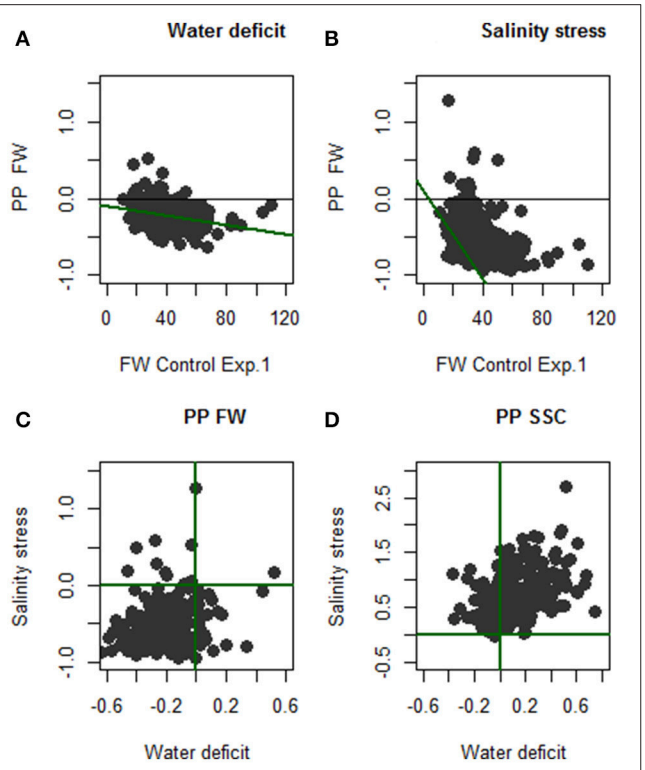

FIGURE 1 | Effect of stress treatments on individual lines for FW and SSC. **(A,B)** plot the FW plasticity— which is the gain (above 0) or loss (below 0) of FW due to stress—against the FW in control treatment of Exp.1. **(C)** (respectively **D**) is the FW (respectively SSC) plasticity in WD against plasticity in SS treatment both compared to the same control in Exp.1.

only 11% of the alleles that could not be strictly assigned to any parent (**Supplemental Figure 3**). Among the parents, Levovil and LA0147, with <10% of the allelic contribution in the MAGIC lines genome deviated, the most from the expected value of 12.5% of each parental allelic contribution.

Considering all treatments, 54 QTL were identified for the seven traits evaluated and their plasticity. The number of QTL per trait varied from four for Flw to 11 for FW (**Supplemental Table 1**). Among these QTL, 19 were found in at least two treatments and around 65% (35 QTL) were treatment specific. Eleven QTL were common to WD and its control condition, while SS and its control condition shared only four QTL (**Figure 2A**).

Some QTL were specifically detected in one treatment or for plasticity traits (interactive QTL; **Supplemental Table 1**). Indeed, irrespective of interactive QTL, we observed eight and four QTL specific to control treatments for Exp.1 and Exp.2, respectively. Nine and 11 QTL were specific to WD and SS respectively, pointing that stress treatments present higher number of specific QTL. For interactive QTL, six were exclusively identified in Exp.2 and one in Exp.1 and no interactive QTL were shared between the two experiments (**Figure 2B**). This outlined the specificity of the interactive QTL. Confidence intervals (CI) of the QTL ranged from 4 to 60 cM (according to genetic distance) and 0.43 to 71.49 Mb (according to physical distance; **Supplemental Table 1**). The high number of recombination occurring in the MAGIC population allowed us to map 24 QTL with CI lower than 2Mb. The chromosome 11 presented the largest number of QTL, each trait except Flw presenting at least one QTL on this chromosome, whereas per trait, FW and SSC had the largest number of QTL (11 and 10, respectively).

Identification of Interactive QTL (QTLxE)

We call interactive QTL (QTLxE) those mapped for plasticity traits in each experiment. Thus, for Exp.1, three QTLxE were detected for RIP (two QTL) and SSC. The RIP QTLs (*RIP9.1* and *RIP10.1*) were also mapped in control for Exp.1 and WD treatment, respectively. The QTLxE *SSC12.1* was specific to the interaction. Likewise, 12 QTLxE were mapped in Exp.2, among which six were specific to the interaction.

Co-Localization of QTL

Clusters of QTL were localized especially on chromosomes 1, 2, 3, 10, and 11 (**Supplemental Figure 4**). Most of these QTL corresponded to correlated traits. For example, around 45 cM on chromosome 1, QTLs linked to phenology traits, FW, SSC, and NFr clustered and could be related to the pleiotropic effect of one QTL. The same observation was noted on chromosome 2 for quality traits and on chromosome 3 for phenology, quality and vegetative traits.

Candidate Gene Selection

After the identification of constitutive and interactive QTLs, the number of genes and polymorphisms within the CI of any QTL mapped in a region lower than 2Mb was assessed using the sequencing information of all parental lines (Causse et al., 2013). For the 24 QTLs that had a CI shorter than 2 Mb, the number of genes within the CI (potential candidate genes) varied from 75 for *Leaf9.1* to 269 genes for *Firm11.1* with 3,804 and 12,530 polymorphisms associated, respectively (**Table 4**). We attempted to reduce the number of candidate genes (CG) by applying a filter in accordance to parental allelic effects at the QTL as described in Materials and Methods. This procedure was efficient for some QTL and allowed us to reduce the number of CG by nearly 80% of the total number of genes within the CI for *Firm11.1* and *Leaf10.1* Nevertheless, for *FW11.3 and RIP4.1* the parental allelic effect filtering wasn't efficient; none of the genes in the CI was discarded as a close haplotype was present in the region (**Supplemental Figure 5**).

The interactive QTL *Firm11.1,* identified in Exp.2 contained the largest number of genes within the CI (269 genes). Regarding the parental allelic effect at this QTL (**Figure 3A**), we filtered the candidates by keeping all polymorphisms that were specific to Cervil parent. This reduced the number of candidates to eight genes and polymorphisms with different effects (**Supplemental Table 2**). For *FW8.1*, we kept all polymorphisms identical between Cervil and Plovdiv and different from Criollo (**Figure 3C**), decreasing the number of CG to 31 genes (**Supplemental Table 2**). Five QTL presented <40 CG after the filtering procedure according to allelic parental effect variation (presented in **Supplemental Table 2** with functional annotation

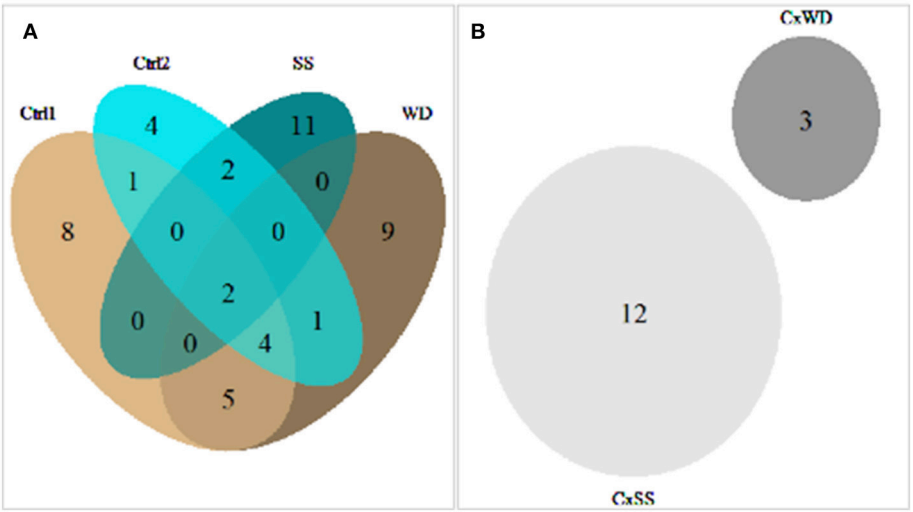

FIGURE 2 | Venn diagram of the number of main effect QTL, detected on mean traits for all treatments **(A)** and interactive QTL, detected on plasticity traits for the two experiments **(B)**.

of the CG). *FW2.2* QTL co-localized with a ripening time QTL *RIP2.1*. These two QTL shared the same CI comprising 1.74 Mb of length and containing 234 genes and 9,957 polymorphisms (**Table 4**). FW and RIP were highly positively correlated and could be impacted by one pleiotropic QTL. Moreover, *RIP2.1* and *FW2.2* presented the same pattern of parental allelic effect, at least for Cervil, Stupicke and LA1420 that had the strongest QTL effect (**Figures 3B,D**).

DISCUSSION

Parental lines of the MAGIC population did not include any wild accession (from the *S. pimpinellifolium* species) but had sufficient genetic diversity to allow QTL mapping on the offspring. The progeny exhibited a large variability with phenotypic transgressions in both directions in every tested condition (**Supplemental Figure 1**), suggesting new favorable allelic combinations obtained in the MAGIC population. Besides, the slight impact of WD and SS on the heritability suggests possibility for marker-assisted selection (MAS). Huang et al. (2015) proposed an interesting MAS approach for MAGIC populations called Multi-parent advanced generation recurrent selection (MAGReS) involving the inter-cross of individuals with the best allelic combinations for one (or more) trait(s) of interest to produce highly performant RILs. The MAGIC population tested here is thus a valuable resource to apply such breeding strategy. However, our results showed high level of GxE for the two experiments that affect also the QTL detection, as 35 QTL (65%) were specifically detected on one condition. Furthermore, FW and SSC, the most important agronomic traits, carried ten or more QTL in all condition tested with only one QTL (*FW2.2*) stable across all treatments. For these traits, MAS may not be of great utility for breeding programs targeting variable cultural areas. Thus, the breeding strategy should take into account the specificity of the QTL to achieve optimal benefit per environment. Applying the MAGReS strategy by selecting genotypes to inter-cross following the performance per environment in order to achieve rapidly performing crop, is an innovative approach to sustain breeding effort.

On average, WD and SS impacted sugar content, fruit weight and leaf length more than the other traits. They both reduced FW and Leaf while SSC was the only trait positively affected by up to 10% increase with respect to control in Exp.1 (**Supplemental Figure 2**). Similar results were frequently found in the literature (Villalta et al., 2007; Huang et al., 2009). The higher SSC under WD and SS was assumed to derive from the fruit water content reduction without necessarily involving higher synthesis of soluble sugar. Indeed, several studies reveal a negative correlation between FW and SSC, pointing a physiological link of these two traits making a simultaneous improvement difficult to be achieved. However, Navarro et al. (2005) showed that when SS occurs, the increased concentrations of sugars and acids were probably both due to the decrease in water content in the fruit and additionally to new sugars synthesis, since concentrations calculated on a dry weight basis also increased. Our results showed 20 and 11 genotypes that increased simultaneously FW and SSC under WD and SS respectively. This may be linked to a positive regulation of SSC during drought and salinity. These genotypes are interesting for quality improvement in tomato with minor impact on FW.

The results of the QTL analyses confirmed the polygenic architecture of fruit quality traits. SSC and FW that are among the most important fruit quality traits had the highest number of QTL identified. Besides this polygenic architecture, the positions of these QTL are distributed along the genome. QTLs related to FW and SSC were identified on six and seven chromosomes respectively, considering all treatments but treatment specific QTL were also identified. In optimal growth condition (Control

TABLE 4 | Characteristics of the 24 QTL with a confidence interval (CI) smaller than 2 Mb.

QTL	CI Mb	Cervil	Levovil	Criollo	Stupicke	Plovdiv	LA1420	Ferum	LA0140	Nb.Genes	Nb.Pol	Filter	Nb.CG	Nb.CP
Firm1.1	1.86	0.608	−1.266	−3.916	2.628	1.655	0.095	−0.629	0.824	245	10991	Criol # Stup	164	620
Firm1.2	1.05	−0.412	−0.539	−0.544	−0.541	−0.372	3.112	−0.428	−0.276	134	5630	LA14 # all	127	1719
Firm11.1	1.87	4.305	−0.651	−0.284	−2.169	−0.821	−0.435	−0.326	0.384	269	11903	Cerv # all	8	3
Firm3.1	1.44	−5.249	4.750	−3.842	3.354	−7.327	0.581	2.679	5.055	171	7051	Plov # (Lev=LA0)	36	29
Firm8.1	1.23	−0.411	−0.421	2.767	−0.815	−0.245	−0.636	−0.009	−0.231	117	7975	Criol # all	27	46
Flw9.1	1.00	0.292	1.523	−0.522	−1.460	3.004	−2.710	3.561	−3.690	119	6375	(Plov=Fer) # LA0	49	35
FW11.2	0.79	−0.131	0.664	−0.043	0.024	0.013	−0.040	0.003	−0.493	91	4478	Lev # LA0	29	32
FW11.3	1.42	−0.155	0.066	−0.049	0.130	−0.001	−0.022	*NA*	0.033	189	11532	Cerv # (Stup=Lev)	189	6989
FW12.1	0.43	0.008	−0.097	0.048	−0.142	−0.038	0.033	0.171	0.020	79	3407	Fer # (Stup=Lev)	77	562
FW2.2	1.74	−0.138	−0.031	0.050	−0.134	0.031	0.082	0.044	0.093	234	9957	(Cerv=Stup) # (LA14 =LA0)	52	1362
FW3.2	0.97	−0.049	−0.004	−0.087	0.056	0.162	−0.078	−0.005	0.003	122	6490	Criol # Plov	109	3026
FW3.3	1.52	−0.095	−0.007	−0.046	−0.038	0.056	−0.083	0.055	0.157	214	10182	(Cer=LA14) # LA0	142	377
FW8.1	1.63	−0.195	0.019	0.111	0.009	−0.132	0.046	0.097	0.047	180	7959	(Cer=Plov) # Criol	31	738
Leaf10.1	1.86	1.565	−0.622	2.628	−2.586	−0.070	3.058	−2.898	−1.073	264	13108	(Criol=LA14) # (Stup=Fer)	42	52
Leaf11.1	1.55	−2.416	2.005	2.040	3.103	−1.464	−2.799	0.890	−1.356	168	10084	Stup # (Cerv =LA14)	94	524
Leaf3.1	1.46	−2.985	2.944	−2.063	1.403	3.224	−1.286	−0.321	−0.918	193	9944	(Lev=Plov) # Cer	184	5803
Leaf9.1	0.76	0.798	−2.351	−1.744	5.031	−4.669	−2.079	3.154	1.861	75	3804	Plov # Stup	52	963
NFr10.1	1.53	−0.129	−0.021	0.039	0.354	0.063	−0.023	0.042	−0.326	212	5506	Stup # LA0	70	80
RIP2.1	1.74	−4.039	1.956	2.022	−3.948	−0.265	3.585	0.654	0.034	234	9957	(Cer=Stup) # LA14	103	1418
RIP4.1	1.21	−0.053	2.639	1.233	−0.053	1.788	−2.420	−0.653	−2.482	150	10794	(LA14 = LA0) # Lev	150	6629
SSC1.2	1.34	0.156	−0.250	−0.670	−0.207	0.194	−0.290	0.121	0.949	197	10528	LA0 # Criol	68	69
SSC11.2	1.56	0.970	−1.916	0.789	−0.594	0.018	0.398	*NA*	0.338	203	11813	(Cer = Criol) # Lev	78	681
SSC12.1	1.52	0.047	0.004	−0.007	−0.094	0.122	0.103	−0.153	−0.019	170	8232	(Plov=LA14) # Fer	110	395
SSC4.1	1.93	−0.792	0.363	0.214	0.441	0.811	0.252	−0.682	−0.606	211	15195	(Cerv=Ferum=LA0) # Plov	65	58

The columns of the eight parents present their respective allelic effect for each QTL. Nb Genes and Nb.Pol count the number of genes and the number of polymorphisms identified—via the Solgenomic database—within the CI. After filtering these genes and polymorphisms according to the allelic effect of parents, the residual numbers of genes are counted as candidate genes (Nb.GC) with the residual number of candidate polymorphisms (N.CP). The parents chosen for the CG filtering are presented in the column "Filter" where the symbols = and # notified respectively parents where identical or divergent polymorphisms were kept.

of Exp.1), seven FW QTL (out of the 11 QTL mapped for FW) were identified, explaining additionally 68.68% of the phenotypic variation, while only one SSC QTL (*SSC2.1*; out of the 10 SSC QTL) was identified, with 6.98% of phenotypic variation. This suggests that SSC QTLs are easier detected in stress than control conditions.

Among all the QTL identified in this study, 35 QTL were treatment specific and only two QTL (*Flw1.1* and *FW2.2*) were stable across every treatment. Depending on the environmental conditions, the main QTL responsible of the observed phenotypic variation are not the same. Only one third of the QTL were detected in at least two treatments. These results reinforce the idea of targeted environment breeding strategy in order to achieve better results per environment.

Fifteen interactive QTL were identified, three in Exp.1 and 12 in Exp.2 but none of them co-localized between the two experiments suggesting different genetic control of the phenotypic plasticity under WD and SS. Two main ideas were developed concerning the genetic control of phenotypic plasticity advocating that: (i) phenotypic plasticity can be caused by environmentally sensitive loci associated with a phenotype, directly influencing the trait value in both environments; (ii) or it can be caused by regulatory genes that simply influence the plasticity of a phenotype. This means that plasticity can be viewed as the result of the action of alleles that have different effects in different environments or being under the control of regulatory loci (Via et al., 1995). Besides, QTL mapping study can be used to address easily which one of these hypotheses is the most probable (Ungerer et al., 2003; Tétard-Jones et al., 2011). When plasticity QTL co-localized with QTL mapped on mean trait value in at least one of the environment tested, they are assumed to be under the control of allelic sensitivity loci. On the contrary, QTL that are specific to plasticity are mainly linked to regulatory genes. In Exp.1 three QTLxE were identified: *RIP9.1, RIP10.1* and *SSC1.2* but only the last one was specific to the interaction. At the same time in Exp.2, among the 12 QTLxE, six were specific to the interaction. One can assume these QTLxE to be under regulation of WD (Exp.1) and SS (Exp.2) response genes, which make them particularly interesting for breeding in stressful environment.

Multi-parental populations offer new insight into fine mapping of quantitative traits (Kover et al., 2009; Milner et al., 2016). The high recombination events occurring in this type of population in addition to the infinite possibility of repeated study are of major interest. One advantage is the high allele segregation compared to bi-parental population and low LD with poor structure compared to GWAS, making them intermediate and complementary between these types of mapping populations (Pascual et al., 2016). Our results were compared to those

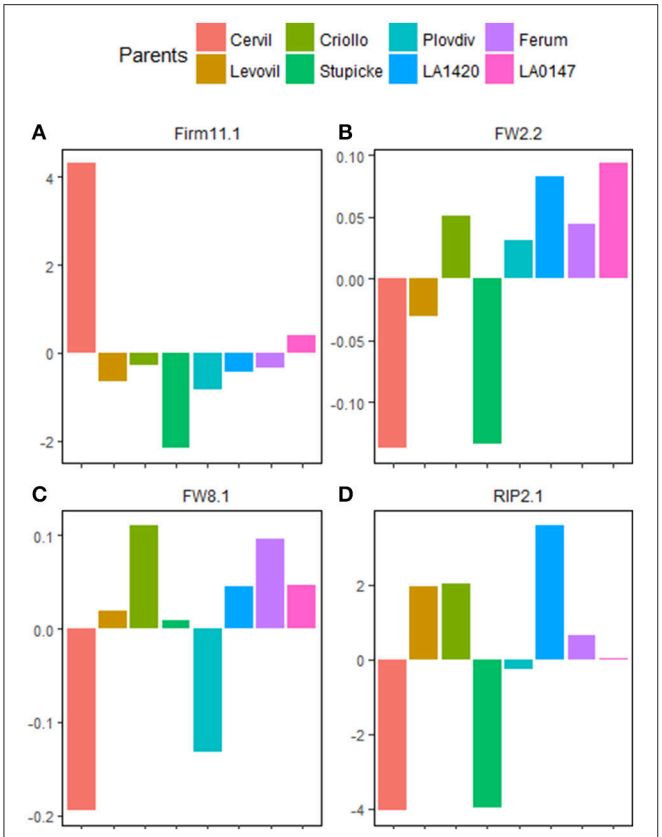

FIGURE 3 | Example of QTL where the parental allelic effect allowed reducing the number of candidate genes. The QTL effects were mean centered to facilitate the visualization of allelic effect difference between parents. **(A)** Allelic effect of the eight parental lines for the QTL Firm11.1. **(B)** Allelic effect of the eight parental lines for the QTL FW2.2. **(C)** Allelic effect of the eight parental lines for the QTL FW8.1. **(D)** Allelic effect of the eight parental lines for the QTL RIP2.1.

of Albert et al. (2016a) and Albert et al. (2016b), that were conducted respectively on bi-parental population and a GWAS panel of tomato grown in similar condition of control and WD treatment than Exp.1. Among the 30 QTL identified in Exp.1, 18 QTL (60%) were also detected in the GWAS or RILs population, but only *Firm11.1* and *SSC11.2* were shared between the three panels. The ability to map QTL considerably depends in the mapping population pointing the relevance of combining different mapping population to identify stable QTL and balanced the advantage and disadvantage of each type of population.

The parental allelic information in the MAGIC population is a real advantage to screen and reduce candidate polymorphisms within the CI of a QTL as first described in Pascual et al., (2015). Indeed, the parents of the MAGIC population present very diverse allelic effects depending on the QTL. Some QTL had very divergent parental allelic effect while some other showed one parent varying differently from others. For example, *Firm1.2*, *Firm8.1,* and *Firm11.1* had all one parent divergent that seem to carry the allele responsible of the phenotypic variation. Besides, those QTL present very strong percentages of variation explained, that makes them interesting targets for breeding. These effects efficiently facilitate the filtering procedure to reduce CG.

On the chromosome 2, in a nearly 8 Mb region ranging from 44.55 to 52.92 Mb, two FW QTL were identified in our study. However, this region contains at least three already known QTL impacting fruit size and fruit shape, two of them positionally cloned: the fruit weight 2.2 (Solyc02g090740) cloned by Frary et al. (2000) and the ovate locus (Solyc02g085500) cloned by Liu et al. (2002). A third FW QTL was fine mapped by Muños et al. (2011) in this region, corresponding to a locule number (lc) locus. The first QTL identified on the chromosome 2 in our study (*FW2.1*) falls in a region of 3.5 Mb covering the *lc* and *ovate* loci. 462 genes and 20,742 polymorphisms were present in this region, and the filtering procedure did not efficiently reduce the CG. The second FW QTL on chromosome 2 (*FW2.2*) felt in a region of 1.74 Mb and covered the QTL fw2.2 cloned by Frary et al. (2000). However, this QTL was discarded when we attempt to reduce CG according to allelic effect of Cervil and Stupicke (**Figure 3B**). This suggests a second FW QTL closely linked to fw2.2. Nevertheless, Pascual et al. (2015) suggested a possible bias in the estimation of allelic parent's effect in regions where many QTL for a given trait are present. Indeed, in this case, the bias of allelic effect estimation may arise if different allelic combinations control different QTL. The QTL were mapped by interval mapping procedure meaning that each interval was tested for linkage with the phenotype. A whole genome mapping method, as proposed by Verbyla et al. (2014) for MAGIC populations, would better capture all small effect QTL and may limit the bias in QTL effect estimation. Anyhow the region of *FW2.2* is of great interest since several studies conducted on different mapping populations identified FW QTL within (Pascual et al., 2015; Albert et al., 2016a).

The number of candidate genes and polymorphisms was reduced using the parental re-sequencing information that allowed comparison of parental genotypes within CI of any detected QTL. Five QTL presented <40 CG after the filtering procedure (**Supplemental Table 2**). For these QTL, the putative functions of CG were screened according to the tomato genome annotation (SL2.50). Eight CG were retained for the QTL *Firm11.1* and all the polymorphisms related to these CG were on intergenic regions (Modifier effect in **Supplemental Table 2**). Among these CG, only Solyc11g006210 was not annotated. The functional annotation of the seven others highlighted one interesting CG (Solyc11g005820) which is a pectinesterase inhibitor. Pectinesterase inhibitors are involved in the rigidification or loosening of the cell wall. Thus, the Solyc11g005820 gene constitutes a good candidate for firmness variation.

FW8.1 presented 31 CG after the filtering procedure but the number of candidate polymorphisms was very high (**Supplemental Table 2**). In this region, most of the CG were affected by more than one polymorphism pointing the need of deeper characterization of our candidate regions to confirm the effectiveness of causal polymorphisms. Nevertheless, this region carried three SNP that had a high effect modifying splice site or start/stop codon whereas most of the candidate polymorphisms remaining after the allelic filtering for other QTL were located in intergenic regions. The three SNP with high effect in the CI of

FW8.1 affected the genes Solyc08g075430, Solyc08g075470, and Solyc08g075510.

We showed in this study the presence of high level of genotype × environment interaction and how these interactions affect the QTL detection according to the environment. Specific and constitutive QTL were identified—in high precision for some—for phenology, vegetative and quality traits and the availability of the parental sequence information was useful for the genetic and genomic characterization of polymorphisms responsible for trait variation. The parental sequences allowed filtering CG and polymorphisms for the QTL mapped on regions carrying divergent parental haplotypes. The transcriptomic response through RNA-sequencing analyses on all parental lines should offer additional information that will be used to improve and support the CG selection. Functional validation could be envisaged afterward in order to detect the exact causal polymorphisms under the QTL of interest.

AUTHOR CONTRIBUTIONS

This work is a part of the Ph.D. project of ID who conducted the statistical analyses and the redaction of the manuscript. LD conducted the experimental trials and phenotyping in Morocco. FB developed the bioinformatics tools to identify the polymorphisms on the MAGIC parental lines. LP reviewed the manuscript and shared a part of the script for QTL mapping analysis. MC supervised all the process of this work, constructed the experimental design and monitored the redaction of the article.

FUNDING

The ANR project ADAPTOM supported this work. ID was supported by the WAAPP (West Africa Agricultural Productivity Project) fellowship and hosted as Ph.D. student in the INRA UR1052, GAFL.

ACKNOWLEDGMENTS

We acknowledge the experimental teams of Gautier SEMENCES for their collaboration in implementing the experimentations and thank the employees of Domaine Margau (Agadir) for the data collection. We thank Christopher Sauvage for proofreading.

SUPPLEMENTARY MATERIAL

The Supplementary Material for this article can be found online at: https://www.frontiersin.org/articles/10.3389/fpls.2018.00279/full#supplementary-material

Supplemental Figure 1 | Distribution of mean values across MAGIC lines for each trait in Exp.1 **(A)** and Exp.2 **(B)**; For each trait, minimum (dotted lines) and maximum (solid lines) parental values are plotted for control (green) and stress (red) treatment.

Supplemental Figure 2 | Average variation caused by water deficit (WD), salinity (SS) and control in Exp.2 (Ctrl2) relative to control in Exp.1. The effect of each treatment was measured in percentage of increase or decrease against control in Exp.1.

Supplemental Figure 3 | Haplotype prediction. Each of the 12 tomato chromosomes is represented with the percentage of allelic contribution of every parental line. NA represented all positions on the chromosomes where the parental allelic origin could not be assigned.

Supplemental Figure 4 | Mapchart representation of detected QTL on the genetic map for all chromosomes where a QTL was identified. The dashes on the chromosomes barchart represent the centimorgan distances between markers along the chromosomes. Each trait has a color code representation.

Supplemental Figure 5 | Allelic effect of parental lines for QTL that were mapped in a confidence interval smaller than 2Mb.

Supplemental Table 1 | QTL detected in the different conditions. For each trait, all the QTL found are identified by a specific name (QTL name column), the treatment where the QTL was found (Treatment), the chromosome (Chr) and the position (Pos) in cM. The peak region encompassing any QTL is defined by a pair of marker (LeftMrk and RightMrk), corresponding to the lower and upper bound expressed in genetic distances (Lower cM & Upper cM) as well as physical distances (Lower Mb & Upper Mb). The confidence interval in centimorgan (CI cM) and Mega-base (CI Mb) represent the corresponding differences between Upper and Lower. R2 is the percentage of phenotypic variation explained by a QTL. Ctrl 1 and Ctrl2 are the controls treatment for Exp.1 and Exp.2 respectively where the QTL were found. WD and SS are the stress treatment for water deficit and salinity. When interactives QTL are identified in Exp.1 (respectively Exp.2) treatment CxWD (respectively (CxSS) are the corresponding treatment designed.

Supplemental Table 2 | Functional annotation of CG retained after the filtering procedure according to allelic parental effect. Only QTL that presented <40 CG were screened. For each QTL, the chromosome and localization (position in pb) were precised. The type of polymorphisms, depending if it is a single nucleotide polymorphism (snp) or insertion deletion (indel) were in the column "Type." The number of snp or indel at a given gene is marked in brackets () when more than one polymorphism affected a given gene. The impact of polymorphisms affecting a gene were defined as MODIFIER when snp or indel are located in upstream or downstream region; MODERATE and LOW when polymorphisms had respectively non-synonymous or synonymous variant effect and HIGH when they affect splice site variant or start/stop codon. The putative function of each CG was checked on the annotation database of the tomato genome assembly (SL2.50).

REFERENCES

Albert, E., Gricourt, J., Bertin, N., Bonnefoi, J., Pateyron, S., Tamby, J. P., et al. (2016a). Genotype by watering regime interaction in cultivated tomato: lessons from linkage mapping and gene expression. *Theor. Appl. Genet.* 129, 395–418. doi: 10.1007/s00122-015-2635-5

Albert, E., Segura, V., Gricourt, J., Bonnefoi, J., Derivot, L., and Causse, M. (2016b). Association mapping reveals the genetic architecture of tomato response to water deficit: focus on major fruit quality traits. *J. Exp. Bot.* 67, 6413–6430. doi: 10.1093/jxb/erw411

Bandillo, N., Raghavan, C., Muyco, P. A., Sevilla, M. A., Lobina, I. T., Dilla-Ermita, C. J., et al. (2013). Multi-parent Advanced Generation Inter-Cross (MAGIC) populations in rice: progress and potential for genetics research and breeding. *Rice* 6:11. doi: 10.1186/1939-8433-6-11

Caro, M., Cruz, V., Cuartero, J., Estañ, M. T., and Bolarin, M. C. (1991). Salinity tolerance of normal-fruited and cherry tomato cultivars. *Plant Soil* 136, 249–255.

Causse, M., Desplat, N., Pascual, L., Le Paslier, M. C., Sauvage, C., Bauchet, G., et al. (2013). Whole genome resequencing in tomato reveals variation associated with introgression and breeding events. *BMC Genomics* 14:791. doi: 10.1186/1471-2164-14-791

Causse, M., Saliba-Colombani, V., Lesschaeve, I., and Buret, M. (2001). Genetic analysis of organoleptic quality in fresh market tomato. 2. Mapping QTLs for sensory attributes. *Theor. Appl. Genet.* 102, 273–283. doi: 10.1007/s001220051644

Chaves, M. M., Maroco, J. P., and Pereira, J. S. (2003). Understanding plant responses to drought - from genes to the whole plant. *Funct. Plant Biol.* 30, 239–264. doi: 10.1071/FP02076

Dai, A. (2011). Drought under global warming: a review. *Wiley Interdiscipl. Rev. Clim. Change* 2, 45–65. doi: 10.1002/wcc.81

de Oliveira, A. B., Alencar, N. L. M., and Gomes-Filho. G. (2013). "Comparison between the water and salt stress effects on plant growth and development," in *Responses of Organisms to Water Stress*, ed S. Akinci (InTech Publisher), 67–94. doi: 10.5772/54223

Du, T., Kang, S., Zhang, J., Li, F., and Yan, B. (2008). Water use efficiency and fruit quality of table grape under alternate partial root-zone drip irrigation. *Agric. Water Manage.* 95, 659–668. doi: 10.1016/j.agwat.2008.01.017

Eduardo, I., Pacheco, I., Chietera, G., Bassi, D., Pozzi, C., Vecchietti, A., et al. (2011). QTL analysis of fruit quality traits in two peach intraspecific populations and importance of maturity date pleiotropic effect. *Tree Genet. Genomes* 7, 323–335. doi: 10.1007/s11295-010-0334-6

El-Soda, M., Malosetti, M., Zwaan, B. J., Koornneef, M., and Aarts, M. G. M. (2014). Genotype X environment interaction QTL mapping in plants: lessons from arabidopsis. *Trends Plant Sci.* 19, 390–398. doi: 10.1016/j.tplants.2014.01.001

Farooq, M., Hussain, M., Wahid, A., and Siddique, K. H. M. (2012). "Drought stress in plants: an overview," in *Plant Responses to Drought Stress*, Vol. 1 (Heidelberg; New York, NY; Dordrecht; London, UK: Springer), 1–33.

Frary, A., Nesbitt, T. C., Grandillo, S., Knaap, E., Cong, B., Liu, J., et al. (2000). fw2.2: a quantitative trait locus key to the evolution of tomato fruit size. *Science* 289, 85–88. doi: 10.1126/science.289.5476.85

Gardner, K. A., Wittern, L. M., and Mackay, I. J. (2016). A highly recombined, high-density, eight-founder wheat MAGIC map reveals extensive segregation distortion and genomic locations of introgression segments. *Plant Biotechnol. J.* 14, 1406–1417. doi: 10.1111/pbi.12504

Gutteling, E. W., Riksen, J. A., Bakker, J., and Kammenga, J. E. (2007). Mapping phenotypic plasticity and genotype-environment interactions affecting life-history traits in caenorhabditis elegans. *Heredity* 98, 28–37. doi: 10.1038/sj.hdy.6800894

Huang, B. E., and George, A. W. (2011). R/mpMap: a computational platform for the genetic analysis of multiparent recombinant inbred lines. *Bioinformatics* 27, 727–729. doi: 10.1093/bioinformatics/btq719

Huang, B. E., George, A. W., Forrest, K. L., Kilian, A., Hayden, M. J., Morell, M. K., et al. (2012). A multiparent advanced generation inter-cross population for genetic analysis in wheat. *Plant Biotechnol. J.* 10, 826–839. doi: 10.1111/j.1467-7652.2012.00702.x

Huang, B. E., Verbyla, K. L., Verbyla, A. P., Raghavan, C., Singh, V. K., Gaur, P., et al. (2015). MAGIC populations in crops: current status and future prospects. *Theor. Appl. Genet.* 128, 999–1017. doi: 10.1007/s00122-015-2506-0

Huang, Y., Tang, R., Cao, Q., and Bie, Z. (2009). Improving the fruit yield and quality of cucumber by grafting onto the salt tolerant rootstock under NaCl stress. *Sci. Hortic.* 122, 26–31. doi: 10.1016/j.scienta.2009.04.004

Kenis, K., Keulemans, J., and Davey, M. W. (2008). Identification and stability of QTLs for fruit quality traits in apple. *Tree Genet. Genomes* 4, 647–661. doi: 10.1007/s11295-008-0140-6

Kover, P. X., Valdar, W., Trakalo, J., Scarcelli, N., Ehrenreich, I. M., Purugganan, M. D., et al. (2009). A multiparent advanced generation inter-cross to fine-map quantitative traits in *Arabidopsis thaliana*. *PLoS Genet.* 5:e1000551. doi: 10.1371/journal.pgen.1000551

Liu, J., Van Eck, J., Cong, B., and Tanksley, S. D. (2002). A new class of regulatory genes underlying the cause of pear-shaped tomato fruit. *Proc. Natl. Acad. Sci. U.S.A.* 99, 13302–13306. doi: 10.1073/pnas.162485999.c

Maas, E. V., and Hoffman, G. J. (1977). Crop salt tolerance - current assesment. *J. Irrigat. Drain. Divis.* 103, 115–134.

Marais, D. L. D., Hernandez, K. M., and Juenger, T. E. (2013). Genotype-by-environment interaction and plasticity: exploring genomic responses of plants to the abiotic environment. *Annu. Rev. Ecol. Evol. Syst.* 44, 5–29. doi: 10.1146/annurev-ecolsys-110512-135806

Milner, S. G., Maccaferri, M., Huang, B. E., Mantovani, P., Massi, A., Frascaroli, E., et al. (2016). A multiparental cross population for mapping QTL for Agronomic Traits in durum wheat (*Triticum turgidum* ssp. durum). *Plant Biotechnol. J.* 14, 735–748. doi: 10.1111/pbi.12424

Mitchell, J. P., Shennan, C., and Grattan, S. R. (1991). Developmental-changes in tomato fruit composition in response to water deficit and salinity. *Physiol. Plant.* 83, 177–185.

Monforte, A. J., Oliver, M., Gonzalo, M. J., Alvarez, J. M., and Dolcet-Sanjuan, R. (2004). Identification of quantitative trait loci involved in fruit quality traits in melon (*Cucumis melo* L.). *Theor. Appl. Genet.* 108, 750–758. doi: 10.1007/s00122-003-1483-x

Munns, R., and Tester, M. (2008). Mechanisms of salinity tolerance. *Annu. Rev. Plant Biol.* 59, 651–681. doi: 10.1146/annurev.arplant.59.032607.092911

Muños, S., Ranc, N., Botton, E., Bérard, A., Rolland, S., Duffé, P., et al. (2011). Increase in tomato locule number is controlled by two single-nucleotide polymorphisms located near WUSCHEL. *Plant Physiol.* 156, 2244–2254. doi: 10.1104/pp.111.173997

Navarro, J. M., Flores, P., Carvajal, M., and Martinez, V. (2005). Changes in quality and yield of tomato fruit with ammonium, bicarbonate and calcium fertilisation under saline conditions. *J. Hortic. Sci. Biotechnol.* 80, 351–357. doi: 10.1080/14620316.2005.11511943

Pascual, L., Albert, E., Sauvage, C., Duangjit, J., Bouchet, J.-P., Bitton, F., et al. (2016). Plant science dissecting quantitative trait variation in the resequencing era : complementarity of bi-parental, multi-parental and association panels. *Plant Sci.* 242, 120–130. doi: 10.1016/j.plantsci.2015.06.017

Pascual, L., Desplat, N., Huang, B. E., Desgroux, A., Bruguier, L., Bouchet, J. P., et al. (2015). Potential of a tomato MAGIC population to decipher the genetic control of quantitative traits and detect causal variants in the resequencing era. *Plant Biotechnol. J.* 13, 565–577. doi: 10.1111/pbi.12282

Ripoll, J., Urban, L., and Bertin, N. (2016). The potential of the MAGIC TOM parental accessions to explore the genetic variability in tomato acclimation to repeated cycles of water deficit and recovery. *Front. Plant Sci.* 6:1172. doi: 10.3389/fpls.2015.01172

Ripoll, J., Urban, L., Staudt, M., Lopez-Lauri, F., Bidel, L. P., and Bertin, N. (2014). Water shortage and quality of fleshy fruits—making the most of the unavoidable. *J. Exp. Bot.* 65, 4097–4117. doi: 10.1093/jxb/eru197

Scholberg, J. M. S., and Locascio, S. J. (1999). Growth response of snap bean and tomato as affected by salinity and irrigation method. *HortScience* 34, 259–264.

Shewfelt, R. L. (1999). What is quality? *Postharvest Biol. Technol.* 15, 197–200.

Shrivastava, P., and Kumar, R. (2015). Soil salinity: a serious environmental issue and plant growth promoting bacteria as one of the tools for its alleviation. *Saudi J. Biol. Sci.* 22, 123–131. doi: 10.1016/j.sjbs.2014.12.001

Tétard-Jones, C., Kertesz, M. A., and Preziosi, R. F. (2011). Quantitative trait loci mapping of phenotypic plasticity and genotype–environment interactions in plant and insect performance. *Philos. Trans. R. Soc. Lond. B Biol. Sci.* 366, 1368–1379. doi: 10.1098/rstb.2010.0356

Threadgill, D. W., Hunter, K. W., and Williams, R. W. (2002). Genetic dissection of complex and quantitative traits: from fantasy to reality via a community effort. *Mamm. Genome* 13, 175–178. doi: 10.1007/s00335-001-4001-y

Tomato Genome Consortium (2012). The tomato genome sequence provides insights into fleshy fruit evolution. *Nature* 485, 635–641. doi: 10.1038/nature11119.

Ungerer, M. C., Halldorsdottir, S. S., Purugganan, M. D., and Mackay, T. F. C. (2003). Genotype-environment interactions at quantitative trait loci affecting inflorescence development in *Arabidopsis thaliana*. *Genetics* 165, 353–365.

Verbyla, A. P., Cavanagh, C. R., and Verbyla, K. L. (2014). Whole-genome analysis of multienvironment or multitrait QTL in MAGIC. *G3* 4, 1569–1584. doi: 10.1534/g3.114.012971

Via, S., Gomulkiewicz, R., De Jong, G., Scheiner, S. M., Schlichting, C. D., and Van Tienderen, P. H. (1995). Adaptive phenotypic plasticity: consensus and controversy. *Trends Ecol Evol.* 10, 212–217.

Villalta, I., Bernet, G. P., Carbonell, E. A., and Asins, M. J. (2007). Comparative QTL analysis of salinity tolerance in terms of fruit yield using two solanum populations of F7 lines. *Theor. Appl. Genet.* 114, 1001–1017. doi: 10.1007/s00122-006-0494-9

Yu, J., Holland, J. B., McMullen, M. D., and Buckler, E. S. (2008). Genetic design and statistical power of nested association mapping in maize. *Genetics* 178, 539–551. doi: 10.1534/genetics.107.074245

Zhu, J. K. (2002). Salt and drought stress signal transduction in plants. *Annu. Rev. Plant Biol.* 53, 247–273. doi: 10.1146/annurev.arplant.53.091401.143329

Conflict of Interest Statement: The authors declare that the research was conducted in the absence of any commercial or financial relationships that could be construed as a potential conflict of interest.

CHAPTER 4

Tomato transcriptome analysis reveals genotype and organ-specific variation under water-deficit stress

Isidore Diouf [a], Elise Albert [a,d], Renaud Duboscq [a], Sylvain Santoni [b], Fréderique Bitton [a], Justine Gricourt [a], Mathilde Causse [a]*

[a] INRA, UR1052, Génétique et Amélioration des Fruits et Légumes, 67 Allée des Chênes, Centre de Recherche PACA, Domaine Saint Maurice, CS60094, Montfavet, 84143, France

[b] NRA, UMR1334, Amélioration génétique et Adaptation des Plantes, Montpellier SupAgro-INRA-IRD-UMII, 2 Place Pierre Viala, Montpellier 34060, France

[c] INRA, UMR1095, Génétique Diversité et Ecophysiologie des Céréales, 5 Chemin de Beaulieu, Clermont-Ferrand 63039, France

[d] present address: Biochemistry & Molecular Biology Department, Michigan State University, 603 Wilson Road East, Lansing, MI, 48823, USA.

In Preparation

Abstract (200 words)

Water deficit (WD) affects tomato growth and fruit quality inducing significant morphological changes. Understanding the molecular mechanisms underlying such phenotypic changes is crucial to develop cultivars with high WD tolerance. Transcriptome response to WD was investigated through RNA sequencing of fruit and leaf on eight genotypes grown in two irrigation conditions, in order to get insight into the complex genetic regulation of drought-response in tomato. Genotype differences in WD response were firstly noticed at the phenotypic level for fruit composition and plant development traits. A total of 14,065 differentially expressed genes under WD were detected among which 7,393 (53%) and 11,059 (79%) were genotype and organ specific, respectively. Water deficit impact on the transcriptome variation was much higher in leaf than in fruit pericarp at the cell expansion stage. A stronger effect of the genetic background, than the WD effect was detected on the transcript abundance, along with the presence of a set of genes showing significant genotype-by-environment interaction. Integrating the DEG with previously identified stress response QTLs allowed us to narrow candidate gene lists within the regions of these QTLs. The results presented outlined valuable resources for further study intended to decipher the complexity of tomato adaptation to WD.

Keywords: RNA sequencing, water deficit stress, Transcriptome, Genotype-by-environment interaction

INTRODUCTION

Drought is among the most common abiotic stress affecting plant growth and crop yield; and more frequent episodes of drought are expected to arise with the climate change (Wang, 2005). Extensive research has been dedicated to understand the mechanisms driving plant adaptation to drought (Chaves et al., 2003). In crops, agricultural water deficit (WD) stress can be defined as a period of plant exposure to dry soil subsequently resulting to reduced crop production and plant growth (Dai, 2011). The morphological changes triggered by WD – encompassing yield decrease – are inherent to the process of plant acclimation through physiological and molecular regulation. Indeed, WD disrupts cellular homeostasis eliciting signaling cascades and the regulation of several physiological processes (Farooq et al., 2012). Plant hormone imbalance following mild to severe WD is associated to changes in gene expression and molecular regulation of different stress responsive genes. For instance, several genes showing susceptibility to WD condition have been characterized in *Arabidopsis thaliana*, which is considered as a model in plant genetics (Bray, 2002). In the same way, the expression level of hundreds of genes is modified under WD as shown in several other plant species (Albert et al., 2018; Ma et al., 2017; Opitz et al., 2016; Zhang et al., 2016).

Cultivated crops usually show high sensitivity to WD, especially when it occurs during the reproductive stage (Daryanto et al., 2017). However, the degree of sensitivity to WD can vary widely between cultivars/genotypes within a species. In tomato, extensive genotype-by-environment interaction (GxE) has been observed in different experimental populations (Albert et al., 2016; Alian et al., 2000; Diouf et al., 2018; Foolad et al., 2003; Sánchez-Rodríguez et al., 2010). These authors showed that phenotypic response to WD significantly differed according to genotypes. The development of drought-adapted crop varieties is a major goal given the expanding drought area regions (Korres et al., 2016). A global understanding of the complex interplay between genetic and environmental factors in tomato adaptation to WD is therefore a key aim, and should help for breeding purposes.

Genetic determinants of plant response to WD have been studied in several species towards this goal. Genotype-phenotype association under WD condition yielded several quantitative trait loci (QTL) affecting plant response to WD across crop species (Gupta et al., 2017; Swamy et al., 2017; Wang et al., 2018), which ultimately pave the way for marker-assisted selection for drought tolerance. In tomato, WD-responsive QTLs have been identified using agronomic traits as well as eco-physiological modelling parameters (Albert et al., 2016; Constantinescu et al., 2016; Diouf et al., 2018). However, the genomic regions covered by the QTL governing WD response usually include many genes, frequently leading to failure to identify the causal genes. Nowadays, the availability of

high-throughput sequencing technologies allows more and more to bridge this gap through the analysis of gene expression regulation.

A significant number of gene expression studies have been reported during the last decades, highlighting the effect of gene expression level on phenotypic variation (Boyes et al., 2001; Liu et al., 2018; Ta et al., 2017). Besides, the changes in the gene expression level could importantly vary under different environmental conditions as well as according to the genetic background (Garg et al., 2016; Lenka et al., 2011; Sarazin et al., 2017). A promising and reliable approach to identify stress-tolerance genes and elucidate clearly the molecular mechanisms and biological pathways involved in abiotic stress adaptation lie therefore in the analysis of transcriptome variation at both genotype and environmental condition levels. There have been few studies depicting the transcriptome variation under WD in tomato and most of them included only one or two genotypes usually characterized as WD-tolerant/susceptible (Iovieno et al., 2016; Lee et al., 2018; Zhang et al., 2019). A recent study however characterized DEG under WD in a large and small tomato fruit accessions and their F1 hybrid, highlighting the presence of GxE at gene expression level and identified interactive expression-QTLs (Albert et al., 2018).

We aimed to assess genotype (G), environment (E) and GxE interaction under fully irrigated and WD conditions at the transcriptome level in eight tomato lines. The genotypes used in this study were the eight parental lines of the MAGIC population firstly presented by Pascual et al., (2015); which display a large genetic variability. Moreover Ripoll et al., (2016a), highlighted different responses to WD for the eight parental MAGIC lines at fruit and leaf level, suggesting genotype-specific adaptive strategies. The eight lines and the MAGIC population were already characterized at phenotypic level for agronomic and physiological response to WD and QTL mapped (Diouf et al., 2018). Differential expression analysis allowed us to identify tomato genes significantly affected by WD in young leaves and fruit pericarp tissue. Genes showing different expression level and a significant GxE interaction were highlighted and examined for their co-location under previously identified WD-response QTLs.

MATERIALS AND METHODS

Plant material

The plant material was constituted by the eight tomato lines used to generate the MAGIC population presented in Pascual et al., (2015). The eight genotypes belong to different genetic groups with four genotypes (Cervil, Criollo, PlovdivXIVa and LA1420) from the *Solanum lycopersicum cerasiforme* group (SLC) and the four others (Levovil, Stupicke Polni Rane, Ferum and LA0147) from the *Solanum*

lycopersicum lycopersicum group (SLL). The experimental design and plant growth conditions are described in details in in Albert et al., (2018). Briefly, the eight lines were grown in the spring-summer 2015 under greenhouse in Avignon under control and water-deficit (WD) conditions. Each plant was replicated at least twice in the greenhouse. The control condition consisted in full irrigation treatment according to evapotranspiration (ETP) while in WD condition; the amount of irrigation was reduced by 40% according to the control. Phenotypic measurements were carried out for different traits related to fruit composition and plant development (**Supplemental Table 1**).

Statistical analyses of phenotypic data

To test for WD effect at phenotypic level, a two-way analysis of variance was performed for each phenotypic trait separately. The level and significance of GxE was assessed through ANOVA analysis with the following model: $y_{ij} = G_i + E_j + GxE_{ij} + \varepsilon_{ijk}$. In this model y_{ij} represents the phenotype of genotype i (G_i) and in environment j (E_j). The environments were constituted by the two watering regime (irrigated and WD). The GxE_{ij} and ε_{ijk} are the genotype-by-environment interaction effect and residual errors, respectively.

RNA extraction

For each genotype total RNA was collected from the young leaves and fruit pericarp (at least five fruits) at the cell expansion stage. Given the differences in their phenological stage, SLC and SLL accessions were sampled for fruit pericarp at 14 days after anthesis (DAA) and 21 DAA, respectively. The samples were immediately frozen after collection then pooled per genotype, organ and condition with two to three biological replicates. Messenger RNA (mRNA) was extracted using the Spectrum Plant Total RNA kit and assessed on Nanodrop 1000 for each replicate. A total of 72 paired-end strand specific libraries were generated from 1µg of the total RNA and sequencing was performed on Hiseq 3000 at the GenoTool platform (INRA Toulouse). Detailed information about the RNA extraction protocol and read sequencing processing are described in Albert et al., (2018). To prevent confounding technical effect for the differential expression analysis, the biological replicates in both conditions were disposed in the same lane for each genotype.

Differential gene-expression analysis

Differential expression (DE) analysis was performed with the Bioconductor R-package *DESeq2 1.14.1* (Love et al., 2014). The impact of WD on transcriptome variation was evaluated for each genotype and for fruit and leaf samples separately. The DE analysis was conducted only on genes with at least 20 read counts, encompassing 23,552 and 22,864 genes for leaf and fruit samples, respectively. To

identify differentially expressed genes (DEG), DESeq2 applied a negative binomial test on the expression level, after normalization process through the estimation of sample size factors across samples. The DE analysis model was constructed by adding an interaction grouping factor such that genotype-specific condition effect could be tested by defining individual contrasts. Thereafter, DEG under WD were selected by setting a threshold p-value of 0.05 after multiple-testing correction with Benjamin and Hochberg method (Benjamini and Hochberg, 1995).

Two-way ANOVA of transcript level variation

Analyses of variance were performed using the normalized pseudo-counts on the gene set used for the DE analysis. For each gene, a fixed two-way ANOVA with interaction was applied and the analyses were conducted for each organ separately. The model used was similar to the one for phenotypic traits with the only difference being that y_{ij} represents this time the transcript abundance of genotype (i) in environment (j) for each single gene included in the analysis. To account for the multiple-testing, adjusted p-value was set to the cut-off of 0.05 to consider significance of any factor. For each organ, the proportion of the sum of square attributed to genotype (G), environment (E) and GxE factors was retrieved and used to estimate the relative contribution of each factor to gene expression variation.

Gene ontology enrichment analysis

Gene ontology (GO) enrichment analysis was performed using the R-Bioconductor package *goseq* (version 1.36.0) (Young et al., 2010). Enriched GO terms were investigated for the set of DEG in fruit and leaf separately. Significant GO terms for biological process (BP) and molecular function (MF) were selected after multiple testing correction by setting a FDR threshold at 5% cutoff with the Benjamin and Hochberg method (Benjamini and Hochberg, 1995). The SL2.50 version of the reference genome 'Heinz' was used and correction for length bias has been carried out with the *nullp* function before GO enrichment testing.

Co-localization of tomato WD-response QTLs and the DEG

A previous study identified stress-response QTLs in the MAGIC population generated from the eight genotypes used in the present study (Diouf et al., 2018). The authors assessed phenotypic plasticity for different plant and fruit related traits by considering the difference between the trait values in stress *vs* control treatments. Stress treatments consisted of WD (-50% of irrigation) and salinity stress (SS: average substrate electro-conductivity of about 6.78 dSm^{-1}). Fourteen QTLs were identified on fruit related plasticity traits. The respective genomic regions of these plasticity QTLs were confronted

to the fruit-DEG identified across the eight parental lines in order to know which DEG under WD were collocated with the reported QTLs. The comparison was made possible using the physical positions of the tomato reference genome (version SL2.50). Correlations between the expression level and allelic effect at the QTL were assessed.

RESULTS

Phenotypic response to WD

Phenotypic traits related to fruit composition and plant development were measured on the eight tomato lines grown under the same greenhouse in control and WD conditions. Considering the average response across genotypes, the dry matter weight (DMW) and fruit-weight (fw) were the most affected traits with +21.4% and -20.7% of variation induced by WD, respectively (**Figure 1**). All the genotypes were negatively affected under WD for fw and diameter while fruit DMW increased in every genotype. However, a large variability was observed among genotypes in their response to WD at the phenotype level. Ferum for instance showed the higher susceptibility to WD compared to the other genotypes for most of the traits (**Supplemental Figure 1**). This strong variability laid to significant genotypic effect for all traits revealed by the ANOVA analysis (**Supplemental Table 2**). The WD treatment significantly affected every trait except flowering time, Glucose, pH and SSC. GxE interaction was only significant for four traits (plant height, stem diameter, fruit weight and glucose content). Thus for flowering time, pH and SSC, only the genotype effect was significant.

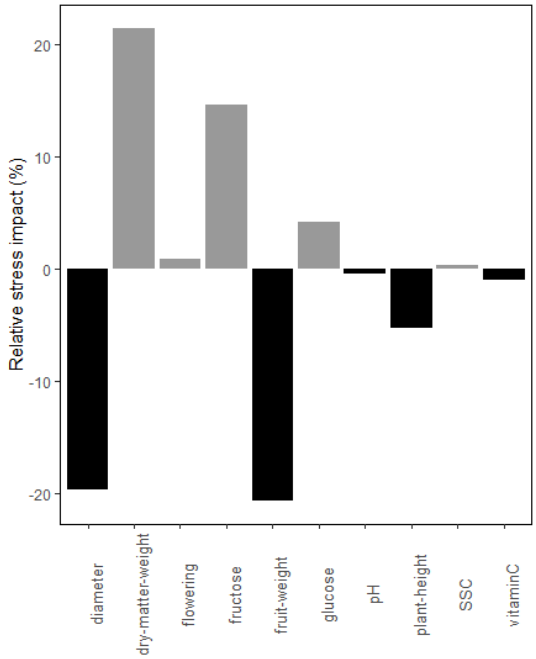

Figure 1: Average impact of WD at phenotypic level across the eight genotypes. The bar plots indicate for each trait the proportion by which WD decreased/increased its average value (across the eight genotypes) against the control.

Transcriptome variability across the eight genotypes

RNA-sequencing was carried out using young leaves and fruit pericarp tissue samples of the eight MAGIC parental lines grown under normal and WD irrigation conditions. Overall, the expression level of 34,718 tomato genes was available after the RNA-sequencing processing. Before analysis, low expressed genes were removed by filtering out all genes with less than 20 read counts across samples, leaving 23,552 (67.8%) and 22,864 (65.8%) genes for leaf and fruit samples, respectively. The total read counts of the remaining set of genes was variable across genotypes and conditions (**Supplemental Figure 2**). Hence, specific sample size factors were computed through the *estimateSizeFactors* function implemented in DESeq2 package, and used for scaling the library size. Gene expression level was highly correlated between repetitions for all the genotype highlighting a good repeatability across biological replicates (**Supplemental Table 3**). Principal component analysis (PCA) on the normalized read counts showed a clear clustering of the samples according to genotypes and conditions (**Figure 2**). Normalized counts were transformed with the regularized log (rlog) transformation. The first two axes of the PCA explained about 51% of the gene expression level variation in fruit and leaf samples. For both organs, variability in the transcript levels according to genotypes was captured by both PC1 and PC2 axes. In addition, for leaf samples the PCA plot separated the conditions following the PC2 axis and Cervil and Levovil appeared as the most discriminant parents. In fruit, transcriptomic variation was highly specific for Cervil as observed on the PCA plot (**Figure 2**).

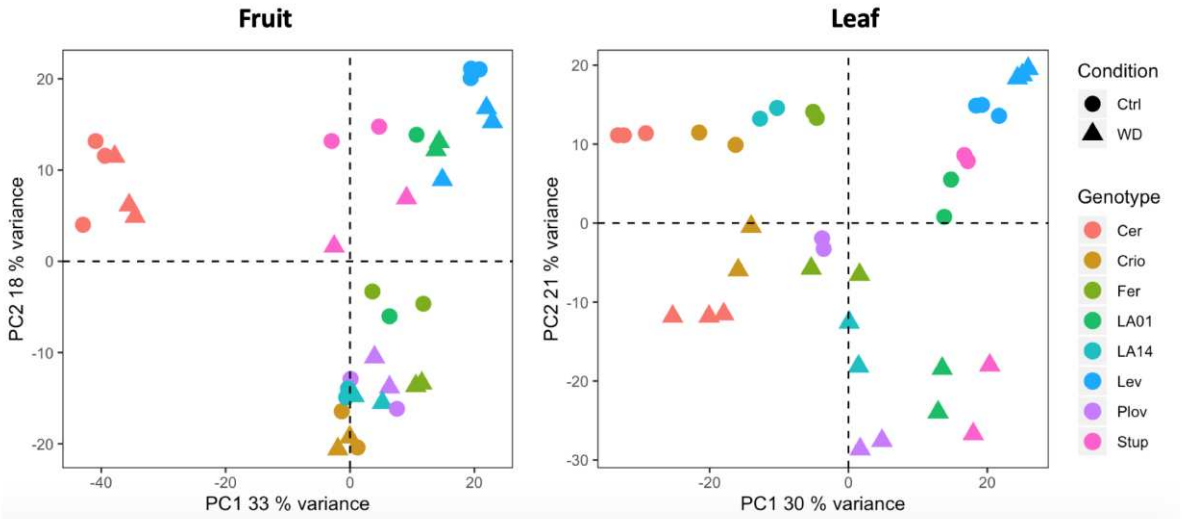

Figure 2: PCA plot of the normalized read counts in fruit and leaf samples.

DEG under WD condition

Considering the eight genotypes together, a total of 4,132 and 12,938 DEG between the two water conditions were identified in the DE analysis in fruit pericarp and young leaf, respectively (**Supplemental Table 4**). The number of DEG was variable among genotypes. In fruit, the number of DEG varied from 0 (Criollo) to 2,978 (Levovil) and in average, the SLL accessions showed a higher number of DEG than SLC genotypes (**Figure 3A**). Levovil and Ferum presented the highest number of DEG under WD, although, the proportion of up/down regulated genes differed. No DEG was detected at the fruit expansion stage for Criollo, which seemed to be the less susceptible genotype to WD. For leaf samples, the number of DEG was less discriminant between genotypes than in fruit. The total number of DEG on leaf varied from 2,240 (Ferum) to 6,177 (LA1420) and the proportion of up/down regulated genes was almost balanced.

We observed an important variability in the transcriptomic response between samples according to the organ. The effect of WD on gene expression variation was more important in leaf than in fruit (**Figure 3B**). Besides, most of the DEG in fruit and leaf were organ-specific. For example, depending on the genotypes, 45 to 82% of the DEG in fruit were not differentially expressed in leaf highlighting organ-specific regulation of gene expression under WD.

Consistent/Divergent patterns of transcriptome regulation (up/down)

A small set of genes has been identified as DEG in both organs (**Figure 3B**), representing 0-13% of the total DEG according to the genotype. For most of the genotypes, the pattern of gene expression regulation was different between leaf and fruit. For instance, for the genotypes with more than 100 consistent DEG between fruit and leaf – notably Cervil, Levovil and Ferum, the proportion of the genes up-regulated in one organ (leaf or fruit) and down-regulated in the other was non negligible representing 47, 44 and 79%, respectively (**Supplemental Figure 3**).

ANOVA of transcript level

A two-way analysis of variance (ANOVA) was performed using the log2 transformation values of normalized transcript level to test the effect of genotype, environment (irrigation condition) and their interaction (GxE) on the regulation of gene expression level. This analysis revealed a total of 16,392 and 19,450 genes that were affected by at least one of the above-mentioned factors in fruit and leaf, respectively. A high proportion of the genes tested showed a significant genotype effect highlighting an important effect of the genetic background on gene expression regulation among the eight lines (**Figure 4**). A much smaller number of genes were specifically affected by WD or the GxE

interaction. For each gene showing a significant effect of the genotype, condition or GxE, the contribution of each factor to the variability was further visualized by computing the proportion of the sum of square attributed to each factor (**Supplemental Figure 4**).

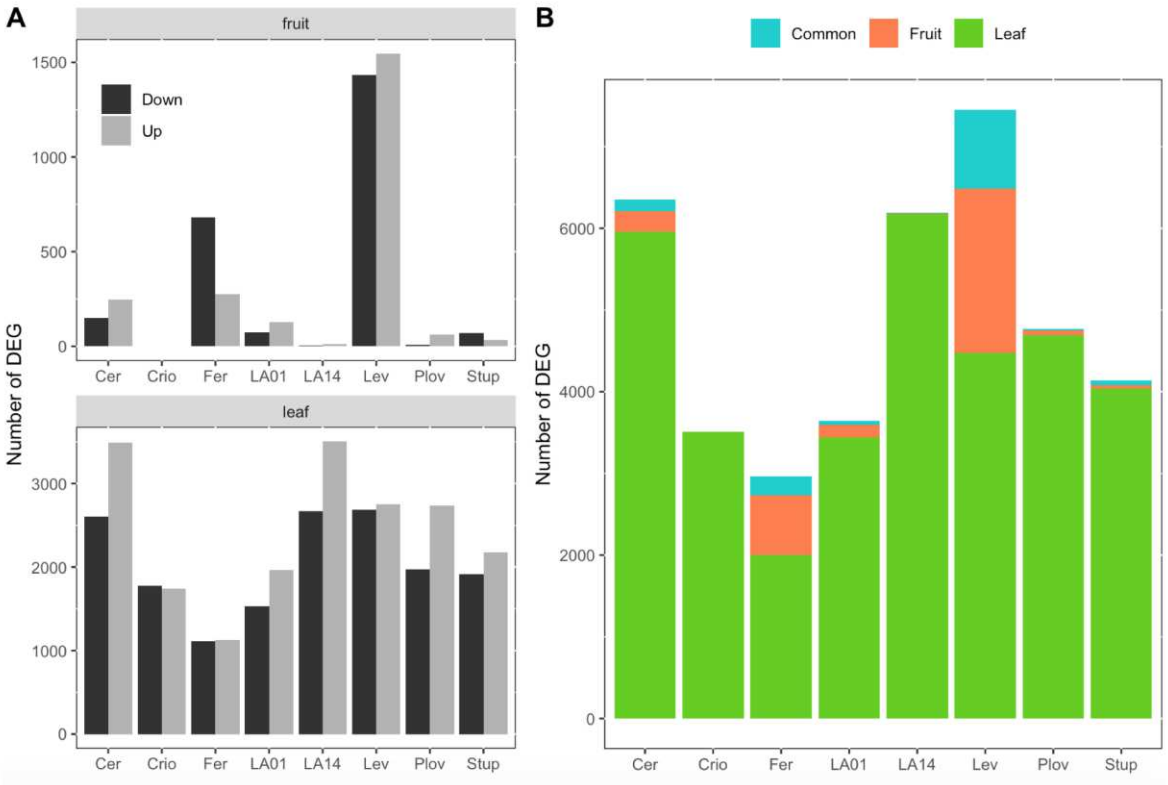

Figure 3: Representation of the number of DEG per genotype. A) Number of DEG under WD in fruit (top) and leaf (down) that were down/up regulated. B) Proportion of DEG that were detected in both organs (blue) and organ specific.

Gene ontology enrichment analysis

GO enrichment analysis was conducted on a set of 3,794 (92% of the total fruit DEG) and 11,804 (92% of the total leaf DEG) DEG in fruit and leaf, respectively; yielding a total of 24 significantly enriched GO categories (**Table 1**). Gene ontology terms associated to 'cell redox homeostasis', 'metabolic process', 'microtubule-based movement' and 'protein phosphorylation' were significantly over-represented regarding the biological process within the DEG in leaf. With reference to the molecular function, three GO terms related to 'chlorophyll binding', 'structural constituent of ribosome' and 'metabolic process' were enriched considering the DEG in fruit and leaf together.

DEG co-location with previously identified WD-responsive QTLs

Combination of gene expression and QTL information was used to identify candidate genes under the plasticity QTLs identified in the MAGIC population. To illustrate the approach, we focused on the 14 QTLs detected in Diouf et al. (2018) which can be considered as WD and SS response QTLs.

Table 1: Enriched gene ontology (GO) terms within the differentially expressed genes under WD in fruit and leaf organs.

Regulation	GO category	Number in DEG	Number in gene space	Ontology	Corrected-pavlue	Description
A) Fruit						
down	GO:0003677	62	558	MF	0.010431148	DNA binding
down	GO:0003735	40	172	MF	3.77E-09	structural constituent of ribosome
down	GO:0005509	24	134	MF	0.004390055	calcium ion binding
down	GO:0005515	210	2233	MF	0.009968992	protein binding
up	GO:0008152	71	609	BP	0.044143524	metabolic process
up	GO:0016168	13	20	MF	2.61E-10	chlorophyll binding
B) Leaf						
down	GO:0003735	117	172	MF	2.98E-42	structural constituent of ribosome
down	GO:0007018	25	45	BP	0.002609063	microtubule-based movement
down	GO:0008017	19	32	MF	0.007931586	microtubule binding
down	GO:0008574	6	6	MF	0.046276125	ATP-dependent microtubule motor activity, plus-end-directed
down	GO:0009922	15	26	MF	0.001886462	fatty acid elongase activity
down	GO:0032183	21	32	MF	1.91E-05	SUMO binding
down	GO:0042802	85	245	MF	0.002057093	identical protein binding
down	GO:0051082	26	55	MF	0.003031927	unfolded protein binding
up	GO:0003700	183	725	MF	0.002891116	DNA-binding transcription factor activity
up	GO:0004364	20	52	MF	0.028991913	glutathione transferase activity
up	GO:0006468	128	430	BP	3.74E-05	protein phosphorylation
up	GO:0008152	161	609	BP	0.002201227	metabolic process
up	GO:0045454	27	75	BP	0.017828078	cell redox homeostasis
up-down	GO:0003735	23	172	MF	0.019020979	structural constituent of ribosome
up-down	GO:0004397	4	5	MF	0.019250117	histidine ammonia-lyase activity
up-down	GO:0016168	8	20	MF	0.003057246	chlorophyll binding
up-down	GO:0031683	5	8	MF	0.006592922	G-protein beta/gamma-subunit complex binding
up-down	GO:0045548	4	6	MF	0.04287232	phenylalanine ammonia-lyase activity

The selected QTLs were mapped on eight out of the 12 tomato chromosomes (**Figure 5**). The confidence interval regions of these QTLs encompassed hundreds of genes. However, the number of DEG within these regions varied from 18 to 104 genes reducing the set of potential candidates by 80-94% according to the QTL (**Figure 5B**). The number of DEG per Mbp was assessed for each of the eight chromosome carrying plasticity QTLs. Interestingly, the genomic regions covered by plasticity QTLs were significantly enriched with DEG for some chromosomes (**Figure 5C**).

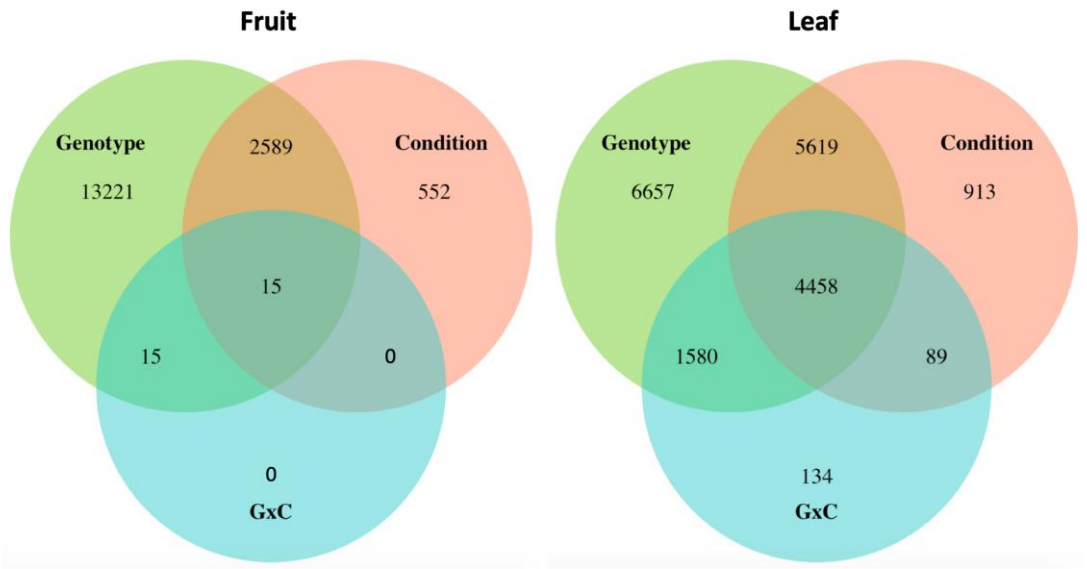

Figure 4: Venn diagram representing the number of genes whose expression level was significantly affected by the genotype, the environment (irrigation treatment) and the GxE interaction for fruit and leaf.

QTL detection using the parental haplotype probabilities in the MAGIC population allows estimation of the allelic effect for each parental line at every QTL position. Correlation analysis was further investigated between the allelic effect and expression level across the eight genotypes. A total of 40 genes – located in 11 plasticity QTLs, showed significant correlation reinforcing their potential implication in regulating fruit phenotype variation under WD (**Supplemental Table 6**). The whole process of the candidate gene selection is depicted for the QTL SSC1.1 as an example on **Figure 6**.

DISCUSSION

Phenotypic response to WD

Plant response to drought is a complex mechanism which ultimately results to morphological changes that can alter agronomic performance in crops. Such responses strongly rely on the genetic background, leading to the necessity of screening different genotypes/accessions. Genotype specificity has been depicted in tomato response to WD for different agronomic traits (Aghaie et al.,

2018; Patanè et al., 2016; Ripoll et al., 2016b) as supported here. The present study highlighted a strong genotype-dependent variation under WD at both phenotype and transcriptome level.

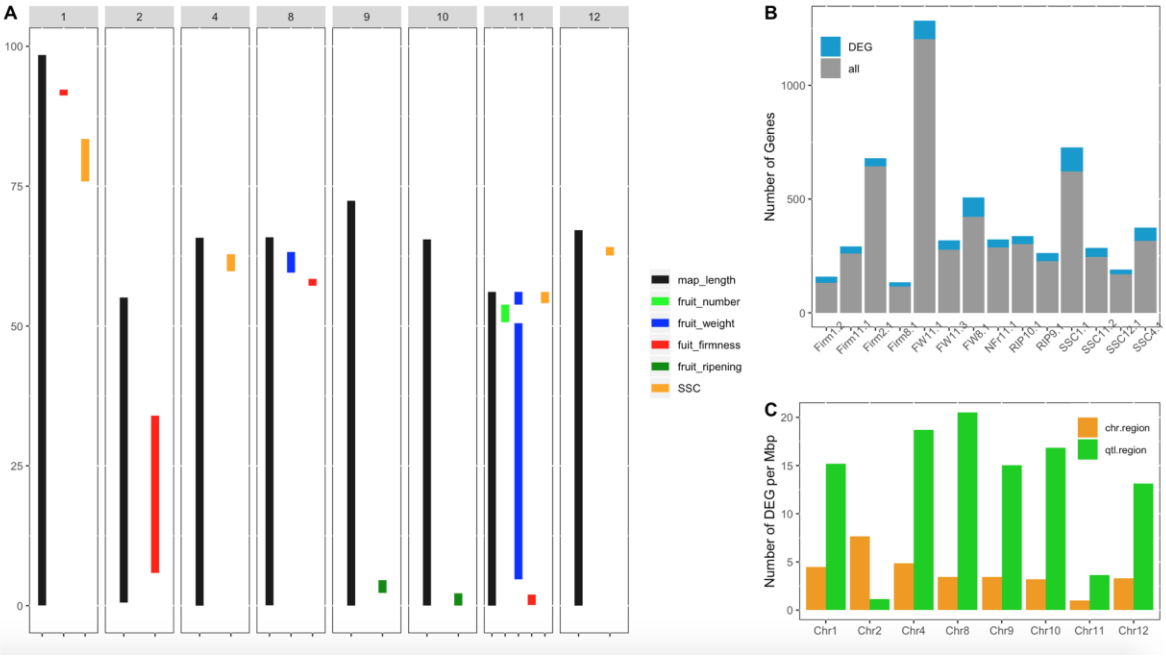

Figure 5: Candidate gene screening for tomato plasticity QTLs. **A)** Position in Mbp of Water deficit and salinity stress plasticity QTLs identified in the MAGIC population in Diouf et al., (2018). Black bars represent the chromosome length and colored bar represent confidence interval regions of the plasticity QTLs according to the phenotypic traits. **B)** Plot the number of genes within the whole CI region of the QTL (in gray) and the number of genes showing significant differential expression under water deficit (in blue). **C)** Represent the number of DEG per Mbp within the whole chromosome (in orange) and within the regions covered by plasticity QTLs per chromosome (in green).

The WD treatment induced a significant variability in the transcriptome across the eight genotypes. The RNA-sequencing design was constructed so that every biological replicates for a given genotype in both conditions were on the same lane, in order to remove potential technical effects. All the differences in the read counts for any genotype can therefore be attributed solely to the water irrigation condition. A total of 14,065 DEG under WD were detected among which 7,393 (53%) were genotype specific. Cervil and Levovil presented the most divergent pattern of gene expression variation at fruit level (**Figure 2**) which was consistent with the phenotypic variation since these two genotypes also presented the smallest and largest fruit weight, representing in average 6.1g and 119g, respectively. Furthermore, these two genotypes were also identified as highly divergent at the whole genome level when comparing their polymorphism sequences against the reference genome (Causse et al., 2013). Moreover, a bi-parental population generated from these two lines yielded significant discovery of genetic loci controlling trait variation in tomato (Causse et al., 2001; Albert et al, 2016; 2018).

Organ and tissue sampling can significantly alter the gene expression profile in plants (Aceituno et al., 2008; Matas et al., 2011; Van Veen et al., 2016). Besides, organ-specific transcript level might be exacerbated by the presence of stress factors occurring especially at a specific growth stage. The WD treatment in our study was applied from the 1st inflorescence appearance until the end of the cropping. Fruit sampling was elaborated to limit differences that might arise from growth stages between the SLL (sampled at 21 DAA) and SLC (sampled at 14 DAA) accessions. The low number of fruit DEG in SLC accessions could have been linked to the sampling strategy we adopted. However, this hypothesis is not supported by the low number of fruit DEG observed for LA0147 and Stupicke which are both SLL accessions.

The process of plant adaptation to drought usually starts with cellular sensing and signaling which activates downstream drought-responsive genes (Farooq et al., 2012). Activation of signaling pathway under WD at the early vegetative growth is hence expected to lead to better adaptation. This may explain the high number of DEG on young leaf organ. Ripoll et al., (2016a) have shown a higher WD impact on leaf than at the fruit level and outlined a prevalence of osmotic adjustment and photosynthetic adaptation in tomato response to WD. The source-sink relationship is highly altered under WD stress condition in tomato (Albacete et al., 2014), which could eventually reflect different transcriptome response.

Comparative analysis of the whole transcriptome variation under WD has been conducted in several species; however most of the time only two genotypes are included (usually tolerant *vs* sensitive genotype). These classical designs are very powerful to detect DEG involved in specific stress response. Yet, the few studies which assessed the impact of a specific stress and the genetic background simultaneously, revealed significant effect of the genotype and GxE (Albert et al., 2018; Van Veen et al., 2016). The eight MAGIC parental lines were selected within a panel of 360 tomato accessions to represent the diversity observed within the cultivated tomato. Our results provide evidence of a strong genotype effect at the transcriptome level, independent of the growing condition. Expression QTL analysis in the MAGIC population should then yield significant results that could help to get more insight into the molecular mechanisms shaping tomato variation.

Integrating QTL information and gene expression variation is a common strategy for candidate gene screening (Lin et al., 2019). This strategy yielded significant results in MAGIC populations in Maize (Septiani et al., 2019) and Cotton (Naoumkina et al., 2019), where the parental haplotypes were besides exploited to drastically narrow the potential candidate genes. We propose a strategy combining DEG and plasticity QTL to identify candidate genes affecting WD and or salinity stress response in tomato. The whole approach depicted in **Figure 6** highlighted 40 CG which showed expression variability in the eight parental MAGIC lines under WD condition. Two interesting CG were indeed identified in the region of SSC1.1 QTL among which Solyc01g074030, a gene coding for Beta-

glucosidase. In the literature, members of the β-glucosidase genes family have been described playing a role in response to drought (Wang et al., 2011) and salinity (Ngara et al., 2012). Regarding the allelic effect of SSC1.1 QTL, salinity stress increased SSC value in all parents except Cervil with the highest effect noticed for Ferum. A total of eight polymorphisms (4 SNPs and 4 INDELs) were identified for Solyc01g074030 among which one INDEL located up-stream the gene region at the position 81,350,515 bp, was discriminant between Ferum (the reference allele) vs all the other parents. A subsequent SNP polymorphism at position 81,363,697 bp also discriminated the parents with Cervil carrying the reference allele against all the other lines. The allelic variants of these polymorphisms are in accordance with the pattern of the gene expression and allelic effects across the eight parental lines. Further studies are however necessary to test the potential implication of these alleles in tomato fruit response to WD.

Similarly, other interesting candidates were identified. For instance, RIP10.1 is a QTL detected on fruit ripening plasticity under WD condition which carried a total of 228 genes within its CI region among which only 34 genes (15%) showed significant differential expression level in fruit pericarp. Some of these last genes presented significant correlation between the plasticity of their expression level under WD and the allelic effect of the QTL across the eight parental lines encompassing Solyc10g006130 annotated as 'Ethylene responsive transcription factor (ERF) 3a' and Solyc10g006650 which is a 'Flavoprotein wrbA'. In tomato, ERF have been described as being involved in fruit maturation process and also as drought inducible transcription factors (Cara and Giovannoni, 2008; Pan et al., 2012). Thus, Solyc10g006130 represents an interesting candidate for studying the interaction between drought and fruit maturation in tomato. Solyc10g006650 also constitute a good candidate; the role of flavoprotein on tolerance to osmotic stress has been depicted in Arabidopsis (Espinosa-Ruiz et al., 1999).

Conclusion

Understanding plant adaptation to drought requires the collection and integration of a great deal of information from phenotypic to omic (transcriptome, metabolome, proteome) responses, to apprehend the complex drought response mechanisms. The investigation of GxE at the transcriptome level has the potential to target interesting candidates for genetical genomic analyses. Collecting and gathering omics data from different organs, tissues, genotypes and conditions is the key step for omics-breeding in the coming years which will certainly help in developing climate resilient crops. The results presented here are then valuable resources for the tomato community for further studies intended to decipher drought response mechanisms.

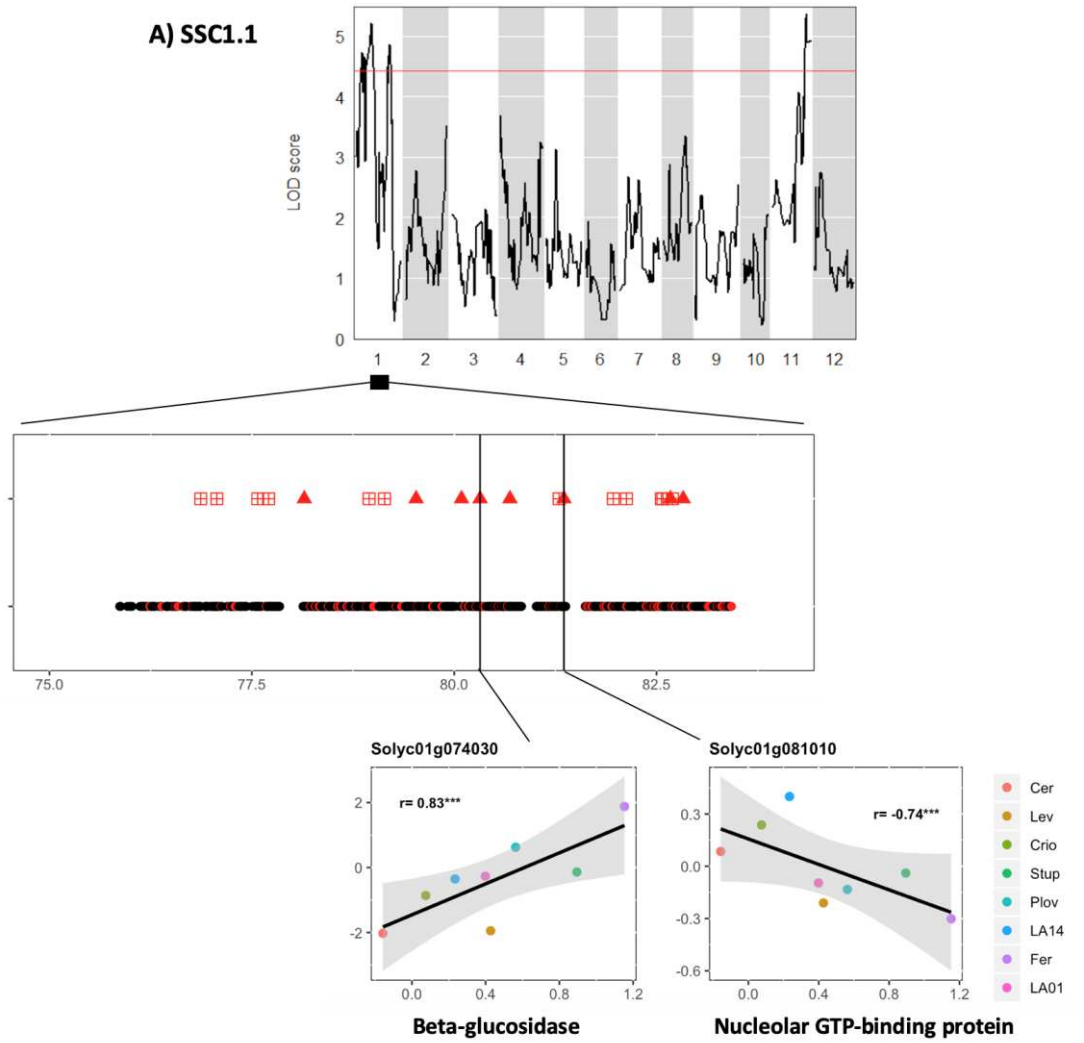

Figure 6: Candidate gene selection for the WD-responsive fruit ripening QTL (SSC1.1) detected in Diouf et al. (2018). **A)** The genome LOD score for QTL detected for soluble sugar content (SSC) response to WD in the MAGIC population. **B)** Genes within the SSC1.1 QTL with all the genes showing differential expression under WD in red color. The DEG showing significant correlation between expression level and the estimated allelic effect for the eight genotypes at the QTL position are squared when the correlation was significant for the expression level in the control or drought condition and in triangles when the correlation related to the delta expression level (expression level in WD – expression level in control). **C)** Correlation between the estimated allelic effect at the QTL and differential expression level for three candidate genes with their functional annotation.

References

Aceituno, F.F., Moseyko, N., Rhee, S.Y., and Gutiérrez, R.A. (2008) The rules of gene expression in plants: Organ identity and gene body methylation are key factors for regulation of gene expression in Arabidopsis thaliana. *BMC Genomics*. 9: 438.

Aghaie, P., Hosseini Tafreshi, S.A., Ebrahimi, M.A., and Haerinasab, M. (2018) Tolerance evaluation and clustering of fourteen tomato cultivars grown under mild and severe drought conditions. *Sci Hortic (Amsterdam)*. 232: 1–12.

Albacete, A.A., Martínez-Andújar, C., and Pérez-Alfocea, F. (2014) Hormonal and metabolic regulation of source–sink relations under salinity and drought: From plant survival to crop yield stability. *Biotechnol Adv*. 32: 12–30.

Albert, E., Duboscq, R., Latreille, M., Santoni, S., Beukers, M., Bouchet, J.-P., et al. (2018) Allele specific expression and genetic determinants of transcriptomic variations in response to mild water deficit in tomato. *Plant J*.

Albert, E., Segura, V., Gricourt, J., Bonnefoi, J., Derivot, L., and Causse, M. (2016) Association mapping reveals the genetic architecture of tomato response to water deficit: focus on major fruit quality traits. *J Exp Bot*. 67: 6413–6430.

Alian, A., Altman, A., and Heuer, B. (2000) Genotypic difference in salinity and water stress tolerance of fresh market tomato cultivars. *Plant Sci*. 152: 59–65.

Benjamini, Y., and Hochberg, Y. (1995) Controlling the False Discovery Rate: A Practical and Powerful Approach to Multiple Testing. *J R Stat Soc Ser B*. 57: 289–300.

Boyes, D.C., Zayed, A.M., Ascenzi, R., McCaskill, A.J., Hoffman, N.E., Davis, K.R., et al. (2001) Growth Stage–Based Phenotypic Analysis of Arabidopsis. *Plant Cell*. 13: 1499–1510.

Bray, E.A. (2002) Classification of Genes Differentially Expressed during Water-deficit Stress in Arabidopsis thaliana: an Analysis using Microarray and Differential Expression Data. *Ann Bot*. 89: 803–811.

Cara, B., and Giovannoni, J.J. (2008) Molecular biology of ethylene during tomato fruit development and maturation. *Plant Sci*. 175: 106–113.

Causse, M., Desplat, N., Pascual, L., Le Paslier, M.-C., Sauvage, C., Bauchet, G., et al. (2013) Whole genome resequencing in tomato reveals variation associated with introgression and breeding events. *BMC Genomics*. 14: 791.

Causse, M., Saliba-Colombani, V., Lesschaeve, I., and Buret, M. (2001) Genetic analysis of organoleptic quality in fresh market tomato. 2. Mapping QTLs for sensory attributes. *TAG Theor Appl Genet*. 102: 273–283.

Chaves, M.M., Maroco, J.P., and Pereira, J.S. (2003) Understanding plant responses to drought - From genes to the whole plant. *Funct Plant Biol*. 30: 239–264.

Constantinescu, D., Memmah, M.-M., Vercambre, G., Génard, M., Baldazzi, V., Causse, M., et al. (2016) Model-Assisted Estimation of the Genetic Variability in Physiological Parameters Related to Tomato Fruit Growth under Contrasted Water Conditions. *Front Plant Sci*. 7: 1841.

Dai, A. (2011) Drought under global warming: A review. *Wiley Interdiscip Rev Clim Chang*. 2: 45–65.

Daryanto, S., Wang, L., and Jacinthe, P.-A. (2017) Global synthesis of drought effects on cereal, legume, tuber and root crops production: A review. *Agric Water Manag*. 179: 18–33.

Diouf, Isidore A., Derivot, L., Bitton, F., Pascual, L., and Causse, M. (2018) Water Deficit and Salinity Stress Reveal Many Specific QTL for Plant Growth and Fruit Quality Traits in Tomato. *Front Plant Sci*. 9: 279.

Diouf, I.A., Derivot, L., Bitton, F., Pascual, L., and Causse, M. (2018) Water deficit and salinity stress reveal many specific QTL for plant growth and fruit quality traits in tomato. *Front Plant Sci*. 9.

Espinosa-Ruiz, A., Belles, J.M., Serrano, R., and Culianez-Macia, F.A. (1999) Arabidopsis thaliana AtHAL3: a

flavoprotein related to salt and osmotic tolerance and plant growth. *Plant J*. 20: 529–539.

Farooq, M., Hussain, M., Wahid, A., and Siddique, K.H.M. (2012) Plant Responses to Drought Stress.

Foolad, M.R., Zhang, L.P., and Subbiah, P. (2003) Genetics of drought tolerance during seed germination in tomato: inheritance and QTL mapping. *Genome*. 46: 536–545.

Garg, R., Shankar, R., Thakkar, B., Kudapa, H., Krishnamurthy, L., Mantri, N., et al. (2016) Transcriptome analyses reveal genotype- and developmental stage-specific molecular responses to drought and salinity stresses in chickpea. *Sci Rep*. 6: 19228.

Gupta, P., Balyan, H., and Gahlaut, V. (2017) QTL Analysis for Drought Tolerance in Wheat: Present Status and Future Possibilities. *Agronomy*. 7: 5.

Iovieno, P., Punzo, P., Guida, G., Mistretta, C., Van Oosten, M.J., Nurcato, R., et al. (2016) Transcriptomic Changes Drive Physiological Responses to Progressive Drought Stress and Rehydration in Tomato. *Front Plant Sci*. 7: 371.

Korres, N.E., Norsworthy, J.K., Tehranchian, P., Gitsopoulos, T.K., Loka, D.A., Oosterhuis, D.M., et al. (2016) Cultivars to face climate change effects on crops and weeds: a review. *Agron Sustain Dev*. 36: 12.

Lee, J., Shim, D., Moon, S., Kim, H., Bae, W., Kim, K., et al. (2018) Genome-wide transcriptomic analysis of BR-deficient Micro-Tom reveals correlations between drought stress tolerance and brassinosteroid signaling in tomato. *Plant Physiol Biochem*. 127: 553–560.

Lenka, S.K., Katiyar, A., Chinnusamy, V., and Bansal, K.C. (2011) Comparative analysis of drought-responsive transcriptome in Indica rice genotypes with contrasting drought tolerance. *Plant Biotechnol J*. 9: 315–327.

Lin, F., Zhou, L., He, B., Zhang, X., Dai, H., Qian, Y., et al. (2019) QTL mapping for maize starch content and candidate gene prediction combined with co-expression network analysis. *Theor Appl Genet*.

Liu, H., Wang, J., Li, C., Qiao, L., Wang, X., Li, J., et al. (2018) Phenotype characterisation and analysis of expression patterns of genes related mainly to carbohydrate metabolism and sporopollenin in male-sterile anthers induced by high temperature in wheat (Triticum aestivum). *Crop Pasture Sci*. 69: 469.

Love, M.I., Huber, W., and Anders, S. (2014) Moderated estimation of fold change and dispersion for RNA-seq data with DESeq2. *Genome Biol*. 15: 550.

Ma, J., Li, R., Wang, H., Li, D., Wang, X., Zhang, Y., et al. (2017) Transcriptomics Analyses Reveal Wheat Responses to Drought Stress during Reproductive Stages under Field Conditions. *Front Plant Sci*. 8: 592.

Matas, A.J., Yeats, T.H., Buda, G.J., Zheng, Y., Chatterjee, S., Tohge, T., et al. (2011) Tissue- and cell-type specific transcriptome profiling of expanding tomato fruit provides insights into metabolic and regulatory specialization and cuticle formation. *Plant Cell*. 23: 3893–910.

Naoumkina, M., Thyssen, G.N., Fang, D.D., Jenkins, J.N., McCarty, J.C., and Florane, C.B. (2019) Genetic and transcriptomic dissection of the fiber length trait from a cotton (Gossypium hirsutum L.) MAGIC population. *BMC Genomics*. 20: 1–14.

Ngara, R., Ndimba, R., Borch-Jensen, J., Jensen, O.N., and Ndimba, B. (2012) Identification and profiling of salinity stress-responsive proteins in Sorghum bicolor seedlings. *J Proteomics*. 75: 4139–4150.

Opitz, N., Marcon, C., Paschold, A., Malik, W.A., Lithio, A., Brandt, R., et al. (2016) Extensive tissue-specific transcriptomic plasticity in maize primary roots upon water deficit. *J Exp Bot*. 67: 1095–1107.

Pan, Y., Seymour, G.B., Lu, C., Hu, Z., Chen, X., and Chen, G. (2012) An ethylene response factor (ERF5) promoting adaptation to drought and salt tolerance in tomato. *Plant Cell Rep*. 31: 349–360.

Pascual, L., Desplat, N., Huang, B.E., Desgroux, A., Bruguier, L., Bouchet, J.-P.P., et al. (2015) Potential of a tomato MAGIC population to decipher the genetic control of quantitative traits and detect causal variants in the resequencing era. *Plant Biotechnol J*. 13: 565–577.

Patanè, C., Scordia, D., Testa, G., and Cosentino, S.L. (2016) Physiological screening for drought tolerance in Mediterranean long-storage tomato. *Plant Sci*. 249: 25–34.

Ripoll, J., Urban, L., and Bertin, N. (2016a) The Potential of the MAGIC TOM Parental Accessions to Explore the Genetic Variability in Tomato Acclimation to Repeated Cycles of Water Deficit and Recovery. *Front Plant Sci*. 6: 1–15.

Ripoll, J., Urban, L., Brunel, B., and Bertin, N. (2016b) Water deficit effects on tomato quality depend on fruit developmental stage and genotype. *J Plant Physiol*. 190: 26–35.

Sánchez-Rodríguez, E., Rubio-Wilhelmi, M., Cervilla, L.M., Blasco, B., Rios, J.J., Rosales, M.A., et al. (2010) Genotypic differences in some physiological parameters symptomatic for oxidative stress under moderate drought in tomato plants. *Plant Sci*. 178: 30–40.

Sarazin, V., Duclercq, J., Guillot, X., Sangwan, B., and Sangwan, R.S. (2017) Water-stressed sunflower transcriptome analysis revealed important molecular markers involved in drought stress response and tolerance. *Environ Exp Bot*. 142: 45–53.

Septiani, P., Lanubile, A., Stagnati, L., Busconi, M., Nelissen, H., Pè, M.E., et al. (2019) Unravelling the genetic basis of fusarium seedling rot resistance in the MAGIC maize population: Novel targets for breeding. *Sci Rep*. 9: 4–13.

Swamy, B.P.M., Shamsudin, N.A.A., Rahman, S.N.A., Mauleon, R., Ratnam, W., Sta. Cruz, M.T., et al. (2017) Association Mapping of Yield and Yield-related Traits Under Reproductive Stage Drought Stress in Rice (Oryza sativa L.). *Rice*. 10: 21.

Ta, K.N., Adam, H., Staedler, Y.M., Schönenberger, J., Harrop, T., Tregear, J., et al. (2017) Differences in meristem size and expression of branching genes are associated with variation in panicle phenotype in wild and domesticated African rice. *Evodevo*. 8: 2.

Van Veen, H., Vashisht, D., Akman, M., Girke, T., Mustroph, A., Reinen, E., et al. (2016) Transcriptomes of eight Arabidopsis thaliana accessions reveal core conserved, genotype- and organ-specific responses to flooding stress. *Plant Physiol*. 172: 668–689.

Wang, G. (2005) Agricultural drought in a future climate: results from 15 global climate models participating in the IPCC 4th assessment. *Clim Dyn*. 25: 739–753.

Wang, H., Zhao, S., Mao, K., Dong, Q., Liang, B., Li, C., et al. (2018) Mapping QTLs for water-use efficiency reveals the potential candidate genes involved in regulating the trait in apple under drought stress. *BMC Plant Biol*. 18: 136.

Wang, P., Liu, H., Hua, H., Wang, L., and Song, C.-P. (2011) A vacuole localized β-glucosidase contributes to drought tolerance in Arabidopsis. *Chinese Sci Bull*. 56: 3538–3546.

Young, M.D., Wakefield, M.J., Smyth, G.K., and Oshlack, A. (2010) Gene ontology analysis for RNA-seq: accounting for selection bias. *Genome Biol*. 11: R14.

Zhang, Z.-F., Li, Y.-Y., and Xiao, B.-Z. (2016) Comparative transcriptome analysis highlights the crucial roles of photosynthetic system in drought stress adaptation in upland rice. *Sci Rep*. 6: 19349.

Zhang, Z., Cao, B., Li, N., Chen, Z., and Xu, K. (2019) Comparative transcriptome analysis of the regulation of ABA signaling genes in different rootstock grafted tomato seedlings under drought stress. *Environ Exp Bot*. 166: 103814.

Supplementary Materials

The supplemental figures and tables of this chapter are presented in Appendix 4.

NB: Supplemental tables 3, 4 and 5 and the supplemental Data can be accessed online:

Supplemental Figure 1: Phenotypic variation under WD for each genotype. Phenotypic traits are represented on the x-axis while the y-axis represents the percentage of increase/decrease of the trait value under the WD condition. In grey and black are all traits affected positively and negatively by WD condition, respectively.

Supplemental Figure 2: Total number of read counts after RNA-sequencing processing for fruit (A) and leaf (B).

Supplemental Figure 3: Expression pattern of the consistent DEG in fruit and leaf. The DEG were classified as up-up when up-regulated in both organs, up-down when up regulated in one organ (leaf or fruit) while down-regulated in the other and down-down when down regulated in both organs.

Supplemental Figure 4: Proportion of the sum of square attributed to each factor (Genotype, Condition or GxC) in fruit and leaf samples through the ANOVA analysis on the normalized transcript level.

Supplemental Table 1: Phenotypic traits evaluated on the eight genotypes under normal irrigation and WD condition. The greenhouse experiment is described in details in Albert et al. (2018).

Supplemental Table 2: Results of the two-way interactive ANOVA analysis on the phenotypic traits. For each factor the associated sum of square and p-value of the test are highlighted. The *ns* p-values for the GxE factor stand for non-significant GxE.

Supplemental Table 3: Correlation between replicates within each genotype. Information regarding the samples names can be found in the **Supplemental Data.**

Supplemental Table 4 & 5: Differentially expressed genes under WD for each of the eight genotypes in fruit and leaf.

Supplemental Table 6: Candidate genes under the plasticity QTLs. The genes presented in this table are all the DEG in fruit under the QTLs regions which besides showed significant correlation between the estimated allelic effect of the QTL and the expression level in control, drought or the expression level plasticity (expression in drought – expression in control). The functional annotation of the genes was retrieved from the reference annotation of SL2.50 version.

Supplemental Data: The normalized read counts for fruit and leaf samples used to conduct the DE analysis.

CHAPTER 5

Genetic architecture of tomato response to heat stress

Estelle Bineau[1, 2, ǂ], Isidore Diouf[1, ǂ], Yolande Carretero[1], Frédérique Bitton[1], Mohamed Zouine[3], Mathilde Causse[1]*

ǂ ***These authors contributed equally***

[1] INRA, UR1052, Génétique et Amélioration des Fruits et Légumes, 67 Allée des Chênes, Centre de Recherche PACA, Domaine Saint Maurice, CS60094, Montfavet, 84143, France

[2] GAUTIER Semences, route d'Avignon, Eyragues, 13630, France

[3] INRA, UMR990 Génomique et Biotechnologie des Fruits, 24 Chemin de Borde Rouge, Castanet-Tolosan, CS 52627, F-31326, France

In Preparation

Abstract (216 words)

Tomato is a widely cultivated crop which can grow in different habitats including high temperature (HT) conditions. However, its reproduction is impaired above 30°C which can lead to significant yield reduction. We assessed the impact of HT-stress in tomato in two experimental populations composed of a multi-parental advanced generation intercross (MAGIC) population and a core-collection (CC) of small fruited tomato accessions. The populations were evaluated in optimal growth conditions and in hot conditions. Yield components, fruit quality and phenology traits were recorded in both populations. Statistical analyses revealed a significant impact of HT-stress condition at the phenotypic level which decreased yield component traits (< 21-35%) and accelerated flowering time for almost all genotypes (96-99%) in both populations. The MAGIC and CC populations were genotyped with SNPs markers and the QTL/association analyses identified 244 QTLs that were in majority (92%) population specific. Phenotypic plasticity in response to HT-stress was computed for each trait and allowed the identification of 70 plasticity QTLs across populations. A high proportion (80 and 91%) of the QTLs identified within population (MAGIC and CC, respectively) was plasticity or condition specific. The present study gave insight into the polygenic architecture and complexity of tomato response to heat stress. Heat-tolerant genotypes were identified, and heat response candidate genes proposed to be used for future studies.

Keywords: Tomato, heat stress, phenotypic plasticity, intraspecific population, QTL, GWAS.

INTRODUCTION

Crop production is nowadays challenged by several environmental constraints – heat stress in particular – hampering the yield potential of cultivated varieties (Wahid et al., 2007). Global climate changes are predicted to raise temperature in most parts of the world and adversely impact crop productivity (Zhao et al., 2017). The urge to maintain acceptable crop yield and productivity under fluctuating temperatures becomes a challenge in breeding programs for most crop species. Hence, several approaches were investigated to better understand the genetic and physiological mechanisms underpinning plant tolerance to high temperature (HT) stress and the ways to breed thermo-tolerant cultivars.

In plants, heat stress is usually declared when temperature rises above a threshold where disruptive effects on plant growth, development and/or homeostasis are perceptible. The upper temperature limit above which HT-stress have detrimental effects in plants is not only variable considering the species but also depends on developmental stages. Anthesis is the most susceptible period to HT-stress (Wahid et al., 2007; Fahad et al., 2019). High temperatures around anthesis generally lead to unsuccessful reproduction (Hall, 1992) and has a direct impact on yield reduction (Nadeem et al., 2018). Besides reproduction impairment, numerous consequences related to HT are documented in the literature. For instance, HT elicits morphological injuries in plants, usually expressed as reduced growth, improper development, leaf senescence and fruit abortion (Hasanuzzaman et al., 2013; Nadeem et al., 2018). The morphological injuries induced by HT generally results from plant responses involving the regulation activity of several heat-response-genes at the molecular level (Mittler et al., 2012).

The development of heat-tolerant varieties requires the identification of genes and/or quantitative trait loci (QTL) associated to heat tolerance (Jha et al., 2014). The genomic era facilitates the identification of single genes responding to variation in environmental condition including heat stress. Hundreds of genes responding to HT were thus pinpointed through transcriptomic analyses. Most of these genes are tightly linked to heat-shock transcription factors (HSFs) across species (Liu et al., 2012; Rienth et al., 2014; Waters et al., 2017). HSFs are considered as master regulators of heat response in plants and their functional mechanisms is well documented, opening an area for engineering thermo-tolerant crops through gene manipulation technologies (Fragkostefanakis et al., 2015; Maruyama et al., 2017). However, HSFs have a broad spectrum of functions and it is necessary to state their pleiotropic effect on stress tolerance with any breeding-trait performance before their suitable use.

Marker-assisted selection remains a promising approach to develop heat-tolerant varieties for quantitative traits and in countries where genetically modified crops are not easily accepted. It requires the identification of molecular markers tightly linked to thermo-tolerance genes/QTLs for the trait of interest. Numerous studies have been dedicated to the identification of heat-tolerant QTLs in several species (Lin et al., 2010; Frey et al., 2016; Bhusal et al., 2017; Shanmugavadivel et al., 2017; Xu et al., 2017a; Paul et al., 2018). Those studies used different indexes for the measurement of heat tolerance to conduct linkage mapping or association analysis including survival rates, growth recovery, physiological parameters or yield performance that remains more interesting in agronomic context. They underlie the complex polygenic nature of heat tolerance. Indeed, heat tolerance is generally viewed as plant's ability to maintain vital functions when exposed to HT; and for breeders, a heat tolerant variety would be considered as the one maintaining a stable or even higher yield and economic quality under HT conditions relatively to control conditions.

Tomato is a widely cultivated crop that can grow in different habitats, from low temperature areas to tropical zones. However its optimal temperature for growing is about 26°C based on crop simulation growth model (Boote et al., 2012). Above 30°C, impaired reproductive development could be observed and final productivity impacted. Xu et al., (2017b) highlighted that tomato reproduction under HT is impaired mainly due to male sterility, notably with higher style exertion and lower pollen viability. Wild relative species contain valuable genetic resources for abiotic stress tolerance and have been exploited for QTL mapping (Foolad, 2007; Driedonks et al., 2018). Yet, a few studies addressed the identification of QTL/association for heat tolerance in tomato (Grilli et al., 2007; Lin et al., 2010; Xu et al., 2017b). All these studies involved intra and inter-specific bi-parental populations. However new tomato experimental populations powerful in QTL mapping analyses are being more available (Rothan et al., 2019).

In this study, tomato tolerance to heat stress was screened in two panels for 11 phenotypic traits. The panels were constituted by an intraspecific 8-way multi-parental (MAGIC) population (Pascual et al., 2015) and a core-collection of unrelated individuals (CC) suitable to genome-wide association study (GWAS) (Albert et al., 2016). The phenotypic responses to HT-stress of the two panels were compared, along with the consequences of HT-stress at the genetic level within each panel. The study was designed to: (i) measure the impact of HT on different breeding traits and genetic materials; (ii): identify useful heat-response QTLs in both panels; (iii) propose heat-response candidate genes controlling tomato phenotypic plasticity.

MATERIALS & METHODS

Plant material & phenotyping

The plant material used in this study was constituted of two populations: an 8-way tomato multi-parental population (MAGIC) and a core-collection (CC) of small, cherry and admixed tomato accessions. The MAGIC population, derived from four large fruit and four small fruit accessions was developed as described in Pascual et al., (2015) and a subset of 265 MAGIC lines was used in the present study. The CC panel consisted of 139 diverse tomato accessions – including the four small fruit parents of the MAGIC population –as described in Albert et al., (2016). The tomato accessions in the CC panel included 108 genotypes from *S. lycopersicum* var *cerasiforme* (SLC), 10 genotypes from *S. pimpinellifolium* (SP) and 21 genotypes forming a mixture group between SLC, SP and S. *lycopersicum* var *lycopersicum*. The MAGIC and CC populations were evaluated in greenhouse the same greenhouse in Avignon (south of France) from March to July in 2017 and 2018, respectively. Each trial was conducted under optimal condition (timely-sown) and HT-stress condition (delayed-sowing). The sowing date for the HT condition was delayed of two months compared to the optimal condition later referred as control. One-month old young seedlings were transferred in the greenhouse in March for optimal condition (control) and in May for HT condition (Heat stress) for each trial. In both conditions, the eight parental MAGIC lines and the four MAGIC-F1 of the first generation were used as control lines and replicated twice. In average, the daily mean/maximal temperatures were of 21.2°C/28.8°C in MAGIC-control, 22.7°C/31°C in CC-control, 26.9°C/34.4°C in MAGIC-heat and 27.5°C/35.5°C in CC-heat stress conditions, respectively. The experimental design in the MAGIC trial was conducted such that one plant per MAGIC line was evaluated in the control condition and one third of the genotypes replicated twice in the HT-stress condition. In the CC trial, all genotypes were randomly duplicated. External genotypes were used as border lines in both trials.

The MAGIC and the CC populations were phenotyped for 11 traits including vegetative and growth traits, fruit quality, plant phenology and yield related traits. Stem diameter (diam) was measured with a digital caliper under the 4^{th} and the 5^{th} truss and for each single plant, two equatorial measurements were recorded. Leaf length (leaf) and plant height (height) were measured with a measuring ruler under the 4^{th} and the 5^{th} truss. Flowering time (flw) was recorded as number of days between the sowing date and the first flower appearance on the 5^{th} truss for the MAGIC and on trusses 4 to 6 for the CC. The number of flowers (nflw = total number of peduncles) and number of fruits (nfr = total number of viable fruits) were measured on the 4^{th} and 5^{th} trusses in the MAGIC population (4^{th} to 6^{th} trusses in the CC). Fruit set was derived as fset = 100*fruit number/number of flowers, with fruit and flower number calculated as the mean value across the different trusses. Ripe

fruits under the 3rd to 6th trusses were weekly harvested and 6 to 10 fruits were used to measure average fruit weight (fw), fruit color (col_a). Fruit color was measured with a Minolta colorimeter using the "a" (red/green) coordinate of the L*a*b* color space. The harvested fruits (on three harvests) were then pooled and crushed, and the juice was used to measure soluble solid content (SSC) with an electronic refractometer and fruit pH with a pH-meter.

Statistical analysis of phenotypic traits

Both populations were submitted to the same statistical analysis. All statistical analyses were performed using R (R Core Team, 2019). First, outliers were removed and skewed data (including fw, nfr and nflw in both populations) log-transformed to meet normality assumptions. A fixed effect analysis of variance was conducted on the subset of 265 MAGIC lines (resp. 139 CC accessions) evaluated in both conditions to test for genotype, condition, and their interaction (gxc) effects with the following model: $y_{ij} = \mu + g_i + c_j + gxc_{ij} + \varepsilon_{ij}$ where y is the trait value, g_i and c_j represent the genotype and condition effects, respectively, gxc_{ij} the genotype-condition interaction and ε_{ijk} the residual effect. Due to the absence of replicates in the control condition of the MAGIC trial, the interaction effect could not be tested for flw, diam, height and leaf. Average trait sensitivity to heat stress was evaluated by computing the relative stress impact (RSI) as: RSI = (mean HT-stress condition – mean control condition)/ (mean control condition). The RSI was computed for every trait, so that a negative RSI value indicates that HT-stress decreased in average the trait value in the population compared to optimal condition and vice-versa.

Broad-sense heritability (h^2) was computed for every trait in each condition separately by using the following linear mixed model: $yij = \mu + gi + \varepsilon ij$ where μ, gi and εij represent the intercept, the random genotype effect, and the random residual effect respectively. Then heritability was derived from the variance components of the model: $h^2 = \sigma^2_g / (\sigma^2_g + \sigma^2_e)$ where σ^2_g and σ^2_e are the genetic and residual variance respectively. Pearson's correlations between traits within a condition and between conditions for every trait were computed by using the mean phenotype values.

Phenotypic plasticity was used to measure the heat susceptibility of individual genotypes. For all MAGIC and CC lines tested in both conditions, plasticity was calculated as (HT-stress value – control value)/ (control value). Phenotypic plasticity was further used as a single trait to perform the QTL mapping and GWAS analyses.

QTL detection in MAGIC population

The use of MAGIC populations in QTL mapping studies has demonstrated its efficiency when the founder probabilities are taken into account. Here we used the recently released package R/qtl2

(Broman et al., 2019) suitable for QTL analysis in multi-parental populations. For every trait, the presence of a QTL was queried by using the mixed linear model option offered by the package that integrates information of relatedness between individuals in the model. The LOCO procedure was thus applied which allows leaving-one-chromosome-out in the kinship matrix when QTLs are screened for that chromosome specifically. The eight MAGIC parental lines were fully re-sequenced and generated a set of 4 million SNPs (Causse et al., 2013). The genetic map used for this purpose was developed by Pascual et al., (2015) and is composed of 1345 SNP markers highly discriminant between the eight parental lines. A 5% Bonferroni threshold was then established to attest for the significance of each QTL. This led to a cut-off LOD score value of 4.12. The phenotypes for the QTL mapping procedure consisted of the mean value per genotype and per condition or for plasticity traits.

GWAS analysis

The GWAS panel was genotyped using the SolCAP Infinium array described in Sim et al., (2012). Quality control was performed through different steps including setting the threshold for minor allele frequency (MAF) at 0.05, fixing the maximum percentage of missing data at 25% per accession and a missing call rate of 10% per marker. A subset of 6099 SNP markers remained after filtering. The *emma.kinship* package (Kang et al., 2008) was used to account for the population stratification by calculating a kinship matrix based on identity by state between the 6099 SNP. The population structure was estimated through a Principal Coordinate Analysis on the genotype matrix (**Supplemental Figure 1**). The coordinates of the accessions on the first three components are available in **Supplemental Table 1**.

The GWAS analysis was conducted using the multi-locus mixed model (MLMM) proposed by Segura et al., (2012). This step by step approach allows for an increased detection power by turning the successive associated markers into fixed effect cofactors, as well as decreasing the False Discovery Rate (FDR) by accounting for both population structure and stratification. Only cofactors displaying a raw P-value < 10^{-4} were kept as significant associated markers. The traits flw, nflw and nfr were first considered for each truss separately and GWAS analysis conducted on each of them, yielding a great number of associations. To avoid redundant information, we focused on a smaller set of associations for these traits by grouping the resulting associations for each condition and for plasticity so that overlapping associations found in the same condition but on different trusses were kept as a single QTL. For any significant association that was detected, the confidence interval (CI) around the pic position was built by calculating the markers pairwise LD for each chromosome with *plink* software. The CI around the significant associated marker was defined as the interval where r^2 was higher than 0.5 in a region of 2Mbp.

Candidate genes screening and comparison of QTLs between populations and

Heat-response candidate genes (CGs) were queried using all the QTLs identified for plasticity traits in both populations. The CI of the QTL in the CC panel was constrained so that most CI region did not exceed 2Mbp. Conversely, the CI in the MAGIC population were defined by decreasing the LOD-score of one unit on both sides of the pic position; additionally, when multiple peaks were detected on a given chromosome, the LOD-score was decreased by two units between peaks to define different QTLs. As a result, large CI could be found for the MAGIC population QTLs. In order to narrow down the set of potential causative genes for these QTLs, we looked for CG in light of the allelic effects estimated for the eight MAGIC parental lines, as described by Pascual et al., (2015).

In order to compare the QTLs found in both populations and look for the underlying candidate genes (CGs), the physical positions of the QTLs were compared using the SL2.50 version of the reference genome. A QTL was considered as being common to both populations when the CI of the QTLs overlapped in the same region.

RESULTS

Phenotypic diversity in the two panels and two temperature conditions

The 11 traits analyzed in the CC panel and in the MAGIC population, respectively showed a broad variability. In the MAGIC population, the phenotypic distribution went beyond parental values and in both directions except for fw. Indeed, all MAGIC lines that were evaluated in both conditions had fw larger than the smallest parent 'Cervil'. Histogram plots were commonly overlapping between conditions for almost all traits but leaf and flw in the MAGIC population, and fset and flw in the CC panel (**Supplemental Figure 2**). These traits were highly impacted by the temperature.

The broad-sense heritability (h^2) was computed for each condition and population separately. Both the MAGIC and the CC populations showed high variability in h^2 according to traits and conditions (**Figure 1**). The population affected h^2 more than the condition notably for fw. The highest h^2 was recorded for height and fw in the MAGIC and CC, respectively, regardless of the condition, highlighting that the traits contributing to the highest h^2 were conserved between populations.

Pearson's correlations were calculated among traits within a condition and for each trait between the two conditions (**Supplemental Table 2**). Results revealed significant correlations between traits in the same condition. For the control condition, the highest correlations were noticed for nfr and nflw that were positively correlated in the MAGIC (0.60) and the CC (0.95) populations. Compared to the

control condition, the HT-stress condition weakened the nfr-nflw correlation although the direction and significance of the correlation remained unchanged. The CC population also showed high correlation between flw and height (0.67) in control condition, meaning that the tallest the plant was, the later the flowers bloomed. This observation was identical in the MAGIC population where flw and height were significantly positively correlated (0.36). The significant correlations found in the CC population were mostly in the same direction as in the MAGIC population underlining consistencies between the different genetic resources regarding the phenotypic links between traits. The same traits evaluated in both conditions additionally showed in majority significant correlations, with correlation coefficients ranging from 0.2 (fset) to 0.60 (height) in the MAGIC and 0.32 (fset) to 0.86 (fw) in the CC populations.

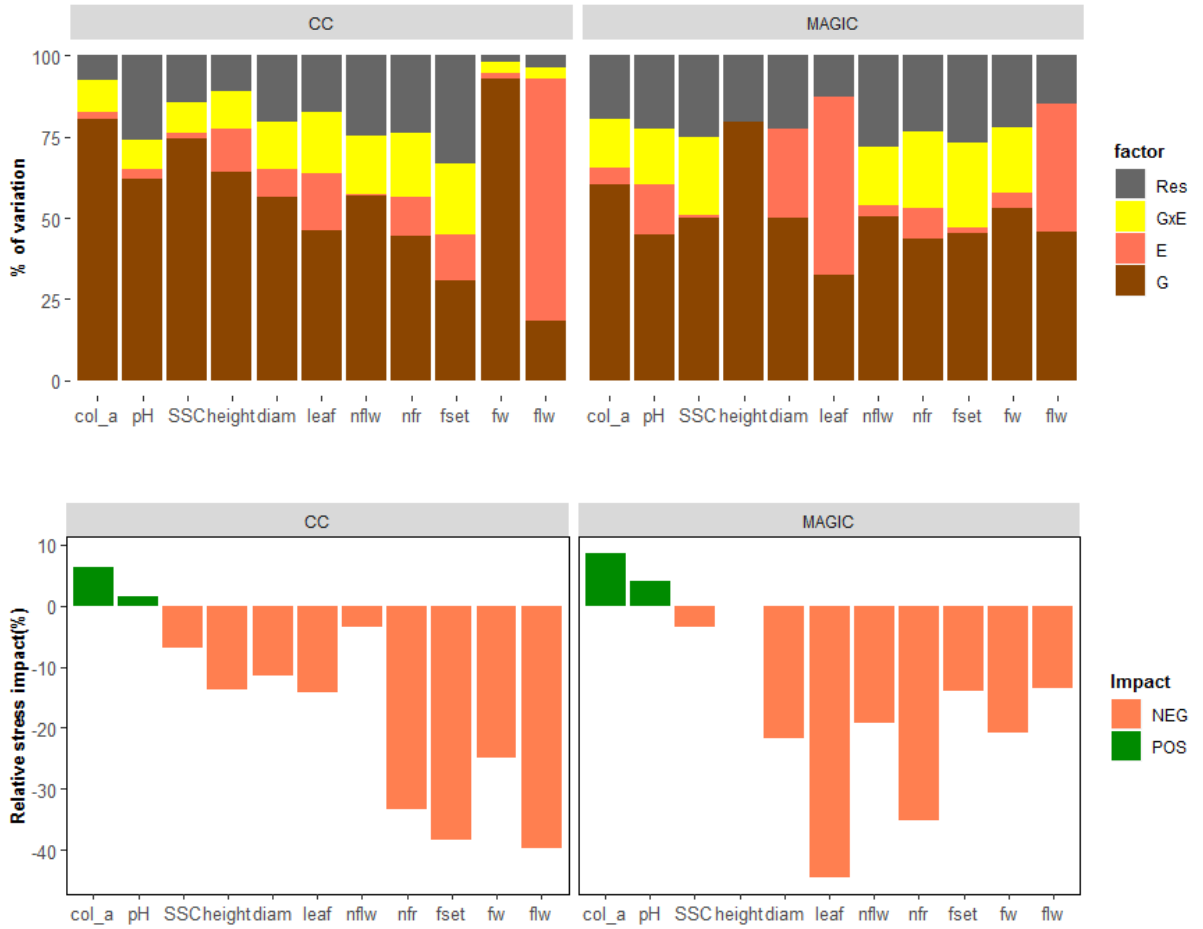

Figure 1: A) Proportion of the total sum of square (SSq) associated to genotype (G), condition (E), genotype-by-condition (GxE) interaction factors and to the residuals (Res) of the ANOVA. The broad-sense heritability of traits is indicated under the graph in the control and HT-stress condition. B) Impact of the HT-stress condition at the population level for all traits evaluated in the CC and MAGIC populations measured by the Relative Stress Impact (RSI). Traits that increased in average under HT-stress condition present a positive RSI and traits that were decreased in average present negative RSI.

Impact of the growth temperature

The analysis of variance was conducted for every trait in each population separately, to measure the contribution and significance of the genotype, condition and their interaction (gxc) effects in the total phenotypic variation. The genotype and condition effects were significant for every trait except for height in the MAGIC where only the genotype effect was significant. A large genetic variability was detected in both panels as the proportion of the sum of square attributed to genotype effects varied from 18-93% in the CC and 32-79% in the MAGIC population. Besides, the gxc interaction effect was significant for every trait but fw and pH in the CC. Given the absence of replicates in MAGIC-control, the gxc effect couldn't be evaluated for diam, flw, leaf and height; nonetheless significant interaction effects were found for all other traits. The proportion of the phenotypic variation attributed to the HT-stress and to the gxc interaction effect was most important for flw and leaf in both populations (**Figure 1**).

The general impact of HT-stress (due to two months delay in the sowing date, leading to plant growth exposed to hot months) was evaluated by calculating a relative-stress-impact index (RSI). In the CC and the MAGIC populations, all the traits were in average impacted in the same direction (**Figure 1**). The lowest average impact was found for height in the MAGIC population, which besides showed non-significant effect of HT-stress in the ANOVA analysis. The strongest impact of HT-stress at the population level was recorded for flw and leaf in the CC and MAGIC population, respectively. Indeed HT-stress decreased flw (-40%) in the CC and leaf (-45%) in the MAGIC population that were besides the traits with the highest proportion of the phenotypic variation explained by the condition effect from the ANOVA analysis. The negative effect of HT-stress on leaf and diam was more remarkable in the MAGIC population than in the CC. The yield related traits (fw and nfr) were affected by HT-stress in the CC and the MAGIC at a rather similar level. The col_a and pH traits were positively impacted in both populations; an increase in col_a value corresponding to more reddish fruit. When considering flowering time which is a heat-susceptible trait in many plant species, the results showed an acceleration of flw with flowering at the 5^{th} truss occurring 9 and 16 days earlier in average under the HT-stress condition, in the MAGIC and CC population, respectively.

Phenotypic plasticity

Individual response to the temperature was measured for each genotype by computing a phenotypic plasticity index. This allowed us to evaluate how much each genotype was impacted by the HT-stress condition. Although fw decreased in average in the MAGIC population, 25% of the MAGIC genotypes had a positive fw plasticity meaning that fw didn't decrease in stress condition for those genotypes. Among them, 17 genotypes showed interesting trend as HT-stress did not reduce the nfr either

(**Supplemental Table 3**). In the CC panel, 79% of the CC lines exhibited a lower fw under HT-stress and 21% (29 genotypes) were positively affected. Based on fw and nfr plasticity, a total of 24 genotypes (5% and 9% of the CC and MAGIC lines, respectively) were considered as heat-tolerant for yield component traits (under the 4^{th} – 6^{th} truss) across the populations. These heat-tolerant genotypes were besides negatively affected for growth traits under HT-stress condition and showed reduced leaf (-33%) and diam (-16%) (**Supplemental Table 3**).

Considering the plasticity of the genotypes across populations, flowering time was the most heat-responsive trait in both populations with 96% and 99% of all the MAGIC and CC genotypes flowering earlier in the HT-stress condition compared to the control condition, respectively. Irrespective of the population, the genotypes were then classified as 'early', 'medium' and 'late' responsive regarding their plasticity value for flw (**Supplemental Figure 3**). Among the 404 MAGIC and CC lines, 29% clustered in the 'early' group (plasticity of flw below -0.3) which flowered in average 18 days earlier in HT-stress condition compared to the control. The 'medium' group was the largest with 65% of the genotypes showing an average early flowering of eight days (plasticity of flw between -0.3 and 0). Only 3% of the genotypes (plasticity of flw above or equal to zero) were in the 'late' group with an average flowering occurring four days later than in the control condition. Comparing the populations, the majority of the CC lines (83%) clustered in the 'early' group and adversely, the MAGIC lines were in high proportion (95% of the MAGIC lines) assigned to the 'medium' group, highlighting population differences regarding flowering heat-susceptibility.

Flowering plasticity was significantly correlated to heat-response for all the growth traits and also with plasticity of pH, fset and col_a (**Figure 2**). Indeed 'early' genotypes showed less susceptibility to HT-stress for diam an leaf compared to 'medium' and 'late' genotypes and the adverse effect was observed for height (**Supplemental Figure 4**). No significant correlation was detected for plasticity of fw and nfr, which are both contributing to final yield in tomato.

QTL mapping in the MAGIC population

QTL analysis was conducted in the MAGIC population first for each condition separately and then for plasticity. The analysis yielded 52 QTLs in control condition, 50 QTLs in HT-stress and 15 QTLs for plasticity traits (**Supplemental Table 4**). A total of 98 QTLs were detected for all the 11 traits among which 36 (37%) were specific to the control condition, 35 (36%) specific to HT-stress and 8 (8%) specific to plasticity. A minor proportion of the QTLs (19%) were common to both conditions, or at least between one condition and plasticity. Frequent QTL co-localizations across traits were found, highlighting some important chromosomal regions having an impact on different traits. The

confidence intervals of the MAGIC QTLs were highly variable according to the QTLs, ranging from 0.58Mbp (leaf9.1) to 78Mbp (fset1.1).

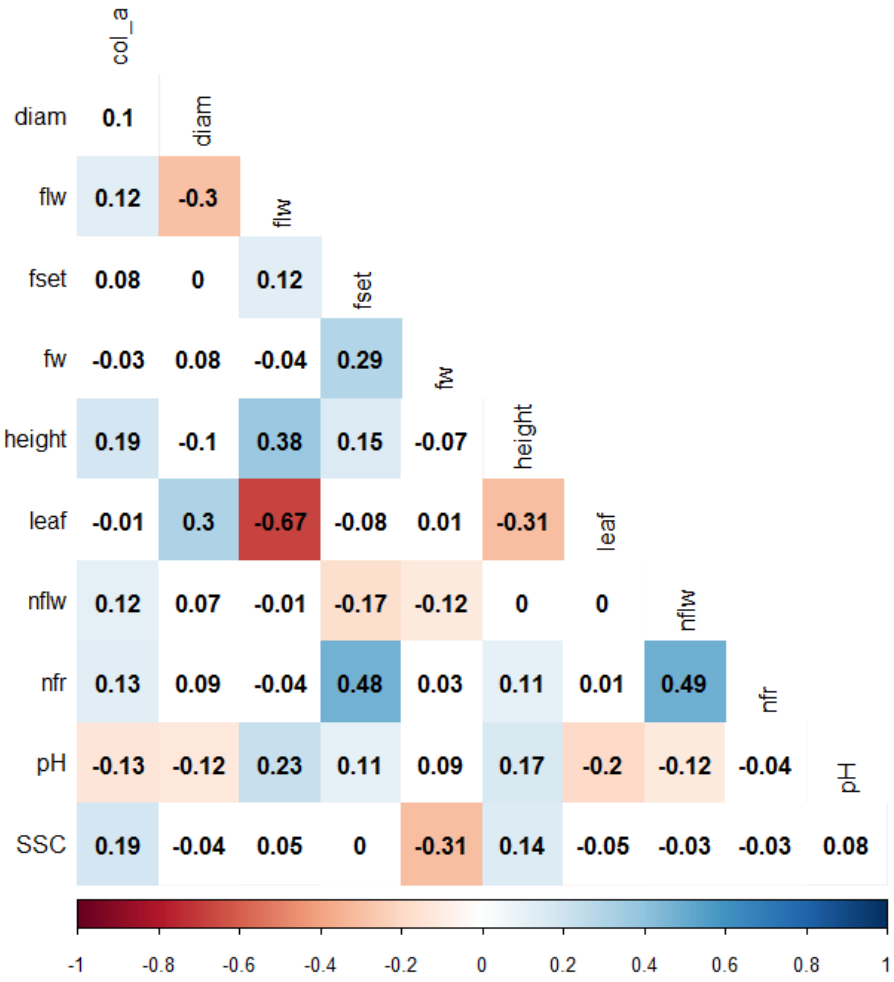

Figure 2: Pearson's correlations between plasticity traits.

GWAS in the CC population

In the CC panel, a total of 166 unique associations were detected for the 11 traits measured with 61, 67 and 55 associations detected for control, HT-stress condition and plasticity, respectively (**Supplemental Table 4**). Among these associations, we identified 151 unique QTLs mapping for one condition or plasticity, and 15 QTLs identified consistently between conditions or between one condition and plasticity. Interestingly, two QTLs (nfr11.5 and nflw11.4) were consistent between the two conditions and plasticity on chromosome 11. Besides, these two QTLs mapped in neighboring regions separated by less than 1Mbp. Confidence interval regions spanning a maximum of 2Mpb

were defined around 88% of the associated markers. The number of significant association per chromosome ranged from 11 (chromosome 9) to 26 (chromosome 11).

Considering the two conditions and plasticity together, the number of QTLs per trait varied from 7 (col_a) to 33 (flw) in the CC population and from 4 (SSC) to 12 (pH) in the MAGIC population. A high proportion of all the QTLs detected across populations were condition-specific or specific to the plasticity (**Figure 3**). However, this trend was highly variable according to the traits. For example, all diam and fset QTLs were specific to a condition or to the plasticity in both populations. The same was found for col_a and height in the CC panel. Conversely 22% of nfr QTLs were commonly detected between the two conditions or between at least one condition and plasticity in the CC. In the MAGIC population, 42% of fw QTLs showed consistency across conditions or between one condition and plasticity (**Supplemental Table 5**).

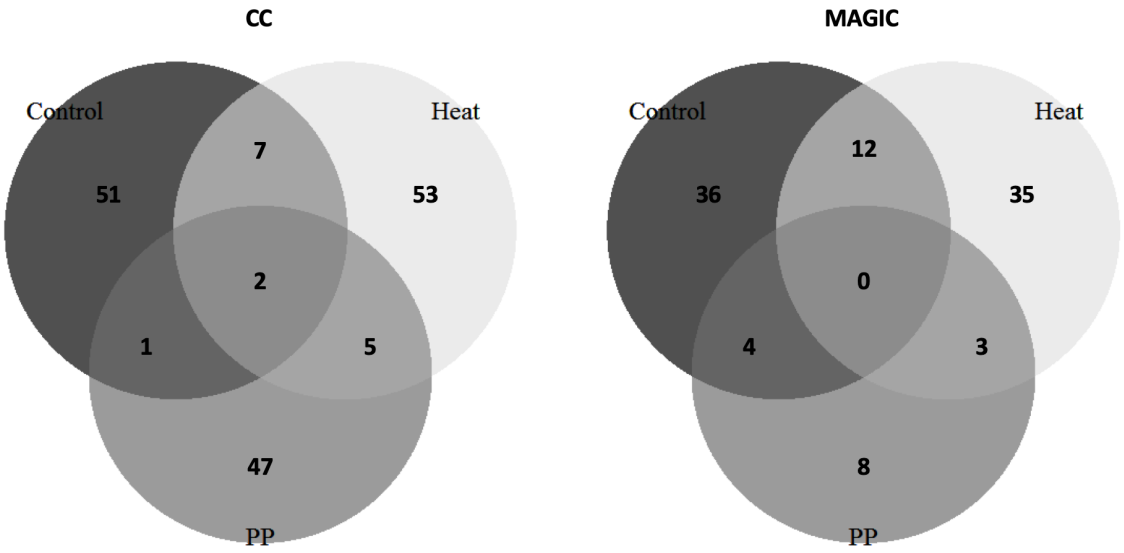

Figure 3: Venn diagram of the number of QTLs per condition. The number of QTLs specific to control, HT-stress condition and to the plasticity is highlighted in the CC panel and the MAGIC population. The numbers in the intersection of the circles represent QTLs that are common in both conditions or between condition and plasticity.

QTLs across populations

Combining both populations and conditions for the common traits, 244 QTLs were identified. The vast majority of these QTLs were population-specific (92% of the QTLs) with only 20 QTLs being simultaneously mapped in both populations. Among these, ten were identified for plasticity, or for the same condition between populations. The QTL SSC9.1 was detected in both populations either for control and HT-stress and its CI interval region covered the *Lin5* gene (Solyc09g010080) which is

described as an Invertase, affecting sugar content in tomato (Fridman et al., 2000). For all the 20 QTLs shared across populations, the CI regions were small, ranging from 7.45 Kbp to 5.07 Mbp and harbored from 2 to 704 genes (**Table 1**).

Table 1: QTLs consistent between populations. For each QTL, the columns 'Control', 'HT-stress' and 'Plasticity' highlight in which condition the QTL was detected and the corresponding population. The columns 'CI_low' and 'CI_high' present the lower and the upper bounds of the collapsing regions between the two panels. The confidence interval (CI) and positions of the lower and upper bounds of the overlapping regions are presented in mega-base-pair (Mbp). For each QTL in the table, the number of candidate genes (CG) and is presented.

QTL-name	Control	HT-stress	Plasticity	Chr	CI low (Mbp)	CI high (Mbp)	Nb CG
ht2.1		MAGIC	CC	2	33,973517	35,214875	77
nflw2.3		MAGIC ; CC	MAGIC	2	44,705571	45,518495	115
col_a3.1	MAGIC	CC		3	53,650069	53,670496	5
flw3.3	MAGIC	MAGIC ; CC	CC	3	65,165483	65,312829	19
fset3.1		MAGIC ; CC		3	63,674517	65,566055	246
nflw3.2		MAGIC	CC	3	63,446585	64,521327	132
nfr3.2		CC	MAGIC ; CC	3	53,08745	54,449864	104
pH3.2	MAGIC	CC		3	64,485318	64,588871	20
diam4.2		MAGIC ; CC		4	65,611502	65,778385	26
ht4.2	CC	MAGIC		4	64,536101	65,778385	163
nfr4.2	CC	MAGIC		4	62,550134	63,900601	178
pH6.2	MAGIC	MAGIC ; CC		6	42,200096	47,27796	704
col_a7.1	MAGIC ; CC			7	4,115593	6,385399	104
fw9.2		MAGIC ; CC		9	30,502912	31,891757	16
nfr9.2	MAGIC	CC		9	66,014053	66,376508	33
SSC9.1	MAGIC ; CC	MAGIC ; CC		9	3,477432	3,48489	2
flw11.5	MAGIC	CC		11	55,330359	56,105593	91
nflw11.3	MAGIC	CC		11	53,964003	54,306131	34
nfr11.4	MAGIC ; CC			11	7,763703	8,414574	45
fw12.1		MAGIC	CC	12	14,640634	15,670729	15

Heat-response QTLs and candidate genes (CGs)

Phenotypic plasticity was used as a trait *per se* to identify HT-response QTLs. Analyses of the two populations revealed 70 plasticity QTLs among which only one (ppnfr3.2) was common to both populations (**Figure 4**). This QTL was mapped in a region of 1.3 Mbp in the CC panel (53.08 – 54.44 Mb), while in the MAGIC population the CI of the QTL spanned about 50 Mbp (region covering the centromere, between 11.26 – 61.92 Mbp). The number of plasticity QTLs varied widely across traits from one (diam) to 13 (flw). Flowering time was the most polygenic trait and all the plasticity QTLs for this trait were identified in the CC and not in the MAGIC population. For almost every trait, the number of plasticity QTLs identified was higher in the CC panel compared to the MAGIC except for

pH. Some regions gathered overlapping plasticity QTLs across traits and panels (**Figure 4**). For example, chromosome 3 carried the plasticity QTLs ppnflw3.2, ppfw3.2, ppflw3.3 and ppfset3.2 that were identified across populations, all of them overlapping in a common region. On chromosome 4, four plasticity QTLs uniquely identified in the CC panel (pppH4.1, ppnfr4.4, ppnflw4.3 and ppfw4.2) mapped in the same region spanning 2 Mbp. Another cluster of five plasticity QTLs (ppnflw11.2, ppflw11.4, ppnfr11.5, ppSSC11.2 and ppnflw11.4) identified in the CC panel were located in a 5 Mbp interval on chromosome 11.

From one to 479 heat-response candidate genes (CGs) were then tagged within the plasticity QTLs by listing all the genes present in the CI of plasticity QTLs and following the filtering procedure described for the MAGIC population in the Materials & Methods section (**Supplemental Table 6**).

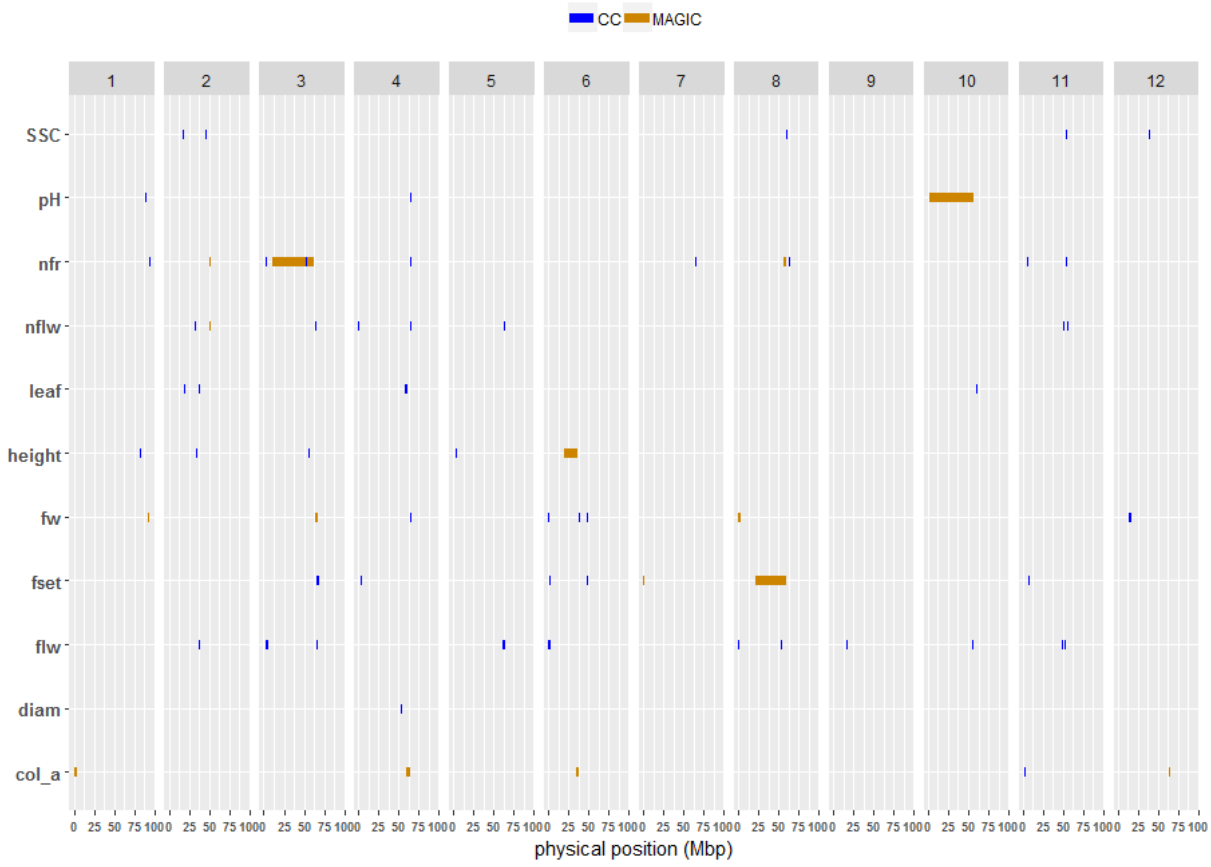

Figure 4: Plasticity QTLs positions in the CC (red) and the MAGIC (blue) populations. Each square represents a chromosome with the number of the chromosome (1 to 12) highlighted. The horizontal bars represent the physical positions of the interval carrying the QTL. The y-axis labelled the different traits for which plasticity QTLs were screened and the x-axis represents the physical positions in Mbp, along the chromosomes. The CI of the CC QTLs were set at 2Mbp interval centered on the pic position for better visualization.

DISCUSSION

Tomato response to heat stress

Plant susceptibility to high temperatures strongly depends on the crop species. However different studies attest that flowering time is the growing period showing the highest susceptibility to heat stress (Wahid et al., 2007; Nadeem et al., 2018). Tomato reproduction is hampered when temperatures exceed the critical value of 30°C, mostly due to susceptibility of male reproductive traits (Xu et al., 2017b). In our experiment, the HT-stress condition was applied by delaying the sowing date of two month compared to the control condition; and the maximal temperatures averaged through the cropping period were 34.4°C and 35.5°C in the MAGIC and CC experiments, respectively. The period surrounding flowering of the parental lines in the HT-stress condition was marked by high temperatures exceeding by about 6°C the control condition (**Supplemental Figure 5**). Besides, no water limitation was applied in the HT-stress conditions in order to avoid confounding effects with drought, and both conditions received the same fertilization solution.

Both tomato populations analyzed showed a large phenotypic variability under control and HT-stress conditions. Differences between the populations were mostly pronounced for fw which showed a coefficient of variation that almost doubled in the CC compared to the MAGIC population (**Supplemental Figure 6**). Indeed, the CC panel included only cherry tomatoes and *S. pimpinellifoliumm* accessions while the MAGIC lines were derived from the cross of cherry and large fruit accessions, which could explain the differences in the fw distribution between the populations. The other traits however showed quite homogeneous distributions across populations.

Most of the traits were characterized by high heritability in both conditions suggesting the possibility to select tomato under heat condition using the resources described here. Heritability was found to vary more between populations than between conditions and in a trait-dependent manner. Fruit weight for example showed very high heritability in the CC compared to the MAGIC population (**Figure 1**) whatever the condition. High fw heritability was already observed in the CC population in a previous study conducted under control and water-deficit condition (Albert et al., 2016). This could be related to the structure in the CC population which is subdivided in three different genetic groups correlated to fw variation. The proportion of the phenotypic variation attributed to genotype effect for fw variation was indeed high (93%) in the CC population compared to the fw variation that was attributed to the condition and gxc effects (about 5%). However, HT-stress condition decreased fw by 25% in the CC population (**Figure 1**). The HT-stress significantly affected all the traits but height in the MAGIC population. The direction of the effect of HT-stress condition was consistent between populations highlighting a similar overall pattern of heat response, with reduced plant development,

reduced fruit number and fw in average but no or little consequence on SSC. However, considering the extent of HT-stress impact, populations showed differences with the MAGIC population being on average more affected for vegetative growth and the CC more affected for yield related traits.

Phenotypic plasticity was calculated to reflect individual response to HT-stress condition in both populations. A set of 24 genotypes were identified as heat-tolerant regarding their plasticity for yield related traits. These genotypes were further screened for their multi-trait plasticity response and most of them showed early flowering phenotypes and impaired growth and leaf development (**Figure 5**). The adaptive behavior of these genotypes seemed to be related to their capacity to reallocate their resources from growth to fruit development by increasing their yield capacity. Some of those genotypes were also positively affected for SSC (**Supplemental Table 3**) highlighting interesting candidates for tomato breeding under high temperature environments. Essentially, the results suggest that heat stress tolerance is a complex mechanism and should be addressed and interpreted in a trait dependent manner since the complex response pathways could result from various phenotypic expressions.

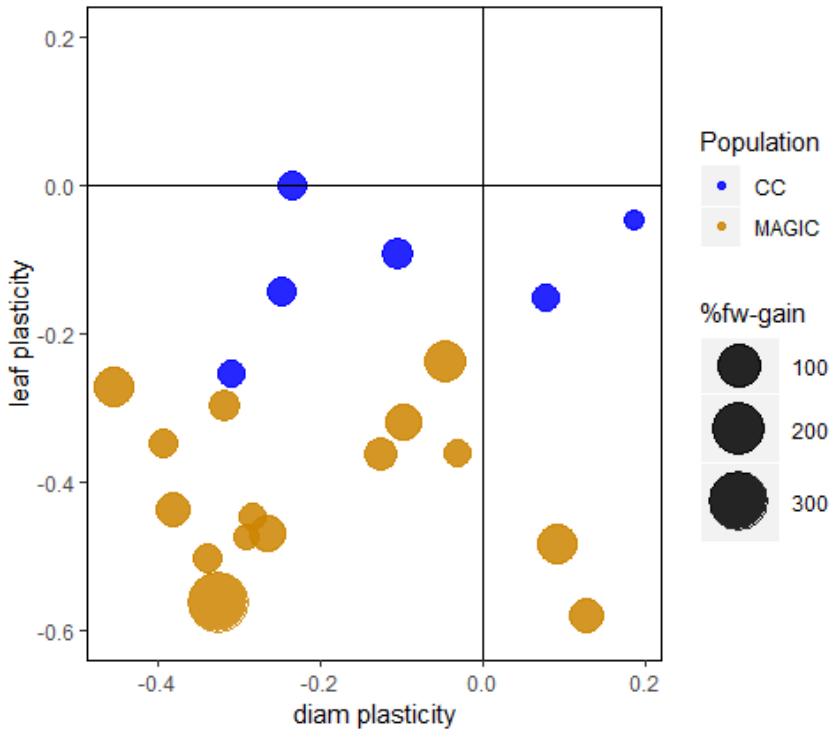

Figure 5: Plasticity of heat-tolerant lines. This plot represents the 24 heat-tolerant lines for fruit weight (17 MAGIC and 7 CC) and their growth response plasticity (diam and leaf). The color represents the population. The size of the circle is proportional to the increase in fruit weight under HT-stress condition. Below the horizontal zero line are plotted all heat-tolerant genotypes that decrease in leaf length under HT-stress condition. The left side of the vertical zero line plot all heat-tolerant genotypes that decrease stem diameter under HT-stress condition.

QTLs common or specific between populations

Considering all traits and conditions, the CC panel yielded a higher number of QTLs than the MAGIC population (166 vs 97, respectively). Besides, we highlighted that the genetic control of heat-response in tomato is highly dependent on the mapping population. Among the 244 unique QTLs identified for the same traits across populations, only 20 QTLs (8%) were consistently identified in both populations. This is in agreement with Pascual et al., (2016), who identified a high proportion of population specific QTLs for fruit and plant related traits under optimal growing condition. The CC panel is composed of lines with diverse geographical origins (**Supplemental Figure 8**) and consisted of genotypes belonging to three distinct genetic groups (SLC, SP and mixture). The high level of population-specific QTLs probably arises from different allele's segregation between the populations.

Plasticity revealed a polygenic control of tomato heat-response

This study was the first using plasticity traits to unravel heat-response QTLs in tomato, to the best of our knowledge. The previous QTL mapping studies on tomato response to high temperature were conducted on traits evaluated in a single heat-stress condition (Grilli et al., 2007; Lin et al., 2010; Xu et al., 2017a). In total, we identified 69 plasticity QTLs specific to populations and one plasticity QTL (ppnfr3.2) shared between the two populations, which denotes the polygenic nature of tomato heat-response. Besides plasticity QTLs, 70 population-specific QTLs and 3 QTLs shared across populations were exclusively detected under the HT-stress condition which may also arise from the heat-response effects (**Figure 3**). Xu et al., (2017a) used SNPs markers from the SolCAP SNP array (Sim et al., 2012) that was also used in our GWAS analysis. This allowed us to compare the physical positions of heat-response QTLs from both study. Interestingly, flw1.5 was identified in the MAGIC population under both control and HT-stress condition, and the region of the QTL overlapped with the previously identified qAL1 from Xu et al., (2017a) that affected variation of anther length under heat. Furthermore, the plasticity QTLs (ppnflw2.3 and ppnfr2.1) mapped in the same region in chromosome 2 and also encompass the positions of two QTLs affecting anther length (qAL2) and style length (qSL2) variation under heat identified in Xu et al., (2017a). The genomic regions holding these QTLs could be important for tomato adaptation to high temperature since heat-response reproductive QTLs were identified within, using different genetic resources.

Focusing only on the plasticity QTLs, from one to 479 candidate genes were proposed per QTL. The plasticity CGs in the MAGIC population were narrowed using the estimated allelic effects of the eight parental lines (**Supplemental Figure 7**). A set of 5657 unique heat-response candidate genes were selected within the CI of the 70 plasticity QTLs (**Supplemental Table 7**). Previous studies identified tomato heat-response genes through expression analysis of male reproductive organs under high

temperature conditions (Fragkostefanakis et al., 2016; Jegadeesan et al., 2018; Keller and Simm, 2018). Thus, tomato heat-inducible genes were then selected from these studies and compared to the candidate genes from our plasticity QTLs. Among the 5657 candidate plasticity genes, 114 genes encompassing 43 plasticity QTLs were selected as their expression in male organs and/or leaf was significantly altered under heat stress (**Supplemental Table 8**). Besides, we identified a set of 60 CGs that are functionally annotated as "chaperon" or "heat-shock" protein within 35 plasticity QTLs, six of which previously identified among the DEG under heat conditions. The candidate genes presented in the **Supplemental Table 8** are thus valuable heat-response candidate genes affecting tomato phenotypic plasticity. Further studies are needed to evaluate in more details the impact of these selected candidate genes, at the phenotype and transcriptome levels in order to better understand the interaction between the regulatory pathways and the phenotypic expression induced by heat stress in tomato.

Conclusion

We identified here tomato genetic resources that are readily usable for breeding purposes and which are useful alternatives to the use of wild germplasm for developing heat tolerant varieties. Both populations broadly showed consistent phenotypic responses while at the genetic level, heat-response QTLs were usually specific. Local adaptation within the CC population and the allelic recombination induced by the crossing design of the parental lines in the MAGIC population induced somewhat different allelic configurations leading to their genetic specificity. Heat-tolerant lines for yield component traits were identified in both populations and could be utilized for further evaluation. Crossing between the heat-tolerant lines from the different populations can be envisaged and could generate allele's combination leading to higher tolerance under hot conditions. We showed that using the phenotypic plasticity as a trait *per se* for QTL identification is a powerful approach for detecting heat-response QTLs. The comparison of plasticity QTLs and QTLs identified in the control or HT-stress conditions identified a high proportion of plasticity QTLs that seem to be controlled by regulatory loci that probably interact with structural genes; besides several HSP located in these regions could be interesting to study in the future if one intended to decipher the molecular mechanisms of tomato heat tolerance.

Authors and Contributors

MC designed the experiments, supervised all the process of this work and monitored the redaction of the article. ID end EB managed the phenotyping, the statistical analyses and the interpretation of the results for the MAGIC and CC populations, respectively. FB developed the bioinformatics tools to identify candidate genes within the QTLs regions. MZ reviewed the manuscript. YC coordinated the trials with the experimental team of the greenhouse facilities.

Acknowledgements

We acknowledge the greenhouse staff of GAFL (Genetics and Breeding of fruit and vegetables) for the trial's management the two successive years of the experiments and the Genetic Resource Center of GAFL for keeping and providing the CC population. We thank very much Esther Pelpoir, Justine Gricourt, Clara Piquot and Mathilde Rigolo for helping in the phenotyping. We also thank Alexandre Hereil for sharing scripts and advices for the GWAS analysis.

Funding

The ANR project TomEpiSet supported this work. ID was supported by the WAAPP (West Africa Agricultural Productivity Project) fellowship and hosted as Ph.D. student in the INRA UR1052, GAFL.

References

Albert, E., Segura, V., Gricourt, J., Bonnefoi, J., Derivot, L., and Causse, M. (2016) Association mapping reveals the genetic architecture of tomato response to water deficit: focus on major fruit quality traits. *J Exp Bot*. 67: 6413–6430.

Bhusal, N., Sarial, A.K., Sharma, P., and Sareen, S. (2017) Mapping QTLs for grain yield components in wheat under heat stress. *PLoS One*. 12: e0189594.

Broman, K.W., Gatti, D.M., Simecek, P., Furlotte, N.A., Prins, P., Sen, Ś., et al. (2019) R/qtl2: Software for Mapping Quantitative Trait Loci with High-Dimensional Data and Multiparent Populations. *Genetics*. 211: 495–502.

Causse, M., Desplat, N., Pascual, L., Le Paslier, M.-C., Sauvage, C., Bauchet, G., et al. (2013) Whole genome resequencing in tomato reveals variation associated with introgression and breeding events. *BMC Genomics*. 14: 791.

Driedonks, N., Wolters-Arts, M., Huber, H., de Boer, G.-J., Vriezen, W., Mariani, C., et al. (2018) Exploring the natural variation for reproductive thermotolerance in wild tomato species. *Euphytica*. 214: 67.

Fahad, S., Adnan, M., Hassan, S., Saud, S., Hussain, S., Wu, C., et al. (2019) Rice Responses and Tolerance to High Temperature. *Adv Rice Res Abiotic Stress Toler*. 201–224.

Foolad, M.R. (2007) Genome mapping and molecular breeding of tomato. *Int J Plant Genomics*. 2007: 64358.

Fragkostefanakis, S., Mesihovic, A., Simm, S., Paupière, M.J., Hu, Y., Paul, P., et al. (2016) HsfA2 Controls the Activity of Developmentally and Stress-Regulated Heat Stress Protection Mechanisms in Tomato Male Reproductive Tissues. *Plant Physiol*. 170: 2461–77.

Fragkostefanakis, S., Röth, S., Schleiff, E., and Scharf, K.-D. (2015) Prospects of engineering thermotolerance in crops through modulation of heat stress transcription factor and heat shock protein networks. *Plant Cell Environ*. 38: 1881–1895.

Frey, F.P., Presterl, T., Lecoq, P., Orlik, A., and Stich, B. (2016) First steps to understand heat tolerance of temperate maize at adult stage: identification of QTL across multiple environments with connected segregating populations. *Theor Appl Genet*. 129: 945–961.

Fridman, E., Pleban, T., and Zamir, D. (2000) A recombination hotspot delimits a wild-species quantitative trait locus for tomato sugar content to 484 bp within an invertase gene. *Proc Natl Acad Sci U S A*. 97: 4718–23.

Grilli, G., Trevizan Braz, L., Gertrudes, E., and Lemos, M. (2007) QTL identification for tolerance to fruit set in tomatoby fAFLP markers. *Crop Breed Appl Biotechnol*. 7: 234–241.

Hall, A.E. (1992) Breeding for Heat Tolerance. In *Plant Breeding Reviews*. pp. 129–168 John Wiley & Sons, Inc., Oxford, UK.

Hasanuzzaman, M., Nahar, K., Alam, M., Roychowdhury, R., Fujita, M., Hasanuzzaman, M., et al. (2013) Physiological, Biochemical, and Molecular Mechanisms of Heat Stress Tolerance in Plants. *Int J Mol Sci*. 14: 9643–9684.

Jegadeesan, S., Chaturvedi, P., Ghatak, A., Pressman, E., Meir, S., Faigenboim, A., et al. (2018) Proteomics of Heat-Stress and Ethylene-Mediated Thermotolerance Mechanisms in Tomato Pollen Grains. *Front Plant Sci*. 9: 1558.

Jha, U.C., Bohra, A., and Singh, N.P. (2014) Heat stress in crop plants: its nature, impacts and integrated breeding strategies to improve heat tolerance. *Plant Breed*. 133: 679–701.

Kang, H.M., Zaitlen, N.A., Wade, C.M., Kirby, A., Heckerman, D., Daly, M.J., et al. (2008) Efficient control of population structure in model organism association mapping. *Genetics*. 178: 1709–23.

Keller, M., and Simm, S. (2018) The coupling of transcriptome and proteome adaptation during development and heat stress response of tomato pollen. *BMC Genomics*. 19: 447.

Kenneth J. Boote; Maria R. Rybak; Johan M.S. Scholberg; James W. Jones (2012) Improving the CROPGRO-Tomato Model for Predicting Growth and Yield Response to Temperature. *HortScience*. 47.

Lin, K.-H., Yeh, W.-L., Chen, H.-M., and Lo, H.-F. (2010) Quantitative trait loci influencing fruit-related characteristics of tomato grown in high-temperature conditions. *Euphytica*. 174: 119–135.

Liu, G.-T., Wang, J.-F., Cramer, G., Dai, Z.-W., Duan, W., Xu, H.-G., et al. (2012) Transcriptomic analysis of grape (Vitis vinifera L.) leaves during and after recovery from heat stress. *BMC Plant Biol*. 12: 174.

Maruyama, K., Ogata, T., Kanamori, N., Yoshiwara, K., Goto, S., Yamamoto, Y.Y., et al. (2017) Design of an optimal promoter involved in the heat-induced transcriptional pathway in Arabidopsis, soybean, rice and maize. *Plant J*. 89: 671–680.

Mittler, R., Finka, A., and Goloubinoff, P. (2012) How do plants feel the heat? *Trends Biochem Sci*. 37: 118–125.

Nadeem, M., Li, J., Wang, M., Shah, L., Lu, S., Wang, X., et al. (2018) Unraveling Field Crops Sensitivity to Heat Stress：Mechanisms, Approaches, and Future Prospects. *Agronomy*. 8: 128.

Pascual, L., Albert, E., Sauvage, C., Duangjit, J., Bouchet, J.-P., Bitton, F., et al. (2016) Dissecting quantitative trait variation in the resequencing era: complementarity of bi-parental, multi-parental and association panels. *Plant Sci*. 242: 120–130.

Pascual, L., Desplat, N., Huang, B.E., Desgroux, A., Bruguier, L., Bouchet, J.-P.P., et al. (2015) Potential of a tomato MAGIC population to decipher the genetic control of quantitative traits and detect causal variants in the resequencing era. *Plant Biotechnol J*. 13: 565–577.

Paul, P.J., Samineni, S., Sajja, S.B., Rathore, A., Das, R.R., Chaturvedi, S.K., et al. (2018) Capturing genetic variability and selection of traits for heat tolerance in a chickpea recombinant inbred line (RIL) population under field conditions. *Euphytica*. 214: 27.

R Core Team (2019).

Rienth, M., Torregrosa, L., Luchaire, N., Chatbanyong, R., Lecourieux, D., Kelly, M.T., et al. (2014) Day and night heat stress trigger different transcriptomic responses in green and ripening grapevine (vitis vinifera) fruit. *BMC Plant Biol*. 14: 108.

Rothan, C., Diouf, I., and Causse, M. (2019) Trait discovery and editing in tomato. *Plant J*. 97: 73–90.

Segura, V., Vilhjálmsson, B.J., Platt, A., Korte, A., Seren, Ü., Long, Q., et al. (2012) An efficient multi-locus mixed-model approach for genome-wide association studies in structured populations. *Nat Genet*. 44: 825–830.

Shanmugavadivel, P., Amitha Mithra, S., Chandra, P., Ramkumar, M., Ratan, T., Trilochan, M., et al. (2017) High Resolution Mapping of QTLs for Heat Tolerance in Rice Using a 5K SNP Array. *Rice*. 10: 28.

Sim, S.-C., Van Deynze, A., Stoffel, K., Douches, D.S., Zarka, D., Ganal, M.W., et al. (2012) High-Density SNP Genotyping of Tomato (Solanum lycopersicum L.) Reveals Patterns of Genetic Variation Due to Breeding. *PLoS One*. 7: e45520.

Wahid, A., Gelani, S., Ashraf, M., and Foolad, M.R. (2007) Heat tolerance in plants: An overview. *Environ Exp Bot*. 61: 199–223.

Waters, A.J., Makarevitch, I., Noshay, J., Burghardt, L.T., Hirsch, C.N., Hirsch, C.D., et al. (2017) Natural variation for gene expression responses to abiotic stress in maize. *Plant J*. 89: 706–717.

Xu, J., Driedonks, N., Rutten, M.J.M., Vriezen, W.H., de Boer, G.-J., and Rieu, I. (2017a) Mapping quantitative trait loci for heat tolerance of reproductive traits in tomato (Solanum lycopersicum). *Mol Breed*. 37: 58.

Xu, J., Wolters-Arts, M., Mariani, C., Huber, H., and Rieu, I. (2017b) Heat stress affects vegetative and reproductive performance and trait correlations in tomato (Solanum lycopersicum). *Euphytica*. 213: 156.

Zhao, C., Liu, B., Piao, S., Wang, X., Lobell, D.B., Huang, Y., et al. (2017) Temperature increase reduces global yields of major crops in four independent estimates. *Proc Natl Acad Sci*. 114: 9326–9331.

Supplementary Materials:

The supplemental figures and tables of this chapter are presented in Appendix 5.

NB: Supplemental tables 1, 6, 7 and 8 can be accessed online:

Supplemental Figure 1: Principal Coordinate Analysis (PCoA) in the CC panel, based on the Kinship matrix.

Supplemental Figure 2: Distribution for all traits evaluated under optimal (light gray) and HT-stress (dark gray) conditions. A) Trait distribution in the CC population with the vertical lines representing the upper-range (solid lines) and lower-range (dashed lines) of the MAGIC parental lines distribution under optimal (green) and HT-stress (red) conditions. Only the four small parental lines included in the CC panel were considered. B) Trait distribution in the MAGIC population; the vertical lines are as in the CC panel but all the eight parental lines were considered.

Supplemental Figure 3: Number of genotypes per group across populations.
The groups were defined according to genotype's susceptibility to HT-stress regarding the flowering time. The "early" (resp. "medium") group clustered genotypes that flowered in average 18 days (resp. 8 days) earlier in the HT-stress condition. The genotypes that flowered later in the HT-stress condition are in the "late" group.

Supplemental Figure 4: Phenotypic plasticity distribution for 404 MAGIC and CC lines regarding the group defined according to flowering time response under HT-stress condition. The stars highlight traits where a significant group effect was detected.

Supplemental Figure 5: Daily temperature fluctuation in the greenhouse for the CC and MAGIC trials. The minimal, mean and maximal temperatures are presented from the plant's transfer into the greenhouse to the end of flowering time. The red and black arrows in the MAGIC figures represent the period covering flowering time of the 5^{th} truss (truss phenotyped for flw) in the MAGIC population.

Supplemental Figure 6: Coefficient of variation (CV) for the 11 traits evaluated in both populations. The green and orange dots represent the Control and HT-stress conditions, respectively. The circle indicates CV in the CC population and the triangle, the MAGIC population.

Supplemental Figure 7: Estimated allelic effects for all plasticity QTLs identified in the MAGIC population.

Supplemental Figure 8: Geographical origin of the CC lines
Each circle represents a country where CC lines were originated and the size of the circle is proportional to the number of genotypes that were selected from a region.

Supplemental Table 1: Principal Coordinate Analysis of the genotype matrix in the CC population. The coordinates of the accessions in the first three axes are displayed. Coordinates of the first three axes are displayed.

Supplemental Table 2: Pearson's correlation between traits and conditions in the CC (A) and the MAGIC (B) populations, resepectively. The upper sides of the table's correspond to trait-correlations

in the HT-stress conditions and the lower sides to trait-correlations in the control condition. The column CorrEnv represents the correlation between HT-stress and control conditions for each single trait. The non-significant correlations were notified by empty cells. When significant at a threshold of 0.05, the coefficient correlations were indicated.

Supplemental Table 3: Heat tolerant genotypes regarding yield component traits in the MAGIC and the CC populations. For each genotype, the plasticity value (heat-response) of the other traits is presented. The flowering group (early, medium or late) of the genotypes is highlighted and for the CC lines, the genetic group and the country of origin are specified.

Supplemental Table 4: List of the QTLs detected in the CC and MAGIC population, under control and HT-stress conditions. For each trait, the detected QTLs are specified in the column 'QTL_name'. The chromosome and the physical position of the QTLs are presented in columns 'Chromosome' and 'Position (Mbp)'. For each QTL, the interval region is presented in mega-base-pair, with the upper interval 'Left_bound (Mbp)' and the lower interval 'Right_bound (Mbp)'. The 'LOD_score' of the QTLs are indicated as well as the 'Marker' name at the pic position of the QTL. LOD scores were calculated as -log10 (P-value). The column 'Condition' indicates if the QTL was detected in control or HT-stress condition, or with the plasticity (PP) phenotype. The population and trait for which the QTL was found are indicated. For each significant QTL/association, the corresponding P-value is reported.

Supplemental Table 5: Summary of the QTLs detected for 11 traits in the CC (A) and the MAGIC (B) populations. The number of QTLs detected per condition and on the plasticity (PP) is indicated for each trait. In brackets is the number of QTLs detected uniquely in one condition or for the plasticity (PP) only. The number of QTLs that co-localized between conditions and or plasticity is presented in the column 'Common'. The column 'Total_QTLs' present the total number of QTLs detected per trait. The last row in bold present the total number of QTLs detected across traits for each condition and for the plasticity and the number of QTLs that were commonly detected. The stars (*) highlight traits for which QTLs were consistently detected in control, HT-stress condition and plasticity within population.

Supplemental Table 6: Plasticity (PP) QTLs across populations. For each PP QTL, the information is as presented in Supplemental Table 4. Besides, the numbers of candidate genes 'NbCG' in the interval region (for the CC QTLs) and the number of candidate genes remaining after the filtering procedure (MAGIC QTLs) are presented. For all plasticity QTLs in the MAGIC population, the estimated allelic effects (see Supplemental Figure 7) were used to narrow the candidate genes and the contrasting parents that were used for this filtering procedure are presented in the column 'Filter'. For each QTLs, the number of genes with unknown function (based on SL2.50 annotation version of the reference genome) is presented in the column NbUG.

Supplemental Table 7: Candidate plasticity genes. For each QTL, the genes within the confidence interval of the QTL (in the CC population) and the genes selected after the filtering procedure (in the MAGIC population) are listed with their Solyc ID. The functional annotation (according to the SL2.50 version of the reference genome) is provided.

Supplemental Table 8: Candidate plasticity genes which are besides differentially expressed under heat (in male reproductive or leaf organs) and/or which functional annotation is related to Chaperone and Heat-shock proteins. The column 'Organ (DE)" indicates in which organ the gene was found differentially expressed. Differentially expressed genes were retrieved from (Fragkostefanakis

et al., 2016; Jegadeesan et al., 2018; Keller and Simm, 2018). The six genes that are identified as Heat shock/Chaperone protein and which altered expression under heat condition has been documented are marked with a star (**) and highlighted in bold.

CHAPTER 6

Genetic basis of phenotypic plasticity and genotype x environment interaction in a multi-parental tomato population

Isidore Diouf [a], Laurent Derivot [b], Shai Koussevitzky [c], Yolande Carretero [a], Frédérique Bitton [a], Laurence Moreau [d], Mathilde Causse [a]*

[a] INRA, UR1052, Génétique et Amélioration des Fruits et Légumes, 67 Allée des Chênes, Centre de Recherche PACA, Domaine Saint Maurice, CS60094, Montfavet, 84143, France

[b] GAUTIER Semences, route d'Avignon, Eyragues, 13630, France

[c] Hazera – Seeds of Growth, Berurim M.P Shikmim, 7983700, Israel

[d] UMR GQE-Le Moulon, INRA, CNRS, AgroParisTech, Université Paris-Saclay, F-91190, Gif-sur-Yvette, France

In preparation

Abstract (296 words)

Abiotic stresses and cultural conditions can lead to different performances of a given genotype when exposed to different environments. This ability is commonly referred as phenotypic plasticity and has received a great interest these last decades. Plant geneticists are aware of the importance of measuring phenotypic plasticity and determining its genetic basis for breeding program purposes. Tomato is a widely cultivated crop that can grow in different geographical habitats and which evinces a great capacity of expressing phenotypic plasticity. We used a multi-parental advanced generation intercross (MAGIC) tomato population to explore trait variation and plasticity in a multi-environment trial (MET) design comprising optimal cultural conditions and water deficit, salinity and heat stress treatments. Genotype x environment interaction (GxE) was evaluated at phenotypic level for a total of ten traits – related to fruit quality, yield component plant growth and phenology traits – and its genetic basis investigated through quantitative trait loci (QTL) mapping analyses. The analyses revealed substantial GxE, explaining 15 to 68% of the phenotypic variance according to the different traits evaluated. A total of 104 unique QTLs were identified for mean phenotypes and different plasticity parameters among which only 21% were common to mean and plasticity. Mixed linear models were further used modelling the MAGIC-MET design to investigate the interactive QTLs (QEI). This analysis yielded 28 QEI which were in majority detected with the QTL analysis using either plasticity or mean phenotypes. The present study highlighted a complex genetic architecture of tomato plasticity and GxE. Plasticity QTLs were in majority distinctly located compared to mean phenotype QTLs for a given trait suggesting the possibility of breeding for plasticity independently. Candidate genes that might be involved in the occurrence of GxE in tomato were proposed, paving the way for functional characterization of stress response genes in tomato.

Keywords: Tomato, MAGIC population, phenotypic plasticity, genotype x environment interaction (GxE), abiotic stresses, QTL.

INTRODUCTION

Plants are sessile organisms which have to cope with environmental fluctuations to ensure species reproduction for persistence in nature. For a given genotype, the expression of different phenotypes according to the growing environment is commonly called phenotypic plasticity (PP) (Bradshaw, 1965). It offers the possibility to plants to adapt to new environments, notably new locations, changes in climatic conditions or seasonal variations. In agriculture, the range of environmental variation for crop cultivation may also include different cultural practices or growing conditions, leading to the expression of PP on agronomic traits and non-stable performance. When different genotypes/accessions are examined for PP within a species, inter-individual variations in their responses usually lead to the common phenomenon of genotype-environment (GxE) interaction (El-Soda et al., 2014). Understanding the genetic mechanisms driving PP and GxE in plants is a crucial step for being able to predict yield performance of crop cultivars and will certainly help to adapt breeding strategies according to the targeted environments.

In plants, the genetic basis of PP has been investigated to assess whether PP has its own genetic regulation and thus could be directly selected. Three main genetic models, widely known as the over-dominance, allelic-sensitivity and gene-regulatory models were proposed in the literature as underlying plant PP (Scheiner, 1993; Via et al., 1995). The over-dominance model suggests that PP is negatively correlated to the number of heterozygous loci (Gillespie and Turelli, 1989). The heterozygous status is favored by allele's complementarity in this case. Allelic-sensitivity and gene-regulatory models are assumed to arise from the differential expression of an allele according to the environment and epistatic interactions between structural and regulatory alleles, respectively. The latter assumes an independent genetic control of mean phenotype and plasticity of a trait. Using a wide range of environmental conditions, the prevalence of the allelic-sensitivity or gene-regulatory model in explaining the genetic architecture of PP was explored in different crop species including barley (Lacaze et al. 2009), maize (Gage et al., 2017; Kusmec et al., 2017), soybean (Xavier et al., 2018) and sunflower (Mangin et al., 2017).

Quantification of PP is however a common question when analyzing the genetic architecture of plasticity since different parameters for PP estimation are available as reviewed by Valladares et al. (2006). At a population level, when multiple genotypes are screened in different environments, different approaches can be used to assess plasticity (Laitinen and Nikoloski, 2019). The most common of these approaches is the joint regression model (Finlay and Wilkinson, 1963) that uses the average performance of the set of tested genotypes in each environment as an index on which the individual phenotypes are regressed. This model, commonly known as the Finlay-Wilkinson

regression model, allows to estimate linear (slopes) and non-linear (from the residual errors) plasticity parameters that presumably have different genetic basis (Kusmec et al., 2017). If the biological description of the environments is available, the environmental index used in the Finlay-Wilkinson regression model can be replaced by environmental covariates such as stress indexes through factorial regression models (Malosetti et al. 2013). Thus plasticity could be estimated as the degree of sensitivity to a given stress continuum (Mangin et al., 2017).

Climate change is predicted to increase the frequency and intensity of abiotic stresses with a high and negative impact on crop yield (Zhao et al., 2017). Plants respond to abiotic stresses by altering their morphology and physiology, reallocating the energy for growth to defense against stress (Munns and Gilliham, 2015). Consequences on agronomic performances are apparent and detrimental to productivity. The most common abiotic stress studied across species are water deficit (WD), salinity stress (SS) and high temperature stress (HT). The negative impact of these stresses on yield have been underlined for major cultivated crops; however, positive effects of WD and SS on fruit quality have been observed in fruit trees and some vegetables notably in tomato (Costa et al. 2007; Mitchell et al. 1991; Ripoll et al. 2014).

Tomato is an economically important crop and a plant model species which led to numerous studies that contributed much in understanding the genetic architecture of the crop and its response to environmental variation. However, most of the studies that addressed the genetic architecture of tomato response to environment were conducted on experimental populations exposed to two conditions (*i.e.* control *vs* stress). Albert et al. (2018) for example identified different WD-response quantitative trait loci (QTL) in a bi-parental population derived from a cross of large and cherry tomato accessions. Tomato heat-response QTLs were also identified in different experimental populations including interspecific and intraspecific populations (Driedonks et al., 2018; Grilli et al., 2007; Xu et al., 2017a). These studies investigated heat-response QTLs using mostly reproductive traits screened under heat stress condition. Villalta et al. (2007) and Diouf et al. (2018) investigated the genetic architecture of tomato response to SS and identified different QTLs for physiological and agronomic traits, involved in salinity tolerance. However, no QTL study has yet been conducted on tomato plasticity assessed under a multiple stress design, although the coincidence of different stress is a more realistic scenario in crop cultivation especially with the climate change.

Tomato benefits of a large panel of genetic resources that have been used in multiple genetic mapping analyses (Grandillo et al. 2013). Bi-parental populations were first used in QTL mapping and permitted the characterization of plenty of QTLs related to yield, disease resistance and fruit quality. In the genomic era, new experimental populations were developed offering higher power and advantages for QTL detection. These include mutant collections, BIL-populations and multi-parent

advanced generation intercross (MAGIC) as described in Rothan et al. (2019). The first tomato MAGIC population was developed at INRA-Avignon in France and was composed of about 400 RILs derived from an 8-way cross (Pascual et al. 2015). This population showed a wide intra-specific genetic variation under control and stress environments and is highly suitable for mapping QTLs.

In the present study, we used the 8-way tomato MAGIC population described above and evaluated its response in a multi-environment trial (MET) design. The population was grown in 12 environments including control and several stress conditions and measured for agronomic traits related to yield, fruit quality, plant growth and phenology. Different plasticity parameters were computed and used together with mean phenotypes to decipher the genetic control of response to environmental variation. Multi-environment QTL analysis was performed in addition to identification of interactive QTLs (QEI) along with QTL mapping for plasticity traits.

MATERIALS AND METHODS

Plant material and phenotyping

The MAGIC population was derived from a cross between eight parental lines that belong to *SL. lycopersicum* and *SL. cerasiforme* groups. More details about the population development can be found in Pascual et al. (2015). Briefly, the population was composed of about 400 8-way MAGIC lines that underwent three generations of selfing before greenhouse evaluations were carried out. In this study, a subset of 241 to 397 lines was grown in each environment (**Supplemental Table 1**).

The full genome sequence of each parental line was available and their comparison with the reference tomato genome ('Heinz 1706') yielded 4 millions of SNPs (Causse et al., 2013). From these polymorphisms, a genetic map of 1345 discriminant SNPs was developed (Pascual et al., 2015) and used in the present study for the QTL analysis.

Experimental design

The MAGIC population was grown in three different geographical regions (France, Israel and Morocco) and four specific stress treatments were applied. Trials were conducted in order that in a given trial any stress treatment was applied aside a control trial (**Supplemental Table 1**). Treatments consisted in water deficit (WD), two levels of salinity – considered here as low salinity (LS) and high salinity (HS) – and high temperature (HT) stress. Water deficit was applied by reducing the water irrigation of about 70% and 30% according to the reference evapotranspiration in Israel in 2014 and

2015, respectively and by 50% in Morocco in 2015. Salinity treatment was managed as described in Diouf et al. (2018) and the average electrical conductivity of the substrate (Ec) in Morocco 2016 was 3.76 and 6.50 $dS.m^{-1}$ for LS and HS, respectively; while the Ec in the control condition in Morocco 2015 was about 1.79 $dS.m^{-1}$. For HT-stress, plants were sown during the late spring and phenotyped in the summer 2014 in Israel (HIs14) and summer 2017 in France (HAvi17). During HT treatments, greenhouse vent opening was managed all along the entire growing season, with opening the vent only when temperatures rose up to 25°C. Average mean/maximal temperatures calculated on daily (24 hours) measurements were 26/34°C for HAvi17 and 33/48°C for HIs14. Besides stress treatments, local conventional cultural conditions were applied for control treatments (as described in Diouf et al. 2018).

Environments were considered as any combination of a geographical region, a year of trial and a treatment applied (**Supplemental Table 1**). Climatic sensors were installed in the greenhouses and climatic parameters recorded hourly in all environments, then stored and managed with a climate computer. From the climatic parameters, seven environmental covariates were defined (**Supplemental Figure 1**) including temperature parameters (mean, minimal and maximal daily temperatures and thermal amplitude), the sum of degree-day (SDD), the vapour-pressure-deficit (Vpd) and the relative humidity (RH) within the greenhouse. To characterize the environments, every covariate was calculated during the period covering flowering time of the population on the fourth truss. Indeed, phenotypic data analyzed here were mostly recorded on the fourth and fifth trusses. Hierarchical clustering was performed with 'FactoMineR' R package (Lê et al., 2008) using the environmental parameters to group environments according to their similarity regarding the within-greenhouse climatic conditions.

The MAGIC population, the eight parental lines and the four first generation hybrids (one hybrid per two-way cross) were evaluated for fruit weight by measuring the average fruit weight (fw) under the third and/or fourth plant truss in each environment. Phenotypic data were recorded across the different environments for nine supplemental traits related to fruit quality – fruit fruit firmness (firm) and soluble solid content (SSC), plant phenology – flowering time (flw), number of flowers (nflw) and fruit setting (fset), plant development – stem diameter (diam), leaf length (leaf) and plant height (height) and fruit number (nfr). Details about the phenotyping measurements are in **Supplemental Table 2**. At least two plants per MAGIC line were replicated in each environment except in Avi17 where the average phenotype was recorded from single plant measurements. Parents and hybrids had more replicates per genotype (at least two) and served as control lines to measure within-environment heterogeneity.

Evaluation of GxE and heritability

Data were first analyzed separately in each environment to remove outliers and correct for spatial heterogeneity within the environment. The model (1) below was applied to test for micro-environmental variation within the greenhouse where y_{ijk} represents the phenotype of the individual *i*, located in row *j* and position *k* in the greenhouse; μ is the overall mean; C_i and L_i represents the fixed effect of control lines and the random effect of the MAGIC lines, respectively. In this model, a 0-1 index t_i was defined to distinguish between control and MAGIC lines; ε_{ijk} is the random residual error.

$$y_{ijk} = \mu + C_i . t_i + L_i . (1-t_i) + R_j + P_k + \varepsilon_{ijk} \quad (1)$$

For every trait where row (R_j) and/or position (P_k) effects were significant, required corrections were applied by removing the BLUP of the significant effects from the raw data. Corrected data were gathered and used in model (2) in order to estimate the broad-sense heritability (h^2_{GxE}) and the proportion of variance associated to the GxE.

$$y_{ij} = \mu + E_j + C_i.t_i + CxE_{ij}.t_i + L_i.(1-t_i) + + LxE_{ij}.(1-t_i) + + \varepsilon_{ij} \quad (2)$$

In model (2), y_{ij} represents the phenotype of the individual *i*, in environment *j*; μ, C_i and L_i are as described in model (1); CxE_{ij} and LxE_{ij} are the fixed control-by-environment interaction effect and the random MAGIC lines-by-environment interaction effect, respectively. Within a given environment, random residuals error terms were assumed to be independent and identically distributed with a variance specific to each environment. From this model, the proportion of the total genotypic and GxE variance explained by the model was calculated as: $prop.\sigma^2{}_{GxE} = \sigma^2{}_{LxE}/\sigma^2{}_{L} + \sigma^2{}_{LxE})$. The significance of GxE was tested with a likelihood ratio test (at 5% level) between the models with and without GxE. The broad-sense heritability at the whole design level (H^2) was derived from variance components of model (2) as: $H^2 = \sigma^2{}_{L}/(\sigma^2{}_{L} + \frac{\sigma^2{}_{LxE}}{nb.E} + \frac{\sigma^2{}_{E}}{nb.R})$, where $\sigma^2{}_{L}$ and $\sigma^2{}_{LxE}$ are the variance components associated to the MAGIC lines and MAGIC lines-by-environment interaction effects, respectively; $nb.E$ and $nb.R$ are the number of environments (*e.g.* 12 for fw) and the average number of repetitions over the whole design; $\sigma^2{}_{E}$ represents the average environmental variance (i.e. $\sum \sigma^2{}_{Ej} / nb.E$).

Phenotypic plasticity

Three different parameters of plasticity were estimated using the Finlay-Wilkinson regression (3) and a factorial regression (4) models.

In model (3), y_{ij} is the phenotype (averaged per environment and genotype) and μ the general intercept, G_i and E_j are the effects of the MAGIC line i and the environment j, respectively; β_i represents the regression coefficient of the model. It measures individual genotypic sensitivity to the environment.

$$y_{ij} = \mu + G_i + \beta_i x E_j + \varepsilon_{ij} \quad (3)$$

Environments are described here as an index that represents the 'quality' of the environment (*i.e.* the average performance of all genotypes in a given environment). The ε_{ij} are the error terms including the GxE and $\varepsilon_{ij} \sim N(0, \sigma^2 R)$. From model (3), three parameters were estimated:

- The mean phenotype (mean) that is equivalent to the sum ($\mu + Gi$) representing the average performance considering all environments.
- The β_i terms (slope), corresponding to genotypic responses to the environments.
- The variance (VAR) of the ε_{ij} terms that is a measurement of non-linear plasticity (Kusmec et al., 2017).

All these parameters were used to characterize the genotypes according to their individual performance and their stability, from control to stress environments. For every trait, reaction norms were then computed from the model (3).

The factorial regression model (4) was further applied to describe the GxE through the response of genotypes to the different environmental covariates (Tmin°, Tmax°, Tm°, Amp.Th°, Vpd, RH and SDD). The environmental covariates defined from the daily recorded climatic variables in the greenhouses were used for this purpose. For each trait, the most significant environmental covariate (p-value > 5%) was first identified – by testing successively the significance of each single covariate – and used as an explanatory variable represented by Cv_j in model (4).

$$y_{ij} = \mu + G_i + E_j + x_i . Cv_j + \varepsilon_{ij}. \quad (4)$$

The x_i terms of the model were extracted and considered as a third plasticity parameter (SCv). They represent genotypic sensitivities to the most impacting environmental covariate for each trait. This measurement of plasticity is of interest as it allows identifying the direction and the intensity of each MAGIC line's sensitivity to a biological meaningful environmental covariate. Throughout the rest of the document, the 'slope' and 'VAR' estimated from the Finlay-Wilkinson model and the 'SCv' from the factorial regression model will be considered as plasticity phenotypes – all of these parameters being trait-specific.

Linkage mapping on the mean and plasticity phenotypes

Linkage mapping was carried out with a set of 1345 SNP markers selected from the genome resequencing of the eight parental lines. All the MAGIC lines were genotyped for those SNPs and at each SNP position, the founder haplotype probability was predicted with the function *calc_genoprob* from R/qtl2 package (Broman et al., 2019). Founder probabilities were then used with the Haley-Knott regression model implemented in R/qtl2 for QTL detection. The response variables were the mean, slope, VAR and SCv for each trait. To attest for significance, the threshold for all phenotypes was set to a LOD = -log10 (α/number of SNPs) where α was fixed at 5% risk level. The VAR plasticity parameter was log transformed for all traits except fset (sqrt transformation) to meet normality assumption before QTL analysis. The function *find_peaks()* of R/qtl2 package was used to detect all peaks exceeding the defined threshold and the LOD threshold was dropped of two and one units to separate two significant peaks as distinct QTLs and to define the confidence interval of the QTLs, respectively.

Multi-environment QTL analysis (QEI)

The strength of QTL dependence on the environment was tested afterward in a second step by identifying QTLs that significantly interact with the environment (QEI). Two multi-environment forward-backward models (5 & 6) were used to test at each marker position the effect of the marker-by-environment interaction.

$$y_{ij} = \mu + E_j + \sum_{p=1}^{8} \alpha_{kp} * x_{ikp} + \sum_{p=1}^{8} \beta_{kpj} * x_{ikp} + G_i + \varepsilon_{ij} \quad (5)$$

$$y_{ij} = \mu + E_j + \sum_{p=1}^{8} \beta_{kpj} * x_{ikp} + G_i + \varepsilon_{ij} \quad (6)$$

For model (5) and (6), y_{ij} represents the phenotype (=mean value per genotype and per environment), *Ej* reflects the fixed environment effect; α_{kp} and β_{kpj} represent the main and interactive parental allelic effects at marker *k* and in environment *j* for β_{kpj}, respectively; x_{ikp} is the probability of the parental allele's origin for the MAGIC line *i*; G_i stands for a random genotype effect and the residual errors ε ~ N (0, $\sigma^2 Rj$) are specific to each environment. The residuals include a part of the GxE that is not explained by the detected QTLs.

Significant QEI were declared in a two-step procedure. First, the main QTL and the QEI effects were tested separately in model (5). The QTL detection process was adapted from the script proposed by Giraud et al., (2017). Every marker showing a significant main-QTL or QEI was added as a fixed cofactor and the significance of the remaining markers tested again until no more significant marker

was found. All markers selected as cofactors are then jointly tested in the backward procedure and only significant QEI after the backward selection are reported. To determine the threshold level for QEI detection, 1000 simulations were performed on the adjusted means with the function *sim.sightr* of mpMap 2.0 R package (Huang and George, 2011). The second procedure used in model (6) to declare QEI consisted in a slight modification of model (5) where α_{kpj} represents now the global effect of the marker. It allowed the detection of markers that had a main-QTL effect or QEI just below the threshold detection but whose global effect is significant when the two components are jointly tested.

RESULTS

Environment description

The 12 environmental conditions were described by the daily climatic parameters recorded until the end of flowering of the 4th truss. Seven environmental covariates were selected, and the environments clustered according to these covariates in four groups (**Figure 1**). The first group included all trials from Morocco that were characterized by high thermal amplitude and low Vpd. The control environments in France (Avi12 and Avi17) clustered together in the 2nd group, defined by low maximal temperatures and high relative humidity. HIs14 clustered alone in the 4th group and formed the most extreme environment showing very high temperatures and dry climate with low relative humidity. The remaining environments clustered together in the 3rd and most disparate group.

Phenotypic distributions were plotted for each trait regarding the environments where it was evaluated (**Supplemental Figure 2**) showing a distribution in accordance with the clustering of the environments for some traits (firm, height, nflw and leaf). Other traits such as fw, nfr, SSC and fset showed a distribution pattern with relatively high within-group variability, notably for environments clustering in group 1 from Morocco.

GxE in the MAGIC population

Genotype-by-environment interaction analysis was carried out after correcting data for micro-environmental heterogeneity and removing outliers. As a first step, variance analysis was conducted with ASReml-R package and the variance components from model (2) used to estimate the proportion of GxE variance ($prop.\sigma^2{}_{GxE}$) and heritability at the whole design level (H^2). Significant GxE was found for every trait and the $prop.\sigma^2{}_{GxE}$ varied from 0.15 (for nflw) to 0.68 (for leaf).

Although GxE was significant, seven out of the ten measured traits showed a higher proportion of genotypic variance compared to GxE (**Supplemental Table 3**). The broad-sense heritability of the whole design H^2 was largely variable according to the trait, varying from 0.18 (nfr) to 0.77 (flw). Its calculation took into account the residual environment-specific variance which showed different range according to the trait, lowering heritability of traits such as nfr and fset (**Supplemental Table 3**). Furthermore ${H^2}_{GxE}$ was lower than the heritability computed in single environments (**Supplemental Figure 3**).

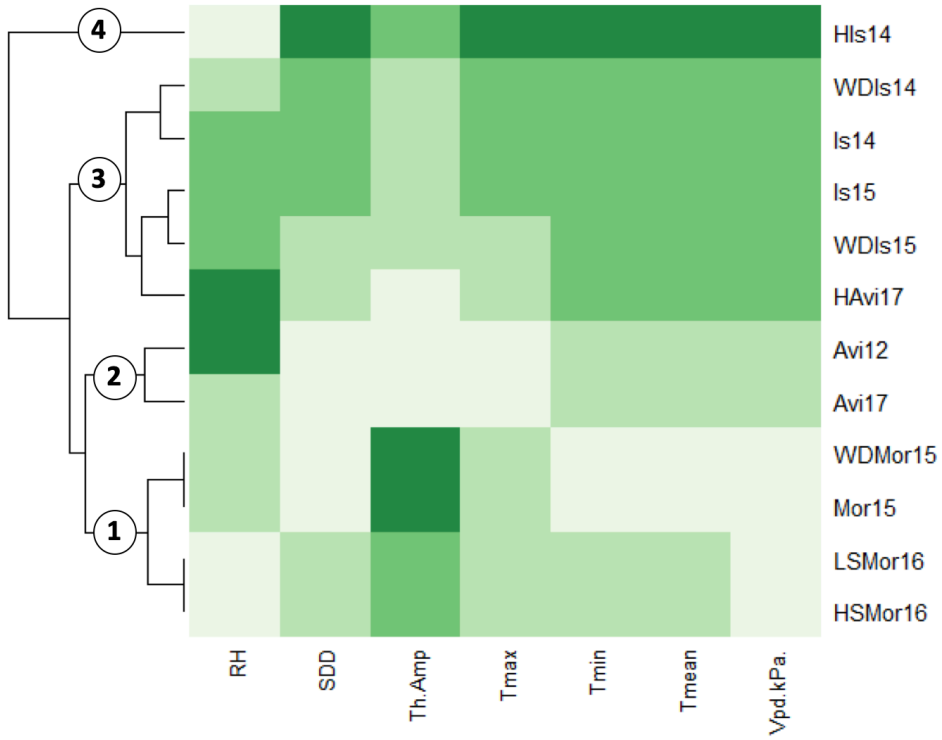

Figure 1: Clustering environments according to seven environmental covariates, measured during the vegetative and flowering stage.

Afterwards, the proportion of the GxE that could be predicted by the environmental covariates was assessed following the factorial regression model (4) (Supplemental Figure 4). Across traits, different environmental covariates significantly explained the GxE. Considering only the most significant covariate, from 18% (fw) to 47% (fset) of the GxE (proportion of the sum of squares) could be reliably attributed to the responses of genotypes to climatic parameters measured within the greenhouses. To perform the factorial regression model (4), the most important environmental covariate was first identified for each trait (Supplemental Figure 4). Growth traits, height and leaf were for example mostly affected by the thermal amplitude and maximal temperature, respectively, while yield component traits, fw and fruit number nfr were particularly sensitive to the sum of degree day. The vapour pressure deficit (Vpd, kPa) was the most important environmental factor affecting fruit

firmness (firm), fruit setting (fset) and soluble sugar content (SSC). Flowering time (flw) and number of flowers (nflw) were mostly affected by minimal temperatures and relative humidity, respectively. Stem diameter was the only trait for which none of the environmental covariates significantly affected the trait; however, the minimal temperature was the covariate that explained the highest proportion of GxE.

Phenotypic plasticity

Three different parameters were used to quantify phenotypic plasticity in the MAGIC-MET design. For each trait, the slope and VAR from the Finlay-Wilkinson regression model and the genotypic sensitivity to the most important environmental covariate (SCv) from the factorial regression model were extracted. A large genetic variability was observed for plasticity of all traits (**Supplemental Figure 5 and Supplemental Figure 6**). Besides, significant correlations were found between the mean phenotypes and plasticity parameters (**Figure 2**) for most of the traits. The best average-performing genotypes were usually the most responsive to environmental variation as highlighted by the positive correlation between mean and the slope parameter from the Finlay-Wilkinson regression model. The majority of the MAGIC lines responded in the same direction to the environmental quality and only a few genotypes (none in the case of height) showed negative reaction norms; however, more divergent shapes of reaction norms were observed from the factorial regression model (**Supplemental Figure 5**).

Figure 2: Pearson's correlation between mean and plasticity parameters.

QTL mapping

We used mean and plasticity measurements for every trait as input phenotypes to decipher the genetic architecture of tomato response to abiotic stresses. Considering the 10 traits, a total of 104 unique QTLs were identified for mean and the plasticity parameters (**Supplemental Table 4**). The proportion of QTLs shared between mean and plasticity was about 21%, lower than QTLs that were plasticity or mean specific (79%). Considering only the 63 plasticity QTLs, 11 and 7 QTLs were specifically detected with the SCv and VAR plasticity parameters. Plasticity QTLs were detected on every chromosome (**Figure 3**); however, the chromosome 1 showed the highest number with 12 plasticity QTLs. In this chromosome, plasticity QTLs were detected at least once for every trait. Chromosome 11 yielded a total of 11 plasticity QTLs and interestingly all these QTL (except ppnflw11.1) co-localized in a portion between 52-55 Mbp of the chromosome. The chromosomes 5, 6 and 10 showed the lowest number (only 3) of plasticity QTLs. For QTLs detected on Mean, the number of QTLs per chromosome varied from 10 QTLs on chromosome 1 to 2 QTLs on chromosomes 6 and 10.

QTL-by-environment analysis (QEI)

A multi-environment forward-backward model was used to assess the significance and the strength of the QTL effects across environments. The QEI analysis was conducted in two steps using the 1345 SNP markers that were also used for the linkage mapping analysis as detailed in Materials and Methods. This analysis yielded 28 QEI (only those showing significant interaction) for the 10 traits (**Supplemental Table 4**). The number of QEI varied from 0 QEI for nfr to 6 QEI for flw. These two traits also demonstrated the lowest and highest ${h^2}_{GxE}$.

All QEI identified in this step were compared with the plasticity and mean QTLs using the physical positions of the QTLs and their confidence intervals. Interestingly, all QEI were also identified using either mean or plasticity parameters, in the linkage mapping analysis except two QEI located on the same region of chromosome 6 (flw6.1 and firm6.1). Among the 106 unique QTLs identified on mean, PP and QEI, a notable number of QTLs were plasticity or mean specific (30 and 32%, respectively) (**Figure 4**). Eight QTLs involving five different traits (flw1.1, fw2.1, fw2.2, fw11.2, leaf6.1, nflw11.2, SSC1.2 and SSC9.1) were identified with all the three approaches highlighting their robustness and sensitivity to environmental variation.

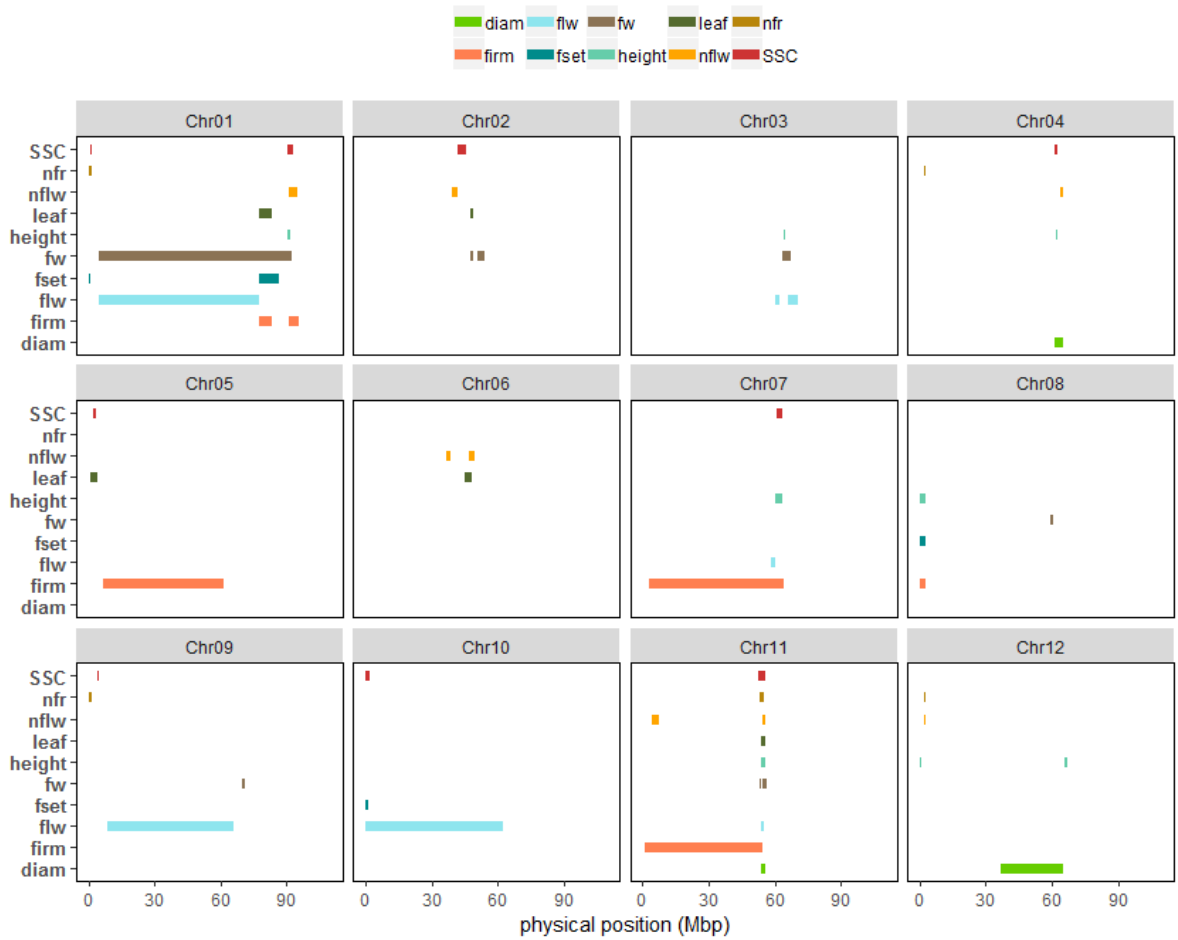

Figure 3: Representation of plasticity QTLs along the genome. Numbers above the square represent the different chromosomes and the colors distinguished the different traits. The x-axis represents the physical distances in mega base pair (Mbp).

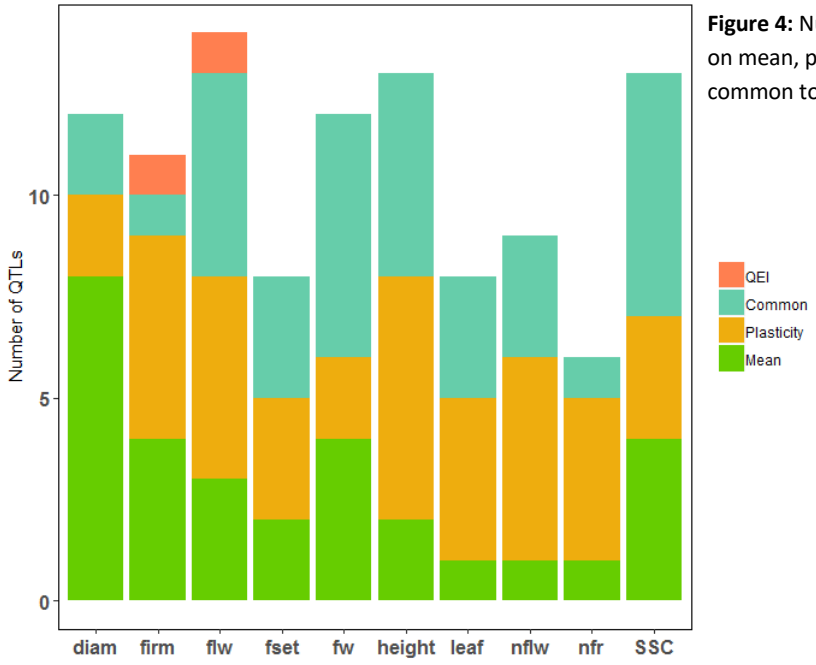

Figure 4: Number of QTLs identified specifically on mean, plasticity or QEI and QTLs that were common to at least two of them.

Genetic location of the MAGIC-MET QTLs

The physical positions based on the SL2.50 version of the reference genome, were used to compare the position of the different QTL category (mean – plasticity – QEI). A recent study has identified different tomato regions (Sweep regions) that were selected during domestication and improvement events (Zhu et al., 2018). These regions were cross checked against the positions of our QTLs. Some QTLs detected in the MAGIC-MET design were located in large regions thus collapsing with a high number of Sweep regions (**Figure 5** & **Supplemental Figure 7**). Considering only the QTLs within less than 2Mbp intervals and all QEI, a total of 61 QTLs were selected and compared with the Sweep regions. Plasticity QTLs appeared to be in majority located within the Sweep regions and only 6% of the selected plasticity QTLs were outside the domestication/improvement selective sweeps (**Supplemental Figure 8**). Interestingly, the Sweep region SW75 located in chromosome 3 (located between 64.76 - 65.01 Mbp) carried a total of five QTLs (ht3.1, fset3.1, flw3.2, leaf3.1, fset3.1). **Supplemental Table 5** presents all the Sweep regions holding at least one MAGIC-MET QTL. Chromosome 11 was highlighted as holding a number of plasticity QTLs for different traits (**Figure 3**). Indeed, seven different QTLs all identified with plasticity parameters, were located within the Sweep regions SW254 and SW255, from 53.81 – 55.62 Mbp on chromosome 11 (**Supplemental Figure 9**). Among the ten QTLs that were outside the Sweep regions, one QTL was identified for mean fw and located on chromosome 5 (fw 5.1) in position 4.52 Mbp. This QTL was mapped in a region holding other QTLs segregating in the MAGIC population for fruit size, fruit width and fruit length (**Supplemental Table 6**; data from the experiment in Pascual et al. (2015)).

Candidate genes

Confidence intervals of the MAGIC-MET QTLs varied from 0.45Mbp to 87Mbp including a variable number of genes. We thus focused on QTLs presenting CI regions smaller than 2Mbp for candidate gene screening. From 49 (nflw12.1) to 256 (diam4.1) genes were within the regions of the selected QTLs. Taking advantage of the parental allelic effect, the CG were narrowed for each QTL by contrasting the allelic effect of the eight parental lines. The selected candidates after the filtering procedure are presented in the **Supplemental Table 7**, highlighting interesting candidates for further studies. Flowering time QTLs for instance included some CG with consistent matching regarding their functional annotation. For example, the QTL ppflw11.1 CI on chromosome 11 included two CG: Solyc11g070100 and Solyc11g071250 corresponding to “Early flowering protein” (ELF) and “EMBYO FLOWERING 1-like protein” (EMF1), respectively. Among other potential flowering candidates, we noticed Solyc12g010490 (AP2-like ERF) for the QTL flw12.1 and Solyc03g114890 and Solyc03g114900 (COBRA-like proteins) for the QTL flw3.2. Aside flowering time, the selected

candidate genes for the QTLs diam4.1 and ppSSC1.1 included the Solyc04g081870 (annotated as an Expansin gene) and Solyc01g006740 (annotated as Sucrose phosphate phosphatase) genes, respectively.

We could identify some plasticity QTLs showing sensitivity to the environmental conditions, notably the QTLs detected using the Scv plasticity parameter. Candidate genes were screened for some QTLs falling into this category. The ppfw9.1 QTL CI for example, showing susceptibility to the SDD day, carried a chaperone candidate (solyc09g091180) which might be involved in regulating fruit weight depending on the SDD variation. Similarly the QTL ppleaf11.1 is affected by the maximal temperature (Supplemental Table 4). Three CG (Solyc11g071830, Solyc11g071930 and Solyc11g071710) belonging to the Chaperone J-domain family, were retained after the filtering procedure in the region of the QTL. Notably, the DnaJ-like zinc-finger gene (Solyc11g071710) was among the candidate genes corresponding to several plasticity QTL including ppflw11.1, ppleaf11.1, ppnflw11.1, ppht11.1 and ppdiam11.2. This gene presented a total of 122 polymorphisms across the eight parental lines among which 35 and 68 are in the up-stream and down-stream gene region. Further investigation regarding this gene is needed to state its potential pleiotropic effect.

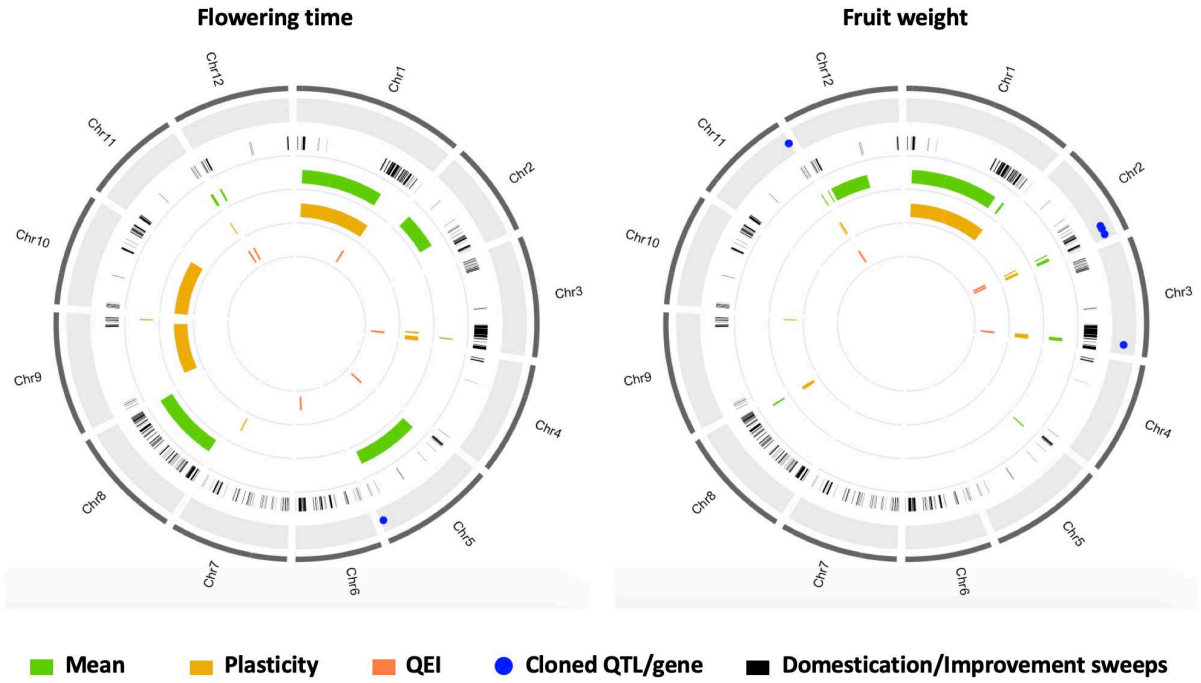

Figure 5: Physical positions of the MAGIC-MET QTLs for fruit weight and flowering time. The following circle with black bars represents the different domestication/ improvement sweep regions identified in (Zhu et al. 2018). The other circles plot the CI of QTLs identified on mean, plasticity or with QEI analysis.

DISCUSSION

Genetic variability in tomato response to environmental variation

Genotype-by-environment interaction has been a long-standing challenge for breeders and the predicted climate change has encouraged plant geneticists to devote more attention into understanding its genetic basis. Tomato is a widely cultivated crop with high adaptability to a variety of environmental conditions (Rothan et al. 2019). However, important incidences of abiotic stress in the final productivity, fruit quality and reproductive performance have been noticed (Mitchell et al. 1991; Estañ et al. 2009; Albert et al. 2016; Xu et al. 2017). We quantified the level of GxE and the subjacent phenotypic plasticity in a multi-environment trial – involving induced water-deficit, salinity and heat stresses – in a highly recombinant tomato population. An important genetic variability was observed for the plasticity traits related to yield, fruit quality, plant growth and phenology (**Supplemental Figure 6**). This highlights an important characteristic of the MAGIC population as a valuable resource for tomato breeding in dynamic changing environments. Tomato wild species have been also characterized as an important reservoir for abiotic stress tolerance genes (Foolad, 2007). However, their effective use in breeding programs could be difficult due to undesirable linkage drag notably for fruit quality. Unlikely, the MAGIC population characterized here is an intra-specific population with high diversity of fruit quality component which provides a great advantage as a breeding resource compared to wild populations.

Several statistical models are available to explore, describe and predict GxE in plants (Yan et al. 2007; Malosetti et al. 2013). Factorial regression model is among the most attractive as it allows to describe the observed GxE regarding relevant environmental information. We used the factorial regression model with different environmental covariates that are readily accessible from year to year, which allowed us to predict a variable proportion of the observed GxE (**Supplemental Figure 4**). Besides, each MAGIC line was characterized for its sensitivity to the growing climatic conditions (**Supplemental Data**); opening avenues to effectively select interesting genotypes for further evaluation in breeding programs targeting stressful environments.

Interestingly we found significant correlation between the genotypic sensitivities to the different environmental covariates and slopes from the Finlay-Wilkinson regression model (**Supplemental Figure 10**). This emphasizes the adequacy of the selected environmental covariates to explain differences observed in the average performance of the genotypes across environments. Conversely, slope and VAR showed less significant correlations, although they were both correlated to mean phenotypes in the same direction – except for SSC (**Figure 2**). This may be induced by distinct genetic regulation of these two plasticity parameters which reflect different types of agronomic stability (Lin

et al. 1986). Indeed, we identified 7 and 14 plasticity QTLs that were specific to VAR and slope, respectively (**Supplemental Table 4**). The correlation pattern of the different plasticity parameters evokes a complex regulation of plasticity which besides is seemingly trait-specific.

Significant correlation at phenotypic level might result from the action of pleiotropic genes. The **Figure 2** displays the correlations between mean and plasticity which were significant for almost every trait at variable degree. These correlations were reflected at the genetic level by 22 QTLs overlapping between mean and plasticity parameters, representing about 21% of all identified QTLs. A high proportion of the QTLs were mean or plasticity specific (**Supplemental Figure 11**) hence suggesting the action of both common and distinct genetic loci in the control of mean and plasticity variation in tomato.

Genomic location of the MAGIC-MET QTLs

The availability of substantial genomic information in tomato enabled the identification of different genomic regions (Sweeps) which were strongly selected during the domestication and improvement process (Lin et al. 2014; Zhu et al. 2018). When projected on the physical positions of the tomato reference genome (SL2.50 version), most of the plasticity QTLs we identified were located within the Sweep regions defined by Zhu et al. (2018). It therefore suggests that plasticity might have been selected together with other interesting agronomic traits during tomato domestication and improvement. For instance, this is corroborated by the positive correlation between slope (from the Finlay-Wilkinson regression model) and mean fruit weight variation. Indeed, genotypes with higher fw slope are characterized by good adaptability in high quality environments and will likely be intended to selection. Co-selection of allelic variants leading to higher performance in optimal condition together with plasticity alleles is a realistic assumption that would explain the significant correlation that we observed between mean and plasticity. In rice for instance, *GhD7* has been described as a key high-yield gene simultaneously involved in the regulation of plasticity of panicle and tiller branching and involved in abiotic stress response (Herath 2019). This example highlights a gene carrying different allelic variants affecting together plasticity and mean phenotypes. Further investigations are needed to assess how domestication and breeding have affected plasticity in tomato and other crop species.

An important genomic region involved in the genetic regulation of plasticity for six different traits was identified in chromosome 11 (**Supplemental Figure 9**). This region is obviously a regulatory hub carrying interesting plasticity genes. It remains to determine if the co-localization of the different plasticity QTLs in this region is due to the action of a pleiotropic gene or different linked genes. Nevertheless, the chromosome 11 region highlighted here is an interesting target for breeding as

well as for understanding the functional mechanisms of plasticity genes.

Allelic-sensitivity vs Gene-regulatory model

Sixty-three plasticity QTLs were identified among which 22 (35%) were identified as well with mean phenotypes and 65% were specific to plasticity. Via et al. (1995) proposed two genetic models – the allelic-sensitivity and gene-regulatory models –among the mechanisms involved in the genetic control of phenotypic plasticity. These two models are distinguishable through QTL analysis (Ungerer et al., 2003) with the expectation that allelic-sensitivity model will lead to co-localization of mean and plasticity QTLs, while a distinct location of QTLs affecting mean and plasticity corresponds to the gene-regulatory model (Kusmec et al., 2017). Regarding our results, both models are suspected to regulate tomato plasticity, even though the gene-regulatory model is predominant with 65% of the plasticity QTLs that did not co-localize with mean QTLs for the same trait. In maize, using a larger number of environments and traits, Kusmec et al. (2017) found similar results and even a higher rate of distinct locations of plasticity and mean QTLs. Studying plasticity as a trait *per se* is therefore of a major interest since breeding in both direction (considering the mean phenotype and its plasticity) is achievable. Through transcriptomic analyses, Albert et al. (2018) observed that genotype-by-water deficit interaction was mostly associated to *trans*-acting genes which we can be assimilated to the gene-regulatory model in agreement with our results.

Although the distinct location of plasticity and mean QTLs could be confidently assigned to the action of genes in interaction, the co-localization of mean and plasticity QTLs is not necessarily a case of allelic-sensitivity regulation, especially if the QTL is in a large region. Indeed, the allelic-sensitivity model assumes that a constitutive gene is directly sensitive to the environment regulating its expression across different environmental conditions, inducing hence phenotypic plasticity. This is a very strong hypothesis regarding the QTLs since the overlapping region between mean and plasticity could carry different causal variants in strong linkage disequilibrium affecting for each either mean or plasticity. Thus, co-locating mean and plasticity QTLs should be not automatically imputed to the allelic-sensitivity model. We found a total of 22 constitutive QTLs between mean and plasticity for the ten measured traits (**Supplemental Table 4**). Considering the estimated QTL effects, the variation patterns of the eight parental allelic classes were compared between mean and PP QTL of the same trait. Only ten QTL showed consistent allelic effects (Spearman correlation significant at 0.05 threshold level) strengthening the hypothesis of the allelic-sensitivity model for these QTLs (**Figure 6**). Further studies should help to elucidate and validate the candidate plasticity genes and to clarify their functional mechanism.

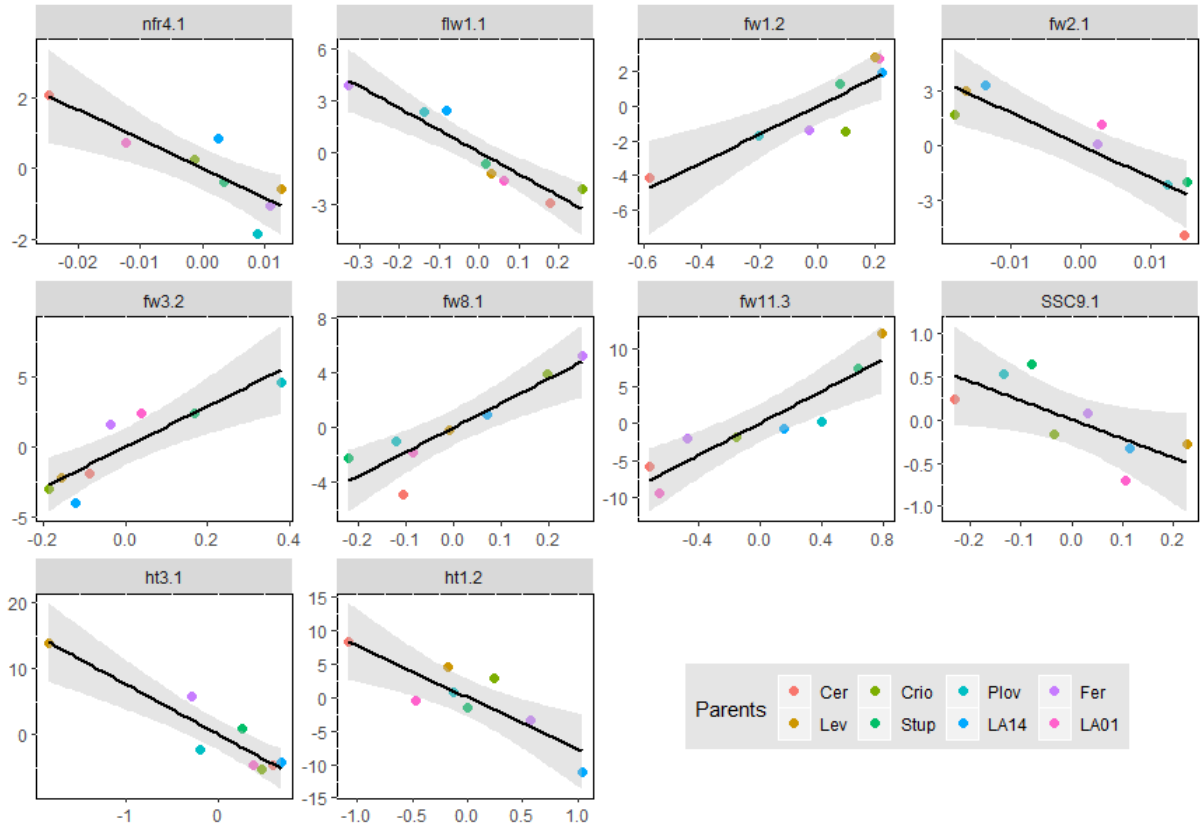

Figure 6: Correlation of the estimated allelic effect for consistent QTLs between mean and plasticity phenotypes.

Complementary methods to identify QTLs sensitive to environmental variation

Different approaches have been proposed in the literature to dissect GxE into its genetic components (Malosetti et al. 2013; El-Soda et al. 2014). We used a mixed linear model with a random genetic effect accounting for the correlation structure of the MAGIC-MET design to identify the QEI. Extending the use of mixed linear models to MAGIC populations in the framework of MET analysis has been very rarely applied in crops. To our knowledge, only Verbyla et al., (2014) applied such approach in wheat and identified QEI for flowering time. Our model was adapted from Giraud et al. (2017) and was adequate to account for the complex mating design of the MAGIC population. Indeed, it allows estimating the QTL effect for each parental allelic class and for each environment at every SNP marker. Overall, 28 QEI were detected showing significant marker x environment interaction for ten traits.

Methods using plasticity as a trait *per se* are also attractive to identify environmentally sensitive QTLs. This strategy was applied in maize, sunflower, barley and soybean to detect the loci governing GxE (Lacaze et al. 2009; Gage et al. 2017; Mangin et al. 2017; Kusmec et al. 2017; Xavier et al. 2018). With different plasticity parameters, we identified a total of 63 plasticity QTLs and only 24% were also identified with the QEI models. Thus both methods, using plasticity or mixed linear models, are

complementary approaches to study the genetic component of GxE.

Candidate genes

Multi-parental populations are powerful for QTL mapping studies (Huang et al. 2012; Kover et al. 2009) and besides are interesting for fine mapping and candidate gene selection. Barrero et al. (2015) for instance considered the variation of the QTL effect estimated for the different parental lines, combined with transcriptomic analyses to efficiently identify candidate genes. Similarly, Septiani et al. (2019) narrowed candidate genes for Fusarium resistance in a maize MAGIC population using allelic effect of the MAGIC parents.

A number of candidate genes were proposed in our study affecting both tomato mean and plasticity variation. These candidate genes were selected based on the parental allelic effect and represent valuable targets for future studies attempting to characterize the molecular mechanisms underlying plasticity genes in tomato. Indeed, relevant candidate genes were proposed for flowering time plasticity including the Solyc11g071250 corresponding to an "EMBYO FLOWERING 1-like protein" (EMF1). The implication of EMF1 in flowering time has been observed in Arabidopsis by Aubert et al., (2001) who highlighted an indirect effect of EMF1 on flowering time and inflorescence. More recently, Luo et al., (2018) outlined the role of EMF1 interacting with CONSTANS proteins in a complex pathway to regulate the expression of flowering time genes in Arabidopsis. Solyc11g070100 which is annotated as "Early flowering protein" (ELF) gene is also an interesting candidate for flowering time regulation. It was observed across species that a consistent expression of ELF3 can extend the rapid transition to flowering (Huang et al., 2017). ELF3 loss of function is therefore expected to trigger early flowering according to these authors. Interestingly, Solyc11g070100 was affected by 69 SNPs and 14 INDELs polymorphisms, among which only one SNP showed polymorphism variation in line with the estimated allelic effect for the eight parental lines at this QTL. This SNP was localized at the position 54,632,225 bp in chromosome 11, upstream the gene Solyc11g070100. The parent LA1420 carried the reference allele at this SNP while the remaining parents held the alternative allele. Considering the estimated allelic effects at this QTL, we could assume that the LA1420 allele variant might induce an early flowering phenotype comparatively to the other parents.

Conclusion

We aimed to dissect the genetic architecture of tomato response to different environments involving control and stress growing conditions. The MAGIC population demonstrated a large genetic variability in response to abiotic stresses which was reflected by the identification of 63 plasticity

QTLs. This was achieved through the use of different plasticity parameter highlighting the importance of plasticity quantification for deciphering its genetic basis. The plasticity QTLs were in majority (65% of the plasticity QTLs) located in distinct regions than the QTLs detected for the mean phenotypes, suggesting a specific genetic control of mean trait variation and plasticity at some extent. Using plasticity as a trait per se in mapping analysis turned out to be a good method for identifying genetic regions underlying GxE. Almost all the QEI were also identified for at least one of the plasticity parameters.

Overall, this study presents the MAGIC population as a powerful resource for tomato breeding under abiotic stress conditions, as well as for understanding the genetic mechanisms regulating tomato response to environmental variation.

References:

Albert, E., Duboscq, R., Latreille, M., Santoni, S., Beukers, M., Bouchet, J.-P., et al. (2018) Allele specific expression and genetic determinants of transcriptomic variations in response to mild water deficit in tomato. *Plant J*.

Albert, E., Segura, V., Gricourt, J., Bonnefoi, J., Derivot, L., and Causse, M. (2016) Association mapping reveals the genetic architecture of tomato response to water deficit: focus on major fruit quality traits. *J Exp Bot*. 67: 6413–6430.

Aubert, D., Chen, L., Moon, Y.H., Martin, D., Castle, L.A., Yang, C.H., et al. (2001) EMF1, a novel protein involved in the control of shoot architecture and flowering in Arabidopsis. *Plant Cell*. 13: 1865–75.

Barrero, J.M., Cavanagh, C., Verbyla, K.L., Tibbits, J.F.G., Verbyla, A.P., Huang, B.E., et al. (2015) Transcriptomic analysis of wheat near-isogenic lines identifies PM19-A1 and A2 as candidates for a major dormancy QTL. *Genome Biol*. 16: 93.

Bradshaw, A.D. (1965) Evolutionary Significance of Phenotypic Plasticity in Plants. *Adv Genet*. 13: 115–155.

Broman, K.W., Gatti, D.M., Simecek, P., Furlotte, N.A., Prins, P., Sen, Ś., et al. (2019) R/qtl2: Software for Mapping Quantitative Trait Loci with High-Dimensional Data and Multiparent Populations. *Genetics*. 211: 495–502.

Causse, M., Desplat, N., Pascual, L., Le Paslier, M.-C., Sauvage, C., Bauchet, G., et al. (2013) Whole genome resequencing in tomato reveals variation associated with introgression and breeding events. *BMC Genomics*. 14: 791.

Costa, J.M., Ortuño, M.F., and Chaves, M.M. (2007) Deficit Irrigation as a Strategy to Save Water: Physiology and Potential Application to Horticulture. *J Integr Plant Biol*. 49: 1421–1434.

Diouf, I.A., Derivot, L., Bitton, F., Pascual, L., and Causse, M. (2018) Water Deficit and Salinity Stress Reveal Many Specific QTL for Plant Growth and Fruit Quality Traits in Tomato. *Front Plant Sci*. 9: 279.

Driedonks, N., Wolters-Arts, M., Huber, H., de Boer, G.-J., Vriezen, W., Mariani, C., et al. (2018) Exploring the natural variation for reproductive thermotolerance in wild tomato species. *Euphytica*. 214: 67.

El-Soda, M., Malosetti, M., Zwaan, B.J., Koornneef, M., and Aarts, M.G.M. (2014) . Trends Plant Sci.

Estañ, M.T., Villalta, I., Bolarín, M.C., Carbonell, E.A., and Asins, M.J. (2009) Identification of fruit yield loci controlling the salt tolerance conferred by solanum rootstocks. *Theor Appl Genet*. 118: 305–312.

Finlay, B.K.W., and Wilkinson, G.N. (1963) THE ANALYSIS OF ADAPTATION IN A PLANT-BREEDING PROGRAMME The ability of some crop varieties to perform well over a wide range of environ - mental conditions has lcng been appreciated by the agronomist and plant breeder . In the cereal belts of southern Au. .

Foolad, M.R. (2007) Genome mapping and molecular breeding of tomato. *Int J Plant Genomics*. 2007: 64358.

Gage, J.L., Jarquin, D., Romay, C., Lorenz, A., Buckler, E.S., Kaeppler, S., et al. (2017) The effect of artificial selection on phenotypic plasticity in maize. *Nat Commun*. 8: 1348.

Gillespie, J.H., and Turelli, M. (1989) Genotype-environment interactions and the maintenance of polygenic variation. *Genetics*. 121.

Giraud, H., Bauland, C., Falque, M., Madur, D., Combes, V., Jamin, P., et al. (2017) Reciprocal Genetics: Identifying QTL for General and Specific Combining Abilities in Hybrids Between Multiparental Populations from Two Maize (Zea mays L.) Heterotic Groups. *Genetics*. 207: 1167–1180.

Grandillo, S., Termolino, P., and van der Knaap, E. (2013) Molecular Mapping of Complex Traits in Tomato. In *Genetics, Genomics, and Breeding of Tomato*. pp. 150–227 Science Publishers.

Grilli, G., Trevizan Braz, L., Gertrudes, E., and Lemos, M. (2007) QTL identification for tolerance to fruit set in tomatoby fAFLP markers. *Crop Breed Appl Biotechnol*. 7: 234–241.

Herath, V. (2019) The architecture of the GhD7 promoter reveals the roles of GhD7 in growth, development and the abiotic stress response in rice. *Comput Biol Chem*. 82: 1–8.

Huang, B.E., and George, A.W. (2011) R/mpMap: A computational platform for the genetic analysis of multiparent recombinant inbred lines. *Bioinformatics*. 27: 727–729.

Huang, B.E., George, A.W., Forrest, K.L., Kilian, A., Hayden, M.J., Morell, M.K., et al. (2012) A multiparent advanced generation inter-cross population for genetic analysis in wheat. *Plant Biotechnol J*. 10: 826–839.

Huang, H., Gehan, M.A., Huss, S.E., Alvarez, S., Lizarraga, C., Gruebbling, E.L., et al. (2017) Cross-species complementation reveals conserved functions for EARLY FLOWERING 3 between monocots and dicots. *Plant Direct*. 1: e00018.

Kover, P.X., Valdar, W., Trakalo, J., Scarcelli, N., Ehrenreich, I.M., Purugganan, M.D., et al. (2009) A multiparent advanced generation inter-cross to fine-map quantitative traits in Arabidopsis thaliana. *PLoS Genet*. 5: e1000551.

Kusmec, A., Srinivasan, S., Nettleton, D., and Schnable, P.S. (2017) Distinct genetic architectures for phenotype means and plasticities in Zea mays. *Nat Plants*. 3: 715–723.

Lacaze, X., Hayes, P.M., and Korol, A. (2009) Genetics of phenotypic plasticity: QTL analysis in barley, Hordeum vulgare. *Heredity (Edinb)*. 102: 163–173.

Laitinen, R.A.E., and Nikoloski, Z. (2019) Genetic basis of plasticity in plants. *J Exp Bot*. 70: 739–745.

Lê, S., Josse, J., and Husson, F. (2008) FactoMineR: An R package for multivariate analysis. *J Stat Softw*. 25: 1–18.

Lin, C.S., Binns, M.R., and Lefkovitch, L.P. (1986) Stability Analysis: Where Do We Stand?1. *Crop Sci*. 26: 894.

Lin, T., Zhu, G., Zhang, J., Xu, X., Yu, Q., Zheng, Z., et al. (2014) Genomic analyses provide insights into the history of tomato breeding. *Nat Genet*. 46: 1220–1226.

Luo, X., Gao, Z., Wang, Y., Chen, Z., Zhang, W., Huang, J., et al. (2018) The NUCLEAR FACTOR-CONSTANS complex antagonizes Polycomb repression to de-repress FLOWERING LOCUS T expression in response to inductive long days in Arabidopsis. *Plant J*. 95: 17–29.

Malosetti, M., Ribaut, J.-M., and van Eeuwijk, F.A. (2013) The statistical analysis of multi-environment data: modeling genotype-by-environment interaction and its genetic basis. *Front Physiol*. 4: 44.

Mangin, B., Casadebaig, P., Cadic, E., Blanchet, N., Boniface, M.-C., Carrère, S., et al. (2017) Genetic control of plasticity of oil yield for combined abiotic stresses using a joint approach of crop modelling and genome-wide association. *Plant Cell Environ*. 40: 2276–2291.

Mitchell, J., Shennan, C., and Grattan, S. (1991) Developmental-Changes in Tomato Fruit Composition in Response To Water Deficit and Salinity. *Physiol Plant*. 83: 177–185.

Munns, R., and Gilliham, M. (2015) Salinity tolerance of crops - what is the cost? *New Phytol*. 208: 668–673.

Pascual, L., Desplat, N., Huang, B.E., Desgroux, A., Bruguier, L., Bouchet, J.-P.P., et al. (2015) Potential of a tomato MAGIC population to decipher the genetic control of quantitative traits and detect causal variants in the resequencing era. *Plant Biotechnol J*. 13: 565–577.

Ripoll, J., Urban, L., Staudt, M., Lopez-Lauri, F., Bidel, L.P.R., and Bertin, N. (2014) Water shortage and quality of fleshy fruits—making the most of the unavoidable. *J Exp Bot*. 65: 4097–4117.

Rothan, C., Diouf, I., and Causse, M. (2019) Trait discovery and editing in tomato. *Plant J*. 97: 73–90.

Scheiner, S.M. (1993) Genetics and Evolution of Phenotypic Plasticity. *Annu Rev Ecol Syst*. 24: 35–68.

Septiani, P., Lanubile, A., Stagnati, L., Busconi, M., Nelissen, H., Pè, M.E., et al. (2019) Unravelling the genetic basis of fusarium seedling rot resistance in the MAGIC maize population: Novel targets for breeding. *Sci*

Rep. 9: 4–13.

Ungerer, M.C., Halldorsdottir, S.S., Purugganan, M.D., and Mackay, T.F.C. (2003) Genotype-environment interactions at quantitative trait loci affecting inflorescence development in Arabidopsis thaliana. *Genetics*. 165: 353–365.

Valladares, F., Sanchez-Gomez, D., and Zavala, M.A. (2006) Quantitative estimation of phenotypic plasticity: bridging the gap between the evolutionary concept and its ecological applications. *J Ecol*. 94: 1103–1116.

Verbyla, A.P., Cavanagh, C.R., and Verbyla, K.L. (2014) Whole-Genome Analysis of Multienvironment or Multitrait QTL in MAGIC. *G3 Genes, Genomes, Genet*. 4.

Via, S., Gomulkiewicz, R., De Jong, G., Scheiner, S.M., Schlichting, C.D., and Van Tienderen, P.H. (1995) Adaptive phenotypic plasticity: consensus and controversy. *Trends Ecol Evol*. 10: 212–7.

Villalta, I., Bernet, G.P., Carbonell, E.A., and Asins, M.J. (2007) Comparative QTL analysis of salinity tolerance in terms of fruit yield using two solanum populations of F7 lines. *Theor Appl Genet*. 114: 1001–1017.

Xavier, A., Jarquin, D., Howard, R., Ramasubramanian, V., Specht, J.E., Graef, G.L., et al. (2018) Genome-Wide Analysis of Grain Yield Stability and Environmental Interactions in a Multiparental Soybean Population. *G3 (Bethesda)*. 8: 519–529.

Xu, J., Driedonks, N., Rutten, M.J.M., Vriezen, W.H., de Boer, G.-J., and Rieu, I. (2017a) Mapping quantitative trait loci for heat tolerance of reproductive traits in tomato (Solanum lycopersicum). *Mol Breed*. 37: 58.

Xu, J., Wolters-Arts, M., Mariani, C., Huber, H., and Rieu, I. (2017b) Heat stress affects vegetative and reproductive performance and trait correlations in tomato (Solanum lycopersicum). *Euphytica*. 213: 156.

Yan, W., Kang, M.S., Ma, B., Woods, S., and Cornelius, P.L. (2007) GGE Biplot vs. AMMI Analysis of Genotype-by-Environment Data. *Crop Sci*. 47: 643.

Zhao, C., Liu, B., Piao, S., Wang, X., Lobell, D.B., Huang, Y., et al. (2017) Temperature increase reduces global yields of major crops in four independent estimates. *Proc Natl Acad Sci*. 114: 9326–9331.

Zhu, G., Wang, S., Huang, Z., Zhang, S., Liao, Q., Zhang, C., et al. (2018) Rewiring of the Fruit Metabolome in Tomato Breeding. *Cell*. 172: 249-261.e12.

Supplementary Materials:

The supplemental figures and tables of this chapter are presented in Appendix 6.

NB: Supplemental tables 6 and 7 and the supplemental Data can be accessed online:

Supplemental Figure 1: Selection of 7 environmental covariates for the factorial regression model. Three periods – each of 20 days – were defined from planting to the end of flowering on the 4th truss. The period from 20 to 60 days after planting (DAP) covered vegetative growth and flowering on the 4th truss and the measured climatic variables averaged during this period. The different environmental covariates are described

Supplemental Figure 2: Boxplot distribution of the traits across environments. The colors of the boxplot are according to the groups defined by clustering of the environments

Supplemental Figure 3: Heritability in the MAGIC-MET design. For each trait, heritability was computed at every environment and plotted with heritability of the full design $\boldsymbol{H^2}$ (in green)

Supplemental Figure 4: Proportion of the sum of square attributed to the different factors in the factorial regression model. For each trait, the orange and green stacked bars represent the proportion of the SSq explained by the Genotype and Environment factors in model (4). The remaining colors represent the effect part of the GxE that could be explained by the different environmental covariates. Only significant covariates were highlighted within the bars.

Supplemental Figure 5: Reaction norms from the Finlay-Wilkinson regression model (A) and the factorial regression model (B). In figure 5 A, the blue and orange lines represent the positive and negative reaction norms. In Figure 5 B, the green and purple lines represent the positive and negative reaction norms

Supplemental Figure 6: Histogram distribution of mean and all plasticity parameters for each trait

Supplemental Figure 7: Physical positions of the MAGIC-MET QTLs for diam, leaf, height, fset, nflw, nfr, firm and SSC. The outer circle with gray font represents the known and cloned QTL/gene for each trait. The following circle with black bars represents the different domestication/improvement sweep regions identified in (Zhu et al. 2018). The other circles plot the CI of QTLs identified on mean (green), plasticity (orange) or with QEI analysis (purple)

Supplemental Figure 8: Number of the MAGIC-MET QTLs identified within or outside the domesticated/improved regions. Only the MAGIC-MET QTLs within short CI (lower than 2Mbp) were considered. The response specific category included QEI and plasticity specific QTLs; the common category correspond to QTLs that were commonly identified on mean, plasticity and QEI or at least two of them

Supplemental Figure 9: Zoom plot on Chromosome 11 region from 53 -57 Mbp. Each color represents a different QTL located in this region and the top black bars are the Sweep regions SW254 and SW255

Supplemental Figure 10: Correlation between the genotypic sensitivities to environmental covariates from the factorial regression model and slopes from the Finlay-Wilkinson regression model

Supplemental Figure 11: Venn diagram of the number of QTL specific or commonly detected with mean, PP or using the QEI models.

Supplemental Table 1: Description of the MAGIC-MET design with the 12 environments and their respective names

Supplemental Table 2: Description of the phenotypic traits evaluated in the MAGIC-MET design

Supplemental Table 3: Estimates of the variance components from model (2)

Supplemental Table 4: Results of QTL and QEI analysis in the MAGIC-MET design

Supplemental Table 5: Genetic location of the MAGIC-MET QTLs overlapping with the Sweep (domestication/improvement) regions.

Supplemental Table 6: QTLs identified for fruit size, fruit width and fruit length in the MAGIC population

Supplemental Table 7: Selected candidate genes for all the mean and plasticity QTLs located within 2Mbp CI region

Chapter 7

General Discussion

Chapter 7 presents a global discussion of the results described in the previous chapters. This chapter presents on overall perspective for deciphering the complexity of the molecular mechanisms underlying plant response to environment. Prospects for breeding tomato under abiotic stresses scenario are suggested.

Outline

Understanding the molecular basis of plant response to environmental stresses is a main goal for breeding in the 21st century due to climate change. Indeed, the recent report of the Intergovernmental Panel on Climate Change (IPPC) emphasizes the need of developing strategies for adapting agriculture and cropping systems to a global increase in temperatures (Hoegh-Guldberg et al., 2019). Genetics and breeding can contribute achieving more sustainable agriculture through the development of climate-smart crops that would show high resilience to environmental variation and adequate yield and nutritional quality of crops intended for human consumption. It is in this context that researchers have deployed so much effort to understand and decipher the genetic basis of plant adaptation to environment for many cultivated crops including tomato. Tomato is among the major consumed vegetables with a high nutritional value (Rothan et al., 2019). It is available worldwide in many different environments. However, yield and quality in tomato are importantly affected by growing conditions notably the irrigation systems and ambient temperatures in either field or greenhouse (Mitchell et al., 1991; Rainwater et al., 1996). We thus conducted this project to get more insight into tomato behavior under water deficit (WD), high temperature (HT) and salinity stress (SS) conditions and its underlying genetic component. The major observation was that tomato is negatively affected by all these stresses regarding yield component traits. However, the reduction in yield is balanced by increasing fruit quality component with higher soluble solid content (SSC) notably, under WD and SS conditions (see Chap III). High temperature importantly affected reproductive and growth traits compared to the other stresses (**Figure 1**). These changes observed in different phenotypic traits were reflected by complex genetic regulation with a polygenic control (see chapter 3, 5 and 6). The chapter 4 also highlighted an important impact of WD on transcriptome variation which besides strongly interact with the genetic background. Bringing these results all together opens new perspectives for future studies attempting to decipher more sharply the molecular mechanisms of phenotypic plasticity in response to abiotic stresses. This also raises questions about the methodological approach to detect the genomic regions associated with plant response to environmental variations. Finally, breeding strategies for developing environmentally adapted crop will be discussed.

1. Statistical modelling for the dissection of loci controlling GxE in MET designs

This study was designed to identify tomato genetic loci involved in GxE in the context of abiotic stresses. A key step forward in the detection of such loci relies on the statistical models applied. El-Soda et al., (2014) presented a number of models available in the literature that could be used in the context of multi-environment trials (MET). The early studies investigating interactive QTL (QEI) just compared QTLs detected in each environment separately (Paterson et al., 1991). Single environment QTL analyses were conducted for every trait and environment but these results were not fully

presented in the earlier chapters. A total of 240 QTLs were detected this way for 18 traits in 12 environments (**Appendix 7**). The stress response QTLs presented in chapter III and V were detected with univariate approaches based on the calculation of plasticity parameters that were later considered as input phenotypes through classical QTL analysis methods. In chapter VI, multivariate mixed models which accounted for the correlation structure between environments were used and tested QTL main effects and QEI using the genotype means per environment data. QEI detection in the MAGIC populations has been scarcely conducted in plants through linear mixed models due to the complex mating design. Verbyla et al., (2014) presented a multivariate approach for multi-environment or multi-trait QTL analysis in MAGIC populations implemented in the R-package *mpwgaim*. This method accounts for probabilities of inheriting founder alleles and is based in a forward QTL selection where the effects of significant QTLs are modelled as random effects (contrary to our model) in the course of the cofactors selection. The univariate and multivariate models are complementary methods to characterize the genetics of GxE. Nevertheless, considering plasticity as a trait per se identified some regions involved in the occurrence of GxE that were not detected using only the multivariate approach.

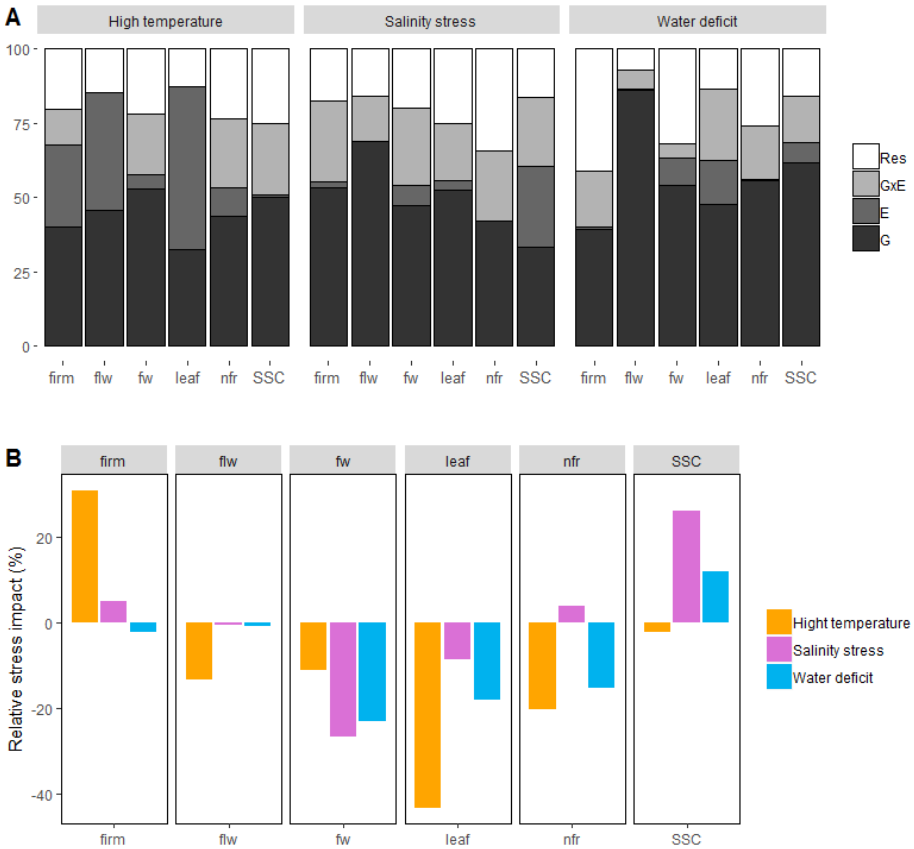

Figure 1: Impact of water deficit (WD) high temperature (HT) and salinity stress (SS) at the phenotypic level**. A)** The proportion of variance attributed to genotype, stress condition and their interaction on different traits commonly measured across stress trials. **B)** Relative stress impact (RSI) induced by stresses on traits related to fruit quality, plant growth and phenology in the MAGIC population.

Environmental characterization was performed in our study by using the available climatic variables that were daily recorded within greenhouses. Although these climactic covariates significantly explained a proportion of the GxE (see Chap VI), they do not fully represent all the environment features. Indeed, most of the studied environmental covariates were associated to temperature parameters measured in the ambient greenhouse environments. The inclusion of other parameters from the substrate conditions (notably the electro-conductivity and soil humidity) would have allowed better characterizing the environments and accounting for all stress-related climatic covariates. We used averaged values of the environmental covariates through the period covering flowering time (on the 4th truss) of the MAGIC population. However, environmental covariates could also be derived by defining different stress thresholds and clustering the environments according to stress limiting factors as presented by (Bouffier et al., 2015).

We identified four different groups through the clustering analysis of the MAGIC-MET design (see Chap VI). These different groups may be considered as representative of an environmental scenario and used directly in the GxE analysis. Prediction of the genotype performances might be possible for new environments that would cluster in one of the defined groups.

2. Genetic control of phenotypic plasticity

We first recall the definition of phenotypic plasticity (PP) which is considered as the ability of an organism to express different phenotypes when exposed to new environmental conditions (Bradshaw, 1965). It obviously play an important role in plant evolution; however distinction between adaptive and non-adaptive PP have been emphasized (Ghalambor et al., 2007). In the agronomic context, plasticity may be undesired as it causes non-stable agronomic performance when environmental variations are important. However, understanding its genetic basis is an important step for developing new cultivars adapted to specific conditions, especially stressful environments.

We emphasized an important genetic variability for plasticity response under WD and SS in the MAGIC population with at least 15 plasticity QTLs (see chapter 3 Diouf et al., (2018)). The MAGIC lines also showed important variability for response to HT stress for which 16 PP QTLs were identified (see Chap V). Six traits (flowering time, leaf length, fruit firmness, SSC, fruit weight and number of fruits) were commonly measured in all the WD, SS and HT trials. Among the 20 PP QTLs detected for these traits no PP QTL was common to the different trials highlighting the presence of stress-specific regions involved in the MAGIC population in response to WD, SS and HT (**Figure 2**). The chapter VI intended to detect tomato genomic regions involved in a general response of environmental variation including controlled and stressed conditions. This analysis revealed 63 plasticity QTLs for a total of 10 phenotypic traits. Considering the six traits commonly measured in WD, SS and HT stress

conditions, a total of 51 plasticity QTLs were detected and a majority of these (82%) were specific (**Figure 2**). Thus we assume that the genetic control of plasticity is highly dependent on the range of the environments (and their characteristics) considered in the analysis and on the measured phenotypic traits. These results altogether revealed that tomato plasticity in response to abiotic stresses has a complex genetic control.

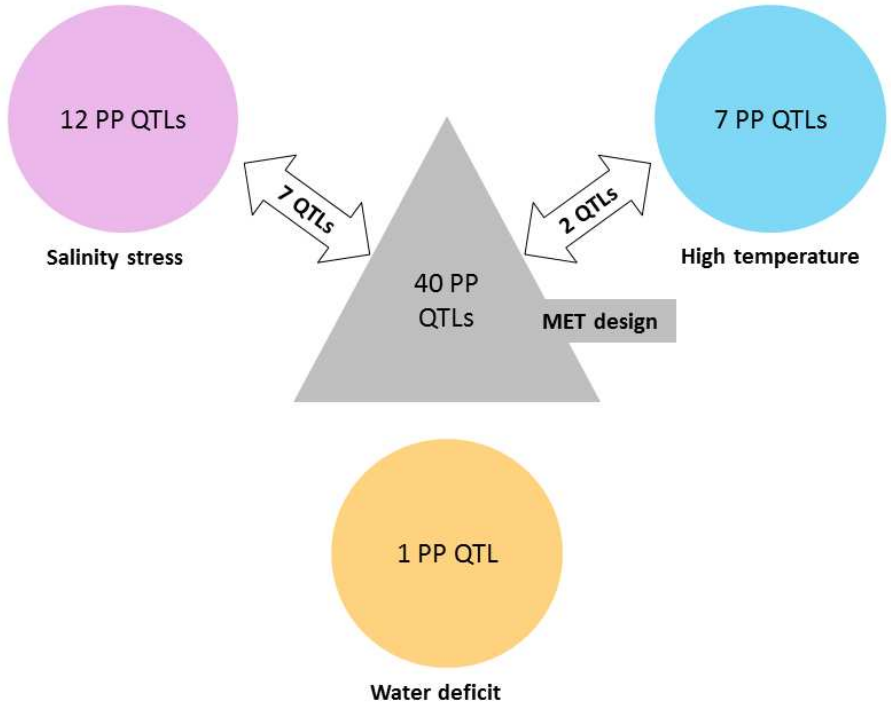

Figure 2: Summary of QTL detection for plasticity traits in the single stress analysis (Water deficit, High temperature and Salinity stress) and in the combined stress analysis (MET design). Numbers in the circles and the triangle indicate the number of plasticity QTLs detected in the single stress analyses and the combined stress analysis, respectively. The double arrows show the number of plasticity QTLs commonly detect between experiments.

2.1. Towards systems biology approach to better characterize genomic control of plasticity

As for any complex trait, the final output of plant responses to the environment is not expected to be clearly and reliably dissected through a single data-type analysis approach. Indeed, complex traits result from the interaction of regulatory mechanisms at different levels as illustrated in **Figure 3**, adapted from Ritchie et al., (2015). We highlighted in the introduction that morphological changes induced by abiotic stress responses generally come from regulation at the physiological, metabolic, transcriptomic and even post-translational levels. These different regulations might importantly affect plasticity response; hence it is necessary to combine multiple data type for a comprehensive understanding of molecular mechanisms underlying plasticity. Systems biology aims to identify regulatory hubs involved in complex networks regulating plant responses, through the integration of

different high throughput omics data such as transcriptomes, metabolomes and proteomes. Such approaches have been successfully used to identify and validate key genes regulating stress tolerance in plants (Cramer et al., 2011).

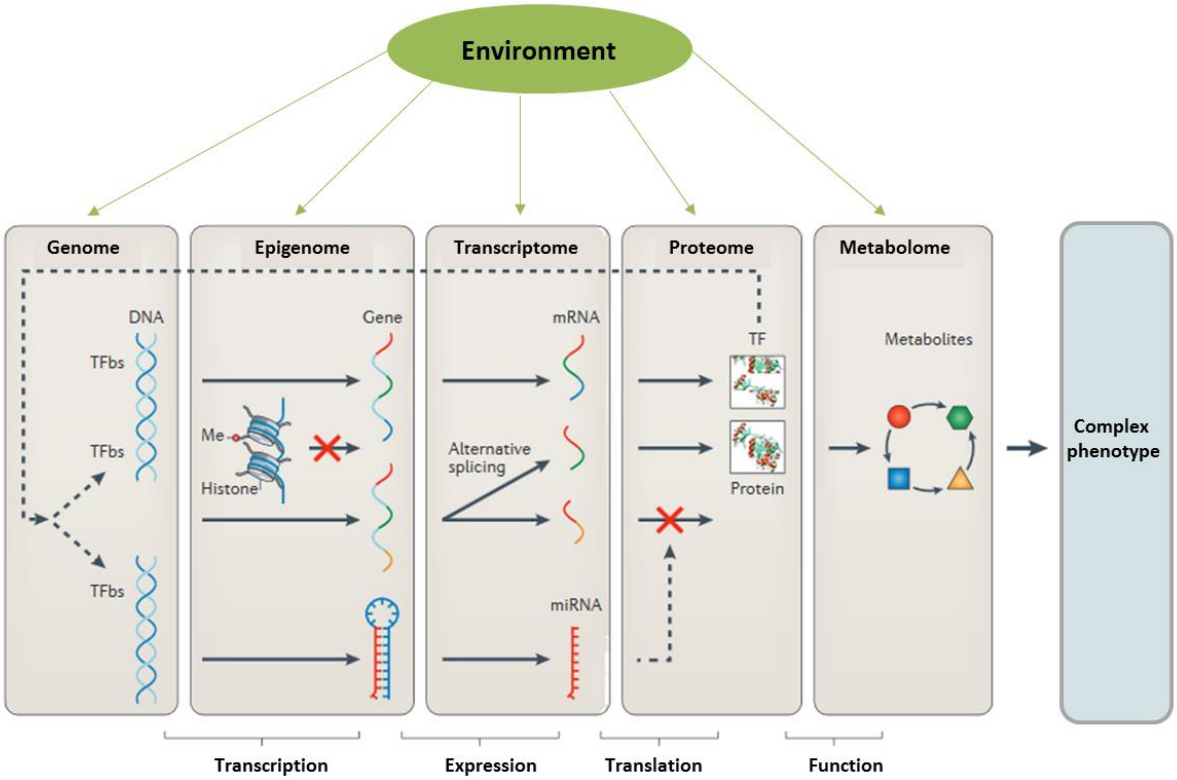

Figure 3: Biological systems multi-omics from the **genome** (single-nucleotide polymorphism, copy number variation, genomic rearrangement such as translocation), **epigenome** (DNA methylation, histone modification, chromatin accessibility, micro RNA (miRNA), transcription factor (TF) binding), **transcriptome** (gene expression and alternative splicing), **proteome** and **metabolome** to the phenome. Bold arrows indicate the flow of genetic information from the genome level to the metabolome level and, ultimately, to the phenome level. The red crosses indicate inactivation of transcription or translation and the green arrows the potential implication of environment at the different levels from genome to phenome. Adapted from (Ritchie et al., 2015).

1.1.1. Combining plasticity QTL information and gene expression data

Transcriptomic data are now routinely produced through microarray and RNA-seq technologies, enhancing our global understanding of plant transcriptome variation. Exploring gene expression variation patterns of the parental lines within QTL interval regions for a given mapping population is a practical approach to shorten the candidate gene list (Wayne and McIntyre, 2002; Lin et al., 2019). However, gene expression regulation have been widely investigated across species revealing a high variability according to genotypes, organs cells and tissues and the stages of RNA sampling (Van Veen et al., 2016; Sarazin et al., 2017). Thus the efficiency of such approach highly relies on the relevance of the gene expression data in relation to the measured phenotype for which QTLs were detected. The MAGIC populations offer besides higher resolution compared to bi-parental populations for narrowing candidate genes. For instance, candidate genes were selected based on the expression

level of genes within the interval region of QTLs for fusarium resistance (Septiani et al., 2019) and fiber length (Naoumkina et al., 2019) combined with polymorphism variations in maize and cotton MAGIC parental lines, respectively. A similar strategy was used in chapter IV where differentially expressed genes (DEG) under WD were selected within the WD and SS plasticity QTLs (Chap III, Diouf et al., (2018)) and candidate genes proposed based on the MAGIC parental haplotype status.

1.1.2. Expression QTL (eQTL) analysis

Another popular strategy combining QTL mapping and gene expression analysis is the expression QTL mapping approach (Waters et al., 2017; Albert et al., 2018). It relies mainly in the identification of genomic loci controlling variation in gene expression level. Early studies investigating eQTL in plants were conducted on Arabidopsis (Lall et al., 2004; Keurentjes et al., 2007). A key feature in eQTL analyses is that the detected regions could be classified as *cis* or *trans* regulatory category furthering our understanding of the regulatory mechanisms underlying gene expression control. *Cis* and *trans*-eQTL are considered when the regulatory alleles are expected to affect the transcript level of the gene itself or other genes located in different genomic position, respectively. This classification can be mirrored to that of plasticity QTLs generally categorized as being under the "allele-sensitivity" or "gene-regulatory" genetic model. These classifications are both based on results from statistical modelling and *cis*-eQTL and allele-sensitivity QTL should be interpreted with the utmost cautious as their definition relies upon threshold used to define confidence interval regions of the e-QTL/QTL. Analyses of eQTL are usually conducted in a subset of genes selected upon the goals of the study. We believe that the genes identified within the interval regions of plasticity QTLs throughout this manuscript are good candidates for first screening and could be selected for further e-QTL mapping study.

1.1.3. Metabolite QTL (mQTL)

The biochemical pathways involved in plant response to abiotic stresses are highly impacted by metabolic regulation upon exposure to stress conditions. It is therefore rational to investigate the genomic regions associated to such changes, which is possible by considering metabolite level as a quantitative trait. The genetic basis of metabolite variation has been studied in plants through linkage and association analyses in order to detect loci involved in metabolic pathways regulation (Keurentjes et al., 2006; Luo, 2015). The physiological status of plants under abiotic stress conditions might be reflected by the metabolites accumulated in different tissues. The characterization of mQTL against specific stress conditions is therefore a straightforward method to detect mQTL affected by stress conditions. For instance Hill et al., (2013) conducted a parallel QTL analysis for 29 agronomic and 205 metabolic traits under WD conditions in wheat and identified several mQTLs coinciding with

QTLs for agronomic traits they interpreted as direct or indirect effects of metabolite flux on agronomic traits. Measuring metabolite accumulation in plants exposed to different environmental conditions could thus help to reliably identify the mQTL associated to GxE.

Overall we believe that deciphering the complexity of plasticity molecular network is feasible and the "generalizing genetical genomics" (GGG) approach proposed by Li et al., (2008) is probably the most effective method to this end. It relies mainly in the identification of QTLs controlling transcript (eQTL), protein (pQTL) and metabolite (mQTL) variations in different environmental conditions. The major limit for such studies is the size of the experiments.

2.2. Fine mapping and functional validation of plasticity candidate genes

Fine mapping the identified plasticity QTLs is also possible using classical genetic approaches. Heterogeneous inbreed families (HIF) have been used for the development of NILs that contrast at specific QTLs for delineating more precisely the region of a QTL (Tuinstra et al., 1997). It requires however the identification of RILs with heterozygous status in the region of the selected QTL. Besides, for traits showing many QTLs, implementing such approach might be difficult and time consuming. Thus, prior screening for selecting the appropriate plasticity QTLs that might be used for fine mapping and candidate gene identification through the HIF approach is crucial. In chapter 6, we identified an interesting region in chromosome 11 (52 – 55 Mbp) which was significantly associated to the plasticity regulation of several phenotypic traits. Defining HIF based on residual heterozygosity in the MAGIC population should be possible. This region probably represents a hub of stress response genes affecting different agronomic traits. It may also hold a key master regulator gene importantly acting for tomato response to the environment. Screening the haplotype status of the MAGIC RILs in this region should help to identify interesting lines for developing different HIFs that might be precisely phenotyped for several traits under WD, SS and HT conditions then submitted to transcriptome and metabolome evaluation. This could be easily coupled with dense genotyping of this region to better characterize its involvement in multiple stress/trait responses.

Fine mapping and the different processes used throughout our study to narrow the candidate genes in the QTL regions are based on statistical analyses. Functional validation is the final step to test for the effects of a given candidate gene. It allows characterizing the function of a gene notably through genetic transformation and different biotechnological tools are available to this end. In tomato, successful genetic transformation have been achieved many years ago and Fischhoff et al., (1987) documented among the first transgenic tomato plants expressing resistance against insects. Indeed, the principle of genetic transformation lies on targeting and modifying the sequence of a given gene and then studies its effect at wide scale. New tools such as Zinc-finger nucleases (ZFNs) and

transcription activator-like effector nucleases (TALENs) have been then used for tomato gene silencing. However, the CRISPR/Cas9 (clustered regularly interspaced short palindromic repeats) technology revealed higher efficiency in several organisms for gene editing (Adli, 2018). CRISPR/Cas9 was first proposed in tomato few years ago (Brooks et al., 2014) and rapidly showed a large potential and wide application for functional gene characterization and applied breeding. CRISPR/Cas9 system can efficiently introduce knockout mutation and is therefore a useful method to analyze candidate genes from forward genetics or natural mutation. It was successfully applied in tomato to characterize different genes related to fruit ripening (Ito et al., 2015; Lang et al., 2017; R. Li et al., 2018), biotic resistance (Nekrasov et al., 2017), plant architecture traits (Rodríguez-Leal et al., 2017) and drought tolerance (Wang et al., 2017). Advances in the CRISPR/Cas9 technology have been achieved in tomato with increased probability of gene insertion and more precise mutation targeting single bases (Danilo et al., 2018, 2019; Veillet et al., 2019). These technologies are now available tools and are ready to use for functional validation of the QTL candidate genes.

3. Breeding in the context of GxE

We identified a large number of plasticity and interactive QTLs (QEI) both affecting the observed GxE interaction in the MAGIC population. From the identification of such QTLs and their estimated effects, different strategies are applicable to develop environmentally-adapted cultivars.

3.1. Multi-parent advanced generation recurrent selection (MAGReS)

The MAGRes strategy was first theorized by Huang et al., (2015) who proposed breeding new varieties based on the segregating QTLs in MAGIC populations. Basically, this strategy lies in identifying and combining the best alleles based on the parental haplotype QTL effects for the trait of interest. Mean and plasticity QTLs should then be combined, and the best allele selection should account for the significance of the QTL (LOD score, PVE), the direction of the allelic effect and the QTL size. Supporting tools (OptiMAS: Valente et al., (2014)) have been developed to help accelerating the identification of the favorable alleles in the multi-allelic context of MAGIC populations. This helpful tool is conceived to characterize the optimal crossing design for best allele combination.

3.2. Targeted-environment breeding strategy

Environment characterization was carried in chapter VI and the 12 environments classified according to the climatic and growing conditions. Breeding strategies for specific group of environments is a possible scenario. A total of 28 QEI were detected in Chapter VI and allelic effects estimated for each parental haplotype in each environment for every QEI positions. Thus, plotting the QTL effects against the environments classified according to the different groups might help identifying the

parental haplotypes with the best alleles-by-environment combination (**Figure 4**). Classical marker assisted selection (MAS) with different strategies according to the targeted group of environments might then be conducted.

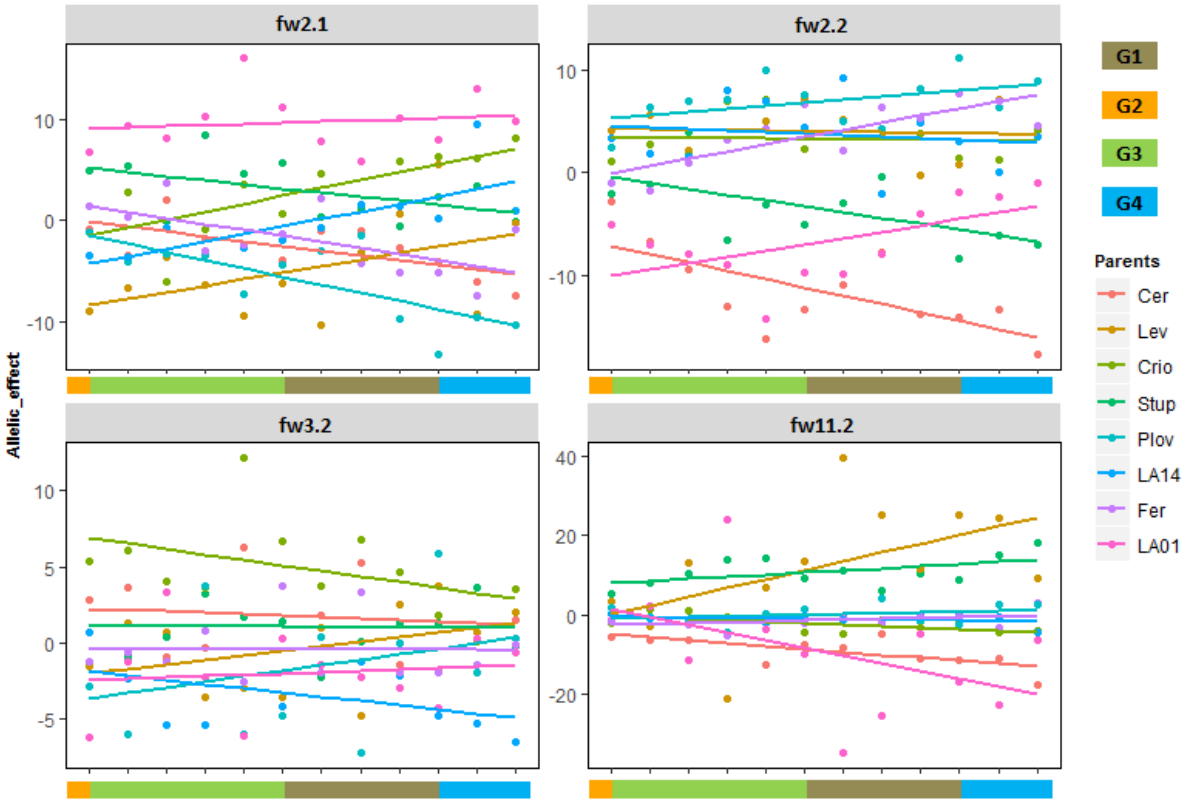

Figure 4: Linear relationship between parental allelic effect and the environments for all the detected fruit weight QEI. Environments are ordered according the groups defined in hierarchical classification (see chapter 6). The estimated allelic effects are retrieved from the QEI model for which an allelic effect was estimated for each parent in each environment for every marker showing significant interaction effect.

3.3. Genomic prediction combined with eco-physiological characterization

Genomic prediction is a powerful tool that has been widely investigated in plants for breeding purposes this last decade. However, its performance might be hampered by environmental variation and statistical models to improve genomic prediction in the context of GxE have been proposed (Crossa et al., 2017). Accurate prediction of GxE for flowering time in Sorghum was documented by Li et al., (2018) who used phenotypic plasticity as a phenotypic trait. The high prediction power was achieved partly due to a good environmental characterization using photothermal time within appropriate phenological stages. Maize yield was also adequately predicted under GxE in a wide range of environmental scenarios by Millet et al., (2019). These authors characterized the environments using genotype-specific indices computed from biological information from the field trials. These studies highlighted opportunities to reach precise prediction of phenotypic plasticity in large panels evaluated in different environments. In our study, environments were characterized on

the basis of climatic variables measured in the greenhouses and the factorial regression model (see chapter 6) applied in a subset of the MAGIC population (genotypes with more than 2/3 of missing values across environments were excluded from the analysis). Genomic prediction in our MAGIC-MET design is achievable and should open the door for genomic selection of plasticity response to abiotic stresses in tomato.

An attractive method combining quantitative genetics and eco-physiological modelling is to conduct QTL/association analysis by using model parameters as input phenotypes. Indeed, model parameters can be viewed as mathematical descriptions of complex traits. It intended to predict a trait variation in a given environmental context. QTLs for model parameters can then be investigated and their positions mirrored to QTLs for agronomic traits. It was proposed in tomato for predicting yield and fruit quality under drought condition by the use of several parameters influencing physiological processes (Constantinescu et al., 2016). However, it necessitates to appropriately define plant models for specific processes. For tomato, plant models were defined for carbon assimilation and allocation among sink sources, water transfer and accumulation, light absorption and photosynthesis and response to temperature (Heuvelink and Bertin, 1994; Boote et al., 2012; Fanwoua et al., 2013; Rybak et al., 2017).

3.4. Implication of phenotypic plasticity in plant breeding

Phenotypic plasticity has been described as an important driver of plant evolution when it triggers adaptive responses in new environments (Ghalambor et al., 2007). Adaptive plasticity indeed refers to environmental responses allowing tending towards the optimal phenotype that will be favored for selection. In the agricultural context, cultivated crops are usually exposed to the optimal conditions and the genotypes capable of expressing the best performance will be favored for selection. Thus, one might presumably imagine that genotypes with high adaptive plasticity regarding the cultural conditions have been selected for years for breeding purposes in crops. Conversely, the more stable genotypes unable of taking advantage of the optimal growing conditions might have been less selected. We discussed in **chapter 6** that co-selection of allelic variants leading to higher performance in optimal condition together with plasticity alleles is a reasonable assumption that would explain the significant correlation that we observed between mean and plasticity, especially for fruit weight which has been a major driver of domestication and breeding in tomato. Gage et al., (2017) evidenced divergent selection that was based on maize plasticity for yield component traits in temperate regions. Alleles governing plasticity of specific traits (notably high performance) are then amenable to operate directional selection according to the growing conditions. This example demonstrates that high crop performance under certain conditions (that could be a specific abiotic stress) can be achieved through directional selection towards better performance in a constant

evaluation of diverse accessions in that specific condition. Mimicking the predicted climate conditions that are expected over the 50 coming years in greenhouses could be a good strategy to select for superior future climate-resilient lines. Long-term directional selection within optimal conditions retained different combinations of high performance alleles in elite varieties and have been probably a key driver of genetic progress. Voss-Fels et al., (2019) showed that wheat lines carrying such genetic configuration also perform better under low agrochemical input and stress conditions. Thus, selection under optimal conditions does not seem to be unfavorable for adaptation to limited conditions. However, if directional selection was operated at the same scale under optimal and stress conditions, genotypes carrying different allele's configuration might arise under low input conditions and outperform the elite varieties. At the end, what is important to remember is that there is not a single variety outperforming all others in every environmental condition. Breeding strategies should always consider the targeted trait and environment and take advantage of what is documented about that specific trait x environment interaction. For several crops, the genetic loci involved in the regulation of GxE or plasticity have been dissected and constitute now valuable species specific resources on which variety improvement in changing environments should be based.

4. Conclusion

Globally, the present study explored tomato variability under different environmental conditions and highlighted a considerable plasticity of the crop, which perhaps explain its wide cultivation in very different geographical regions. We used a MAGIC population carrying an important intraspecific diversity of the cultivated tomato that revealed significant GxE. This emphasizes that breeding for environmentally adapted tomato is possible without reclaiming the wild reservoir. Tomato plasticity has been described throughout this document as being trait specific and heavily depending on the range of environmental conditions considered. However, the genetic architecture of tomato plasticity is very complex and deserves to be more precisely dissected at the molecular level. Several candidate genes that might be involved in plasticity regulation have been proposed. Overall, upon the results presented in the different chapters of this document, phenotypic plasticity may now be considered as a trait per se for which selection can be conducted. We identified common and distinct loci controlling mean phenotypes and plasticity in tomato. The work presented here clearly depicted potential avenues for the molecular characterization of plasticity genes in tomato and for the integration of phenotypic plasticity in breeding for environment resilient cultivars.

References:

Adli, M. (2018) The CRISPR tool kit for genome editing and beyond. *Nat Commun*. 9: 1911.

Albert, E., Duboscq, R., Latreille, M., Santoni, S., Beukers, M., Bouchet, J.-P., et al. (2018) Allele specific expression and genetic determinants of transcriptomic variations in response to mild water deficit in tomato. *Plant J*.

Bouffier, B., Derory, J., Murigneux, A., Reynolds, M., and Le Gouis, J. (2015) Clustering of Environmental Parameters Discriminates Drought and Heat Stress Bread Wheat Trials. *Agron J*. 107: 1489.

Bradshaw, A.D. (1965) Evolutionary Significance of Phenotypic Plasticity in Plants. *Adv Genet*. 13: 115–155.

Brooks, C., Nekrasov, V., Lippman, Z.B., and Van Eck, J. (2014) Efficient gene editing in tomato in the first generation using the clustered regularly interspaced short palindromic repeats/CRISPR-associated9 system. *Plant Physiol*. 166: 1292–7.

Constantinescu, D., Memmah, M.-M., Vercambre, G., Génard, M., Baldazzi, V., Causse, M., et al. (2016) Model-Assisted Estimation of the Genetic Variability in Physiological Parameters Related to Tomato Fruit Growth under Contrasted Water Conditions. *Front Plant Sci*. 7: 1841.

Cramer, G.R., Urano, K., Delrot, S., Pezzotti, M., and Shinozaki, K. (2011) Effects of abiotic stress on plants: a systems biology perspective. *BMC Plant Biol*. 11: 163.

Danilo, B., Perrot, L., Botton, E., Nogué, F., and Mazier, M. (2018) The DFR locus: A smart landing pad for targeted transgene insertion in tomato. *PLoS One*. 13: e0208395.

Danilo, B., Perrot, L., Mara, K., Botton, E., Nogué, F., and Mazier, M. (2019) Efficient and transgene-free gene targeting using Agrobacterium-mediated delivery of the CRISPR/Cas9 system in tomato. *Plant Cell Rep*. 38: 459–462.

Diouf, I.A., Derivot, L., Bitton, F., Pascual, L., and Causse, M. (2018) Water Deficit and Salinity Stress Reveal Many Specific QTL for Plant Growth and Fruit Quality Traits in Tomato. *Front Plant Sci*. 9: 279.

El-Soda, M., Malosetti, M., Zwaan, B.J., Koornneef, M., and Aarts, M.G.M. (2014) . Trends Plant Sci.

Fanwoua, J., de Visser, P.H.B., Heuvelink, E., Yin, X., Struik, P.C., and Marcelis, L.F.M. (2013) A dynamic model of tomato fruit growth integrating cell division, cell growth and endoreduplication. *Funct Plant Biol*. 40: 1098.

Fischhoff, D.A., Bowdish, K.S., Perlak, F.J., Marrone, P.G., McCormick, S.M., Niedermeyer, J.G., et al. (1987) Insect Tolerant Transgenic Tomato Plants. *Nat Biotechnol*. 5: 807–813.

Gage, J.L., Jarquin, D., Romay, C., Lorenz, A., Buckler, E.S., Kaeppler, S., et al. (2017) The effect of artificial selection on phenotypic plasticity in maize. *Nat Commun*. 8: 1348.

GHALAMBOR, C.K., McKAY, J.K., CARROLL, S.P., and REZNICK, D.N. (2007) Adaptive versus non-adaptive phenotypic plasticity and the potential for contemporary adaptation in new environments. *Funct Ecol*. 21: 394–407.

Heuvelink, E., and Bertin, N. (1994) Dry-matter partitioning in a tomato crop: Comparison of two simulation models. *J Hortic Sci*. 69: 885–903.

Hill, C.B., Taylor, J.D., Edwards, J., Mather, D., Bacic, A., Langridge, P., et al. (2013) Whole-genome mapping of agronomic and metabolic traits to identify novel quantitative trait Loci in bread wheat grown in a water-limited environment. *Plant Physiol*. 162: 1266–81.

Hoegh-Guldberg, O., D. Jacob, M. Taylor, M. Bindi, S. Brown, I. Camilloni, A. Diedhiou, R. Djalante, K.L. Ebi, F. Engelbrecht, J. Guiot, Y. Hijioka, S. Mehrotra, A. Payne, S.I. Seneviratne, A. Thomas, R. Warren, and G. Zhou, 2018 (2019) Impacts of 1.5°C Global Warming on Natural and Human Systems.

Huang, B.E., Verbyla, K.L., Verbyla, A.P., Raghavan, C., Singh, V.K., Gaur, P., et al. (2015) MAGIC populations in crops: current status and future prospects. *Theor Appl Genet*. 128: 999–1017.

Ito, Y., Nishizawa-Yokoi, A., Endo, M., Mikami, M., and Toki, S. (2015) CRISPR/Cas9-mediated mutagenesis of the RIN locus that regulates tomato fruit ripening. *Biochem Biophys Res Commun*. 467: 76–82.

Kenneth J. Boote; Maria R. Rybak; Johan M.S. Scholberg; James W. Jones (2012) Improving the CROPGRO-Tomato Model for Predicting Growth and Yield Response to Temperature. *HortScience*. 47.

Keurentjes, J.J.B., Fu, J., Terpstra, I.R., Garcia, J.M., van den Ackerveken, G., Snoek, L.B., et al. (2007) Regulatory network construction in Arabidopsis by using genome-wide gene expression quantitative trait loci. *Proc Natl Acad Sci U S A*. 104: 1708–13.

Keurentjes, J.J.B., Fu, J., de Vos, C.H.R., Lommen, A., Hall, R.D., Bino, R.J., et al. (2006) The genetics of plant

metabolism. *Nat Genet*. 38: 842–849.

Lall, S., Nettleton, D., DeCook, R., Che, P., and Howell, S.H. (2004) Quantitative trait loci associated with adventitious shoot formation in tissue culture and the program of shoot development in Arabidopsis. *Genetics*. 167: 1883–92.

Lang, Z., Wang, Y., Tang, K., Tang, D., Datsenka, T., Cheng, J., et al. (2017) Critical roles of DNA demethylation in the activation of ripening-induced genes and inhibition of ripening-repressed genes in tomato fruit. *Proc Natl Acad Sci U S A*. 114: E4511–E4519.

Li, R., Fu, D., Zhu, B., Luo, Y., and Zhu, H. (2018) CRISPR/Cas9-mediated mutagenesis of lncRNA1459 alters tomato fruit ripening. *Plant J*. 94: 513–524.

Li, X., Guo, T., Mu, Q., Li, Xianran, and Yu, J. (2018) Genomic and environmental determinants and their interplay underlying phenotypic plasticity. *Proc Natl Acad Sci U S A*. 115: 6679–6684.

Li, Y., Breitling, R., and Jansen, R.C. (2008) Generalizing genetical genomics: getting added value from environmental perturbation. *Trends Genet*. 24: 518–524.

Lin, F., Zhou, L., He, B., Zhang, X., Dai, H., Qian, Y., et al. (2019) QTL mapping for maize starch content and candidate gene prediction combined with co-expression network analysis. *Theor Appl Genet*.

Luo, J. (2015) Metabolite-based genome-wide association studies in plants. *Curr Opin Plant Biol*. 24: 31–38.

Millet, E.J., Kruijer, W., Coupel-Ledru, A., Alvarez Prado, S., Cabrera-Bosquet, L., Lacube, S., et al. (2019) Genomic prediction of maize yield across European environmental conditions. *Nat Genet*. 51: 952–956.

Mitchell, J., Shennan, C., and Grattan, S. (1991) Developmental-Changes in Tomato Fruit Composition in Response To Water Deficit and Salinity. *Physiol Plant*. 83: 177–185.

Naoumkina, M., Thyssen, G.N., Fang, D.D., Jenkins, J.N., McCarty, J.C., and Florane, C.B. (2019) Genetic and transcriptomic dissection of the fiber length trait from a cotton (Gossypium hirsutum L.) MAGIC population. *BMC Genomics*. 20: 1–14.

Nekrasov, V., Wang, C., Win, J., Lanz, C., Weigel, D., and Kamoun, S. (2017) Rapid generation of a transgene-free powdery mildew resistant tomato by genome deletion. *Sci Rep*. 7: 482.

Paterson, A.H., Damon, S., Hewitt, J.D., Zamir, D., Rabinowitch, H.D., Lincoln, S.E., et al. (1991) Mendelian factors underlying quantitative traits in tomato: comparison across species, generations, and environments. *Genetics*. 127.

Rainwater, D.T., Gossetp, D.R., Millhollon, E.P., Hanna, H.Y., Banks, S.W., and Lucas, M.C. (1996) The Relationship Between Yield and the Antioxidant Defense System in Tomatoes Grown Under Heat Stress. *Free Radic Res*. 25: 421–435.

Ritchie, M.D., Holzinger, E.R., Li, R., Pendergrass, S.A., and Kim, D. (2015) Methods of integrating data to uncover genotype–phenotype interactions. *Nat Rev Genet*. 16: 85–97.

Rodríguez-Leal, D., Lemmon, Z.H., Man, J., Bartlett, M.E., and Lippman, Z.B. (2017) Engineering Quantitative Trait Variation for Crop Improvement by Genome Editing. *Cell*. 171: 470-480.e8.

Rothan, C., Diouf, I., and Causse, M. (2019) Trait discovery and editing in tomato. *Plant J*. 97: 73–90.

Rybak, M.R., Boote, K.J., Jones, J.W., and Zotarelli, L. (2017) Simulating growth, fresh weight and size of individual fruits under water and nitrogen limitations with the CROPGRO-Tomato model. *Acta Hortic*. 137–144.

Sarazin, V., Duclercq, J., Guillot, X., Sangwan, B., and Sangwan, R.S. (2017) Water-stressed sunflower transcriptome analysis revealed important molecular markers involved in drought stress response and tolerance. *Environ Exp Bot*. 142: 45–53.

Septiani, P., Lanubile, A., Stagnati, L., Busconi, M., Nelissen, H., Pè, M.E., et al. (2019) Unravelling the genetic basis of fusarium seedling rot resistance in the MAGIC maize population: Novel targets for breeding. *Sci Rep*. 9: 4–13.

Tuinstra, M.R., Ejeta, G., and Goldsbrough, P.B. (1997) Heterogeneous inbred family (HIF) analysis: a method for developing near-isogenic lines that differ at quantitative trait loci. *Theor Appl Genet*. 95: 1005–1011.

Valente, F., Gauthier, F., Bardol, N., Blanc, G., Joets, J., Charcosset, A., et al. (2014) OptiMAS: A Decision Support Tool to Conduct Marker-Assisted Selection Programs pp. 97–116 Humana Press, New York, NY.

Van Veen, H., Vashisht, D., Akman, M., Girke, T., Mustroph, A., Reinen, E., et al. (2016) Transcriptomes of eight Arabidopsis thaliana accessions reveal core conserved, genotype- and organ-specific responses to flooding stress. *Plant Physiol*. 172: 668–689.

Veillet, F., Perrot, L., Chauvin, L., Kermarrec, M.-P., Guyon-Debast, A., Chauvin, J.-E., et al. (2019) Transgene-

Free Genome Editing in Tomato and Potato Plants Using Agrobacterium-Mediated Delivery of a CRISPR/Cas9 Cytidine Base Editor. *Int J Mol Sci*. 20: 402.

Verbyla, A.P., Cavanagh, C.R., and Verbyla, K.L. (2014) Whole-Genome Analysis of Multienvironment or Multitrait QTL in MAGIC. *G3 Genes, Genomes, Genet*. 4.

Voss-Fels, K.P., Stahl, A., Wittkop, B., Lichthardt, C., Nagler, S., Rose, T., et al. (2019) Breeding improves wheat productivity under contrasting agrochemical input levels. *Nat Plants*. 5: 706–714.

Wang, L., Chen, L., Li, R., Zhao, R., Yang, M., Sheng, J., et al. (2017) Reduced Drought Tolerance by CRISPR/Cas9-Mediated SlMAPK3 Mutagenesis in Tomato Plants. *J Agric Food Chem*. 65: 8674–8682.

Waters, A.J., Makarevitch, I., Noshay, J., Burghardt, L.T., Hirsch, C.N., Hirsch, C.D., et al. (2017) Natural variation for gene expression responses to abiotic stress in maize. *Plant J*. 89: 706–717.

Wayne, M.L., and McIntyre, L.M. (2002) Combining mapping and arraying: An approach to candidate gene identification. *Proc Natl Acad Sci U S A*. 99: 14903–6.

Appendices

- **Appendix 1:** French summary of the manuscript
- **Appendix 2:** Review article: Rothan C, Diouf I and Causse M ***"Trait discovery and editing in tomato". Plant J***
- **Appendix 3:** Supplementary materials from chapter 3
- **Appendix 4:** Supplementary materials from chapter 4
- **Appendix 5:** Supplementary materials from chapter 5
- **Appendix 6:** Supplementary materials from chapter 6
- **Appendix 7:** List of all the QTLs identified in the MAGIC population throughout this thesis (published and unpublished QTLs)

NB: *large excel files that are in Supplementary Materials for the different chapters are available online in a local database that can be accessed online*

Annexe 1

Résumé Substantiel de la thèse à la demande de l'Ecole Doctorale

Introduction

Les plantes sont des organismes immobiles, fréquemment soumis à d'importantes fluctuations environnementales dans leurs habitats. La survie à long terme de ces organismes nécessite des mécanismes adaptatifs bien élaborés pour limiter les effets néfastes induits par les variations environnementales tout au long de leur cycle de vie. On parle généralement de stress abiotique lorsque les variations environnementales entraînent des perturbations importantes du métabolisme et de l'homéostasie des plantes (Munns and Gilliham, 2015). Lorsqu'elles sont exposées à un stress abiotique, les plantes activent des mécanismes de régulation à différent niveaux d'organisation cellulaire (régulations physiologique, métabolique, biochimique et moléculaire), résultant à des changements morphologiques visibles. La baisse du rendement est notamment un caractère symptomatique des conséquences des stress abiotique chez les espèces cultivés.

Comprendre les mécanismes qui sous-tendent la réponse des plantes aux stress abiotiques revêt donc une importance capitale pour la sélection et l'amélioration variétale en conditions de cultures constamment variables ; d'autant plus que risques potentiels d'importantes pertes de rendement des cultures principales sont attendues avec les prédictions récentes sur une augmentation des températures de 1,5 à 2 ° C à l'échelle du globe (Hoegh-Guldberg et al., 2019).

Ainsi, les biologistes des plantes ont fourni des efforts importants pour mieux caractériser la réaction des plantes face aux stress abiotiques, notamment par l'étude des processus physiologiques majeurs et de la régulation moléculaire à la base de l'adaptation des plantes aux stress abiotiques. Le Déficit hydrique, les hautes températures et à la salinité font partie des principaux stress abiotiques décrites dans la littérature, affectant la production agricole chez les espèces cultivées dont la tomate (*Solanum lycopersicum L.*).

La tomate est une culture d'importance économique majeure, produite partout à travers le monde et fait partie des principaux légumes consommés à haute valeur nutritionnelle (Rothan et al., 2019). Elle appartient à la grande famille des solanacées. Il s'agit d'une culture autogame ayant un génome moyen (~ 950 Mb), un cycle rapide (2 à 3 cycles par an) et un taux intéressant de succès pour la transformation génétique. Tous ces attributs en font une plante modèle pour les études en génétique. Le rendement et la qualité du fruit chez la tomate sont fortement influencés par les conditions de croissance, notamment les systèmes d'irrigation et les températures ambiantes en champ ou en serre (Mitchell et al., 1991; Rainwater et al., 1996). Nous avons donc dans ce projet de thèse, souhaité étudier le comportement de la tomate dans les conditions de culture de déficit hydrique (WD), de fortes températures (HT) et de stress salin (SS) dans le but de mieux caractériser la composante génétique de la réponse de la tomate à différents stress abiotiques.

Objectifs de l'étude

Cette étude avait pour objectif général d'identifier les QTLs/gènes, génotypes et phénotypes impliqués dans l'adaptation de la tomate aux différents stress énumérés ci-dessus (WD, HT et SS). Cela, dans le cadre de différents projets (ADAPTOM et TomEpiset), en partie financés par l'Agence National de la Recherche française (ANR) et avec la contribution de plusieurs groupes de recherche et de compagnies de sélection privées.

Dans cette thèse, nous avons souhaité évaluer l'impact des stress abiotiques sur la qualité du fruit, la phénologie et le développement des plantes et le rendement de la tomate et d'étudier son architecture génétique.

Plus spécifiquement, trois questions scientifiques ont été proposées pour atteindre cet objectif :

1. Quelles variations phénotypiques sont induites par le déficit hydrique, la salinité et le stress thermique chez la tomate ?
2. Comment le transcriptome de la tomate est-il affecté par le déficit hydrique mais aussi par différents génotypes ?
3. Quelles sont les bases génétiques de la plasticité phénotypique et des interactions génotype x environnement (GxE) chez la tomate en réponse aux stress abiotiques ?

Matériel et Méthodes

Pour réaliser ce travail, nous avons utilisé une population multi-parentale (MAGIC) issue du croisement de huit lignées de tomate dont quatre de gros calibre et quatre tomates cerise. Une description détaillée du développement de la population est fournie au **chapitre 2**. La population MAGIC a été évaluée dans trois sites géographiques différents (France, Israël et Maroc) et quatre conditions de culture spécifiques ont été appliquées. Les essais ont été réalisés de sorte que dans un essai donné, un traitement contrôle (condition optimale de culture) soit toujours opposé à un traitement de stress (WD, HT ou SS). Une description détaillée des traitements est présentée au **chapitre 3** (pour WD et SS) et au **chapitre 5** (pour stress HT). Pour chaque essai, différents traits phénotypiques ont été mesurés. Les variables climatiques dans les serres ont été enregistrées quotidiennement dans chaque essai, à partir desquels des co-variables environnementales ont calculées pour caractériser les environnements (voir le **chapitre 6** pour plus de détails). L'impact des différents stress a ainsi été

évaluée au niveau phénotypique, génétique et transcriptomique (uniquement pour WD : **chapitre 4**). Par la suite, des gènes candidats de réponse aux stress ont été proposés.

Résultats et discussion

Au cours de ce travail, nous avons pu mettre en évidence la complexité de la réponse de la tomate aux stress abiotique qui apparaît être sous le contrôle de plusieurs gènes encore non identifiés singulièrement pour la plupart, mais dont nous avons pu proposer des candidats.

Dans le **chapitre 3** nous avons évalué l'impact du déficit hydrique et de la salinité sur la qualité du fruit et la croissance de la tomate. Au total, 250 lignées individuelles de la population MAGIC ont été utilisées pour identifier les QTLs en lien avec le poids et le nombre de fruits, la teneur en sucre, la fermeté du fruit, le temps de floraison et de maturité et la longueur des feuilles. Tous ces traits présentaient une variation phénotypique importante attribuée en majorité à l'effet du génotype (33 à 86% de la variation phénotypique totale). Ces traits ont par ailleurs montré héritabilité importante autant dans les conditions contrôle que dans les conditions de stress, signalant la capacité d'opérer de la sélection variétale sur ce trait en condition limitante. D'autre part des interactions significatives génotype × condition de culture ont été détectées pour la majorité des traits. Les QTLs ont été cartographiés à l'aide de 1345 marqueurs SNPs. Un total de 54 QTLs ont été trouvés parmi lesquels 15 ont révélés des interactions génotype × environnement et 65% (35 QTLs) étaient spécifiques au traitement. Les intervalles de confiance des QTL ont été projetés sur la carte physique du génome ; ce qui a permis d'identifier les régions de co-localisations des QTLs, suggérant une régulation pléiotropique. Nous avons ensuite appliqué une stratégie de recherche des gènes candidats basée sur la cartographie à haute résolution offerte par la population MAGIC, l'effet allélique estimé des différentes lignées parentales pour chaque QTL détecté et les informations de polymorphisme de séquence des huit lignées parentales.

Le **chapitre 4** s'est focalisé sur l'étude de la variation du transcriptome en réponse au déficit hydrique chez la tomate. Les données transcriptomiques ont été recueillies par séquençage de l'ARN totale de jeunes feuilles et de fruits au stade d'expansion cellulaire en condition contrôle (irrigation optimale) et en condition de déficit hydrique (-40% ETP). Huit génotypes couvrant une importante diversité allélique des tomates cultivées ont été utilisés pour ce faire. Ces génotypes ont d'abord montré des différences importantes de réponse au déficit hydrique au niveau phénotypique. En examinant l'expression des gènes dans les deux conditions, un total de 14 065 gènes différentiellement exprimés (DEG) en condition de déficit hydrique a été détecté, dont 7 393 (53%) et 11 059 (79%) spécifiques au

génotype et à l'organe, respectivement. L'impact du déficit hydrique sur la variation du transcriptome était plus important au niveau des feuilles que pour le péricarpe du fruit en expansion cellulaire. Cette étude a également mis en évidence un très fort effet du génotype sur le niveau d'expression des gènes ainsi que la présence d'un ensemble de gènes présentant une interaction significative génotype x environnement au niveau transcriptomique. L'intégration des DEG aux QTLs de réponse au stress hydrique et salin, précédemment identifiés dans le **chapitre 3**, nous a permis de réduire la liste de gènes candidats dans les régions de ces QTLs. Les résultats présentés ont mis en évidence des ressources intéressantes pour des études ultérieures visant à décrypter la complexité de l'adaptation de la tomate au stress hydrique.

Dans le **chapitre 5**, nous avons évalué l'impact du stress thermique sur la tomate dans deux populations expérimentales constituées d'une population multi-parentale (MAGIC) et d'une collection (CC) regroupant plusieurs accessions de tomates cerise. Ces populations ont été évaluées dans des conditions de culture optimale et de stress lié à des températures élevées. Des traits liés au rendement, à la qualité du fruit et à la croissance phénologie des plantes ont été phénotypés dans les deux populations. Les analyses statistiques ont révélé un impact significatif des conditions de stress thermique au niveau phénotypique, qui a entraîné une diminution des traits de composante du rendement (<21-35%) et accélérer la floraison pour presque l'ensemble des génotypes (96-99%) dans les deux populations. Les deux populations ont été génotypées ave des marqueurs SNPs et les analyses de QTL et d'association ont identifié 244 QTLs dont la majorité (92%) était spécifique ç l'une des populations. La plasticité phénotypique en réponse au stress thermique a été calculée pour chaque caractère et a permis l'identification de 70 QTLs de plasticité. Une forte proportion (80 et 91%) des QTL identifiés au sein des populations MAGIC et CC, respectivement, était spécifique ou à la plasticité ou à une des deux conditions. La présente étude a permis de mieux comprendre l'architecture polygénique et la complexité de la réponse de la tomate au stress thermique. Des génotypes tolérants aux températures élevées ont été identifiés et des gènes candidats de réponse au stress thermique mis en évidence.

Au **chapitre 6**, les données issues de l'évaluation de la population MAGIC dans le dispositif multi-environnement (MET) ont été conjointement analysées. Au total, 10 traits phénotypique ont été analysés dans 5 à 12 environnements différents suivant le dispositif décrit dans le tableau 2 du chapitre 2 des Matériels et Méthodes. Il a été mis en évidence une importante présence d'interactions GxE expliquant 15 à 68% de la variance phénotypique en fonction des différents traits évalués. Les analyses de cartographie génétique ont révélé au total 104 QTLs uniques identifiés en utilisant les phénotypes moyens et la plasticité phénotypique parmi lesquels, seul 221% étaient communs. Des modèles

linéaires mixtes ont par la suite été utilisés pour modéliser la complexité du dispositif MAGIC-MET afin d'étudier les QTL interactifs (QEI). Cette analyse a identifié 28 QEI dont la majorité a aussi été détecté avec l'analyse QTL sur plasticité et les phénotypes moyens. Le chapitre 6 a permis de mettre en évidence une architecture génétique complexe de la plasticité phénotypique et des interactions GxE chez la tomate. Les QTLs de plasticité ont été détectés majoritairement dans des régions distinctes par rapport aux QTLs de phénotype moyen pour un caractère donné ; ce qui suggère la possibilité d'une sélection indépendante pour la plasticité. Des gènes candidats potentiellement impliqués dans l'occurrence du GxE chez la tomate ont été proposés, ouvrant la voie à la caractérisation fonctionnelle des gènes de réponse aux stress chez la tomate.

Conclusion

En conclusion, cette thèse nous a permis d'explorer la variabilité de la tomate dans différentes conditions environnementales et a mis en évidence une plasticité phénotypique considérable chez cette espèce ; ce qui peut expliquer qu'elle soit cultivée partout dans le monde dans différentes régions géographiques et sous diverses conditions de culture. Nous avons utilisé une population MAGIC renfermant une importante diversité allélique intra-spécifique des tomates cultivées. Cette population a révélé une forte présence d'interactions GxE. Cela souligne que la sélection de tomates adaptées à l'environnement est possible sans aller puiser dans le réservoir des espèces sauvages qui généralement contiennent des fragments importants non désirables pour la sélection variétale. La plasticité phénotypique de la tomate a été décrite tout au long de ce document comme un caractère qui soit spécifique en fonction du trait étudié, et fortement dépendante de la gamme de variation environnemental considérée. De toute évidence, l'architecture génétique de la plasticité de la tomate est très complexe et mérite d'être étudié de façon plus précise au niveau moléculaire. Plusieurs gènes candidats potentiellement impliqués dans la régulation de la plasticité ont été proposés. Globalement, sur la base des résultats présentés dans les différents chapitres de ce document, la plasticité phénotypique peut maintenant être considérée comme un trait en soi pour lequel la sélection variétale peut être opérée. Nous avons identifié des locus communs et distincts contrôlant les phénotypes moyens et la plasticité chez la tomate. Les travaux présentés ici présentent clairement des pistes potentielles pour la caractérisation moléculaire des gènes de plasticité chez la tomate et l'intégration de la plasticité phénotypique dans les programmes de sélection variétale visant à développer des cultivars résilients.

Références

Hoegh-Guldberg, O., D. Jacob, M. Taylor, M. Bindi, S. Brown, I. Camilloni, A. Diedhiou, R. Djalante, K.L. Ebi, F. Engelbrecht, J. Guiot, Y. Hijioka, S. Mehrotra, A. Payne, S.I. Seneviratne, A. Thomas, R. Warren, and G. Zhou, 2018 (2019) Impacts of 1.5ºC Global Warming on Natural and Human Systems.

Mitchell, J., Shennan, C., and Grattan, S. (1991) Developmental-Changes in Tomato Fruit Composition in Response To Water Deficit and Salinity. *Physiol Plant*. 83: 177–185.

Munns, R., and Gilliham, M. (2015) Salinity tolerance of crops - what is the cost? *New Phytol*. 208: 668–673.

Rainwater, D.T., Gossetp, D.R., Millhollon, E.P., Hanna, H.Y., Banks, S.W., and Lucas, M.C. (1996) The Relationship Between Yield and the Antioxidant Defense System in Tomatoes Grown Under Heat Stress. *Free Radic Res*. 25: 421–435.

Rothan, C., Diouf, I., and Causse, M. (2019) Trait discovery and editing in tomato. *Plant J*. 97: 73–90.

Appendix 2

the plant journal

SEB Society for Experimental Biology

The Plant Journal (2019) **97,** 73–90 doi: 10.1111/tpj.14152

SI GENOME TO PHENOME

Trait discovery and editing in tomato

Christophe Rothan[1]*, Isidore Diouf[2] and Mathilde Causse[2]

[1]INRA and University of Bordeaux, UMR 1332 Biologie du Fruit et Pathologie, F-33140, Villenave d'Ornon, France, and
[2]INRA, UR1052, Génétique et Amélioration des Fruits et Légumes, CS60094, F-84143, Montfavet, France

Received 3 September 2018; revised 8 October 2018; accepted 30 October 2018; published online 11 November 2018.
*For correspondence (e-mail: christophe.rothan@inra.fr).

SUMMARY

Tomato (*Solanum lycopersicum*), which is used for both processing and fresh markets, is a major crop species that is the top ranked vegetable produced over the world. Tomato is also a model species for research in genetics, fruit development and disease resistance. Genetic resources available in public repositories comprise the 12 wild related species and thousands of landraces, modern cultivars and mutants. In addition, high quality genome sequences are available for cultivated tomato and for several wild relatives, hundreds of accessions have been sequenced, and databases gathering sequence data together with genetic and phenotypic data are accessible to the tomato community. Major breeding goals are productivity, resistance to biotic and abiotic stresses, and fruit sensorial and nutritional quality. New traits, including resistance to various biotic and abiotic stresses and root architecture, are increasingly being studied. Several major mutations and quantitative trait loci (QTLs) underlying traits of interest in tomato have been uncovered to date and, thanks to new populations and advances in sequencing technologies, the pace of trait discovery has considerably accelerated. In recent years, clustered regularly interspaced short palindromic repeats (CRISPR)/Cas9 gene editing (GE) already proved its remarkable efficiency in tomato for engineering favorable alleles and for creating new genetic diversity by gene disruption, gene replacement, and precise base editing. Here, we provide insight into the major tomato traits and underlying causal genetic variations discovered so far and review the existing genetic resources and most recent strategies for trait discovery in tomato. Furthermore, we explore the opportunities offered by CRISPR/Cas9 and their exploitation for trait editing in tomato.

Keywords: tomato, *Solanum lycopersicum*, natural diversity and mutants, stress, QTL, GWAS, mapping-by-sequencing, CRISPR/Cas9 gene editing, 'omics.

INTRODUCTION

Tomato is the top ranked vegetable grown over the world. It accounts for more than 15% of world vegetable production (over 177 million metric tons in 2016; www.fao.org/faostat). Tomato is grown for both processing and fresh markets. It is a rich source of micronutrients in the human diet. The major goals of tomato breeding (high productivity, tolerance to biotic and abiotic stresses, and high sensory and health value of the fruit) require a good comprehension and management of tomato genetic resources and diversity. Tomato is also an acknowledged model species for research in genetics, fruit development and disease resistance. It has a short life cycle, is easy to cross and self-pollinate, has a medium-sized genome (approximately 900 Mb), can be transformed with a high success rate, and benefits from a lot of genetic and genomic resources. Furthermore, the tomato community has access to several databases, gathering sequence data together with genetic and phenotypic data.

Tomato and its 12 closely related species belong to the *Solanum* genus in the large *Solanaceae* family (Peralta *et al.*, 2008). All these species come from the Andean region of South America. Exploration of the tomato center of origin has permitted major advances in the characterization of its diversity. In parallel, *ex situ* conservation of genetic resources in large national collections has ensured the conservation of landraces and wild species (Labate *et al.*, 2007) and new artificially induced genetic diversity has been generated (Meissner *et al.*, 1997; Menda *et al.*,

2004; Just *et al.*, 2013). Modern genetics and breeding methods have not only contributed to the understanding of the genetic control of agronomical traits, but have also contributed to the development of thousands of new cultivars.

The advent of molecular biology in the 1980s raised great hopes in terms of characterization of the genetic diversity present in both wild and cultivated compartments. The development of molecular biological techniques allowed pinpointing of genomic regions involved in targeted traits (Paterson *et al.*, 1988). Dissection of the genetic control of complex traits, using *ad hoc* techniques from quantitative genetics, has led to the identification of key alleles involved in many agronomic traits, originating from several wild relatives (Tanksley, 2004). Quantitative trait locus (QTL) mapping techniques in natural populations or, more recently, genome-wide association studies (GWAS) also facilitated the understanding of the genetic architecture of complex traits and germplasm management of both wild and cultivated tomatoes. Tomato has been one of the first crops for gene and QTL cloning by a map-based approach (Martin *et al.*, 1993; Frary *et al.*, 2000; Fridman *et al.*, 2000). Several reviews have reported the numerous genes and QTL cloned (Labate *et al.*, 2007; Foolad and Panthee, 2012; Sato *et al.*, 2012; Causse and Grandillo, 2016; Grandillo and Cammareri, 2016).

The tomato genome is now fully sequenced, providing a high quality reference genome (Sato *et al.*, 2012). In addition, hundreds of new accessions have been resequenced (Aflitos *et al.*, 2014; Lin *et al.*, 2014; Zhu *et al.*, 2018) and large transcriptome and metabolome datasets have been made available (Tohge *et al.*, 2015; Fernie and Tohge, 2017; Zouine *et al.*, 2017; Shinozaki *et al.*, 2018). Progress in deep sequencing technologies have triggered, in parallel, new developments such as GWAS (Bauchet *et al.*, 2017; Tieman *et al.*, 2017; Zhu *et al.*, 2018), QTL-seq (Illa-Berenguer *et al.*, 2015) and mapping-by-sequencing (MBS) (Garcia *et al.*, 2016) for the exploitation of natural and induced genetic diversity, thus accelerating gene/allele discovery. Together with the very recently developed CRISPR/Cas9 gene editing (GE) system, which is highly successful in tomato, these advances have contributed to the promotion of tomato not only as a model crop species but also as a model to further our understanding of plant biology. In this review, we will present the recent progresses leading to the identification and characterization of genes and QTLs of interest as well as the advances in tomato GE and their exploitation for tomato breeding.

DISCOVERY OF GENETIC VARIATIONS UNDERLYING MAJOR TRAITS IN TOMATO

Important traits in tomato breeding

Tomato is grown all over the world under much contrasted conditions (from open field to soil-free greenhouses), so there are many traits of interest for this species (Figure 1). Apart from fruit size and yield, breeding efforts have focused on fruit shape and composition, disease resistance, adaptation to new growth conditions, and abiotic stresses. Tomato is remarkable for the number of traits used in the cultivated species that are controlled by a unique locus (Figure 1). Since the early works of Steve Tanksley and his colleagues who constructed the first high density map of molecular markers (Tanksley *et al.*, 1992), many genes controlling such mutations have been mapped and positionally cloned (Causse and Grandillo, 2016; see Supplementary Table S1 for synthesis). These genes are involved in plant architecture (*sp* mutation; Pnueli *et al.*, 1998), fruit color (*del*; Ronen *et al.*, 1999; *Gr*; Barry *et al.*, 2005; *wf*; Galpaz *et al.*, 2006), fruit ripening and shelf life (*rin;* Vrebalov *et al.*, 2002; *Gr;* Barry *et al.*, 2005), and abscission (*j*; Mao *et al.*, 2000). Since the first cloning of the *Pto* gene, responsible for resistance to *Pseudomonas tomato*, more than 30 genes responsible for disease resistance have been mapped and most of these have been positionally cloned (Foolad and Panthee, 2012).

In addition to these major mutations, several QTLs controlling fruit size, shape, color intensity, firmness, and composition were mapped. With the development of high throughput metabolome studies, the content of hundreds primary and secondary metabolites was assessed (Carrari *et al.*, 2006; Bauchet *et al.*, 2017; Tieman *et al.*, 2017). Concerning tomato sensory quality, many QTLs for sensory traits were mapped as well as QTLs for volatile organic compounds (Causse *et al.*, 2002; Tieman *et al.*, 2007) and a few were positionally cloned (Supplementary Table S1).

Environmental conditions diversely affect tomato phenotype

Several studies have evidenced a genetic variability in tomato response to its environment among wild related species and within the cultivated clade (Bai and Lindhout, 2007; Bolger *et al.*, 2014). Indeed, environmental stress, such as from drought, cold, salinity, or heat, generally impairs tomato yield but can enhance to some extent fruit quality (Ripoll *et al.*, 2016). These responses depend on the genotypes and the stress duration, intensity and stage of application, as well as the trait under consideration. Genotype (G) $\times$ environment (E) interactions that arise from the differential sensitivity of tomato cultivars to given environmental conditions, and of the underlying genetic determinism, were studied for several physiological and/or agronomic traits and yielded hundreds of QTLs (see Grandillo and Cammareri, 2016 for a recent review). Since the pioneering work of Paterson *et al.* (1990), who compared QTLs detected in three single environments, and showed that different QTLs were detected for a same trait, QTL and GWAS results have frequently presented variable effects according to the environment (Sauvage *et al.*, 2014;

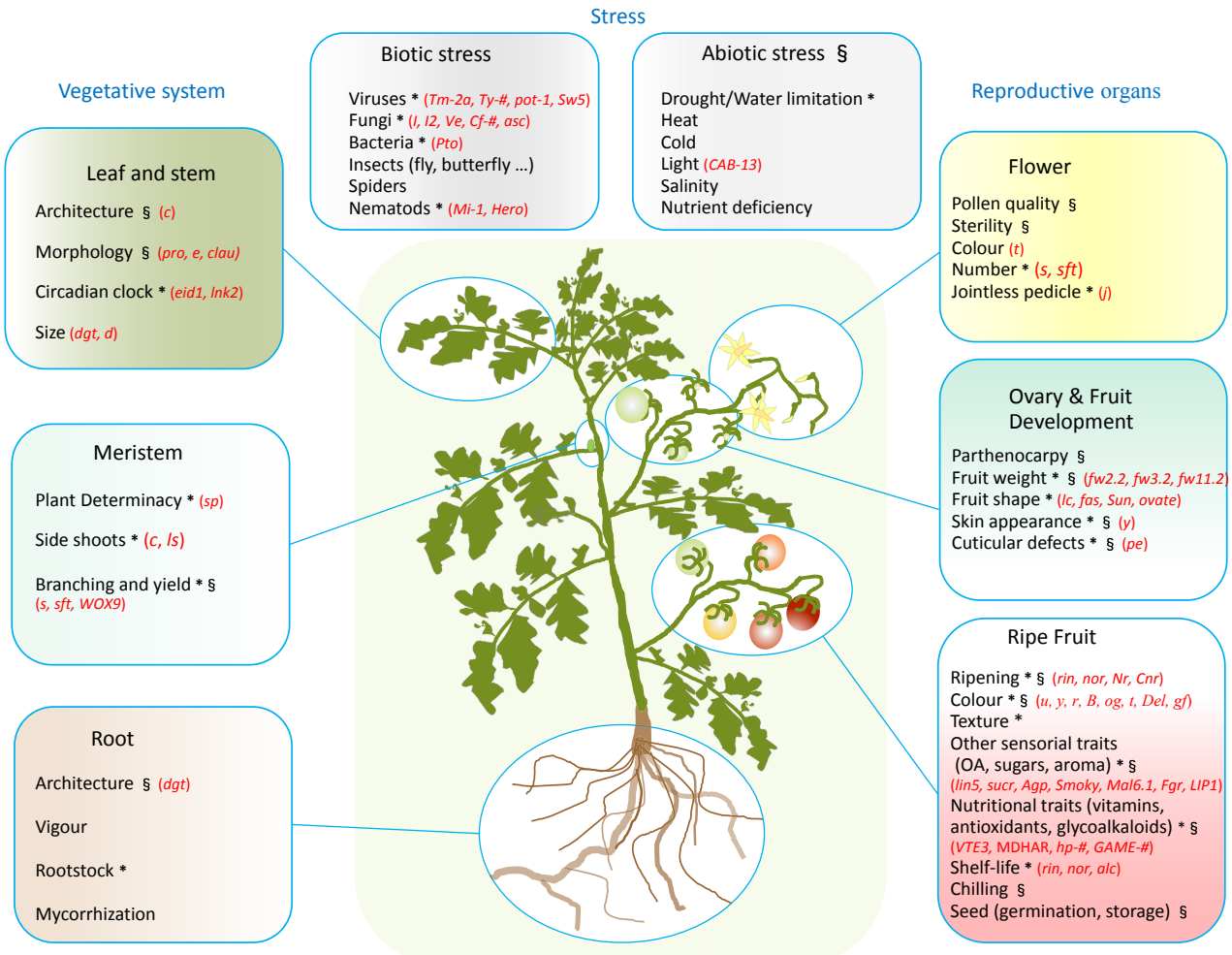

Figure 1. Main phenotypic traits studied in tomato.
Left and right boxes: main tissues and associated phenotypic traits studied in tomato for their agricultural importance. Center boxes: main stresses that tomato is facing. *, traits selected during tomato domestication and improvement. §, traits highly susceptible to variations in environmental conditions. In brackets, nonexhaustive list of major genes and QTLs identified in natural genetic diversity (see Supplementary Table S1; Sato *et al.*, 2012). Tomato phyllotaxis is not faithfully represented for convenience.

Zhang *et al.*, 2015). Recent studies on the impact of controlled abiotic stresses (water or salt stress) identified specific QTLs controlling the GxE interaction (QTLxE; Albert *et al.*, 2016; Diouf *et al.*, 2018). Therefore, to assess QTLxE effects and identify the genes controlling their variation, future studies should include a wide range of environmental conditions coupled with appropriate statistical methods (Malosetti *et al.*, 2013). With the current availability of high-resolution populations, the impact of the environment on candidate loci controlling important traits can be deciphered. This information could be used both in breeding programs, by allowing the accurate choice of the QTL transferred into elite lines, and for functional validation studies.

While most QTLxE studies have involved two contrasting environments (i.e. a single stress condition vs its control), there is a knowledge gap in the identification of QTLs involved in responses to combined stress. This aspect is of capital importance as it was shown that stress combination in tomato (biotic and/or abiotic) does not always have an additive effect regarding physiological, morphological, or biochemical responses compared with single stress (Rivero *et al.*, 2014; Bai *et al.*, 2018; Martinez *et al.*, 2018).

Mapping populations for gene discovery in tomato

Mapping populations used for gene discovery in tomato are very diverse and display specific and complementary features (Labate *et al.*, 2007). The genomic era with cheaper and high-throughput sequencing capacity has facilitated access to large number of polymorphisms between individuals even between closely related varieties.

This has led to the development of new designs of mapping populations in tomato with saturated genetic maps that amplify the power and precision of QTL detection. Apart from the traditional bi-parental populations and introgression line (IL) sets used to discover genes and QTLs, new segregating populations were recently developed in tomato including backcross inbred lines (BILs) and multi-parent advanced generation intercross (MAGIC) populations. In addition, several panels of naturally evolved accessions were used for GWAS. These populations have different benefits and limits (Figure 2).

From the first ILs developed in tomato from *S. lycopersicum* (cv M82) and the wild *S. pennellii* (LA716) (Eshed and Zamir, 1995), Ofner *et al.* (2016) created a BIL population sustained over 11 generations of selfing and carrying smaller introgressions. The 446 BILs were densely genotyped with the 10k Solcap Single Nucleotide Polymorphism (SNP) array. The authors identified 1049 unique bins at the whole-genome level with half of the bins presenting less than 10 genes. Using two well known QTL/gene, *fw2.2* and *beta-carotene* (*B*), they demonstrated the high-resolution mapping offered by the population. The genome of the *S. pennellii* accession was sequenced (Bolger *et al.*, 2014) and BILs enabled the characterization of QTL involved in yield (Soyk *et al.*, 2017a), leaf shape (Fulop *et al.*, 2016), leaf thickness (Coneva *et al.*, 2017), and day length response (Müller *et al.*, 2016; Soyk *et al.*, 2017b).

To date, only one multi-parental population was developed in tomato with eight parental lines belonging to the cultivated clade *S. lycopersicum var lycopersicum*. This population demonstrated its potential to suitably decipher the genetic architecture of fruit quality traits (Pascual *et al.*, 2015). It did not present any structure and had linkage disequilibrium (LD) decay making it appropriate for linkage/

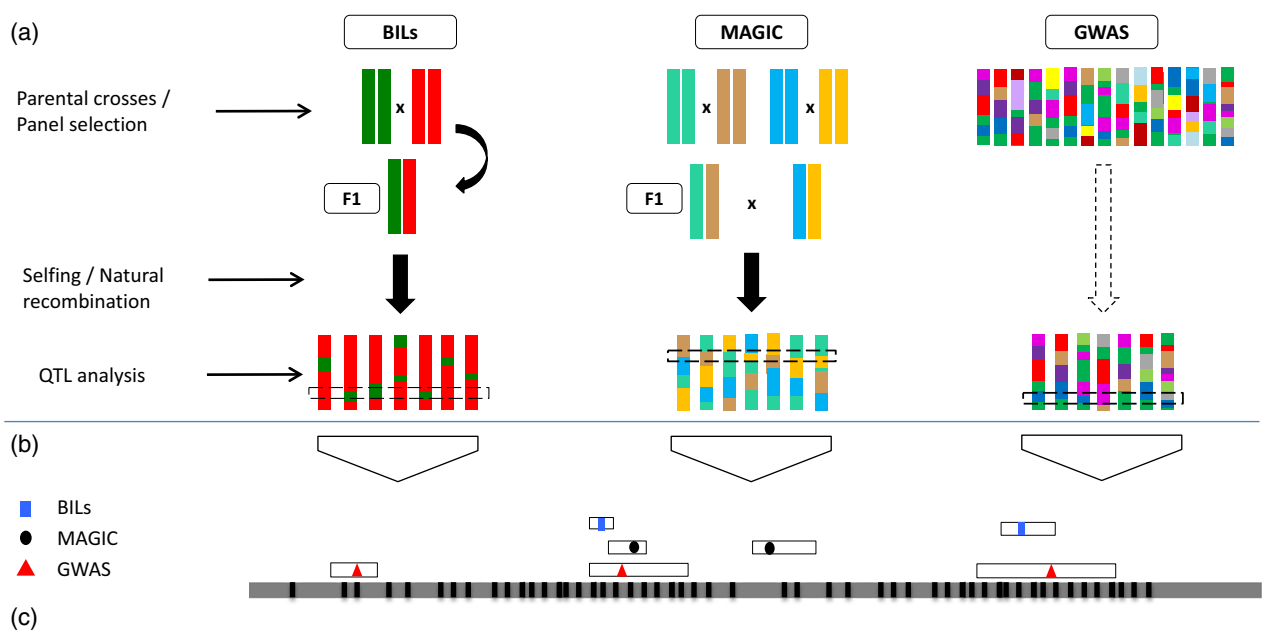

Time to set up	Time consuming	Time consuming	Short time
Allelic diversity	+	++	++++
Population structure	No structure	No structure	Structure
Marker density required	++	+	+++
Mapping resolution	+++	+	variable

Figure 2. New populations developed in tomato for gene/QTL mapping and identification.
(a) Mapping population development and linkage/association analysis. BILs are created by backrossing the F1 hybrid into the recurrent parent, followed by several selfing generations. A single (or a few) portion of the wild recurrent parent is introgressed. MAGIC population here involved crossing four parental lines producing two F1 hybrids thereafter crossed together. The derived progeny then follows several generations of selfing to reach inbred MAGIC lines. GWAS panels are constitued by natural accessions each of which has its own recombination history. For each population and the GWAS panel, appropriate statistical models are used to decipher the linkage/association between DNA polymorphism and the observed phenotypic variation.
(b) The confidence intervals around the identified QTL can be aligned onto the physical map of the reference tomato genome and compared according to their positions. Candidate genes can be suggested when the intervals are not too large.
(c) Key characteristics differentiating BIL, MAGIC and GWAS populations.

association mapping. It was also used for testing environmental effects on traits of interest and for deciphering the genetic basis of GxE interactions (Diouf *et al.*, 2018). This population was also used in a comparative study showing its complementarity to bi-parental populations and GWAS panels (Pascual *et al.*, 2016). GWAS panels accumulate a large diversity, notably if some wild accessions are included in the panel, and therefore allow identification of more loci significantly associated with the trait variation than in the bi-parental and MAGIC populations.

After the release of the tomato reference genome, GWAS has been rapidly applied to the exploration of various traits including fruit composition and plant architecture. The first panel studied included accessions of cultivated tomato, cherry tomato and wild *S. pimpinellifolium* accessions (Sauvage *et al.*, 2014). Collections of unrelated accessions usually present some structure pattern that can hamper the detection of significant associations or conduct false-positive associations, limiting the potential of GWAS to detect reliable associations. Statistical modeling correcting for the effect of population structure can solve this problem, but may lead to missing some true associations for traits correlated to the structure such as fruit weight (Xu *et al.*, 2013). To limit the impact of panel structure, Albert *et al.* (2016) studied a new panel composed of cherry fruit accessions that showed a limited structure. Large panels of resequenced accessions also allowed the identification of several genes related to domestication traits (Lin *et al.*, 2014) or composition (Zhu *et al.*, 2018). Other GWAS studies showed that associations could be identified using a panel of landrace accessions but this led to a limited number of associations (Ruggieri *et al.*, 2014; Sacco *et al.*, 2015).

Important genes and QTLs recently discovered

The genetic basis of many agronomic important traits has been dissected using segregating populations (as described above). The availability of the genome sequence allowed the identification of many new candidate genes, but just a few mutations corresponding to major phenotypes or QTLs have been identified and functionally validated so far. The function of several genes previously cloned was also specified. Several fruit shape and size mutations were described. Among the four genes responsible for fruit shape diversity (Rodríguez *et al.*, 2011), Soyk *et al.* (2017a) showed that the fasciated (*fas*) locus, which leads to increased locule number and fruit size during tomato domestication, results from a regulatory mutation in *CLAVATA*3 (*SlCLV3*), which interacts with *WUSCHEL* (*SlWUS*) in the region harboring two SNPs responsible for the *lc* mutation (Muños *et al.*, 2011; Rodríguez-Leal *et al.*, 2017). Two fruit weight QTLs were newly cloned, corresponding respectively to a cytochrome P450 (*fw3.2*; Chakrabarti *et al.*, 2013) and to a novel protein (cell size regulator), which increases fruit weight predominantly through enlargement of the pericarp areas (*fw11.2*; Bardol *et al.*, 2013; Mu *et al.*, 2017).

In addition to fruit size increase, domestication has led to many changes (Sauvage *et al.*, 2017). Two mutations involved in day length response were cloned. Müller *et al.* (2016) showed that the circadian clock of cultivated tomato has slowed following domestication due to a variation in the *EID1* gene encoding a phytochrome A-associated F-box protein. The other gene was the florigen paralog and flowering repressor *SELF-PRUNING 5G* (*SP5G*). This was identified following a QTL-seq approach on an F2 population and was validated by CRISPR/Cas9 (Soyk *et al.*, 2017a). The evolution of the inflorescence architecture was also dissected and two transcription factors influencing the truss ramification identified (Xu *et al.*, 2015; Soyk *et al.*, 2017b). The two genes interact together, but exploiting natural and engineered alleles for these genes produced a continuum of inflorescence complexity that can be used by breeders for increasing yield.

The mutation controlling fruit uniform ripening, which is now used in every modern accession was characterized (Powell *et al.*, 2012). It is encoded by a Golden 2-like transcription factor regulating chloroplast development in fruit. With a lower photosynthetic capacity, the mutation was shown to affect fruit sugar content, suggesting a role in the poorer taste of modern varieties. Since cloning of long shelf-life genes (Vrebalov *et al.*, 2002), very few genes controlling variation in fruit firmness have been discovered, apart from a mutation in pectate lyase, which was shown to correspond to a QTL for fruit firmness (Uluisik *et al.*, 2016; Wang *et al.*, 2018).

Investigation of fruit sensorial and nutritional quality was considerably aided by the large scale inventory of fruit metabolites (metabolome) (Fernie and Tohge, 2017). Increased analytical throughput and widening of the range of metabolites identified and of genetic diversity studied led to the detection of hundreds of metabolite QTLs (mQTLs) controlling fruit composition (primary and specialized metabolites, volatiles, cuticle components, etc.) (Alseekh *et al.*, 2015, 2017; Ballester *et al.*, 2016; Ofner *et al.*, 2016; Tieman *et al.*, 2017; Albert *et al.*, 2018; Garbowicz *et al.*, 2018; Zhu *et al.*, 2018). This was the first step for identification by map-based cloning of genes involved in metabolite variations such as a glycosyltransferase controlling smoky aroma (Tikunov *et al.*, 2013) and a MYB transcription factor responsible for pink fruit color (Ballester *et al.*, 2010). The genetic control of fruit anti-nutritional alkaloids was also deciphered (Itkin *et al.*, 2013). GWAS studies coupled with mQTL analyses further identified several loci of interest for improving major fruit quality traits such as malic acid content (Ye *et al.*, 2017) or aromas (Bauchet *et al.*, 2017; Tieman *et al.*, 2017). More recently, Zhu *et al.* (2018) showed, by screening a large set of lines, that

selection for agronomical traits (fruit size, fruit color, virus resistance) during domestication and improvement led to the modification of fruit metabolome through hitchhiking.

GENETIC RESOURCES FOR TRAIT DISCOVERY IN TOMATO

Investigating the wild reservoir of genetic diversity

The 12 wild species related to tomato were rapidly used to set up segregating populations and discover new traits or genes of interest. All these populations allowed mapping and characterization of a myriad of major genes and QTLs involved in various traits (recent synthesis in Grandillo and Cammareri, 2016). ILs, notably the set developed between *S. pennellii* and *S. lycopersicum* (Eshed and Zamir, 1995), were used to map many QTLs for fruit composition (Schauer *et al.*, 2006; Alseekh *et al.*, 2015). A unique QTL was shown to improve at the heterozygous level harvest index, earliness and metabolite content (sugars and amino acids) in processing tomatoes (Gur *et al.*, 2010, 2011). ILs were also used to fine map and positionally clone several genes and QTL of interest. A natural mutation in the *SFT* gene, involved in flowering time, was shown to correspond to a single overdominant gene that increases yield in hybrids of processing tomato (Krieger *et al.*, 2010). The BILs developed from this population were then used to clone several genes (see above).

The comparison of whole genome SNP distribution in the wild *S. pimpinellifolium* and the domesticated *S. l. cerasiforme* (*S.l.c.*) or cultivated accessions identified regions of genetic bottleneck, which occurred during domestication and selection (Lin *et al.*, 2014; Blanca *et al.*, 2015). The potential of other species was shown but to a lesser extent. For instance an allelic variant increasing sugar content was identified in the promoter of a gene encoding an ADP-glucose pyrophosphorylase from *S. habrochaites* (Petreikov *et al.*, 2006). The mutation allowing an extended gene expression led to higher starch accumulation during fruit development and subsequent increase in soluble solid content in ripe fruit. More recently a mutation in a SWEET transporter in wild species was shown to be responsible for a higher fructose to glucose ratio compared with that in *S. lycopersicum* (Shammai *et al.*, 2018).

Wild relative species were particularly useful as a source of disease resistance. More than 100 pathogens attack cultivated tomato. As landrace varieties are susceptible to every pathogen, most of the resistance sources come from the crop wild relatives. This has resulted in a large number of genes mapped for marker-assisted selection and cloning (Foolad and Panthee, 2012; Causse and Grandillo, 2016). In recent years, the first gene conferring resistance to late blight was cloned by Zhang *et al.* (2014) as well as several genes conferring resistance to the Tomato Yellow Leaf Curl virus: the allelic genes *Ty1* and *Ty3* (Verlaan *et al.*, 2013); *Ty-5* (Lapidot *et al.*, 2015);. *Ty-2* (Yamaguchi *et al.*, 2018). Defense against insects remains challenging. Analysis of natural and induced variation in tomato glandular trichome flavonoids identified a myricetin *O*-methyltransferase gene absent in the reference genome (Kim *et al.*, 2014). The acylsugars metabolism in trichomes and their role in insect defense were also deciphered and the role of an isopropylmalate synthase and of acyltransferases underlined (Ning *et al.*, 2015; Schilmiller *et al.*, 2015). Screening for the discovery of markers for new resistance genes has also continued with a higher efficiency thanks to the availability of reference genome sequences (Bao *et al.*, 2015; Haggard *et al.*, 2015; Kim *et al.*, 2016, 2017, 2018; Wang *et al.*, 2016; Hameed *et al.*, 2017).

Artificially induced genetic diversity: an additional genetic resource for trait discovery in cultivated tomato

Mutant collections offer a complementary alternative for trait discovery in tomato and provide an allelic series on a uniform genetic background. In tomato, the main physical mutagenic agents are fast-neutron, which causes large deletions and translocations, and gamma-ray bombardments, which provoke small deletions and point mutations (Meissner *et al.*, 1997; Emmanuel and Levy, 2002; Shirasawa *et al.*, 2016). The most widely used chemical mutagen is EMS, which induces point mutations (SNPs) evenly distributed at high frequency over the genome. Because up to 10 000 mutations per plant can be obtained in highly mutagenized tomato populations (Garcia *et al.*, 2016; Petit *et al.*, 2016; Shirasawa *et al.*, 2016; Musseau *et al.*, 2017; Pulungan *et al.*, 2018), a limited number of lines (<3000 lines) is sufficient to reach saturation mutagenesis. Therefore, large allelic series, including strong and hypomorphic alleles producing a range of phenotypic alterations (Park *et al.*, 2014; Musseau *et al.*, 2017), can be obtained for a given gene of interest. It is noteworthy that several traits found in natural germplasm are not likely to be observed in mutant collections, including the traits caused by transposition of mobile elements (Xiao *et al.*, 2008) or by epigenetic alterations (Manning *et al.*, 2006; Kanazawa *et al.*, 2011; Chen *et al.*, 2015).

Both determinate and indeterminate tomato cultivars have been used for generating fast-neutron and EMS mutant collections in the last decades (Meissner *et al.*, 1997; Menda *et al.*, 2004; Minoia *et al.*, 2010; Okabe *et al.*, 2011; Just *et al.*, 2013). Mutant collections of the determinate processing tomato cultivar M82 and model miniature tomato Micro-Tom, well suited for laboratory use, have been systematically screened for tens of phenotypic descriptors of traits such as yield, plant architecture, leaf shape and complexity, flower and fruit morphology, color and ripening, etc. (Menda *et al.*, 2004; Saito *et al.*, 2011; Just *et al.*, 2013). Data stored in publicly available databases (http://tomatoma.nbrp.jp/; http://zamir.sgn.cornell.ed

u/mutants/) can be mined for mutants harboring specific traits and the corresponding seeds can be ordered. Tomato mutant collections have been successfully used for identification by Targeting Induced Local Lesions IN Genomes (TILLING) of allelic series for genes involved in a wide range of biological processes (reviewed in Rothan *et al.*, 2016). Over the last few years, a growing number of mutations that underlie remarkable tomato traits have been isolated by forward genetics approaches. They proved to be very efficient for (1) deciphering pathways controlling plant architecture and yield heterosis (*sft* alleles; Krieger *et al.*, 2010; Park *et al.*, 2014); and (2) for discovering new functions involved in inflorescence branching and fruit size (*fab* and *fin* alleles; Xu *et al.*, 2015), leaf development (*curl*; Pulungan *et al.*, 2018), male and female sterility (*Slses*; Hao *et al.*, 2017), carotenoid sequestration in plastoglobules (*pyp*; Ariizumi *et al.*, 2014), and regulation of cutin formation (*cd2*; Isaacson *et al.*, 2009), biosynthesis (*cd3/cyp86a69* and *gpat6*; Shi *et al.*, 2013; Petit *et al.*, 2016), and polymerization (*cd1/gdsl1/cus1*; Yeats *et al.*, 2012; Petit *et al.*, 2014).

ACCELERATING TRAIT DISCOVERY IN TOMATO USING DEEP SEQUENCING STRATEGIES

The natural and artificially induced genetic diversity available in tomato is considerable and holds a great potential for trait discovery. However, while hundreds of QTLs controlling various traits have been mapped, comparatively few genetic variants that underlie QTLs have been identified to date (see above). Actually, until very recently, linking trait to genetic variations relied mostly on map-based cloning approaches using DNA markers and on the development of specific populations. Once the chromosomal region harboring the trait has been identified, its subsequent break-down to identify the causal polymorphism can be a daunting task because of the high number of candidate genetic variants or, at the opposite end, the absence of obvious candidate genes as well as the possible high LD and low meiotic recombination in the target region. The availability of high quality tomato reference genome sequences and cheap deep sequencing technologies has accelerated trait discovery via approaches such as QTL-seq and MBS or integration of multiomics data.

Bulk segregant analysis coupled with whole-genome sequencing approaches

By allowing comparison with reference genome sequences, whole-genome sequencing (WGS) has enabled the discovery of all polymorphisms in a given genotype, including causal genetic variation. Association with fine mapping reduced the number of polymorphisms to a chromosomal region (Illa-Berenguer *et al.*, 2015; Petit *et al.*, 2016; Hao *et al.*, 2017). Usually, the target region still holds a large number of candidate SNPs/indels and it is therefore necessary to confirm their function by studying additional alleles or by functional analyses. This strategy has been successfully employed by Ariizumi *et al.* (2014) who detected EMS tomato mutants that harbored pale colored flowers, performed allelic tests to demonstrate that mutants complement each other and demonstrated by WGS sequencing that independent mutations in the *PYP1* gene were responsible for the flower color trait.

Bulk segregant analysis (BSA) coupled with WGS alleviates the need for previous mapping of the trait. Here QTL-seq is used for BSA-WGS mapping of natural quantitative variations (Illa-Berenguer *et al.*, 2015; Bazakos *et al.*, 2017); MBS is used for mutation mapping (Schneeberger, 2014) and is illustrated in Figure 3. Once the trait of interest has been detected and its inheritance pattern is determined, the line harboring the trait is crossed to either another tomato genotype (QTL-seq) or to a wild-type (non-mutagenized) parental line (MBS) to produce an F2 progeny segregating for the trait. For QTL-seq, the line of interest can be outcrossed with a not-too-distantly related genotype, typically *S. pimpinellifolium*, or even cherry tomato (*S.l.c.*), because WGS allows the detection of all polymorphisms in tomato genome, *c.* millions of SNPs in *S.l.c.* (Causse *et al.*, 2013), and therefore produces enough DNA markers for trait mapping (Illa-Berenguer *et al.*, 2015). The limitations of outcrossing the line of interest with a distantly related genotype are then avoided and the progeny phenotyping is facilitated. In the MBS strategy, because the mutant is backcrossed with the wild-type parental line, the SNPs detected by WGS, (<10 000 SNPs per plant; Garcia *et al.*, 2016; Pulungan *et al.*, 2018), are only due to mutagenesis. Following phenotyping, F2 plants displaying the same phenotype are pooled, DNA bulks are sequenced, WGS reads are aligned to the reference genome and SNP variants are filtered to exclude polymorphisms linked to the parental genomes (Garcia *et al.*, 2016). An alternative strategy is to first select the exome (Pulungan *et al.*, 2018). This reduces sequencing effort but limits the information to coding regions and exclude *cis*-regulatory regions. Allele frequencies are then analyzed to delineate the chromosomal region harboring the causal genetic variant.

Mapping precision will depend on the extent of recombination in the chromosomal region harboring the genetic variant and on the size of the population studied. Pericentromeric regions, which may account for 75% of the chromosomes in tomato, display high LD and low recombination rates, while chromosome ends are usually highly recombigenic in this species (Sato *et al.*, 2012). To date, reported sizes for QTL-seq encompass several Mb and several tens or hundreds of candidate genes (Illa-Berenguer *et al.*, 2015; Soyk *et al.*, 2017a; Zheng and Kawabata, 2017). DNA markers derived from WGS-detected SNPs are then used to fine map the trait by recombinant analysis. This may remain a tedious task, depending on

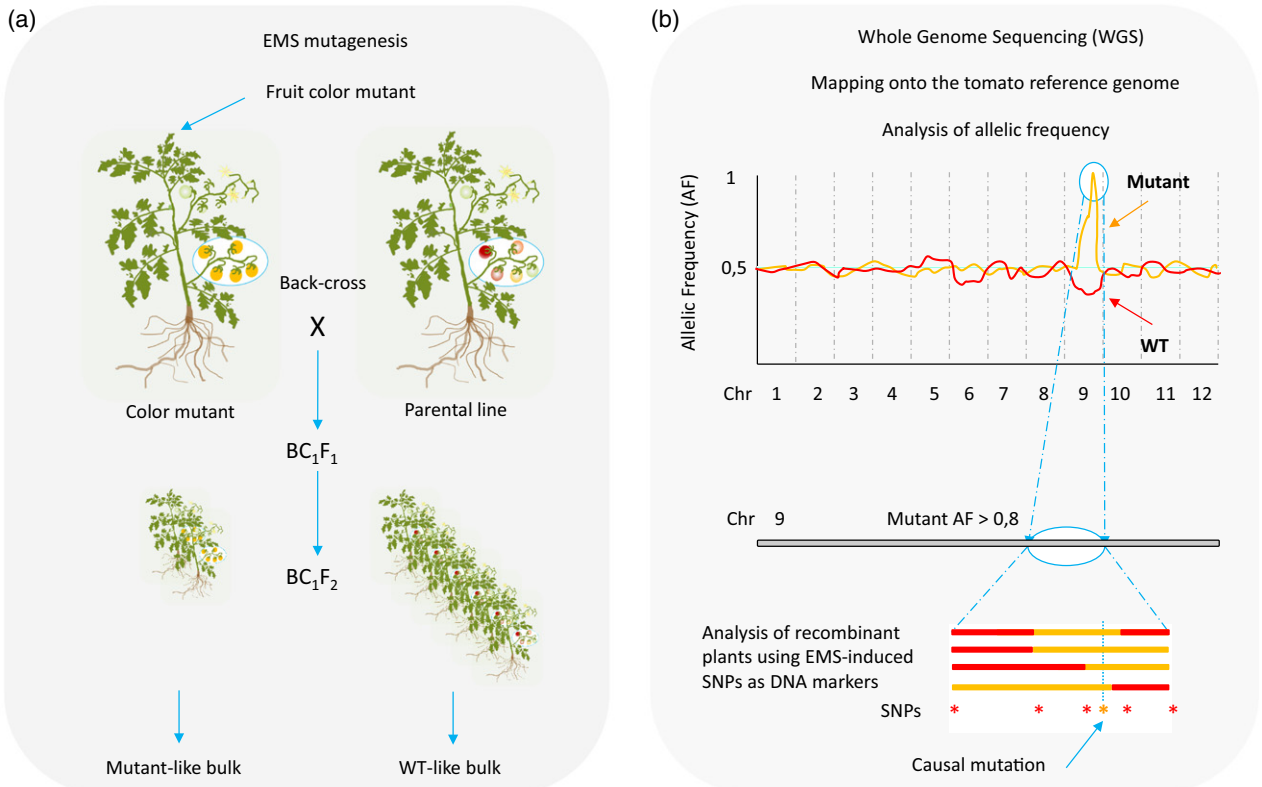

Figure 3. Identification of causal mutation by mapping-by-sequencing (MBS).
(a) Fruit colour mutant (here a recessive orange fruit trait) is detected by screening a tomato EMS mutant collection. Homozygous mutant line is back-crossed to parental (non-mutagenized) line, the BC_1F_1 hybrid is selfed and a BC_1F_2 population segregating for the orange fruit trait is generated. Tomato plants displaying either the wild type trait (red fruit) or the mutant trait (orange fruit) are pooled and DNA is extracted from the bulks.
(b) DNA bulks are sequenced by whole-genome sequencing (WGS). Sequences are mapped onto the tomato reference genome, filtered, and allelic frequencies (AF) of WT and mutant alleles are determined. In case of recessive mutation, genomic region carrying the causal mutation displays an AF > 0.8 for mutant alleles (orange line) and < 0.5 for WT alleles (red line). EMS-induced single nucleotide polymorphisms (SNPs) detected within the genomic region of interest are then used as genetic markers to detect recombinants in the BC_1F_2 segregating population. BC_1F_2 plants homozygous for the mutant allele (orange bars) have orange fruits, while plants heterozygous or homozygous for the WT allele (red bars) have red fruits. Genotype-to-phenotype association allows the unambiguous identification of the mutation responsible for the orange fruit trait in the fruit colour mutant.

the number of SNPs and indels and extent of LD found in the candidate region (Illa-Berenguer *et al.*, 2015; Zhu *et al.*, 2018). One possible way to alleviate this limitation is to combine QTL mapping data with gene expression data and/or with the predicted biological function of the protein. Regarding MBS, because of the comparatively low number of EMS-induced SNPs, reducing the candidate genetic variants to few SNPs or possibly to a single SNP when present in a highly recombigenic region, can be straightforward. Reported sizes for MBS-mapped traits are typically in the 1–4 Mb range and the number of candidate mutations is <10, as indicated for the fruit color mutant *psy1, cutin deficient* mutant *gpat6-a* and fruit parthenocarpy mutation in *SlAGL6* gene (Garcia *et al.*, 2016; Petit *et al.*, 2016; Klap *et al.*, 2017). Recombinant analysis is then usually performed to unequivocally identify the causal mutation (Figure 3). The findings can also be strengthened by studying independent allelic variants from the same population as carried out for the *curly leaf* mutants (Pulungan *et al.*, 2018), or by reverse genetics strategies including CRISPR-Cas9 mutagenesis.

In the very near future, the efficiency and precision of trait mapping using classical map-based cloning or BSA-WGS-based strategies will be accelerated by increased meiotic recombination in tomato. The recent demonstration that an EMS-induced truncation mutation in the anti-crossover DNA helicase RECQ4 increases crossovers in tomato by approximately three-fold (Mieulet *et al.*, 2018) paves the way for such improvement. However, as the *RECQ4* mutation does not increase crossovers in the pericentromeric regions, work is still needed to extend this finding to the whole tomato genome, including low recombigenic regions.

Multiomics analyses

For nearly two decades, 'omics technologies including transcriptomics, proteomics, and metabolomics have been used alone or in combination to discover genes and

networks underlying various traits of interest in tomato. Examples of these are rootstock grafting (Ntatsi *et al.*, 2017), effect of root mycorhization on fruit quality (Zouari *et al.*, 2014), meristem maturation and inflorescence architecture (Park *et al.*, 2012; Soyk *et al.*, 2017a), leaf morphology and thickness (Koenig *et al.*, 2013; Coneva *et al.*, 2017), glandular trichome metabolism (Balcke *et al.*, 2017), seed composition (Toubiana *et al.*, 2015), fruit set and parthenocarpy (Wang *et al.*, 2009; Ruiu *et al.*, 2015), and fruit development, ripening, and composition (Carrari *et al.*, 2006; Faurobert *et al.*, 2007; Mintz-Oron *et al.*, 2008; Mounet *et al.*, 2009; Matas *et al.*, 2011; Osorio *et al.*, 2011; Itkin *et al.*, 2013; Pan *et al.*, 2013; Pattison *et al.*, 2015; Fernandez-Moreno *et al.*, 2016; Szymanski *et al.*, 2017; Li *et al.*, 2018b; Shinozaki *et al.*, 2018; Stevens *et al.*, 2018). While fruit studies outnumber all others, considerable efforts have also been devoted to the study of abiotic stress, including heat (Keller and Simm, 2018), cold (Cruz-Mendívil *et al.*, 2015; Barrero-Gil *et al.*, 2016; Ntatsi *et al.*, 2017), water limitation (Albert *et al.*, 2018), salinity stress (Zhang *et al.*, 2018) and nutrient deficiency (Zamboni *et al.*, 2012), and of plant reaction to biotic stress, causes of which include viruses (Ramesh *et al.*, 2017), bacteria (French *et al.*, 2018), fungi (Blanco-Ulate *et al.*, 2013; Ghosh *et al.*, 2016), and nematodes (Święcicka *et al.*, 2017).

However, large scale 'omics analyses typically produce tens or hundreds of candidate genes, which cannot all be analyzed by reverse genetics. Even the precise knowledge of when, where, and in response to what stimuli a gene or a protein is expressed and/or to which pathway or network it belongs is usually not sufficient to confidently predict its implication in a trait of interest. In recent years, integration of 'omics data with additional phenotypic and genetic information, aided by the establishment of bi-parental and multi-parental tomato populations and the mapping of metabolic QTL (mQTL) and/or expression QTL (eQTL) (Toubiana *et al.*, 2012; Alseekh *et al.*, 2015; Ranjan *et al.*, 2016; Albert *et al.*, 2018; Garbowicz *et al.*, 2018), has considerably helped linking gene to phenotype. To cite a few traits, candidate genes underlying tolerance to continuous light (Velez-Ramirez *et al.*, 2014) and to water limitation (Albert *et al.*, 2018), and fruit metabolic variations in cuticle compounds (Ofner *et al.*, 2016), fructose to glucose ratio (Shammai *et al.*, 2018), steroidal glycoalkaloids (Itkin *et al.*, 2013) and other secondary metabolites (Alseekh *et al.*, 2015), carotenoids (Lee *et al.*, 2012), and flavor volatiles (Garbowicz *et al.*, 2018) have been uncovered and, for several of these, functionally validated, using various combinations of 'omics technologies, genetics, and functional analysis.

The increased availability and low cost of deep sequencing now enabled the integration of 'omics and genetics information. Over the last few years, GWAS combined with extensive mapping of various traits including fruit metabolite content (mGWAS) of up to 398 tomato genotypes enabled both the identification of domestication and improvement sweeps (see for example Tieman *et al.*, 2017) along the genome and the dissection of genetic and biochemical bases of fruit primary metabolite and ascorbate contents (Sauvage *et al.*, 2014), malate content (Ye *et al.*, 2017), pink fruit color (Lin *et al.*, 2014), and flavor components (Bauchet *et al.*, 2017; Tieman *et al.*, 2017). Very recently, association studies were brought to an unprecedented resolution level by integrating SNP data (~26 million SNPs) with fruit transcriptome (RNA-seq, ~30 000 genes) and metabolome (362 annotated metabolites) datasets from between 399 and 610 accessions of wild tomato species, *S. pimpinellifolium*, *S. lycopersicum* var. *cerasiforme,* and *S. lycopersicum* (Zhu *et al.*, 2018). In this study, mapping of mQTLs and eQTLs and the study of their association with SNPs by building a multiomics correlation network revealed new metabolic genes and pathways underlying major fruit metabolic traits such as the content in anti-nutritional glycoalkaloids or the pink fruit color. In addition, this study emphasized the metabolic selection sweeps that modern tomato underwent along its history and highlighted the contribution to fruit composition of linkage drags associated with the introgression of fruit weight QTLs and of seemingly unrelated traits such as virus resistance.

We may expect that such powerful forward genetic strategy will be used for the discovery of genetic variations underlying many other tomato traits, for example plant responses to various environmental stresses or pathogens. We may also expect that it will be extended to the discovery of traits under epigenetic regulation by analyzing the methylome of germplasm collections. Recent studies have paved the way for such advances by demonstrating that fruit development and ripening was dependent upon the methylation status of key regulatory and structural genes (Manning *et al.*, 2006; Kanazawa *et al.*, 2011; Zhong *et al.*, 2013; Chen *et al.*, 2015; Liu *et al.*, 2015; Lang *et al.*, 2017; Corem *et al.*, 2018) as was the accumulation of vitamin E (Quadrana *et al.*, 2014) and the production of flavor volatiles in fruits submitted to chilling stress (Zhang *et al.*, 2016). Given the prominent role of epigenetics in developmental processes and stress responses (Giovannoni *et al.*, 2017), it is likely that integration of phenotypic data with information on the transcriptome, genome, and epigenome will, in the very near future, give access to heritable epigenetic changes underlying trait variation in tomato.

FROM TRAIT DISCOVERY TO TRAIT ENGINEERING: GENE EDITING

Once a trait has been discovered, the genotype–phenotype relationship must be established by screening tomato germplasm for additional alleles or through reverse genetic strategies such as gene complementation, gene

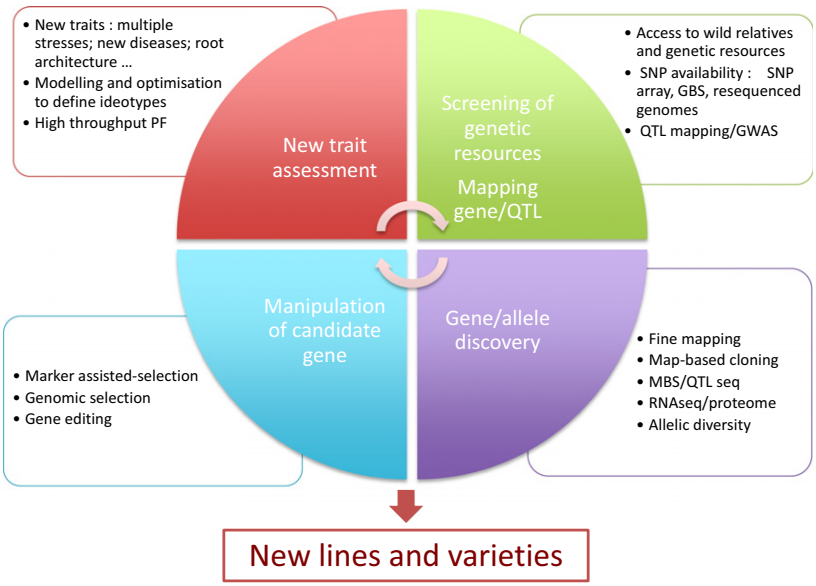

Figure 4. General strategy to breed a new trait of interest.
(1) New traits may be complex to assess, notably the response to multiple biotic and abiotic stresses or root-related traits. Automated high-throughput phenotypic platforms (PF) may contribute to phenotyping and ecophysiological modeling may help to define new ideotypes. (2) Once the target phenotype is defined, genetic resources are screened and mapping populations or GWAS panels are used to map the genes/QTLs controlling the trait variation. For this purpose, many SNP resources are available. (3) The discovery of the gene/allele underlying a specific QTL or a mutation requires either fine mapping and map-based cloning or MBS/QTL-seq. Screening allelic diversity in genetic resources and mining 'omics data (RNA-seq, proteome) and literature may provide additional information on the candidate gene. (4) Manipulation of the candidate gene through targeted gene editing of *cis*-regulatory or coding sequences can be used to validate its role in the trait. Finally, the creation of a new cultivar will follow a combination of marker-assisted selection, genomic selection and gene editing (when possible).

disruption, or gene silencing (Figure 4). Over the last three decades, various gene silencing (co-suppression, antisense RNA and RNA interference) and gene complementation strategies based on stable genetic transformation have been used for functional analysis of target genes and played crucial roles in the establishment of genotype–phenotype relationships in tomato (Frary *et al.*, 2000; Fernandez *et al.*, 2009; Grierson, 2016). Over the last 15 years, fast transient assay systems based on the use of viruses such as the virus-induced gene complementation (VIGC) (Zhou *et al.*, 2012; Kong *et al.*, 2013) or the widely used virus-induced gene silencing (VIGS) (Liu *et al.*, 2002) technologies were effectively developed in tomato for functional analysis and validation of candidate genes. Virus-based technologies have also been used for inducing stably inherited mutational epi-modifications to target genes in tomato (Kanazawa *et al.*, 2011). In the last 5 years, CRISPR/Cas9 system has been successfully established in tomato and has undergone, since then, an overwhelming development. All these technologies have already proved their large interest for establishing genotype–phenotype relationships. In this review, we will purposely focus on the most recent applications of GE to tomato and more specifically on the CRISPR/Cas9 system, which now allows precise gene disruption, base editing and even targeted gene replacement in tomato.

Once the genotype–phenotype relationship has been validated *in planta*, the trait can be exploited for tomato improvement e.g. by pyramiding favorable alleles by marker-assisted selection for constructing superior tomato varieties combining yield, fruit quality and stress resistance. However, even with the help of advanced genotyping technologies and of recombination engineering (Mieulet *et al.*, 2018), this task can remain difficult as unfavorable genes with large pleiotropic effects may be introgressed together with the favorable alleles (Zhu *et al.*, 2018). Then, the ideal would be to reproduce directly in elite lines the allelic variation(s) responsible for improvement of the trait(s) of interest. Thanks to the recent advances in GE technologies, reaching this objective can be expected in the very near future, as very recently demonstrated by several studies (Rodríguez-Leal *et al.*, 2017; Li *et al.*, 2018c; Zsögön *et al.*, 2018).

Gene editing systems used for tomato mutagenesis

Zinc finger nucleases (ZFNs), transcription activator-like effector nucleases (TALENs), and clustered regularly interspaced short palindromic repeats (CRISPR) and its associated nuclease Cas (CRISPR-associated system) have been successfully applied to tomato (Van Eck, 2018; Yamamoto *et al.*, 2018). All three technologies are designed to target and edit a given sequence using sequence-specific binding

domains fused to a non-specific nuclease that creates double-stranded breaks (DSB) in adjacent sequences. Because DNA DSBs, which occur naturally in the plant, may be extremely damaging when left unrepaired, plants have developed DSB repair mechanisms. DSBs can be repaired by error prone non-homologous end joining (NHEJ), which can introduce point mutations and/or small insertions/deletions, or by homology-directed homologous recombination (HR) (Puchta, 2017). Because of inherent complexity and incidence of off-targets, the use of ZFN (Hilioti *et al.*, 2016) and of TALEN (Lor *et al.*, 2014; Čermák *et al.*, 2015) for tomato genome engineering has been limited, in contrast with the CRISPR/Cas9 system. Studied for decades for its role in bacterial antiviral defense, CRISPR-Cas has been recently developed into a simple, versatile, and cheap technology for cleaving and editing DNA sequences in eukaryotes. CRISPR/Cas9 relies on the combination of the *Streptococcus* Cas9 endonuclease with an engineered single-guide RNA (gRNA) that can find a given DNA target. Soon after its development, CRISPR/Cas9 was successfully used in tomato either via *Agrobacterium rhizogenes* root transformation (Ron *et al.*, 2014) or via *Agrobacterium tumefaciens* cotyledon transformation that generates heritable mutations (Brooks *et al.*, 2014).

Gene disruption with CRISPR/Cas9 in tomato

Since the early applications of CRISPR/Cas9 GE to tomato, the number of tomato traits engineered with this system has exploded (see for review Scheben *et al.*, 2017; Van Eck, 2018; Yamamoto *et al.*, 2018). To date, CRISPR/Cas9 has been chiefly used to knock out genes by creating NHEJ-repaired DSBs in target coding regions. A dominant gain-of-function mutation was also reported for a DELLA protein (Tomlinson *et al.*, 2018). In tomato, in which genetic transformation is carried out via somatic embryogenesis, very high frequencies of bi-allelic and homozygous heritable mutations can be obtained in the first generation (up to 100%; Brooks *et al.*, 2014; Pan *et al.*, 2016; Ueta *et al.*, 2017), meaning that CRISPR engineered tomato plants can be studied a few months after tissue culture. To further fix the mutation and exploit it for breeding, the transgenes have to be segregated out in the progeny (Yu *et al.*, 2017; Van Eck, 2018). The efficiency of gene disruption can be improved using Cas9 nuclease with paired gRNAs targeting the two ends of a specific sequence (Puchta, 2017). Standard protocols for *Agrobacterium*-mediated transformation have been published for main tomato varieties (Van Eck, 2018) and can be adapted for recalcitrant genotypes. User-friendly tools such as CRISPOR (http://crispor.tefor.net/; Haeussler *et al.*, 2016) , which takes into account GC content and possible tomato off-targets for designing gRNAs, are publicly available. In addition, non-profit plasmid repositories such as AddGene (https://www.addgene.org/) provide plasmids useful for CRISPR/Cas9 editing of tomato, including plant-optimized Cas9 (Li *et al.*, 2013) and modular cloning systems for multiplexing (Weber *et al.*, 2011).

In the recent years, many tomato genes have been successfully targeted by CRISPR/Cas9, resulting in alteration of traits such as root development (Ron *et al.*, 2014), leaf development (Brooks *et al.*, 2014; Pan *et al.*, 2016), day neutrality and yield (Soyk *et al.*, 2017a), meristem size and inflorescence architecture (Xu *et al.*, 2015), pollen development (Chen *et al.*, 2018; Qin *et al.*, 2018), fruit parthenocarpy (Klap *et al.*, 2017), fruit ripening (Ito *et al.*, 2015; Li *et al.*, 2018b), fruit composition (Nonaka *et al.*, 2017), fruit shelf life (Yu *et al.*, 2017), chilling temperature tolerance (Li *et al.*, 2018d) as well as in enhanced resistance to the fungal pathogen powdery mildew (Nekrasov *et al.*, 2017). In addition, the combination of natural and gene-edited mutations of regulators of meristem maturation successfully enabled the development of weakly branched tomato hybrids with higher flower and fruit production (Soyk *et al.*, 2017a). Multiplex genome editing of up to six genes with multiple gRNAs was also effective in increasing fruit nutritional value by rewiring lycopene (Li *et al.*, 2018a) and GABA (Li *et al.*, 2017) metabolic pathways.

Recent developments of CRISPR/Cas9 system and exploitation for tomato breeding

The NHEJ mechanism was also harnessed for creating new allelic diversity. Many natural variations favored by domestication and improvement are found in *cis*-regulatory regions because mutations in coding regions may have undesirable pleiotropic effects (Swinnen *et al.*, 2016). By targeting with many gRNAs the *cis*-regulatory regions of *SlWUS* and *SlCLV3* that are involved in the control of tomato carpel number and thus of fruit size (Muños *et al.*, 2011; Xu *et al.*, 2015), Rodríguez-Leal *et al.* (2017) could produce a series of mutations including deletions, insertions, inversion, and point mutations. The *cis*-regulatory alleles, which induced a range of phenotypic changes recapitulating the quantitative variations in carpel number/ fruit size observed in cultivated tomato resources, could be further combined and fixed in the progeny. Additionally, they also showed that plant architecture and inflorescence production could be engineered by targeting promoters from COMPOUND INFLORESCENCE and SELF PRUNING, two genes already known to control tomato yield (Park *et al.*, 2014).

Such a strategy, which produces transgene-free plants that can be integrated into a breeding programme after evaluation of their phenotypic value, can be extended to the engineering of a wide range of traits in a single tomato variety (Zsögön *et al.*, 2017). Of special interest are those traits that should be fine tuned because there is a trade-off between plant fitness/productivity/quality and adaptation to abiotic stresses (water limitation, salinity,

etc.) (Mickelbart *et al.*, 2015) or to biotic stresses e.g. viruses (Gauffier *et al.*, 2016). Very recently, Zsögön *et al.* (2018) and Li *et al.* (2018c) engineered the *S. pimpinellifolium* wild ancestor of cultivated tomato by CRISPR multiplexing with six gRNAs, which resulted in the generation of gene-edited plants with characteristics similar to those of cultivated tomato, i.e. increased fruit yield and nutritional value. GE targets were *cis*-regulatory regions, coding regions or upstream μORF of domestication genes involved in the regulation of plant architecture, fruit carpel number, size and shape, and synthesis of lycopene and ascorbate. In addition, the various accessions of *S. pimpinellifolium* gene edited by Li *et al.* (2018c) displayed salt tolerance and, for two of these, resistance to bacterial spot disease.

A second recent breakthrough in tomato (GE) and engineering of agricultural traits is the demonstration that the HR mechanism can be effectively harnessed for gene replacement. HR enables the integration of an intended mutation into the target site, providing that a DNA repair template is available. However, because HR is much less efficient than NHEJ in somatic plant cells, it requires considerable efforts for screening large numbers of transformed plants or the use of selection markers. Recently, geminivirus amplicons were shown to considerably increase the efficiency of donor template delivery for HR DNA repair in tomato (Čermák *et al.*, 2015, 2017). Dahan-Meir *et al.* (2018) combined, in a single vector designed for *Agrobacterium*-mediated transformation, the CRISPR/Cas9 DSB induction system with a geminivirus replicon carrying a WT 3′ truncated *CAROTENOID ISOMERASE* (*CRTISO*) gene as donor. The defective deletion allele responsible for *tangerine* mutation was effectively replaced by the WT allele, thus restoring the red fruit color phenotype. Although these achievements still require confirmation for additional targets, the very high proportion of HR observed in this study (25% of first generation plants), without selection during tissue culture, is very promising. Prospects such as the reproduction of natural genetic diversity in tomato elite lines, the precise editing *in planta* of *cis*-regulating elements or of proteins with the desired properties, e.g. for creating new virus resistance (Bastet *et al.*, 2018), can now be considered.

The application for crop improvement of CRISPR/Cas9 system is expanding continuously (Scheben *et al.*, 2017). New Cas enzymes offer increased fidelity or RNA targeting possibilities (Puchta, 2017). Marker-free and new multiplexing systems have been developed for tomato (Čermák *et al.*, 2017). One possible exploitation of Cas9 is the generation of a deactivated dCas9 or a nickase nCas9, which recognizes a DNA−gRNA complex but does not induce DSBs. Cytidine deaminase fused to dCas9 or nCas9 induces point mutations at cytidines within the target range, as successfully established in several crops including tomato (Shimatani *et al.*, 2017). Recently, a dCas9 fused to a human demethylase was shown to induce heritable epigenetic changes at specific loci in Arabidopsis (Gallego-Bartolomé *et al.*, 2018) opening the way for epigenome editing of gene regulation in tomato.

CONCLUSION

The pace of trait discovery in tomato has considerably accelerated in the recent years. Whole genome sequencing and RNA-seq has enabled easier mapping and narrowing down of the region harboring the traits of interest or even the direct identification of EMS-induced causal mutations. Genes, SNPs, indels, or methylation patterns underlying remarkable phenotypes are currently being identified for major fruit traits. In addition, current technologies allow the integration of SNP, transcriptome, and metabolome data gathered at genome-wide level from hundreds of tomato genotypes for discovering and tracing back the history of genetic variations that underlie complex traits. At last, the tomato EMS and gene-edited recombination mutants now available, which increase meiotic crossovers by at least three-fold (Mieulet *et al.*, 2018), should considerably reduce the work necessary to identify genetic variants and accelerate trait discovery.

In the very near future, genetic variations that underlie additional phenotypic variations will continue to be discovered, including for environment-dependent traits. One of the main limitations is now the availability and throughput of phenotyping technologies, notably for the study of environmental stress impact. The availability of high-density genotyping techniques and large collections of resequenced collections may help to set up genomic selection for quantitative traits (Duangjit *et al.*, 2016; Yamamoto *et al.*, 2017), which should be combined with single mutations for breeding purposes (Figure 4).

Tomato is ideally suited for trait engineering by GE and several techniques can now be exploited for breeding superior tomato varieties. However, the exploitation of CRISPR/Cas9 technologies for breeding is facing huge regulatory issues in several countries. While the USA considers that CRISPR-edited organisms are not genetically modified organisms (GMOs) (Waltz, 2016), the European Union (EU) has very recently considered, in a preliminary judgment, that CRISPR mutagenesis constitutes alterations made to the genetic material and therefore satisfies the definition of a GMO (Callaway, 2018). In practice, new tomato varieties obtained through GE technologies ,including CRISPR, will have to undertake the long process of GMO authorization and will face social acceptance issues in Europe. This caveat will probably prohibit their use within the EU market over the coming years, while other tomato markets will be largely open to GE tomato varieties.

ACKNOWLEDGEMENTS

This work was supported by the TomGEM H2020 EU project (679796), the Traditom (634561) H2020 EU project and Région Nouvelle Aquitaine AgirClim project. We would like to thank JP Mauxion for helpful discussions on the implementation of CRISPR/Cas9 system in tomato.

CONFLICT OF INTEREST

The authors declare that they have no competing interests.

SUPPORTING INFORMATION

Additional Supporting Information may be found in the online version of this article.

Table S1. Identified genes and QTLs underlying tomato traits.

a) Genes corresponding to a phenotyped mutation mapped on the tomato genome.

b) Disease resistance traits.

c) Flower, ovary and fruit development and yield traits.

d) Metabolite traits.

REFERENCES

Aflitos, S., Schijlen, E., de Jong, H. *et al.* (2014) Exploring genetic variation in the tomato (*Solanum* section *lycopersicon*) clade by whole-genome sequencing. *Plant J.* **80**, 136–148.

Albert, E., Segura, V., Gricourt, J., Bonnefoi, J., Derivot, L. and Causse, M. (2016) Association mapping reveals the genetic architecture of tomato response to water deficit: focus on major fruit quality traits. *J. Exp. Bot.* **67**, 6413–6430.

Albert, E., Duboscq, R., Latreille, M. *et al.* (2018) Allele specific expression and genetic determinants of transcriptomic variations in response to mild water deficit in tomato. *Plant J.* **96**, 635–650.

Alseekh, S., Tohge, T., Wendenberg, R. *et al.* (2015) Identification and mode of inheritance of quantitative trait loci for secondary metabolite abundance in tomato. *Plant Cell*, **27**, 485–512.

Alseekh, S., Tong, H., Scossa, F. *et al.* (2017) Canalization of tomato fruit metabolism. *Plant Cell*, **29**, 2753–2765.

Ariizumi, T., Kishimoto, S., Kakami, R. *et al.* (2014) Identification of the tomato carotenogenic gene PALE YELLOW PETAL 1 as an essential factor in xanthophyll esterification and yellow flower pigmentation. *Plant J.* **79**, 453–465.

Bai, Y. and Lindhout, P. (2007) Domestication and breeding of tomatoes: what have we gained and what can we gain in the future? *Ann. Bot.* **100**, 1085–1094.

Bai, Y., Kissoudis, C., Yan, Z., Visser, R.G.F. and van der Linden, G. (2018) Plant behaviour under combined stress: tomato responses to combined salinity and pathogen stress. *Plant J.* **93**, 781–793.

Balcke, G.U., Bennewitz, S., Bergau, N., Athmer, B., Henning, A., Majovsky, P., Jiménez-Gómez, J.M., Hoehenwarter, W. and Tissier, A. (2017) Multi-omics of tomato glandular trichomes reveals distinct features of central carbon metabolism supporting high productivity of specialized metabolites. *Plant Cell*, **29**, 960–983.

Ballester, A.R., Molthoff, J., de Vos, R. *et al.* (2010) Biochemical and molecular analysis of pink tomatoes: deregulated expression of the gene encoding transcription factor SlMYB12 leads to pink tomato fruit color. *Plant Physiol.* **152**, 71–84.

Ballester, A.R., Tikunov, Y., Molthoff, J., Grandillo, S., Viquez-Zamora, M., de Vos, R., de Maagd, R.A., van Heusden, S. and Bovy, A.G. (2016) Identification of loci affecting accumulation of secondary metabolites in tomato fruit of a *Solanum lycopersicum* × *Solanum chmielewskii* introgression line population. *Front. Plant Sci.* **7**, 1428.

Bao, Z., Meng, F., Strickler, S.R., Dunham, D.M., Munkvold, K.R. and Martin, G.B. (2015) Identification of a candidate gene in for resistance to a race 1 strain of pv. *Plant Genome*, **8**, 1–15.

Bardol, N., Ventelon, M., Mangin, B. *et al.* (2013) Combined linkage and linkage disequilibrium QTL mapping in multiple families of maize (*Zea mays* L.) line crosses highlights complementarities between models based on parental haplotype and single locus polymorphism. *Theor. Appl. Genet.* **126**, 2717–2736.

Barrero-Gil, J., Huertas, R., Rambla, J.L., Granell, A. and Salinas, J. (2016) Tomato plants increase their tolerance to low temperature in a chilling acclimation process entailing comprehensive transcriptional and metabolic adjustments. *Plant, Cell Environ.* **39**, 2303–2318.

Barry, C.S., McQuinn, R.P., Thompson, A.J., Seymour, G.B., Grierson, D. and Giovannoni, J.J. (2005) Ethylene insensitivity conferred by the green-ripe and never-ripe 2 ripening mutants of tomato. *Plant Physiol.* **138**, 267–275.

Bastet, A., Lederer, B., Giovinazzo, N. *et al.* (2018) Trans-species synthetic gene design allows resistance pyramiding and broad-spectrum engineering of virus resistance in plants. *Plant Biotechnol. J.* **16**, 1569–1581.

Bauchet, G., Grenier, S., Samson, N. *et al.* (2017) Identification of major loci and genomic regions controlling acid and volatile content in tomato fruit: implications for flavor improvement. *New Phytol.* **215**, 624–641.

Bazakos, C., Hanemian, M., Trontin, C., Jiménez-Gómez , J., **Loudet, O. and Merchant, S.** (2017) New strategies and tools in quantitative genetics: how to go from the phenotype to the genotype. *Annu. Rev. Plant Biol.* **68**, 435–455.

Blanca, J., Montero-Pau, J., Sauvage, C. *et al.* (2015) Genomic variation in tomato, from wild ancestors to contemporary breeding accessions. *BMC Genom.* **16**, 257.

Blanco-Ulate, B., Vincenti, E., Powell, A.L. and Cantu, D. (2013) Tomato transcriptome and mutant analyses suggest a role for plant stress hormones in the interaction between fruit and *Botrytis cinerea*. *Front. Plant Sci.* **14**, 142.

Bolger, A., Scossa, F., Bolger, M.E. *et al.* (2014) The genome of the stress-tolerant wild tomato species *Solanum pennellii*. *Nat. Genet.* **46**, 1034–1038.

Brooks, C., Nekrasov, V., Lippman, Z.B. and Van Eck, J. (2014) Efficient gene editing in tomato in the first generation using the clustered regularly interspaced short palindromic repeats/CRISPR-associated9 system1. *Plant Physiol.* **166**, 1292–1297.

Callaway, E. (2018) EU law deals blow to CRISPR crops. *Nature*, **560**, 16.

Carrari, F., Baxter, C., Usadel, B. *et al.* (2006) Integrated analysis of metabolite and transcript levels reveals the metabolic shifts that underlie tomato fruit development and highlight regulatory aspects of metabolic network behavior. *Plant Physiol.* **142**, 1380–1396.

Causse, M. and Grandillo, S. (2016) Gene mapping in tomato. In *The tomato genome*. (Causse, M., Giovannoni, J., Bouzayen, M. and Zouine, M., eds). Berlin, Heidelberg: Springer, pp. 23–37.

Causse, M., Saliba-Colombani, V., Lecomte, L., Duffé, P., Rousselle, P. and Buret, M. (2002) QTL analysis of fruit quality in fresh market tomato: a few chromosome regions control the variation of sensory and instrumental traits. *J. Exp. Bot.* **53**, 2089–2098.

Causse, M., Desplat, N., Pascual, L. *et al.* (2013) Whole genome resequencing in tomato reveals variation associated with introgression and breeding events. *BMC Genom.*, **14**, 791.

Čermák, T., Baltes, N.J., Čegan, R., Zhang, Y. and Voytas, D.F. (2015) High-frequency, precise modification of the tomato genome. *Genome Biol.* **16**, 232.

Čermák, T., Curtin, S.J., Gil-Humanes, J. *et al.* (2017) A multipurpose toolkit to enable advanced genome engineering in plants. *Plant Cell*, **29**, 1196–1217.

Chakrabarti, M., Zhang, N., Sauvage, C. *et al.* (2013) A cytochrome P450 regulates a domestication trait in cultivated tomato. *Proc. Natl Acad. Sci. USA* **110**, 17125–17130.

Chen, W., Kong, J., Qin, C. *et al.* (2015) Requirement of CHROMOMETHYLASE3 for somatic inheritance of the spontaneous tomato epimutation colourless non-ripening. *Sci. Rep.* **5**, 9192.

Chen, L., Yang, D., Zhang, Y. *et al.* (2018) Evidence for a specific and critical role of mitogen-activated protein kinase 20 in uni-to-binucleate transition of microgametogenesis in tomato. *New Phytol.* **219**, 176–194.

Coneva, V., Frank, M.H., Balaguer, M.A.D.L., Li, M., Sozzani, R. and Chitwood, D.H. (2017) Genetic architecture and molecular networks underlying leaf thickness in desert-adapted tomato *Solanum pennellii*. *Plant Physiol.* **175**, 376–391.

Corem, S., Doron-Faigenboim, A., Jouffroy, O., Maumus, F., Arazi, T. and Bouché, N. (2018) Redistribution of CHH methylation and small

interfering RNAs across the genome of tomato ddm1 mutants. *Plant Cell* **30**, 1628–1644.

Cruz-Mendívil, A., López-Valenzuela, J.A., Calderón-Vázquez, C.L. *et al.* (2015) Transcriptional changes associated with chilling tolerance and susceptibility in 'Micro-Tom' tomato fruit using RNA-Seq. *Postharvest Biol. Technol.* **99**, 141–151.

Dahan-Meir, T., Filler-Hayut, S., Melamed-Bessudo, C., Bocobza, S., Czosnek, H., Aharoni, A. and Levy, A.A. (2018) Efficient in planta gene targeting in tomato using geminiviral replicons and the CRISPR/Cas9 system. *Plant J.* **95**, 5–16.

Diouf, I.A., Derivot, L., Bitton, F., Pascual, L. and Causse, M. (2018) Water deficit and salinity stress reveal many specific QTL for plant growth and fruit quality traits in tomato. *Front. Plant Sci.* **9**, 279.

Duangjit, J., Causse, M. and Sauvage, C. (2016) Efficiency of genomic selection for tomato fruit quality. *Mol. Breed.* **36**, 29.

Emmanuel, E. and Levy, A.A. (2002) Tomato mutants as tools for functional genomics. *Curr. Opin. Plant Biol.* **5**, 112–117.

Eshed, Y. and Zamir, D. (1995) An introgression line population of *Lycopersicon pennellii* in the cultivated tomato enables the identification and fine mapping of yield-associated QTL. *Genetics*, **141**, 1147–1162.

Faurobert, M., Mihr, C., Bertin, N., Pawlowski, T., Negroni, L., Sommerer, N. and Causse, M. (2007) Major proteome variations associated with cherry tomato pericarp development and ripening. *Plant Physiol.* **143**, 1327–1346.

Fernandez, A.I., Viron, N., Alhagdow, M. *et al.* (2009) Flexible tools for gene expression and silencing in tomato. *Plant Physiol.* **151**, 1729–1740.

Fernandez-Moreno, J.P., Tzfadia, O., Forment, J., Presa, S., Rogachev, I., Meir, S., Orzaez, D., Aharoni, A. and Granell, A. (2016) Characterization of a new pink-fruited tomato mutant results in the identification of a null allele of the SlMYB12 transcription factor. *Plant Physiol.* **171**, 1821–1836.

Fernie, A.R. and Tohge, T. (2017) The genetics of plant metabolism. *Annu. Rev. Genet.* **51**, 287–310.

Foolad, M.R. and Panthee, D.R. (2012) Marker-assisted selection in tomato breeding. *CRC. Crit. Rev. Plant Sci.* **31**, 93–123.

Frary, A., Nesbitt, T.C., Grandillo, S. *et al.* (2000) fw2.2: a quantitative trait locus key to the evolution of tomato fruit size. *Science*, **289**, 85–88.

French, E., Kim, B.S., Rivera-Zuluaga, K. and Iyer-Pascuzzi, A.S. (2018) Whole root transcriptomic analysis suggests a role for auxin pathways in resistance to *Ralstonia solanacearum* in tomato. *Mol. Plant Microbe Interact.* **31**, 432–444.

Fridman, E., Pleban, T. and Zamir, D. (2000) A recombination hotspot delimits a wild-species quantitative trait locus for tomato sugar content to 484 bp within an invertase gene. *Proc. Natl Acad. Sci. USA* **97**, 4718–4723.

Fulop, D., Ranjan, A., Ofner, I. *et al.* (2016) A new advanced backcross tomato population enables high resolution leaf QTL mapping and gene identification. *G3–Genes Genom. Genet.* **13**, 3169–3184.

Gallego-Bartolomé, J., Gardiner, J., Liu, W., Papikian, A., Ghoshal, B., Kuo, H.Y., Zhao, J.M., Segal, D.J. and Jacobsen, S.E. (2018) Targeted DNA demethylation of the Arabidopsis genome using the human TET1 catalytic domain. *Proc. Natl Acad. Sci. USA* **115**, E2125–E2134.

Galpaz, N., Ronen, G., Khalfa, Z., Zamir, D. and Hirschberg, J. (2006) A chromoplast-specific carotenoid biosynthesis pathway is revealed by cloning of the tomato white-flower locus. *Plant Cell*, **18**, 1947–1960.

Garbowicz, K., Liu, Z., Alseekh, S. *et al.* (2018) Quantitative trait loci analysis identifies a prominent gene involved in the production of fatty-acid-derived flavor volatiles in tomato. *Mol Plant.* **11**, 1147–1165.

Garcia, V., Bres, C., Just, D. *et al.* (2016) Rapid identification of causal mutations in tomato EMS populations via mapping-by-sequencing. *Nat. Protoc.* **11**, 2401–2418.

Gauffier, C., Lebaron, C., Moretti, A., Constant, C., Moquet, F., Bonnet, G., Caranta, C. and Gallois, J.L. (2016) A TILLING approach to generate broad-spectrum resistance to potyviruses in tomato is hampered by eIF4E gene redundancy. *Plant J.* **85**, 717–729.

Ghosh, S., Narula, K., Sinha, A., Ghosh, R., Jawa, P., Chakraborty, N. and Chakraborty, S. (2016) Proteometabolomic study of compatible interaction in tomato fruit challenged with *Sclerotinia rolfsii* illustrates novel protein network during disease progression. *Front. Plant Sci.* **7**, 1034.

Giovannoni, J., Nguyen, C., Ampofo, B., Zhong, S. and Fei, Z. (2017) The epigenome and transcriptional dynamics of fruit ripening. *Annu. Rev. Plant Biol.* **68**, 61–84.

Grandillo, S. and Cammareri, M. (2016) Molecular mapping of quantitative trait loci in tomato. In *The tomato genome* (Causse, M., Giovannoni, J., Bouzayen, M. and Zouine, M. eds). Berlin, Heidelberg: Springer, pp. 39–73.

Grierson, D. (2016) Identifying and silencing tomato ripening genes with antisense genes. *Plant Biotechnol. J.* **14**, 835–838.

Gur, A., Osorio, S., Fridman, E., Fernie, A.R. and Zamir, D. (2010) hi2-1, A QTL which improves harvest index, earliness and alters metabolite accumulation of processing tomatoes. *Theor. Appl. Genet.* **121**, 1587–1599.

Gur, A., Semel, Y., Osorio, S. *et al.* (2011) Yield quantitative trait loci from wild tomato are predominately expressed by the shoot. *Theor. Appl. Genet.* **122**, 405–420.

Haeussler, M., Schönig, K., Eckert, H. *et al.* (2016) Evaluation of off-target and on-target scoring algorithms and integration into the guide RNA selection tool CRISPOR. *Genome Biol.* **17**, 148.

Haggard, J.E., Johnson, E.B. and Clair, D.A.St (2015) Multiple QTL for horticultural traits and quantitative resistance to *Phytophthora infestans* linked on *Solanum habrochaites* chromosome 11. *G3 – Genes. Genom. Genet.* **5**, 219–233.

Hameed, A., Saleem, M.Y., Akhtar, K.P., Shoaib, M., Iqbal, Q. and Asghar, M. (2017) Molecular confirmation of intraspecific tomato (*Solanum lycopersicum*) hybrids and their evaluation against late blight and cucumber mosaic virus. *Mol. Biotechnol.* **59**, 234–240.

Hao, S., Ariizumi, T. and Ezura, H. (2017) Sexual sterility is essential for both male and female gametogenesis in tomato. *Plant Cell Physiol.* **58**, 22–34.

Hilioti, Z., Ganopoulos, I., Ajith, S., Bossis, I. and Tsaftaris, A. (2016) A novel arrangement of zinc finger nuclease system for in vivo targeted genome engineering: the tomato LEC1-LIKE4 gene case. *Plant Cell Rep.* **35**, 2241–2255.

Illa-Berenguer, E., Van Houten, J., Huang, Z. and van der Knaap, E. (2015) Rapid and reliable identification of tomato fruit weight and locule number loci by QTL-seq. *Theor. Appl. Genet.* **128**, 1329–1342.

Isaacson, T., Kosma, D., Matas, A. *et al.* (2009) Cutin deficiency in the tomato fruit cuticle consistently affects resistance to microbial infection and biomechanical properties, but not transpirational water loss. *Plant J.* **60**, 363–377.

Itkin, M., Heinig, U., Tzfadia, O. *et al.* (2013) Biosynthesis of antinutritional alkaloids in solanaceous crops is mediated by clustered genes. *Science*, **341**, 175–179.

Ito, Y., Nishizawa-Yokoi, A., Endo, M., Mikami, M. and Toki, S. (2015) CRISPR/Cas9-mediated mutagenesis of the RIN locus that regulates tomato fruit ripening. *Biochem. Biophys. Res. Comm.* **467**, 76–82.

Just, D., Garcia, V., Fernandez, L. *et al.* (2013) Micro-Tom mutants for functional analysis of target genes and discovery of new alleles in tomato. *Plant Biotechnol.* **30**, 225–231.

Kanazawa, A., Inaba, J.I., Shimura, H., Otagaki, S., Tsukahara, S., Matsuzawa, A., Kim, B.M., Goto, K. and Masuta, C. (2011) Virus-mediated efficient induction of epigenetic modifications of endogenous genes with phenotypic changes in plants. *Plant J.* **65**, 156–168.

Keller, M., SPOT-ITN Consortium, Simm, S. (2018) The coupling of transcriptome and proteome adaptation during development and heat stress response of tomato pollen. *BMC Genom.* **19**, 447.

Kim, J., Matsuba, Y., Ning, J., Schilmiller, A.L., Hammar, D., Jones, A.D., Pichersky, E. and Last, R.L. (2014) Analysis of natural and induced variation in tomato glandular trichome flavonoids identifies a gene not present in the reference genome. *Plant Cell*, **26**, 3272–3285.

Kim, B., Kim, N., Kim, J.Y., Kim, B.S., Jung, H.-J., Hwang, I., Noua, I.-S., Sim, S.-C. and Park, Y. (2016) Development of a high-resolution melting marker for selecting Fusarium crown and root rot resistance in tomato. *Genome*, **59**, 173–183.

Kim, B., Hwang, I.S., Lee, H.-J. and Oh, C.-S. (2017) Combination of newly developed SNP and InDel markers for genotyping the Cf-9 locus conferring disease resistance to leaf mold disease in the tomato. *Mol. Breed.* **37**, 59.

Kim, D., Jin, B., Je, B.Il, Choi, Y., Kim, B.S., Jung, H.-J., Nou, I.-S. and Park, Y. (2018) Development of DNA markers for SlMlo1.1, a new mutant allele of the powdery mildew resistance gene SlMlo1 in tomato (*Solanum lycopersicum*). *Genome*, **61**, 703–712.

Klap, C., Yeshayahou, E., Bolger, A.M., Arazi, T., Gupta, S.K., Shabtai, S., Usadel, B., Salts, Y. and Barg, R. (2017) Tomato facultative

parthenocarpy results from SlAGAMOUS-LIKE 6 loss of function. *Plant Biotechnol. J.* **15**, 634–647.

Koenig, D., Jiménez-Gómez, J.M., Kimura, S. *et al.* (2013) Comparative transcriptomics reveals patterns of selection in domesticated and wild tomato. *Proc. Natl Acad. Sci. USA* **110**, E2655–E2662.

Kong, J., Chen, W., Shen, J., Qin, C., Lai, T., Zhang, P., Wang, Y., Wu, C., Yang, X. and Hong, Y. (2013) Virus-induced gene complementation in tomato. *Plant Signal Behav.* **8**, e27142.

Krieger, U., Lippman, Z. and Zamir, D. (2010) The flowering gene SINGLE FLOWER TRUSS drives heterosis for yield in tomato. *Nat. Genet.* **42**, 459–463.

Labate, J.A., Grandillo, S., Fulton, T. *et al.* (2007) In *Genome Mapping and Molecular Breeding in Plants, Volume 5, Vegetables*. (Kole, C., ed). Berlin Heidelberg: Springer-Verlag, pp. 11–135.

Lang, Z., Wang, Y., Tang, K., Tang, D., Datsenka, T., Cheng, J., Zhang, Y., Handa, A.K. and Zhu, J. (2017) Critical roles of DNA demethylation in the activation of ripening-induced genes and inhibition of ripening-repressed genes in tomato fruit. *Proc. Natl Acad. Sci. USA*, **114**, E4511–E4519.

Lapidot, M., Karniel, U., Gelbart, D. *et al.* (2015) A novel route controlling begomovirus resistance by the messenger RNA surveillance factor pelota. *PLoS Genet.* **11**, e1005538.

Lee, J.M., Joung, J.G., McQuinn, R., Chung, M.Y., Fei, Z., Tieman, D., Klee, H. and Giovannoni, J. (2012) Combined transcriptome, genetic diversity and metabolite profiling in tomato fruit reveals that the ethylene response factor SlERF6 plays an important role in ripening and carotenoid accumulation. *Plant J.* **70**, 191–204.

Li, J.R., Aach, J., Norville, J.E., McCormack, M., Zhang, D., Bush, J., Church, G.M. and Sheen, J. (2013) Multiplex and homologous recombination-mediated plant genome editing via guide RNA/Cas9. *Nat. Biotechnol.* **31**, 688–691.

Li, R., Li, R., Li, X., Fu, D., Zhu, B., Tian, H., Luo, Y. and Zhu, H. (2017) Multiplexed CRISPR/Cas9-mediated metabolic engineering of γ-aminobutyric acid levels in *Solanum lycopersicum*. *Plant Biotechnol. J.* **16**, 415–427.

Li, X., Wang, Y., Chen, S., Tian, H., Fu, D., Zhu, B., Luo, Y. and Zhu, H. (2018a) Lycopene is enriched in tomato fruit by CRISPR/Cas9-mediated multiplex genome editing. *Front. Plant Sci.* **9**, 559.

Li, S., Xu, H., Ju, Z., Cao, D., Zhu, H., Fu, D., Grierson, D., Qin, G., Luo, Y. and Zhu, B. (2018b) The RIN-MC fusion of MADS-box transcription factors has transcriptional activity and modulates expression of many ripening genes. *Plant Physiol.* **176**, 891–909.

Li, T., Yang, X., Yu, Y., Si, X., Zhai, X., Zhang, H., Dong, W., Gao, C. and Xu, C. (2018c) Domestication of wild tomato is accelerated by genome editing. *Nat. Biotechnol.* https://doi.org/10.1038/nbt.4273. [Epub ahead of print]

Li, R., Zhang, L., Wang, L., Chen, L., Zhao, R., Sheng, J. and Shen, L. (2018d) CRISPR/Cas9-mediated SlCBF1 mutagenesis reduces tomato plant chilling tolerance. *J. Agric. Food Chem.* **66**, 9042–9051.

Lin, T., Zhu, G., Zhang, J. *et al.* (2014) Genomic analyses provide insights into the history of tomato breeding. *Nat. Genet.* **46**, 1220–1226.

Liu, Y., Schiff, M. and Dinesh-Kumar, S.P. (2002) Virus-induced gene silencing in tomato. *Plant J.* **31**, 777–786.

Liu, R., How-Kit, A., Stammitti, L. *et al.* (2015) A DEMETER-like DNA demethylase governs tomato fruit ripening. *Proc. Natl Acad. Sci. USA* **112**, 10804–10809.

Lor, V.S., Starker, C.G., Voytas, D.F., Weiss, D. and Olszewski, N.E. (2014) Targeted mutagenesis of the tomato PROCERA gene using transcription activator-like effector nucleases. *Plant Physiol.* **166**, 1288–1291.

Malosetti, M., Ribaut, J.M. and van Eeuwijk, F. (2013) The statistical analysis of multi-environment data: modeling genotype-by-environment interaction and its genetic basis. *Front. Physiol.* **4**, 44.

Manning, K., Tör, M., Poole, M., Hong, Y., Thompson, A.J., King, G.J., Giovannoni, J.J. and Seymour, G.B. (2006) A naturally occurring epigenetic mutation in a gene encoding an SBP-box transcription factor inhibits tomato fruit ripening. *Nat. Genet.* **38**, 948–952.

Mao, L., Begum, D., Chuang, H., Budiman, M.A., Szymkowiak, E.J., Irish, E.E. and Wing, R.A. (2000) JOINTLESS is a MADS-box gene controlling tomato flower abscission zone development. *Nature*, **406**, 910–913.

Martin, G.B., Brommonschenkel, S.H., Chunwongse, J., Frary, A., Ganal, M.W., Spivey, R., Wu, T., Earle, E.D. and Tanksley, S.D. (1993) Map-based cloning of a protein kinase gene conferring disease resistance in tomato. *Science*, **262**, 1432–1436.

Martinez, V., Nieves-Cordones, M., Lopez-Delacalle, M. *et al.* (2018) Tolerance to stress combination in tomato plants: new insights in the protective role of melatonin. *Molecules*, **23**, 535.

Matas, A.J., Yeats, T.H., Buda, G.J. *et al.* (2011) Tissue- and cell-type specific transcriptome profiling of expanding tomato fruit provides insights into metabolic and regulatory specialization and cuticle formation. *Plant Cell*, **23**, 3893–3910.

Meissner, R., Jacobson, Y., Melamed, S., Levyatuv, S., Shalev, G., Ashri, A., Elkind, Y. and Levy, A.A. (1997) A new model system for tomato genetics. *Plant J.* **12**, 1465–1472.

Menda, N., Semel, Y., Peled, D., Eshed, Y. and Zamir, D. (2004) In silico screening of a saturated mutation library of tomato. *Plant J.* **38**, 861–872.

Mickelbart, M.V., Hasegawa, P.M. and Bailey-Serres, J. (2015) Genetic mechanisms of abiotic stress tolerance that translate to crop yield stability. *Nat. Rev. Genet.* **16**, 237–251.

Mieulet, D., Aubert, G., Bres, C. *et al.* (2018) Unleashing meiotic crossovers in crops. *Nat. Plants* https://doi.org/10.1038/s41477-018-0311-x. [Epub ahead of print]

Minoia, S., Petrozza, A., D'Onofrio, O., Piron, F., Mosca, G., Sozio, G., Cellini, F., Bendahmane, A. and Carriero, F. (2010) A new mutant genetic resource for tomato crop improvement by TILLING technology. *BMC Res. Notes*, **3**, 69.

Mintz-Oron, S., Mandel, T., Rogachev, I. *et al.* (2008) Gene expression and metabolism in tomato fruit surface tissues. *Plant Physiol.* **147**, 823–851.

Mounet, F., Moing, A., Garcia, V. *et al.* (2009) Gene and metabolite regulatory network analysis of early developing fruit tissues highlights new candidate genes for the control of tomato fruit composition and development. *Plant Physiol.* **149**, 1505–1528.

Mu, Q., Huang, Z., Chakrabarti, M., Illa-Berenguer, E., Liu, X., Wang, Y., Ramos, A. and van der Knaap, E. (2017) Fruit weight is controlled by cell size regulator encoding a novel protein that is expressed in maturing tomato fruits. *PLoS Genet.* **13**, 1–26.

Müller, N.A., Wijnen, C.L., Srinivasan, A. *et al.* (2016) Domestication selected for deceleration of the circadian clock in cultivated tomato. *Nat. Genet.* **48**, 89–93.

Muños, S., Ranc, N., Botton, E. *et al.* (2011) Increase in tomato locule number is controlled by two single-nucleotide polymorphisms located near WUSCHEL. *Plant Physiol.* **156**, 2244–2254.

Musseau, C., Just, D., Jorly, J., Gevaudant, F., Moing, A., Chevalier, C., Lemaire-Chamley, M., Rothan, C. and Fernandez, L. (2017) Identification of two new mechanisms that regulate fruit growth by cell expansion in tomato. *Front. Plant Sci.* **8**, 988.

Nekrasov, V., Wang, C., Win, J., Lanz, C., Weigel, D. and Kamoun, S. (2017) Rapid generation of a transgene-free powdery mildew resistant tomato by genome deletion. *Sci. Rep.* **7**, 482.

Ning, J., Moghe, G., Leong, B. *et al.* (2015) A feedback insensitive isopropylmalate synthase affects acylsugar composition in cultivated and wild tomato. *Plant Physiol.* **169**, 1821–1835.

Nonaka, S., Arai, C., Takayama, M., Matsukura, C. and Ezura, H. (2017) Efficient increase of ɣ-aminobutyric acid (GABA) content in tomato fruits by targeted mutagenesis. *Sci. Rep.* **7**, 7057.

Ntatsi, G., Savvas, D., Papasotiropoulos, V., Katsileros, A., Zrenner, R.M., Hincha, D.K., Zuther, E. and Schwarz, D. (2017) Rootstock sub-optimal temperature tolerance determines transcriptomic responses after long-term root cooling in rootstocks and scions of grafted tomato plants. *Front. Plant Sci.* **8**, 911.

Ofner, I., Lashbrooke, J., Pleban, T., Aharoni, A. and Zamir, D. (2016) *Solanum pennellii* backcross inbred lines (BILs) link small genomic bins with tomato traits. *Plant J.* **87**, 151–160.

Okabe, Y., Asamizu, E., Saito, T., Matsukura, C., Ariizumi, T., Bres, C., Rothan, C., Mizoguchi, T. and Ezura, H. (2011) Tomato TILLING technology: development of a reverse genetics tool for the efficient isolation of mutants from Micro-Tom mutant libraries. *Plant Cell Physiol.* **52**, 1994–2005.

Osorio, S., Alba, R., Damasceno, C.M. *et al.* (2011) Systems biology of tomato fruit development: combined transcript, protein, and metabolite analysis of tomato transcription factor (nor, rin) and ethylene receptor

(Nr) mutants reveals novel regulatory interactions. *Plant Physiol.* **157**, 405–425.

Pan, Y., Bradley, G., Pyke, K. *et al.* (2013) Network inference analysis identifies an APRR2-like gene linked to pigment accumulation in tomato and pepper fruits. *Plant Physiol.* **161**, 1476–1485.

Pan, C., Ye, L., Qin, L. *et al.* (2016) CRISPR/Cas9-mediated efficient and heritable targeted mutagenesis in tomato plants in the first and later generations. *Sci. Rep.* **6**, 24765.

Park, S.J., Jiang, K., Schatz, M.C. and Lippman, Z.B. (2012) Rate of meristem maturation determines inflorescence architecture in tomato. *Proc. Natl Acad. Sci. USA* **109**, 639–644.

Park, S.J., Jiang, K., Tal, L., Yichie, Y., Gar, O., Zamir, D., Eshed, Y. and Lippman, Z.B. (2014) Optimization of crop productivity in tomato using induced mutations in the florigen pathway. *Nat. Genet.* **46**, 1337–1342.

Pascual, L., Desplat, N., Huang, B.E. *et al.* (2015) Potential of a tomato MAGIC population to decipher the genetic control of quantitative traits and detect causal variants in the resequencing era. *Plant Biotechnol. J.* **13**, 565–577.

Pascual, L., Albert, E., Sauvage, C. *et al.* (2016) Dissecting quantitative trait variation in the resequencing era: complementarity of bi-parental, multi-parental and association panels. *Plant Sci.* **242**, 120–130.

Paterson, A.H., Lander, E.S., Hewitt, J.D., Peterson, S., Lincoln, S.E. and Tanksley, S.D. (1988) Resolution of quantitative traits into Mendelian factors by using a complete linkage map of restriction fragment length polymorphisms. *Nature*, **335**, 721–726.

Paterson, A.H., DeVerna, J.W., Lanini, B. and Tanksley, S.D. (1990) Fine mapping of quantitative trait loci using selected overlapping recombinant chromosomes, in an interspecies cross of tomato. *Genetics*, **124**, 735–742.

Pattison, R.J., Csukasi, F., Zheng, Y., Fei, Z., van der Knaap, E. and Catalá, C. (2015) Comprehensive tissue-specific transcriptome analysis reveals distinct regulatory programs during early tomato fruit development. *Plant Physiol.* **168**, 1684–1701.

Peralta, I., Spooner, D.M. and Knapp, S. (2008) Taxonomy of wild tomatoes and their relatives (*Solanum* sections *lycopersicoides*, Juglandilolia, Lycopersicon; Solanaceae). *Syst. Bot. Monogr.* **84**, 1–186.

Petit, J., Bres, C., Just, D., Garcia, V., Mauxion, J., Marion, D., Bakan, B., Joubès , J., **Domergue, F. and Rothan, C.** (2014) Analyses of tomato fruit brightness mutants uncover both cutin-deficient and cutin-abundant mutants and a new hypomorphic allele of GDSL lipase. *Plant Physiol.* **164**, 888–906.

Petit, J., Bres, C., Mauxion, J.-P., Wong Jun Tai, F., Martin, L.B.B., Fich, E.A., Joubès, J., Rose, J.K.C., Domergue, F. and Rothan, C. (2016) The glycerol-3-phosphate acyltransferase GPAT6 from tomato plays a central role in fruit cutin biosynthesis. *Plant Physiol.* **171**, 894–913.

Petreikov, M., Shen, S., Yeselson, Y., Levin, I., Bar, M. and Schaffer, A.A. (2006) Temporally extended gene expression of the ADP-Glc pyrophosphorylase large subunit (AgpL1) leads to increased enzyme activity in developing tomato fruit. *Planta*, **224**, 1465–1479.

Pnueli, L., Carmel-Goren, L., Hareven, D., Gutfinger, T., Alvarez, J., Ganal, M., Zamir, D. and Lifschitz, E. (1998) The SELF-PRUNING gene of tomato regulates vegetative to reproductive switching of sympodial meristems and is the ortholog of CEN and TFL1. *Development*, **125**, 1979–1989.

Powell, A.L.T., Nguyen, C.V., Hill, T. *et al.* (2012) Uniform ripening encodes a golden 2-like transcription factor regulating tomato fruit chloroplast development. *Science*, **336**, 1711–1715.

Puchta, H. (2017) Applying CRISPR/Cas for genome engineering in plants: the best is yet to come. *Curr. Opin. Plant Biol.* **36**, 1–8.

Pulungan, S.I., Yano, R., Okabe, Y., Ichino, T., Kojima, M., Takebayashi, Y., Sakakibara, H., Ariizumi, T. and Ezura, H. (2018) SlLAX1 is required for normal leaf development mediated by balanced adaxial and abaxial pavement cell growth in tomato. *Plant Cell Physiol.* **59**, 1170–1186.

Qin, X., Li, W., Liu, Y., Tan, M., Ganal, M. and Chetelat, R.T. (2018) A farnesyl pyrophosphate synthase gene expressed in pollen functions in S-RNase-independent unilateral incompatibility. *Plant J.* **93**, 417–430.

Quadrana, L., Almeida, J., Asís, R. *et al.* (2014) Natural occurring epialleles determine vitamin E accumulation in tomato fruits. *Nat. Commun.* **5**, 3027.

Ramesh, S.V., Williams, S., Kappagantu, M., Mitter, N. and Pappu, H.R. (2017) Transcriptome-wide identification of host genes targeted by tomato spotted wilt virus-derived small interfering RNAs. *Virus Res.* **238**, 13–23.

Ranjan, A., Budke, J.M., Rowland, S.D. *et al.* (2016) eQTL regulating transcript levels associated with diverse biological processes in tomato. *Plant Physiol.* **172**, 328–340.

Ripoll, J., Urban, L., Brunel, B. and Bertin, N. (2016) Water deficit effects on tomato quality depend on fruit developmental stage and genotype. *J. Plant Physiol.* **190**, 26–35.

Rivero, R.M., Mestre, T.C., Mittler, R., Rubio, F., Garcia-Sanchez, F. and Martinez, V. (2014) The combined effect of salinity and heat reveals a specific physiological, biochemical and molecular response in tomato plants. *Plant, Cell Environ.* **37**, 1059–1073.

Rodríguez, G.R., Muños, S., Anderson, C., Sim, S.-C., Michel, A., Causse, M., Gardener, B.B.M., Francis, D. and van der Knaap, E. (2011) Distribution of SUN, OVATE, LC, and FAS in the tomato germplasm and the relationship to fruit shape diversity. *Plant Physiol.* **156**, 275–285.

Rodríguez-Leal, D., Lemmon, Z.H., Man, J., Bartlett, M.E. and Lippman, Z.B. (2017) Engineering quantitative trait variation for crop improvement by genome editing. *Cell*, **171**, 470–480.

Ron, M., Kajala, K., Pauluzzi, G. *et al.* (2014) Hairy root transformation using *Agrobacterium rhizogenes* as a tool for exploring cell type-specific gene expression and function using tomato as a model. *Plant Physiol.* **166**, 455–469.

Ronen, G., Cohen, M., Zamir, D. and Hirschberg, J. (1999) Regulation of carotenoid biosynthesis during tomato fruit development: expression of the gene for lycopene epsilon-cyclase is down-regulated during ripening and is elevated in the mutant Delta. *Plant J.* **17**, 341–351.

Rothan, C., Bres, C., Garcia, V. and Just, D. (2016) Tomato resources for functional genomics. In *The tomato genome* (Causse, M., Giovannoni, J., Bouzayen, M. and Zouine, M., eds). Berlin, Heidelberg: Springer, pp. 75–94.

Ruggieri, V., Francese, G., Sacco, A. *et al.* (2014) An association mapping approach to identify favourable alleles for tomato fruit quality breeding. *BMC Plant Biol.* **14**, 337.

Ruiu, F., Picarella, M.E., Imanishi, S. and Mazzucato, A. (2015) A transcriptomic approach to identify regulatory genes involved in fruit set of wild-type and parthenocarpic tomato genotypes. *Plant Mol. Biol.* **89**, 263–278.

Sacco, A., Ruggieri, V., Parisi, M., Festa, G., Rigano, M.M., Picarella, M.E., Mazzucato, A. and Barone, A. (2015) Exploring a tomato landraces collection for fruit-related traits by the aid of a high-throughput genomic platform. *PLoS ONE*, **10**, e0137139.

Saito, T., Ariizumi, T., Okabe, Y., Asamizu, E., Hiwasa-Tanase, K., Fukuda, N., Mizoguchi, T., Yamazaki, Y., Aoki, K. and Ezura, H. (2011) TOMATOMA: a novel tomato mutant database distributing Micro-Tom mutant collections. *Plant Cell Physiol.* **52**, 283–296.

Sato, S., Tabata, S., Hirakawa, H. *et al.* (2012) The tomato genome sequence provides insights into fleshy fruit evolution. *Nature*, **485**, 635–641.

Sauvage, C., Segura, V., Bauchet, G., Stevens, R., Do, P.T., Nikoloski, Z., Fernie, A.R. and Causse, M. (2014) Genome-wide association in tomato reveals 44 candidate loci for fruit metabolic traits. *Plant Physiol.* **165**, 1120–1132.

Sauvage, C., Rau, A., Aichholz, C. *et al.* (2017) Domestication rewired gene expression and nucleotide diversity patterns in tomato. *Plant J.* **91**, 631–645.

Schauer, N., Semel, Y., Roessner, U. *et al.* (2006) Comprehensive metabolic profiling and phenotyping of interspecific introgression lines for tomato improvement. *Nat. Biotechnol.* **24**, 447–454.

Scheben, A., Wolter, F., Batley, J., Puchta, H. and Edwards, D. (2017) Towards CRISPR/Cas crops - bringing together genomics and genome editing. *New Phytol.* **216**, 682–698.

Schilmiller, A.L., Moghe, G.D., Fan, P., Ghosh, B., Ning, J., Jones, A.D. and Last, R.L. (2015) Functionally divergent alleles and duplicated loci encoding an acyltransferase contribute to acylsugar metabolite diversity in *Solanum* trichomes. *Plant Cell*, **27**, 1002–1017.

Schneeberger, K. (2014) Using next-generation sequencing to isolate mutant genes from forward genetic screens. *Nat. Rev. Genet.*, **15**, 662–676.

Shammai, A., Petreikov, M., Yeselson, Y. *et al.* (2018) Natural genetic variation for expression of a SWEET transporter among wild species of tomato determines the hexose composition of ripening tomato fruit. *Plant J.*, **96**, 343–357.

Shi, J.X., Adato, A., Alkan, N. *et al.* (2013) The tomato SISHINE3 transcription factor regulates fruit cuticle formation and epidermal patterning. *New Phytol.*, **197**, 468–480.

Shimatani, Z., Kashojiya, S., Takayama, M. *et al.* (2017) Targeted base editing in rice and tomato using a CRISPR-Cas9 cytidine deaminase fusion. *Nat. Biotechnol.*, **35**, 441–443.

Shinozaki, Y., Nicolas, P., Fernandez-Pozo, N. *et al.* (2018) High-resolution spatiotemporal transcriptome mapping of tomato fruit development and ripening. *Nat. Commun.*, **9**, 364.

Shirasawa, K., Hirakawa, H., Nunome, T., Tabata, S. and Isobe, S. (2016) Genome-wide survey of artificial mutations induced by ethyl methanesulfonate and gamma rays in tomato. *Plant Biotechnol. J.*, **14**, 51–60.

Soyk, S., Lemmon, Z.H., Oved, M. *et al.* (2017a) Bypassing negative epistasis on yield in tomato imposed by a domestication gene. *Cell*, **169**, 1142–1155.

Soyk, S., Müller, N.A., Park, S.J., Schmalenbach, I., Jiang, K., Hayama, R., Zhang, L., Van Eck, J., Jiménez-Gómez, J.M. and Lippman, Z.B. (2017b) Variation in the flowering gene SELF PRUNING 5G promotes day-neutrality and early yield in tomato. *Nat. Genet.*, **49**, 162–168.

Stevens, R.G., Baldet, P., Bouchet, J.P. *et al.* (2018) A Systems biology study in tomato fruit reveals correlations between the ascorbate pool and genes involved in ribosome biogenesis, translation, and the heat-shock response. *Front. Plant Sci.*, **9**, 137.

Święcicka, M., Skowron, W., Cieszyński, P., Dąbrowska-Bronk, J., Matuszkiewicz, M., Filipecki, M. and Koter, M.D. (2017) The suppression of tomato defence response genes upon potato cyst nematode infection indicates a key regulatory role of miRNAs. *Plant Physiol. Biochem.*, **113**, 51–55.

Swinnen, G., Goossens, A. and Pauwels, L. (2016) Lessons from domestication: targeting Cis-regulatory elements for crop improvement. *Trends Plant Sci.*, **21**, 506–515.

Szymanski, J., Levin, Y., Savidor, A., Breitel, D., Chappell-Maor, L., Heinig, U., Töpfer, N. and Aharoni, A. (2017) Label-free deep shotgun proteomics reveals protein dynamics during tomato fruit tissues development. *Plant J.*, **90**, 396–417.

Tanksley, S.D. (2004) The genetic, developmental, and molecular bases of fruit size and shape variation in tomato. *Plant Cell*, **16**, 181–189.

Tanksley, S.D., Ganal, M.W., Prince, J.P. *et al.* (1992) High density molecular linkage maps of the tomato and potato genomes. *Genetics*, **132**, 1141–1160.

Tieman, D.M., Loucas, H.M., Kim, J.Y., Clark, D.G. and Klee, H.J. (2007) Tomato phenylacetaldehyde reductases catalyze the last step in the synthesis of the aroma volatile 2-phenylethanol. *Phytochemistry*, **68**, 2660–2669.

Tieman, D., Zhu, G., Resende, M.F. Jr *et al.* (2017) A chemical genetic roadmap to improved tomato flavor. *Science*, **355**, 391–394.

Tikunov, Y.M., Molthoff, J., de Vos, R.C.H. *et al.* (2013) Non-smoky glycosyltransferase1 prevents the release of smoky aroma from tomato fruit. *Plant Cell*, **25**, 3067–3078.

Tohge, T., Scossa, F. and Fernie, A.R. (2015) Integrative approaches to enhance understanding of plant metabolic pathway structure and regulation. *Plant Physiol.* **169**, 1499–1511.

Tomlinson, L., Yang, Y., Emenecker, R., Smoker, M., Taylor, J., Perkins, S., Smith, J., MacLean, D., Olszewski, N.E. and Jones, J.D.G. (2018) Using CRISPR/Cas9 genome editing in tomato to create a gibberellin-responsive dominant dwarf DELLA allele. *Plant Biotechnol. J.* https://doi.org/10.1111/pbi.12952. [Epub ahead of print]

Toubiana, D., Semel, Y., Tohge, T., Beleggia, R., Cattivelli, L., Rosental, L., Nikoloski, Z., Zamir, D., Fernie, A.R. and Fait, A. (2012) Metabolic profiling of a mapping population exposes new insights in the regulation of seed metabolism and seed, fruit, and plant relations. *PLoS Genet.* **8**, e1002612.

Toubiana, D., Batushansky, A., Tzfadia, O., Scossa, F., Khan, A., Barak, S., Zamir, D., Fernie, A.R., Nikoloski, Z. and Fait, A. (2015) Combined correlation-based network and mQTL analyses efficiently identified loci for branched-chain amino acid, serine to threonine, and proline metabolism in tomato seeds. *Plant J.* **81**, 121–133.

Ueta, R., Abe, C., Watanabe, T., Sugano, S.S., Ishihara, R., Ezura, H., Osakabe, Y. and Osakabe, K. (2017) Rapid breeding of parthenocarpic tomato plants using CRISPR/Cas9. *Sci. Rep.* **7**, 507.

Uluisik, S., Chapman, N.H., Smith, R. *et al.* (2016) Genetic improvement of tomato by targeted control of fruit softening. *Nat. Biotechnol.* **34**, 950–952.

Van Eck, J. (2018) Genome editing and plant transformation of solanaceous food crops. *Curr. Opin. Biotechnol.* **49**, 35–41.

Velez-Ramirez, A.I., van Ieperen, W., Vreugdenhil, D., van Poppel, P.M., Heuvelink, E. and Millenaar, F.F. (2014) A single locus confers tolerance to continuous light and allows substantial yield increase in tomato. *Nat Commun.* **5**, 4549.

Verlaan, M.G., Hutton, S.F., Ibrahem, R.M., Kormelink, R., Visser, R.G.F., Scott, J.W., Edwards, J.D. and Bai, Y. (2013) The tomato yellow leaf curl virus resistance genes Ty-1 and Ty-3 are allelic and code for DFDGD-class RNA–dependent RNA polymerases. *PLoS Genet.* **9**, e1003399.

Vrebalov, J., Ruezinsky, D., Padmanabhan, V., White, R., Medrano, D., Drake, R., Schuch, W. and Giovannoni, J. (2002) A MADS-box gene necessary for fruit ripening at the tomato ripening-inhibitor (rin) locus. *Science*, **296**, 343–346.

Waltz, E. (2016) Gene-edited CRISPR mushroom escapes US regulation. *Nature*, **532**, 293.

Wang, H., Schauer, N., Usadel, B., Frasse, P., Zouine, M., Hernould, M., Latché, A., Pech, J.C., Fernie, A.R. and Bouzayen, M. (2009) Regulatory features underlying pollination-dependent and -independent tomato fruit set revealed by transcript and primary metabolite profiling. *Plant Cell*, **21**, 1428–1452.

Wang, Y.-Y., Chen, C.-H., Hoffmann, A., Hsu, Y.-C., Lu, S.-F., Wang, J.-F. and Hanson, P. (2016) Evaluation of the Ph-3 gene-specific marker developed for marker-assisted selection of late blight-resistant tomato P. Wehling, ed. *Plant Breed.* **135**, 636–642.

Wang, D., Yeats, T.H., Uluisik, S., Rose, J.K.C. and Seymour, G.B. (2018) Fruit softening: revisiting the role of pectin. *Trends Plant Sci.* **23**, 302–310.

Weber, E., Engler, C., Gruetzner, R., Werner, S. and Marillonnet, S.A. (2011) Modular cloning system for standardized assembly of multigene constructs. *PLoS ONE*, **6**, e16765.

Xiao, H., Jiang, N., Schaffner, E., Stockinger, E.J. and van der Knaap, E. (2008) A retrotransposon-mediated gene duplication underlies morphological variation of tomato fruit. *Science*, **319**, 1527–1530.

Xu, J., Ranc, N., Muños, S., Rolland, S., Bouchet, J.P., Desplat, N., Le Paslier, M.C. and Causse, M. (2013) Association mapping for fruit quality traits in cultivated tomato and wild related species. *Theor. Appl. Genet.* **126**, 567–581.

Xu, C., Liberatore, K.L., MacAlister, C.A. *et al.* (2015) A cascade of arabinosyltransferases controls shoot meristem size in tomato. *Nat. Genet.* **47**, 784–792.

Yamaguchi, H., Ohnishi, J., Saito, A., Ohyama, A., Nunome, T., Miyatake, K. and Fukuoka, H. (2018) An NB-LRR gene, TYNBS1, is responsible for resistance mediated by the Ty-2 Begomovirus resistance locus of tomato. *Theor. Appl. Genet.* **131**, 1345–1362.

Yamamoto, E., Matsunaga, H., Onogi, A., Ohyama, A., Miyatake, K., Yamaguchi, H., Nunome, T., Iwata, H. and Fukuoka, H. (2017) Efficiency of genomic selection for breeding population design and phenotype prediction in tomato. *Heredity (Edinb)*, **118**, 202–209.

Yamamoto, T., Kashojiya, S., Kamimura, S., Kameyama, T., Ariizumi, T., Ezura, H. and Miura, K. (2018) Application and development of genome editing technologies to the Solanaceae plants. *Plant Physiol. Biochem.* **131**, 37–46.

Ye, J., Wang, X., Hu, T. *et al.* (2017) An InDel in the promoter of Al-ACTIVATED MALATE TRANSPORTER9 selected during tomato domestication determines fruit malate contents and aluminum tolerance. *Plant Cell*, **29**, 2249–2268.

Yeats, T.H., Martin, L.B., Viart, H.M. *et al.* (2012) The identification of cutin synthase: formation of the plant polyester cutin. *Nat. Chem. Biol.* **8**, 609–611.

Yu, Q., Wang, B., Li, N., Tang, Y., Yang, S., Yang, T. and Xu, J. (2017) CRISPR/Cas9-induced targeted mutagenesis and gene replacement to generate long-shelf life tomato lines. *Sci. Rep.* **7**, 11874.

Zamboni, A., Zanin, L., Tomasi, N., Pezzotti, M., Pinton, R., Varanini, Z. and Cesco, S. (2012) Genome-wide microarray analysis of tomato roots showed defined responses to iron deficiency. *BMC Genom.* **13**, 101.

Zhang, C., Liu, L., Wang, X. *et al.* (2014) The Ph-3 gene from *Solanum pimpinellifolium* encodes CC-NBS-LRR protein conferring resistance to *Phytophthora infestans*. *Theor. Appl. Genet.* **127**, 1353–1364.

Zhang, J., Zhao, J., Xu, Y., Liang, J., Chang, P., Yan, F., Li, M., Liang, Y. and Zou, Z. (2015) Genome-wide association mapping for tomato volatiles positively contributing to tomato flavor. *Front. Plant Sci.* **6**, 1042.

Zhang, B., Tieman, D.M., Jiao, C., Xu, Y., Chen, K., Fei, Z., Giovannoni, J.J. and Klee, H.J. (2016) Chilling-induced tomato flavor loss is associated with altered volatile synthesis and transient changes in DNA methylation. *Proc. Natl Acad. Sci. USA* **113**, 12580–12585.

Zhang, J., Zeng, L., Chen, S., Sun, H. and Ma, S. (2018) Transcription profile analysis of *Lycopersicum esculentum* leaves, unravels volatile emissions and gene expression under salinity stress. *Plant Physiol. Biochem.* **126**, 11–21.

Zheng, H. and Kawabata, S. (2017) Identification and validation of new alleles of FALSIFLORA and COMPOUND INFLORESCENCE genes controlling the number of branches in tomato inflorescence. *Int. J. Mol. Sci.* **18**, E1572.

Zhong, S., Fei, Z., Chen, Y.R. *et al.* (2013) Single-base resolution methylomes of tomato fruit development reveal epigenome modifications associated with ripening. *Nat. Biotechnol.* **31**, 154–159.

Zhou, T., Zhang, H., Lai, T. *et al.* (2012) Virus-induced gene complementation reveals a transcription factor network in modulation of tomato fruit ripening. *Sci. Rep.* **2**, 836.

Zhu, G., Wang, S., Huang, Z. *et al.* (2018) Rewiring of the fruit metabolome in tomato breeding. *Cell*, **172**, 249–261.e12.

Zouari, I., Salvioli, A., Chialva, M., Novero, M., Miozzi, L., Tenore, G.C., Bagnaresi, P. and Bonfante, P. (2014) From root to fruit: RNA-Seq analysis shows that arbuscular mycorrhizal symbiosis may affect tomato fruit metabolism. *BMC Genom.* **15**, 221.

Zouine, M., Maza, E., Djari, A., Lauvernier, M., Frasse, P., Smouni, A., Pirrello, J. and Bouzayen, M. (2017) TomExpress, a unified tomato RNA-Seq platform for visualization of expression data, clustering and correlation networks. *Plant J.* **92**, 727–735.

Zsögön, A., Čermák , T., Voytas, D. and Peres, L.E. (2017) Genome editing as a tool to achieve the crop ideotype and de novo domestication of wild relatives: case study in tomato. *Plant Sci.* **256**, 120–130.

Zsögön, A., Čermák, T., Naves, E.R., Notini, M.M., Edel, K.H., Weinl, S., Freschi, L., Voytas, D.F., Kudla, J. and Peres, L.E.P. (2018) De novo domestication of wild tomato using genome editing. *Nat. Biotechnol.* https://doi.org/10.1038/nbt.4272. [Epub ahead of print]

Appendix 3

Supplemental Figures

A)

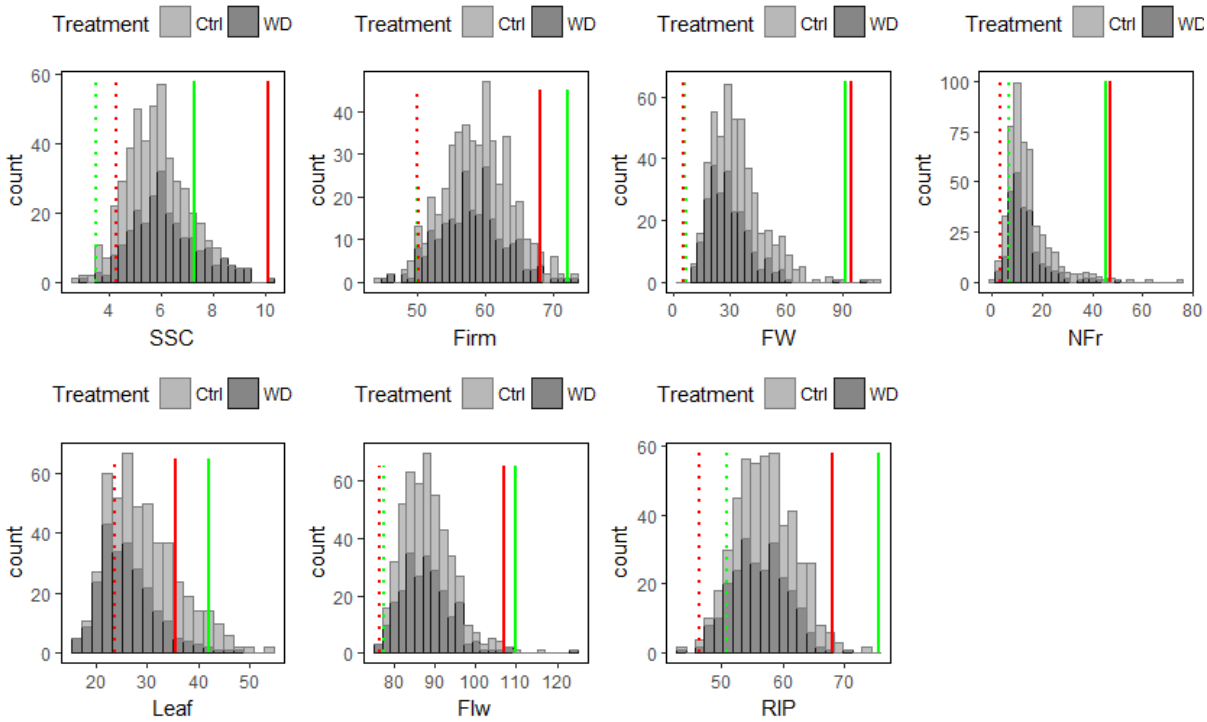

B)

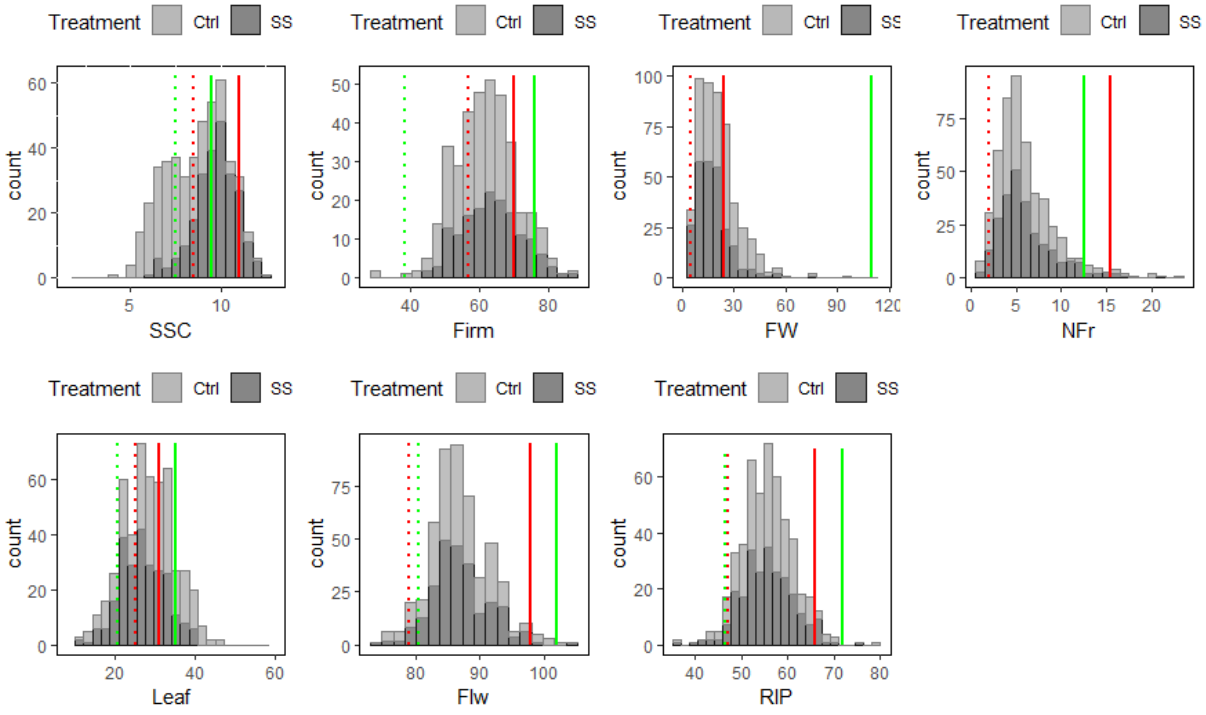

Supplemental Fig. 1: distribution of mean values within magic lines for each trait in Exp.1 (A) and Exp.2 (B); For each trait, minimum (dotted lines) and maximum (solid lines) parental values are plotted for control (green) and stress (red) treatment.

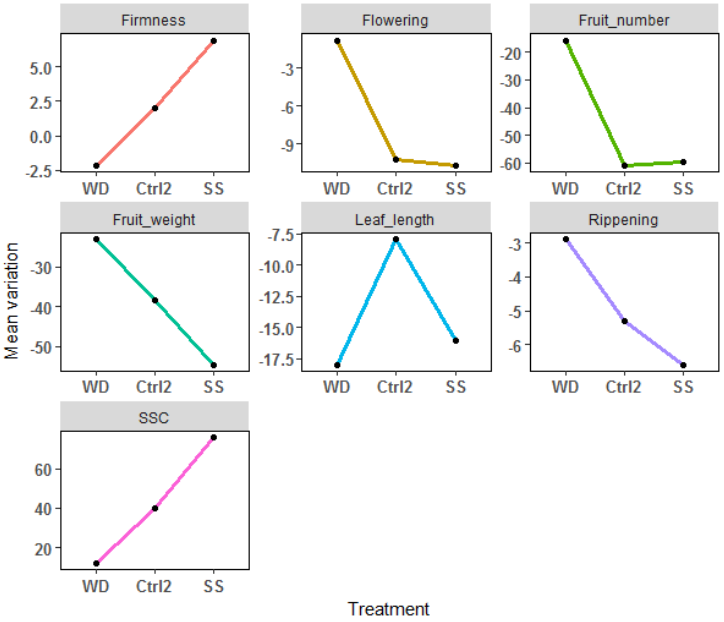

Supplemental Fig. 2: Average variation caused by water deficit (WD), salinity (SS) and control in Exp.2 (Ctrl2) relatively to control in Exp.1. The effect of each treatment was measured in percentage of increase or decrease against control in Exp.1.

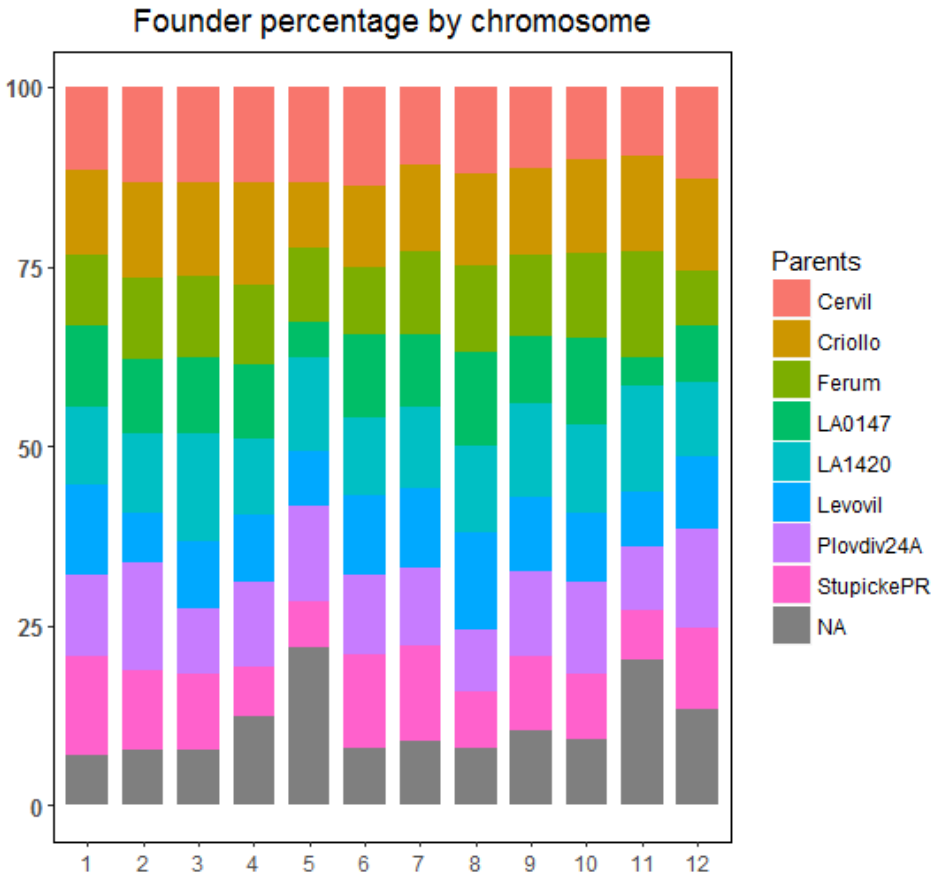

Supplemental Fig. 3: Haplotypes prediction. Each of the 12 tomato chromosome is represented with the percentage of allelic contribution of every parental line. NA represented all positions on the chromosomes where the parental allelic provenance could not be assigned

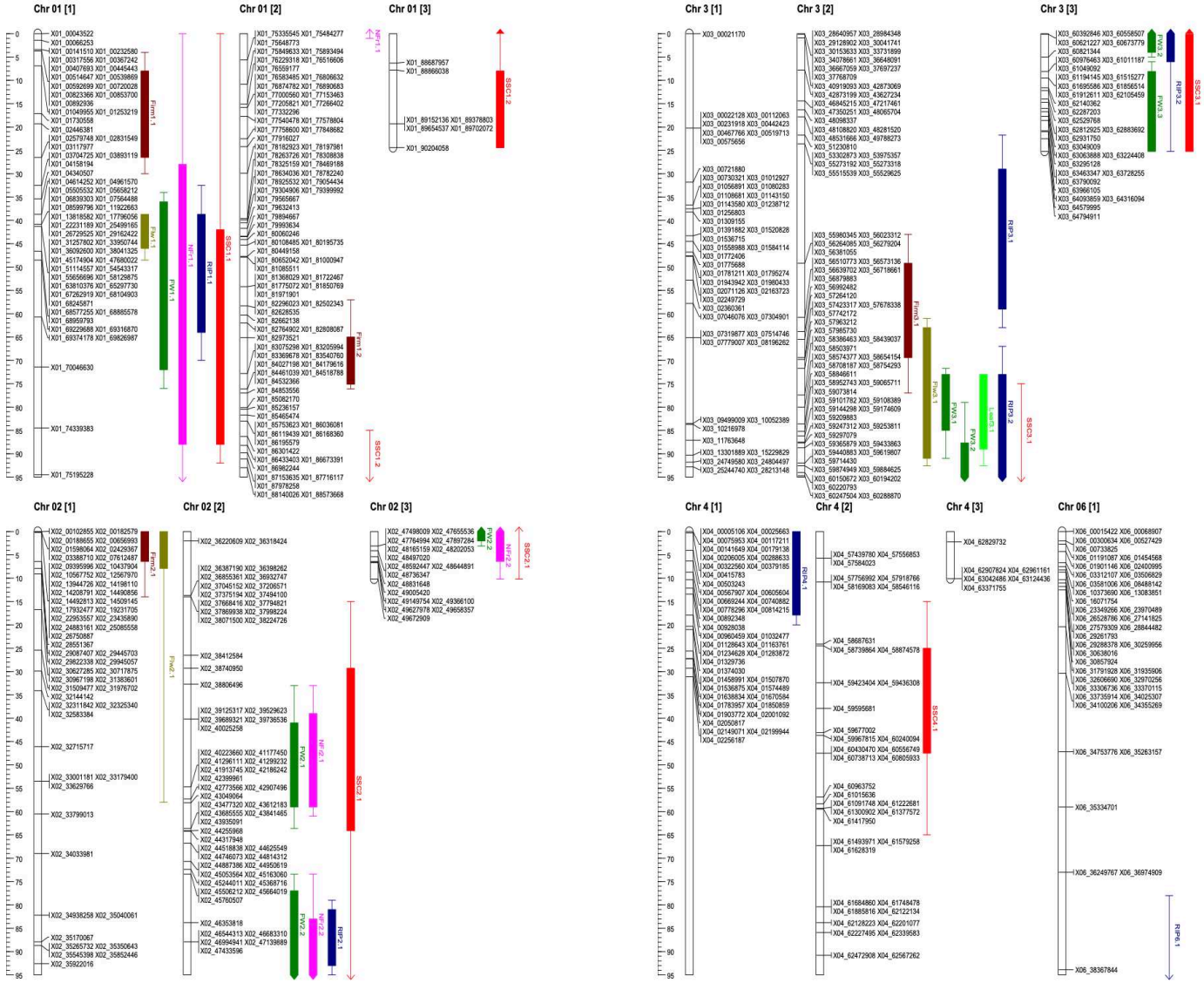

Supplemental Fig. 4: Mapchart representation of detected QTL on the genetic map for all chromosomes where a QTL was identified. The dashes on the chromosomes barchart represent the centimorgan distances between markers along the chromosomes. Each trait has a color code representation.

Appendix 3: Supplementary materials of Chapter 3

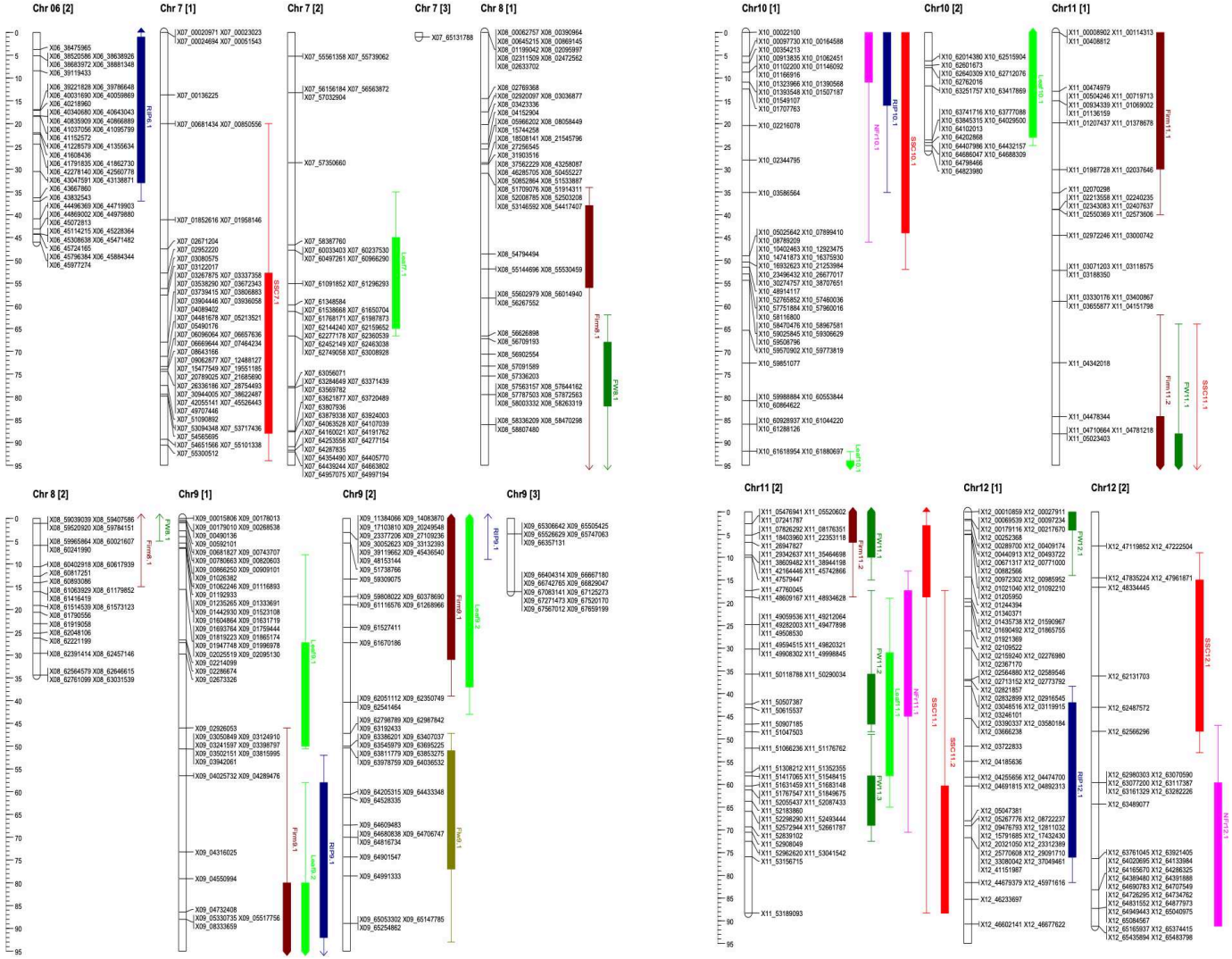

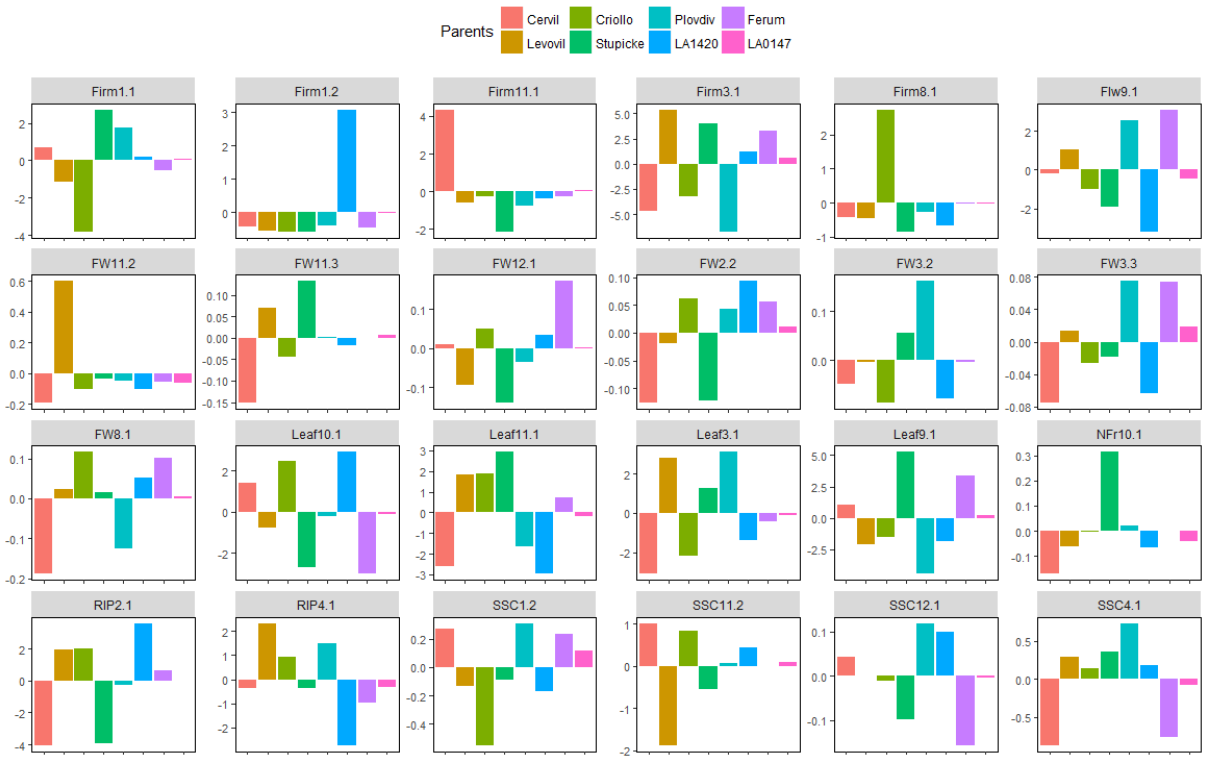

Supplemental Fig. 5: Allelic effect for parental lines for QTL that were mapped in a region of < 2Mb of confidence interval.

Supplemental Tables:

Supplemental Table 1: QTL detected in the different conditions

QTL name	Treatment	Chr	Pos	Lower cM	Upper cM	CI cM	LeftMrk	RightMrk	pvalue	Lower Mb	Upper Mb	CI Mb	R2
Firmness (Firm)													
Firm1.1	WD	1	19,28	8,00	26,54	18,54	Y01_01730558	Y01_2446381	0,000917	1,25	3,12	1,86	7
Firm1.2	CxSS	1	164,00	160,07	170,00	9,93	Y01_91212721	Y01_91314498	2,10E-05	91,21	92,27	1,05	25,39
Firm2.1	CxSS	2	0,24	0,00	6,44	6,44	Y02_19236455	Y02_19860103	0,000931	5,86	33,97	28,12	9,86
Firm3.1	SS	3	160,54	144,22	164,44	20,22	Y03_63211070	Y03_63370267	0,000637	61,93	63,37	1,44	14,35
Firm8.1	CxSS	8	44,00	38,00	56,00	18,00	Y08_57208257	Y08_57585344	0,000864	57,21	58,44	1,23	18,48
Firm8.1	Ctrl2	8	84,00	52,00	111,13	59,13	Y08_61097319	Y08_61170209	0,000532	58,36	64,25	5,89	10,98
Firm9.1	Ctrl1	9	96,00	80,00	126,00	46,00	Y09_8333659	Y09_11384066	0,000345	4,55	66,55	62,00	7,87
Firm11.1	CxSS	11	22,00	0,00	30,00	30,00	Y11_1378678	Y11_01987728	9,77E-07	0,11	1,99	1,87	30,09
Firm11.2	WD	11	98,00	84,33	101,73	17,40	Y11_7241787	Y11_7826292	0,000127	4,48	41,47	36,99	8,74
Flowering time (Flw)													
Flw1.1	WD	1	40,80	38,73	48,00	9,27	Y01_29162422	Y01_31257802	1,20E-11	4,61	76,84	72,22	19,6
Flw1.1	Ctrl2	1	40,80	38,73	46,00	7,27	Y01_29162422	Y01_31257802	4,59E-14	4,61	76,19	71,57	22,19
Flw1.1	Ctrl1	1	42,00	40,00	48,00	8,00	Y01_75855371	Y01_76186755	3,11E-15	4,96	76,84	71,88	24,09
Flw1.1	SS	1	66,00	38,73	80,00	41,27	Y01_77436487	Y01_77656130	8,82E-07	4,61	82,58	77,96	11,95
Flw2.1	Ctrl1	2	2,00	0,00	7,92	7,92	Y02_2784466	Y02_33973517	0,00027	5,86	34,87	29,01	7,87
Flw3.1	Ctrl1	3	160,54	148,00	186,00	38,00	Y03_63211070	Y03_63370267	0,000964	62,33	65,39	3,06	6,76
Flw3.1	WD	3	178,00	158,00	186,00	28,00	Y03_64701243	Y03_64793561	0,000142	62,94	65,39	2,45	8,41
Flw9.1	WD	9	155,58	145,00	178,00	33,00	Y09_68638813	Y09_68807596	2,09E-06	68,30	69,71	1,41	11,72
Flw9.1	Ctrl1	9	162,30	145,41	188,00	42,59	Y09_69261614	Y09_69332969	4,39E-05	68,41	69,96	1,54	9,37
Flw9.1	Ctrl2	9	165,03	146,00	172,00	26,00	Y09_69468865	Y09_69553678	0,000991	68,64	69,64	1,00	6,56
Fruit Weight (FW)													
FW1.1	WD	1	60,67	36,00	72,00	36,00	Y01_77436487	Y01_77656130	4,04E-05	4,34	82,58	78,24	9,44
FW1.1	Ctrl2	1	60,67	38,73	76,00	37,27	Y01_77436487	Y01_77656130	1,15E-05	4,61	82,58	77,96	11,45
FW1.1	Ctrl1	1	62,00	36,00	74,00	38,00	Y01_77436487	Y01_77656130	1,40E-05	4,34	82,58	78,24	10,39
FW2.1	Ctrl1	2	149,75	136,00	154,00	18,00	Y02_47822111	Y02_48195716	1,16E-05	45,45	48,90	3,45	10,54
FW2.1	WD	2	152,00	132,00	159,14	27,14	Y02_47822111	Y02_48195716	3,30E-06	44,55	49,68	5,13	11,38
FW2.2	Ctrl2	2	172,00	164,00	188,00	24,00	Y02_51182657	Y02_51775968	2,82E-05	50,24	52,92	2,68	9,44
FW2.2	Ctrl1	2	182,95	172,00	192,00	20,00	Y02_52855746	Y02_52920159	4,36E-08	51,18	52,92	1,74	14,61
FW2.2	WD	2	184,00	172,00	194,00	22,00	Y02_52855746	Y02_52920159	7,95E-08	51,18	53,92	2,74	14,04
FW2.2	SS	2	194,00	176,00	200,16	24,16	Y02_53919170	Y02_54014597	2,54E-05	51,18	55,10	3,91	9,73
FW3.2	WD	3	174,00	168,00	189,68	21,68	Y03_64450921	Y03_64521327	0,000152	63,93	66,10	2,16	8,35
FW3.2	Ctrl1	3	175,02	168,00	180,00	12,00	Y03_64450921	Y03_64521327	4,65E-05	63,93	64,90	0,97	9,43

FW3.3	SS	3	189,68	182,73	194,00	11,27	Y03_66167743	Y03_66194454	3,80E-05	65,24	66,77	1,52	9,42
FW3.4	SS	3	215,20	198,13	215,20	17,07	Y03_70526945	Y03_70741861	0,000278	67,00	70,74	3,75	7,61
FW8.1	Ctrl2	8	74,00	68,00	82,00	14,00	Y08_59925589	Y08_60170203	2,20E-05	59,54	61,17	1,63	9,6
FW8.1	CxSS	8	98,00	68,00	104,00	36,00	Y08_62618151	Y08_62799864	0,000958	59,54	63,24	3,69	6,77
FW11.1	Ctrl1	11	82,00	66,00	100,00	34,00	Y11_04342018	Y11_4478344	0,000103	4,15	21,80	17,65	8,78
FW11.1	WD	11	92,00	64,00	100,00	36,00	Y11_5023403	Y11_5476941	1,54E-05	4,15	21,80	17,65	10,2
FW11.1	Ctrl2	11	96,00	88,13	112,00	23,87	Y11_5023403	Y11_5476941	0,000102	4,71	50,68	45,97	8,43
FW11.1	CxSS	11	97,56	88,13	104,97	16,85	Y11_7241787	Y11_7826292	0,000722	4,71	50,50	45,79	6,91
FW11.2	Ctrl2	11	134,00	125,19	141,67	16,48	Y11_53206534	Y11_53423887	1,64E-05	52,51	53,82	1,31	9,82
FW11.2	Ctrl1	11	137,34	130,70	141,67	10,97	Y11_53423887	Y11_53532037	0,000312	53,04	53,82	0,79	7,84
FW11.2	WD	11	137,34	130,70	141,67	10,97	Y11_53423887	Y11_53532037	6,95E-05	53,04	53,82	0,79	9
FW11.3	CxSS	11	155,27	142,00	183,33	41,33	Y11_54599648	Y11_54684047	0,000582	53,82	56,11	2,28	6,88
FW11.3	Ctrl2	11	155,27	152,35	164,00	11,65	Y11_54599648	Y11_54684047	1,34E-06	54,27	55,76	1,49	11,27
FW11.3	WD	11	158,66	153,09	164,00	10,91	Y11_55100360	Y11_55214790	2,36E-06	54,33	55,76	1,42	11,22
FW12.1	Ctrl1	12	1,89	0,00	4,00	4,00	Y12_252368	Y12_289700	0,000732	0,01	0,44	0,43	7,09
Leaf lenght (Leaf)													
Leaf3.1	WD	3	178,00	168,00	184,00	16,00	Y03_64701243	Y03_64793561	0,000292	63,93	65,39	1,46	7,81
leaf7.1	CxSS	7	150,06	140,00	160,00	20,00	Y07_63972793	Y07_64025084	0,000576	60,03	64,92	4,89	7,11
Leaf9.1	Ctrl1	9	46,01	27,27	50,00	22,73	Y09_02673326	Y09_2926053	0,000109	2,29	3,05	0,76	8,63
Leaf9.2	Ctrl2	9	120,00	80,00	132,00	52,00	Y09_66029792	Y09_66172567	0,000478	4,55	66,55	62,00	7,08
Leaf10.1	SS	10	102,00	94,00	118,00	24,00	Y10_63191372	Y10_63277141	0,000197	62,56	64,42	1,86	8,01
Leaf11.1	WD	11	138,12	126,00	153,09	27,09	Y11_53532037	Y11_53823685	0,000732	52,92	54,46	1,55	7,01
Fruit Number (NFr)													
NFr1.1	SS	1	72,00	28,00	88,00	60,00	Y01_77656130	Y01_82578583	0,000857	3,12	83,43	80,32	6,71
NFr2.1	WD	2	108,70	94,00	152,00	58,00	Y02_42916250	Y02_43090566	0,000419	41,34	48,33	6,99	7,5
NFr2.1	Ctrl1	2	150,00	134,00	154,00	20,00	Y02_47822111	Y02_48195716	0,000153	44,55	48,90	4,35	8,51
NFr2.2	SS	2	188,00	178,77	196,43	17,66	Y02_52855746	Y02_52920159	1,19E-05	51,78	54,43	2,65	10,44
NFr10.1	SS	10	6,00	0,00	10,89	10,89	Y10_164588	Y10_354213	0,000773	0,02	1,55	1,53	6,99
NFr11.1	CxSS	11	113,75	112,27	140,00	27,73	Y11_51851128	Y11_51976036	0,000634	50,68	53,82	3,15	7,33
NFr12.1	SS	12	166,00	154,63	186,18	31,55	Y12_65148027	Y12_65419995	0,000372	64,13	67,14	3,02	10,19
Time to ripe (RIP)													
RIP1.1	Ctrl1	1	42,00	38,73	64,00	25,27	Y01_75855371	Y01_76186755	1,76E-05	4,61	77,66	73,04	10,17
RIP1.1	Ctrl2	1	48,00	38,73	64,00	25,27	Y01_76569293	Y01_76839188	5,01E-05	4,61	77,66	73,04	9,13
RIP2.1	Ctrl1	2	182,95	176,00	188,00	12,00	Y02_52855746	Y02_52920159	2,70E-10	51,18	52,92	1,74	17,86
RIP2.1	WD	2	182,95	176,00	188,00	12,00	Y02_52855746	Y02_52920159	1,62E-11	51,18	52,92	1,74	19,48
RIP3.1	Ctrl1	3	142,00	124,00	154,00	30,00	Y03_43631616	Y03_61927295	6,61E-05	43,63	62,46	18,83	9,11
RIP3.2	SS	3	189,04	168,00	196,00	28,00	Y03_65831575	Y03_66097622	0,000459	63,93	66,92	2,99	7,3
RIP4.1	WD	4	12,05	0,00	17,94	17,94	Y04_892348	Y04_928038	0,000207	0,12	1,33	1,21	6,9
RIP6.1	Ctrl1	6	117,29	96,00	128,00	32,00	Y06_45218536	Y06_45401935	0,000959	41,98	47,28	5,30	6,82

RIP9.1	CxWD	9	36,00	26,72	78,00	51,28	Y09_02673326	Y09_2926053	0,000772	2,29	4,55	2,26	7,04
RIP9.1	Ctrl1	9	73,23	58,00	92,00	34,00	Y09_04289476	Y09_04316025	0,000771	4,29	11,38	7,09	7,02
RIP10.1	CxWD	10	8,66	0,00	18,00	18,00	Y10_1166916	Y10_01323966	5,85E-05	0,02	2,22	2,19	9,24
RIP10.1	WD	10	34,00	5,25	48,00	42,75	Y10_02344795	Y10_3586564	0,00021	0,16	5,03	4,86	8,12
RIP12.1	WD	12	64,00	42,00	76,00	34,00	Y12_4892313	Y12_5047381	0,000533	3,25	38,65	35,40	7,32
Sugar Content (SSC)													
SSC1.1	CxSS	1	74,00	42,00	88,00	46,00	Y01_77656130	Y01_82578583	0,00082	75,86	83,43	7,58	10,55
SSC1.2	WD	1	209,26	198,00	214,45	16,45	Y01_97105238	Y01_97391336	0,000735	97,11	98,44	1,34	7,03
SSC2.1	Ctrl1	2	148,00	124,29	159,14	34,85	Y02_45447408	Y02_45645810	0,000825	44,16	49,68	5,52	6,98
SSC3.1	SS	3	206,74	190,06	215,20	25,14	Y03_68995959	Y03_69010838	0,000347	66,34	70,74	4,40	7,81
SSC4.1	CxSS	4	116,00	100,71	142,00	41,29	Y04_60952746	Y04_61094261	0,000138	59,79	62,84	3,05	9,41
SSC4.1	SS	4	127,40	120,00	142,51	22,51	Y04_61842938	Y04_62002311	0,000128	61,28	63,21	1,93	8,66
SSC4.1	Ctrl2	4	130,00	88,00	142,00	54,00	Y04_61842938	Y04_62002311	9,00E-04	58,90	62,84	3,94	7,22
SSC7.1	SS	7	73,31	52,81	88,00	35,19	Y07_5490176	Y07_6096064	0,000242	2,95	57,33	54,38	10,89
SSC10.1	WD	10	14,00	0,00	44,00	44,00	Y10_1707763	Y10_02216078	0,000282	0,02	5,03	5,00	7,86
SSC11.1	Ctrl2	11	104,45	98,00	113,75	15,75	Y11_41466599	Y11_39071789	0,000417	7,24	51,85	44,61	7,93
SSC11.2	Ctrl2	11	162,00	155,27	183,33	28,06	Y11_55578287	Y11_55755602	9,56E-05	54,55	56,11	1,56	9,27
SSC11.2	CxSS	11	164,00	148,00	183,33	35,33	Y11_55578287	Y11_55755602	0,000976	54,09	56,11	2,01	9,86
SSC11.2	SS	11	164,00	155,27	183,33	28,06	Y11_55578287	Y11_55755602	4,40E-05	54,55	56,11	1,56	9,18
SSC12.1	CxWD	12	130,00	110,00	143,30	33,30	Y12_62976697	Y12_63690753	0,000326	62,60	64,13	1,52	7,83

For each trait, all the QTL found are identified by a specific name (QTL name column), the treatment where the QTL was found (Treatment), the chromosome (Chr) and the position (Pos) in cM. The peak region encompassing any QTL is defined by a pair of marker (LeftMrk and RightMrk), corresponding to the lower and upper bound expressed in genetic distances (Lower cM & Upper cM) as well as physical distances (Lower Mb & Upper Mb). The confidence interval in centimorgan (CI cM) and Mega-base (CI Mb) represent the corresponding differences between Upper and Lower. R2 is the percentage of phenotypic variation explained by a QTL. Ctrl 1 and Ctrl2 are the controls treatment for Exp.1 and Exp.2 respectively where the QTL were found. WD and SS are the stress treatment for water deficit and salinity. When interactives QTL are identified in Exp.1 (respectively Exp.2) treatment CxWD (respectively (CxSS) are the corresponding treatment designed.

Supplemental Table 2: Functional annotation of CG retained after the filtering procedure according to allelic parental effect.

Chromosome	Localization	Type	impact	gene	Function
***Firm11.1* specific to CxSS (8GC & 3 pol)**					
SL2.50ch11	668462	snp	MODIFIER	Solyc11g005820	Pectinesterase inhibitor
SL2.50ch11	668462	snp	MODIFIER	Solyc11g005830	NifS-like protein Aminotransferase class V family
SL2.50ch11	668462	snp	MODIFIER	Solyc11g005840	Cysteine desulfurase
SL2.50ch11	901124	indel	MODIFIER	Solyc11g006130	Methyltransferase-like protein 6
SL2.50ch11	901124	indel	MODIFIER	Solyc11g006140	DNAJ heat shock N-terminal domain-containing protein
SL2.50ch11	958779	indel	MODIFIER	Solyc11g006200	Homeobox transcription factor Hox7-like protein
SL2.50ch11	958779	indel	MODIFIER	Solyc11g006210	Unknown Protein
SL2.50ch11	958779	indel	MODIFIER	Solyc11g006220	Myosin XI
***Firm8.1* common to CxSS and Ctrl2 (27GC & 46 Pol)**					
SL2.50ch08	57391527 - 57393693	snp (3)	MODIFIER	Solyc08g068290	Os01g0786800 protein
SL2.50ch08	57392863 - 57407143	snp (3) ; indel (1)	MODIFIER	Solyc08g068300	Coiled-coil domain-containing protein 25
SL2.50ch08	57405098 - 57413668	snp (5) ; indel (1)	MODIFIER	Solyc08g068310	RNA-binding La domain protein
SL2.50ch08	57413668 - 57429092	snp (3)	MODIFIER	Solyc08g068320	Transcription factor myb
SL2.50ch08	57424926 - 57435833	snp (3)	MODIFIER	Solyc08g068330	Aspartate aminotransferase
SL2.50ch08	57435833 - 57446365	snp (2)	MODIFIER	Solyc08g068340	Eukaryotic translation initiation factor 3 subunit 6-interacting protein
SL2.50ch08	57446365	snp	MODIFIER	Solyc08g068350	Unknown Protein
SL2.50ch08	57460516	snp	MODIFIER	Solyc08g068370	Class E vacuolar protein-sorting machinery protein HSE1
SL2.50ch08	57513432 - 57525807	snp (3)	MODIFIER	Solyc08g068390	Fatty acid oxidation complex subunit alpha
SL2.50ch08	57518954 - 57525807	snp (2)	MODIFIER	Solyc08g068400	Dienelactone hydrolase domain protein
SL2.50ch08	57531214 - 57897103	snp (4)	MODIFIER	Solyc08g068410	Unknown Protein
SL2.50ch08	57564151 - 57570883	snp (4)	MODIFIER	Solyc08g068420	FAD-linked oxidoreductase
SL2.50ch08	57574499 - 57578506	snp (2); indel (1)	MODIFIER	Solyc08g068430	Galactosylgalactosylxylosylprotein 3-beta-glucuronosyltransferase 1
SL2.50ch08	57868081 - 57909685	snp	MODIFIER	Solyc08g068720	Tyramine hydroxycinnamoyl transferase
SL2.50ch08	57868081	snp	MODIFIER	Solyc08g068730	N-acetyltransferase
SL2.50ch08	57897103	snp	MODIFIER	Solyc08g068750	Unknown Protein
SL2.50ch08	57897103	snp	MODIFIER	Solyc08g068760	Growth-regulating factor 3
SL2.50ch08	57897103 - 57902392	snp (3)	MODIFIER	Solyc08g068770	N-acetyltransferase
SL2.50ch08	57902308 - 57902392	snp (2)	LOW	Solyc08g068780	N-acetyltransferase
SL2.50ch08	57902308	snp (3); indel (1)	MODIFIER	Solyc08g068790	Tyramine hydroxycinnamoyl transferase
SL2.50ch08	57909549 - 57916200	snp (10) ; indel (1)	MODIFIER	Solyc08g068800	Glutathione peroxidase
SL2.50ch08	57909549 - 57917666	snp (11) ; indel (1)	MODIFIER	Solyc08g068810	Ubiquitin carboxyl-terminal hydrolase
SL2.50ch08	57917666 - 57921322	snp (2)	MODIFIER	Solyc08g068820	Zinc finger CCCH domain-containing protein 18
SL2.50ch08	57921322 - 57929734	snp (2)	MODIFIER	Solyc08g068830	Zinc finger CCCH-type with G patch domain-containing protein
SL2.50ch08	57929734 - 57935634	snp (2)	MODIFIER	Solyc08g068840	Transcription factor IIIB 90 kDa subunit
SL2.50ch08	57929734 - 57935634	snp (2)	MODIFIER	Solyc08g068850	Proton pump interactor 1
SL2.50ch08	57935634	snp	MODIFIER	Solyc08g068860	Aspartic proteinase nepenthesin-1

***Firm3.1* specific to SS (36 CG & 29 Pol)**					
SL2.50ch03	61944128	indel	MODIFIER	Solyc03g111330.2	UPF0235 protein yggU
SL2.50ch03	61944128 - 61955812	indel (2)	MODIFIER	Solyc03g111340.2	Ubiquitin-like modifier-activating enzyme 5
SL2.50ch03	61955812	indel	MODIFIER	Solyc03g111350.2	Deoxycytidylate deaminase-like
SL2.50ch03	61955812	indel	MODIFIER	Solyc03g111360.2	Oxygen-independent coproporphyrinogen III oxidase-like protein sll1917
SL2.50ch03	61955812	indel	MODIFIER	Solyc03g111370.2	Zinc finger protein
SL2.50ch03	61994574	indel	MODIFIER	Solyc03g111400.1	Xanthine/uracil permease family protein
SL2.50ch03	61994574 - 62005711	indel (2)	MODIFIER	Solyc03g111410.2	B3 domain-containing protein Os01g0905400
SL2.50ch03	62028535	indel	MODIFIER	Solyc03g111430.1	Unknown Protein
SL2.50ch03	62028535	indel	MODIFIER	Solyc03g111440.1	DNAJ heat shock N-terminal domain-containing protein
SL2.50ch03	62064922	indel	MODIFIER	Solyc03g111460.1	Nuclear transcription factor Y subunit C-2
SL2.50ch03	62099020	snp	MODIFIER	Solyc03g111490.1	Ulp1 protease family C-terminal catalytic domain containing protein
SL2.50ch03	62099020	snp	MODIFIER	Solyc03g111500.2	B3 domain-containing protein Os01g0905400
SL2.50ch03	62117618 - 62117956	indel (3)	MODIFIER	Solyc03g111510.2	Zinc finger family protein
SL2.50ch03	62131267 - 62131953	indel (2)	MODIFIER	Solyc03g111530.2	Cysteine-rich receptor-like protein kinase
SL2.50ch03	62415608 - 62418765	indel (4)	MODIFIER	Solyc03g111780.1	WD-40 repeat family protein
SL2.50ch03	62415608 - 62418765	indel (4)	MODIFIER	Solyc03g111790.2	Centromere protein X
SL2.50ch03	62418765	indel	MODIFIER	Solyc03g111800.2	Receptor like kinase%2C RLK
SL2.50ch03	62594981	indel	MODIFIER	Solyc03g112050.2	Serine/threonine kinase
SL2.50ch03	62594981	indel	MODIFIER	Solyc03g112060.2	Quinolinate synthase A
SL2.50ch03	62689442	indel	MODIFIER	Solyc03g112190.2	Pentatricopeptide repeat-containing protein
SL2.50ch03	62689442	indel	MODIFIER	Solyc03g112200.1	Unknown Protein
SL2.50ch03	62689442	indel	MODIFIER	Solyc03g112210.1	Unknown Protein
SL2.50ch03	62689442	indel	MODIFIER	Solyc03g112220.1	Unknown Protein
SL2.50ch03	62765101	indel	MODIFIER	Solyc03g112330.2	U-box domain-containing protein 33
SL2.50ch03	62765101	indel	MODIFIER	Solyc03g112340.1	Ring H2 finger protein
SL2.50ch03	62869719	indel	MODIFIER	Solyc03g112460.2	Alliinase
SL2.50ch03	62889969	indel	MODIFIER	Solyc03g112490.1	Unknown Protein
SL2.50ch03	62928738 - 62933195	indel (2)	MODIFIER	Solyc03g112540.2	Retinol dehydrogenase 12
SL2.50ch03	62933195	indel	MODIFIER	Solyc03g112550.2	Kinetochore protein Spc25
SL2.50ch03	62965799	indel	MODIFIER	Solyc03g112580.2	Receptor like kinase%2C RLK
SL2.50ch03	63001033	indel	MODIFIER	Solyc03g112600.2	JmjC domain-containing protein
SL2.50ch03	63001033	indel	MODIFIER	Solyc03g112610.1	Unknown Protein
SL2.50ch03	63001033 - 63002483	indel (2)	MODIFIER	Solyc03g112620.2	Carboxyl-terminal proteinase
SL2.50ch03	63016924	indel	MODIFIER	Solyc03g112630.2	Fas-associated factor 1-like protein
SL2.50ch03	63016924	indel	MODIFIER	Solyc03g112640.2	CRAL/TRIO domain containing protein
SL2.50ch03	63231925 - 63239632	indel (2)	MODIFIER	Solyc03g112940.2	Serine/threonine-protein kinase ATM
***FW8.1* common to CxSS and Ctrl2 (31GC & 738 Pol)**					
SL2.50ch08	59544733 - 59546703	indel (3); snp (20)	MODIFIER	Solyc08g075390	Isopentenyl-diphosphate delta-isomerase family protein

SL2.50ch08	59544733 - 59550417	indel (3); snp (30)	MODIFIER/MODERATE	Solyc08g075400	SWIB/MDM2 domain protein
SL2.50ch08	59544733 - 59553646	indel (3); snp (38)	MODIFIER	Solyc08g075410	50S ribosomal protein L2
SL2.50ch08	59546159 - 59561420	indel (5); snp (54)	MODIFIER	Solyc08g075420	Uncharacterized zinc finger CCHC domain-containing protein At4g19190
SL2.50ch08	59560930 _ 59572063	indel (6); snp (45)	MODIFIER/LOW/MODERATE/HIGH	Solyc08g075430	ABC transporter G family member 14
SL2.50ch08	59586672 - 59600670	indel (6); snp (54)	MODIFIER/MODERATE/LOW	Solyc08g075440	Conserved oligomeric Golgi complex subunit 6
SL2.50ch08	59594411 - 59614436	indel (8); snp (72)	MODIFIER	Solyc08g075450	Nodulin-like protein
SL2.50ch08	59610214 - 59622431	indel (7); snp (49)	MODIFIER/MODERATE	Solyc08g075460	Nodulin-like protein
SL2.50ch08	59615722 - 59630904	indel (12); snp(67)	MODIFIER/MODERATE/LOW/HIGH	Solyc08g075470	Nodulin-like protein
SL2.50ch08	59622559 - 59630904	indel (10); snp(45)	MODIFIER/MODERATE/LOW	Solyc08g075480	Carotenoid cleavage dioxygenase 4A
SL2.50ch08	59640117 - 59651492	indel (13); snp (61)	MODIFIER/MODERATE/LOW	Solyc08g075490	Carotenoid cleavage dioxygenase 4B
SL2.50ch08	59655124 - 59662369	indel (5); snp (54)	MODIFIER/MODERATE/LOW/HIGH	Solyc08g075500	Pentatricopeptide repeat-containing protein
SL2.50ch08	59656921 - 59669780	indel (9); snp (39)	MODIFIER/MODERATE	Solyc08g075510	JmjC domain protein
SL2.50ch08	59667562 - 59681711	indel (6); snp (50)	MODIFIER/MODERATE/LOW	Solyc08g075520	Binding protein
SL2.50ch08	59687841 - 59713033	indel (10); snp (60)	MODIFIER/LOW	Solyc08g075530	Alpha glucosidase-like protein
SL2.50ch08	59707355 - 59718596	indel (9); snp (36)	MODIFIER/LOW	Solyc08g075540	Alternative oxidase
SL2.50ch08	59712704 - 59723088	indel (17); snp (49)	MODIFIER/MODERATE/LOW	Solyc08g075550	Alternative oxidase
SL2.50ch08	59723852 - 59733339	indel (11); snp (39)	MODIFIER/MODERATE/LOW	Solyc08g075560	Unknown Protein
SL2.50ch08	59729935 - 59742458	indel (13); snp (58)	MODIFIER/MODERATE/LOW	Solyc08g075570	Urea active transporter-like protein
SL2.50ch08	59734828 - 59742458	indel (7) ; (41)	MODIFIER	Solyc08g075580	DNA-directed RNA polymerase III subunit F
SL2.50ch08	59735219 - 59742458	indel (4); snp (33)	MODIFIER/MODERATE/LOW	Solyc08g075590	Receptor like kinase%2C RLK
SL2.50ch08	60630281 - 60630307	snp (2)	MODIFIER	Solyc08g076690	Inositol-tetrakisphosphate 1-kinase 1
SL2.50ch08	60793358	indel	MODIFIER	Solyc08g076870	Unknown Protein
SL2.50ch08	60897111 _ 60897121	indel; snp	MODIFIER	Solyc08g076960	Abscisic acid receptor PYR1
SL2.50ch08	60907932	indel	MODIFIER	Solyc08g076970	Acetylornithine deacetylase or succinyl-diaminopimelate desuccinylase
SL2.50ch08	60923434 - 60926657	indel (4)	MODIFIER	Solyc08g076980	Acetylornithine deacetylase or succinyl-diaminopimelate desuccinylase
SL2.50ch08	60926657 - 60936272	indel (2)	MODIFIER	Solyc08g076990	Acetylornithine deacetylase
SL2.50ch08	61065341	indel	MODIFIER	Solyc08g077160	NAD
SL2.50ch08	61101245	indel	MODIFIER	Solyc08g077190	Unknown Protein
SL2.50ch08	61101245 - 61102430	indel (3)	MODIFIER	Solyc08g077200	Ribose-phosphate pyrophosphokinase
SL2.50ch08	61131025	indel	MODIFIER	Solyc08g077220	Tetraspanin family protein
***FW11.2* common to Ctrl1, WD and Ctrl2 (29 CG & 32 Pol)**					
SL2.50ch11	53040997	indel	MODIFIER	Solyc11g067300.1	Lipid A export ATP-binding/permease protein msbA
SL2.50ch11	53124062	indel	MODIFIER	Solyc11g068370.1	BZIP transcription factor
SL2.50ch11	53158885 - 53159771	snp (1) ; indel (1)	MODIFIER	Solyc11g068430.1	Ferredoxin
SL2.50ch11	53171810 - 53177163	snp (2) ; indel (3)	MODIFIER	Solyc11g068440.1	Glucan endo-1 3-beta-glucosidase 7
SL2.50ch11	53177163	indel	MODIFIER	Solyc11g068450.1	Biogenesis of lysosome-related organelles complex-1 subunit 1
SL2.50ch11	53177163	indel	MODIFIER	Solyc11g068460.1	Calpain-2 catalytic subunit
SL2.50ch11	53225598 - 53225601	snp (1) ; indel (1)	MODIFIER	Solyc11g068520.1	Rho GTPase activating protein 2

SL2.50ch11	53225598 - 53225601	snp (1) ; indel (1)	MODIFIER	Solyc11g068530.1	Genomic DNA chromosome 5 P1 clone MWD9
SL2.50ch11	53225598 - 53225601	snp (1) ; indel (1)	MODIFIER	Solyc11g068540.1	N-carbamoylputrescine amidase
SL2.50ch11	53336896 - 53337562	indel (3)	MODIFIER	Solyc11g068700.1	Unknown Protein
SL2.50ch11	53336896 - 53343358	snp (1) ; indel (3)	MODIFIER	Solyc11g068710.1	F-box family protein
SL2.50ch11	53356856 - 53358330	snp (1) ; indel (1)	MODIFIER	Solyc11g068720.1	Os04g0625000 protein
SL2.50ch11	53358330 - 53372493	snp (1) ; indel (1)	MODIFIER	Solyc11g068730.1	Nitrilase 4A
SL2.50ch11	53372493	indel	MODIFIER	Solyc11g068740.1	Methyl binding domain protein
SL2.50ch11	53400655	indel	MODIFIER	Solyc11g068760.1	Unknown Protein
SL2.50ch11	53415455	indel	MODIFIER	Solyc11g068780.1	Plant-specific domain TIGR01568 family protein
SL2.50ch11	53415455	indel	MODIFIER	Solyc11g068790.1	Chromosome 20 open reading frame 108 ortholog
SL2.50ch11	53425133	indel	MODIFIER	Solyc11g068800.1	Transcription factor
SL2.50ch11	53425133	indel	MODIFIER	Solyc11g068810.1	Unknown Protein
SL2.50ch11	53494458	indel	MODIFIER	Solyc11g068930.1	Autophagy-related 7
SL2.50ch11	53494458	indel	MODIFIER	Solyc11g068940.1	U-box domain-containing protein 24
SL2.50ch11	53547091 - 53549750	indel (3)	MODIFIER	Solyc11g068970.1	Aluminum-activated malate transporter
SL2.50ch11	53556394	indel	MODIFIER	Solyc11g068980.1	Mitochondrial import inner membrane translocase subunit tim22
SL2.50ch11	53601247 - 53603756	indel (2)	MODIFIER	Solyc11g069030.1	MYB transcription factor
SL2.50ch11	53668484	indel	MODIFIER	Solyc11g069080.1	Os09g0549700 protein
SL2.50ch11	53682719	indel	MODIFIER	Solyc11g069090.1	ATP-binding cassette protein
SL2.50ch11	53731840	indel	MODIFIER	Solyc11g069130.1	Unknown Protein
SL2.50ch11	53759795	indel	MODIFIER	Solyc11g069150.1	Proteasome subunit beta type
SL2.50ch11	53759795	indel	MODIFIER	Solyc11g069160.1	Sumo ligase

Only QTL that presented less than 40 CG were screened. For each QTL, the chromosome and localization (position in pb) were precised. The type of polymorphisms, depending if it is a single nucleotide polymorphism (snp) or insertion deletion (indel) were in the column "Type". The number of snp or indel at a given gene is marked in brackets () when more than one polymorphism affected a given gene. The impact of polymorphisms affecting a gene were defined as MODIFIER when snp or indel are located in upstream or downstream region; MODERATE and LOW when polymorphisms had respectively non-synonymous or synonymous variant effect and HIGH when they affect splice site variant or start/stop codon. The putative function of each CG was checked on the annotation database of the tomato genome assembly (SL2.50)

Appendix 4

Supplemental Figures:

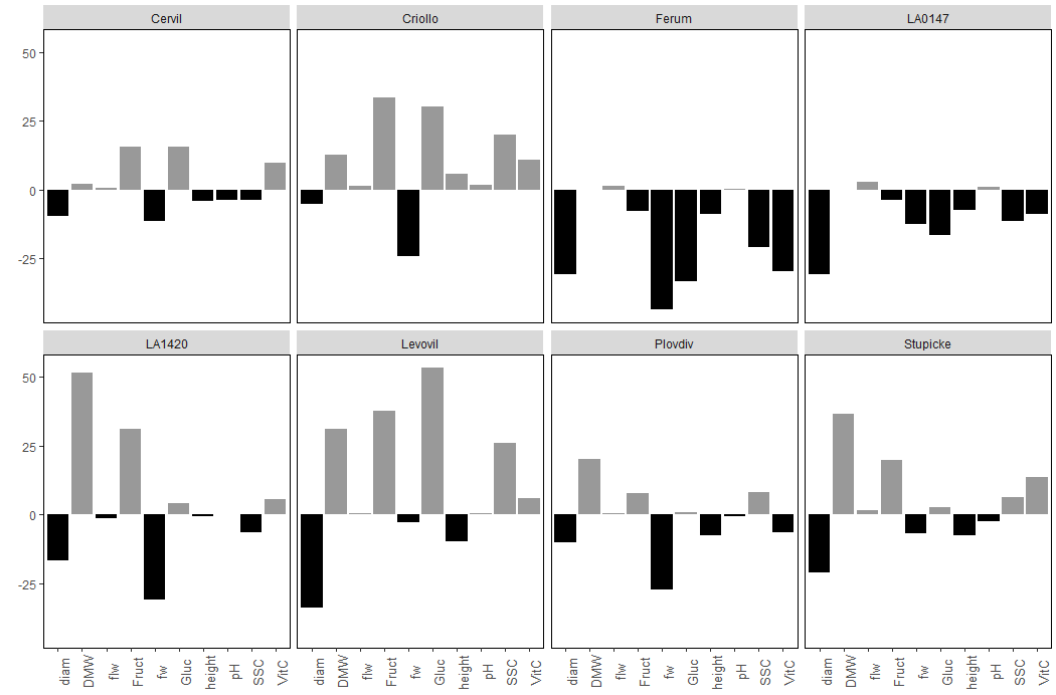

Supplemental Figure 1: Phenotypic variation under WD for each genotype. Phenotypic traits are represented on the x-axis while the y-axis represents the percentage of increase/decrease of the trait value under the WD condition. In grey and black are all traits affected positively and negatively by WD condition, respectively.

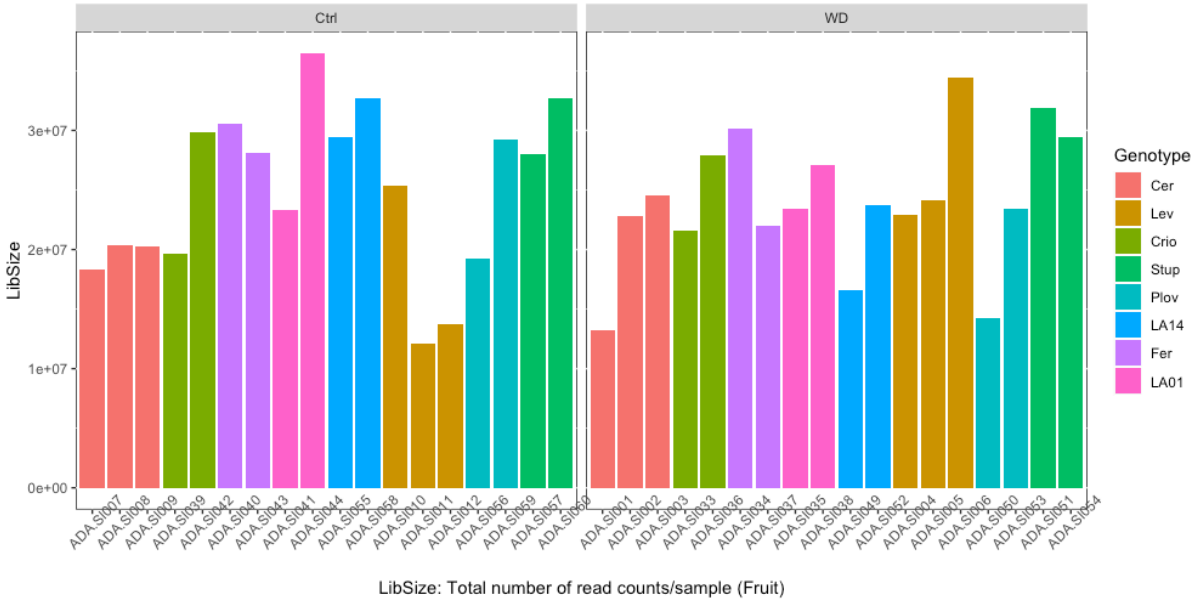

Supplemental Figure 2 A): Total number of read counts after RNA-sequencing processing for fruit.

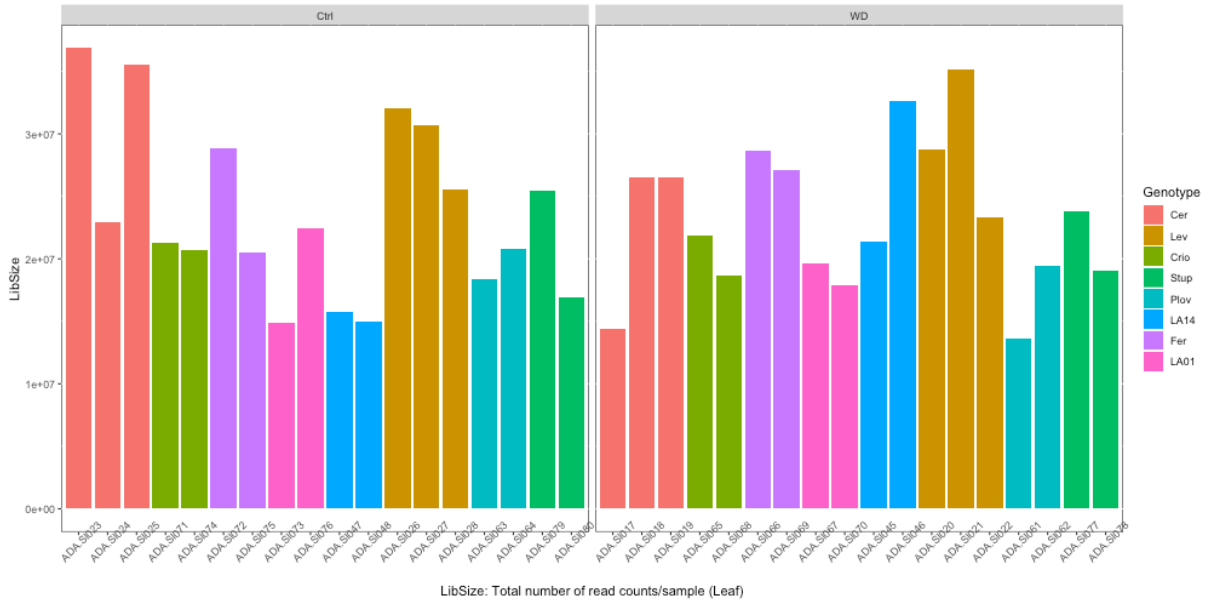

Supplemental Figure 2 B): Total number of read counts after RNA-sequencing processing for leaf.

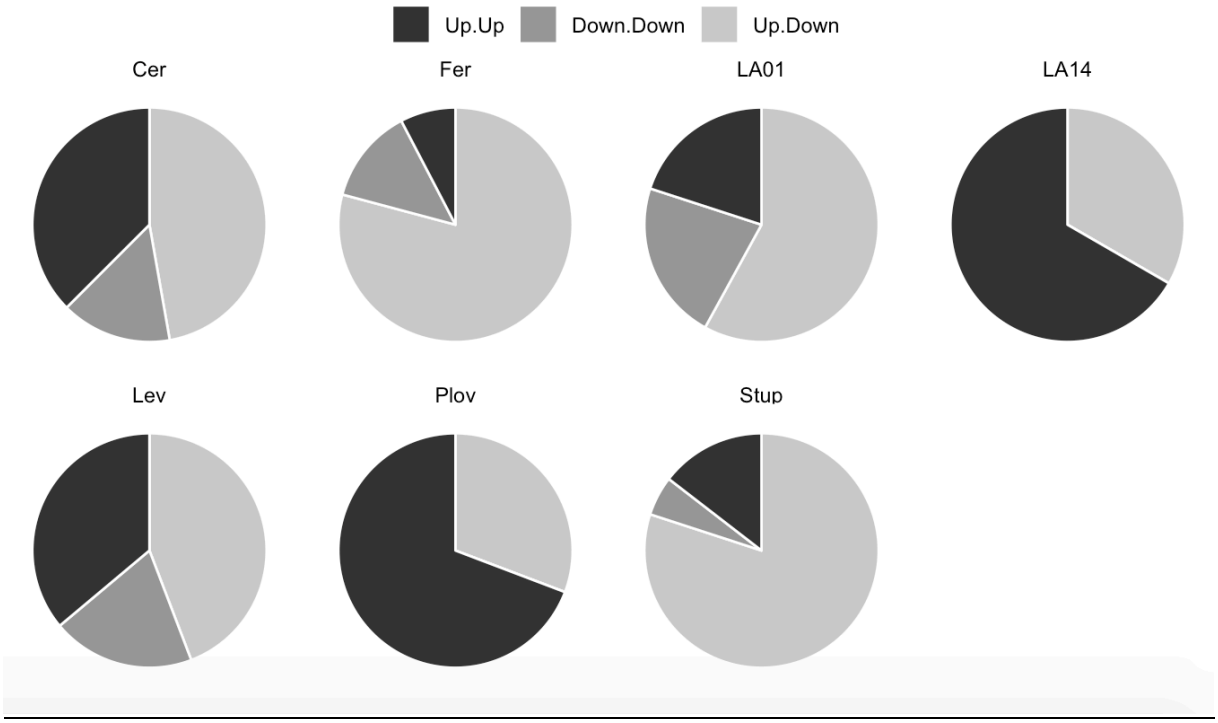

Supplemental Figure 3: Expression pattern of the consistent DEG in fruit and leaf. The DEG were classified as up-up when up-regulated in both organs, up-down when up regulated in one organ (leaf or fruit) while down-regulated in the other and down-down when down regulated in both organs.

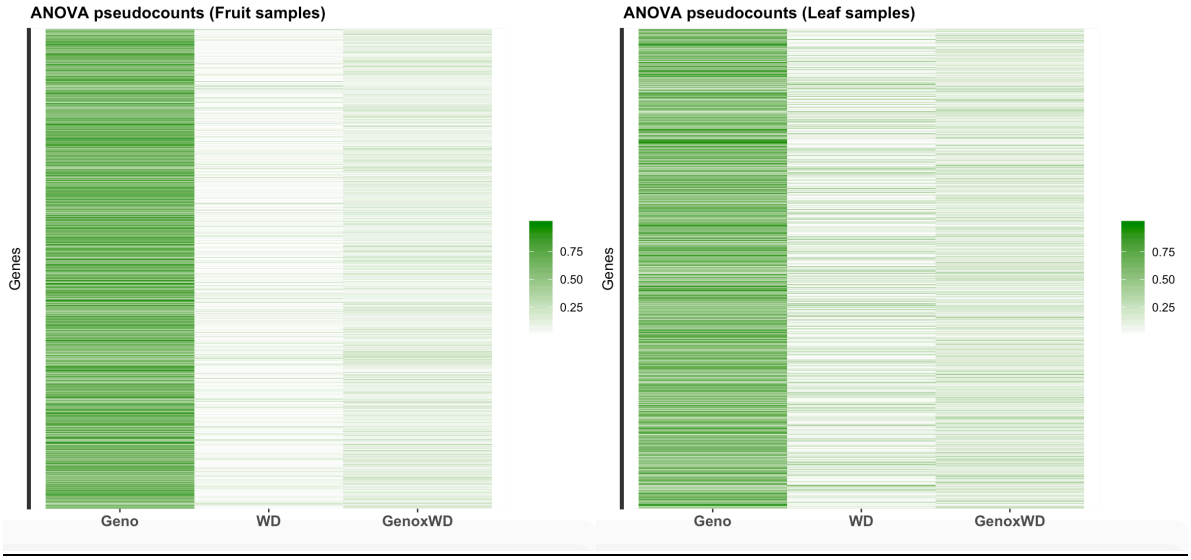

Supplemental Figure 4: Proportion of the sum of square attributed to each factor (Genotype, Condition or GxC) in fruit and leaf samples through the ANOVA analysis on the normalized transcript level.

Supplemental Tables:

Supplemental Table 1: Phenotypic traits evaluated on the eight genotypes under normal irrigation and WD condition. The greenhouse experiment is described in details in Albert et al. (2018).

Trait	Abbreviation	Truss phenotyped	Measurements
Flowering time	flw	T4	Number of days from the 1st of january
Plant height	height	T4	Plant height in cm at the 4th truss
Stem diameter	diam	T4	Equatorial measurement os stem diameter (in mm) under the 4th truss
Soluble solid content	SSC	T3-to-T6	Brix of pooled fruits from the 3rd to the 6th truss
fruit weight	fw	T3-to-T6	Average fruit weight (in grams) of pooled fruits from the 3rd to the 6th truss
pH	pH	T3-to-T6	Brix of pooled fruits from the 3rd to the 6th truss
Dry matter weight	DMW	T3-to-T6	Percentage of dry matter after fruit samples dried in an oven for 4 days. Fruits were pooled from the 3rd to 6th truss
Glucose content	Gluc	T3-to-T6	g 100 g-1 of fresh matter from a pool of fruits harvested on the 3rd - 6th truss
Fructose content	Fruct	T3-to-T6	g 100 g-1 of fresh matter from a pool of fruits harvested on the 3rd - 6th truss
Vitamine C	VitC	T3-to-T6	mg 100 g-1 of fresh matter from a pool of fruits harvested on the 3rd - 6th truss

Supplemental Table 2: Results of the two-way interactive ANOVA analysis on the phenotypic traits. For each factor the associated sum of square and p-value of the test are highlighted. The *ns* p-values for the GxE factor stand for non-significant GxE.

Trait	Factor	SSQ	p-value
diameter	Geno	182,497536	1,29E-16
diameter	Env	166,796934	1,15E-19
diameter	GxE	50,1595955	2,22E-05
DMW	Geno	161,146561	4,56E-09
DMW	Env	16,0913547	0,0014867
DMW	GxE	31,592869	*ns*
flw	Geno	2701,3381	1,08E-55
flw	Env	1,42074058	0,39463091
flw	GxE	194,378776	*ns*
Fructose	Geno	12,9844224	5,78E-12
Fructose	Env	1,09974856	0,00077117
Fructose	GxE	3,31885506	*ns*
fw	Geno	65400,9879	1,46E-22
fw	Env	2519,56424	1,22E-07
fw	GxE	3296,64439	6,96E-06
Glucose	Geno	16,0933101	3,60E-16
Glucose	Env	0,09180106	0,15403216
Glucose	GxE	2,12293183	3,75E-05
height	Geno	35211,5739	1,61E-42
height	Env	1549,16667	3,04E-07
height	GxE	1038,54167	0,00876656
pH	Geno	0,53180262	3,90E-06
pH	Env	0,00832775	0,34551452
pH	GxE	0,34683558	*ns*
SSC	Geno	100,780933	4,75E-13
SSC	Env	4,67E-05	0,99259824
SSC	GxE	20,87862	*ns*
vitamin C	Geno	651,71389	0,0001262
vitamin C	Env	1,28027436	0,77898539
vitamin C	GxE	608,99548	*ns*

Supplemental Table 6: Candidate genes under the plasticity QTLs. The genes presented in this table are all the DEG in fruit under the QTLs regions which besides showed significant correlation between the estimated allelic effect of the QTL and the expression level in control, drought or the expression level plasticity (expression in drought – expression in control). The functional annotation of the genes was retrieved from the reference annotation of SL2.50 version.

QTL_name	Candidate genes	Chr	Start2.5	End2.5	r2 (expression in control)	r2 (expression in WD)	r2 (plasticity expression)	Annotation
SSC1.1	Solyc01g067890	1	76868469	76872760	-0,786	0,262	0,667	1-deoxy-D-xylulose 5-phosphate synthase 1
SSC1.1	Solyc01g068030	1	77067061	77069661	-0,810	-0,357	0,714	Cyclase/dehydrase
SSC1.1	Solyc01g068360	1	77571932	77576464	-0,524	0,786	0,690	Receptor like kinase%2C RLK
SSC1.1	Solyc01g068470	1	77706812	77716549	-0,738	-0,143	0,190	CM0216.540.nc protein
SSC1.1	Solyc01g073950	1	81294817	81299295	0,762	0,119	-0,333	Bromodomain protein
SSC1.1	Solyc01g074030	1	81355107	81362077	-0,667	0,810	0,833	Beta-glucosidase 01
SSC1.1	Solyc01g079080	1	78147650	78153323	-0,238	0,833	0,762	Coiled-coil protein
SSC1.1	Solyc01g079820	1	78948285	78952100	-0,738	0,214	0,643	Redoxin domain protein
SSC1.1	Solyc01g080010	1	79139189	79140725	0,810	-0,190	-0,500	Xylanase inhibitor
SSC1.1	Solyc01g080280	1	79528933	79534220	-0,667	0,738	0,786	Glutamine synthetase
SSC1.1	Solyc01g080810	1	80090183	80113075	-0,810	0,190	0,738	Isoleucyl-tRNA synthetase
SSC1.1	Solyc01g081010	1	80319039	80322870	0,667	-0,095	-0,738	Nucleolar GTP-binding protein
SSC1.1	Solyc01g081490	1	80688400	80694078	-0,738	0,595	0,762	RNA polymerase sigma factor
SSC1.1	Solyc01g087040	1	81964948	81965916	-0,214	0,762	0,643	Thylakoid lumenal 19 kDa protein%2C chloroplastic
SSC1.1	Solyc01g087200	1	82128176	82131412	-0,476	-0,762	-0,310	Cc-nbs-lrr%2C resistance protein
SSC1.1	Solyc01g087610	1	82558349	82575296	-0,762	0,000	0,452	Alpha-N-acetylglucosaminidase
SSC1.1	Solyc01g087620	1	82578141	82582009	0,786	0,095	-0,619	Unknown Protein
SSC1.1	Solyc01g087750	1	82671716	82676297	-0,833	0,095	0,762	Homology to unknown gene
SSC1.1	Solyc01g087810	1	82696867	82699405	0,786	0,381	-0,262	Subtilisin-like protease
SSC1.1	Solyc01g087980	1	82828688	82829937	0,429	-0,381	-0,762	Unknown Protein
Firm1.2	Solyc01g102450	1	91256276	91257499	-0,167	-0,738	-0,357	Transmembrane protein 34
Firm1.2	Solyc01g103350	1	91979041	91985730	0,357	-0,143	-0,738	Cell division protein kinase 13
Firm2.1	Solyc02g021270	2	22396831	22398073	0,738	0,571	-0,119	Unknown Protein
SSC4.1	Solyc04g076110	4	61064632	61068969	0,500	-0,119	-0,810	Genomic DNA chromosome 5 TAC clone K2I5
SSC4.1	Solyc04g077140	4	62081239	62083601	0,762	0,310	-0,190	Unknown Protein
SSC4.1	Solyc04g077470	4	62384500	62387723	-0,071	0,238	0,857	Cellulose synthase-like C1-2 glycosyltransferase family 2 protein
SSC4.1	Solyc04g077670	4	62603103	62610325	-0,143	0,762	0,595	Serine carboxypeptidase 1
Firm8.1	Solyc08g068180	8	57296261	57299703	0,190	0,905	0,357	Ribosomal protein L37
Firm8.1	Solyc08g068300	8	57396636	57404421	0,381	0,762	0,429	Coiled-coil domain-containing protein 25

Firm8.1	Solyc08g068320	8	57418440	57426724	0,405	0,833	0,262	Transcription factor myb
Firm8.1	Solyc08g068600	8	57730921	57733032	-0,095	-0,738	-0,524	Decarboxylase family protein
Firm8.1	Solyc08g068680	8	57812621	57814771	0,333	-0,833	-0,667	Decarboxylase family protein
Firm8.1	Solyc08g068690	8	57820371	57821093	-0,476	-0,762	-0,762	N-acetyltransferase
Firm8.1	Solyc08g069010	8	58091099	58104720	0,000	0,762	0,262	Pentatricopeptide repeat-containing protein
FW8.1	Solyc08g075540	8	59711798	59713604	-0,810	0,619	0,881	Alternative oxidase
FW8.1	Solyc08g075840	8	59923376	59927498	0,810	-0,119	-0,762	Single-stranded DNA-binding replication protein A large subunit
FW8.1	Solyc08g075960	8	60037421	60047282	-0,810	0,357	0,476	Mps one binder kinase activator-like 1A
FW8.1	Solyc08g076170	8	60199376	60199624	0,905	-0,238	-0,310	Unknown Protein
FW8.1	Solyc08g076200	8	60216924	60225205	-0,881	-0,095	0,429	ATP dependent RNA helicase
FW8.1	Solyc08g076250	8	60252381	60254194	0,762	0,738	-0,167	Cytochrome P450
FW8.1	Solyc08g076420	8	60428964	60437672	-0,952	0,238	0,714	Poly polymerase catalytic domain containing protein expressed
FW8.1	Solyc08g076650	8	60585195	60590640	0,643	-0,167	-0,833	Alpha alpha-trehalose-phosphate synthase
FW8.1	Solyc08g076810	8	60710899	60723537	0,786	0,190	-0,048	GPI-anchored wall transfer protein 1
FW8.1	Solyc08g077440	8	61326655	61336566	-0,833	0,048	0,738	ATP-dependent protease La
FW8.1	Solyc08g078040	8	61908800	61911939	-0,810	-0,214	0,143	Monooxygenase FAD-binding
FW8.1	Solyc08g078050	8	61911855	61912154	-0,719	-0,286	0,000	CTF2A
FW8.1	Solyc08g078100	8	61950808	61952214	0,762	-0,262	-0,667	Amino acid permease-like protein
FW8.1	Solyc08g078670	8	62449831	62451757	0,810	0,238	-0,310	Aspartyl protease
FW8.1	Solyc08g079260	8	62866686	62872031	-0,738	0,000	0,238	Serine/threonine-protein phosphatase
FW8.1	Solyc08g079280	8	62887252	62889535	0,905	0,119	-0,429	cytochrome P450
FW8.1	Solyc08g079450	8	62967637	62975950	0,238	-0,381	-0,833	Maspardin
FW8.1	Solyc08g083410	8	62913369	62915364	0,405	0,786	-0,238	cytochrome P450
RIP9.1	Solyc09g009030	9	2377785	2382402	-0,786	-0,095	0,619	Histone deacetylase 2a-like
RIP9.1	Solyc09g009510	9	2924885	2929510	0,619	-0,524	-0,810	Hydrolase alpha/beta fold family protein
RIP9.1	Solyc09g010520	9	3897831	3901988	-0,381	0,357	0,905	ADP-ribosylation factor GTPase activating protein 1
RIP9.1	Solyc09g010630	9	3965253	3968837	-0,619	-0,048	0,810	heat shock protein
RIP9.1	Solyc09g010700	9	4021734	4024116	0,810	0,024	-0,238	CM0545.320.nc protein
RIP9.1	Solyc09g010870	9	4200163	4209478	0,762	-0,024	-0,619	Exoribonuclease R/ribonuclease II
RIP9.1	Solyc09g011140	9	4499977	4502723	0,429	-0,095	-0,810	Tropinone reductase I
RIP10.1	Solyc10g005100	10	92148	94188	-0,252	-0,802	-0,575	Salt stress root protein RS1
RIP10.1	Solyc10g006130	10	863907	864572	0,359	-0,371	-0,755	Ethylene responsive transcription factor 3a
RIP10.1	Solyc10g006180	10	887356	891118	0,731	-0,731	-0,826	Unknown Protein
RIP10.1	Solyc10g006190	10	899319	905588	-0,431	-0,743	-0,299	Cell differentiation protein rcd1
RIP10.1	Solyc10g006650	10	1157432	1161954	0,216	-0,335	-0,731	Flavoprotein wrbA
Firm11.1	Solyc11g005700	11	547491	548753	0,119	-0,762	-0,429	U-box domain-containing protein
FW11.1	Solyc11g011910	11	4841188	4847641	0,333	0,881	0,714	Transmembrane 9 superfamily protein member 1
FW11.1	Solyc11g017440	11	8383387	8384626	0,143	-0,786	-0,714	Snakin-2

FW11.1	Solyc11g017470	11	8422146	8423170	-0,619	0,190	0,762	NAC domain protein IPR003441
FW11.1	Solyc11g020040	11	10015582	10019521	-0,500	0,310	0,833	Chaperone DnaK
FW11.1	Solyc11g020610	11	11747788	11752875	-0,238	-0,738	-0,333	Neutral invertase like protein
FW11.1	Solyc11g040050	11	40024447	40028245	-0,738	0,000	0,548	RNA binding protein
FW11.1	Solyc11g040180	11	39214219	39232913	-0,143	0,810	0,619	mRNA-capping enzyme subunit alpha
FW11.1	Solyc11g044510	11	32553978	32555063	-0,524	0,833	0,905	Unknown Protein
FW11.1	Solyc11g062420	11	49461521	49461894	0,881	-0,299	-0,976	Unknown Protein
NFr11.1	Solyc11g065520	11	50941268	50942947	0,738	-0,262	-0,786	Unknown Protein
NFr11.1	Solyc11g065700	11	51233185	51238585	-0,762	0,000	0,310	Nuclear transcription factor Y subunit A-1
NFr11.1	Solyc11g065930	11	51514472	51526784	0,357	-0,833	-0,810	Xanthine dehydrogenase/oxidase
NFr11.1	Solyc11g066380	11	52152003	52154883	0,857	-0,690	-0,833	Auxin-regulated protein
NFr11.1	Solyc11g067080	11	52823676	52828937	-0,381	-0,833	-0,071	Protein kinase like protein
NFr11.1	Solyc11g068540	11	53230361	53236610	-0,786	-0,071	0,524	N-carbamoylputrescine amidase
FW11.3	Solyc11g069570	11	54189529	54193187	0,000	0,881	0,619	Cytokinin riboside 5%26apos%3B-monophosphate phosphoribohydrolase LOG
FW11.3	Solyc11g069600	11	54231913	54237114	0,738	0,786	0,310	Inter-alpha-trypsin inhibitor heavy chain H4
SSC11.2	Solyc11g069800	11	54429028	54430560	0,119	-0,762	-0,405	cytochrome P450
SSC11.2	Solyc11g071270	11	54800949	54808782	0,000	-0,357	-0,762	Class E vacuolar protein-sorting machinery protein HSE1
FW11.3	Solyc11g071620	11	55041360	55048950	0,762	-0,167	-0,405	Aldehyde oxidase
SSC11.2	Solyc11g071620	11	55041360	55048950	-0,524	0,738	0,690	Aldehyde oxidase
FW11.3	Solyc11g071920	11	55240769	55250182	0,762	0,357	-0,381	Serine/threonine-protein phosphatase
SSC12.1	Solyc12g057020	12	63099371	63100778	0,833	0,156	-0,524	Acetyl xylan esterase A
SSC12.1	Solyc12g088400	12	63800346	63800636	0,524	0,810	0,714	Zinc-finger protein
SSC12.1	Solyc12g088430	12	63811082	63811432	0,262	-0,714	-0,762	Unknown Protein

Appendix 5

Supplemental Figures

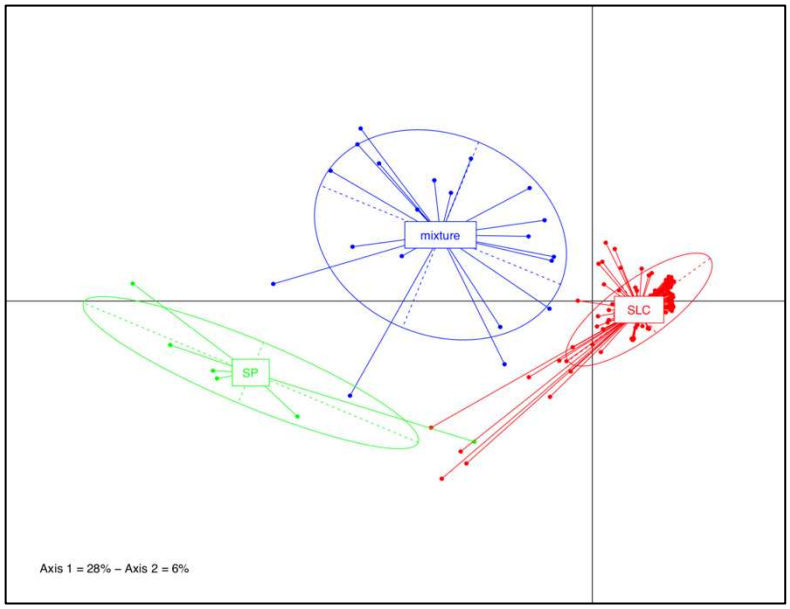

Supplemental Figure 1: Principal Coordinate Analysis (PCoA) in the CC panel, based on the Kinship matrix.

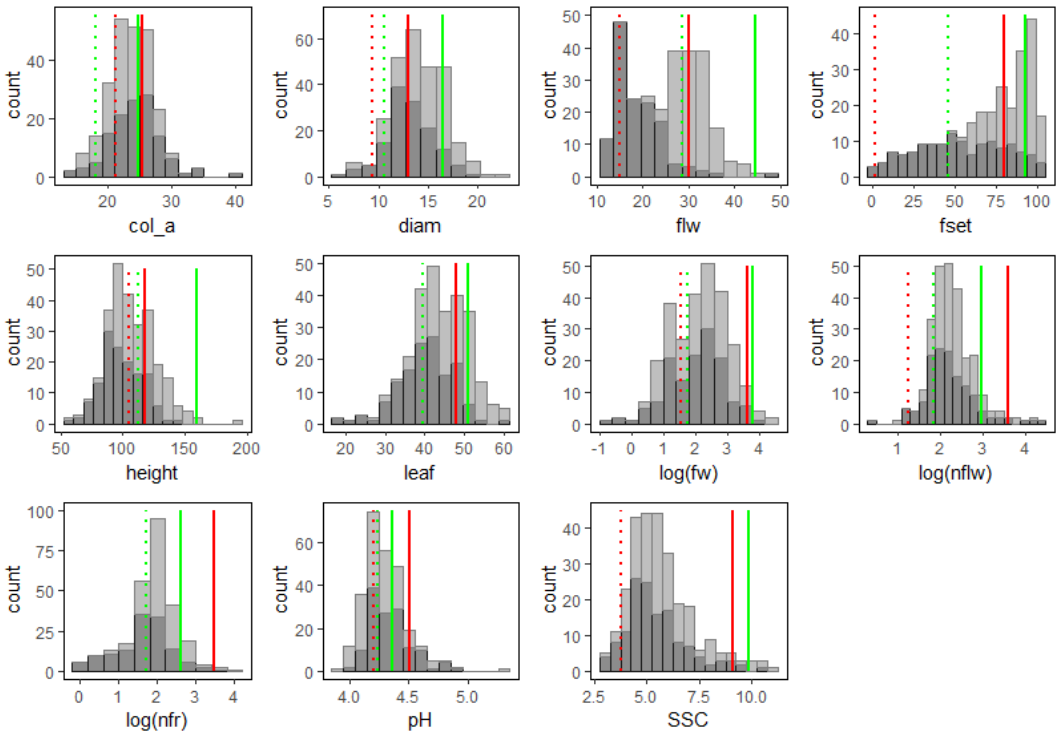

Supplemental Figure 2 A): Distribution for all traits evaluated under optimal (light gray) and HT-stress (dark gray) conditions, in the CC population with the vertical lines representing the upper-range (solid lines) and lower-range (dashed lines) of the MAGIC parental lines distribution under optimal (green) and HT-stress (red) conditions. Only the four small parental lines included in the CC panel were considered.

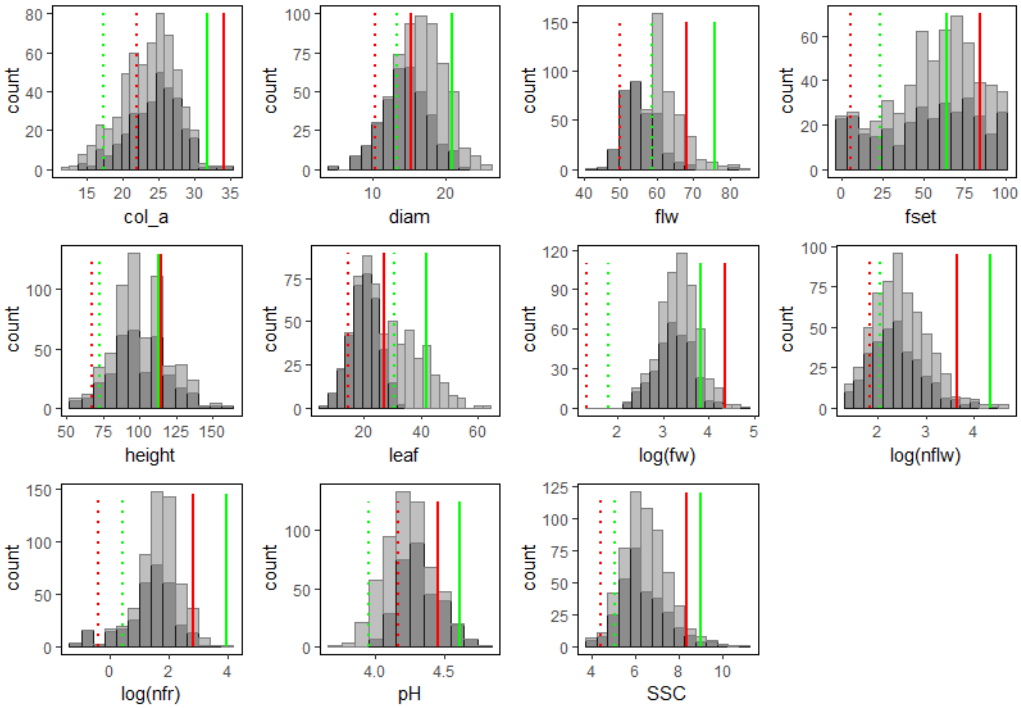

Supplemental Figure 2 B): Distribution for all traits evaluated under optimal (light gray) and HT-stress (dark gray) conditions, in the MAGIC population; the vertical lines are as in the CC panel, but all the eight parental lines were considered.

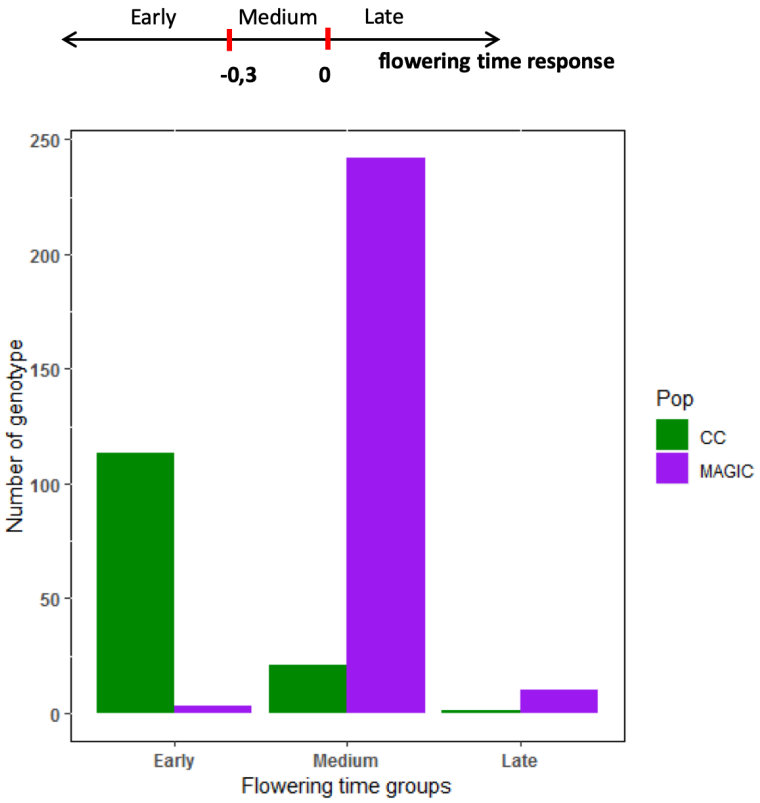

Supplemental Figure 3: Number of genotypes per group across populations. The groups were defined according to genotype's susceptibility to HT-stress regarding the flowering time. The "early" (resp. "medium") group clustered genotypes that flowered in average 18 days (resp. 8 days) earlier in the HT-stress condition. The genotypes that flowered later in the HT-stress condition are in the "late" group.

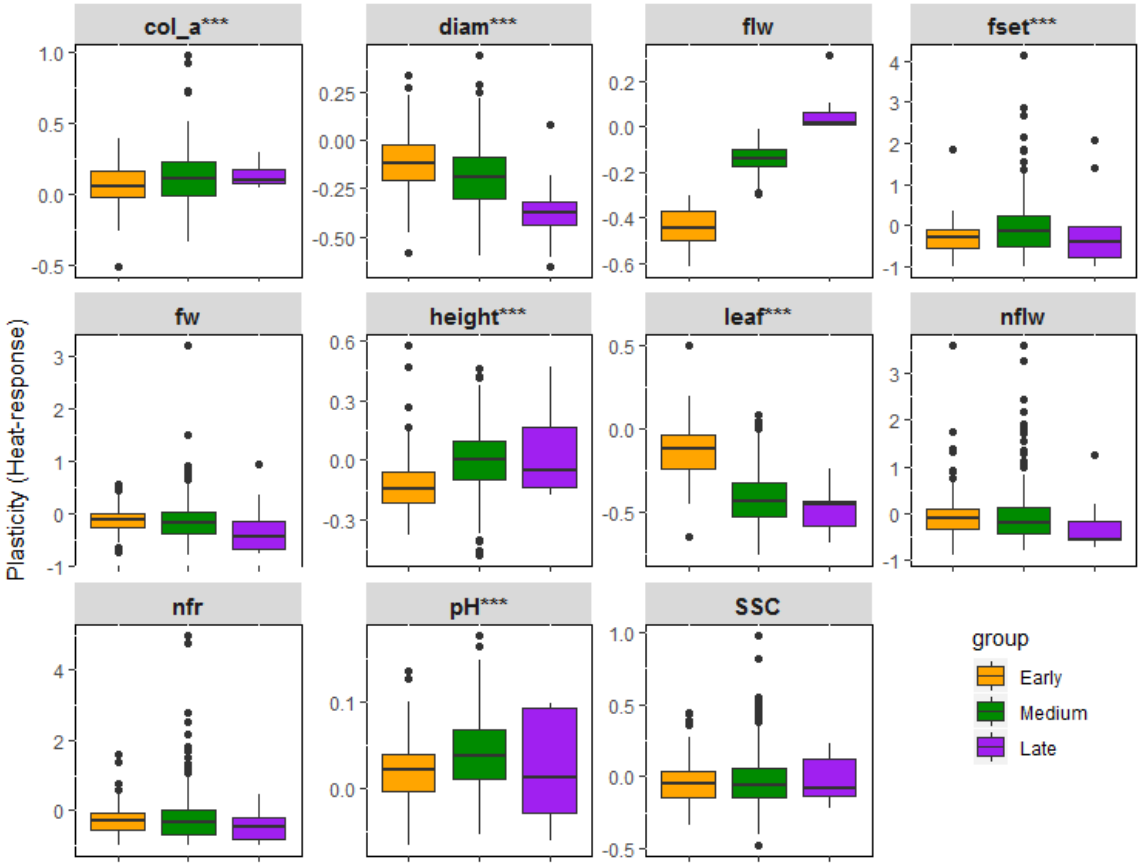

Supplemental Figure 4: Phenotypic plasticity distribution for 404 MAGIC and CC lines regarding the group defined according to flowering time response under HT-stress condition. The stars highlight traits where a significant group effect was detected.

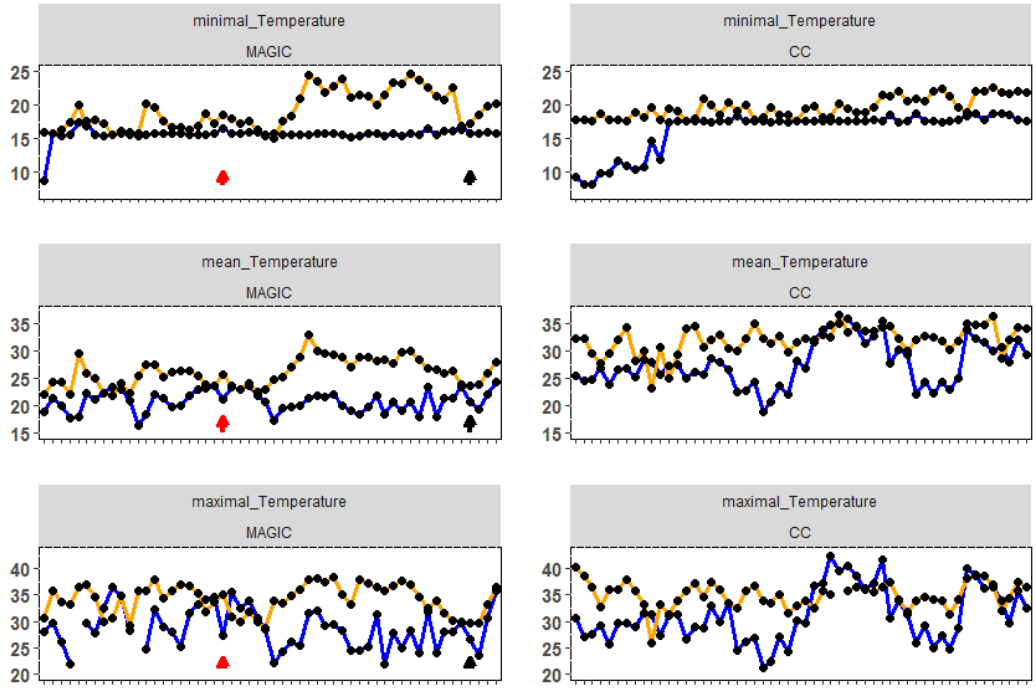

Supplemental Figure 5: Daily temperature fluctuation in the greenhouse for the CC and MAGIC trials. The minimal, mean and maximal temperatures are presented from the plant's transfer into the greenhouse to the end of flowering time. The red and black arrows in the MAGIC figures represent the period covering flowering time of the 5th truss (truss phenotyped for flw) in the MAGIC population.

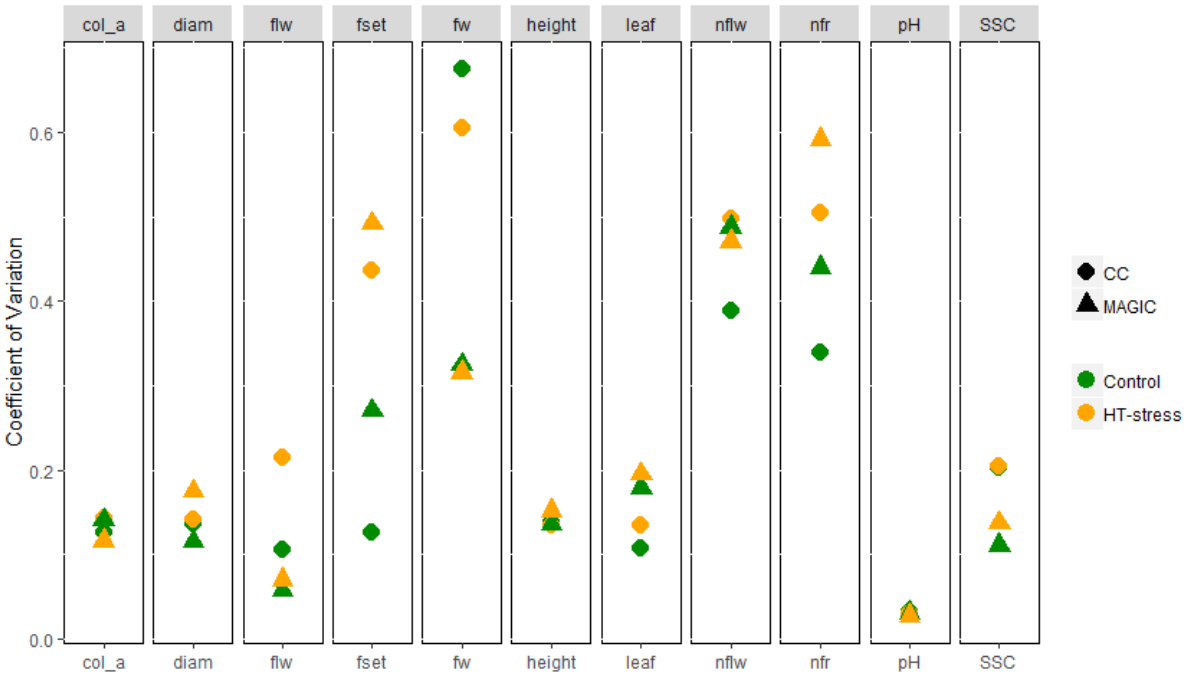

Supplemental Figure 6: Coefficient of variation (CV) for the 11 traits evaluated in both populations. The green and orange dots represent the Control and HT-stress conditions, respectively. The circle indicates CV in the CC population and the triangle, the MAGIC population.

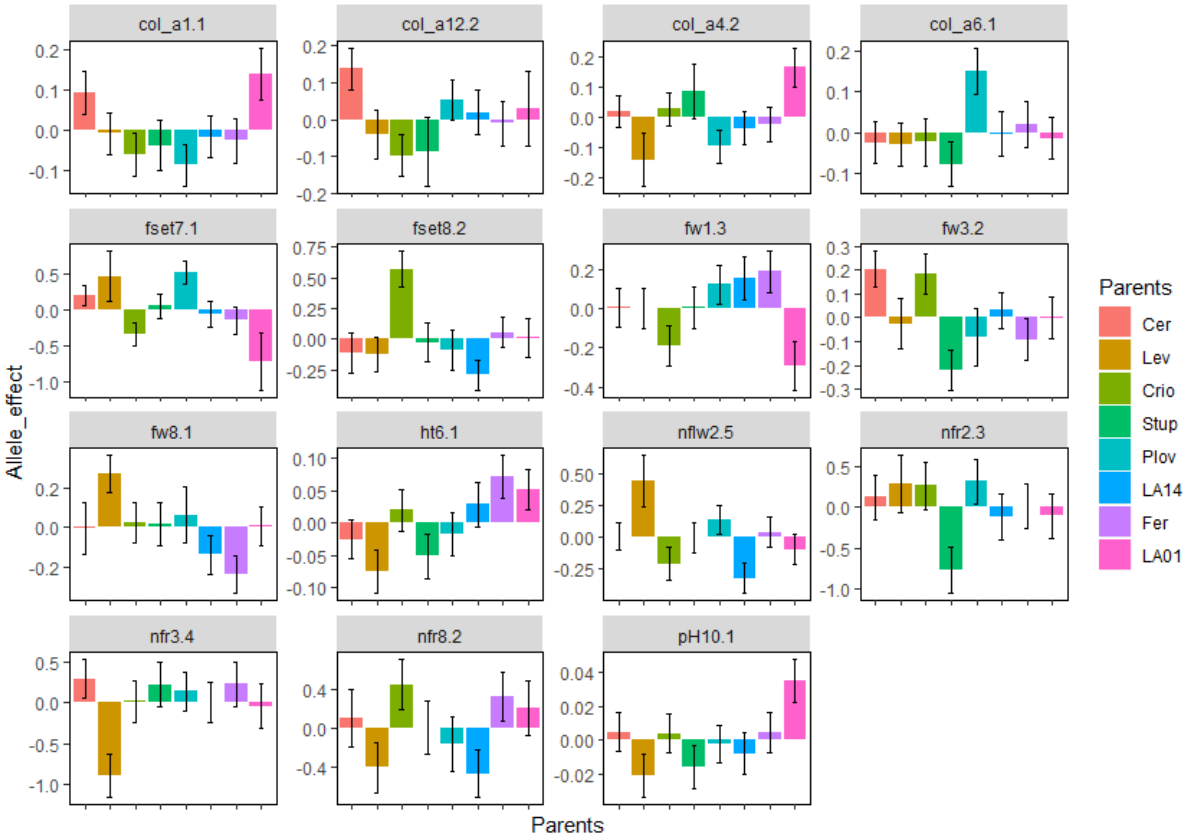

Supplemental Figure 7: Estimated allelic effects for all plasticity QTLs identified in the MAGIC population.

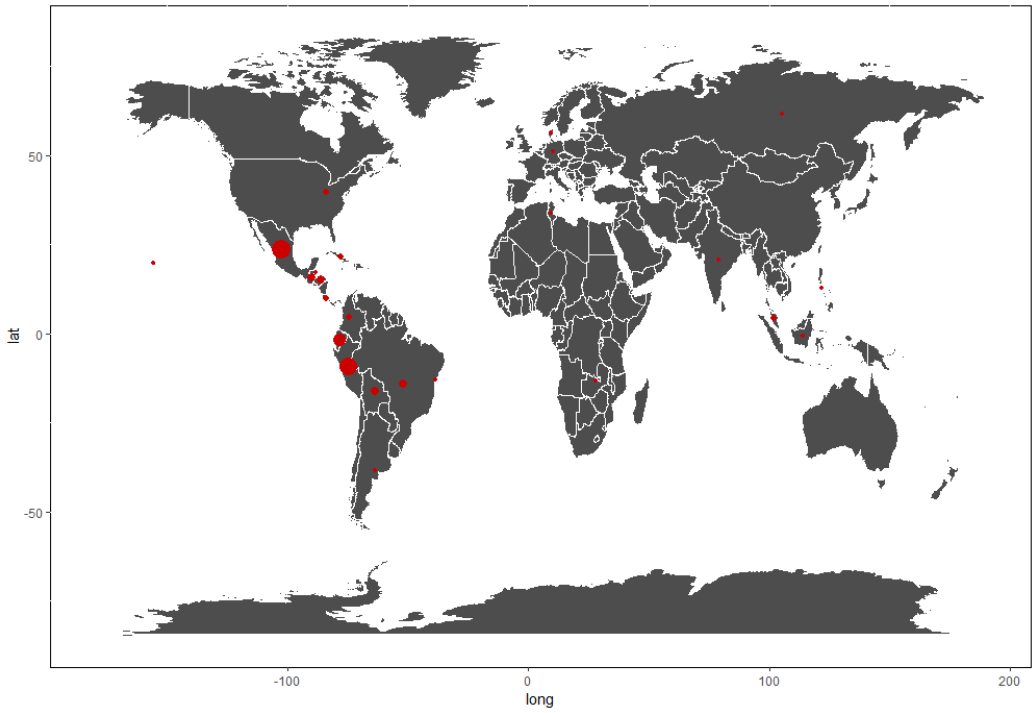

Supplemental Figure 8: Geographical origin of the CC lines. Each circle represents a country where CC lines were originated, and the size of the circle is proportional to the number of genotypes that were selected from a region.

Supplemental Tables

Supplemental Table 2: Pearson's correlation between traits and conditions in the CC (A) and the MAGIC (B) populations, respectively. The upper sides of the table's correspond to trait-correlations in the HT-stress conditions and the lower sides to trait-correlations in the control condition. The column CorrEnv represents the correlation between HT-stress and control conditions for each single trait. The non-significant correlations were notified by empty cells. When significant at a threshold of 0.05, the coefficient correlations were indicated.

A) CC

Traits	leaf	diam	height	flw	nflw	nfr	fset	fw	col_a	SSC	pH	CorrEnv
leaf	**leaf**	0.286		-0.417			0.218		-0.184			0.343
diam	0.36	**diam**			-0.192	-0.195		0.297		-0.207		0.471
height			**height**	0.3						-0.195		0.524
flw	-0.227		0.674	**flw**		-0.324	-0.607			-0.246		0.7
nflw		-0.27		-0.207	**nflw**	0.641						0.57
nfr		-0.228		-0.201	0.95	**nfr**	0.402	-0.256		0.389	0.186	0.475
fset					-0.293		**fset**			0.492	0.237	0.321
fw		0.268		0.213		-0.2255	-0.227	**fw**		-0.352	-0.364	0.861
col_a			-0.181	-0.207					**col_a**			0.786
SSC		-0.225		-0.23	0.282	0.338		-0.504		**SSC**	0.49	0.826
pH						0.204		-0.24	-0.196	0.529	**pH**	0.706

B) MAGIC

Traits	diam	height	leaf	pH	SSC	fw	col	nflw	nfr	fset	flw	CorrEnv
diam	**diam**	-0.127	0.145						0.138	0.158	-0.341	0.435
height		**height**	-0.18		0.136		0.128	0.108			0.287	0.602
leaf	0.133		**leaf**				0.12		0.116	0.179	-0.115	0.505
pH				**pH**	0.205	-0.119						0.385
SSC		0.154			**SSC**	-0.286	0.148					0.291
fw					-0.227	**fw**			-0.136			0.331
col	0.12	0.164		-0.147			**col**		-0.136			0.54
nflw	-0.151					-0.158		**nflw**	0.438	-0.224		0.352
nfr						-0.231	-0.19	0.604	**nfr**	0.495	-0.292	0.4
fset	0.226	0.148						-0.364	0.26	**fset**	-0.377	0.187
flw		0.358		-0.134	0.147		0.282				**flw**	0.536

Supplemental Table 3: Heat tolerant genotypes regarding yield component traits in the MAGIC and the CC populations. For each genotype, the plasticity value (heat-response) of the other traits is presented. The flowering group (early, medium or late) of the genotypes is highlighted and for the CC lines, the genetic group and the country of origin are specified.

Genotype	col_a	diam	flw	fset	fw	height	leaf	nflw	nfr	pH	SSC	Pop	group	SeedBank	Country	Genetic_group
H10_136	0.02	-0.03	-0.10	0.33	0.09	-0.07	-0.36	0.61	1.75	0.04	0.21	MAGIC	Medium	NA	NA	mixture
H10_148	0.11	-0.10	-0.17	1.80	0.44	0.05	-0.32	-0.57	0.17	0.01	-0.09	MAGIC	Medium	NA	NA	mixture
H10_185	0.15	0.13	-0.10	1.04	0.41	0.10	-0.58	0.14	1.09	0.01	0.14	MAGIC	Medium	NA	NA	mixture
H10_207	-0.18	-0.45	-0.01	0.47	0.66	-0.06	-0.27	-0.14	0.18	-0.02	-0.47	MAGIC	Medium	NA	NA	mixture
H10_225	-0.02	-0.39	-0.14	0.41	0.15	-0.13	-0.35	-0.19	0.09	0.06	-0.12	MAGIC	Medium	NA	NA	mixture
H10_256	0.00	-0.29	-0.13	0.45	0.03	0.18	-0.47	-0.13	0.33	-0.03	-0.22	MAGIC	Medium	NA	NA	mixture
H10_52	0.39	-0.28	-0.22	-0.04	0.09	0.21	-0.45	-0.25	0.00	0.18	0.09	MAGIC	Medium	NA	NA	mixture
H10_53	-0.12	-0.33	-0.14	4.13	3.20	-0.14	-0.56	-0.78	0.00	0.11	-0.22	MAGIC	Medium	NA	NA	mixture
H10_77	-0.02	-0.13	-0.18	2.13	0.25	0.10	-0.36	0.44	4.75	0.01	-0.17	MAGIC	Medium	NA	NA	mixture
LA1456	0.40	NA	NA	-0.50	1.37	-0.13	-0.20	0.80	0.33	0.05	-0.42	CC	Undefined	TGRC	Mexico	SP
LA1464	-0.02	-0.25	-0.52	-0.24	0.14	-0.23	-0.14	0.00	0.00	-0.01	-0.26	CC	Early	TGRC	Honduras	SLC
LA1482	-0.08	-0.23	-0.55	-0.17	0.11	-0.12	0.00	0.56	0.60	0.03	0.03	CC	Early	TGRC	Malaysia	SLC
LA2670	-0.03	-0.31	-0.48	-0.39	0.07	-0.12	-0.26	1.40	0.75	0.02	0.05	CC	Early	TGRC	Peru	SLC
Mex-104	0.27	0.19	-0.46	0.07	0.00	-0.12	-0.05	0.00	0.08	-0.07	-0.10	CC	Early	MALAGA	Mexico	SLC
Mex-85	0.03	0.08	-0.45	-0.01	0.07	-0.05	-0.15	0.08	0.10	-0.01	0.01	CC	Early	MALAGA	Mexico	SLC
MT_148	0.01	-0.32	-0.20	1.84	0.21	-0.11	-0.30	0.17	1.80	-0.04	-0.06	MAGIC	Medium	NA	NA	mixture
MT_149	0.03	-0.27	-0.16	-0.21	0.45	-0.12	-0.47	0.24	0.01	0.02	0.09	MAGIC	Medium	NA	NA	mixture
MT_166	0.12	0.09	-0.14	0.54	0.71	0.25	-0.48	0.07	0.75	0.10	-0.14	MAGIC	Medium	NA	NA	mixture
MT_177	0.08	-0.38	0.05	-0.14	0.34	0.16	-0.44	0.20	0.44	0.09	-0.18	MAGIC	Late	NA	NA	mixture
MT_234	0.24	-0.04	-0.20	0.11	0.85	-0.32	-0.24	0.36	0.45	0.07	0.08	MAGIC	Medium	NA	NA	mixture
MT_277	0.02	-0.34	-0.10	0.44	0.13	0.46	-0.50	-0.23	0.17	0.16	0.09	MAGIC	Medium	NA	NA	mixture
MT_41	0.47	0.05	-0.13	-0.25	0.41	0.00	-0.61	3.59	2.53	-0.02	-0.20	MAGIC	Medium	NA	NA	mixture
MT_84	0.10	0.00	-0.07	-0.68	0.23	-0.07	NA	1.74	0.00	-0.03	0.00	MAGIC	Medium	NA	NA	mixture
Piguti	0.22	-0.10	-0.52	-0.23	0.17	-0.20	-0.09	0.06	0.07	-0.01	-0.14	CC	Early	INRA UR1075	NA	SLC

Supplemental Table 4: List of the QTLs detected in the CC and MAGIC population, under control and HT-stress conditions. For each trait, the detected QTLs are specified in the column 'QTL_name'. The chromosome and the physical position of the QTLs are presented in columns 'Chromosome' and 'Position (Mbp)'. For each QTL, the interval region is presented in mega-base-pair, with the upper interval 'Left_bound (Mbp)' and the lower interval 'Right_bound (Mbp)'. The 'LOD_score' of the QTLs are indicated as well as the 'Marker' name at the pic position of the QTL. LOD scores were calculated as -log10 (P-value). The column 'Condition' indicates if the QTL was detected in control or HT-stress condition, or with the plasticity (PP) phenotype. The population and trait for which the QTL was found are indicated. For each significant QTL/association, the corresponding P-value is reported.

QTL_name	Chromosome	Position(Mb)	Left_bound(Mb)	Right_bound(Mb)	LOD_score	Marker	Trait	Condition	Panel
ppcol_a1.1	1	2.446381	1.253219	3.704725	4.66	X01_2446381	col_a	PP	MAGIC
col_a2.1	2	36.853283	36.076859	37.733992	5.42	S02_36853283	col_a	Control	CC
col_a2.2	2	40.332255	40.289804	40.915583	5.93	S02_40332255	col_a	HT-stress	CC
col_a3.1	3	53.298712	5.936744	54.662217	4.89	X03_48065704	col_a	Control	MAGIC
col_a3.1	3	53.670389	53.650069	53.670496	4.40	S03_53670389	col_a	HT-stress	CC
col_a3.2	3	64.701243	63.21107	65.387833	5.34	X03_58654154	col_a	Control	MAGIC
col_a4.1	4	53.86254	52.381185	58.89901	6.80	X04_53010310	col_a	HT-stress	MAGIC
col_a4.2	4	59.84641	59.334003	60.163622	8.36	X04_57439780	col_a	Control	MAGIC
ppcol_a4.2	4	61.830034	59.990653	63.900601	4.63	X04_59423404	col_a	PP	MAGIC
ppcol_a6.1	6	36.880315	34.368124	38.363876	4.48	X06_32606690	col_a	PP	MAGIC
col_a7.1	7	4.481678	0.020971	55.770848	4.44	X07_5213521	col_a	Control	MAGIC
col_a7.1	7	4.925959	4.115593	6.385399	3.01	S07_04925959	col_a	Control	CC
col_a7.2	7	65.692641	65.041543	65.926032	4.03	S07_65692641	col_a	HT-stress	CC
col_a8.1	8	3.613518	2.645233	34.267974	3.07	S08_03613518	col_a	HT-stress	CC
col_a8.2	8	60.397157	59.101552	61.873039	4.60	X08_57644162	col_a	HT-stress	MAGIC
col_a9.1	9	4.316025	2.926053	4.732408	5.86	X09_4316025	col_a	Control	MAGIC
ppcol_a11.1	11	2.068777	1.152677	2.850057	3.68	S11_02068777	col_a	PP	CC
col_a11.2	11	4.478344	4.151798	5.476941	5.75	X11_4478344	col_a	HT-stress	MAGIC
col_a12.1	12	3.722833	2.821857	5.047381	5.05	X12_3722833	col_a	HT-stress	MAGIC
ppcol_a12.2	12	64.941176	64.125346	65.419995	4.73	X12_63282226	col_a	PP	MAGIC
col_a12.2	12	66.385245	64.125346	66.824887	4.70	X12_64734762	col_a	Control	MAGIC
diam1.1	1	75.879505	75.093616	76.687312	4.54	S01_75879505	diam	Control	CC
diam1.2	1	96.218696	96.217112	96.277795	3.59	S01_96218696	diam	HT-stress	CC
diam3.1	3	53.105002	52.536734	53.82511	4.46	S03_53105002	diam	HT-stress	CC
diam3.2	3	64.899693	64.450921	65.312829	8.55	X03_58952743	diam	HT-stress	MAGIC
ppdiam4.1	4	54.067864	52.291246	55.127267	3.88	S04_54067864	diam	PP	CC
diam4.2	4	65.236362	63.82458	65.778385	6.12	X04_62829732	diam	HT-stress	MAGIC

diam4.2	4	66.063525	65.611502	66.446769	6.47	S04_66063525	diam	HT-stress	CC
diam5.1	5	8.403486	5.638011	60.985149	5.00	X05_8403486	diam	Control	MAGIC
diam7.1	7	60.093644	59.849207	60.884595	3.82	S07_60093644	diam	Control	CC
diam9.1	9	2.445969	2.411368	2.446934	3.13	S09_02445969	diam	Control	CC
diam9.2	9	4.550994	4.289476	63.711556	4.58	X09_4550994	diam	HT-stress	MAGIC
diam10.1	10	54.449604	54.294074	54.449899	3.43	S10_54449604	diam	Control	CC
diam11.1	11	5.023403	4.342018	41.466599	5.37	X11_5023403	diam	Control	MAGIC
diam11.2	11	54.931292	54.076798	55.686487	3.64	S11_54931292	diam	HT-stress	CC
diam12.1	12	3.246101	2.109522	3.722833	4.68	X12_3246101	diam	HT-stress	MAGIC
diam12.2	12	37.115899	37.08155	37.253156	4.07	S12_37115899	diam	Control	CC
flw1.1	1	2.461631	2.371872	2.463253	4.32	S01_02461631	flw	Control	CC
flw1.5	1	4.96157	4.340507	82.578583	8.23	X01_4961570	flw	Control	MAGIC
flw1.2	1	5.087451	4.597945	5.726521	3.59	S01_05087451	flw	HT-stress	CC
flw1.3	1	6.843787	6.229659	7.576706	5.09	S01_06843787	flw	Control	CC
flw1.4	1	69.368609	69.260744	69.594028	4.98	S01_69368609	flw	Control	CC
flw1.5	1	77.65613	75.855371	82.578583	7.51	X01_70046630	flw	HT-stress	MAGIC
flw1.6	1	93.702068	93.123997	93.899137	3.52	S01_93702068	flw	HT-stress	CC
flw2.1	2	36.741888	36.696643	36.790187	4.57	S02_36741888	flw	HT-stress	CC
ppflw2.2	2	37.702336	36.853283	38.543388	4.09	S02_37702336	flw	PP	CC
flw2.3	2	48.095271	47.122672	49.257681	3.66	S02_48095271	flw	HT-stress	CC
flw2.4	2	53.624203	52.855746	54.014597	5.61	X02_47897284	flw	HT-stress	MAGIC
ppflw3.1	3	2.735111	1.877032	2.913577	6.43	S03_02735111	flw	PP	CC
ppflw3.2	3	4.277648	3.805614	5.431516	3.18	S03_04277648	flw	PP	CC
flw3.3	3	64.793561	63.93268	65.312829	5.32	X03_58846611	flw	Control	MAGIC
flw3.3	3	64.793561	64.450921	65.312829	9.44	X03_58846611	flw	HT-stress	MAGIC
flw3.3	3	66.062007	65.165483	66.277952	14.15	S03_66062007	flw	HT-stress	CC
ppflw3.3	3	66.062007	65.165483	66.277952	3.57	S03_66062007	flw	PP	CC
flw4.1	4	55.462759	53.669515	58.245959	3.68	S04_55462759	flw	Control	CC
flw5.1	5	2.246416	1.337513	3.386465	9.67	S05_02246416	flw	HT-stress	CC
flw5.2	5	8.354789	8.156622	8.400766	3.58	S05_08354789	flw	Control	CC
ppflw5.3	5	62.636863	62.34382	62.699296	7.84	S05_62636863	flw	PP	CC
ppflw5.4	5	63.309656	62.957456	63.954891	4.97	S05_63309656	flw	PP	CC
ppflw6.1	6	1.240331	1.240271	1.240605	8.08	S06_01240331	flw	PP	CC
flw6.2	6	38.363876	34.368124	39.859867	4.95	X06_35263157	flw	Control	MAGIC
flw7.1	7	63.768352	60.02716	64.92064	4.68	X07_61296293	flw	HT-stress	MAGIC
ppflw8.1	8	0.393921	0.362038	0.417491	6.41	S08_00393921	flw	PP	CC
flw8.2	8	4.744584	4.103562	34.267974	8.09	S08_04744584	flw	HT-stress	CC

ppflw8.3	8	53.749644	53.08483	54.694932	3.59	S08_53749644	flw	PP	CC
flw8.4	8	62.964944	62.865804	63.270879	5.97	S08_62964944	flw	Control	CC
flw8.5	8	65.140992	65.055799	65.158843	3.65	S08_65140992	flw	Control	CC
flw9.1	9	2.314204	2.279826	2.557959	4.93	S09_02314204	flw	HT-stress	CC
ppflw9.2	9	17.882178	17.564933	18.302492	5.18	S09_17882178	flw	PP	CC
flw9.3	9	68.297506	67.694814	68.807596	6.62	X09_63545979	flw	Control	MAGIC
flw9.4	9	69.805632	69.805632	69.822374	6.03	S09_69805632	flw	Control	CC
flw9.4	9	69.805632	69.767245	69.822374	6.41	S09_69805632	flw	HT-stress	CC
ppflw10.1	10	56.027008	55.950776	56.778945	4.24	S10_56027008	flw	PP	CC
flw11.1	11	3.393788	3.158623	3.457164	6.39	S11_03393788	flw	Control	CC
flw11.2	11	6.627532	6.622017	7.104482	4.87	S11_06627532	flw	Control	CC
ppflw11.3	11	48.733611	47.291349	50.328082	5.08	S11_48733611	flw	PP	CC
ppflw11.4	11	52.448642	51.489767	53.375561	3.19	S11_52448642	flw	PP	CC
flw11.5	11	54.684047	53.823685	56.105593	4.63	X11_52087433	flw	Control	MAGIC
flw11.5	11	56.227124	55.330359	56.151029	6.34	S11_56227124	flw	HT-stress	CC
flw12.1	12	0.608247	0.60074	0.714884	3.50	S12_00608247	flw	HT-stress	CC
flw12.2	12	1.701268	1.374935	2.870235	4.00	S12_01701268	flw	HT-stress	CC
flw12.2	12	2.494987	1.461833	3.475605	4.41	S12_02494987	flw	Control	CC
fset1.1	1	77.436487	4.158194	82.578583	4.60	X01_69374178	fset	Control	MAGIC
fset1.2	1	94.540622	91.047287	96.379226	4.78	X01_86301422	fset	Control	MAGIC
fset2.1	2	50.666161	48.471214	51.775968	5.32	X02_45368716	fset	Control	MAGIC
fset2.2	2	54.663481	54.024321	54.758149	3.28	S02_54663481	fset	Control	CC
fset3.1	3	63.93268	63.21107	66.339796	5.95	X03_57985730	fset	HT-stress	MAGIC
fset3.1	3	64.689793	63.674517	65.566055	3.69	S03_64689793	fset	HT-stress	CC
ppfset3.2	3	67.512964	66.978561	68.413314	7.06	S03_67512964	fset	PP	CC
ppfset4.1	4	2.936538	2.915842	2.97985	5.07	S04_02936538	fset	PP	CC
fset4.2	4	26.12367	26.123473	27.392008	4.87	S04_26123670	fset	HT-stress	CC
fset4.3	4	62.8371	61.281208	63.82458	5.54	X04_60805933	fset	HT-stress	MAGIC
fset4.4	4	65.853888	65.828262	66.446769	6.20	S04_65853888	fset	Control	CC
ppfset6.1	6	1.453632	0.488346	1.807844	6.55	S06_01453632	fset	PP	CC
fset6.2	6	32.798578	2.400995	36.11689	4.58	X06_30638016	fset	Control	MAGIC
ppfset6.3	6	48.24401	48.167692	48.740122	4.05	S06_48244010	fset	PP	CC
ppfset7.1	7	0.136225	0.051543	1.852616	4.85	X07_136225	fset	PP	MAGIC
fset7.2	7	66.986639	66.431183	67.729281	6.66	S07_66986639	fset	Control	CC
fset8.1	8	0.849696	0.029999	0.98595	3.22	S08_00849696	fset	HT-stress	CC
ppfset8.2	8	59.460898	21.047529	59.925589	5.11	X08_56626898	fset	PP	MAGIC
fset9.1	9	64.781171	8.333659	66.029792	5.36	X09_59808022	fset	HT-stress	MAGIC

fset10.1	10	0.354213	0.0221	1.323966	4.98	X10_354213	fset	HT-stress	MAGIC
fset11.1	11	0.496383	0.436089	0.719356	3.16	S11_00496383	fset	Control	CC
ppfset11.2	11	7.254423	6.544596	8.14031	3.57	S11_07254423	fset	PP	CC
fset11.3	11	55.10036	54.599648	56.105593	7.61	X11_52183860	fset	Control	MAGIC
fset12.1	12	0.621594	0.60074	0.714884	3.10	S12_00621594	fset	HT-stress	CC
fset12.2	12	39.287937	39.24928	39.418026	3.84	S12_39287937	fset	HT-stress	CC
fw1.1	1	91.314498	91.212721	93.092756	4.85	X01_83540760	fw	Control	MAGIC
ppfw1.1	1	92.266398	91.77996	93.992823	4.82	X01_84027198	fw	PP	MAGIC
fw2.1	2	37.817429	37.184874	37.817539	7.02	S02_37817429	fw	Control	CC
lc2	2	47.822111	44.228646	51.966463	7.24	X02_42399961	fw	HT-stress	MAGIC
lc2	2	48.471214	47.822111	48.89947	7.62	X02_43049064	fw	Control	MAGIC
fw2.2	2	51.966463	51.182657	54.014597	11.18	X02_47139889	fw	Control	MAGIC
fw2.3	2	54.663481	54.024321	54.758149	4.11	S02_54663481	fw	HT-stress	CC
fw3.1	3	54.485146	54.449864	54.903836	3.45	S03_54485146	fw	Control	CC
fw3.2	3	65.121559	63.93268	67.141095	5.62	X03_59209883	fw	Control	MAGIC
ppfw3.2	3	66.768294	64.701243	67.141095	4.45	X03_60821344	fw	PP	MAGIC
fw4.1	4	0.928038	0.005106	2.926444	6.52	X04_928038	fw	HT-stress	MAGIC
ppfw4.2	4	65.703025	65.518119	66.290484	7.17	S04_65703025	fw	PP	CC
fw5.1	5	4.527122	4.01884	4.96699	4.90	X05_4829681	fw	Control	MAGIC
fw5.2	5	7.251936	5.638011	60.985149	5.98	X05_7143867	fw	HT-stress	MAGIC
ppfw6.1	6	1.006581	0.056871	1.999894	3.72	S06_01006581	fw	PP	CC
ppfw6.2	6	38.323491	38.006394	39.276193	8.04	S06_38323491	fw	PP	CC
ppfw6.3	6	48.545669	48.343798	48.940051	4.55	S06_48545669	fw	PP	CC
fw7.1	7	6.05398	4.478922	6.385399	4.18	S07_06053980	fw	HT-stress	CC
fw7.2	7	57.37349	57.31849	57.465601	3.89	S07_57373490	fw	Control	CC
fw7.3	7	63.768352	60.02716	64.92064	7.60	X07_61091852	fw	HT-stress	MAGIC
ppfw8.1	8	2.095997	0.062757	2.769368	5.05	X08_645215	fw	PP	MAGIC
fw8.2	8	60.195041	60.170203	60.405484	5.13	S08_60195041	fw	HT-stress	CC
fw9.1	9	2.445969	2.411368	2.446934	4.28	S09_02445969	fw	Control	CC
fw9.1	9	2.445969	2.411368	2.446934	5.10	S09_02445969	fw	HT-stress	CC
fw9.2	9	30.503025	30.502912	31.891757	4.87	S09_30503025	fw	HT-stress	CC
fw9.2	9	56.141247	4.289476	66.172567	5.17	X09_51738766	fw	HT-stress	MAGIC
fw11.1	11	4.342018	3.18835	55.21479	4.48	X11_4342018	fw	Control	MAGIC
fw11.1	11	53.206534	52.915345	53.823685	11.04	X11_50290034	fw	HT-stress	MAGIC
fw12.1	12	1.244394	0.493722	63.690753	4.57	X12_1244394	fw	HT-stress	MAGIC
ppfw12.1	12	15.121088	14.640634	15.670729	3.25	S12_15121088	fw	PP	CC
fw12.2	12	64.046622	61.864756	65.148027	4.75	X12_62487572	fw	Control	MAGIC

ht1.1	1	4.96157	4.158194	76.983678	6.15	X01_4614252	height	HT-stress	MAGIC
ht1.1	1	75.855371	3.117977	76.186755	4.80	X01_65297730	height	Control	MAGIC
ppht1.2	1	82.521565	82.448405	82.528806	4.78	S01_82521565	height	PP	CC
ht1.3	1	88.232834	86.437181	88.891242	7.45	X01_79993634	height	HT-stress	MAGIC
ht1.3	1	88.688358	87.871613	89.607229	5.41	X01_80449158	height	Control	MAGIC
ppht2.1	2	34.220988	30.577483	35.214875	10.52	S02_34220988	height	PP	CC
ht2.2	2	36.696643	36.076859	37.733992	3.05	S02_36696643	height	HT-stress	CC
ht2.3	2	41.120028	40.334709	42.323124	6.13	S02_41120028	height	Control	CC
ht2.1	2	44.1631	33.973517	44.547467	4.62	X02_38740950	height	HT-stress	MAGIC
ht2.4	2	51.182657	50.236462	51.775968	5.84	X02_45760507	height	HT-stress	MAGIC
ht3.1	3	2.071126	0.575656	2.360361	4.76	X03_2163723	height	Control	MAGIC
ppht3.2	3	56.592085	55.547354	59.338993	3.07	S03_56592085	height	PP	CC
ht3.3	3	64.655137	64.450921	65.048732	6.66	X03_58708187	height	Control	MAGIC
ht3.3	3	64.793561	63.910162	65.387833	4.99	X03_58846611	height	HT-stress	MAGIC
ht4.1	4	55.472455	53.669515	58.218186	4.50	S04_55472455	height	Control	CC
ht4.2	4	63.900601	2.865239	65.778385	4.57	X04_61493971	height	HT-stress	MAGIC
ht4.2	4	65.396498	64.536101	66.324715	3.92	S04_65396498	height	Control	CC
ppht5.1	5	3.877262	3.580143	4.164928	4.72	S05_03877262	height	PP	CC
ht6.1	6	31.089509	1.454568	45.401935	4.68	X06_28844482	height	HT-stress	MAGIC
ppht6.1	6	32.354682	19.382154	36.11689	5.22	X06_28844482	height	PP	MAGIC
ht6.2	6	45.218536	44.762672	45.401935	4.98	X06_41608436	height	Control	MAGIC
ht9.1	9	1.38199	1.221555	1.38199	5.99	S09_01381990	height	HT-stress	CC
ht9.2	9	2.498892	2.314204	2.557959	3.20	S09_02498892	height	Control	CC
ht9.3	9	4.645709	4.561644	4.666246	4.83	S09_04645709	height	Control	CC
ht11.1	11	50.280765	49.226488	51.334347	3.39	S11_50280765	height	HT-stress	CC
ht11.2	11	55.489444	55.003933	56.105593	4.90	X11_52298290	height	Control	MAGIC
ht12.1	12	0.440913	0.010859	0.972302	4.48	X12_440913	height	HT-stress	MAGIC
ht12.2	12	4.162345	3.240286	5.158348	4.08	S12_04162345	height	HT-stress	CC
leaf1.1	1	83.434428	77.65613	84.468518	7.77	X01_75195228	leaf	HT-stress	MAGIC
ppleaf2.1	2	20.334143	20.334143	20.375312	5.78	S02_20334143	leaf	PP	CC
leaf2.2	2	36.741888	36.696643	36.790187	6.36	S02_36741888	leaf	Control	CC
ppleaf2.3	2	37.733992	36.853283	38.543388	4.87	S02_37733992	leaf	PP	CC
leaf3.1	3	63.910162	43.631616	64.521327	7.45	X03_57963212	leaf	Control	MAGIC
ppleaf4.1	4	59.199728	59.104097	60.179408	3.79	S04_59199728	leaf	PP	CC
leaf4.2	4	61.146494	60.952746	63.900601	4.44	X04_58739864	leaf	HT-stress	MAGIC
leaf5.1	5	7.143867	0.990309	60.985149	4.80	X05_7251936	leaf	Control	MAGIC
leaf6.1	6	45.401935	45.218536	46.657691	12.92	X06_42278140	leaf	Control	MAGIC

leaf6.1	6	46.170878	45.218536	46.657691	20.77	X06_41791835	leaf	HT-stress	MAGIC
leaf7.1	7	57.777838	4.089402	61.06426	4.65	X07_54651566	leaf	Control	MAGIC
leaf7.2	7	67.237086	66.333377	67.582423	4.76	S07_67237086	leaf	Control	CC
leaf8.1	8	54.324737	4.252804	57.585344	6.65	X08_46285705	leaf	HT-stress	MAGIC
leaf9.1	9	2.09513	1.631719	2.214099	4.76	X09_1759444	leaf	HT-stress	MAGIC
leaf9.2	9	9.225943	9.225943	10.504685	8.87	S09_09225943	leaf	Control	CC
ppleaf10.1	10	60.664352	60.586463	60.966693	3.35	S10_60664352	leaf	PP	CC
leaf10.2	10	63.48653	62.687551	64.603497	3.35	S10_63486530	leaf	Control	CC
leaf11.1	11	54.921323	53.960745	55.766399	3.88	S11_54921323	leaf	HT-stress	CC
leaf12.1	12	63.784031	63.772969	63.854913	4.72	S12_63784031	leaf	Control	CC
leaf12.1	12	63.784031	63.772969	63.854913	4.52	S12_63784031	leaf	HT-stress	CC
ppnflw2.1	2	33.742091	30.577483	34.220988	4.80	S02_33742091	nflw	PP	CC
nflw2.2	2	40.332187	40.289804	40.915583	4.99	S02_40332187	nflw	HT-stress	CC
nflw2.3	2	44.228646	39.456131	50.309536	4.56	X02_38806496	nflw	HT-stress	MAGIC
nflw2.3	2	45.515428	44.705571	45.518495	4.20	S02_45515428	nflw	HT-stress	CC
ppnflw2.3	2	50.58521	50.236462	51.775968	4.77	X02_45163060	nflw	PP	MAGIC
nflw3.1	3	4.407686	4.011014	4.427906	4.85	S03_04407686	nflw	Control	CC
nflw3.2	3	63.689122	62.939432	64.521327	6.63	X03_57678338	nflw	HT-stress	MAGIC
ppnflw3.2	3	64.348252	63.446585	65.147049	3.20	S03_64348252	nflw	PP	CC
nflw3.3	3	68.476718	66.996042	69.242078	4.80	X03_62529768	nflw	Control	MAGIC
ppnflw4.1	4	0.767236	0.744896	0.845631	5.95	S04_00767236	nflw	PP	CC
nflw4.2	4	2.926444	2.001092	55.861058	5.05	X04_2926444	nflw	Control	MAGIC
ppnflw4.3	4	65.17345	64.717474	66.152971	5.73	S04_65173450	nflw	PP	CC
nflw5.1	5	8.403486	6.932595	61.248466	4.88	X05_7251936	nflw	HT-stress	MAGIC
ppnflw5.2	5	63.13104	62.159914	63.954891	3.77	S05_63131040	nflw	PP	CC
nflw5.2	5	64.214037	63.217046	65.176391	5.32	S05_64214037	nflw	HT-stress	CC
nflw6.1	6	45.953573	45.03513	47.223776	5.79	S06_45953573	nflw	HT-stress	CC
nflw8.1	8	54.072286	53.749644	54.074828	4.13	S08_54072286	nflw	Control	CC
nflw8.2	8	55.964915	55.937442	56.07594	3.14	S08_55964915	nflw	Control	CC
nflw8.3	8	60.793734	60.730948	60.811459	3.60	S08_60793734	nflw	Control	CC
nflw8.3	8	60.967774	59.9886	61.910573	3.28	S08_60967774	nflw	HT-stress	CC
nflw9.1	9	65.618957	63.711556	66.553493	5.90	X09_61268966	nflw	HT-stress	MAGIC
nflw9.1	9	65.771347	0.015806	66.553493	4.46	X09_61116576	nflw	Control	MAGIC
nflw9.2	9	66.751411	66.562001	66.926136	4.58	S09_66751411	nflw	HT-stress	CC
nflw9.3	9	69.587566	68.423124	70.467811	5.02	S09_69587566	nflw	Control	CC
nflw10.1	10	54.449899	54.449604	54.523401	3.72	S10_54449899	nflw	HT-stress	CC
nflw10.2	10	58.195213	57.237943	58.307818	3.73	S10_58195213	nflw	HT-stress	CC

nflw11.1	11	5.667281	4.912781	6.227985	6.75	S11_05667281	nflw	Control	CC
ppnflw11.2	11	51.503469	50.764231	52.281041	5.11	S11_51503469	nflw	PP	CC
nflw11.3	11	53.472342	52.780186	54.306131	4.53	S11_53472342	nflw	HT-stress	CC
nflw11.3	11	55.10036	53.964003	56.105593	4.86	X11_52183860	nflw	Control	MAGIC
nflw11.4	11	55.958042	55.766807	56.005145	4.41	S11_55958042	nflw	HT-stress	CC
ppnflw11.4	11	56.008109	55.023449	56.151029	3.19	S11_56008109	nflw	PP	CC
nflw11.4	11	56.078411	55.146006	56.151029	7.32	S11_56078411	nflw	Control	CC
nflw12.1	12	1.690492	1.20595	2.109522	5.14	X12_1590967	nflw	HT-stress	MAGIC
nflw12.2	12	9.91793	9.150573	9.972015	4.12	S12_09917930	nflw	Control	CC
ppnfr1.1	1	94.722622	94.705626	94.72345	4.93	S01_94722622	nfr	PP	CC
ppnfr2.1	2	51.182657	50.58521	51.966463	5.70	X02_45506212	nfr	PP	MAGIC
nfr2.1	2	52.920159	51.182657	54.42757	5.30	X02_48202053	nfr	HT-stress	MAGIC
nfr3.1	3	2.735111	1.877032	2.913577	5.72	S03_02735111	nfr	HT-stress	CC
ppnfr3.1	3	2.735111	1.877032	2.913577	7.05	S03_02735111	nfr	PP	CC
ppnfr3.2	3	49.326696	11.265495	61.927295	5.76	X03_42873199	nfr	PP	MAGIC
nfr3.2	3	53.670496	53.08745	54.449864	7.32	S03_53670496	nfr	HT-stress	CC
ppnfr3.2	3	53.670496	53.08745	54.449864	5.67	S03_53670496	nfr	PP	CC
nfr4.1	4	0.767236	0.744896	0.845631	8.70	S04_00767236	nfr	HT-stress	CC
nfr4.2	4	62.8371	61.281208	63.900601	4.81	X04_60556749	nfr	HT-stress	MAGIC
nfr4.2	4	63.225199	62.550134	64.09501	8.51	S04_63225199	nfr	Control	CC
ppnfr4.3	4	65.17872	64.536101	66.152971	3.69	S04_65178720	nfr	PP	CC
nfr4.3	4	66.063525	65.611502	66.446769	5.37	S04_66063525	nfr	HT-stress	CC
nfr6.1	6	42.4926	41.602831	44.387315	8.05	S06_42492600	nfr	Control	CC
nfr7.1	7	65.161289	64.45	65.926032	4.08	S07_65161289	nfr	Control	CC
ppnfr7.1	7	65.168391	64.45	65.692641	3.72	S07_65168391	nfr	PP	CC
nfr8.1	8	53.08483	52.904532	53.749644	5.24	S08_53084830	nfr	HT-stress	CC
nfr8.2	8	54.372654	54.296663	54.444193	5.25	S08_54372654	nfr	Control	CC
ppnfr8.3	8	59.460898	57.208257	59.736554	4.91	X08_56626898	nfr	PP	MAGIC
ppnfr8.4	8	64.275214	64.156513	64.630487	3.21	S08_64275214	nfr	PP	CC
nfr9.1	9	0.835037	0.447776	1.221555	4.62	S09_00835037	nfr	HT-stress	CC
nfr9.2	9	64.781171	56.141247	67.30117	5.58	X09_59808022	nfr	Control	MAGIC
nfr9.2	9	66.103125	66.014053	66.376508	5.88	S09_66103125	nfr	HT-stress	CC
nfr10.1	10	54.449604	54.294074	54.449899	3.41	S10_54449604	nfr	HT-stress	CC
nfr10.2	10	58.003053	57.397425	58.189616	3.89	S10_58003053	nfr	HT-stress	CC
nfr10.3	10	63.245547	62.249522	64.218704	3.98	S10_63245547	nfr	HT-stress	CC
nfr11.1	11	1.163118	1.152677	1.182112	3.12	S11_01163118	nfr	HT-stress	CC
nfr11.2	11	5.667281	4.912781	6.227985	7.31	S11_05667281	nfr	Control	CC

ppnfr11.3	11	6.627532	6.622017	7.104482	3.06	S11_06627532	nfr	PP	CC
nfr11.4	11	7.863337	7.763703	8.414574	3.41	S11_07863337	nfr	Control	CC
nfr11.4	11	50.495947	7.241787	51.525667	5.34	X11_47579447	nfr	Control	MAGIC
nfr11.5	11	53.320055	52.428128	54.429101	9.47	S11_53320055	nfr	HT-stress	CC
ppnfr11.5	11	53.90264	53.88505	53.906868	5.60	S11_53902640	nfr	PP	CC
nfr11.5	11	54.429488	52.030767	55.475645	6.16	S11_54429488	nfr	Control	CC
nfr12.1	12	62.343961	62.08802	62.975968	3.21	S12_62343961	nfr	Control	CC
pH1.1	1	2.446381	1.253219	2.579748	4.98	X01_2446381	pH	Control	MAGIC
pH1.2	1	76.839188	4.340507	82.578583	4.81	X01_69316870	pH	Control	MAGIC
pppH1.3	1	90.225849	90.111583	90.240188	3.18	S01_90225849	pH	PP	CC
pH2.1	2	44.1631	41.740574	50.309536	5.89	X02_38740950	pH	Control	MAGIC
pH3.1	3	3.34422	3.334661	3.510178	4.77	S03_03344220	pH	Control	CC
pH3.2	3	62.520086	43.631616	64.899693	5.19	X03_56718661	pH	Control	MAGIC
pH3.2	3	64.512996	64.485318	64.588871	4.27	S03_64512996	pH	HT-stress	CC
pppH4.1	4	65.664182	64.360786	66.290965	3.08	S04_65664182	pH	PP	CC
pH5.1	5	63.43264	63.422638	63.449989	3.77	S05_63432640	pH	HT-stress	CC
pH5.1	5	63.85689	63.212646	63.880865	4.64	S05_63856890	pH	Control	CC
pH6.1	6	40.544466	39.549809	41.363544	4.63	S06_40544466	pH	Control	CC
pH6.2	6	41.977944	40.585009	45.218536	4.76	X06_38367844	pH	Control	MAGIC
pH6.2	6	43.189771	42.200096	44.272401	3.38	S06_43189771	pH	HT-stress	CC
pH6.2	6	44.965734	44.762672	47.27796	6.03	X06_41355634	pH	HT-stress	MAGIC
pH8.1	8	0.849696	0.029999	0.98595	8.98	S08_00849696	pH	HT-stress	CC
pH8.2	8	65.055199	63.651251	65.865539	4.50	X08_62221199	pH	Control	MAGIC
pH9.1	9	0.413648	0.41189	0.754579	3.59	S09_00413648	pH	Control	CC
pH9.2	9	68.169953	67.468084	68.174329	5.84	S09_68169953	pH	HT-stress	CC
pH9.3	9	69.906993	68.638813	69.958773	5.20	X09_65147785	pH	HT-stress	MAGIC
pppH10.1	10	5.025642	2.216078	57.291194	5.38	X10_7899410	pH	PP	MAGIC
pH11.1	11	5.023403	4.342018	5.476941	5.22	X11_5023403	pH	Control	MAGIC
pH11.2	11	52.128564	50.676545	53.035288	4.71	X11_49508530	pH	Control	MAGIC
pH12.1	12	8.722237	4.892313	38.647373	6.43	X12_8722237	pH	HT-stress	MAGIC
pH12.2	12	66.050838	65.580355	66.385245	5.49	X12_64391888	pH	HT-stress	MAGIC
SSC1.1	1	82.549018	82.128743	82.552739	3.80	S01_82549018	SSC	Control	CC
ppSSC2.1	2	17.652025	17.651901	17.970996	3.89	S02_17652025	SSC	PP	CC
ppSSC2.2	2	46.637841	45.546741	47.717105	4.41	S02_46637841	SSC	PP	CC
SSC2.3	2	48.89947	47.822111	51.775968	4.54	X02_43612183	SSC	Control	MAGIC
SSC3.1	3	54.662217	5.936744	59.85627	4.95	X03_49788273	SSC	HT-stress	MAGIC
SSC4.1	4	61.830034	59.990653	62.8371	7.19	X04_59423404	SSC	HT-stress	MAGIC

SSC4.1	4	62.374445	60.952746	63.900601	4.47	X04_59967815	SSC	Control	MAGIC
SSC4.2	4	66.307772	66.300765	66.446769	9.64	S04_66307772	SSC	Control	CC
SSC5.1	5	64.464346	64.457548	64.593171	4.88	S05_64464346	SSC	HT-stress	CC
SSC8.1	8	54.500456	53.749644	55.175977	5.15	S08_54500456	SSC	Control	CC
SSC8.2	8	57.724788	56.88112	57.899064	8.47	S08_57724788	SSC	Control	CC
ppSSC8.3	8	60.195041	60.170203	60.405484	4.43	S08_60195041	SSC	PP	CC
SSC9.1	9	2.673326	2.09513	3.942061	5.93	X09_2673326	SSC	Control	MAGIC
SSC9.1	9	3.398797	2.926053	4.550994	7.57	X09_3502151	SSC	HT-stress	MAGIC
SSC9.1	9	3.477979	3.477432	3.48489	7.47	S09_03477979	SSC	Control	CC
SSC9.1	9	3.477979	3.477432	3.48489	9.74	S09_03477979	SSC	HT-stress	CC
SSC10.1	10	54.449604	54.294074	54.449899	4.91	S10_54449604	SSC	HT-stress	CC
SSC11.1	11	2.589031	2.585263	2.5937	12.02	S11_02589031	SSC	HT-stress	CC
ppSSC11.2	11	54.93092	53.960745	55.766399	5.62	S11_54930920	SSC	PP	CC
ppSSC12.1	12	39.287937	39.24928	39.418026	7.40	S12_39287937	SSC	PP	CC

Supplemental Table 5: Summary of the QTLs detected for 11 traits in the CC (A) and the MAGIC (B) populations. The number of QTLs detected per condition and on the plasticity (PP) is indicated for each trait. In brackets is the number of QTLs detected uniquely in one condition or for the plasticity (PP) only. The number of QTLs that co-localized between conditions and or plasticity is presented in the column 'Common'. The column 'Total_QTLs' present the total number of QTLs detected per trait. The last row in bold present the total number of QTLs detected across traits for each condition and for the plasticity and the number of QTLs that were commonly detected. The stars (*) highlight traits for which QTLs were consistently detected in control, HT-stress condition and plasticity within population.

A) CC POPULATION

Trait	Control	HT_stress	PP	Common	Total_QTLs
col	2 (2)	4 (4)	1 (1)	0	7
diam	5 (5)	4 (4)	1 (1)	0	10
flw	11 (9)	12 (9)	13 (12)	3	33
fset	4 (4)	5 (5)	5 (5)	0	14
fw	4 (3)	5 (4)	5 (5)	1	13
height	5 (5)	4 (4)	4 (4)	0	13
leaf	5 (4)	2 (1)	4 (4)	1	10
nflw	8 (6)	10 (7)	7 (5)	3*	21
nfr	8 (6)	12 (8)	8 (3)	5*	22
pH	4 (3)	5 (4)	2 (2)	1	10
SSC	5 (4)	4 (3)	5 (5)	1	13
Total	**61 (51)**	**67 (53)**	**55 (47)**	**15**	**166**

B) MAGIC POPULATION

Trait	Control	HT_stress	PP	Common	Total_QTLs
col	6 (4)	4 (4)	4 (2)	2	12
diam	2 (2)	4 (4)	0	0	6
flw	5 (3)	4 (2)	0	2	7
fset	5 (5)	4 (4)	2 (2)	0	11
fw	7 (**3**)	7 (**5**)	3 (1)	4	**13**
height	6 (3)	8 (4)	1 (0)	4	11
leaf	4 (3)	5 (4)	0	1	8
nflw	4 (3)	5 (3)	1 (0)	2	8
nfr	2 (2)	2 (1)	3 (2)	1	6
pH	8 (7)	4 (3)	1 (1)	1	12
SSC	3 (1)	3 (1)	0	2	4
Total	**52 (36)**	**50 (35)**	**15 (8)**	**19**	**98**

Appendix 6

Supplemental Figures

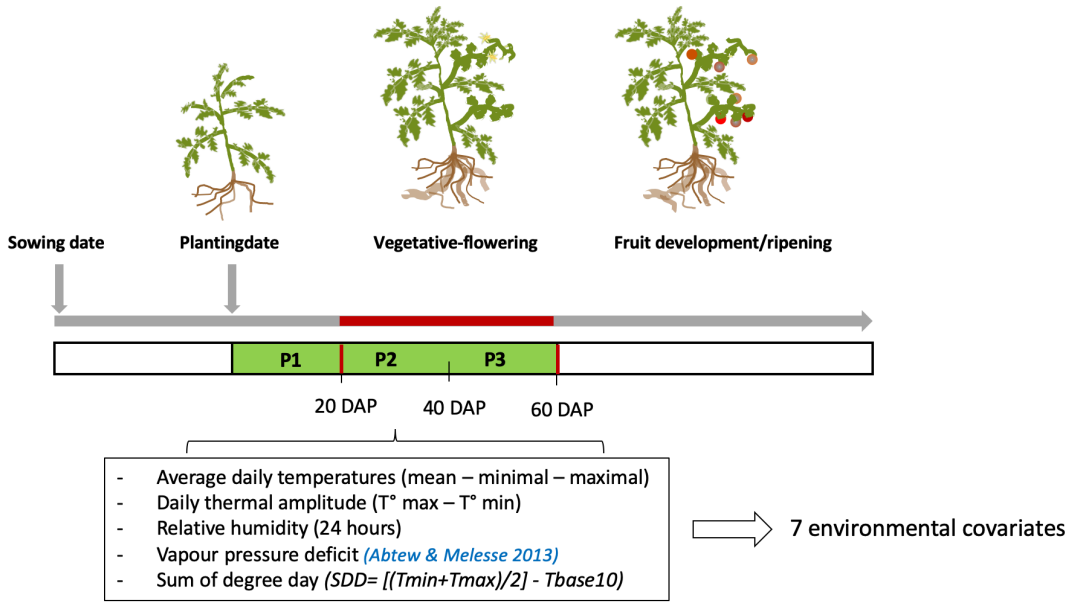

DAP = Days after plantation

Period covering the flowering time (under the 4th truss) of the MAGIC population

Supplemental Figure 1: Selection of 7 environmental covariates for the factorial regression model. Three periods – each of 20 days – were defined from planting to the end of flowering on the 4th truss. The period from 20 to 60 days after planting (DAP) covered vegetative growth and flowering on the 4th truss and the measured climatic variables averaged during this period. The different environmental covariates are described

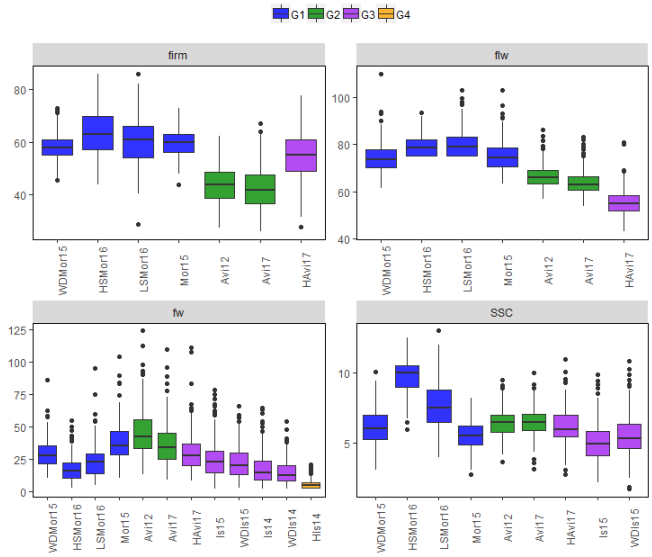

Supplemental Figure 2: Boxplot distribution of the traits across environments. The colors of the boxplot are according to the groups defined by clustering of the environments

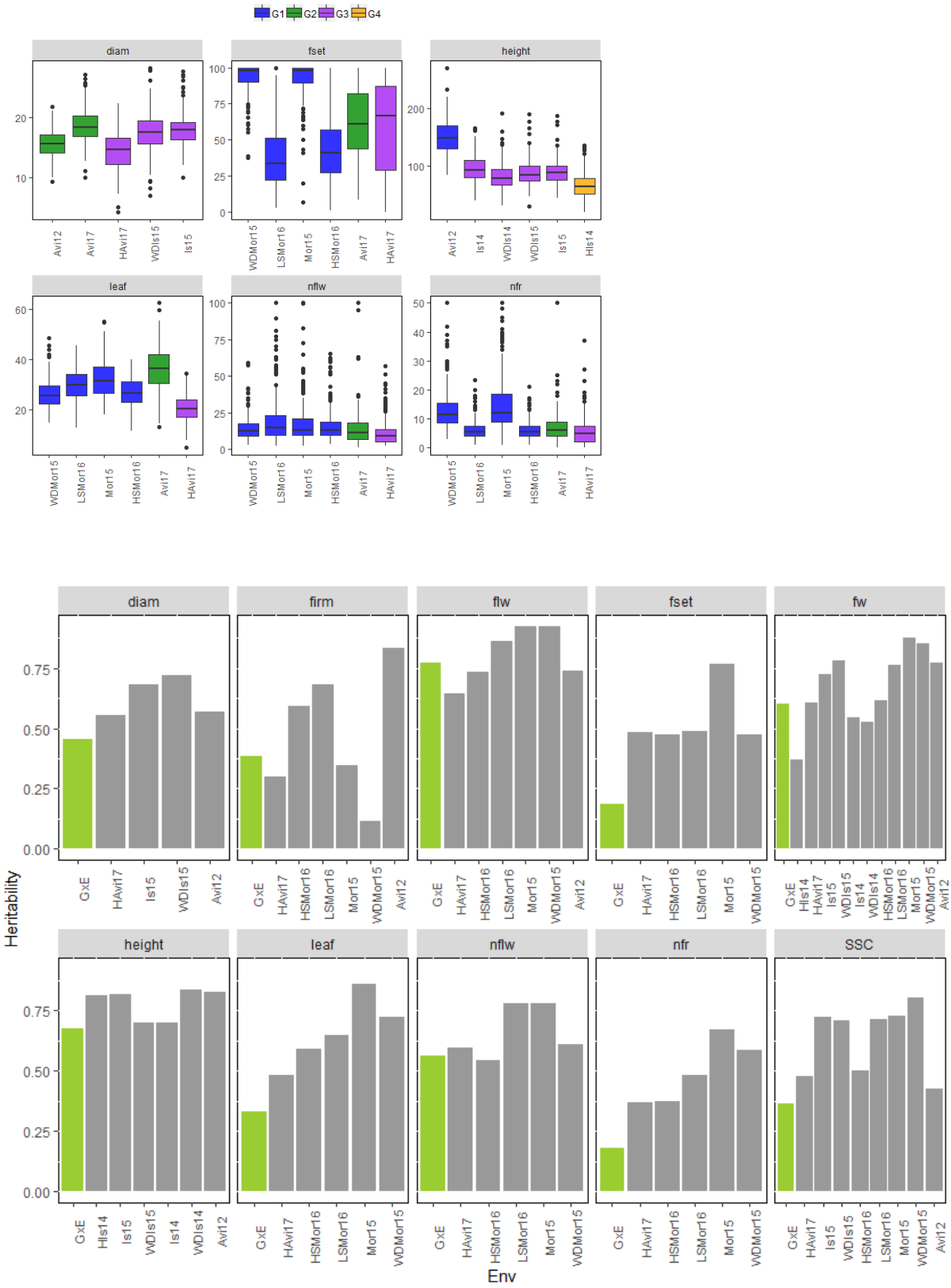

Supplemental Figure 3: Heritability in the MAGIC-MET design. For each trait, heritability was computed at every environment and plotted with heritability of the full design H^2 (in green)

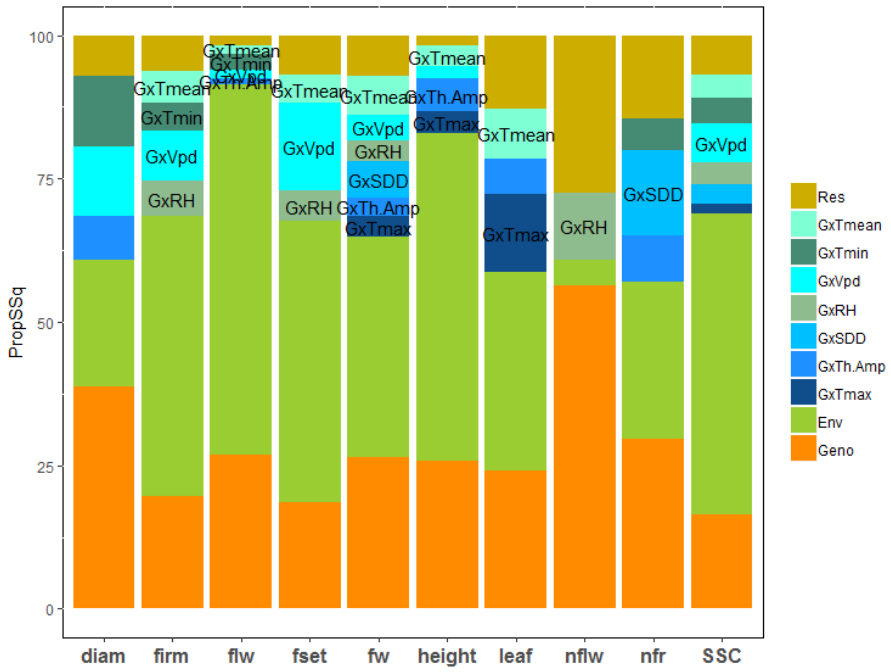

Supplemental Figure 4: Proportion of the sum of square attributed to the different factors in the factorial regression model. For each trait, the orange and green stacked bars represent the proportion of the SSq explained by the Genotype and Environment factors in model (4). The remaining colors represent the effect part of the GxE that could be explained by the different environmental covariates. Only significant covariates were highlighted within the bars.

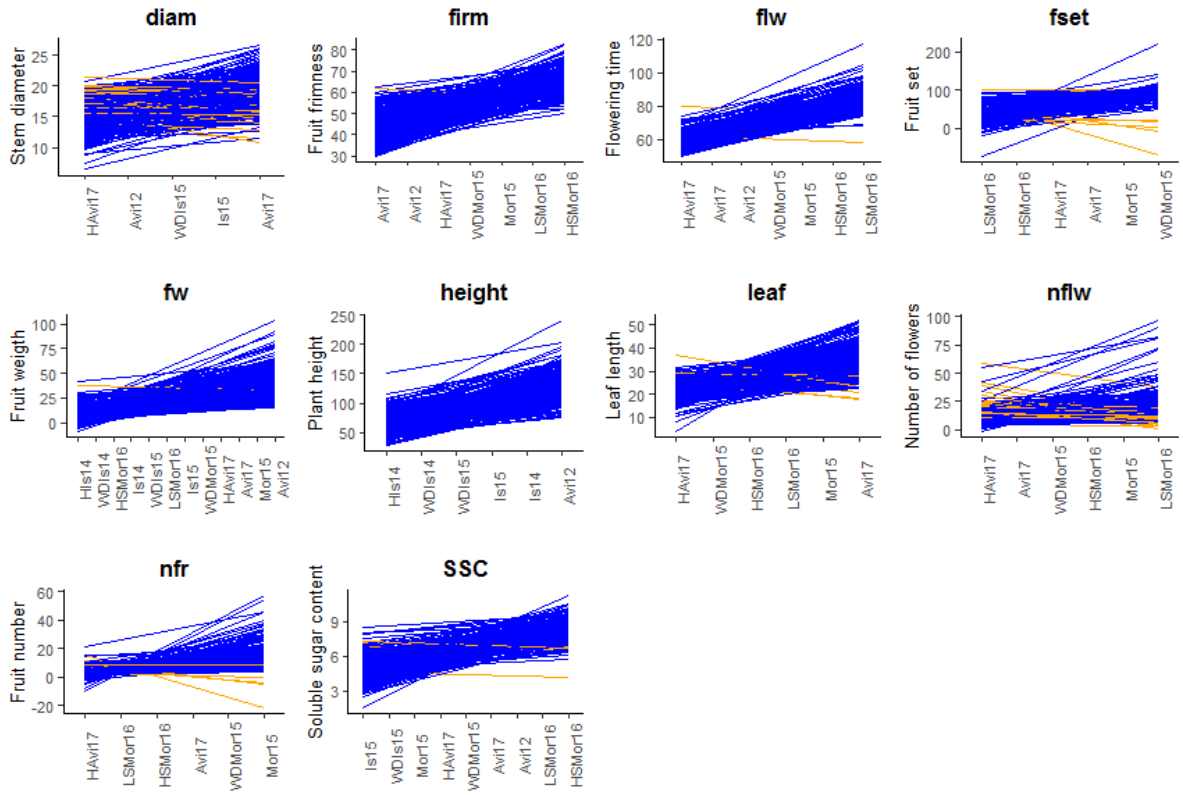

Supplemental Figure 5-A: Reaction norms from the Finlay-Wilkinson regression model. Blue and orange lines represent the positive and negative reaction norms

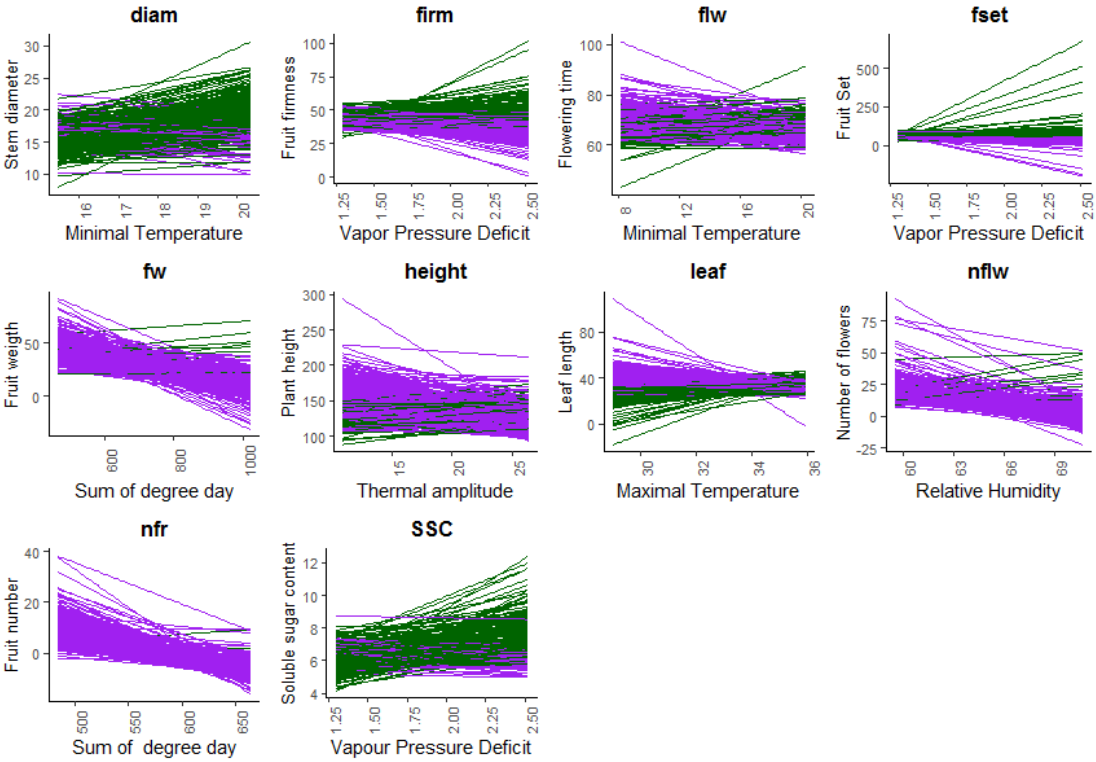

Supplemental Figure 5-B: Reaction norms from the factorial regression model. Green and purple lines represent the positive and negative reaction norms

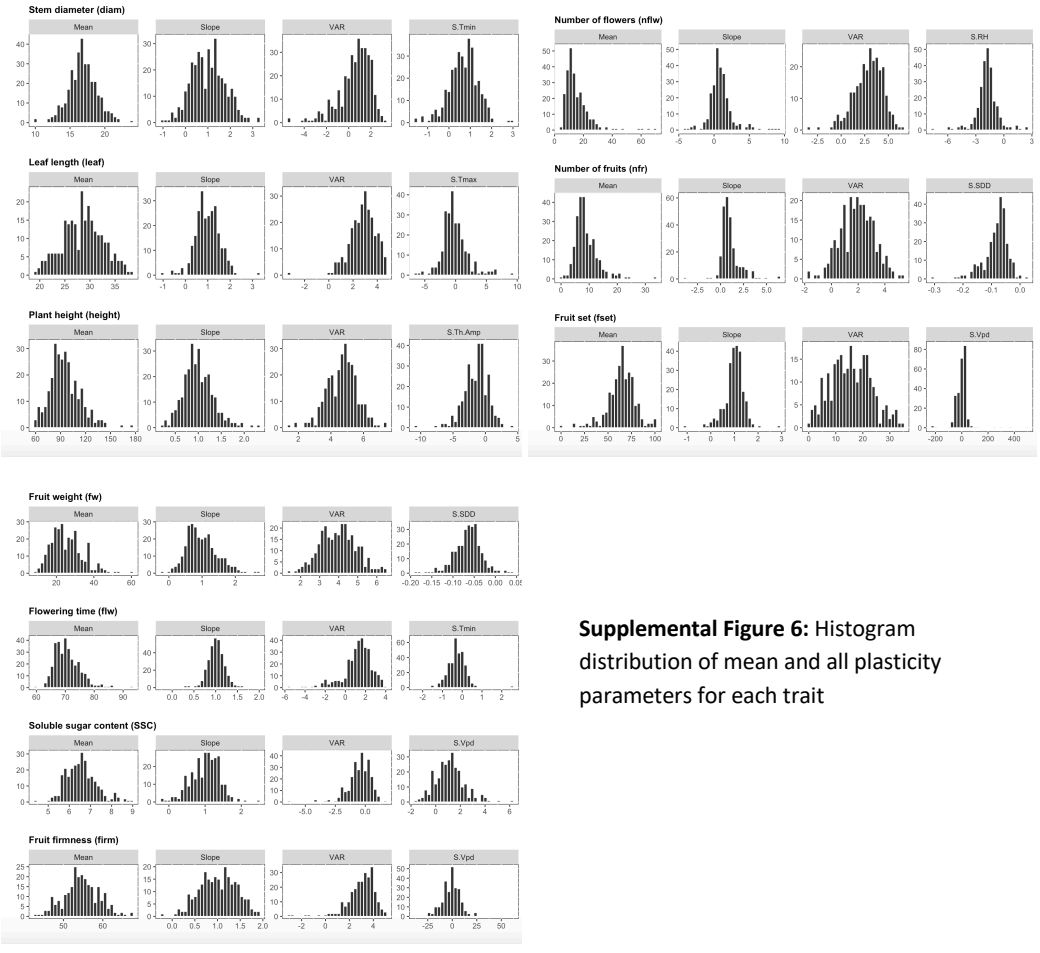

Supplemental Figure 6: Histogram distribution of mean and all plasticity parameters for each trait

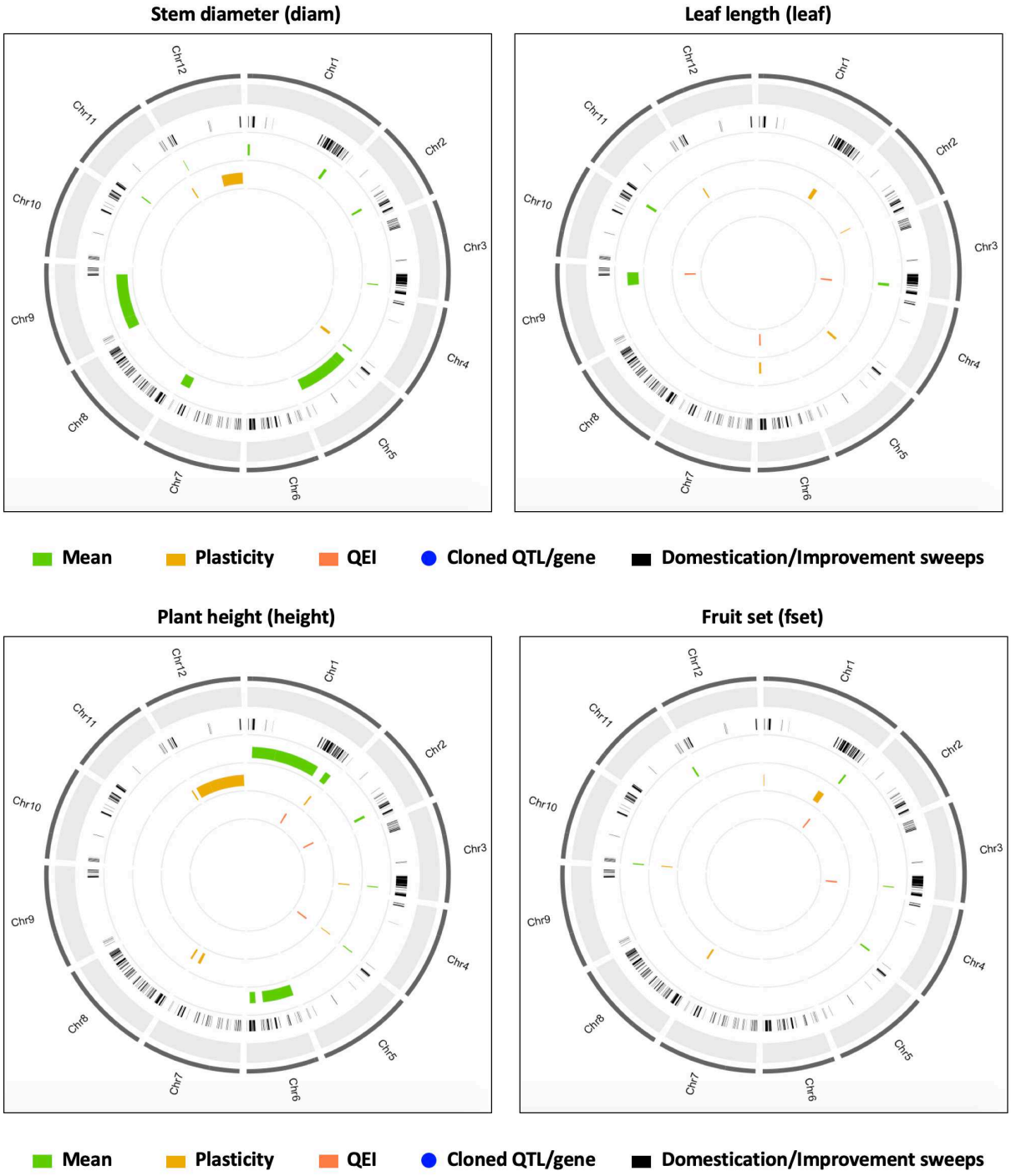

Supplemental Figure 7: Physical positions of the MAGIC-MET QTLs for diam, leaf, height, fset, nflw, nfr, firm and SSC. The outer circle with gray font represents the known and cloned QTL/gene for each trait. The following circle with black bars represents the different domestication/improvement sweep regions identified in (Zhu et al. 2018). The other circles plot the CI of QTLs identified on mean, plasticity or with QEI analysis.

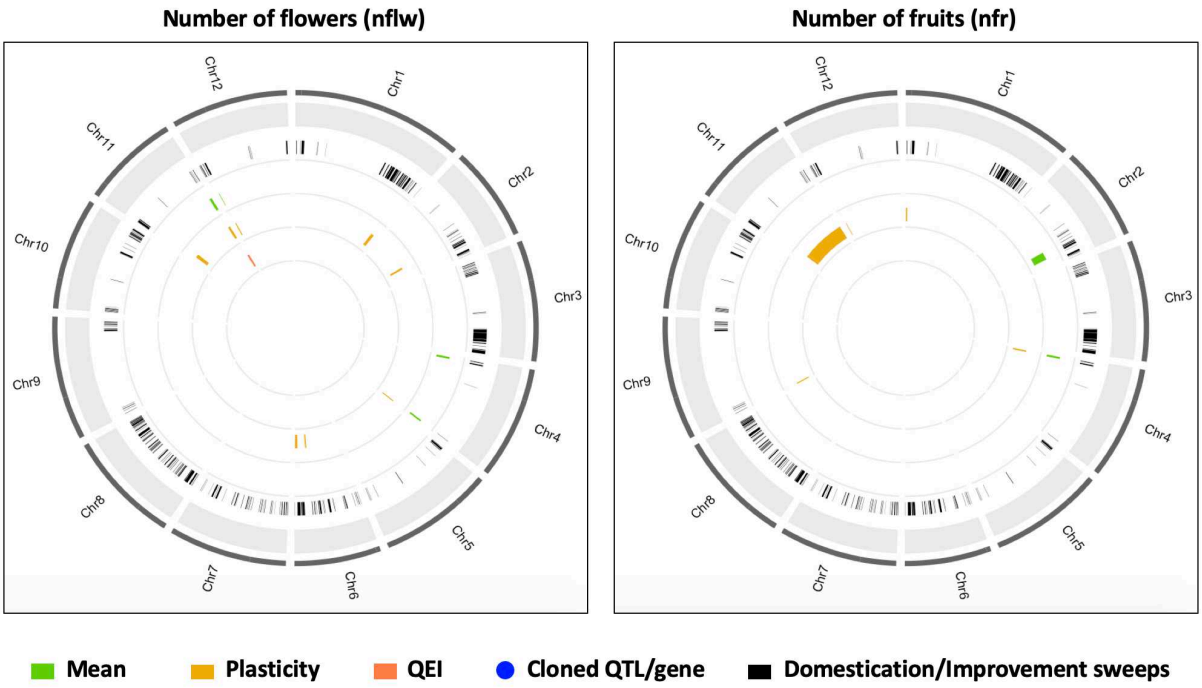
Number of flowers (nflw)
Number of fruits (nfr)
Chr1
Chr2
Chr3
Chr4
Chr5
Chr6
Chr7
Chr8
Chr9
Chr10
Chr11
Chr12
Mean
Plasticity
QEI
Cloned QTL/gene
Domestication/Improvement sweeps

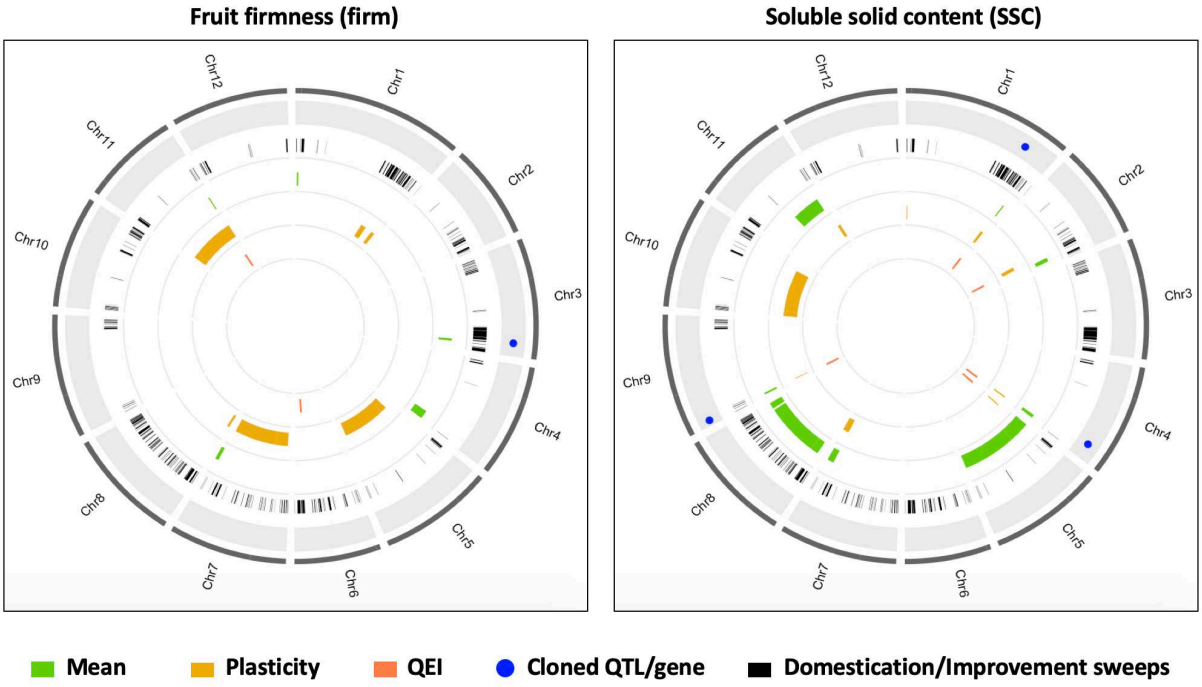
Fruit firmness (firm)
Soluble solid content (SSC)
Chr1
Chr2
Chr3
Chr4
Chr5
Chr6
Chr7
Chr8
Chr9
Chr10
Chr11
Chr12
Mean
Plasticity
QEI
Cloned QTL/gene
Domestication/Improvement sweeps

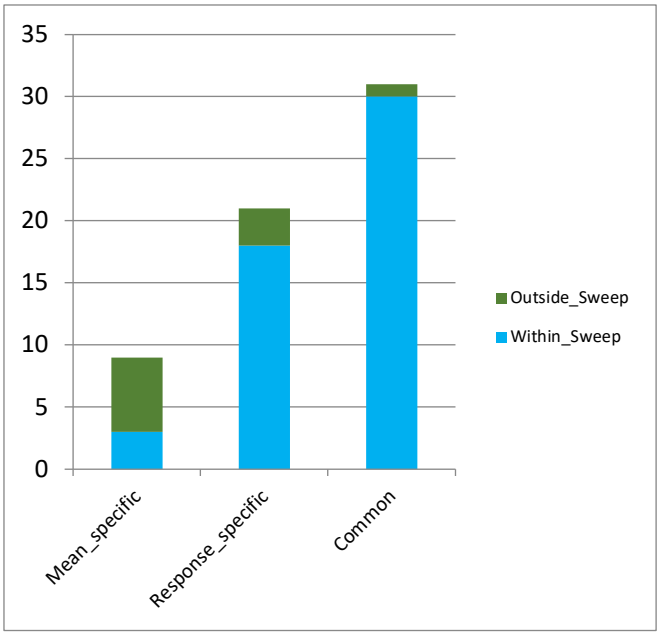

Supplemental Figure 8: Number of the MAGIC-MET QTLs identified within or outside the domesticated/improved regions. Only the MAGIC-MET QTLs within short CI (lower than 2Mbp) were considered. The response specific category included QEI and plasticity specific QTLs; the common category correspond to QTLs that were commonly identified on mean, plasticity and QEI or at least two of them

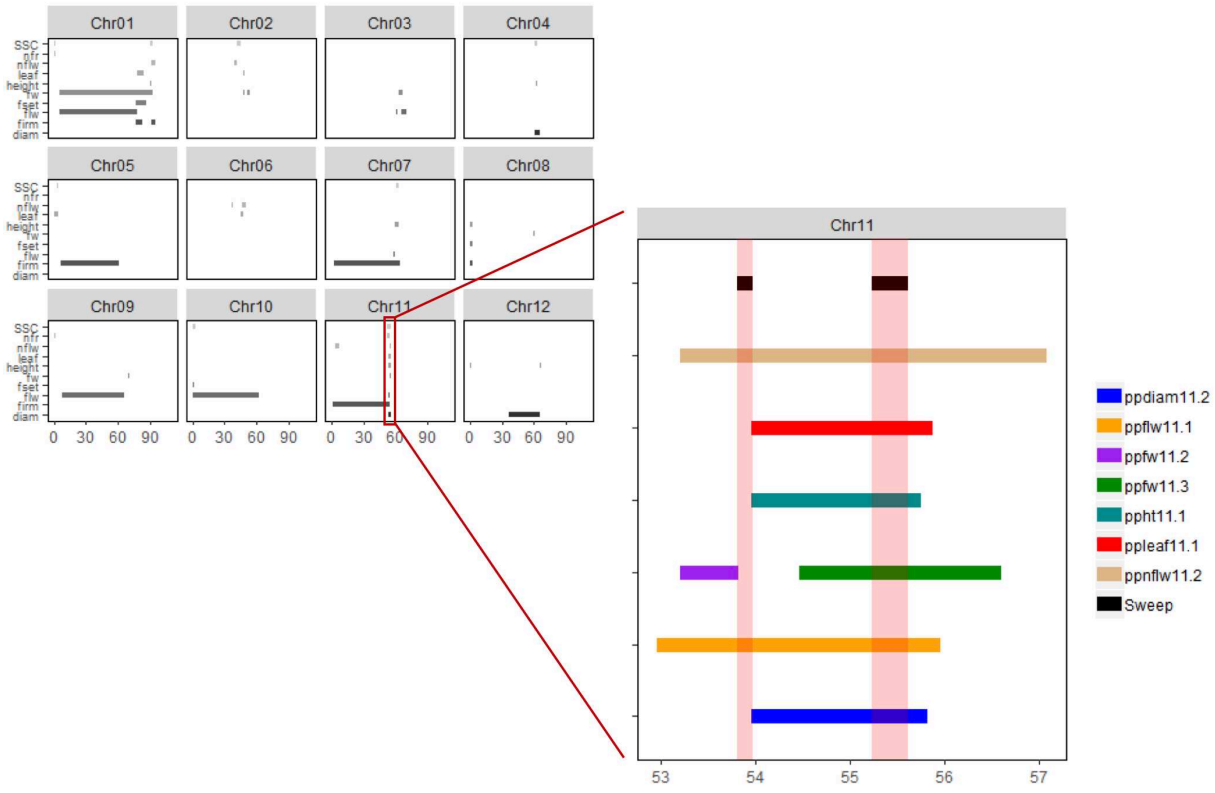

Supplemental Figure 9: Zoom plot on Chromosome 11 region from 53 -57 Mbp. Each color represents a different QTL located in this region and the top black bars are the Sweep regions SW254 and SW255

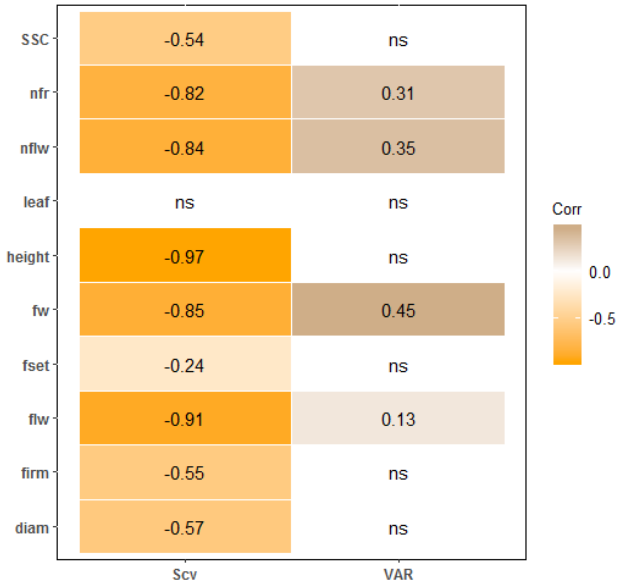

Supplemental Figure 10: Correlation between the genotypic sensitivities to environmental covariates from the factorial regression model and slopes from the Finlay-Wilkinson regression model

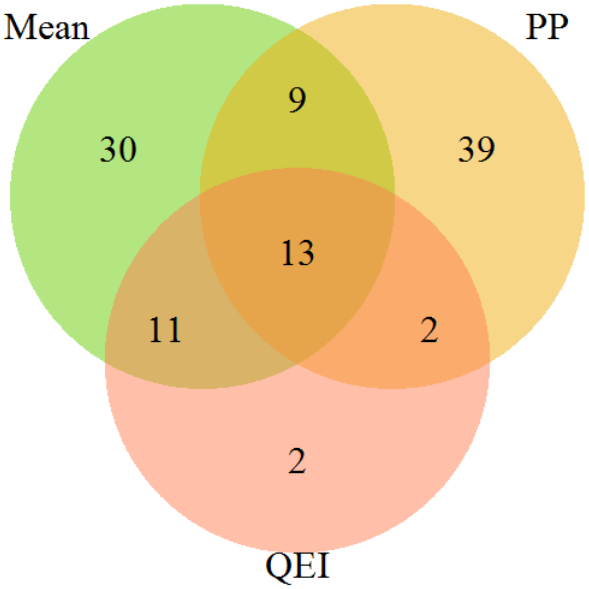

Supplemental Figure 11: Venn diagram of the number of QTL specific or commonly detected with mean, PP or using the QEI models

Supplemental Tables

Supplemental Table 1: Description of the MAGIC-MET design with the 12 environments and their respective names

Environ-ments	Location	Water irrigation (%ETP)	Treatment	EC (dS/m)	Tmin (°C)	Tm (°C)	Tmax (°C)	Amp.Th (°C)	RH (%)	Vpd (kPa)	Sum of degree day (SDD)	Number of Genotypes
Avi12	France	100%	Control	1.33	15.48	20.5	26.4	10.92	70.83	1.71	466.94	397
Avi17	France	100%	Control	1.65	16.05	21.44	29.02	12.97	63.73	1.62	496.4	280
HAvi17	France	100%	Heat	1.47	20.35	26.9	34.34	13.99	70.72	2.52	664.06	356
Is14	Israel	100%	Control	NA	20.16	28.6	38.72	18.56	67.4	2.64	800.23	288
HIs14	Israel	100%	Heat	NA	21.92	33.05	48.33	26.41	55.02	2.78	1022.73	288
WDIs14	Israel	-70%	Water deficit	NA	20.53	29.28	40.83	20.3	63.48	2.59	835.57	288
Is15	Israel	100%	Control	NA	17.39	26.78	37.54	20.15	65.38	2.3	685.12	288
WDIs15	Israel	-30%	Water deficit	NA	17.27	25.97	35.38	18.11	65.94	2.21	638.54	288
Mor15	Morocco	100%	Control	2.17	8.11	18.17	35.91	27.8	62.42	1.3	484.9	241
WDMor15	Morocco	-50%	Water deficit	1.42	8.11	18.17	35.91	27.8	62.42	1.3	484.9	241
LSMor16	Morocco	100%	Salinity	3.76	11.54	19.99	34.11	22.57	59.56	1.39	583.06	253
HSMor16	Morocco	100%	Salinity	6.5	11.54	19.99	34.11	22.57	59.56	1.39	583.06	253

Supplemental Table 2: Description of the phenotypic traits evaluated in the MAGIC-MET design

Trait	Truss Phenotyped	Trait Description
diam	T4	Stem diameter (mm) measured on individual plants (two measures)
firm	T4	Mean firmness of viable fruits harvested (3-10 fruits per individual plant)
flw	T4	Number of days between plant sowing and first flower appareance on the truss
fset	T4-T5	Fruit set was calculated as: 100*(number of viable fruits / number of peduncles)/truss
fw	T4	Mean weight (g) of viable fruits harvested (3-10 fruits per individual plant)
height	T6	Height (cm) of the plant at 6th truss
leaf	T5	Length (cm) of the leaf under the 5th truss
nflw	T4-T5	Total number of flowers per truss
nfr	T4	Total number of viable fruits per truss
SSC	T4	Soluble Solid content (°Brix) of a pool of at least 3 fruits (when avalaible) per genotype.

Supplemental Table 3: Estimates of the variance components from model (2)

Trait	Geno	GxE	Res.E	min Res.E	max Res.E	prop. σ^2GxE	h^2GxE	nb.Env	nb.MAGIC
diam	2.74	2	4.56	2.62	6.57	0.42	0.46	5	334
firm	17.36	13.49	4.11	16.29	62.37	0.44	0.38	7	251
flw	17.46	5.04	7.6	4.6	10.62	0.22	0.77	7	327
fset	59.11	59.74	402.03	81.41	947.34	0.5	0.19	6	252
fw	69.93	52.4	93.34	15.26	186.1	0.43	0.6	12	283
height	281.02	128.57	214.13	136.94	296.91	0.31	0.68	6	286
leaf	8.27	17.57	23.36	12.75	38.95	0.68	0.33	6	253
nflw	68.75	12.06	84.08	41.11	135.75	0.15	0.56	6	253
nfr	4.69	1.82	34.35	10.01	96.38	0.3	0.18	6	253
SSC	0.35	0.53	0.86	0.33	1.57	0.6	0.36	9	274

Supplemental Table 4: Results of QTL and QEI analysis in the MAGIC-MET design

Trait	QTL_ID	Type	Pheno	Chromosome	-log10(pvalue)	Pos (Mbp)	ci_lo (Mbp)	ci_hi (Mbp)	marker
height	ht1.1	QEI	QEI	1	4.30	75.855371	74.355371	77.355371	X01_68245871
fw	fw1.1	Mean	Mean	1	4.44	77.436487	4.96157	82.578583	X01_69826987
fset	ppfset1.2	PP	VAR	1	4.50	84.468518	77.436487	86.422123	X01_76229318
fw	ppfw1.2	PP	VAR	1	4.53	90.867735	4.96157	92.266398	X01_82628535
height	ht1.2	Mean	Mean	1	4.64	88.232834	87.293634	93.992823	X01_79993634
fw	fw1.2	Mean	Mean	1	4.65	90.535223	90.211101	92.266398	X01_82296023
nflw	ppnflw1.1	PP	Slope	1	4.72	93.992823	91.212721	94.672603	X01_85753623
fset	ppfset1.1	PP	Slope	1	4.76	0.066253	0.043522	1.049955	X01_66253
diam	diam1.2	Mean	Mean	1	4.92	86.437181	85.571496	88.688358	X01_78197981
SSC	ppSSC1.1	PP	Slope	1	4.94	1.253219	0.892936	1.730558	X01_1253219
diam	diam1.1	Mean	Mean	1	4.98	1.730558	0.23258	2.579748	X01_1730558
nfr	ppnfr1.1	PP	S.SDD	1	5.04	1.049955	0.066253	1.730558	X01_1049955
height	ppht1.2	PP	S.Th.Amp	1	5.14	91.047287	90.211101	92.266398	X01_82808087
fset	fset1.3	QEI	QEI	1	5.29	93.092756	91.592756	94.592756	X01_84853556
flw	ppflw1.1	PP	Slope	1	5.33	76.186755	4.96157	84.468518	X01_68577255
firm	ppfirm1.3	PP	Slope	1	5.34	93.475357	91.212721	95.392835	X01_85236157
firm	firm1.1	Mean	Mean	1	5.42	2.446381	1.253219	2.579748	X01_2446381
SSC	ppSSC1.2	PP	S.Vpd	1	5.45	91.608878	90.211101	93.092756	X01_83369678
leaf	ppleaf1.1	PP	VAR	1	5.49	82.578583	77.65613	83.574745	X01_74339383
fset	fset1.3	Mean	Mean	1	5.62	93.092756	91.212721	93.32137	X01_84853556
height	ppht1.2	PP	Slope	1	6.07	91.047287	90.211101	91.314498	X01_82808087
flw	flw1.1	QEI	QEI	1	6.25	76.569293	75.069293	78.069293	X01_68959793
firm	ppfirm1.2	PP	S.Vpd	1	6.40	82.578583	77.436487	83.434428	X01_74339383
flw	ppflw1.1	PP	S.Tmin	1	6.87	76.186755	4.96157	77.65613	X01_68577255
height	ht1.1	Mean	Mean	1	8.16	75.855371	4.96157	77.65613	X01_68245871
SSC	SSC1.2	Mean	Mean	1	10.94	91.608878	91.212721	92.266398	X01_83369678
SSC	SSC1.2	QEI	QEI	1	12.14	91.77996	90.27996	93.27996	X01_83540760
flw	flw1.1	Mean	Mean	1	19.25	76.186755	4.96157	77.65613	X01_68577255
diam	diam2.1	QEI	QEI	2	4.00	40.592217	39.092217	42.092217	X02_35170067
SSC	SSC2.1	QEI	QEI	2	4.15	45.158686	43.658686	46.658686	X02_39736536
diam	diam2.1	Mean	Mean	2	4.66	40.592217	39.456131	41.80934	X02_35170067
nflw	ppnflw2.1	PP	Slope	2	4.71	40.592217	39.456131	41.642759	X02_35170067
nfr	nfr2.1	Mean	Mean	2	4.88	41.740574	41.274596	48.195716	X02_36318424
leaf	ppleaf2.1	PP	Slope	2	5.05	48.329646	47.822111	48.89947	X02_42907496
fw	fw2.1	Mean	Mean	2	5.14	48.329646	47.822111	48.89947	X02_42907496
height	ht2.1	QEI	QEI	2	5.22	47.822111	46.322111	49.322111	X02_42399961
SSC	ppSSC2.1	PP	Slope	2	5.39	44.547467	41.740574	45.64581	X02_39125317
SSC	SSC2.2	Mean	Mean	2	5.60	50.666161	48.471214	51.966463	X02_45244011

fw	fw2.1	QEI	QEI	2	5.72	48.195716	46.695716	49.695716	X02_42773566
flw	flw2.1	Mean	Mean	2	5.92	27.224828	5.855256	38.423331	X02_17932477
fw	fw2.2	QEI	QEI	2	7.17	52.10546	50.60546	53.60546	X02_46683310
fw	ppfw2.2	PP	S.SDD	2	7.29	52.920159	51.775968	54.014597	X02_47498009
fw	ppfw2.2	PP	VAR	2	7.48	52.920159	51.182657	54.014597	X02_47498009
fw	ppfw2.1	PP	S.SDD	2	7.95	48.195716	47.822111	48.89947	X02_42773566
height	ht2.1	Mean	Mean	2	8.61	47.822111	45.447408	48.195716	X02_42399961
fw	fw2.2	Mean	Mean	2	8.96	51.775968	51.182657	54.014597	X02_46353818
fw	ppfw2.2	PP	Slope	2	9.02	52.920159	51.182657	54.014597	X02_47498009
fw	ppfw2.1	PP	Slope	2	9.63	48.195716	47.822111	48.89947	X02_42773566
fw	fw3.2	QEI	QEI	3	4.38	64.793561	63.293561	66.293561	X03_58846611
flw	ppflw3.1	PP	Slope	3	4.52	62.328005	60.528754	62.457723	X03_56381055
flw	ppflw3.3	PP	VAR	3	4.87	70.040809	65.831575	70.741861	X03_64093859
leaf	leaf3.1	QEI	QEI	3	5.11	64.450921	62.950921	65.950921	X03_58503971
fw	ppfw3.2	PP	Slope	3	5.29	68.052409	63.93268	68.476718	X03_62105459
height	ht3.1	Mean	Mean	3	5.75	64.701243	63.93268	64.899693	X03_58754293
firm	firm3.1	Mean	Mean	3	5.80	62.520086	62.328005	64.333413	X03_56573136
fw	ppfw3.2	PP	VAR	3	6.14	65.387833	63.21107	67.141095	X03_59440883
diam	diam3.1	Mean	Mean	3	6.18	63.93268	63.21107	64.333413	X03_57985730
flw	flw3.2	Mean	Mean	3	6.25	64.793561	64.450921	65.387833	X03_58846611
leaf	leaf3.1	Mean	Mean	3	6.46	64.450921	62.328005	65.244029	X03_58503971
fset	fset3.1	Mean	Mean	3	6.49	64.701243	63.93268	64.899693	X03_58754293
fw	fw3.2	Mean	Mean	3	6.82	64.701243	63.93268	66.923413	X03_58754293
height	ppht3.1	PP	S.Th.Amp	3	7.63	64.521327	63.93268	65.387833	X03_58574377
fset	fset3.1	QEI	QEI	3	7.80	64.601104	63.101104	66.101104	X03_58654154
height	ppht3.1	PP	Slope	3	8.05	64.521327	63.93268	64.899693	X03_58574377
flw	flw3.2	QEI	QEI	3	14.61	64.793561	63.293561	66.293561	X03_58846611
nfr	ppnfr4.1	PP	S.SDD	4	4.55	1.850859	1.37403	2.926444	X04_1850859
nfr	nfr4.1	Mean	Mean	4	4.58	1.850859	1.670584	3.481942	X04_1850859
diam	ppdiam4.1	PP	Slope	4	4.67	62.374445	61.281208	65.236362	X04_59967815
SSC	SSC4.1	Mean	Mean	4	5.15	62.374445	59.990653	62.8371	X04_59967815
firm	firm4.1	Mean	Mean	4	5.24	61.830034	55.727428	63.370382	X04_59423404
nflw	ppnflw4.2	PP	S.RH	4	5.42	64.634125	64.034949	64.879538	X04_62227495
fset	fset4.1	Mean	Mean	4	5.57	62.002311	60.952746	62.8371	X04_59595681
nflw	nflw4.1	Mean	Mean	4	5.60	2.050817	1.670584	3.481942	X04_2050817
nflw	nflw4.2	Mean	Mean	4	5.81	64.534853	63.422266	64.879538	X04_62128223
SSC	ppSSC4.1	PP	Slope	4	5.88	61.842938	61.281208	62.8371	X04_59436308
nfr	ppnfr4.1	PP	VAR	4	6.50	2.149071	2.050817	2.926444	X04_2149071
height	ht4.2	QEI	QEI	4	6.93	64.034949	62.534949	65.534949	X04_61628319
height	ppht4.1	PP	S.Th.Amp	4	7.02	62.083632	61.842938	62.8371	X04_59677002
height	ppht4.1	PP	Slope	4	7.20	62.083632	62.002311	62.8371	X04_59677002

nflw	ppnflw4.2	PP	Slope	4	7.79	64.634125	64.034949	64.879538	X04_62227495
diam	diam4.1	QEI	QEI	4	8.58	64.034949	62.534949	65.534949	X04_61628319
SSC	SSC4.1	QEI	QEI	4	9.16	61.842938	60.342938	63.342938	X04_59436308
height	ht4.2	Mean	Mean	4	10.46	64.034949	63.82458	64.879538	X04_61628319
diam	diam4.1	Mean	Mean	4	11.17	64.034949	63.82458	65.778385	X04_61628319
SSC	SSC5.1	QEI	QEI	5	4.30	2.02052	0.52052	3.52052	X05_2020520
SSC	SSC5.1	Mean	Mean	5	4.48	65.774446	0.11876	65.870042	X05_64920796
firm	ppfirm5.1	PP	Slope	5	4.50	7.143867	6.932595	61.632828	X05_7143867
flw	flw5.1	Mean	Mean	5	4.64	56.142303	5.638011	61.248466	X05_55288653
leaf	ppleaf5.1	PP	S.Tmax	5	4.79	4.322124	0.990309	4.373269	X05_4322124
fw	fw5.1	Mean	Mean	5	4.79	4.527122	4.01884	5.180595	X05_4527122
diam	diam5.1	Mean	Mean	5	4.97	6.932595	5.638011	60.985149	X05_6932595
flw	flw5.1	QEI	QEI	5	5.47	7.251936	5.751936	8.751936	X05_7251936
SSC	ppSSC5.1	PP	S.Vpd	5	6.16	2.538011	2.339908	3.669112	X05_2538011
flw	flw6.1	QEI	QEI	6	4.30	42.249026	40.749026	43.749026	X06_38638926
height	ht6.2	Mean	Mean	6	4.55	45.218536	40.585009	46.657691	X06_41608436
firm	firm6.1	QEI	QEI	6	4.55	40.585009	39.085009	42.085009	X06_36974909
nflw	ppnflw6.2	PP	Slope	6	4.65	48.782813	46.748971	49.687274	X06_45072813
nflw	ppnflw6.1	PP	Slope	6	5.08	37.965369	36.880315	38.363876	X06_34355269
leaf	ppleaf6.1	PP	S.Tmax	6	5.32	46.657691	45.218536	48.206369	X06_43047591
height	ht6.1	Mean	Mean	6	5.37	0.733825	0.015422	32.798578	X06_733825
leaf	leaf6.1	QEI	QEI	6	12.32	46.170878	44.670878	47.670878	X06_42560778
firm	ppfirm7.1	PP	S.Vpd	7	4.52	4.481678	3.122017	64.215168	X07_4481678
SSC	ppSSC7.1	PP	Slope	7	4.57	67.773594	61.06426	67.908188	X07_64997194
SSC	SSC7.1	Mean	Mean	7	4.68	63.768352	60.02716	65.832471	X07_61091852
height	ppht7.1	PP	S.Th.Amp	7	4.84	61.06426	60.02716	63.768352	X07_58387760
diam	diam7.1	Mean	Mean	7	4.88	63.972793	57.242195	67.908188	X07_61296293
SSC	ppSSC7.1	PP	S.Vpd	7	4.90	63.64279	61.06426	63.768352	X07_60966290
height	ppht7.1	PP	Slope	7	5.14	61.06426	60.02716	63.768352	X07_58387760
firm	firm7.2	Mean	Mean	7	5.78	67.029958	64.764273	67.908188	X07_64253558
flw	ppflw7.1	PP	VAR	7	6.11	59.709404	58.415562	60.02716	X07_57032904
height	ppht8.1	PP	Slope	8	4.45	1.199042	0.062757	2.769368	X08_1199042
SSC	SSC8.2	Mean	Mean	8	4.45	61.170209	59.101552	64.624556	X08_58336209
fset	ppfset8.1	PP	S.Vpd	8	4.47	0.390964	0.062757	2.769368	X08_390964
firm	ppfirm8.1	PP	S.Vpd	8	4.54	0.062757	0.062757	2.769368	X08_62757
fw	ppfw8.1	PP	VAR	8	4.64	59.736554	57.208257	61.170209	X08_56902554
flw	flw8.1	Mean	Mean	8	4.95	28.732034	3.036877	65.225414	X08_15744258
fw	ppfw8.1	PP	Slope	8	5.17	59.736554	59.101552	60.397157	X08_56902554
SSC	SSC8.1	Mean	Mean	8	5.18	21.047529	3.523236	57.585344	X08_31903516
fw	fw8.1	Mean	Mean	8	5.97	60.170203	59.543193	61.170209	X08_57336203
leaf	leaf9.1	QEI	QEI	9	4.06	63.711556	62.211556	65.211556	X09_59309075

nfr	ppnfr9.1	PP	Slope	9	4.58	0.490136	0.015806	1.235265	X09_490136
diam	diam9.1	Mean	Mean	9	4.86	56.141247	4.289476	64.210503	X09_51738766
flw	ppflw9.1	PP	S.Tmin	9	5.09	63.711556	8.333659	65.618957	X09_59309075
SSC	ppSSC9.1	PP	Slope	9	5.43	4.550994	3.942061	4.732408	X09_4550994
fw	ppfw9.1	PP	S.SDD	9	5.71	69.958773	69.906993	71.056445	X09_65306642
leaf	leaf9.1	Mean	Mean	9	5.88	66.172567	52.555625	66.553493	X09_61670186
flw	flw9.2	Mean	Mean	9	7.65	69.553678	69.130616	69.958773	X09_64901547
SSC	SSC9.1	Mean	Mean	9	8.93	4.316025	2.926053	4.550994	X09_4316025
SSC	SSC9.1	QEI	QEI	9	9.67	3.398797	1.898797	4.898797	X09_3398797
flw	ppflw10.1	PP	S.Tmin	10	4.58	1.146092	0.164588	62.294422	X10_1146092
leaf	leaf10.1	Mean	Mean	10	4.59	63.191372	62.556165	65.499448	X10_62515904
fset	fset10.1	Mean	Mean	10	4.88	0.164588	0.0221	1.323966	X10_164588
SSC	ppSSC10.1	PP	S.Vpd	10	5.01	0.354213	0.0221	2.216078	X10_354213
fset	ppfset10.1	PP	Slope	10	5.31	1.166916	0.0221	1.323966	X10_1166916
SSC	ppSSC10.1	PP	Slope	10	5.74	3.586564	1.707763	53.439459	X10_3586564
flw	flw11.1	QEI	QEI	11	3.75	54.464915	52.964915	55.964915	X11_51548415
nflw	ppnflw11.2	PP	VAR	11	4.46	53.532037	53.206534	55.21479	X11_50615537
flw	ppflw11.1	PP	Slope	11	4.59	54.224712	53.964003	55.21479	X11_51308212
nflw	nflw11.2	QEI	QEI	11	4.63	55.578287	54.078287	57.078287	X11_52661787
nfr	ppnfr11.1	PP	VAR	11	4.63	7.241787	5.023403	55.21479	X11_51849675
height	ppht11.1	PP	Slope	11	4.72	54.766175	53.964003	55.755602	X11_51849675
nfr	ppnfr11.1	PP	Slope	11	4.76	54.766175	52.915345	55.21479	X11_51849675
leaf	ppleaf11.1	PP	S.Tmax	11	4.83	55.10036	53.964003	55.87912	X11_52183860
fset	fset11.1	Mean	Mean	11	4.84	55.003933	53.823685	55.824549	X11_52087433
nflw	nflw11.2	Mean	Mean	11	4.91	55.10036	53.532037	55.755602	X11_52183860
height	ppht11.1	PP	S.Th.Amp	11	5.04	55.10036	53.964003	55.755602	X11_52183860
firm	ppfirm11.1	PP	S.Vpd	11	5.25	53.423887	1.136159	54.224712	X11_50507387
flw	flw11.1	Mean	Mean	11	5.48	54.599648	53.206534	55.755602	X11_51683148
diam	diam11.1	Mean	Mean	11	5.64	4.781218	4.151798	5.476941	X11_4781218
nflw	ppnflw11.1	PP	S.RH	11	6.15	7.241787	4.151798	7.826292	X11_7241787
fw	ppfw11.2	PP	S.SDD	11	6.37	53.423887	53.206534	53.823685	X11_50507387
diam	ppdiam11.2	PP	Slope	11	6.40	55.578287	53.964003	55.824549	X11_52661787
nflw	ppnflw11.2	PP	S.RH	11	7.00	55.10036	54.599648	55.755602	X11_52183860
SSC	ppSSC11.2	PP	VAR	11	7.61	54.599648	52.42503	55.824549	X11_51683148
nflw	ppnflw11.1	PP	Slope	11	7.72	5.476941	4.151798	7.826292	X11_5476941
nflw	ppnflw11.2	PP	Slope	11	7.81	55.10036	54.599648	55.755602	X11_52183860
SSC	SSC11.1	Mean	Mean	11	8.38	48.659366	25.747752	50.676545	X11_45742866
fw	ppfw11.2	PP	Slope	11	8.48	53.423887	53.206534	53.823685	X11_50507387
fw	fw11.3	QEI	QEI	11	8.65	55.10036	53.60036	56.60036	X11_52183860
fw	fw11.3	Mean	Mean	11	8.86	55.10036	54.268855	55.21479	X11_52183860
firm	firm11.1	QEI	QEI	11	8.93	50.495947	48.995947	51.995947	X11_47579447

fw	ppfw11.3	PP	VAR	11	9.88	55.003933	54.464915	56.105593	X11_52087433
firm	firm11.1	Mean	Mean	11	11.74	53.035288	52.42503	53.423887	X11_50118788
fw	fw12.2	Mean	Mean	12	4.45	4.892313	3.666238	37.355136	X12_4892313
nflw	ppnflw12.1	PP	S.RH	12	4.45	2.15924	1.921369	2.821857	X12_2159240
height	ppht12.2	PP	Slope	12	4.54	65.945275	65.580355	67.142748	X12_64286325
nflw	ppnflw12.1	PP	Slope	12	4.75	2.36717	1.921369	2.821857	X12_2367170
diam	ppdiam12.2	PP	VAR	12	4.86	64.125346	36.724611	65.419995	X12_62566296
fw	fw12.1	Mean	Mean	12	4.87	0.409174	0.010859	0.972302	X12_409174
nfr	ppnfr12.1	PP	VAR	12	4.99	2.36717	2.109522	2.821857	X12_2367170
height	ppht12.1	PP	S.Th.Amp	12	5.07	0.882566	0.493722	66.824887	X12_882566
flw	flw12.1	Mean	Mean	12	5.23	2.821857	1.921369	3.722833	X12_2821857
height	ppht12.1	PP	Slope	12	5.28	0.882566	0.493722	0.972302	X12_882566
nflw	nflw12.1	Mean	Mean	12	5.31	2.713152	2.36717	2.821857	X12_2713152
flw	flw12.1	QEI	QEI	12	5.45	2.821857	1.321857	4.321857	X12_2821857
diam	diam12.1	Mean	Mean	12	5.86	2.15924	1.921369	2.56488	X12_2159240

Supplemental Table 5: Genetic location of the MAGIC-MET QTLs overlapping with the Sweep (domestication/improvement) regions.

Region	Chromosome	Start	End	QEI	Mean	Plasticity
SW8	Chr1	420000	520000			fset1.1; nfr1.1
SW9	Chr1	870000	1220000			fset1.1; nfr1.1; SSC1.1
SW22	Chr1	75720000	77870000	ht1.1; flw1.1		
SW34	Chr1	90290000	90580000			ht1.2
SW35	Chr1	91440000	91650000		SSC1.2	
SW36	Chr1	93170000	93700000	fset1.3		
SW37	Chr1	93900000	94000000	fset1.3		
SW47	Chr2	40940000	41180000	diam2.1		
SW49	Chr2	44300000	45020000	SSC2.1		
SW50	Chr2	45420000	46660000	SSC2.1		
SW51	Chr2	46830000	46970000	ht2.1		
SW52	Chr2	48130000	48280000	ht2.1	fw2.1	fw2.1; leaf2.1
SW54	Chr2	52990000	53290000	fw2.2		
SW55	Chr2	53740000	53890000	fw2.2		
SW74	Chr3	62310000	62950000			flw3.1
SW75	Chr3	64760000	65010000	leaf3.1; fset3.1; fw3.2	ht3.1; fset3.1; flw3.2	ht3.1
SW78	Chr4	1470000	1960000		nflw4.1	
SW79	Chr4	2780000	2880000		nfr4.1; nflw4.1	nfr4.1
SW80	Chr4	3280000	4130000		nflw4.1	
SW82	Chr4	64300000	64500000	diam4.1; ht4.2	diam4.1; ht4.2; nflw4.2	nflw4.2
SW85	Chr5	2160000	2530000	SSC5.1		
SW86	Chr5	7670000	7820000	flw5.1		
SW114	Chr6	42230000	43700000	flw6.1		
SW116	Chr6	45370000	47400000	leaf6.1		
SW152	Chr7	59360000	59500000			flw7.1
SW207	Chr8	59490000	59960000		fw8.1	fw8.1
SW208	Chr8	60240000	60630000		fw8.1	fw8.1
SW213	Chr9	1000000	1220000			nfr9.1
SW215	Chr9	4530000	4890000			SSC9.1
SW217	Chr9	63490000	64600000	leaf9.1		
SW222	Chr9	69020000	69260000		flw9.2	
SW223	Chr9	69460000	69570000		flw9.2	
SW224	Chr9	69990000	70570000			fw9.1
SW225	Chr10	610000	850000		fset10.1	fset10.1
SW226	Chr10	1150000	1450000		fset10.1	fset10.1
SW253	Chr11	52740000	53040000	firm11.1	firm11.1	
SW254	Chr11	53810000	53980000	flw11.1		fw11.2; flw11.1; ht11.1; leaf11.1; diam11.2
SW255	Chr11	55240000	55620000	flw11.1; fw11.3	fw11.3	flw11.1; fw11.3; nflw11.2; ht11.1; leaf11.1; diam11.2

SW256	Chr12	50000	350000		fw12.1	
SW257	Chr12	790000	1310000		fw12.1;	ht12.1
SW258	Chr12	2710000	3070000	flw12.1	nflw12.1; flw12.1	nflw12.1; nfr12.1
SW263	Chr12	65270000	66040000			ht12.2